doi.org/10.26434/chemrxiv.12624869.v1

Palladium-Catalyzed Carboformylation Enabled by a Molecular Shuffling Process

Yong Ho Lee, Elliott Denton, Bill Morandi

Submitted date: 08/07/2020 • Posted date: 09/07/2020

Citation information: Lee, Yong Ho; Denton, Elliott; Morandi, Bill (2020): Palladium-Catalyzed Carboformylation Enabled by a Molecular Shuffling Process. ChemRxiv. Preprint. https://doi.org/10.26434/chemrxiv.12624869.v1

Hydroformylation, a reaction which installs both a C–H bond and an aldehyde group across an unsaturated substrate, is one of the most important catalytic reactions both in industry and academia. Given the synthetic importance of creating new C–C bonds, and the widespread academic and industrial impact of hydroformylation, the development of carboformylation reactions, wherein a new C–C bond is formed instead of a C–H bond, would bear enormous synthetic potential to rapidly increase molecular complexity in the synthesis of valuable aldehydes. However, the demanding complexity inherent in a four-component reaction, utilizing an exogenous CO source, has made the development of a direct carboformylation reaction a formidable challenge. Here, we describe a molecular shuffling strategy featuring the use of readily available aroyl chlorides as a carbon electrophile and CO source, in tandem with a sterically congested hydrosilane, to perform a stereoselective carboformylation of alkynes under palladium catalysis. An extension of this protocol to four chemodivergent carbonylations further highlights the creative opportunity offered by this molecular shuffling strategy in carbonylation chemistry.

Palladium-catalyzed carboformylation enabled by a molecular shuffling process

Yong Ho Lee, Elliott H. Denton, Bill Morandi*

ETH Zürich, Vladimir-Prelog-Weg 3, HCI, 8093 Zürich, Switzerland.

*Correspondence to: bill.morandi@org.chem.ethz.ch

Abstract

Hydroformylation, a reaction which installs both a C–H bond and an aldehyde group across an unsaturated substrate, is one of the most important catalytic reactions both in industry and academia. Given the synthetic importance of creating new C–C bonds, and the widespread academic and industrial impact of *hydroformylation*, the development of *carboformylation* reactions, wherein a new C–C bond is formed instead of a C–H bond, would bear enormous synthetic potential to rapidly increase molecular complexity in the synthesis of valuable aldehydes. However, the demanding complexity inherent in a four-component reaction, utilizing an exogenous CO source, has made the development of a direct carboformylation reaction a formidable challenge. Here, we describe a molecular shuffling strategy featuring the use of readily available aroyl chlorides as a carbon electrophile and CO source, in tandem with a sterically congested hydrosilane, to perform a stereoselective carboformylation of alkynes under palladium catalysis. An extension of this protocol to four chemodivergent carbonylations further highlights the creative opportunity offered by this molecular shuffling strategy in carbonylation chemistry.

Carbonylation reactions using carbon monoxide (CO) constitute an industrial core technology. They provide a direct and atom-economic strategy to convert, on a multimillion ton-scale per year, bulk chemicals to various carbonyl-containing compounds and their derivatives, which are essential commodity products in daily life[1–4]. Due to the importance of these reactions in preparative chemistry, intense academic and industrial research has been dedicated to the development of more environmentally benign and robust catalyst systems as well as highly chemo-, regio- and stereoselective carbonylation reactions[5–13]. Simultaneously, significant research has focused on vanquishing the hazards associated with the use of toxic and highly flammable CO, as well as avoiding the use of pressurized reactors to facilitate laboratory use. Among these strategies, the use of CO surrogates and two-chamber systems operating under mild conditions, as well as CO transfer by shuttle catalysis and single bond metathesis strategies, have emerged as valuable alternatives[14–21].

Among all carbonylation reactions, catalytic hydroformylation, the addition of CO and H_2 across unsaturated substrates, is an essential reaction to access a wide set of functionalized aldehyde products. Both the industrial and academic importance of this reaction are clearly highlighted by the large volumes of aldehydes it generates annually (>12 million tons), as well as the continuous filing and publication of new patents and manuscripts in this area (>10,000)[2]. A key feature of hydroformylation is the possibility to introduce an aldehyde group, arguably one of the most versatile functional groups in target-oriented synthesis, alongside the formation of a new C–H bond (Fig. 1A, top)[2,22–24]. Given the importance of creating new C–C bonds[25] and the widespread academic and industrial impact of *hydroformylation*, the development of *carboformylation* reactions, wherein a new C–C bond is formed instead of a C–H bond, would bear enormous synthetic potential as a tool to rapidly prepare densely functionalized aldehydes which are widespread synthetic intermediates (Fig. 1a, bottom).

Despite the promises offered by a carboformylation paradigm, only a single isolated example of carboformylation has been disclosed thus far by Grigg (Fig. 1b)[26–28]. This report clearly captures the challenge of developing such a reaction, as it relies on a carefully designed intramolecular iodoarylalkene substrate undergoing a "molecular queuing" process, involving a hydrosilane and CO, to surgically manipulate the selective formation of three sequential bonds and generate the desired cyclized aldehyde product (Fig. 1b, top). The severity of the method´s limitations can be illustrated in an example where shortening the tether length by a single atom led to a different product arising from double insertion of CO (Fig. 1b, bottom)[29]. This extremely limited reactivity clearly highlights the universal challenges which have plagued the development of intermolecular carboformylation reactions (Fig. 1c): (1) the need for a catalyst system that can delicately mediate a single and selective incorporation of one molecule of CO in the presence of an excess of CO gas; (2) the nearly impossible task to orchestrate an intermolecular, chemoselective four-component reaction (an electrophile, CO, a hydride source and an unsaturated substrate), a process which can potentially lead to the formation of more than 10 different products[24,29–34]; (3) the use of toxic and highly flammable CO itself, which has likely limited further research on this topic.

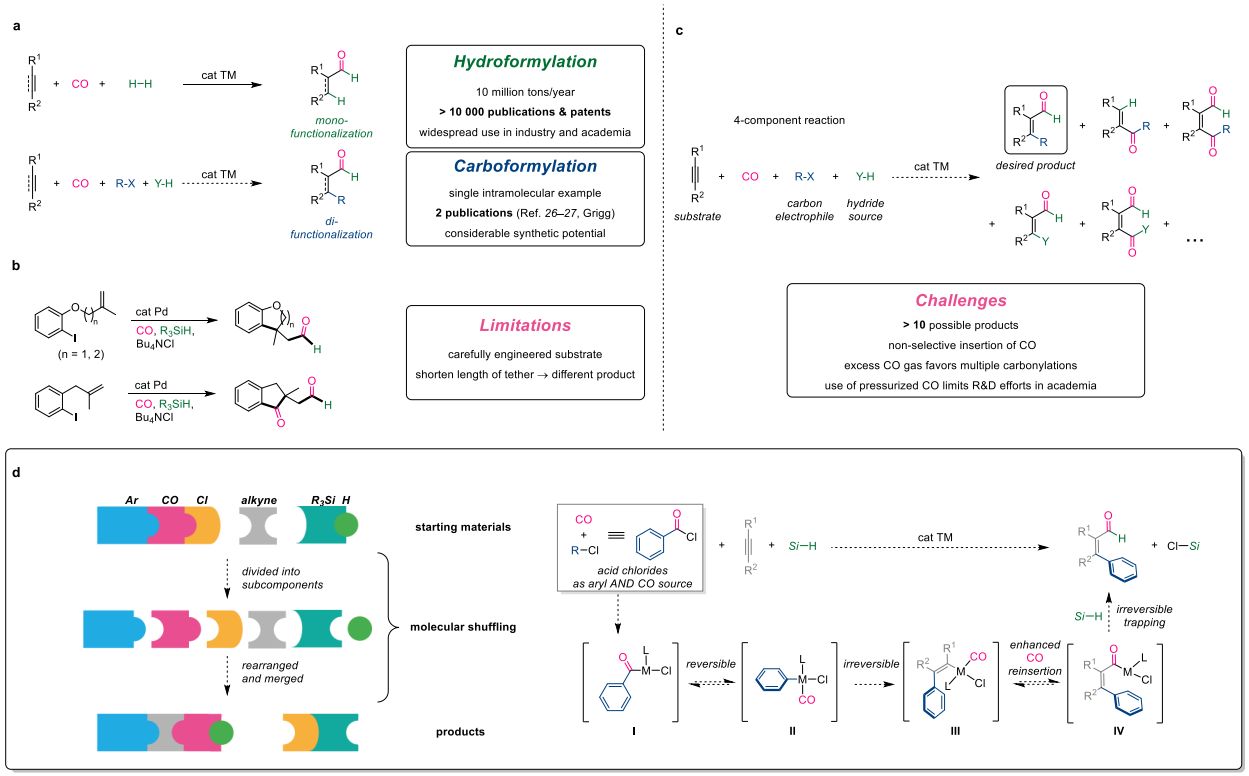

Fig. 1. Comparison between conventional hydroformylation and carboformylation. a, Hydroformylation versus carboformylation. **b**, Intramolecular carboformylation developed by Grigg (1995). **c**, Challenges for intermolecular carboformylation using a conventional approach. **d**, Our strategy - molecular shuffling using acid chlorides as aryl and CO source. cat TM, transition metal catalyst. R–X, carbon electrophile. Y–H, hydride source. cat Pd, palladium catalyst. *Si*–H, hydrosilane. Cl–*Si*, chlorosilane. L, ligand.

We hypothesized that the challenges of developing an intermolecular carboformylation reaction could potentially be addressed by using acid chlorides as reagents[19–21]. We reasoned that they could simultaneously act as an atom-economic source of a carbon electrophile and CO in a catalytic carboformylation reaction proceeding through a molecular shuffling process involving a sequence of C–C bond cleavage and formation events, mediated by a transition metal catalyst (Fig. 1d)[35,36]. The use of acid chlorides appeared ideal for several reasons: (1) only 1 equivalent of CO would be present in the entire reaction system, preventing additional insertions often observed using excess CO gas as a reagent; (2) acid chlorides can rapidly react with a low valent transition metal to generate the corresponding aryl–M complex (**II**, *e.g.* M = Pd), which can then add across a triple bond; (3) the intermediacy of a M–Cl bond should significantly slow down any undesirable C–Cl reductive elimination prior to the programmed CO reinsertion[37–40]. These essential features should lead to the formation of the final acyl complex (**IV**) which can then be irreversibly trapped by a hydride, to develop a general platform for the elusive carboformylation reaction[12,13]. However, a daunting challenge to be addressed in this strategy is to prevent any premature trapping of several closely related organopalladium intermediates (**I**, **II** and **III**) generated under the reaction conditions.

Herein, we report an intermolecular carboformylation reaction of internal alkynes using aroyl chlorides as a dual aryl and CO source. We describe a molecular shuffling process in which an aromatic acid chloride is formally deconstructed to aryl, CO and Cl subcomponents by a Pd catalyst. The individual subcomponents are then "shuffled" and merged with an alkyne and silane in a programmed order, providing a conceptual framework for the realization of a carboformylation reaction (Fig. 1d). Using bulky hydrosilane reductants, we were able to transform a broad range of alkynes into the corresponding functionalized, tetrasubstituted α,β-unsaturated aldehydes. The generality of this shuffling concept is further demonstrated by an extension of this reactivity, to the chemodivergent formation of three other valuable carbonyl derivatives, highlighting the potential of this strategy to unlock novel carbonylation reactions.

Results and discussion

To test our initial hypothesis, we chose internal alkynes and aromatic acid chlorides as test substrates to prepare highly functionalized α,β-unsaturated aldehydes which are normally accessed through tedious multi-step synthesis[23,41]. After observing small amounts of the product using a wide variety of different phosphine ligands (see Supplementary Section 2), we reasoned that selectively intercepting the right Pd intermediate (**IV**) with a hydride source would be crucial to improve the yield of the product. We took advantage of the vast palette of commercially available hydrosilanes exhibiting different steric profiles to probe their influence on the reactivity. A clear correlation between the yield of the desired product relative to the steric bulk of the silane could be observed. Using smaller silanes, a larger amount of the undesired aromatic aldehyde was generated, presumably due to premature reduction of Pd intermediate **I** (Fig. 1d), whereas sterically congested silanes, $i\text{Pr}_3\text{SiH}$ and $(i\text{Pr}_2\text{HSi})_2\text{O}$, resulted in the highest yields of the desired product. After systematic fine-tuning, two phosphine ligands, BISBI (2,2'-

bis(diphenylphosphinomethyl)-1,1'-biphenyl) and TDMPP (tris(2,6-dimethoxyphenyl)phosphine), were found to be optimal, therefore resulting in two complementary conditions for the reaction depending on the steric confinement of the aroyl chloride substrate (**1**, **14**, **18**)[42,43].

With the optimized conditions in hand, we set out to investigate the scope of this carboformylation. Various (hetero)aroyl chlorides bearing *ortho*-substituents successfully participate in this Pd-catalyzed carboformylation with 4-octyne, producing the desired α,β-unsaturated aldehydes with excellent (*Z*)-selectivities and in good yields (Table 1)[20,37,44]. Sterically less hindered aroyl chlorides provided moderate yields accompanied by 5–20% of the corresponding (*E*)-isomer, suggesting that the *ortho*-substituents of aroyl chlorides impede *E*/*Z* isomerization[11,12]. Methyl-, ethyl-, benzyl- and trifluoromethyl ethers (**3**, **5**, **21**, **22**), esters (**4**, **24**), nitriles (**6**, **26**), trifluoromethyl groups (**7**, **28**), ketones (**10**) and sulfonamides (**29**) are tolerated. Aryl halogenides (Cl (**8**, **15**), Br (**25**)) and aryl boronate esters (**23**), which are, respectively, ubiquitous carbon electrophiles and nucleophiles in conventional cross-coupling reactions, are compatible. Furthermore, a benzyl protecting group (**22**) remained intact under the reducing reaction conditions, namely a Pd catalyst and a hydride source, illustrating the orthogonality and chemoselectivity of this new reaction. Heteroaromatic acid chlorides, including thiophene (**11**), benzofuran (**12**), pyridine (**13**), isoxazole (**16**) and thiazole (**30**) derivatives, are also effective reaction partners. In addition, two derivatives of carboxylic acid-containing pharmaceutical compounds (probenecid (**29**) and febuxostat (**30**)) participated in this carboformylation. Notably, aroyl chlorides bearing electron-withdrawing substituents showed moderate yields and diminished stereoselectivity. GC analysis of the crude reaction mixtures showed an increased yield of a side product arising from competing hydroarylation, indicating that CO reinsertion (**III** to **IV**) is less favored with electron-poor substrates. Finally, using isotopically labelled reagents, the D and ^{13}C labels were efficiently incorporated into the desired products (**2**, **20**), highlighting the synthetic potential of this method as an addition to medicinal chemistry's toolbox for the preparation of isotopically labelled α,β-unsaturated aldehydes[16,45]. Gratifyingly, the reaction could be performed on a multi-gram scale (25 mmol), delivering the product (**1**) in excellent yield (83%, 4.8 g) with complete stereoselectivity. This result clearly demonstrates the potential of this reaction for preparative synthesis without the need for any specialized equipment[46], such as autoclaves or two-chamber reaction vessels.

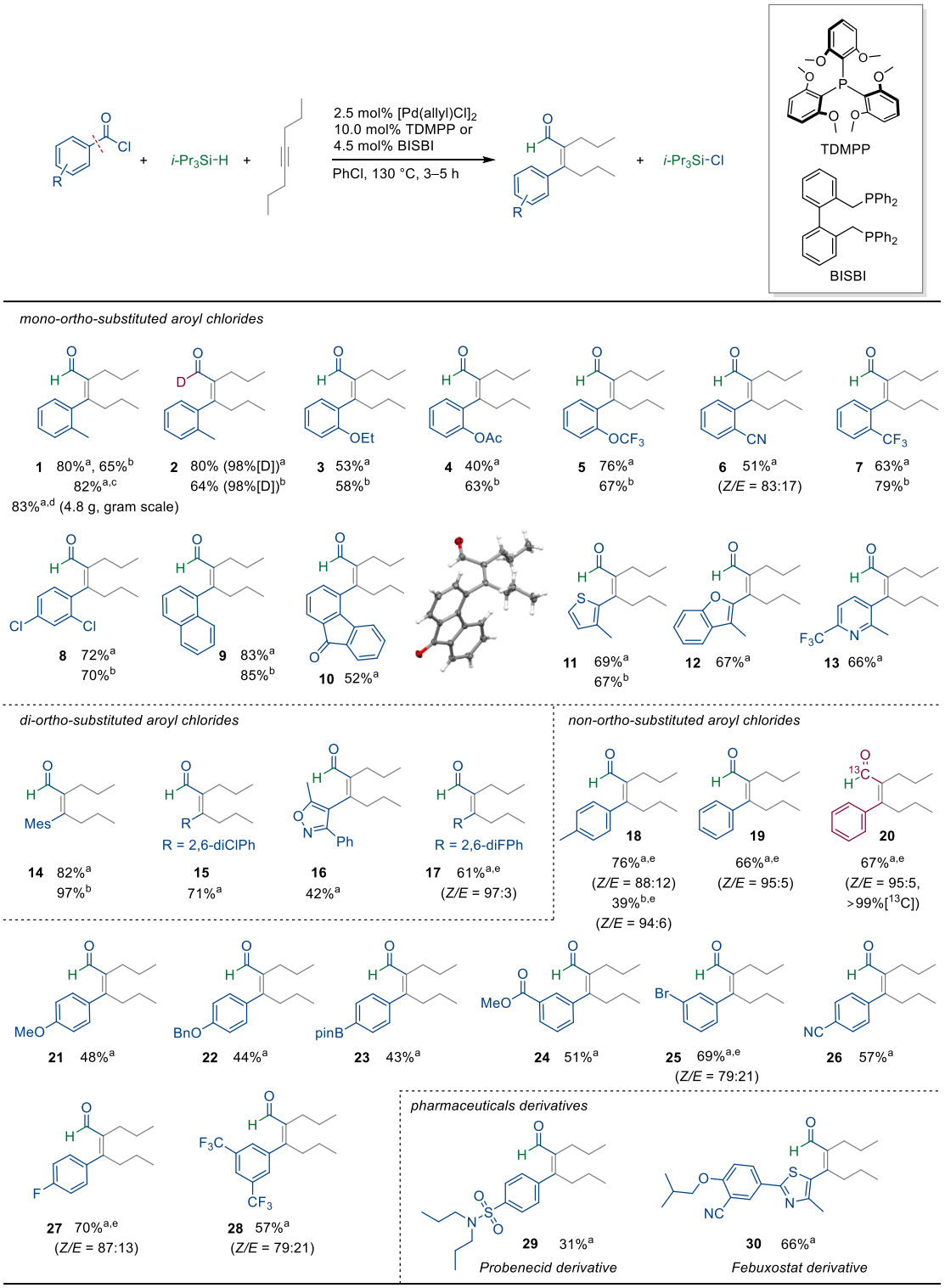

Table 1. Scope with respect to aroyl chlorides. All yields are isolated as a single stereoisomer unless otherwise stated. [a]TDMPP. [b]BISBI. [c]Open system. [d]Open system, 25 mmol scale. [e]Isolated as an inseparable mixture of stereoisomers. Mes, Mesityl. 2,6-diClPh, 2,6-Dichlorophenyl. 2,6-diFPh, 2,6-Difluorophenyl. For details, see Supplementary Section 3 and 11.

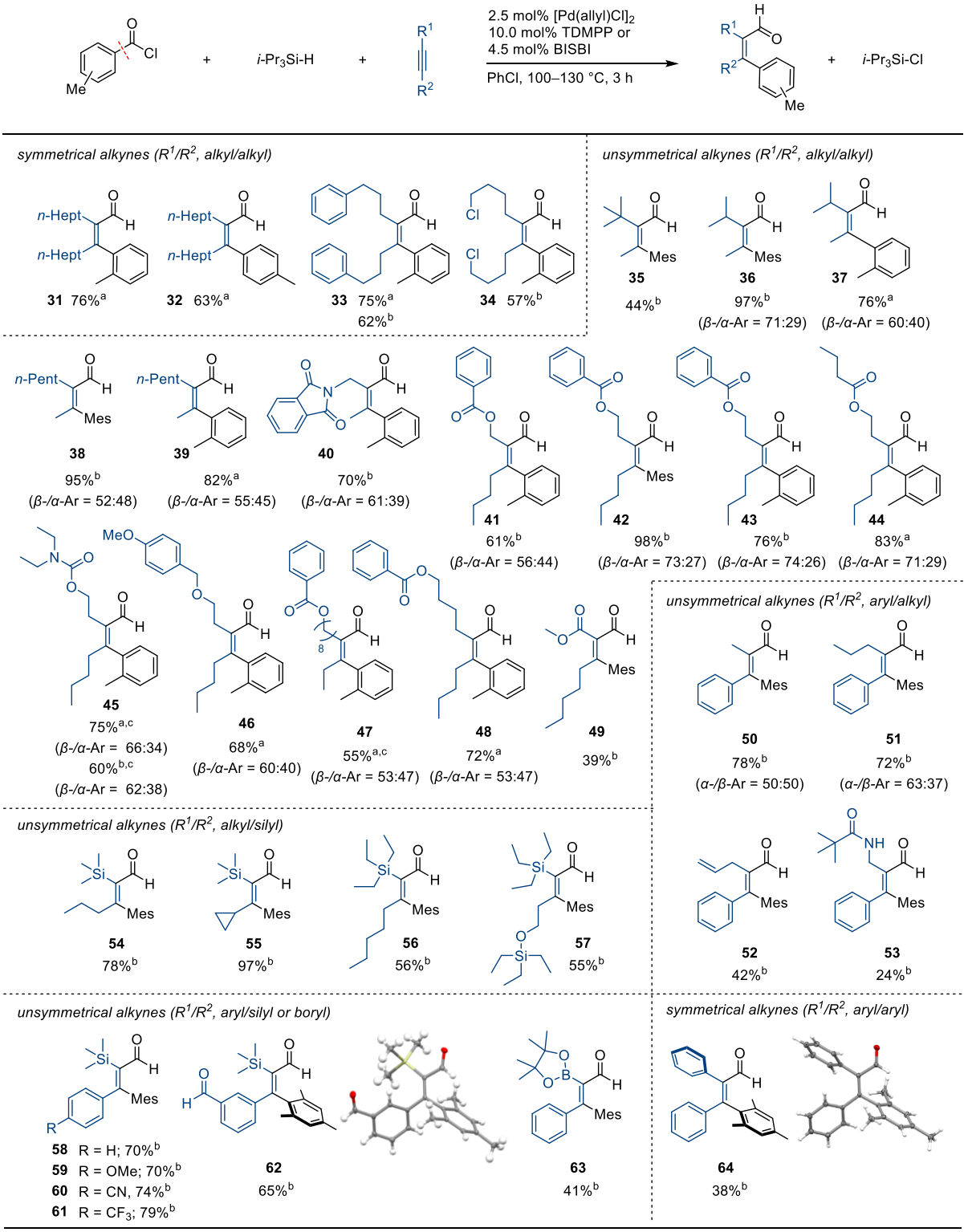

Table 2. Scope with respect to internal alkynes. All yields are isolated as a single stereo- and regioisomer unless otherwise stated. [a]TDMPP. [b]BISBI. [c]Isolated as an inseparable mixture of regioisomers. *n*-Hept, *n*-Heptyl. *n*-Pent, *n*-Pentyl. Mes, Mesityl. For details, see Supplementary Section 3.

Next, the generality of this method with respect to symmetrical and unsymmetrical internal alkynes was explored using *o*-, *p*-toluoyl and mesitoyl chlorides as representative acid chloride substrates (Table 2). Alkyl chlorides (**34**), phthalimides (**40**), esters (**41**–**44**, **47**–**49**), carbamates (**45**), alkenes (**52**), amides (**53**), silyl ethers (**57**) and aldehydes (**62**) were all tolerated. Several internal alkynes tethered with a polar functional group such as phthalimides, esters, carbamates and ethers were also probed to explore whether directing effects could influence the reaction´s regioselectivity. While most of them resulted in only slightly improved or negligible regioselectivity, an ester at the β-position relative to the alkyne led to a synthetically useful ratio of separable isomers (up to 3:1, **42**–**44**)[18]. Additionally, high regioselectivity was obtained when a highly sterically encumbered alkyne is reacted with a bulky aroyl chloride (**35**), displaying preferential aryl insertion at the distal position relative to the bulky group, presumably to minimize steric repulsion. Next, aryl-alkyl and diaryl alkynes (**50**–**53**, **64**) were shown to be suitable substrates for this transformation, offering new opportunities to access novel conjugated aldehydes with potential applications in imaging and organic materials[47–50]. With regards to the regioselectivity in this class of substrates, electronic effects seem to prevail slightly over steric effects since arylation occurred at the more hindered position of an alkyne, resulting in geminal diaryl functionalities (**51**). While terminal alkynes failed to deliver the anticipated product, likely because of polyinsertion side-reactions[43], we found that a number of alkyl-silyl (**54**–**57**), aryl-silyl alkynes (**58**–**62**), and even an aryl-boryl alkyne (**63**) reacted with complete regio- and stereoselectivity. While being valuable products in their own right, they also grant access, after deprotection, to synthetically desirable products not directly accessible through the direct carboformylation of terminal alkynes.

We next investigated whether our molecular shuffling concept would allow for the inclusion of alternative nucleophiles, other than a hydride, as well as different skeletal shuffling processes depending on the structure of the acid chloride reagent. Such extensions would allow for a chemodivergent and modular process, which is enabled by the discovery of our molecular shuffling strategy. As a proof-of-concept, we were interested in replacing both the hydride with an aryl nucleophile, to generate either an aldehyde or a ketone, as well as the aroyl chloride electrophile with an aliphatic acid chloride, to allow for potential reactivity divergences in the shuffling process. Such a set of experiments involving all the permutations would enable us to transform the same alkyne substrate into four kinds of diversified products under a nearly identical set of reaction conditions (Fig. 2, top). Remarkably, with only subtle modification of the reaction conditions, four different carbonylated products could indeed be obtained in good yields and excellent stereoselectivities, making this molecular shuffling concept a modular tool for the realization of diverse carbonylation reactions (Fig. 2, bottom). Apart from carboformylation, a CO-free carboacylation could also be realized by using an aryl stannane as a nucleophile in place of the silane (**66**). Furthermore, the use of aliphatic acid chlorides, which can undergo molecular shuffling to release an alkene, CO and a hydride, unlocked the corresponding hydroformylation and hydroacylation processes (**65**, **67**), thus significantly expanding the breadth of the strategy.

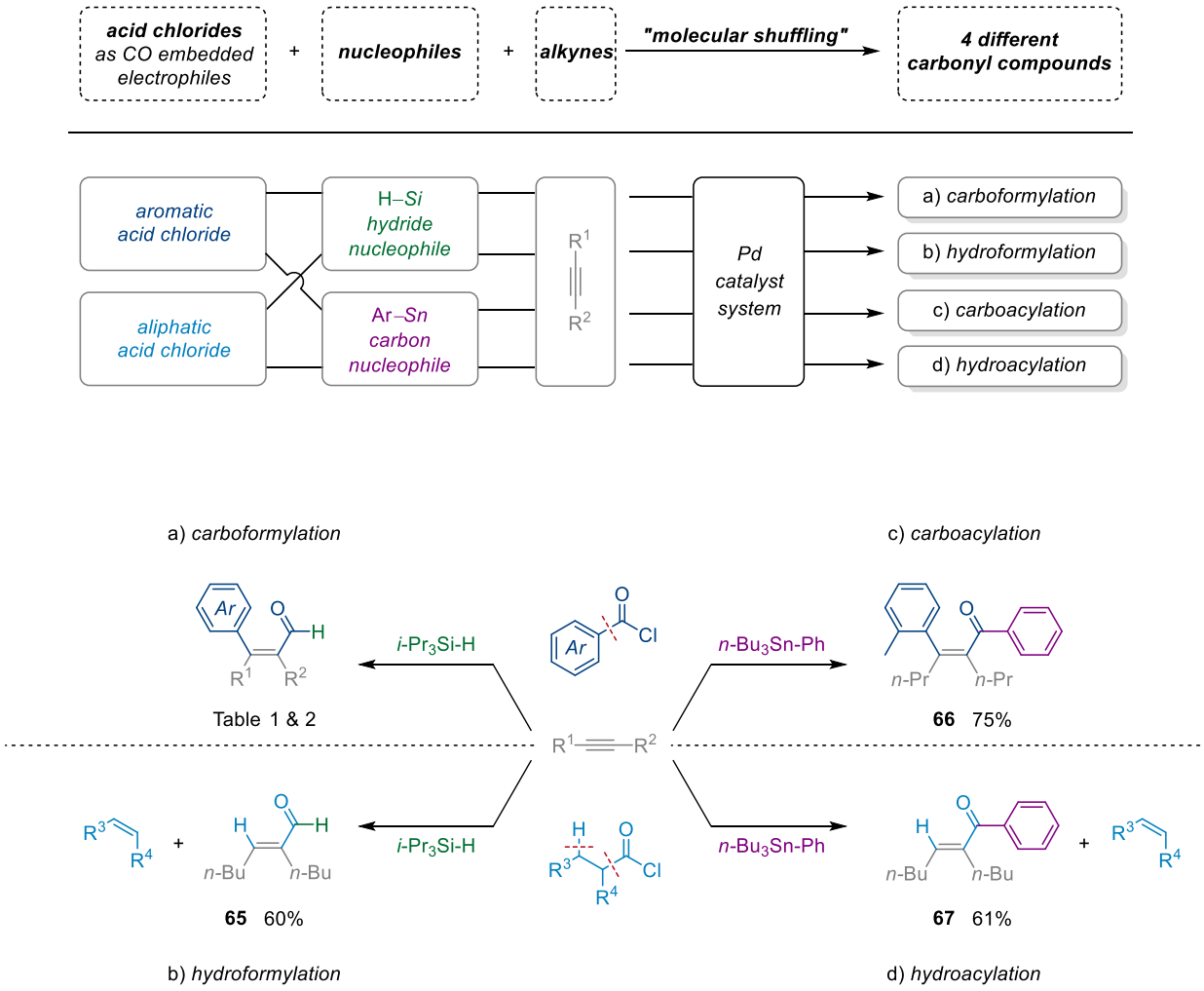

Fig. 2. Chemodivergent carbonylations by molecular shuffling. All yields are isolated as a single stereoisomer unless otherwise stated. For details, see Supplementary Section 4, 5 and 6. H–*Si*, hydrosilane. Ar–*Sn*, aryl stannane.

In summary, we have developed a reaction for the carboformylation of alkynes. Not only does this reaction add a versatile aldehyde moiety across an alkyne, but it does so concomitantly while forming a new C–C bond, offering a facile route to densely functionalized aldehydes which are otherwise challenging to access. The enabling feature of this reaction is the use of an aroyl chloride as both a carbon electrophile and CO source through a molecular shuffling strategy. In a broader context, this reactivity clearly highlights the potential of this approach for the development of a vast array of new, CO-free carbonylation reactions as demonstrated in a striking example of chemodivergent catalysis.

References

1. Bertleff, W., Roeper, M. & Sava, X. in *Ullmann's Encyclopedia of Industrial Chemistry* 73–95 (Wiley-VCH, Weinheim, 2007).
2. Börner, A. & Franke, R. *Hydroformylation: Fundamentals, Processes, and Applications in Organic Synthesis* (Wiley-VCH, Weinheim, 2016).
3. Cornils, B., Herrmann, W. A. & Rasch, M. Otto Roelen, pioneer in industrial homogeneous catalysis. *Angew. Chem. Int. Ed.* **33,** 2144–2163 (1994).
4. Kiss, G. Palladium-catalyzed Reppe carbonylation. *Chem. Rev.* **101,** 3435–3456 (2001).
5. Peng, J.-B., Wu, F.-P. & Wu, X.-F. First-row transition-metal-catalyzed carbonylative transformations of carbon electrophiles. *Chem. Rev.* **119,** 2090–2127 (2019).
6. Bai, Y., Davis, D. C. & Dai, M. Natural product synthesis via palladium-catalyzed carbonylation. *J. Org. Chem.* **82,** 2319–2328 (2017).
7. Hood, D. M. et al. Highly active cationic cobalt(II) hydroformylation catalysts. *Science* **367,** 542–548 (2020).
8. Yang, J. et al. Direct synthesis of adipic acid esters via palladium-catalyzed carbonylation of 1,3-dienes. *Science* **366,** 1514–1517 (2019).
9. Willcox, D. et al. A general catalytic β-C–H carbonylation of aliphatic amines to β-lactams. *Science* **354,** 851–857 (2016).
10. Kinney, R. G. et al. A general approach to intermolecular carbonylation of arene C–H bonds to ketones through catalytic aroyl triflate formation. *Nat. Chem.* **10,** 193–199 (2018).
11. Schoenberg, A. & Heck, R. F. Palladium-catalyzed formylation of aryl, heterocyclic, and vinylic halides. *J. Am. Chem. Soc.* **96,** 7761–7764 (1974).
12. Baillargeon, V. P. & Stille, J. K. Palladium-catalyzed formylation of organic halides with carbon monoxide and tin hydride. *J. Am. Chem. Soc.* **108,** 452–461 (1986).
13. Pri-Bar, I. & Buchman, O. Reductive formylation of aromatic halides under low carbon monoxide pressure catalyzed by transition-metal compounds. *J. Org. Chem.* **49,** 4009–4011 (1984).

14. Wu, L., Liu, Q., Jackstell, R. & Beller, M. Carbonylations of alkenes with CO surrogates. *Angew. Chem. Int. Ed.* **53,** 6310–6320 (2014).

15. Morimoto, T. & Kakiuchi, K. Evolution of carbonylation catalysis: no need for carbon monoxide. *Angew. Chem. Int. Ed.* **43,** 5580–5588 (2004).

16. Friis, S. D., Lindhardt, A. T. & Skrydstrup, T. The development and application of two-chamber reactors and carbon monoxide precursors for safe carbonylation reactions. *Acc. Chem. Res.* **49,** 594–605 (2016).

17. Murphy, S. K., Park, J.-W., Cruz, F. A. & Dong, V. M. Rh-catalyzed C–C bond cleavage by transfer hydroformylation. *Science* **347,** 56–60 (2015).

18. Tan, G., Wu, Y., Shi, Y. & You, J. Syngas-free rhodium-catalyzed highly regioselective transfer hydroformylation of alkynes to α,β-unsaturated aldehydes. *Angew. Chem. Int. Ed.* **58,** 7440–7444 (2019).

19. Fang, X., Cacherat, B. & Morandi, B. CO- and HCl-free synthesis of acid chlorides from unsaturated hydrocarbons via shuttle catalysis. *Nat. Chem.* **9,** 1105–1109 (2017).

20. Lee, Y. H. & Morandi, B. Metathesis-active ligands enable a catalytic functional group metathesis between aroyl chlorides and aryl iodides. *Nat. Chem.* **10,** 1016–1022 (2018).

21. De La Higuera Macias, M. & Arndtsen, B. A. Functional group transposition: a palladium-catalyzed metathesis of Ar–X σ-bonds and acid chloride synthesis. *J. Am. Chem. Soc.* **140,** 10140–10144 (2018).

22. Johnson, J. R., Cuny, G. D. & Buchwald, S. L. Rhodium-catalyzed hydroformylation of internal alkynes to α,β-unsaturated aldehydes. *Angew. Chem. Int. Ed.* **34,** 1760–1761 (1995).

23. Zhang, S., Neumann, H. & Beller, M. Synthesis of α,β-unsaturated carbonyl compounds by carbonylation reactions. *Chem. Soc. Rev.* https://doi.org/10.1039/C9CS00615J (2020).

24. Matsuda, I., Ogiso, A., Sato, S. & Izumi, Y. An efficient silylformylation of alkynes catalyzed by $Rh_4(CO)_{12}$. *J. Am. Chem. Soc.* **111,** 2332–2333 (1989).

25. Marek, I., Chinkov, N. & Banon-Tenne, D. in *Metal-Catalyzed Cross-Coupling Reactions* (eds de Meijere, A. & Diederich, F.) 395–478 (Wiley-VCH, Weinheim, 2004).

26. Brown, S., Clarkson, S., Grigg, R. & Sridharan, V. Palladium-catalysed cyclisation-carboformylation. molecular queuing cascades. *J. Chem. Soc., Chem. Commun.* 1135–1136 (1995).

27. Brown, S. et al. Palladium catalysed queuing processes. part 1: termolecular cyclization-anion capture employing carbon monoxide as a relay switch and hydride, organotin(IV) or boron reagents. *Tetrahedron* **57,** 1347–1359 (2001).

28. Negishi, E., Copéret, C. in *Handbook of Organopalladium Chemistry for Organic Synthesis* (ed Negishi, E.) 1431–1448 (Wiley, New York, 2002).

29. Van den Hoven, B. G. & Alper, H. Innovative synthesis of 4-carbaldehydepyrrolin-2-ones by zwitterionic rhodium catalyzed chemo- and regioselective tandem cyclohydrocarbonylation/CO insertion of α-Imino alkynes. *J. Am. Chem. Soc.* **123,** 10214–10220 (2001).

30. Fuji, K., Morimoto, T., Tsutsumi, K. & Kakiuchi, K. Rh(I)-catalyzed CO gas-free cyclohydrocarbonylation of alkynes with formaldehyde to α,β-butenolides. *Chem. Commun.* 3295–3297 (2005).

31. Peng, J.-B., Wu, F.-P., Spannenberg, A. & Wu, X.-F. Palladium-catalyzed tunable carbonylative synthesis of enones and benzofulvenes. *Chem. Eur. J.* **25,** 8696–8700 (2019).

32. Fujihara, T., Tatsumi, K., Terao, J. & Tsuji, Y. Palladium-catalyzed formal hydroacylation of allenes employing acid chlorides and hydrosilanes. *Org. Lett.* **15,** 2286–2289 (2013).

33. Kokubo, K., Matsumasa, K., Miura, M. & Nomura, M. Rhodium-catalyzed reaction of aroyl chlorides with alkynes. *J. Org. Chem.* **61,** 6941–6946 (1996).

34. Yasukawa, T., Satoh, T., Miura, M. & Nomura, M. Iridium-catalyzed reaction of aroyl chlorides with internal alkynes to produce substituted naphthalenes and anthracenes. *J. Am. Chem. Soc.* **124,** 12680–12681 (2002).

35. Wang, P., Rao, H., Zhou, F., Hua, R. & Li, C.-J. Ruthenium-catalyzed aldehyde functionality reshuffle: selective synthesis of *E*-2-arylcinnamaldehydes from *E*-β-bromostyrenes and aryl aldehydes. *J. Am. Chem. Soc.* **134,** 16468–16471 (2012).

36. Chen, P., Billett, B. A., Tsukamoto, T. & Dong, G. "Cut and Sew" Transformations via transition-metal-catalyzed carbon−carbon bond activation. *ACS Catal.* **7,** 1340–1360 (2017).

37. Tsuji, J. in *Handbook of Organopalladium Chemistry for Organic Synthesis* (ed Negishi, E.) 2643–2653 (Wiley, New York, 2002).

38. Shen, X., Hyde, A. M. & Buchwald, S. L. Palladium-catalyzed conversion of aryl and vinyl triflates to bromides and chlorides. *J. Am. Chem. Soc.* **132,** 14076–14078 (2010).

39. Petrone, D. A., Ye, J. & Lautens, M. Modern transition-metal-catalyzed carbon–halogen bond formation. *Chem. Rev.* **116,** 8003–8104 (2016).

40. Malapit, C. A., Ichiishi, N. & Sanford, M. S. Pd-catalyzed decarbonylative cross-couplings of aroyl chlorides, *Org. Lett.* **19,** 4142–4145 (2017).

41. Flynn, A. B. & Ogilvie, W. W. Stereocontrolled synthesis of tetrasubstituted olefins. *Chem. Rev.* **107,** 4698–4745 (2007).

42. Casey, C. P. et al. Diphosphines with natural bite angles near 120° increase selectivity for *n*-aldehyde formation in rhodium-catalyzed hydroformylation. *J. Am. Chem. Soc.* **114,** 5535–5543 (1992).

43. Trost, B. M., Sorum, M. T., Chan, C., Harms, A. E. & Rühter, G. Palladium-catalyzed additions of terminal alkynes to acceptor alkynes. *J. Am. Chem. Soc.* **119,** 698–708 (1997).

44. El-Khawaga, A. M., Roberts, R. M. & Sweeney, K. M. Transacylations between sterically hindered aromatic ketones and various arenes. *J. Org. Chem.* **50,** 2055–2058 (1985).

45. Gauthier, Jr., D. R., Rivera, N. R., Yang, H., Schultz, D. M. & Shultz, C. S. Palladium-catalyzed carbon isotope exchange on aliphatic and benzoic acid chlorides. *J. Am. Chem. Soc.* **140,** 15596–15600 (2018).

46. Natta, G., Ercoli, R., Castellano, S. & Barbieri, F. H. The influence of hydrogen and carbon monoxide partial pressures on the rate of the hydroformylation reaction. *J. Am. Chem. Soc.* **76,** 4049–4050 (1954).

47. Cnossen, A., Browne, W. R. & Feringa, B. L. in *Molecular Machines and Motors* (eds Credi, A., Silvi, S. & Venturi, M.) 139–162 (Springer, Berlin, 2014).

48. Meier, H. The photochemistry of stilbenoid compounds and their role in materials technology. *Angew. Chem. Int. Ed.* **31,** 1399–1420 (1992).

49. Mei, J., Leung, N. L. C., Kwok, R. T. K., Lam, J. W. Y. & Tang, B. Z. Aggregation-induced emission: together we shine, united we soar! *Chem. Rev.* **115,** 11718–11940 (2015).

50. Chan, J., Dodani, S. C. & Chang, C. J. Reaction-based small-molecule fluorescent probes for chemoselective bioimaging. *Nat. Chem.* **4,** 973–984 (2012).

Data availability

Crystallographic data are available free of charge from the Cambridge Crystallographic Data Centre, under reference numbers CCDC 1998285 (**10**), 2000217 (**36**, **minor**), 2000218 (**53**), 1998290 (**62**), 1998292 (**64**), 1998293 (**L08**) and 1998299 (**69**). All other data are available in the main text or the Supplementary Information.

Acknowledgements

We acknowledge the ETH Zürich, the European Research Council under the European Union's Horizon 2020 research and innovation program (Shuttle Cat, Project ID: 757608), and LG Chem (fellowship to Y.H.L.) for financial support. We thank the NMR, MS (MoBiAS) and X-ray (SMoCC) service departments at ETH Zürich for technical assistance.

Author contributions

Y.H.L. designed and discovered the reaction. Y.H.L. and E.H.D. performed the scope of the reaction. B.M. supervised the research. All authors contributed to manuscript writing and editing.

Competing interests

The authors declare no competing interests.

Supplementary Information

Palladium-catalyzed carboformylation enabled by a molecular shuffling process

Yong Ho Lee, Elliott H. Denton, Bill Morandi*

ETH Zürich, Vladimir-Prelog-Weg 3, HCI, 8093 Zürich, Switzerland.

**Correspondence to: bill.morandi@org.chem.ethz.ch*

Table of contents

1. General information

Unless otherwise noted, all reactions were carried out under argon in oven-dried 4 mL screw-top glass vials using anhydrous solvents. The anhydrous solvents were prepared by distillation over appropriate drying agents or by using solvent purification system (LC Technology Solutions, Inc.) under N_2 atmosphere (H_2O content: below 10 ppm, as determined by Karl Fischer titration) and stored over molecular sieves prior to use. All commercially available compounds were used as received from common suppliers (Sigma-Aldrich, Strem Chemicals, abcr, TCI, Fluorochem, Acros Organics, Alfa Aesar and Apollo Scientific).

Thin layer chromatography (TLC): Aluminum TLC plate, silica gel coated with fluorescent indicator F254 (TLC Silica gel 60 F254, Merck). Visualization was accomplished using UV light (254 nm) or $KMnO_4$ stain.

Flash column chromatography: SiliaFlash P60 silica gel (60 Å, 40−63 μm, SiliCycle Inc.) with reagent grade solvents.

NMR: Spectra were recorded on Bruker AVANCE III 400, Neo 400, Neo 500, or 600 spectrometers at room temperature, unless indicated otherwise; the chemical shifts are reported with respect to internal solvent: δH = 7.26 ppm, and δC = 77.16 (t) ppm ($CDCl_3$); δH = 7.16 ppm, and δC = 128.06 (t) ppm (C_6D_6); δH = 2.50 (p) ppm, and δC = 39.52 (hept) ppm (DMSO-d6). Multiplicities are indicated by s (singlet), d (doublet), t (triplet), q (quartet), p (quintet), h (sextet), hept (septet), m(multiplet), br (broad), or combinations thereof. All 2D NMR measurements were performed by the NMR service in the Laboratorium für Organische Chemie at ETH Zürich.

GC/FID and GC/MS: Shimadzu GC-2025 (capillary column: Macherey-Nagel OPTIMA 5, 30.0 m× 0.25 mm × 0.25 μm; carrier gas: H_2); To determine GC yields, calibration curves were generated using *n*-dodecane as an internal standard. Shimadzu GCMS-QP2020 (capillary column: Macherey-Nagel OPTIMA 5, 30.0 m× 0.25 mm × 0.25 μm; carrier gas: He).

High-resolution MS (HRMS): Thermo scientific Q-Exactive GC Orbitrap for EI. Bruker Daltonics maXis ESI-QTOF or solariX ESI-FTICR-MS for ESI. HRMS data were obtained by the mass spectrometry service (MoBiAS, Molecular and Biomolecular Analysis Service) in the Laboratorium für Organische Chemie at ETH Zürich.

X-ray crystal structure: Bruker SMART Platform with Apex I CCD-detector, Bruker-Nonius Kappa-CCD, Bruker-Nonius Mach III/ Apex II CCD-detector, Rigaku Oxford Synergy with Dual-Microsource and Dectris Pilatus 300K. X-ray single crystal structure analyses were provided by the Small Molecule Crystallography Center (SMoCC) of Department of Chemistry and Applied Biosciences at ETH Zürich.

2. Reaction optimization

2.1. Phosphine Ligands

General procedure for ligand screening

In a glovebox, a 4 mL screw-cap vial equipped with a stirring bar was charged with $[Pd(allyl)Cl]_2$ (2.5 mol%, 6.25 µmol, 2.29 mg) and the indicated bisphosphine ligand (**L01-L35**, 4.5 mol%, 11.25 µmol) or the indicated monophosphine ligand (**L36-L65**, 9.0 mol%, 22.50 µmol) and then PhCl (2 mL). The solution was stirred at room temperature for 10 min. To a pre-mixed solution were added o-toluoyl chloride (3 equiv, 0.75 mmol), 4-octyne (1.0 equiv, 0.25 mmol) and triisopropylsilane (*i*Pr_3SiH, 3 equiv, 0.75 mmol). The reaction mixture was stirred at 130 °C for 3 h. The reaction was cooled to room temperature then diluted with DCM (2 mL) and *n*-dodecane was added as an internal standard. The resulting solution was filtered through a celite/silica plug and the filtrate was analyzed by GC/FID and GC/MS.

Supplementary Eq. 1. Ligand screening - bisphosphine ligands.

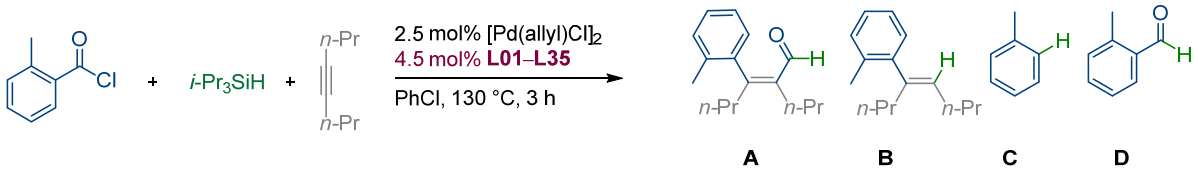

Supplementary Eq. 2. Ligand screening - monophosphine ligands.

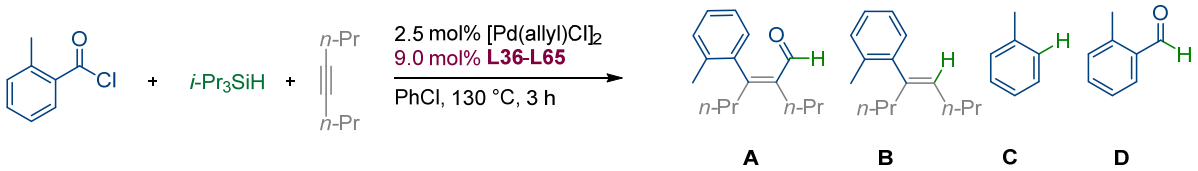

Supplementary Table 1. Ligand screening - bisphosphine ligands.

					Yield (%)[b]
Ligand	A	B	C	D	A+B+C+D
L01	67	1	149	42	258
L02	39	17	19	157	232
L03	43	15	27	157	243
L04	51	11	29	151	242
L05	41	3	44	142	230
L06	55	1	164	37	257
L07[a]	20	n.d.	137	3	160
L08[a]	21	n.d.	149	3	173
L09	70	5	62	113	249
L10	39	17	18	155	229
L11	45	13	17	162	237
L12	49	2	104	81	235
L13	54	3	115	70	241
L14	33	2	132	38	204
L15	52	1	153	48	255
L16	30	21	5	165	221
L17	9	6	31	79	125
L18	50	13	22	156	241
L19	34	20	12	171	237
L20	59	1	180	16	257
L21	27	23	6	169	224
L22	37	21	12	172	242
L23	46	1	199	13	260
L24	65	1	159	42	268
L25	62	4	84	100	250
L26	62	4	88	99	253
L27	64	1	107	81	254
L28	52	5	90	97	244
L29	59	2	137	48	247
L30	49	11	37	141	237
L31	46	15	23	156	240
L32	47	13	38	144	242
L33	57	3	84	101	244
L34	53	9	40	146	248
L35	35	9	32	148	224

[a]In a control experiment using 1.0 equivalents of both aroyl chloride and hydrosilane versus alkyne, both DBFphos (**L07)** and U-DNFphos (**L08)** gave a comparable yield of **A** (Supplementary Eq. 1) to BISBI (**L24)**. However, in Supplementary Table 1, the systems using **L7** and **L8** showed a remarkable decrease in conversion when 3.0 equivalents of aroyl chloride were employed, indicating that those ligand systems are more susceptible to higher concentration of aroyl chloride. [b]The GC yields are based on the moles of a limiting reagent, 4-octyne (0.25 mmol, 1 equiv.).

Supplementary Fig. 1. Ligand screening - bisphosphine ligands.

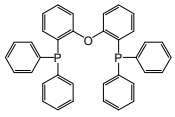

L01 DPEphos

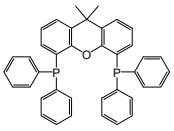

L02 Xantphos

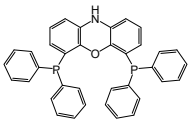

L03 4,6-Bis(diphenylphosphino)phenoxazine

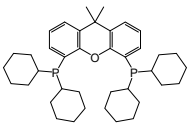

L04 4,5-Bis(dicyclohexylphosphino)-9,9-dimethylxanthene

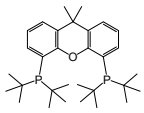

L05 9,9-Dimethyl-4,5-bis(di-t-butylphosphino)xanthene

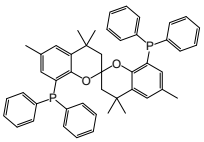

L06 SPANphos

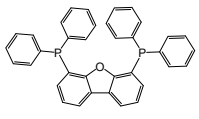

L07 DBFphos

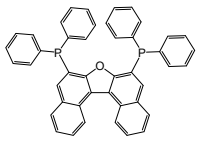

L08 6,8-bis(diphenylphosphaneyl)dinaphtho[2,1-*b*:1',2'-*d*]furan
U-DNFphos

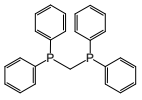

L09 dppm

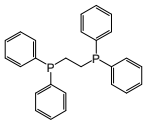

L10 dppe

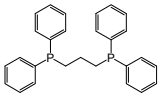

L11 dppp

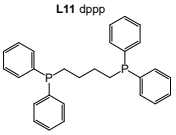

L12 dppb

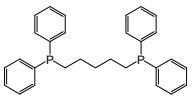

L13 dpppent

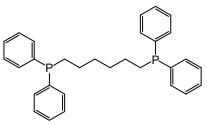

L14 dpphex

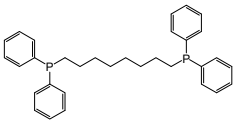

L15 dppoct

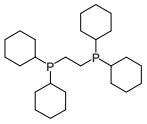

L16 dcype

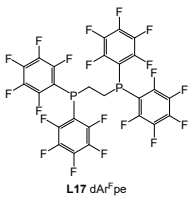

L17 dAr^{F}pe

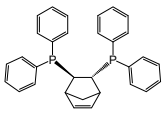

L18 (R,R)-NORPHOS
71042-55-2

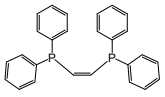

L19 cis-1,2-Bis(diphenylphosphino)ethylene

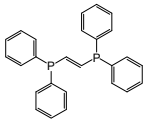

L20 trans-1,2-Bis(diphenylphosphino)ethylene

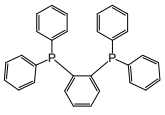

L21 1,2-Bis(diphenylphosphino)benzene

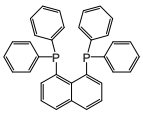

L22 1,8-(Diphenylphosphino)naphthalene

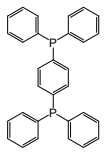

L23 1,4-bis(diphenylphosphaneyl)benzene

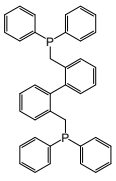

L24 BISBI

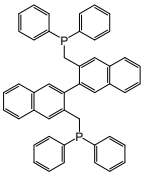

L25 VNAphos

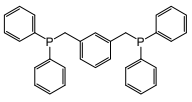

L26 1,3-Bis(diphenylphosphinomethyl)benzene

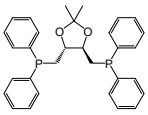

L27 (R,R)-DIOP

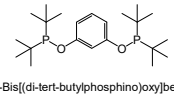

L28 1,3-Bis[(di-tert-butylphosphino)oxy]benzene

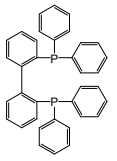

L29 BIPHEP

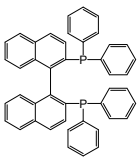

L30 rac-BINAP

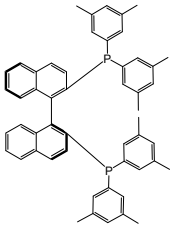

L31 (S)-(-)-2,2'-Bis[di(3,5-xylyl)phosphino]-1,1'-binaphthyl

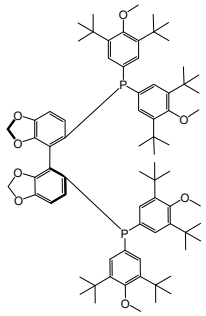

L32 (S)-DTBM-SEGPHOS

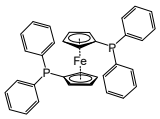

L33 dppf

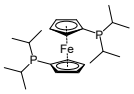

L34 1,1'-Bis(diisopropylphosphino)ferrocene

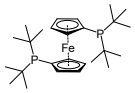

L35 1,1'-Bis(di-t-butylphosphino)ferrocene

Supplementary Table 2. Ligand screening - monophosphine ligands.

					Yield[a] (%)
	A	B	C	D	A+B+C+D
L36	82	2	103	69	256
L37	69	3	61	114	247
L38	66	3	184	15	268
L39	32	1	105	73	210
L40	36	1	222	5	264
L41	50	14	22	169	255
L42	26	4	62	80	171
L43	60	1	189	17	267
L44	39	15	29	153	237
L45	36	20	22	173	251
L46	32	17	24	160	233
L47	18	1	64	51	134
L48	6	n.d.	35	14	56
L49	55	2	170	35	262
L50	44	2	140	47	233
L51	44	9	48	134	235
L52	59	5	98	86	247
L53	43	1	187	32	264
L54	32	1	222	15	270
L55	32	1	214	21	268
L56	48	1	214	8	270
L57	60	4	189	6	260
L58	59	2	199	6	267
L59	54	2	191	27	275
L60	19	6	80	94	199
L61	14	6	4	54	78
L62	3	1	87	105	196
L63	16	1	107	100	224
L64	11	1	120	111	243
L65	n.d.	n.d.	70	167	236

[a]The GC yields are based on the moles of a limiting reagent, 4-octyne (0.25 mmol, 1 equiv.).

Supplementary Fig. 2. Ligand screening - monophosphine ligands.

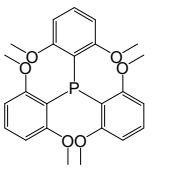

L36 TDMPP

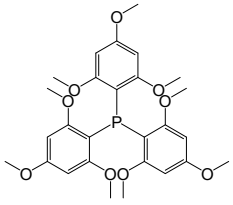

L37 TTMPP

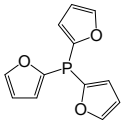

L38 Tri(2-furyl)phosphine

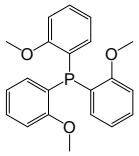

L39 Tris(o-methoxyphenyl)phosphine

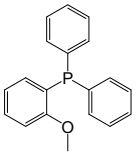

L40 Diphenyl(2-methoxyphenyl)-phosphine

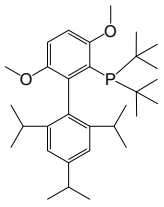

L41 tBuBrettPhos

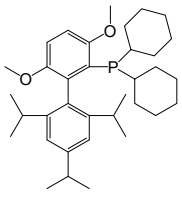

L42 BrettPhos

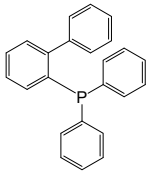

L43 2-(Diphenylphosphino)biphenyl

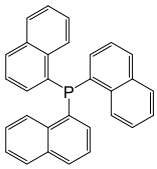

L44 Tri-1-naphthylphosphine

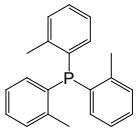

L45 Tri(o-tolyl)phosphine

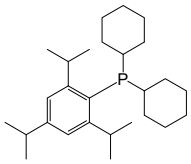

L46
Dicyclohexyl(2,4,6-triisopropylphenyl)-phosphine

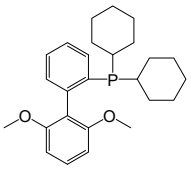

L47 Sphos

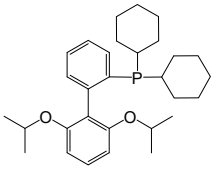

L48 RuPhos

L62 Tri-tert-butylphosphine

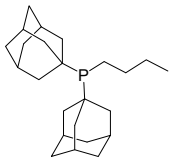

L63
Di(1-adamantyl)-n-butylphosphine

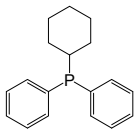

L49 Cyclohexyldiphenylphosphine

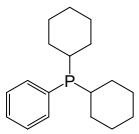

L50 Dicyclohexylphenylphosphine

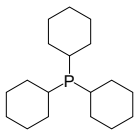

L51 Tricyclohexylphosphine

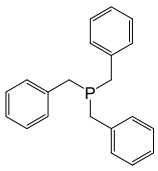

L52 Tribenzylphosphine

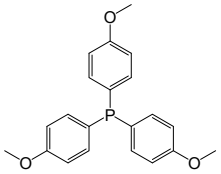

L53 Tris(4-methoxyphenyl)phosphine

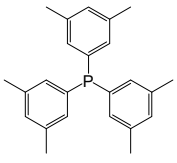

L54 Tris(3,5-dimethylphenyl)phosphine

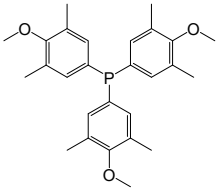

L55 Tris(4-methoxy-3,5-dimethylphenyl)-phosphine

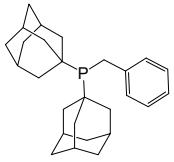

L64 Di(1-adamantyl)benzylphosphine

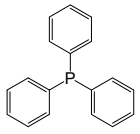

L56 Triphenylphosphine

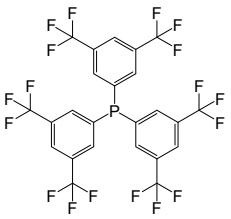

L57 Tris[3,5-bis(trifluoromethyl)phenyl]-phosphine

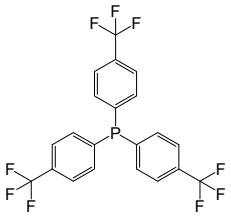

L58 Tris(4-trifluoromethylphenyl)phosphine

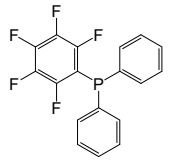

L59 (Pentafluorophenyl)diphenylphosphine

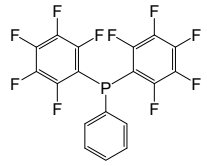

L60 Bis(pentafluorophenyl)phenylphosphine

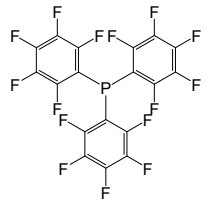

L61 Tris(pentafluorophenyl)phosphine

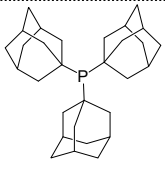

L65 Tris(1-adamantyl)phosphine

Supplementary Eq. 3. Comparison between chelating and non-chelating bisphosphine ligands.

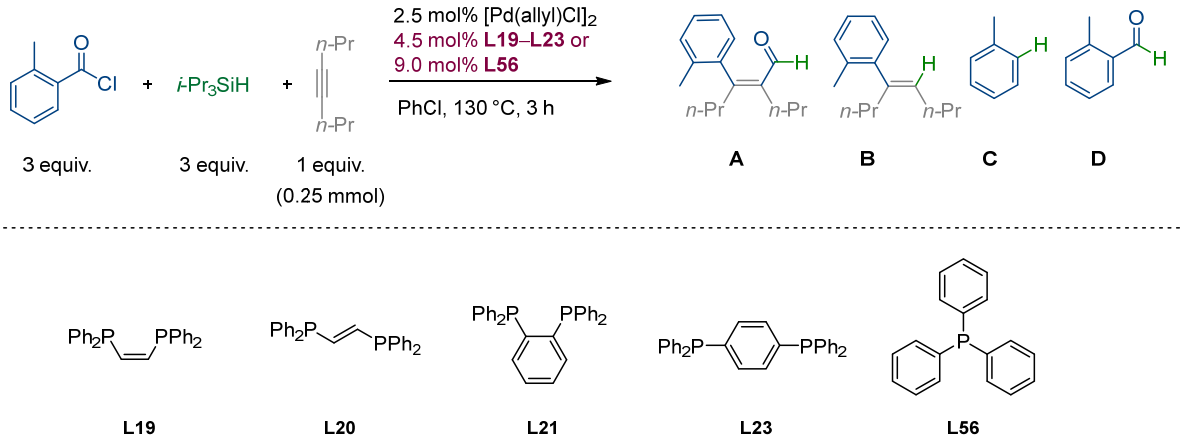

Supplementary Fig. 3. Chelating vs. non-chelating bisphosphine ligands.

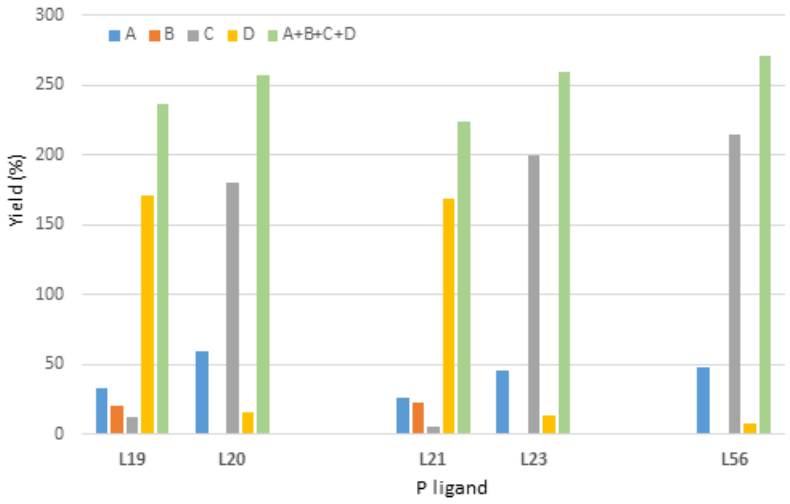

2.2 Transition metal precursors

General procedure for transition metal precursor screening

In a glovebox, a 4 mL screw-cap vial equipped with a stirring bar was charged with a transition metal (5 mol%, 12.50 μmol as a metal atom) and tris(2,6-dimethoxyphenyl)phosphine (TDMPP, **L36**, 10.0 mol%, 0.0250 mmol) and then PhCl (2 mL). The solution was stirred at room temperature for 10 min. To a pre-mixed solution were added o-toluoyl chloride (3 equiv, 0.75 mmol), 4-octyne (1.0 equiv, 0.25 mmol) and triisopropylsilane (iPr$_3$SiH, 3 equiv, 0.75 mmol). The reaction mixture was stirred at 130 °C for 3 h. The reaction was cooled to room temperature then quenched with sodium methoxide (3 equiv, 0.75 mmol, 0.14 mL of 5.4M solution in MeOH) and diluted with DCM (2 mL) and *n*-dodecane was added as an internal standard. The resulting solution was filtered through a celite/silica plug and the filtrate was analyzed by GC/FID and GC/MS.

Supplementary Eq. 4. Transition metal precursor screening.

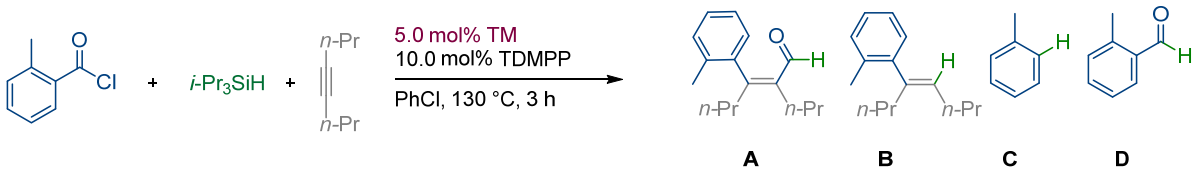

Supplementary Table 3. Transition metal precursor screening

						Yield[a] (%)
entry	transition metals	A	B	C	D	*i*Pr$_3$SiH (unreacted)
1	[Pd(allyl)Cl]$_2$	83	3	111	63	16
2	[(cinnamyl)PdCl]$_2$	82	3	105	68	18
3	Pd(acac)$_2$	82	3	109	63	20
4	Pd(OPiv)$_2$	77	3	107	64	22
5	Pd(OAc)$_2$	71	3	94	78	25
6	Pd(TFA)$_2$	69	3	88	81	26
7	PdBr$_2$	54	2	86	125	5
8	PdCl$_2$	62	2	94	75	39
9	(PhCN)$_2$PdCl$_2$	74	3	112	67	18
10	PdCl$_2$(cod)	80	3	115	61	15
11	Pd$_2$(dba)$_3$	76	3	97	71	31
12	(cod)Pd(CH$_2$SiMe$_3$)$_2$	86	3	116	51	19
13	Pd(PPh$_3$)$_4$	4	1	139	2	124
14	[Pd^{I}(μ-I)P(*t*Bu)$_3$]$_2$	12	n.d.	176	62	18
15	[Pd^{I}(μ-I)P(*t*Bu)$_3$]$_2$ (w/o **L36**)	13	8	23	222	n.d.
16	[Rh(cod)Cl]$_2$	n.d.	n.d.	15	18	209
17	[RhCl(CO)$_2$]$_2$	n.d.	n.d.	9	14	239
18	[Ir(cod)Cl]$_2$	n.d.	n.d.	8	26	214
19	Ir(acac)(CO)$_2$	n.d.	n.d.	4	18	238
20	no metal precursor	n.d.	n.d.	n.d.	n.d.	271
21[b]	no metal precursor	n.d.	n.d.	n.d.	n.d.	263

[a]The GC yields are based on the moles of a limiting reagent, 4-octyne (0.25 mmol, 1 equiv.).
[b]BISBI (4.5 mol%) was used instead of TDMPP (10.0 mol%).

2.3 P/Pd ratio

General procedure for P/Pd atomic ratio screening

In a glovebox, a 4 mL screw-cap vial equipped with a stirring bar was charged with $[Pd(allyl)Cl]_2$ (2.5 mol%, 6.25 µmol, 2.29 mg) and the indicated P ligand (BISBI (**L24**), TDMPP (**L36**), TTMPP (**L37**) or $(2\text{-furyl})_3P$ (**L38**), 0.0 to 15.0 mol% as a P atom) and then PhCl (2 mL). The solution was stirred at room temperature for 10 min. To a pre-mixed solution were added o-toluoyl chloride (3 equiv, 0.75 mmol), 4-octyne (1.0 equiv, 0.25 mmol) and triisopropylsilane ($i\text{Pr}_3\text{SiH}$, 3 equiv, 0.75 mmol). The reaction mixture was stirred at 130 °C for 3 h. The reaction was cooled to room temperature then diluted with DCM (2 mL) and *n*-dodecane was added as an internal standard. The resulting solution was filtered through a celite/silica plug and the filtrate was analyzed by GC/FID and GC/MS.

Initially, the ligand screening revealed reactivity for a diverse range of phosphine ligands, regardless of their electronic or steric properties. In an attempt to develop a rationale, we next evaluated the effect of varying the P to Pd ratio in the reaction (Supplementary Fig. 4). First, a Pd precursor ($[Pd(allyl)Cl]_2$) was examined as a sole catalyst without the employment of phosphines. Therein, no desired product formation was observed and a considerable amount of starting materials remained. Thus, in order to bridge the discrepancy between the phosphine ligand-free and optimized reaction conditions, a set of experiments to evaluate the effect of the P to Pd ratio was undertaken using BISBI and TDMPP (Supplementary Fig. 4a and 4b). For TDMPP, a dramatic change in reactivity and product distribution was found which showed an increase in conversion and yield when the ratio of P to Pd was increased up to 2.0 (Supplementary Fig. 4b). When testing BISBI, a similar tendency as with TDMPP was observed with a distinction, there was a more gradual increase of the desired product relative to TDMPP (Supplementary Fig. 4a). Notably, the maximum yield was observed at a ratio of 1.8 to 1.9. Higher ratios resulted in dramatically decreased conversion, likely a result of catalyst inhibition by Pd chelation of the surplus P ligand (Supplementary Fig. 3 and 4a).

Supplementary Fig. 4. P/Pd atomic ratio screening, **a,** BISBI (**L24**). **b,** TDMPP (**L36**). **c,** TTMPP (**L37**). **d,** (2-furyl)$_3$P (**L38**).

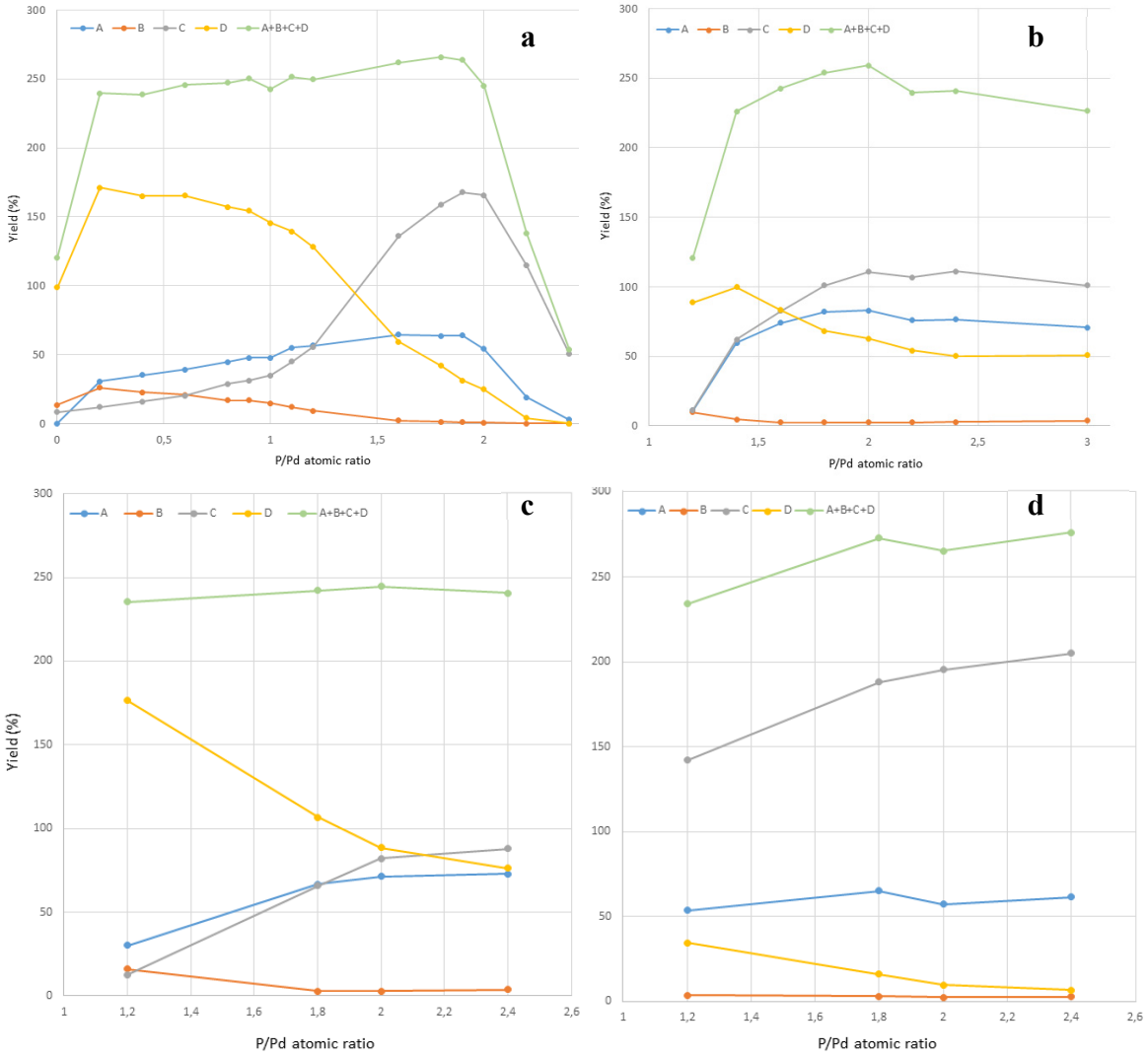

Supplementary Eq. 5. P/Pd atomic ratio screening, BISBI (**L24**).

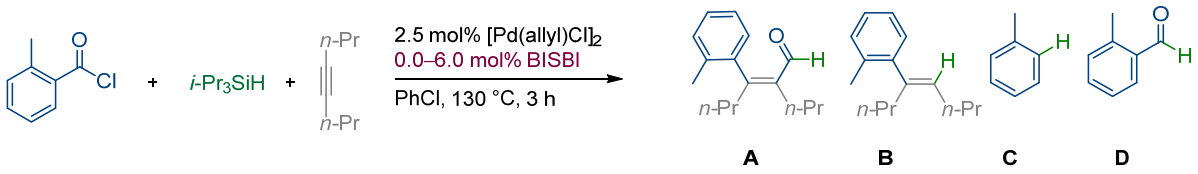

Supplementary Table 4. P/Pd atomic ratio screening, BISBI (**L24**).

						Yield[a] (%)
entry	P/Pd atomic ratio (BISBI)	A	B	C	D	A+B+C+D
1	0.0	n.d.	13	8	99	120
2	0.2	31	26	12	171	240
3	0.4	35	23	16	165	239
4	0.6	39	21	20	165	246
5	0.8	45	17	29	157	247
6	0.9	48	17	31	154	250
7	1.0	48	15	35	145	243
8	1.1	55	12	45	140	252
9	1.2	57	9	56	128	250
10	1.6	65	2	136	59	262
11	1.8	64	1	159	42	266
12	1.9	64	1	168	31	264
13	2.0	54	1	166	25	245
14	2.2	19	n.d.	115	4	138
15	2.4	3	n.d.	51	n.d.	53

[a]The GC yields are based on the moles of a limiting reagent, 4-octyne (0.25 mmol, 1 equiv.).

Supplementary Eq. 6. P/Pd atomic ratio screening, TDMPP (**L36**).

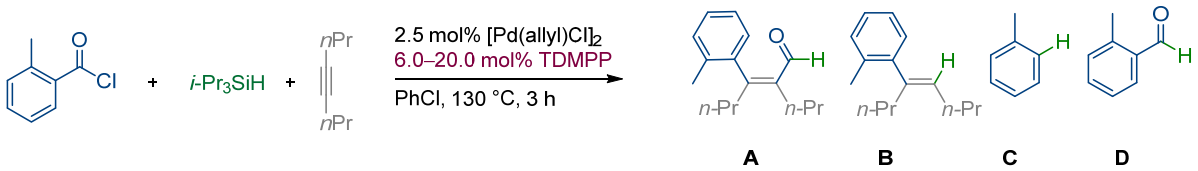

Supplementary Table 5. P/Pd atomic ratio screening, TDMPP (**L36**).

						Yield[a] (%)
entry	P/Pd ratio (TDMPP)	A	B	C	D	A+B+C+D
1	1.2	11	10	11	89	121
2	1.4	60	5	62	100	226
3	1.6	74	3	83	83	243
4	1.8	82	2	101	68	254
5	2.0	83	3	111	63	259
6	2.2	76	2	107	54	240
7	2.4	77	3	111	50	241
8	3.0	71	4	101	51	226
9	4.0	57	5	89	63	213

[a]The GC yields are based on the moles of a limiting reagent, 4-octyne (0.25 mmol, 1 equiv.).

Supplementary Eq. 7. P/Pd atomic ratio screening. **a,** TTMPP (**L37**). **b,** (2-furyl)$_3$P (**L38**).

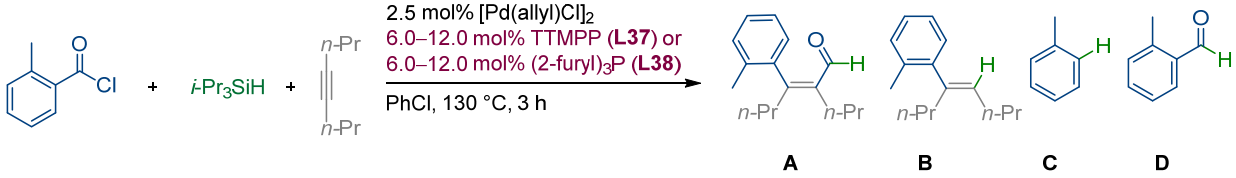

Supplementary Table 6. P/Pd atomic ratio screening. **a,** TTMPP (**L37**). **b,** (2-furyl)$_3$P (**L38**).

a						Yield[a] (%)
entry	P/Pd ratio (TTMPP)	A	B	C	D	A+B+C+D
1	1.2	30	16	13	176	235
2	1.8	67	3	66	107	242
3	2.0	71	3	82	88	245
4	2.4	73	4	88	76	241
b						
entry	P/Pd ratio ((2-furyl)$_3$P)	A	B	C	D	A+B+C+D
1	1.2	54	4	142	34	234
2	1.8	65	3	188	16	273
3	2.0	57	3	195	10	265
4	2.4	62	3	205	7	276

[a]The GC yields are based on the moles of a limiting reagent, 4-octyne (0.25 mmol, 1 equiv.).

2.4. Hydrosilanes

General procedure for hydrosilane screening

In a glovebox, a 4 mL screw-cap vial equipped with a stirring bar was charged with $[Pd(allyl)Cl]_2$ (2.5 mol%, 6.25 μmol, 2.29 mg) and TDMPP (10.0 mol%) or BISBI (4.5 mol%) and then PhCl (2 mL). The solution was stirred at room temperature for 10 min. To a pre-mixed solution were added *o*-toluoyl chloride (3 equiv, 0.75 mmol), 4-octyne (1.0 equiv, 0.25 mmol) and a hydrosilane (3 equiv, 0.75 mmol). The reaction mixture was stirred at 130 °C for 3 h. The reaction was cooled to room temperature then diluted with DCM (2 mL) and *n*-dodecane was added as an internal standard. The resulting solution was filtered through a celite/silica plug and the filtrate was analyzed by GC/FID and GC/MS.

Investigations using electronically and sterically differentiated hydrosilanes revealed a positive correlation between yield of a desired product and the steric bulk of the hydrosilane. In contrast, a negative correlation between the yield of an aromatic aldehyde and the steric bulk (Supplementary Table 7 and 8). This observation suggested that the intrinsic reactivity of hydride sources could influence the rate of H/Cl transfer with respect to a set of Pd intermediates (Fig. 1, **I**, **II**, **III**, and **IV**) and thus the distribution of resulting products. This outcome illustrates the optimal steric balance of a hydrosilane is key to suppress premature trapping of reaction intermediates (Fig. 1, **I**, **II** and **III**).

Supplementary Eq. 8. Hydrosilane screening, TDMPP.

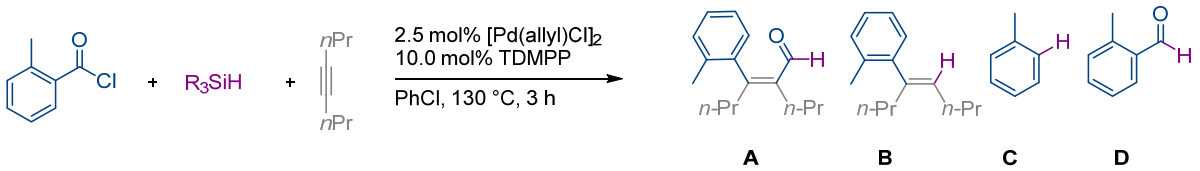

Supplementary Table 7. Hydrosilane screening, TDMPP.

							Yield[b] (%)
entry	hydrosilane, CAS no.	A	B	C	D	A+B+C	A+B+C+D
Si01	tBu$_2$MeSiH, 56310-20-4	54	7	55	91	116	208
Si02	iPr$_3$SiH, 6485-79-6	83	3	111	63	196	259
Si03[a]	(iPr$_2$HSi)$_2$O, 18043-71-5	91	2	82	75	175	250
Si04	iBu$_3$SiH, 6485-81-0	83	3	97	67	183	250
Si05	tBu$_2$SiH$_2$, 30736-07-3	66	3	76	102	145	248
Si06	(iPr)$_2$OctSiH, 129536-19-2	52	1	125	68	178	246
Si07	tBuMe$_2$SiH, 29681-57-0	30	1	140	85	171	256
Si08	nOct$_3$SiH, 18765-09-8	10	n.d.	93	136	103	239
Si09	nHex$_3$SiH, 2929-52-4	15	n.d.	79	146	94	240
Si10	nBu$_3$SiH, 998-41-4	12	n.d.	96	137	108	245
Si11	nPr$_3$SiH, 998-29-8	15	n.d.	97	139	113	251
Si12	Et$_3$SiH, 617-86-7	8	n.d.	82	168	90	259
Si13[a]	[(Me$_2$HSi)CH$_2$]$_2$, 20152-11-8	6	n.d.	81	169	87	256
Si14[a]	(Me$_2$HSi)$_2$O, 3277-26-7	4	n.d.	45	222	49	271
Si15	Ph$_3$SiH, 789-25-3	59	5	75	118	139	256
Si16	Ph$_2$MeSiH 776-76-1	23	1	84	150	108	259
Si17	PhMe$_2$SiH 766-77-8	5	n.d.	90	170	95	265
Si18	(Me$_3$SiO)$_3$SiH 1873-89-8	32	30	30	110	93	203
Si19	(EtO)$_3$SiH 998-30-1	12	19	38	66	69	135
Si20	(EtO)$_2$MeSiH 2031-62-1	6	2	32	143	40	183
Si21	(MeO)$_2$MeSiH 16881-77-9	5	1	24	169	31	199
Si22	tBu$_2$SiHCl 56310-18-0	29	10	38	66	77	143
Si23	iPr$_2$SiHCl 2227-29-4	8	2	10	237	19	256

entry	hydrosilane, CAS no.	A	B	C	D	o-MePhCOCl (unreacted)
Si24[c]	no hydrosilane	n.d.	n.d.	n.d.	n.d.	265
Si25[c]	iPr$_3$SiCl instead of a hydrosilane	n.d.	n.d.	n.d.	n.d.	275

[a]1.5 equiv. of the silane was used. [b]The GC yields are based on the moles of a limiting reagent, 4-octyne (0.25 mmol, 1 equiv.). [c]For o-toluoyl chloride, GC yield was determined using the corresponding methyl ester after quenching with NaOMe.

Supplementary Eq. 9. Hydrosilane screening, BISBI.

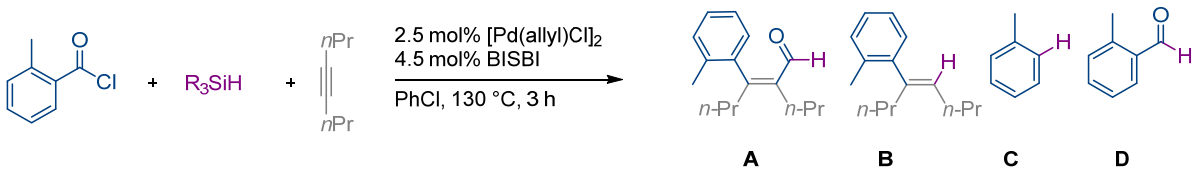

Supplementary Table 8. Hydrosilane screening, BISBI.

							Yield[b] (%)
entry	hydrosilane, CAS no.	A	B	C	D	A+B+C	A+B+C+D
Si01	tBu$_2$MeSiH, 56310-20-4	47	8	42	102	97	199
Si02	iPr$_3$SiH, 6485-79-6	65	1	159	42	226	268
Si03[a]	(iPr$_2$HSi)$_2$O, 18043-71-5	68	n.d.	146	39	215	254
Si04	iBu$_3$SiH, 6485-81-0	57	1	161	37	219	256
Si05	tBu$_2$SiH$_2$, 30736-07-3	51	1	145	50	197	248
Si06	(iPr)$_2$OctSiH, 129536-19-2	34	n.d.	193	28	227	255
Si07	tBuMe$_2$SiH, 29681-57-0	33	1	208	27	242	269
Si08	nOct$_3$SiH, 18765-09-8	9	n.d.	234	14	242	257
Si09	nHex$_3$SiH, 2929-52-4	9	n.d.	237	9	247	256
Si10	nBu$_3$SiH, 998-41-4	9	n.d.	236	16	245	262
Si11	nPr$_3$SiH, 998-29-8	12	n.d.	235	19	247	265
Si12	Et$_3$SiH, 617-86-7	7	n.d.	245	24	252	276
Si13[a]	[(Me$_2$HSi)CH$_2$]$_2$, 20152-11-8	6	n.d.	204	45	210	255
Si14[a]	(Me$_2$HSi)$_2$O, 3277-26-7	9	n.d.	206	45	215	260
Si15	Ph$_3$SiH, 789-25-3	12	6	78	80	97	177
Si16	Ph$_2$MeSiH 776-76-1	21	1	217	32	239	271
Si17	PhMe$_2$SiH 766-77-8	9	n.d.	219	31	228	259
Si18	(Me$_3$SiO)$_3$SiH 1873-89-8	29	32	53	90	114	204
Si19	(EtO)$_3$SiH 998-30-1	10	20	75	60	105	165
Si20	(EtO)$_2$MeSiH 2031-62-1	19	2	129	98	149	248
Si21	(MeO)$_2$MeSiH 16881-77-9	8	1	128	86	137	224
Si22	tBu$_2$SiHCl 56310-18-0	23	7	43	52	73	125
Si23	iPr$_2$SiHCl 2227-29-4	16	n.d.	154	84	170	255

entry	hydrosilane, CAS no.	A	B	C	D	o-MePhCOCl (unreacted)
Si24[c]	no hydrosilane	n.d.	n.d.	n.d.	n.d.	298
Si25[c]	iPr$_3$SiCl instead of a hydrosilane	n.d.	n.d.	n.d.	n.d.	286

[a]1.5 equiv. of the silane was used. [b]The GC yields are based on the moles of a limiting reagent, 4-octyne (0.25 mmol, 1 equiv.). [c]For o-toluoyl chloride, GC yield was determined using the corresponding methyl ester after quenching with NaOMe.

2.5. Solvents

General procedure for solvent screening

In a glovebox, a 4 mL screw-cap vial equipped with a stirring bar was charged with $[Pd(allyl)Cl]_2$ (2.5 mol%, 6.25 μmol, 2.29 mg) and TDMPP (10.0 mol%) or BISBI (4.5 mol%) and then the indicated solvent (2 mL). The solution was stirred at room temperature for 10 min. To a pre-mixed solution were added *o*-toluoyl chloride (3 equiv, 0.75 mmol), 4-octyne (1.0 equiv, 0.25 mmol) and triisopropylsilane (iPr$_3$SiH, 3 equiv, 0.75 mmol). The reaction mixture was stirred at 130 °C for 3 h. The reaction was cooled to room temperature then diluted with DCM (2 mL) and *n*-dodecane was added as an internal standard. The resulting solution was filtered through a celite/silica plug and the filtrate was analyzed by GC/FID and GC/MS.

Supplementary Eq. 10. Solvent screening, TDMPP.

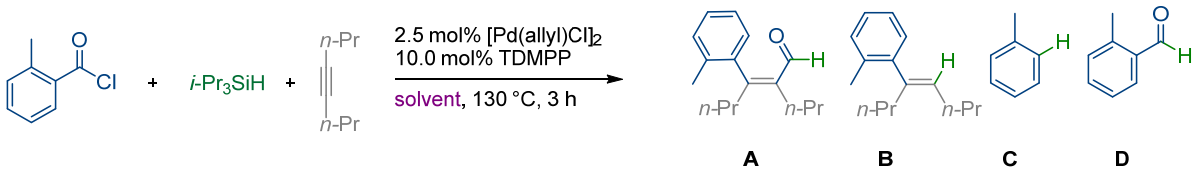

Supplementary Table 9. Solvent screening, TDMPP.

						Yield[b] (%)
entry		A	B	C	D	4-octyne
1	PhCl	83	3	111	63	-[a]
2	dioxane	84	3	106	88	14
3	CPME	72	5	-[a]	75	20
4	$PhCF_3$	72	5	100	67	7
5	diglyme	69	3	97	83	17
6	PhMe	68	3	-[a]	79	13
7	*p*-xylene	67	3	89	73	17
8	DCE	41	8	42	160	18
9	octane	17	10	17	28	57
10	DMI	9	3	46	173	36
11	CH_3CN	n.d.	3	19	49	68
12	$MeNO_2$	n.d.	n.d.	3	44	40

[a]The GC retention time overlapped with the solvent. [b]The GC yields are based on the moles of a limiting reagent, 4-octyne (0.25 mmol, 1 equiv.).

Supplementary Eq. 11. Solvent screening, BISBI.

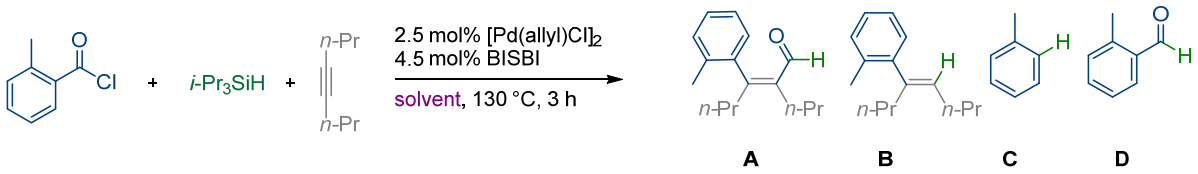

Supplementary Table 10. Solvent screening, BISBI.

						Yield[b] (%)
entry	solvent	A	B	C	D	4-octyne
1	PhCl	65	1	159	42	-[a]
2	$PhCF_3$	67	4	144	52	12
3	CPME	63	2	-[a]	30	31
4	THF	63	1	193	33	28
5	dioxane	59	1	187	48	37
6	*p*-xylene	59	1	210	26	31
7	DCE	56	3	115	94	22
8	diglyme	56	1	160	67	33
9	PhMe	56	1	-[a]	22	33
10	octane	40	3	156	47	45
11	DMI	31	1	93	107	27
12	MeCN	12	4	143	48	30
13	$MeNO_2$	n.d.	3	55	46	29

[a]The GC retention time overlapped with the solvent. [b]The GC yields are based on the moles of a limiting reagent, 4-octyne (0.25 mmol, 1 equiv.).

2.6. Further optimization (other variations)

Supplementary Eq. 12. Substrates equivalent ratio, TDMPP.

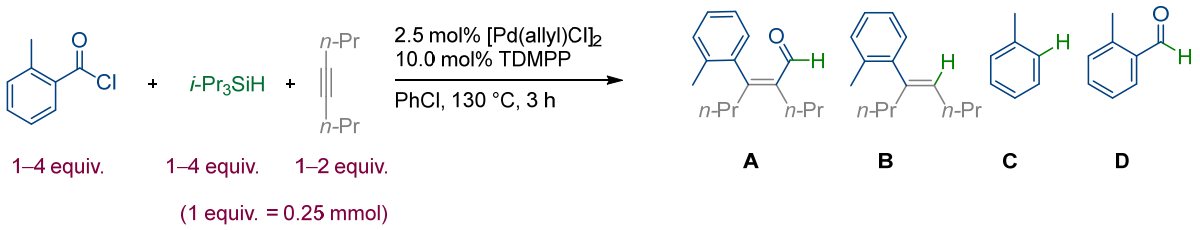

Supplementary Table 11. Substrates equivalent ratio, TDMPP.

					Yield[a] (%)
aroyl chloride / hydrosilane / alkyne equivalent ratio	A	B	C	D	A+B+C+D
1 / 1 / 2	34	10	8	4	56
2 / 1 / 1	31	6	23	8	67
1 / 2 / 1	31	2	29	5	67
1 / 1 / 1	44	5	16	4	69
2 / 2 / 1	71	3	62	20	156
3 / 3 / 1[b]	83	3	111	63	259
4 / 4 / 1	78	2	140	110	331

[a]The GC yields are based on the moles of a limiting reagent, 4-octyne (0.25 mmol, 1 equiv.). [b]Standard condition.

Supplementary Eq. 13. Substrates equivalent ratio, BISBI.

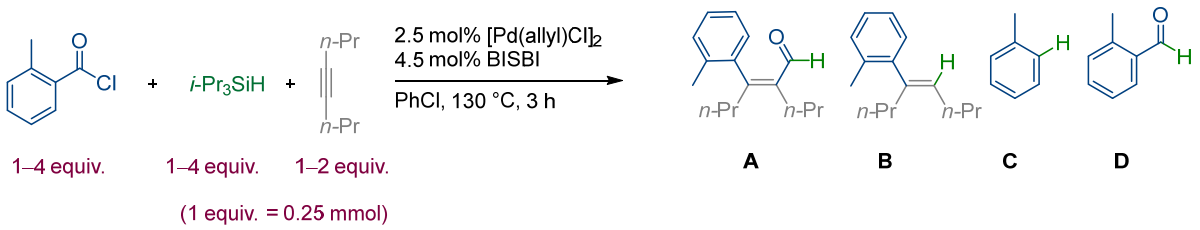

Supplementary Table 12. Substrates equivalent ratio, BISBI.

					Yield[a] (%)
aroyl chloride / hydrosilane / alkyne equivalent ratio	A	B	C	D	A+B+C+D
1 / 1 / 2	45	4	30	1	80
2 / 1 / 1	21	3	42	4	69
1 / 2 / 1	19	n.d.	72	2	94
1 / 1 / 1	41	2	43	2	88
2 / 2 / 1	55	1	124	9	188
3 / 3 / 1[b]	65	1	159	42	268
4 / 4 / 1	64	1	221	87	374

[a]The GC yields are based on the moles of a limiting reagent, 4-octyne (0.25 mmol, 1 equiv.). [b]Standard condition.

Supplementary Eq. 14. Optimization, TDMPP. **a,** Catalyst loading. **b,** Solvent volume. **c,** Reaction temperature and time.

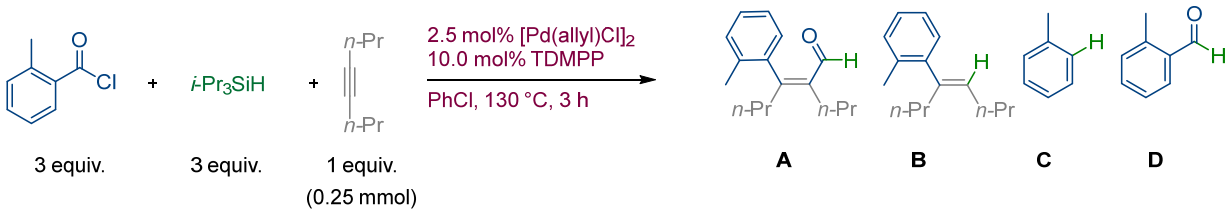

Supplementary Table 13. Optimization, TDMPP. **a,** Catalyst loading. **b,** Solvent volume. **c,** Reaction temperature and time.

a							Yield[a] (%)
entry	catalyst loading (mol% as Pd)	A	B	C	D	A+B+C+D	
1	1.0 mol% Pd, 2.0 mol% TDMPP	6	7	10	45	68	
2	2.5 mol% Pd, 5.0 mol% TDMPP	68	4	74	92	238	
3	5.0 mol% Pd, 10.0 mol% TDMPP	83	3	111	63	259	standard condition
4	10.0 mol% Pd, 20.0 mol% TDMPP	70	3	89	65	227	
b							
entry	solvent volume						
1	1 mL PhCl (ca. 0.250 M)	84	5	108	57	253	
2	2 mL PhCl (ca. 0.125 M)	83	3	111	63	259	standard condition
3	3 mL PhCl (ca. 0.083 M)	72	1	83	82	238	
c							
entry	reaction temperature and reaction time	A	B	C	D	A+B+C+D	
1	150 °C, 3 h	77	4	103	57	241	
2	130 °C, 3 h	83	3	111	63	259	standard condition
3	120 °C, 3 h	62	2	83	63	210	
4	110 °C, 3 h	14	1	27	31	75	
5	120 °C, 12 h	76	2	93	74	246	
6	110 °C, 12 h	61	2	67	93	223	

[a]The GC yields are based on the moles of a limiting reagent, 4-octyne (0.25 mmol, 1 equiv.).

Supplementary Eq. 15. Optimization, BISBI. **a,** Catalyst loading. **b,** Solvent volume. **c,** Reaction temperature and time.

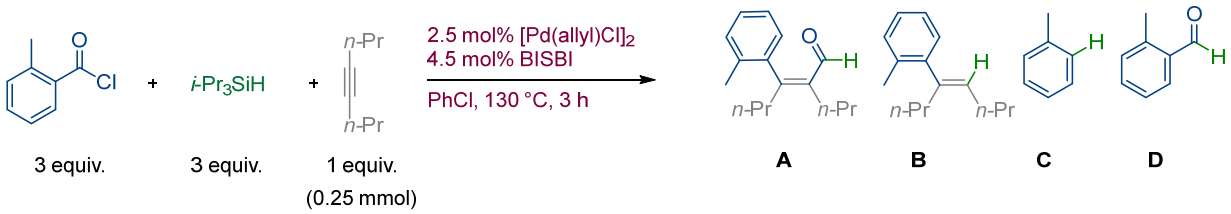

Supplementary Table 14. Optimization, BISBI. **a,** Catalyst loading. **b,** Solvent volume. **c,** Reaction temperature and time.

a							Yield (%)
entry	catalyst loading (mol% as Pd)	A	B	C	D	A+B+C+D	
1	1.0 mol% Pd, 0.90 mol% BISBI	54	6	82	115	257	
2	2.5 mol% Pd, 2.25 mol% BISBI	62	2	142	59	265	
3	5.0 mol% Pd, 4.50 mol% BISBI	65	1	159	42	268	standard condition
4	10.0 mol% Pd, 9.00 mol% BISBI	65	1	188	19	273	
b							
entry	solvent volume	A	B	C	D	A+B+C+D	
1	1 mL PhCl (ca. 0.250 M)	67	2	179	25	273	
2	2 mL PhCl (ca. 0.125 M)	65	1	159	42	268	standard condition
3	3 mL PhCl (ca. 0.083 M)	62	1	145	50	259	
c							
entry	reaction temperature and time	A	B	C	D	A+B+C+D	
1	150 °C, 3 h	69	3	160	47	279	
2	140 °C, 3 h	67	2	167	43	279	
3	130 °C, 3 h	65	1	159	42	268	standard condition
4	120 °C, 3 h	48	1	139	41	229	
5	110 °C, 3 h	20	n.d.	106	18	144	
6	120 °C, 12 h	62	1	159	47	269	

[a]The GC yields are based on the moles of a limiting reagent, 4-octyne (0.25 mmol, 1 equiv.).

3. Carboformylation of internal alkynes

General procedure for mono-*ortho*-substituted aroyl chloride

Method 1: In a glovebox, a 4 mL screw-cap vial equipped with a stirring bar was charged with $[Pd(allyl)Cl]_2$ (2.5 mol%, 6.25 μmol, 2.29 mg or 1.0 mL as 6.25 mM stock solution in PhCl) and TDMPP (10.0 mol%, 0.025 mmol, 11.06 mg, or 221.0 mg as 5.0wt% stock solution in PhCl, **Method 1A**) or BISBI (4.5 mol%, 6.19 mg, or 61.9 mg as 10.0wt% stock solution in PhCl, **Method 1B**) and then PhCl (2 mL, or 1mL when stock solutions were used). The solution was stirred at room temperature for 10 min. To a pre-mixed solution were added aroyl chloride (3 equiv, 0.75 mmol), alkyne (1.0 equiv, 0.25 mmol) and iPr$_3$SiH (3 equiv, 0.75 mmol, 118.77 mg). The reaction mixture was stirred at 130 °C for 3 h. The reaction was cooled to room temperature then quenched with sodium methoxide (3 equiv, 0.75 mmol, 0.14 mL of 5.4M solution in MeOH, note: the quenching step could be omitted for substrates bearing a base-labile functional group) and diluted with DCM (2 mL). The resulting solution was filtered through a celite/silica plug and concentrated under reduced pressure. The crude product was purified by column chromatography on silica gel (pentane/DCM, pentane/EA or pentane/MTBE).

General procedure for di-*ortho*-substituted aroyl chloride

Method 2A: In a glovebox, a 4 mL screw-cap vial equipped with a stirring bar was charged with $[Pd(allyl)Cl]_2$ (2.5 mol%, 6.25 μmol, 2.29 mg) and TDMPP (10.0 mol%, 11.06 mg) and then PhCl (2 mL). The solution was stirred at room temperature for 10 min. To a pre-mixed solution were added aroyl chloride (2.0 equiv, 0.50 mmol), alkyne (1.0 equiv, 0.25 mmol) and iPr$_3$SiH (2.0 equiv, 0.50 mmol, 79.18 mg). The reaction mixture was stirred at 120 °C for 3 h. The reaction was cooled to room temperature then quenched with sodium methoxide (2.0 equiv, 0.50 mmol, 0.09 mL of 5.4M solution in MeOH, note: the quenching step could be omitted for substrates bearing a base-labile functional group) and diluted with DCM (2 mL). The resulting solution was filtered through a celite/silica plug and concentrated under reduced pressure. The crude product was purified by column chromatography on silica gel (pentane/DCM, pentane/EA or pentane/MTBE).

Method 2B: In a glovebox, a 4 mL screw-cap vial equipped with a stirring bar was charged with $[Pd(allyl)Cl]_2$ (2.5 mol%, 6.25 μmol, 2.29 mg) and BISBI (4.5 mol%, 6.19 mg) and then PhCl (2 mL). The solution was stirred at room temperature for 10 min. To a pre-mixed solution were added aroyl chloride (1.5 equiv, 0.375 mmol), alkyne (1.0 equiv, 0.250 mmol) and tBu$_2$SiH$_2$ (1.5 equiv, 0.375 mmol, 54.12 mg). The reaction mixture was stirred at 100 °C for 3 h. The reaction was cooled to room temperature then quenched with sodium methoxide (1.5 equiv, 0.375 mmol, 0.07 mL of 5.4M solution in MeOH, note: the quenching step could be omitted for substrates bearing a base-labile functional group) and diluted with DCM (2 mL). The resulting solution was filtered through a celite/silica plug and concentrated under reduced pressure. The crude product was purified by column chromatography on silica gel (pentane/DCM, pentane/EA or pentane/MTBE).

General procedure for non-*ortho*-substituted aroyl chloride

Method 3: In a glovebox, a 4 mL screw-cap vial equipped with a stirring bar was charged with $[Pd(allyl)Cl]_2$ (2.5 mol%, 6.25 μmol, 2.29 mg) and TDMPP (10.0 mol%, 11.06 mg, **Method 3A**) or BISBI (4.5 mol%, 6.19 mg, **Method 3B**) and then PhCl (2 mL). The solution was stirred at room temperature for 10 min. To a pre-mixed solution were added aroyl chloride (2.0 equiv, 0.50 mmol), alkyne (1.0 equiv, 0.25 mmol) and $(i\text{Pr}_2\text{HSi})_2\text{O}$ (1.0 equiv, 0.25 mmol, 61.64 mg). The reaction mixture was stirred at 130 °C for 5 h. The reaction was cooled to room temperature then quenched with sodium methoxide (2.0 equiv, 0.50 mmol, 0.09 mL of 5.4M solution in MeOH, note: the quenching step could be omitted for substrates bearing a base-labile functional group) and diluted with DCM (2 mL). The resulting solution was filtered through a celite/silica plug and concentrated under reduced pressure. The crude product was purified by column chromatography on silica gel (pentane/DCM, pentane/EA or pentane/MTBE).

Supplementary Eq. 16. Disproving of a probable side product formation (**E**) by hydroacylation.

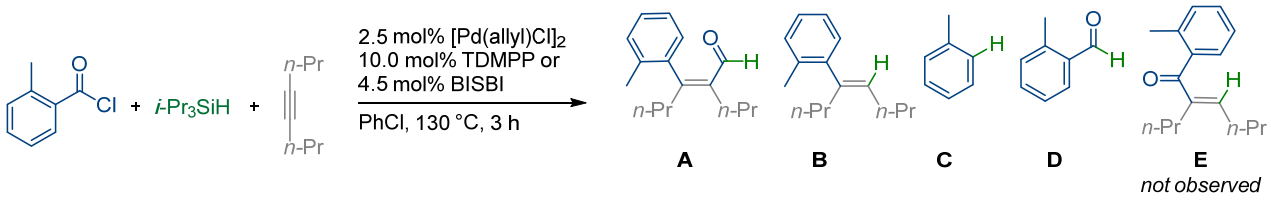

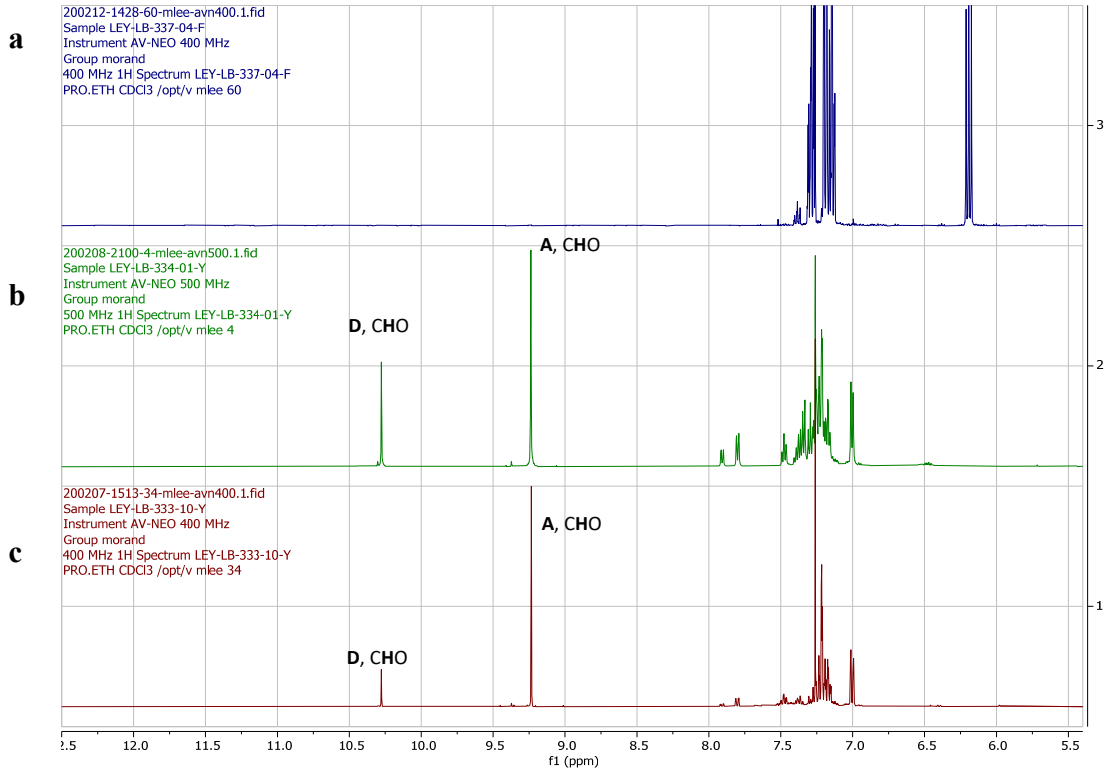

Supplementary Fig. 5. Disproving of a probable side product formation (**E**) by hydroacylation. **a,** ^{1}H NMR spectrum of compound **E**. **b,** ^{1}H NMR spectrum of the crude product mixture (Supplementary Eq. 16, Method 1A, TDMPP). **c,** ^{1}H NMR spectrum of the crude product mixture (Supplementary Eq. 16, Method 1B, BISBI).

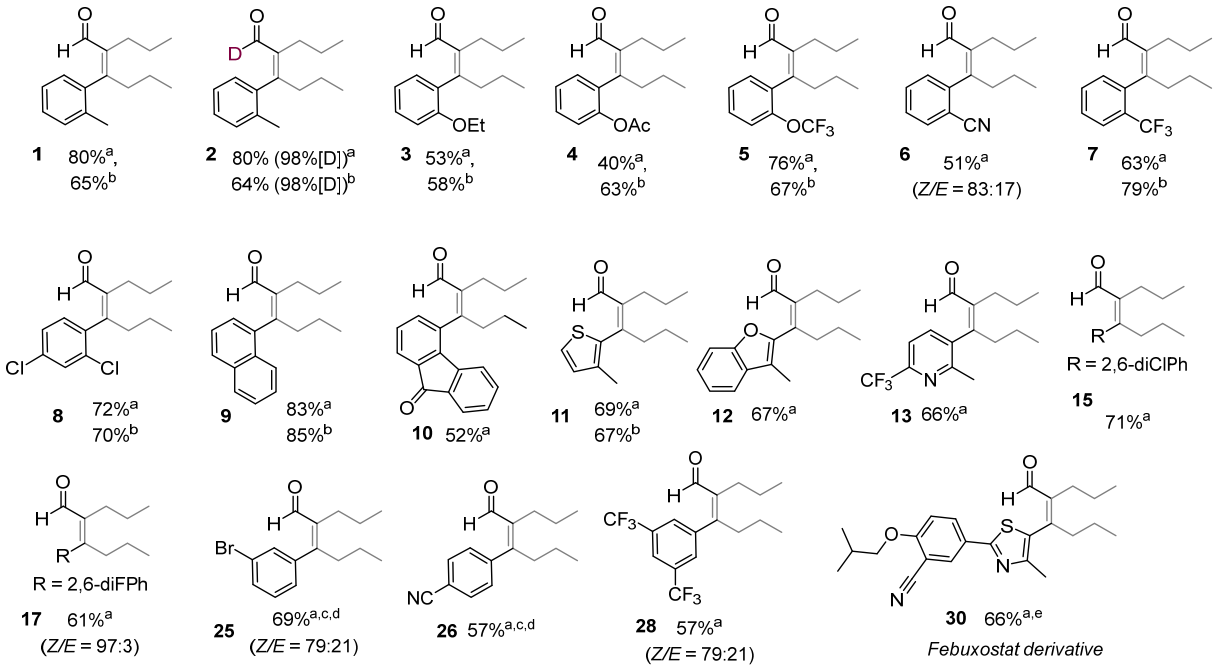

Supplementary Fig. 6. Reaction conditions: [a]Method 1A. [b]Method 1B. [c]$(i\mathrm{Pr_2HSi})_2O$ (1.5 equiv.). [d]12 h. [e]5 h.

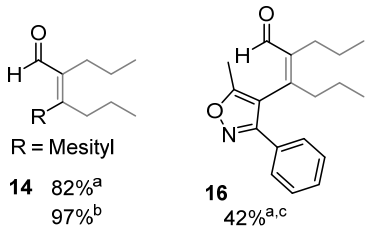

Supplementary Fig. 7. Reaction conditions: [a]Method 2A. [b]Method 2B. [c]130 °C.

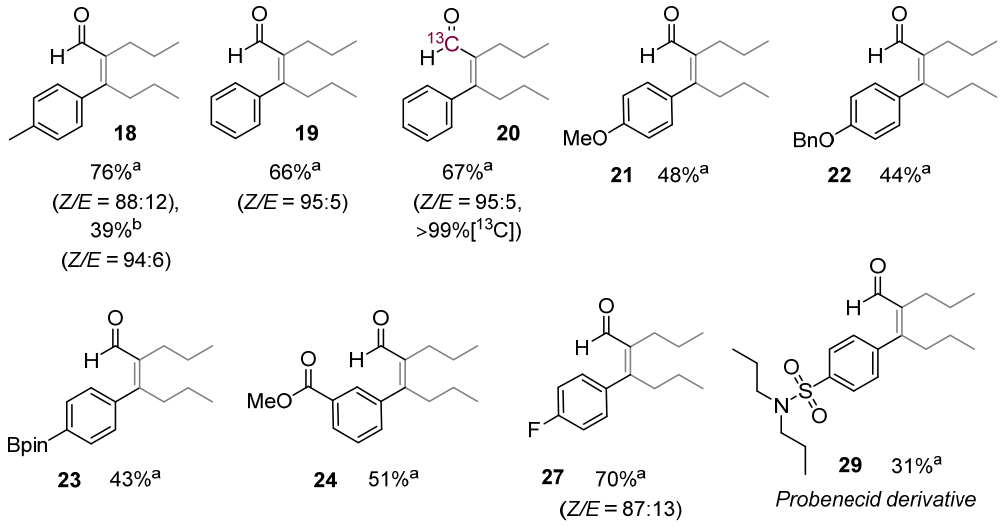

Supplementary Fig. 8. Reaction conditions: [a]Method 3A. [b]Method 3B.

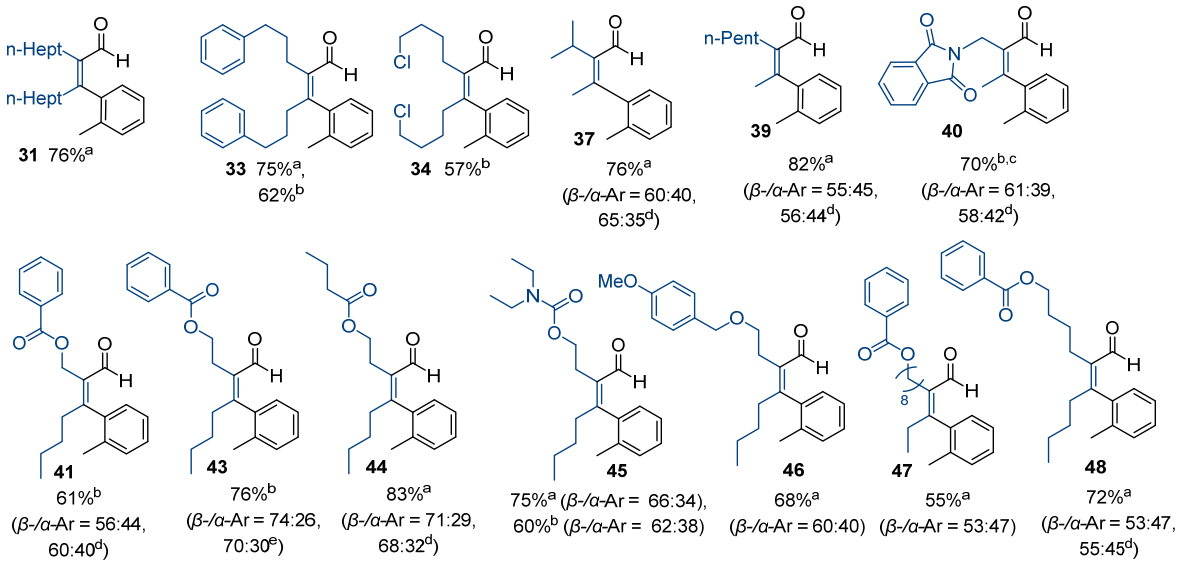

Supplementary Fig. 9. Reaction conditions: [a]Method 1A. [b]Method 1B. [c]12 h. [d]Determined by GC analysis of a crude mixture. [e]Determined by ^{1}H NMR analysis of a crude mixture.

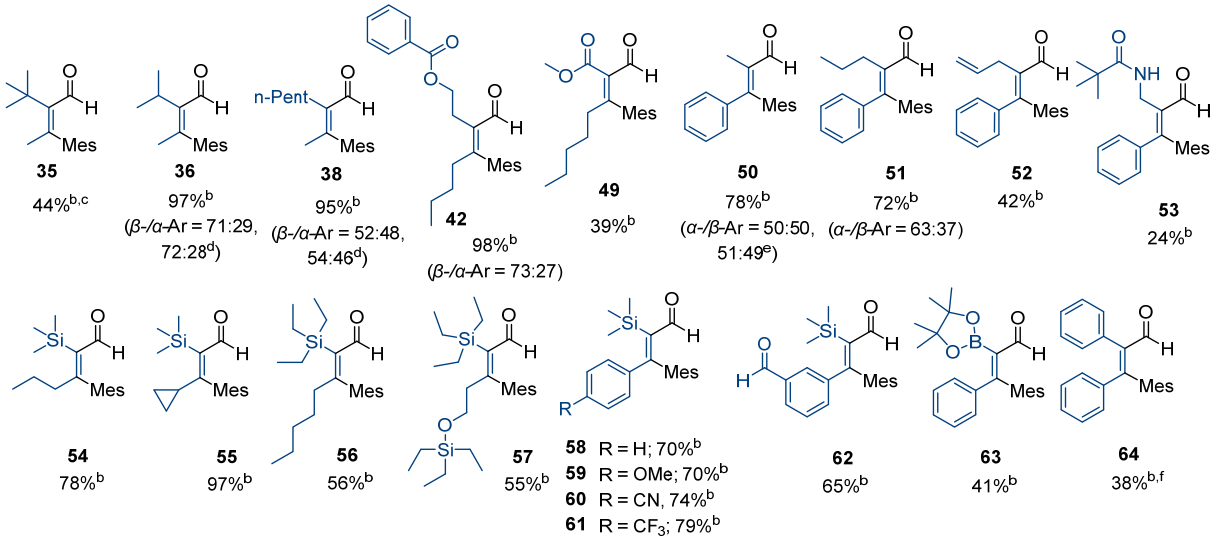

Supplementary Fig. 10. Reaction conditions: [a]Method 2A. [b]Method 2B. [c]12 h. [d]Determined by GC analysis of a crude mixture. [e]Determined by ^{1}H NMR analysis of a crude mixture. [f]Aroyl chloride (0.25 mmol, 1 equiv.), tBu$_2$SiH$_2$ (1 equiv.), alkyne (2 equiv.), 100 °C, 12 h.

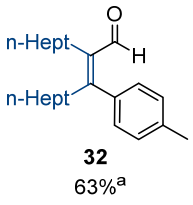

Supplementary Fig. 11. Reaction conditions: [a]Method 3A.

(*Z*)-2-propyl-3-(*o*-tolyl)hex-2-enal (**1**)**.** Colorless oil. 65% yield (38 mg, BISBI). 80% yield (46 mg, TDMPP), 82% yield (47 mg, TDMPP, open), 83% yield (4.8 g, TDMPP, 25 mmol scale).

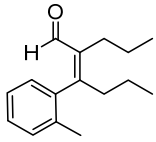

^{1}H NMR (600 MHz, $CDCl_3$) δ 9.24 (s, 1H), 7.25 – 7.20 (m, 2H), 7.19 – 7.15 (m, 1H), 7.00 (dd, *J* = 7.5, 1.4 Hz, 1H), 2.61 (ddd, *J* = 13.1, 10.6, 5.9 Hz, 1H), 2.47 – 2.29 (m, 3H), 2.19 (s, 3H), 1.53 – 1.29 (m, 4H), 0.99 (t, *J* = 7.4 Hz, 3H), 0.94 (t, *J* = 7.3 Hz, 3H). **^{13}C NMR** (151 MHz, $CDCl_3$) δ 194.42, 161.98, 138.86, 138.65, 135.38, 130.30, 129.28, 127.87, 125.50, 37.97, 27.00, 22.78, 20.97, 19.89, 14.62, 14.45. **HRMS** (EI, m/z): $[M-H]^+$ calcd. for $C_{16}H_{21}O_1$, 229.1587; found 229.1593. The stereochemistry of the product was determined by 2D-NMR analysis.

(*Z*)-2-propyl-3-(*o*-tolyl)hex-2-enal-1-*d* (**2**). Colorless oil. 64% yield (37 mg, 98% [D], BISBI). 80% yield (46 mg, 98% [D], TDMPP)

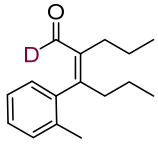

^{1}H NMR (500 MHz, $CDCl_3$) δ 7.27 – 7.14 (m, 3H), 7.00 (ddt, *J* = 7.5, 1.3, 0.5 Hz, 1H), 2.61 (ddd, *J* = 13.1, 10.5, 6.0 Hz, 1H), 2.48 – 2.29 (m, 3H), 2.19 (s, 3H), 1.53 – 1.28 (m, 4H), 0.99 (t, *J* = 7.4 Hz, 3H), 0.94 (t, *J* = 7.3 Hz, 3H). **^{2}H NMR** (77 MHz, $CDCl_3$) δ 9.27. **^{13}C NMR** (126 MHz, $CDCl_3$) δ 194.07 (t, *J* = 27.0 Hz), 162.00, 138.79 (t, *J* = 3.1 Hz), 138.66, 135.37, 130.30, 129.27, 127.87, 125.51, 37.96, 26.95, 22.78, 20.97, 19.89, 14.62, 14.45. **HRMS** (ESI, m/z): $[M+H]^+$ calcd. for $C_{16}H_{22}O_1D_1$, 232.1806; found 232.1808. The stereochemistry of the product was determined by 2D and ^{2}H-NMR analysis.

(*Z*)-3-(2-ethoxyphenyl)-2-propylhex-2-enal (**3**). Colorless oil. 58% yield (38 mg, BISBI). 53% yield (34 mg, TDMPP).

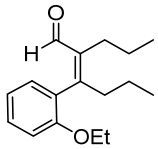

^{1}H NMR (400 MHz, $CDCl_3$) δ 9.31 (s, 1H), 7.31 – 7.25 (m, 1H), 7.00 (dd, *J* = 7.4, 1.8 Hz, 1H), 6.92 (td, *J* = 7.4, 1.0 Hz, 1H), 6.87 (dd, *J* = 8.3, 1.0 Hz, 1H), 3.99 (q, *J* = 7.0 Hz, 2H), 2.66 – 2.48 (m, 2H), 2.48 – 2.28 (m, 2H), 1.51 – 1.41 (m, 2H), 1.40 – 1.25 (m, 5H), 0.97 (t, *J* = 7.4 Hz, 3H), 0.90 (t, *J* = 7.4 Hz, 3H). **^{13}C NMR** (101 MHz, $CDCl_3$) δ 194.87, 159.77, 156.05, 138.71, 130.83, 129.29, 128.02, 120.02, 111.59, 63.71, 37.24, 27.09, 22.62, 21.13, 14.85, 14.42, 14.24. **HRMS** (ESI, m/z): $[M+H]^+$ calcd. for $C_{17}H_{25}O_2$, 261.1849; found 261.1847. The stereochemistry of the product was determined by 2D-NMR analysis.

(*Z*)-2-(5-formyloct-4-en-4-yl)phenyl acetate (**4**). Pale yellow oil. 63% yield (43 mg, BISBI). 40% yield (27 mg, TDMPP).

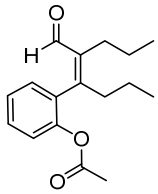

^{1}H NMR (600 MHz, $CDCl_3$) δ 9.30 (s, 1H), 7.37 (ddd, *J* = 8.0, 7.4, 1.7 Hz, 1H), 7.24 (td, *J* = 7.6, 1.2 Hz, 1H), 7.13 (td, *J* = 7.8, 1.4 Hz, 2H), 2.59 (ddd, *J* = 13.3, 10.0, 6.4 Hz, 1H), 2.48 – 2.39 (m, 2H), 2.29 (dddd, *J* = 13.0, 9.3, 6.3, 0.7 Hz, 1H), 2.18 (s, 3H), 1.51 – 1.27 (m, 4H), 0.97 (t, *J* = 7.4 Hz, 3H), 0.92 (t, *J* = 7.3 Hz, 3H). **^{13}C NMR** (151 MHz, $CDCl_3$) δ 194.08, 169.01, 156.61, 148.02, 139.87, 132.23, 131.00, 129.31, 125.83, 123.08, 37.21, 27.12, 22.77, 21.21, 20.90, 14.41, 14.33. **HRMS** (ESI, m/z): $[M+Na]^+$ calcd. for $C_{17}H_{22}Na_1O_3$, 297.1461; found 297.1463. The stereochemistry of the product was determined by 2D-NMR analysis.

(*Z*)-2-propyl-3-(2-(trifluoromethoxy)phenyl)hex-2-enal (**5**). Pale yellow oil. 67% yield (50 mg, BISBI). 76% yield (57 mg, TDMPP).

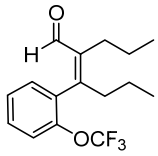

^{1}H NMR (400 MHz, $CDCl_3$) δ 9.29 (s, 1H), 7.40 (ddd, *J* = 8.4, 7.3, 1.7 Hz, 1H), 7.34 – 7.26 (m, 2H), 7.15 (ddd, *J* = 7.6, 1.7, 0.4 Hz, 1H), 2.66 (ddd, *J* = 13.6, 9.9, 6.5 Hz, 1H), 2.55 – 2.40 (m, 2H), 2.30 (dddd, *J* = 13.1, 8.3, 7.3, 0.7 Hz, 1H), 1.53 – 1.21 (m, 4H), 0.97 (t, *J* = 7.4 Hz, 3H), 0.92 (t, *J* = 7.3 Hz, 3H). **^{13}C NMR** (151 MHz, $CDCl_3$) δ 193.47, 156.72, 146.51 (q, *J* = 1.5 Hz), 140.34, 132.10, 132.07, 129.72, 126.39, 120.67 (q, *J* = 1.6 Hz), 120.63 (q, *J* = 258.3 Hz), 37.01, 27.17, 22.48, 21.01, 14.34, 14.21. ^{19}F NMR (376 MHz, CDCl3) δ -56.74. **HRMS** (ESI, m/z): $[M+H]^+$ calcd. for $C_{16}H_{20}F_3O_2$, 301.1410; found 301.1413. The stereochemistry of the product was determined by 2D-NMR analysis.

(*Z*)-2-(5-formyloct-4-en-4-yl)benzonitrile (**6-*Z***). Colorless oil. 43% yield (26 mg)

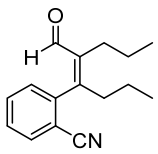

^{1}H NMR (400 MHz, $CDCl_3$) δ 9.24 (s, 1H), 7.73 (ddd, *J* = 7.7, 1.4, 0.6 Hz, 1H), 7.61 (td, *J* = 7.7, 1.4 Hz, 1H), 7.47 (td, *J* = 7.7, 1.3 Hz, 1H), 7.29 – 7.26 (m, 1H), 2.65 (ddd, *J* = 8.7, 6.9, 1.4 Hz, 2H), 2.54 – 2.44 (m, 1H), 2.42 – 2.32 (m, 1H), 1.56 – 1.26 (m, 4H), 1.00 (t, *J* = 7.4 Hz, 3H), 0.95 (t, *J* = 7.3 Hz, 3H). **^{13}C NMR** (126 MHz, $CDCl_3$) δ 192.43, 157.30, 143.38, 141.14, 133.15, 132.48, 130.34, 128.48, 117.52, 112.77, 37.81, 27.32, 22.58, 21.01, 14.37, 14.35. **HRMS** (ESI, m/z):

$[M+Na]^+$ calcd. for $C_{16}H_{19}N_1Na_1O_1$, 264.1359; found 264.1359. The stereochemistry of the product was determined by 2D-NMR analysis and by analogy to previously reported literature[1,2].

(*E*)-2-(5-formyloct-4-en-4-yl)benzonitrile (**6-*E***). Colorless oil. 8% yield (5 mg)

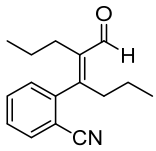

^{1}H NMR (400 MHz, $CDCl_3$) δ 10.30 (s, 1H), 7.75 (ddd, *J* = 7.8, 1.3, 0.6 Hz, 1H), 7.64 (td, *J* = 7.7, 1.3 Hz, 1H), 7.46 (td, *J* = 7.7, 1.2 Hz, 1H), 7.21 (ddd, *J* = 7.8, 1.2, 0.6 Hz, 1H), 3.01 (ddd, *J* = 13.5, 9.6, 6.6 Hz, 1H), 2.74 (ddd, *J* = 14.2, 9.5, 5.6 Hz, 1H), 2.05 (ddd, *J* = 13.0, 10.1, 5.5 Hz, 1H), 1.88 (ddd, *J* = 13.0, 10.0, 5.9 Hz, 1H), 1.59 – 1.36 (m, 2H), 1.36 – 1.13 (m, 2H), 0.96 (t, *J* = 7.3 Hz, 3H), 0.70 (t, *J* = 7.4 Hz, 3H). **^{13}C NMR** (126 MHz, $CDCl_3$) δ 191.30, 155.40, 145.47, 140.18, 133.28, 132.75, 128.56, 128.20, 117.63, 111.19, 34.47, 29.60, 22.31, 22.19, 14.31, 13.97. **HRMS** (ESI, m/z): $[M+Na]^+$ calcd. for $C_{16}H_{19}N_1Na_1O_1$, 264.1359; found 264.1358. The stereochemistry of the product was determined by 2D-NMR analysis and by analogy to previously reported literature[1,2].

(*Z*)-2-propyl-3-(2-(trifluoromethyl)phenyl)hex-2-enal (**7**). Colorless oil. 79% yield (56 mg, BISBI). 63% yield (45 mg, TDMPP)

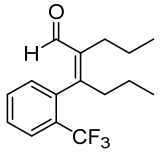

^{1}H NMR (400 MHz, $CDCl_3$) δ 9.17 (s, 1H), 7.77 – 7.69 (m, 1H), 7.54 (tdd, J = 7.6, 1.5, 0.7 Hz, 1H), 7.47 (dddd, J = 7.6, 6.7, 1.5, 0.8 Hz, 1H), 7.15 (ddt, J = 7.6, 1.5, 0.8 Hz, 1H), 2.77 (ddd, J = 13.7, 11.0, 6.0 Hz, 1H), 2.48 (dt, J = 13.0, 7.7 Hz, 1H), 2.37 – 2.20 (m, 2H), 1.55 – 1.27 (m, 4H), 0.98 (t, *J* = 7.4 Hz, 3H), 0.95 (t, *J* = 7.3 Hz, 3H). **^{13}C NMR** (151 MHz, $CDCl_3$) δ 193.26, 158.40, 139.80 (q, *J* = 1.3 Hz), 137.89 (q, *J* = 2.0 Hz), 131.32 (q, *J* = 1.1 Hz), 131.17, 128.39 (q, J = 30.0 Hz), 128.14, 126.83 (q, *J* = 5.1 Hz), 124.15 (q, *J* = 274.0 Hz), 38.02 (q, *J* = 1.9 Hz), 27.05, 22.21, 21.01, 14.54, 14.36. **^{19}F NMR** (376 MHz, $CDCl_3$) δ -58.63. **HRMS** (ESI, m/z): $[M+Na]^+$ calcd. for $C_{16}H_{19}F_3Na_1O_1$, 307.1280; found 307.1283. The stereochemistry of the product was determined by 2D-NMR analysis.

(*Z*)-3-(2,4-dichlorophenyl)-2-propylhex-2-enal (**8**). Pale yellow oil. 70% yield (50 mg, BISBI). 72% yield (51 mg, TDMPP).

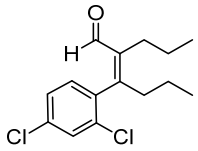

^{1}H NMR (400 MHz, $CDCl_3$) δ 9.25 (s, 1H), 7.46 (d, *J* = 2.1 Hz, 1H), 7.27 (dd, *J* = 8.1, 2.1 Hz, 1H), 7.06 (d, *J* = 8.2 Hz, 1H), 2.63 – 2.40 (m, 3H), 2.38 – 2.27 (m, 1H), 1.52 – 1.26 (m, 4H), 1.01 – 0.96 (m, 3H), 0.93 (d, *J* = 7.4 Hz, 3H). **^{13}C NMR** (151 MHz, $CDCl_3$) δ 193.14, 157.53, 140.11, 136.41, 134.58, 133.83, 131.75, 129.77, 126.97, 37.20, 27.08, 22.51, 20.90, 14.47, 14.33. **HRMS** (ESI, m/z): $[M+Na]^+$ calcd. for $C_{15}H_{18}Cl_2Na_1O_1$, 307.0627; found 307.0627. The stereochemistry of the product was determined by 2D-NMR analysis.

(*Z*)-3-(naphthalen-1-yl)-2-propylhex-2-enal (**9**). Colorless oil. 85% yield (57 mg, BISBI). 83% yield (55 mg, TDMPP).

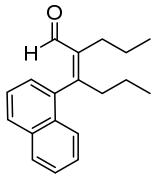

^{1}H NMR (400 MHz, $CDCl_3$) δ 9.19 (s, 1H), 7.91 – 7.82 (m, 2H), 7.74 – 7.67 (m, 1H), 7.54 – 7.43 (m, 3H), 7.22 (dd, *J* = 7.0, 1.3 Hz, 1H), 2.77 (ddd, *J* = 13.0, 10.3, 6.2 Hz, 1H), 2.61 – 2.50 (m, 2H), 2.50 – 2.40 (m, 1H), 1.64 – 1.52 (m, 2H), 1.49 – 1.28 (m, 2H), 1.06 (t, *J* = 7.3 Hz, 3H), 0.91 (t, *J* = 7.3 Hz, 3H). **^{13}C NMR** (151 MHz, $CDCl_3$) δ 194.21, 160.64, 140.42, 136.70, 133.67, 131.88, 128.67, 128.32, 126.88, 126.74, 126.28, 125.58, 124.97, 38.42, 27.25, 22.94, 21.65, 14.58, 14.50. **HRMS** (ESI, m/z): $[M+H]^+$ calcd. for $C_{19}H_{23}O_1$, 267.1743; found 267.1744. The stereochemistry of the product was determined by 2D-NMR analysis.

(*Z*)-3-(9-oxo-9H-fluoren-4-yl)-2-propylhex-2-enal (**10**). 52% yield (41 mg).

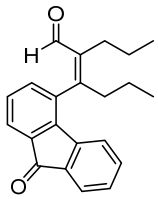

^{1}H NMR (400 MHz, $CDCl_3$) δ 9.49 (s, 1H), 7.72 – 7.65 (m, 2H), 7.40 (td, *J* = 7.5, 1.3 Hz, 1H), 7.36 – 7.27 (m, 3H), 7.16 (dd, *J* = 7.7, 1.2 Hz, 1H), 2.78 (ddd, *J* = 13.0, 10.6, 6.0 Hz, 1H), 2.59 – 2.39 (m, 3H), 1.66 – 1.36 (m, 4H), 1.06 (t, *J* = 7.3 Hz, 3H), 0.96 (t, *J* = 7.3 Hz, 3H). **^{13}C NMR** (126 MHz, $CDCl_3$) δ 193.31, 193.27, 158.83, 143.76, 141.44, 139.93, 136.27, 134.90, 134.85, 134.52, 134.50, 129.34, 128.76, 124.74, 123.90, 123.08, 37.68, 27.28, 22.54, 21.16, 14.67, 14.60. **HRMS** (ESI, m/z): $[M+Na]^+$ calcd. for $C_{22}H_{22}Na_1O_2$, 341.1512; found 341.1512. The absolute configuration of the product was determined by 2D-NMR analysis and X-ray crystallography.

(*Z*)-3-(3-methylthiophen-2-yl)-2-propylhex-2-enal (**11**). Colorless oil. 67% yield (39 mg, BISBI). 69% yield (41 mg, TDMPP).

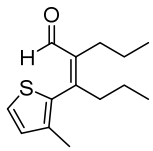

^{1}H NMR (400 MHz, $CDCl_3$) δ 9.37 (s, 1H), 7.28 (d, *J* = 5.1 Hz, 1H), 6.85 (d, *J* = 5.1 Hz, 1H), 2.65 – 2.46 (m, 2H), 2.39 (dd, *J* = 9.1, 6.8 Hz, 2H), 2.06 (s, 3H), 1.53 – 1.32 (m, 4H), 0.97 (t, *J* = 7.4 Hz, 3H), 0.93 (t, *J* = 7.4 Hz, 3H). **^{13}C NMR** (151 MHz, $CDCl_3$) δ 194.12, 153.64, 141.41, 137.53, 134.74, 129.83, 125.25, 39.21, 27.91, 22.91, 21.56, 14.77, 14.47, 14.36. **HRMS** (ESI, m/z): $[M+Na]^+$ calcd. for $C_{14}H_{20}Na_1O_1S_1$, 259.1127; found 259.1128. The stereochemistry of the product was determined by 2D-NMR analysis.

(*Z*)-3-(3-methylbenzofuran-2-yl)-2-propylhex-2-enal (**12**). Pale yellow oil. 67% yield (46 mg).

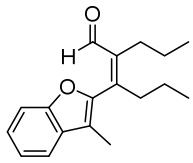

^{1}H NMR (400 MHz, $CDCl_3$) δ 9.49 (s, 1H), 7.52 (ddd, *J* = 7.7, 1.4, 0.7 Hz, 1H), 7.46 (dt, *J* = 8.2, 0.9 Hz, 1H), 7.35 (ddd, *J* = 8.2, 7.2, 1.4 Hz, 1H), 7.29 (dd, *J* = 7.6, 1.0 Hz, 1H), 2.74 – 2.68 (m, 2H), 2.49 – 2.43 (m, 2H), 2.13 (s, 3H), 1.56 – 1.43 (m, 2H), 1.43 – 1.31 (m, 2H), 1.00 (t, *J* = 7.4 Hz, 3H), 0.91 (t, *J* = 7.4 Hz, 3H). **^{13}C NMR** (126 MHz, $CDCl_3$) δ 193.27, 154.60, 148.81, 148.32, 142.54, 129.62, 125.57, 122.85, 119.89, 118.94, 111.33, 34.73, 28.14, 22.92, 21.85, 14.50, 14.16, 9.47. **HRMS** (ESI, m/z): $[M+Na]^+$ calcd. for $C_{18}H_{22}Na_1O_2$, 293.1512; found 293.1503. The stereochemistry of the product was determined by 2D-NMR analysis.

(*Z*)-3-(2-methyl-6-(trifluoromethyl)pyridin-3-yl)-2-propylhex-2-enal (**13**). Pale yellow oil. 66% yield (49 mg).

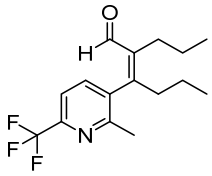

^{1}H NMR (400 MHz, $CDCl_3$) δ 9.22 (s, 1H), 7.57 – 7.48 (m, 2H), 2.66 (ddd, *J* = 13.3, 10.5, 6.1 Hz, 1H), 2.52 (s, 3H), 2.51 – 2.31 (m, 3H), 1.55 – 1.24 (m, 4H), 1.00 (t, *J* = 7.3 Hz, 3H), 0.96 (t, *J* = 7.3 Hz, 3H). **^{13}C NMR** (126 MHz, $CDCl_3$) δ 192.37, 157.35, 156.92, 147.24 (q, *J* = 34.7 Hz), 140.43, 138.04, 137.21 (d, *J* = 1.2 Hz), 121.53 (q, *J* = 274.1 Hz), 117.41 (q, *J* = 2.8 Hz), 37.50, 27.14, 22.99, 22.64, 20.90, 14.47, 14.42. **^{19}F NMR** (376 MHz, $CDCl_3$) δ -68.00. **HRMS** (ESI, m/z): $[M+H]^+$ calcd. for $C_{16}H_{21}F_3N_1O_1$, 300.1570; found 300.1571. The stereochemistry of the product was determined by 2D-NMR analysis.

(*Z*)-3-mesityl-2-propylhex-2-enal (**14**). Colorless oil. 97% yield (63 mg, BISBI). 82% yield (53 mg, TDMPP).

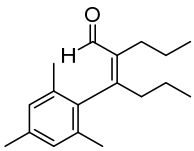

^{1}H NMR (400 MHz, $CDCl_3$) δ 9.21 (s, 1H), 6.87 (s, 2H), 2.54 – 2.45 (m, 2H), 2.43 – 2.35 (m, 2H), 2.28 (s, 3H), 2.11 (s, 6H), 1.54 – 1.42 (m, 2H), 1.41 – 1.30 (m, 2H), 0.99 (t, J = 7.4 Hz, 3H), 0.94 (t, J = 7.3 Hz, 3H). **^{13}C NMR** (101 MHz, $CDCl_3$) δ 194.46, 161.72, 138.97, 137.03, 135.30, 135.22, 128.50, 38.19, 26.96, 22.62, 21.14, 21.10, 20.49, 15.03, 14.57. **HRMS** (EI, m/z): $[M]^+$ calcd. for $C_{18}H_{26}O_1$, 258.1978; found 258.1979. The stereochemistry of the product was determined by 2D-NMR analysis.

(*Z*)-3-(2,6-dichlorophenyl)-2-propylhex-2-enal (**15**). White solid. 71% yield (50 mg).

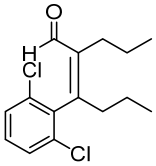

^{1}H NMR (400 MHz, $CDCl_3$) δ 9.22 (s, 1H), 7.36 (d, J = 8.1 Hz, 2H), 7.23 (dd, J = 8.6, 7.4 Hz, 1H), 2.64 – 2.57 (m, 2H), 2.46 – 2.39 (m, 2H), 1.56 – 1.46 (m, 2H), 1.46 – 1.36 (m, 2H), 0.99 (t, J = 7.4 Hz, 3H), 0.96 (t, J = 7.3 Hz, 3H). **^{13}C NMR** (126 MHz, $CDCl_3$) δ 192.94, 155.88, 140.13, 136.91, 134.69, 129.63, 128.28, 36.93, 26.98, 22.22, 21.00, 14.86, 14.36. **HRMS** (ESI, m/z): $[M+Na]^+$ calcd. for $C_{15}H_{18}Cl_2Na_1O_1$, 307.0627; found 307.0624. The stereochemistry of the product was determined by 2D-NMR analysis.

(*Z*)-3-(5-methyl-3-phenylisoxazol-4-yl)-2-propylhex-2-enal (**16**). White solid. 42% yield (31 mg).

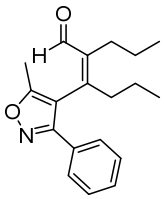

^{1}H NMR (400 MHz, $CDCl_3$) δ 9.64 (s, 1H), 7.66 – 7.59 (m, 2H), 7.46 – 7.38 (m, 3H), 2.62 – 2.49 (m, 2H), 2.37 – 2.26 (m, 1H), 2.31 (s, 3H), 1.92 (dddd, J = 13.3, 9.9, 5.5, 0.8 Hz, 1H), 1.56 – 1.41 (m, 2H), 1.34 – 1.14 (m, 2H), 1.00 (t, J = 7.4 Hz, 3H), 0.82 (t, J = 7.3 Hz, 3H). **^{13}C NMR** (101 MHz, $CDCl_3$) δ 193.01, 168.25, 160.45, 150.50, 142.75, 130.13, 129.03, 128.96, 127.67, 112.34, 36.85, 27.59, 22.67, 21.57, 14.46, 14.31, 11.60. **HRMS** (ESI, m/z): $[M+H]^+$ calcd. for $C_{19}H_{24}N_1O_2$, 298.1802; found 298.1801. The stereochemistry of the product was determined by 2D-NMR analysis.

(*Z*)-3-(2,6-difluorophenyl)-2-propylhex-2-enal (**17**). Colorless oil. 61% yield (39 mg with an *E* isomer, *Z*/*E* = 97:3).

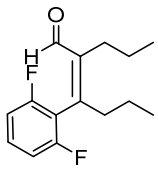

^{1}H NMR (400 MHz, $CDCl_3$) δ 9.38 (s, 1H), 7.36 – 7.27 (m, 1H), 6.98 – 6.90 (m, 2H), 2.62 – 2.53 (m, 2H), 2.47 – 2.38 (m, 2H), 1.54 – 1.42 (m, 2H), 1.42 – 1.30 (m, 2H), 0.97 (t, *J* = 7.4 Hz, 3H), 0.94 (t, *J* = 7.3 Hz, 3H). **^{13}C NMR** (126 MHz, $CDCl_3$) δ 192.97, 159.99 (dd, *J* = 247.4, 7.2 Hz), 149.11, 141.42, 130.12 (t, *J* = 10.0 Hz), 115.63 (t, *J* = 21.2 Hz), 111.66 – 111.40 (m), 36.79 (t, *J* = 1.2 Hz), 27.27, 22.52, 21.07, 14.24, 14.20. **^{19}F NMR** (376 MHz, $CDCl_3$) δ -111.39. **HRMS** (ESI, m/z): $[M+Na]^+$ calcd. for $C_{15}H_{18}F_2Na_1O_1$, 275.1218; found 275.1214. The stereochemistry of the mixture of products was determined by 2D-NMR analysis and by analogy to previously reported literature[1,2].

(*E*) isomer: **^{1}H NMR** (500 MHz, $CDCl_3$) δ 10.30 (s, 1H), 2.82 – 2.77 (m, 2H), 2.03 – 1.98 (m, 2H), 0.71 (t, *J* = 7.4 Hz, 3H). **^{19}F NMR** (376 MHz, $CDCl_3$) δ -111.73. The stereochemistry of the product was determined by 2D-NMR analysis and by analogy to previously reported literature[1,2]. Where assignments of C or H atoms within the isomers are ambiguous, no peak assignment is given.

(*Z*)-2-propyl-3-(p-tolyl)hex-2-enal (**18**). Pale yellow oil. 39% yield (23 mg with an *E* isomer, *Z*/*E* = 94:6, BISBI). 76% yield (44 mg with an *E* isomer, *Z*/*E* = 88:12, TDMPP).

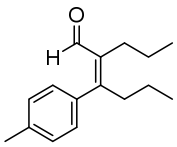

^{1}H NMR (400 MHz, $CDCl_3$) δ 9.36 (s, 1H), 7.19 – 7.14 (m, 2H), 7.08 – 7.04 (m, 2H), 2.64 – 2.53 (m, 2H), 2.43 – 2.32 (m, 2H), 2.37 (s, 3H), 1.49 – 1.38 (m, 2H), 1.38 – 1.27 (m, 2H), 0.97 (t, *J* = 7.3 Hz, 3H), 0.89 (t, *J* = 7.4 Hz, 3H). **^{13}C NMR** (126 MHz, $CDCl_3$) δ 194.61, 162.21, 138.83, 138.19, 135.96, 129.33, 128.91, 37.94, 27.73, 22.82, 21.38, 21.34, 14.45, 14.25. **HRMS** (ESI, m/z): $[M+Na]^+$ calcd. for $C_{16}H_{22}Na_1O_1$, 253.1563; found 253.1564. The stereochemistry of the mixture of products was determined by 2D-NMR analysis and by analogy to previously reported literature[1,2].

(*E*) isomer: **^{1}H NMR** (400 MHz, $CDCl_3$) δ 10.26 (s, 1H), 2.85 – 2.77 (m, 2H), 2.07 – 2.01 (m, 2H), 0.72 (t, *J* = 7.3 Hz, 3H). The stereochemistry of the product was determined by 2D-NMR analysis and by analogy to previously reported literature[1,2]. Where assignments of C or H atoms within the isomers are ambiguous, no peak assignment is given.

(*Z*)-3-phenyl-2-propylhex-2-enal (**19**). Colorless oil. 66% yield (36 mg with an *E* isomer, *Z*/*E* = 95:5).

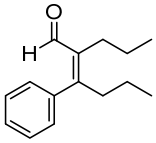

^{1}H NMR (400 MHz, $CDCl_3$) δ 9.35 (s, 1H), 7.41 – 7.31 (m, 3H), 7.21 – 7.14 (m, 2H), 2.64 – 2.55 (m, 2H), 2.42 – 2.34 (m, 2H), 1.52 – 1.39 (m, 2H), 1.39 – 1.26 (m, 2H), 0.98 (t, *J* = 7.4 Hz, 3H), 0.90 (t, *J* = 7.4 Hz, 3H). **^{13}C NMR** (101 MHz, $CDCl_3$) δ 194.52, 162.14, 138.99, 138.91, 129.32, 128.23, 128.21, 37.99, 27.62, 22.81, 21.28, 14.45, 14.25. **HRMS** (ESI, m/z): $[M+H]^+$ calcd. for $C_{15}H_{21}O_1$, 217.1587; found 217.1589. The stereochemistry of the mixture of products was determined by 2D-NMR analysis and by analogy to previously reported literature[1,2].

(*E*) isomer: **^{1}H NMR** (500 MHz, $CDCl_3$) δ 10.27 (s, 1H), 2.85 – 2.79 (m, 2H), 2.06 – 2.00 (m, 2H), 0.71 (t, *J* = 7.4 Hz, 3H). The stereochemistry of the product was determined by 2D-NMR analysis and by analogy to previously reported literature[1,2]. Where assignments of C or H atoms within the isomers are ambiguous, no peak assignment is given.

(*Z*)-3-phenyl-2-propylhex-2-enal-1-^{13}C (**20**). Colorless oil. 67% yield (36 mg with an *E* isomer, *Z*/*E* = 95:5, >99% [^{13}C]).

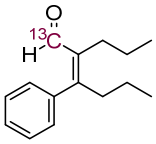

^{1}H NMR (500 MHz, $CDCl_3$) δ 9.35 (d, *J* = 176.1 Hz, 1H), 7.40 – 7.32 (m, 3H), 7.21 – 7.14 (m, 2H), 2.63 – 2.56 (m, 2H), 2.43 – 2.34 (m, 2H), 1.50 – 1.40 (m, 2H), 1.39 – 1.29 (m, 2H), 0.98 (t, *J* = 7.4 Hz, 3H), 0.90 (t, *J* = 7.4 Hz, 3H). **^{13}C NMR** (126 MHz, $CDCl_3$) δ 194.50, 162.10 (d, *J* = 4.5 Hz), 139.08 (d, *J* = 11.5 Hz), 138.86 (d, *J* = 35.1 Hz), 129.32, 128.22, 128.22, 38.00 (d, *J* = 4.1 Hz), 27.63 (d, *J* = 1.8 Hz), 22.81, 21.28, 14.44, 14.25. **HRMS** (ESI, m/z): $[M+H]^+$ calcd. for $C_{14}{}^{13}C_1H_{21}O_1$, 218.162; found 218.1625. The stereochemistry of the mixture of products was determined by 2D-NMR analysis and by analogy to previously reported literature[1,2].

(*E*) isomer **^{1}H NMR** (500 MHz, CDCl3) δ 10.27 (d, *J* = 172.2 Hz, 1H), 2.86 – 2.79 (m, 2H), 2.07 – 2.00 (m, 2H), 0.71 (t, *J* = 7.4 Hz, 3H). **^{13}C NMR** (126 MHz, $CDCl_3$) δ 192.10. The stereochemistry of the product was determined by 2D-NMR analysis and by analogy to previously reported literature[1,2]. Where assignments of C or H atoms within the isomers are ambiguous, no peak assignment is given.

(*Z*)-3-(4-methoxyphenyl)-2-propylhex-2-enal (**21**). Pale yellow oil. 48% yield (30 mg).

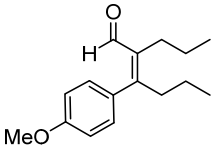

^{1}H NMR (400 MHz, $CDCl_3$) δ 9.37 (s, 1H), 7.14 – 7.07 (m, 2H), 6.92 – 6.86 (m, 2H), 3.83 (s, 3H), 2.62 – 2.53 (m, 2H), 2.41 – 2.32 (m, 2H), 1.49 – 1.37 (m, 2H), 1.37 – 1.27 (m, 2H), 0.97 (t,

J = 7.4 Hz, 3H), 0.89 (t, J = 7.3 Hz, 3H). **^{13}C NMR** (126 MHz, $CDCl_3$) δ 194.60, 161.80, 159.82, 138.88, 131.08, 130.75, 113.65, 55.46, 37.87, 27.89, 22.83, 21.51, 14.47, 14.23. **HRMS** (ESI, m/z): $[M+Na]^+$ calcd. for $C_{16}H_{22}Na_1O_2$, 269.1512; found 269.1499. The stereochemistry of the product was determined by 2D-NMR analysis.

(*Z*)-3-(4-(benzyloxy)phenyl)-2-propylhex-2-enal (**22**). White solid. 44% yield (36 mg).

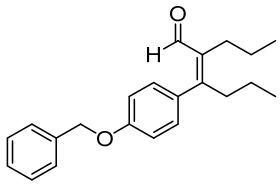

^{1}H NMR (400 MHz, $CDCl_3$) δ 9.38 (s, 1H), 7.48 – 7.32 (m, 5H), 7.14 – 7.09 (m, 2H), 7.00 – 6.94 (m, 2H), 5.08 (s, 2H), 2.61 – 2.55 (m, 2H), 2.40 – 2.34 (m, 2H), 1.49 – 1.38 (m, 2H), 1.38 – 1.27 (m, 2H), 0.97 (t, J = 7.4 Hz, 3H), 0.89 (t, J = 7.4 Hz, 3H). **^{13}C NMR** (126 MHz, $CDCl_3$) δ 194.59, 161.75, 159.05, 138.91, 136.83, 131.36, 130.77, 128.80, 128.26, 127.67, 114.55, 70.25, 37.87, 27.88, 22.83, 21.51, 14.46, 14.24. **HRMS** (ESI, m/z): $[M+Na]^+$ calcd. for $C_{22}H_{26}Na_1O_2$, 345.1825; found 345.1823. The stereochemistry of the product was determined by 2D-NMR analysis.

(*Z*)-2-propyl-3-(4-(4,4,5,5-tetramethyl-1,3,2-dioxaborolan-2-yl)phenyl)hex-2-enal (**23**). Colorless oil. 43% yield (37 mg).

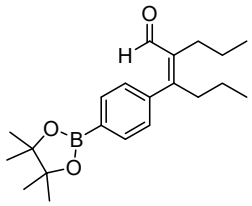

^{1}H NMR (400 MHz, $CDCl_3$) δ 9.34 (s, 1H), 7.83 – 7.77 (m, 2H), 7.21 – 7.16 (m, 2H), 2.63 – 2.55 (m, 2H), 2.41 – 2.33 (m, 2H), 1.49 – 1.40 (m, 2H), 1.35 (s, 12H), 1.34 – 1.27 (m, 2H), 0.97 (t, J = 7.4 Hz, 3H), 0.88 (t, J = 7.3 Hz, 3H). **^{13}C NMR** (101 MHz, $CDCl_3$) δ 194.33, 161.98, 141.95, 138.93, 135.36, 134.59, 128.69, 84.11, 37.90, 27.59, 25.03, 22.80, 21.22, 14.46, 14.24. **HRMS** (ESI, m/z): $[M+Na]^+$ calcd. for $C_{21}H_{31}B_1Na_1O_3$, 365.2262; found 365.2262. The stereochemistry of the product was determined by analogy to related products and previously reported literature[1,2].

Methyl (*Z*)-3-(5-formyloct-4-en-4-yl)benzoate (**24**). Colorless oil. 51% yield (35 mg).

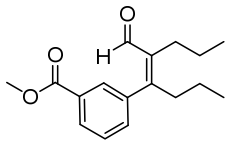

^{1}H NMR (400 MHz, $CDCl_3$) δ 9.32 (s, 1H), 8.03 (ddd, J = 7.8, 1.7, 1.3 Hz, 1H), 7.86 (td, J = 1.8, 0.6 Hz, 1H), 7.46 (td, J = 7.7, 0.6 Hz, 1H), 7.36 (ddd, J = 7.6, 1.8, 1.3 Hz, 1H), 3.93 (s, 3H), 2.64 – 2.57 (m, 2H), 2.43 – 2.36 (m, 2H), 1.50 – 1.39 (m, 2H), 1.37 – 1.26 (m, 2H), 0.98 (t, J = 7.4 Hz,

3H), 0.90 (t, J = 7.3 Hz, 3H). **^{13}C NMR** (126 MHz, $CDCl_3$) δ 193.85, 166.77, 160.70, 139.52, 139.36, 133.74, 130.37, 130.03, 129.39, 128.42, 52.46, 37.96, 27.62, 22.77, 21.18, 14.45, 14.23. **HRMS** (ESI, m/z): $[M+Na]^+$ calcd. for $C_{17}H_{22}Na_1O_3$, 297.1461; found 297.1461. The stereochemistry of the product was determined by 2D-NMR analysis.

(*Z*)-3-(3-bromophenyl)-2-propylhex-2-enal (**25**). Pale yellow oil. 69% yield (51 mg with an *E* isomer, *Z*/*E* = 79:21).

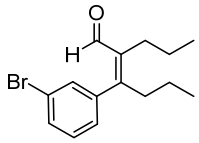

^{1}H NMR (400 MHz, $CDCl_3$) δ 9.35 (s, 1H), 7.49 (ddd, J = 8.0, 2.0, 1.1 Hz, 1H), 7.34 (ddd, J = 2.0, 1.6, 0.4 Hz, 1H), 7.25 – 7.21 (m, 1H), 7.10 (ddd, J = 7.6, 1.6, 1.1 Hz, 1H), 2.61 – 2.52 (m, 2H), 2.41 – 2.33 (m, 2H), 1.50 – 1.38 (m, 2H), 1.38 – 1.28 (m, 2H), 0.97 (t, J = 7.3 Hz, 3H), 0.91 (t, J = 7.3 Hz, 3H). **^{13}C NMR** (126 MHz, $CDCl_3$) δ 193.82, 160.05, 141.19, 139.54, 131.86, 131.31, 129.77, 128.09, 122.59, 37.91, 27.59, 22.74, 21.19, 14.43, 14.23. **HRMS** (EI, m/z): $[M]^+$ calcd. for $C_{15}H_{19}Br_1O_1$, 294.0614; found 294.0615. The stereochemistry of the product was determined by 2D-NMR analysis and by analogy to previously reported literature[1,2].

(*E*) isomer: **^{1}H NMR** (400 MHz, CDCl3) δ 10.25 (s, 1H), 7.47 (ddd, J = 8.1, 2.0, 1.0 Hz, 1H), 7.31 – 7.26 (m, 1H), 7.29 – 7.22 (m, 1H), 7.06 (ddd, J = 7.6, 1.7, 1.0 Hz, 1H), 2.83 – 2.75 (m, 2H), 2.08 – 1.97 (m, 2H), 1.50 – 1.19 (m, 4H), 0.92 (t, J = 7.4 Hz, 3H), 0.73 (t, J = 7.4 Hz, 3H). **^{13}C NMR** (126 MHz, $CDCl_3$) δ 191.79, 158.44, 143.75, 138.92, 130.81, 130.06, 130.04, 125.91, 122.58, 34.73, 29.28, 22.76, 22.22, 14.30, 13.85. The stereochemistry of the product was determined by 2D-NMR analysis and by analogy to previously reported literature[1,2]. Where assignments of C or H atoms within the isomers are ambiguous, no peak assignment is given.

(*Z*)-4-(5-formyloct-4-en-4-yl)benzonitrile (**26**). Pale yellow oil. 57% yield (35 mg).

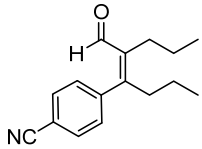

^{1}H NMR (400 MHz, $CDCl_3$) δ 9.30 (s, 1H), 7.72 – 7.64 (m, 2H), 7.34 – 7.27 (m, 2H), 2.62 – 2.54 (m, 2H), 2.42 – 2.34 (m, 2H), 1.49 – 1.38 (m, 2H), 1.36 – 1.25 (m, 2H), 0.97 (t, J = 7.4 Hz, 3H), 0.91 (t, J = 7.3 Hz, 3H). **^{13}C NMR** (101 MHz, $CDCl_3$) δ 193.08, 159.37, 144.14, 139.98, 132.11, 129.98, 118.47, 112.23, 37.76, 27.61, 22.72, 21.12, 14.41, 14.18. **HRMS** (ESI, m/z): $[M+Na]^+$ calcd. for $C_{16}H_{19}N_1Na_1O_1$, 264.1359; found 264.1363. The stereochemistry of the product was determined by 2D-NMR analysis.

(*Z*)-3-(4-fluorophenyl)-2-propylhex-2-enal (**27**). Yellow oil. 70% yield (41 mg with an *E* isomer, *Z*/*E* = 87:13).

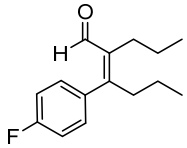

^{1}H NMR (400 MHz, $CDCl_3$) δ 9.35 (s, 1H), 7.18 – 7.12 (m, 2H), 7.10 – 7.03 (m, 2H), 2.61 – 2.54 (m, 2H), 2.41 – 2.34 (m, 2H), 1.48 – 1.37 (m, 2H), 1.36 – 1.27 (m, 2H), 0.97 (t, *J* = 7.4 Hz, 3H), 0.90 (t, *J* = 7.4 Hz, 3H). **^{13}C NMR** (101 MHz, $CDCl_3$) δ 194.12, 162.72 (d, *J* = 248.0 Hz), 160.79, 139.38, 134.82 (d, *J* = 3.5 Hz), 130.99 (d, *J* = 8.1 Hz), 115.34 (d, *J* = 21.5 Hz), 38.01, 27.71, 22.78, 21.27, 14.45, 14.21. **^{19}F NMR** (376 MHz, $CDCl_3$) δ -113.48. **HRMS** (ESI, m/z): $[M+Na]^+$ calcd. for $C_{15}H_{19}F_1Na_1O_1$, 257.1312; found 257.1309. The stereochemistry of the product was determined by analogy to related products and previously reported literature[1,2].

(*E*) isomer: **^{1}H NMR** (400 MHz, $CDCl_3$) δ 10.25 (s, 1H), 7.20 – 7.01 (m, 4H), 2.84 – 2.76 (m, 2H), 2.06 – 1.98 (m, 2H), 1.52 – 1.24 (m, 4H), 0.92 (t, *J* = 7.4 Hz, 3H), 0.72 (t, *J* = 7.4 Hz, 3H). **^{13}C NMR** (101 MHz, $CDCl_3$) δ 191.93, 128.92 (d, *J* = 8.0 Hz), 115.49 (d, *J* = 21.5 Hz), 34.98, 29.22, 22.22, 17.18, 14.32, 13.83. **^{19}F NMR** (376 MHz, CDCl3) δ -114.29. The stereochemistry of the product was determined by analogy to related products and previously reported literature[1,2]. Where assignments of C or H atoms within the isomers are ambiguous, no peak assignment is given.

(*Z*)-3-(3,5-bis(trifluoromethyl)phenyl)-2-propylhex-2-enal (**28-*Z***). 45% yield (39 mg).

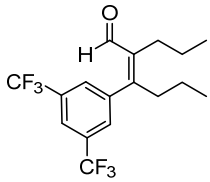

^{1}H NMR (400 MHz, CDCl3) δ 9.28 (s, 1H), 7.89 (s, 1H), 7.62 (s, 2H), 2.66 – 2.57 (m, 2H), 2.47 – 2.37 (m, 2H), 1.52 – 1.40 (m, 2H), 1.39 – 1.28 (m, 2H), 1.00 (t, *J* = 7.4 Hz, 3H), 0.94 (t, *J* = 7.3 Hz, 3H). **^{13}C NMR** (101 MHz, $CDCl_3$) δ 192.54, 157.90, 141.40, 140.76, 132.13, 131.80, 129.37, 129.15 – 128.96 (m), 124.50, 122.30 – 122.13 (m), 121.79, 37.97, 27.66, 22.70, 21.09, 14.48, 14.20. **^{19}F NMR** (376 MHz, $CDCl_3$) δ -62.81. **HRMS** (ESI, m/z): $[M+H]^+$ calcd. for $C_{17}H_{19}F_6O_1$, 353.1335; found 353.1339. The stereochemistry of the product was determined by analogy to related products and previously reported literature[1,2].

(*E*)-3-(3,5-bis(trifluoromethyl)phenyl)-2-propylhex-2-enal (**28-*E***). 12% yield (10 mg).

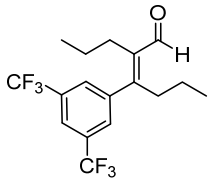

^{1}H NMR (400 MHz, $CDCl_3$) δ 10.28 (s, 1H), 7.88 (s, 1H), 7.59 (s, 2H), 2.89 – 2.79 (m, 2H), 2.00 – 1.91 (m, 2H), 1.51 – 1.38 (m, 2H), 1.32 – 1.21 (m, 2H), 0.96 (t, *J* = 7.3 Hz, 3H), 0.73 (t, *J* = 7.4 Hz, 3H). **^{13}C NMR** (151 MHz, $CDCl_3$) δ 191.27, 155.85, 143.71, 139.81, 132.09 (q, J =

33.5 Hz), 127.53 (dd, J = 3.7, 1.1 Hz), 123.24 (q, J = 272.9 Hz), 121.78 (p, J = 3.8 Hz), 34.55, 29.50, 22.82, 22.32, 14.15, 13.83. **^{19}F NMR** (376 MHz, $CDCl_3$) δ -62.88. **HRMS** (ESI, m/z): $[M+Na]^+$ calcd. for $C_{17}H_{18}F_6Na_1O_1$, 375.1154; found 375.1150. The stereochemistry of the product was determined by 2D-NMR analysis and by analogy to related products and previously reported literature[1,2].

(*Z*)-4-(5-formyloct-4-en-4-yl)-*N,N*-dipropylbenzenesulfonamide (**29**). Yellow oil. 31% yield (29 mg).

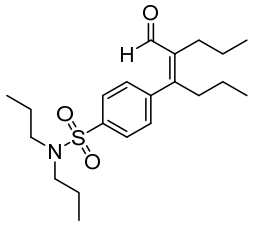

^{1}H NMR (400 MHz, $CDCl_3$) δ 9.31 (s, 1H), 7.84 – 7.78 (m, 2H), 7.34 – 7.29 (m, 2H), 3.15 – 3.07 (m, 4H), 2.63 – 2.55 (m, 2H), 2.43 – 2.35 (m, 2H), 1.63 – 1.51 (m, 4H), 1.50 – 1.39 (m, 2H), 1.37 – 1.26 (m, 2H), 0.98 (t, *J* = 7.4 Hz, 3H), 0.91 (t, *J* = 7.3 Hz, 3H), 0.87 (t, *J* = 7.4 Hz, 6H). **^{13}C NMR** (126 MHz, $CDCl_3$) δ 193.43, 160.00, 143.33, 140.18, 139.82, 129.81, 127.03, 50.13, 37.85, 27.61, 22.74, 22.16, 21.12, 14.42, 14.19, 11.32. **HRMS** (ESI, m/z): $[M+H]^+$ calcd. for $C_{21}H_{34}N_1O_3S_1$, 380.2254; found 380.2257. The stereochemistry of the product was determined by 2D-NMR analysis.

(*Z*)-5-(5-(5-formyloct-4-en-4-yl)-4-methylthiazol-2-yl)-2-isobutoxybenzonitrile (**30**). Yellow oil. 66% yield (68 mg).

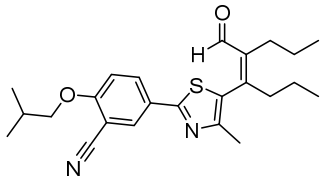

^{1}H NMR (400 MHz, $CDCl_3$) δ 9.50 (s, 1H), 8.11 (dd, *J* = 2.3, 0.4 Hz, 1H), 8.05 (dd, *J* = 8.8, 2.3 Hz, 1H), 7.01 (dd, *J* = 8.8, 0.5 Hz, 1H), 3.89 (d, *J* = 6.5 Hz, 2H), 2.55 (t, *J* = 7.7 Hz, 2H), 2.47 – 2.37 (m, 2H), 2.28 (s, 3H), 2.26 – 2.13 (m, 1H), 1.53 – 1.37 (m, 4H), 1.09 (d, *J* = 6.7 Hz, 6H), 0.99 (t, *J* = 7.4 Hz, 3H), 0.96 (t, *J* = 7.3 Hz, 3H). **^{13}C NMR** (101 MHz, $CDCl_3$) δ 192.98, 164.81, 162.17, 153.11, 150.18, 142.62, 132.25, 131.81, 128.92, 126.41, 115.71, 112.73, 102.97, 75.76, 39.09, 28.31, 28.01, 22.85, 21.63, 19.22, 16.16, 14.48, 14.31. **HRMS** (ESI, m/z): $[M+Na]^+$ calcd. for $C_{24}H_{30}N_2Na_1O_2S_1$, 433.1920; found 433.1923. The stereochemistry of the product was determined by 2D-NMR analysis.

(*Z*)-2-heptyl-3-(*o*-tolyl)dec-2-enal (**31**). Colorless oil. 76% yield (65 mg).

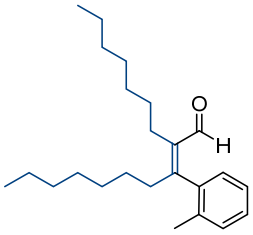

^{1}H NMR (500 MHz, $CDCl_3$) δ 9.22 (s, 1H), 7.27 – 7.14 (m, 3H), 7.00 (dd, *J* = 7.4, 1.4 Hz, 1H), 2.62 (ddd, *J* = 13.0, 10.2, 4.9 Hz, 1H), 2.47 – 2.29 (m, 3H), 2.18 (s, 3H), 1.47 – 1.16 (m, 20H), 0.90 (t, *J* = 7.3 Hz, 3H), 0.86 (t, *J* = 7.0 Hz, 3H). **^{13}C NMR** (126 MHz, $CDCl_3$) δ 194.39, 162.03, 138.98, 138.72, 135.39, 130.28, 129.27, 127.84, 125.50, 35.97, 32.00, 31.87, 30.12, 30.05, 29.62, 29.33, 29.19, 27.63, 25.08, 22.82, 22.74, 19.90, 14.26, 14.19. **HRMS** (ESI, m/z): $[M+H]^+$ calcd. for $C_{24}H_{39}O_1$, 343.2995; found 343.2992. The stereochemistry of the product was determined by 2D-NMR analysis.

(*Z*)-2-heptyl-3-(*p*-tolyl)dec-2-enal (**32**). Colorless oil. 63% yield (54 mg).

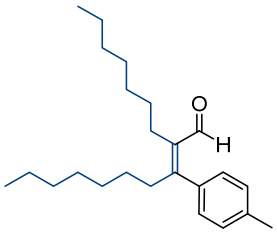

^{1}H NMR (500 MHz, $CDCl_3$) δ 9.35 (s, 1H), 7.18 – 7.15 (m, 2H), 7.08 – 7.04 (m, 2H), 2.62 – 2.53 (m, 2H), 2.41 – 2.33 (m, 2H), 2.38 (s, 3H), 1.44 – 1.16 (m, 20H), 0.89 (t, *J* = 7.0 Hz, 3H), 0.85 (t, *J* = 7.1 Hz, 3H). **^{13}C NMR** (126 MHz, $CDCl_3$) δ 194.59, 162.31, 138.91, 138.16, 136.05, 129.33, 128.90, 36.07, 32.00, 31.84, 30.05, 29.81, 29.69, 29.33, 29.17, 28.12, 25.81, 22.82, 22.73, 21.35, 14.26, 14.19. **HRMS** (ESI, m/z): $[M+Na]^+$ calcd. for $C_{24}H_{38}Na_1O_1$, 365.2815; found 365.2815. The stereochemistry of the product was determined by 2D-NMR analysis.

(*Z*)-6-phenyl-2-(3-phenylpropyl)-3-(*o*-tolyl)hex-2-enal (**33**). White solid. 62% yield (60 mg, BISBI). 75% yield (72 mg, TDMPP).

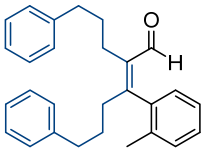

^{1}H NMR (500 MHz, $CDCl_3$) δ 9.23 (s, 1H), 7.33 – 7.25 (m, 4H), 7.25 – 7.15 (m, 7H), 7.11 – 7.07 (m, 2H), 6.98 (dd, *J* = 7.5, 1.4 Hz, 1H), 2.69 – 2.61 (m, 2H), 2.58 – 2.51 (m, 3H), 2.46 – 2.27 (m, 3H), 2.16 (s, 3H), 1.78 – 1.65 (m, 3H), 1.64 – 1.56 (m, 1H). **^{13}C NMR** (126 MHz, $CDCl_3$) δ 194.09, 161.81, 142.34, 141.62, 138.84, 138.38, 135.32, 130.39, 129.22, 128.59, 128.55, 128.50, 128.48, 128.03, 126.17, 125.99, 125.62, 36.30, 36.16, 35.41, 31.37, 29.30, 24.78, 19.92. **HRMS** (ESI, m/z): $[M+Na]^+$ calcd. for $C_{28}H_{30}Na_1O_1$, 405.2189; found 405.2189. The stereochemistry of the

product was determined by 2D-NMR analysis and by analogy to related products and previously reported literature[1,2].

(*Z*)-7-chloro-2-(4-chlorobutyl)-3-(o-tolyl)hept-2-enal (**34**). Light brown oil. 57% yield (46 mg).

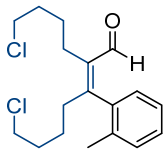

^{1}H NMR (500 MHz, $CDCl_3$) δ 9.26 (s, 1H), 7.32 – 7.22 (m, 2H), 7.22 (dddd, *J* = 7.5, 6.9, 1.9, 0.6 Hz, 1H), 7.04 (dd, *J* = 7.4, 1.3 Hz, 1H), 3.63 (t, *J* = 6.5 Hz, 2H), 3.53 (t, *J* = 6.5 Hz, 2H), 2.70 (ddd, *J* = 13.1, 10.8, 5.9 Hz, 1H), 2.53 – 2.38 (m, 3H), 1.93 – 1.78 (m, 4H), 1.66 – 1.47 (m, 4H). **^{13}C NMR** (126 MHz, $CDCl_3$) δ 194.01, 161.42, 138.63, 138.00, 135.33, 130.49, 129.22, 128.20, 125.72, 44.92, 44.55, 35.05, 32.72, 32.65, 26.69, 24.86, 24.19, 19.93. **HRMS** (ESI, m/z): $[M+H]^+$ calcd. for $C_{18}H_{25}Cl_2O_1$, 327.1277; found 327.1274. The stereochemistry of the product was determined by 2D-NMR analysis and by analogy to related products and previously reported literature[1,2].

(*Z*)-2-(*tert*-butyl)-3-mesitylbut-2-enal (**35**). Colorless oil. 44% yield (27 mg).

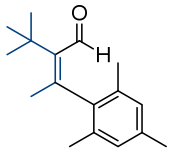

^{1}H NMR (500 MHz, $CDCl_3$) δ 9.27 (s, 1H), 6.84 (dt, *J* = 1.3, 0.7 Hz, 2H), 2.26 (s, 3H), 2.20 (s, 3H), 2.12 (s, 6H), 1.38 (s, 9H). **^{13}C NMR** (126 MHz, $CDCl_3$) δ 196.57, 151.87, 145.62, 139.21, 136.77, 133.87, 128.62, 35.56, 31.00, 23.53, 21.08, 19.52. **HRMS** (ESI, m/z): $[M+Na]^+$ calcd. for $C_{17}H_{24}Na_1O_1$, 267.1719; found 267.1719. The regio- and stereochemistry of the product was determined by 2D-NMR analysis.

(*Z*)-2-isopropyl-3-mesitylbut-2-enal, A (**36-β-Ar, major**). Colorless oil. 69% yield (40 mg).

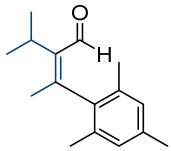

^{1}H NMR (600 MHz, $CDCl_3$) δ 9.22 (d, *J* = 1.7 Hz, 1H), 6.87 (dq, *J* = 1.3, 0.7 Hz, 2H), 3.10 (heptd, *J* = 7.1, 1.7 Hz, 1H), 2.28 (s, 3H), 2.14 (s, 3H), 2.12 (s, 6H), 1.28 (d, *J* = 7.1 Hz, 6H). **^{13}C NMR** (151 MHz, $CDCl_3$) δ 194.31, 157.08, 143.36, 137.40, 136.98, 134.26, 128.47, 27.18, 21.67, 21.09, 20.43, 19.67. **HRMS** (ESI, m/z): $[M+Na]^+$ calcd. for $C_{16}H_{22}Na_1O_1$, 253.1563; found 253.1565. The regio- and stereochemistry of the product was determined by 2D-NMR analysis.

(*Z*)-3-mesityl-2,4-dimethylpent-2-enal, B (**36-α-Ar, minor**). 28% yield (16 mg).

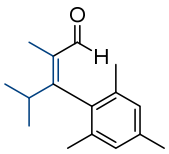

^{1}H NMR (500 MHz, $CDCl_3$) δ 9.19 (s, 1H), 6.87 (dq, *J* = 1.3, 0.7 Hz, 2H), 3.17 – 3.05 (m, 1H), 2.28 (s, 3H), 2.09 (s, 6H), 1.95 (d, *J* = 0.6 Hz, 3H), 1.05 (d, *J* = 7.0 Hz, 6H). **^{13}C NMR** (126 MHz, $CDCl_3$) δ 194.81, 167.05, 136.83, 135.64, 134.73, 134.22, 128.40, 33.46, 21.37, 21.23, 21.06, 10.70. **HRMS** (ESI, m/z): $[M+Na]^+$ calcd. for $C_{16}H_{22}Na_1O_1$, 253.1563; found 253.1560. The regio- and stereochemistry of the product was determined by 2D-NMR analysis and X-ray crystallography.

(*Z*)-2-isopropyl-3-(*o*-tolyl)but-2-enal, A (**37-β-Ar, major**). Colorless oil. 46% yield (23 mg).

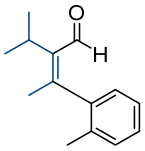

^{1}H NMR (500 MHz, $CDCl_3$) δ 9.25 (d, *J* = 1.7 Hz, 1H), 7.25 – 7.14 (m, 3H), 7.06 – 7.00 (m, 1H), 3.08 (heptd, *J* = 7.1, 1.7 Hz, 1H), 2.19 (s, 3H), 2.19 (s, 3H), 1.29 (d, *J* = 2.7 Hz, 3H), 1.27 (d, *J* = 2.7 Hz, 3H). **^{13}C NMR** (126 MHz, $CDCl_3$) δ 194.27, 157.32, 143.33, 141.01, 134.59, 130.35, 128.19, 127.82, 125.95, 27.33, 22.91, 20.58, 20.45, 19.48. **HRMS** (ESI, m/z): $[M+H]^+$ calcd. for $C_{14}H_{19}O_1$, 203.1430; found 203.1429. The regio- and stereochemistry of the product was determined by 2D-NMR analysis.

(*Z*)-2,4-dimethyl-3-(*o*-tolyl)pent-2-enal, B (**37-α-Ar, minor**). Colorless oil. 31% yield (16 mg).

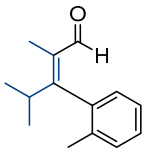

^{1}H NMR (500 MHz, $CDCl_3$) δ 9.20 (s, 1H), 7.26 – 7.20 (m, 2H), 7.20 – 7.15 (m, 1H), 7.00 – 6.97 (m, 1H), 3.23 (hept, *J* = 6.9 Hz, 1H), 2.15 (s, 3H), 1.93 (s, 3H), 1.15 (d, *J* = 7.0 Hz, 3H), 0.87 (d, *J* = 6.8 Hz, 3H). **^{13}C NMR** (126 MHz, $CDCl_3$) δ 194.94, 166.22, 136.32, 136.18, 133.66, 130.18, 129.01, 127.76, 125.25, 32.85, 21.30, 20.77, 19.50, 10.15. **HRMS** (ESI, m/z): $[M+H]^+$ calcd. for $C_{14}H_{19}O_1$, 203.1430; found 203.1430. The regio- and stereochemistry of the product was determined by 2D-NMR analysis.

(*Z*)-2-(1-mesitylethylidene)heptanal, A (**38-β-Ar, major**). Colorless oil. 50% yield (32 mg).

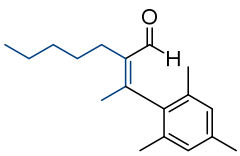

^{1}H NMR (500 MHz, $CDCl_3$) δ 9.23 (s, 1H), 6.90 – 6.86 (m, 2H), 2.44 – 2.37 (m, 2H), 2.29 (s, 3H), 2.13 (s, 3H), 2.11 (s, 6H), 1.49 – 1.40 (m, 2H), 1.40 – 1.33 (m, 4H), 0.94 – 0.89 (m, 3H). **^{13}C NMR** (126 MHz, $CDCl_3$) δ 193.72, 157.89, 139.43, 137.11, 136.68, 134.56, 128.47, 32.23, 28.63, 24.85, 22.70, 21.59, 21.10, 19.81, 14.22. **HRMS** (ESI, m/z): $[M+H]^+$ calcd. for $C_{18}H_{27}O_1$, 259.2056; found 259.2055. The regio- and stereochemistry of the product was determined by 2D-NMR analysis.

(*Z*)-3-mesityl-2-methyloct-2-enal, B (**38-α-Ar, minor**). Colorless oil. 46% yield (30 mg).

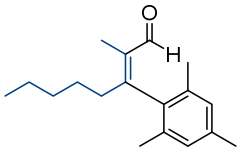

^{1}H NMR (500 MHz, $CDCl_3$) δ 9.23 (s, 1H), 6.88 (dd, *J* = 1.3, 0.7 Hz, 2H), 2.53 – 2.46 (m, 2H), 2.29 (s, 3H), 2.10 (s, 6H), 1.91 (s, 3H), 1.41 – 1.31 (m, 2H), 1.33 – 1.24 (m, 4H), 0.89 – 0.84 (m, 3H). **^{13}C NMR** (126 MHz, $CDCl_3$) δ 194.31, 162.03, 137.09, 135.55, 135.35, 134.34, 128.52, 36.70, 32.62, 26.90, 22.56, 21.10, 20.54, 14.13, 10.17. **HRMS** (ESI, m/z): $[M+H]^+$ calcd. for $C_{18}H_{27}O_1$, 259.2056; found 259.2054. The regio- and stereochemistry of the product was determined by 2D-NMR analysis.

(*Z*)-2-(1-(*o*-tolyl)ethylidene)heptanal, A (**39-β-Ar, major**). Colorless oil. 45% yield (26 mg).

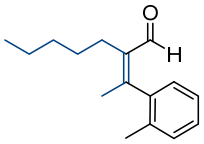

^{1}H NMR (500 MHz, $CDCl_3$) δ 9.27 (s, 1H), 7.25 – 7.17 (m, 3H), 7.03 (dd, *J* = 7.3, 1.4 Hz, 1H), 2.39 (dddd, *J* = 20.0, 13.0, 8.4, 6.6 Hz, 2H), 2.20 (s, 3H), 2.19 (s, 3H), 1.48 – 1.40 (m, 2H), 1.40 – 1.33 (m, 4H), 0.94 – 0.89 (m, 3H). **^{13}C NMR** (126 MHz, $CDCl_3$) δ 193.69, 158.06, 140.28, 139.32, 134.77, 130.35, 128.46, 127.94, 125.91, 32.15, 28.70, 25.00, 22.85, 22.71, 19.61, 14.22. **HRMS** (ESI, m/z): $[M+Na]^+$ calcd. for $C_{16}H_{22}Na_1O_1$, 253.1563; found 253.1562. The regio- and stereochemistry of the product was determined by 2D-NMR analysis.

(*Z*)-2-methyl-3-(*o*-tolyl)oct-2-enal, B (**39-α-Ar, minor**). Colorless oil. 37% yield (21 mg).

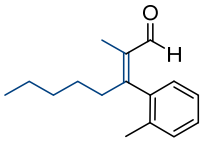

^{1}H NMR (500 MHz, $CDCl_3$) δ 9.26 (s, 1H), 7.28 – 7.18 (m, 2H), 7.18 (dddd, *J* = 7.4, 6.8, 2.0, 0.6 Hz, 1H), 7.01 (dd, *J* = 7.4, 1.4 Hz, 1H), 2.64 (ddd, *J* = 13.0, 10.2, 5.8 Hz, 1H), 2.38 (dddd, *J* = 13.0, 10.2, 5.6, 0.7 Hz, 1H), 2.18 (s, 3H), 1.91 (s, 3H), 1.46 – 1.33 (m, 2H), 1.33 – 1.25 (m, 4H), 0.89 – 0.83 (m, 3H). **^{13}C NMR** (126 MHz, $CDCl_3$) δ 194.34, 162.30, 138.89, 135.43, 134.19, 130.33, 129.28, 127.92, 125.53, 36.44, 32.21, 26.77, 22.59, 19.95, 14.09, 10.36. **HRMS** (ESI,

m/z): $[M+Na]^+$ calcd. for $C_{16}H_{22}Na_1O_1$, 253.1563; found 253.1562. The regio- and stereochemistry of the product was determined by 2D-NMR analysis.

(*Z*)-2-((1,3-dioxoisoindolin-2-yl)methyl)-3-(o-tolyl)but-2-enal, B (**40-β-Ar, major**). Colorless oil. 43% yield (34 mg).

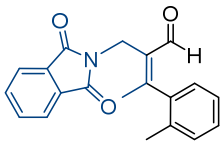

^{1}H NMR (500 MHz, $CDCl_3$) δ 9.26 (s, 1H), 7.84 (dd, *J* = 5.4, 3.0 Hz, 2H), 7.70 (dd, *J* = 5.5, 3.0 Hz, 2H), 7.27 – 7.15 (m, 3H), 7.05 (dd, *J* = 7.4, 1.4 Hz, 1H), 4.73 (d, *J* = 14.5 Hz, 1H), 4.64 (d, *J* = 14.4 Hz, 1H), 2.38 (s, 3H), 2.21 (s, 3H). **^{13}C NMR** (126 MHz, $CDCl_3$) δ 191.97, 167.97, 162.72, 139.49, 134.59, 134.07, 132.60, 132.17, 130.52, 128.36, 128.13, 125.97, 123.42, 33.18, 23.36, 19.59. **HRMS** (ESI, m/z): $[M+H]^+$ calcd. for $C_{20}H_{18}N_1O_3$, 320.1281; found 320.1283. The regio- and stereochemistry of the product was determined by 2D-NMR analysis.

(*E*)-4-(1,3-dioxoisoindolin-2-yl)-2-methyl-3-(*o*-tolyl)but-2-enal, A (**40-α-Ar, minor**). Colorless oil. 27% yield (22 mg).

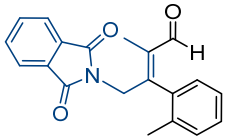

^{1}H NMR (500 MHz, CDCl3) δ 9.29 (s, 1H), 7.74 – 7.69 (m, 2H), 7.67 – 7.63 (m, 2H), 7.12 – 7.05 (m, 2H), 6.97 – 6.89 (m, 2H), 4.87 – 4.78 (m, 2H), 2.22 (s, 3H), 2.12 (t, *J* = 0.9 Hz, 3H). **^{13}C NMR** (126 MHz, $CDCl_3$) δ 193.53, 167.69, 154.11, 136.44, 135.77, 134.27, 134.17, 131.70, 130.27, 129.54, 128.60, 125.43, 123.39, 40.28, 19.71, 10.44. **HRMS** (ESI, m/z): $[M+Na]^+$ calcd. for $C_{20}H_{17}N_1Na_1O_3$, 342.1101; found 342.1102. The regio- and stereochemistry of the product was determined by 2D-NMR analysis.

(*Z*)-2-formyl-3-(*o*-tolyl)hept-2-en-1-yl benzoate, B (**41-β-Ar, major**). Colorless oil. 34% yield (29 mg).

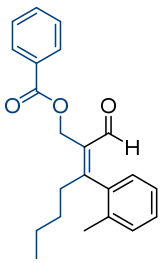

^{1}H NMR (500 MHz, $CDCl_3$) δ 9.30 (s, 1H), 8.07 – 8.00 (m, 2H), 7.60 – 7.52 (m, 1H), 7.48 – 7.40 (m, 2H), 7.33 – 7.20 (m, 3H), 7.08 (dd, *J* = 7.5, 1.4 Hz, 1H), 5.22 (d, *J* = 1.6 Hz, 2H), 2.79 (ddd, *J* = 13.0, 10.6, 5.3 Hz, 1H), 2.62 – 2.53 (m, 1H), 2.23 (s, 3H), 1.47 – 1.26 (m, 4H), 0.81 (t, *J* = 7.1

Hz, 3H). **^{13}C NMR** (126 MHz, $CDCl_3$) δ 192.43, 168.39, 166.55, 137.50, 135.09, 133.17, 133.13, 130.57, 130.22, 129.78, 128.65, 128.50, 128.50, 125.74, 57.00, 36.42, 30.01, 23.18, 19.81, 13.88. **HRMS** (ESI, m/z): $[M+Na]^+$ calcd. for $C_{22}H_{24}Na_1O_3$, 359.1618; found 359.1613. The regio- and stereochemistry of the product was determined by 2D-NMR analysis.

(*E*)-3-formyl-2-(*o*-tolyl)hept-2-en-1-yl benzoate, A (**41-α-Ar, minor**). Colorless oil. 27% yield (22 mg).

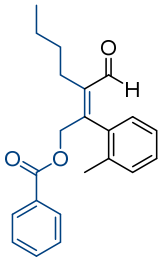

^{1}H NMR (500 MHz, $CDCl_3$) δ 9.36 (s, 1H), 7.80 – 7.75 (m, 2H), 7.52 (ddt, *J* = 8.8, 7.2, 1.3 Hz, 1H), 7.40 – 7.34 (m, 2H), 7.25 – 7.20 (m, 2H), 7.17 (td, *J* = 7.1, 6.6, 2.2 Hz, 1H), 7.12 (dd, *J* = 7.3, 1.4 Hz, 1H), 5.33 (d, *J* = 13.8 Hz, 1H), 5.27 (d, *J* = 13.8 Hz, 1H), 2.59 – 2.45 (m, 2H), 2.26 (s, 3H), 1.51 – 1.39 (m, 4H), 0.94 (t, *J* = 7.1 Hz, 3H). **^{13}C NMR** (126 MHz, $CDCl_3$) δ 193.66, 166.17, 153.38, 141.24, 136.10, 135.40, 133.29, 130.23, 129.76, 129.65, 129.60, 128.57, 128.49, 125.81, 64.26, 31.77, 25.10, 23.09, 20.05, 14.06. **HRMS** (ESI, m/z): $[M+Na]^+$ calcd. for $C_{22}H_{24}Na_1O_3$, 359.1618; found 359.1618. The regio- and stereochemistry of the product was determined by 2D-NMR analysis.

(*Z*)-3-formyl-4-mesityloct-3-en-1-yl benzoate, B (**42-β-Ar, major**). Pale yellow oil. 72% yield (68 mg).

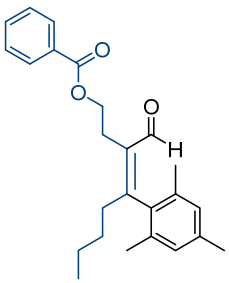

^{1}H NMR (600 MHz, $CDCl_3$) δ 9.24 (s, 1H), 8.07 – 8.02 (m, 2H), 7.59 – 7.53 (m, 1H), 7.47 – 7.40 (m, 2H), 6.86 (q, *J* = 0.8 Hz, 2H), 4.45 (t, *J* = 6.8 Hz, 2H), 2.94 (t, *J* = 6.8 Hz, 2H), 2.63 – 2.55 (m, 2H), 2.28 (s, 3H), 2.07 (s, 6H), 1.34 – 1.25 (m, 4H), 0.83 (t, *J* = 7.0 Hz, 3H). **^{13}C NMR** (151 MHz, $CDCl_3$) δ 193.86, 166.73, 164.61, 137.31, 135.11, 134.78, 134.57, 133.08, 130.39, 129.74, 128.60, 128.47, 63.65, 35.99, 29.69, 24.77, 23.50, 21.09, 20.47, 13.89. **HRMS** (ESI, m/z): $[M+Na]^+$ calcd. for $C_{25}H_{30}Na_1O_3$, 401.2087; found 401.2086. The regio- and stereochemistry of the product was determined by 2D-NMR analysis.

(*Z*)-4-formyl-3-mesityloct-3-en-1-yl benzoate, A (**42-α-Ar, minor**). Colorless oil. 26% yield (25 mg).

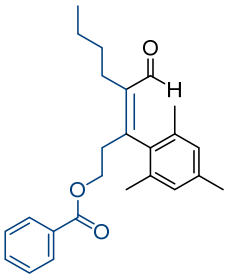

^{1}H NMR (500 MHz, $CDCl_3$) δ 9.27 (s, 1H), 7.97 – 7.92 (m, 2H), 7.58 – 7.53 (m, 1H), 7.46 – 7.40 (m, 2H), 6.89 – 6.88 (m, 2H), 4.28 (t, *J* = 6.8 Hz, 2H), 3.04 (t, *J* = 6.8 Hz, 2H), 2.49 (dd, *J* = 8.5, 6.6 Hz, 2H), 2.28 (s, 3H), 2.14 (s, 6H), 1.50 – 1.37 (m, 4H), 0.92 (t, *J* = 7.1 Hz, 3H). **^{13}C NMR** (126 MHz, $CDCl_3$) δ 193.94, 166.51, 156.22, 141.33, 137.61, 135.46, 133.69, 133.23, 130.00, 129.67, 128.83, 128.53, 62.26, 34.27, 31.58, 25.01, 23.22, 21.08, 20.30, 14.08. **HRMS** (ESI, m/z): $[M+Na]^+$ calcd. for $C_{25}H_{30}Na_1O_3$, 401.2087; found 401.2085. The regio- and stereochemistry of the product was determined by 2D-NMR analysis.

(*Z*)-3-formyl-4-(*o*-tolyl)oct-3-en-1-yl benzoate, B (**43-β-Ar, major**). Pale yellow oil. 56% yield (49 mg).

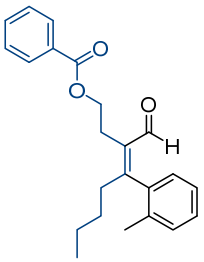

^{1}H NMR (400 MHz, $CDCl_3$) δ 9.26 (s, 1H), 8.09 – 8.01 (m, 2H), 7.61 – 7.52 (m, 1H), 7.49 – 7.40 (m, 2H), 7.29 – 7.14 (m, 3H), 7.02 – 6.95 (m, 1H), 4.50 – 4.37 (m, 2H), 3.01 – 2.83 (m, 2H), 2.79 – 2.65 (m, 1H), 2.52 – 2.40 (m, 1H), 2.14 (s, 3H), 1.40 – 1.20 (m, 4H), 0.82 (t, *J* = 7.0 Hz, 3H). **^{13}C NMR** (151 MHz, $CDCl_3$) δ 193.82, 166.72, 164.78, 138.19, 135.24, 134.29, 133.10, 130.40, 130.39, 129.74, 129.05, 128.50, 128.13, 125.62, 63.61, 35.99, 29.69, 24.86, 23.20, 19.86, 13.93. **HRMS** (ESI, m/z): $[M+Na]^+$ calcd. for $C_{23}H_{26}Na_1O_3$, 373.1774; found 373.1777. The regio- and stereochemistry of the product was determined by 2D-NMR analysis.

(*Z*)-4-formyl-3-(*o*-tolyl)oct-3-en-1-yl benzoate, A (**43-α-Ar, minor**)**.** Colorless oil. 20% yield (18 mg).

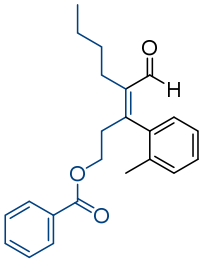

^{1}H NMR (500 MHz, $CDCl_3$) δ 9.29 (s, 1H), 7.98 – 7.92 (m, 2H), 7.56 (ddt, *J* = 8.8, 7.1, 1.3 Hz, 1H), 7.46 – 7.39 (m, 2H), 7.30 – 7.16 (m, 3H), 7.07 (dd, *J* = 7.5, 1.4 Hz, 1H), 4.31 (dd, *J* = 6.9, 6.2 Hz, 2H), 3.16 (dt, *J* = 14.0, 6.9 Hz, 1H), 2.94 (dt, *J* = 14.1, 6.2 Hz, 1H), 2.55 – 2.40 (m, 2H), 2.21 (s, 3H), 1.51 – 1.34 (m, 4H), 0.91 (t, *J* = 7.1 Hz, 3H). **^{13}C NMR** (126 MHz, $CDCl_3$) δ 193.91, 166.49, 156.53, 141.24, 137.22, 135.62, 133.26, 130.60, 129.98, 129.67, 129.36, 128.56, 128.39, 125.96, 62.08, 34.60, 31.79, 25.04, 23.15, 19.79, 14.08. **HRMS** (ESI, m/z): $[M+Na]^+$ calcd. for $C_{23}H_{26}Na_1O_3$, 373.1774; found 373.1773. The regio- and stereochemistry of the product was determined by 2D-NMR analysis.

(*Z*)-3-formyl-4-(*o*-tolyl)oct-3-en-1-yl butyrate, B (**44-β-Ar, major**). Colorless oil. 59% yield (47 mg).

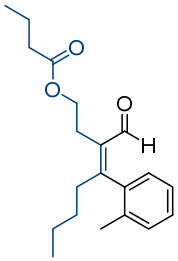

^{1}H NMR (500 MHz, $CDCl_3$) δ 9.22 (s, 1H), 7.27 – 7.16 (m, 3H), 7.03 – 6.97 (m, 1H), 4.23 – 4.10 (m, 2H), 2.85 – 2.71 (m, 2H), 2.74 – 2.64 (m, 1H), 2.50 – 2.41 (m, 1H), 2.29 (dd, *J* = 7.7, 7.2 Hz, 2H), 2.18 (s, 3H), 1.67 (h, *J* = 7.4 Hz, 2H), 1.44 – 1.27 (m, 4H), 0.96 (t, *J* = 7.4 Hz, 3H), 0.87 (t, *J* = 7.0 Hz, 3H). **^{13}C NMR** (126 MHz, $CDCl_3$) δ 193.75, 173.76, 164.69, 138.25, 135.19, 134.32, 130.41, 129.05, 128.13, 125.63, 62.91, 36.37, 35.97, 29.72, 24.71, 23.23, 19.84, 18.53, 13.99, 13.87. **HRMS** (ESI, m/z): $[M+Na]^+$ calcd. for $C_{20}H_{28}Na_1O_3$, 339.1931; found 339.1929. The regio- and stereochemistry of the product was determined by 2D-NMR analysis.

(*Z*)-4-formyl-3-(*o*-tolyl)oct-3-en-1-yl butyrate, A (**44-α-Ar, minor**). Colorless oil. 24% yield (19 mg).

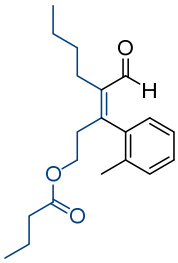

^{1}H NMR (500 MHz, $CDCl_3$) δ 9.26 (s, 1H), 7.27 – 7.16 (m, 3H), 7.04 – 7.00 (m, 1H), 4.12 – 4.00 (m, 2H), 3.01 (ddd, *J* = 14.1, 7.4, 6.7 Hz, 1H), 2.78 (dt, *J* = 14.1, 6.4 Hz, 1H), 2.51 – 2.33 (m, 2H), 2.26 – 2.19 (m, 2H), 2.19 (s, 3H), 1.62 (dt, *J* = 14.9, 7.5 Hz, 2H), 1.47 – 1.36 (m, 4H), 0.97 – 0.90 (m, 6H). **^{13}C NMR** (126 MHz, $CDCl_3$) δ 193.90, 173.55, 156.51, 141.16, 137.26, 135.59, 130.55, 129.30, 128.35, 125.88, 61.31, 36.21, 34.52, 31.71, 24.97, 23.15, 19.75, 18.45, 14.13, 13.81. **HRMS** (ESI, m/z): $[M+Na]^+$ calcd. for $C_{20}H_{28}Na_1O_3$, 339.1931; found 339.1927. The regio- and stereochemistry of the product was determined by 2D-NMR analysis.

(*Z*)-3-formyl-4-(*o*-tolyl)oct-3-en-1-yl diethylcarbamate, A (**45-β-Ar, major**)**.** Colorless oil. 60% yield (52 mg as an inseparable mixture of regioisomers, **β-Ar**/α-Ar = 62:38, BISBI). 75% yield (65 mg as an inseparable mixture of regioisomers, **β-Ar**/α-Ar = 66:34, TDMPP).

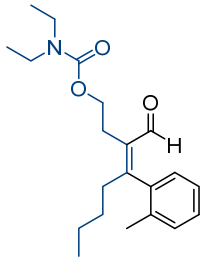

^{1}H NMR (600 MHz, $CDCl_3$) δ 9.23 (s, 1H), 7.26 – 7.20 (m, 3H), 7.00 (dd, *J* = 7.6, 1.4 Hz, 1H), 4.19 – 4.13 (m, 2H), 3.33 – 3.23 (br, 4H), 2.82 (dt, *J* = 13.7, 7.0 Hz, 1H), 2.79 – 2.73 (m, 1H), 2.69 (ddt, *J* = 9.8, 7.7, 5.0 Hz, 1H), 2.50 – 2.43 (m, 1H), 2.18 (s, 3H), 1.45 – 1.24 (m, 4H), 1.12 (br, 6H), 0.86 (t, *J* = 7.0 Hz, 3H). **^{13}C NMR** (151 MHz, $CDCl_3$) δ 193.79, 164.35, 156.05, 138.33, 135.27, 134.63, 130.36, 129.09, 128.07, 125.59, 63.68, 41.77, 41.23, 35.93, 29.69, 25.14, 23.21, 19.87, 13.98, 14.17, 13.63. **HRMS** (ESI, m/z): $[M+H]^+$ calcd. for $C_{21}H_{32}N_1O_3$, 346.2377; found 346.2378. The regio- and stereochemistry of the product was determined by 2D-NMR analysis.

(*Z*)-4-formyl-3-(o-tolyl)oct-3-en-1-yl diethylcarbamate, B (**45-α-Ar, minor**).

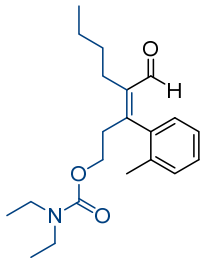

^{1}H NMR (600 MHz, $CDCl_3$) δ 9.26 (s, 1H), 7.18 (td, *J* = 7.3, 1.7 Hz, 3H), 7.03 (dd, *J* = 7.6, 1.3 Hz, 1H), 4.11 – 4.02 (m, 2H), 3.33 – 3.14 (br, 4H), 3.03 (ddd, *J* = 13.9, 7.7, 6.2 Hz, 1H), 2.79 – 2.74 (m, 1H), 2.49 – 2.43 (m, 1H), 2.42 – 2.37 (m, 1H), 2.19 (s, 3H), 1.43 – 1.28 (m, 4H), 1.06 (br, 6H), 0.95 (t, *J* = 7.1 Hz, 3H). **^{13}C NMR** (151 MHz, $CDCl_3$) δ 193.96, 157.21, 155.68, 141.07, 137.41, 135.55, 130.51, 129.33, 128.27, 125.85, 62.07, 41.89, 35.16, 31.71, 24.88, 23.13, 19.71, 14.17, 14.17, 14.10, 13.58. The regio- and stereochemistry of the product was determined by 2D-NMR analysis. Where assignments of C or H atoms within the isomers are ambiguous, no peak assignment is given.

(*Z*)-2-(2-((4-methoxybenzyl)oxy)ethyl)-3-(*o*-tolyl)hept-2-enal, B (**46-β-Ar, major**). Colorless oil. 41% yield (37 mg).

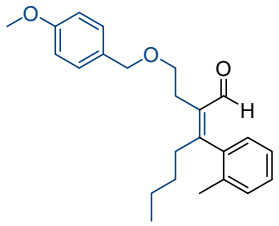

^{1}H NMR (500 MHz, $CDCl_3$) δ 9.22 (s, 1H), 7.29 – 7.25 (m, 2H), 7.24 – 7.15 (m, 3H), 7.01 – 6.98 (m, 1H), 6.90 – 6.86 (m, 2H), 4.46 (s, 2H), 3.81 (s, 3H), 3.57 – 3.49 (m, 2H), 2.83 – 2.65 (m, 3H), 2.46 – 2.39 (m, 1H), 2.16 (s, 3H), 1.38 – 1.22 (m, 4H), 0.84 (t, *J* = 7.0 Hz, 3H). **^{13}C NMR** (126 MHz, $CDCl_3$) δ 194.14, 164.30, 159.25, 138.59, 135.36, 135.13, 130.77, 130.30, 129.34, 129.06, 127.94, 125.51, 113.87, 72.73, 68.89, 55.41, 36.09, 29.69, 25.83, 23.24, 19.87, 14.00. **HRMS** (ESI, m/z): $[M+Na]^+$ calcd. for $C_{24}H_{30}Na_1O_3$, 389.2087; found 389.2093. The regio- and stereochemistry of the product was determined by 2D-NMR analysis.

(*Z*)-2-(3-((4-methoxybenzyl)oxy)-1-(o-tolyl)propylidene)hexanal, A (**46-α-Ar, minor**). Colorless oil. 27% yield (25 mg).

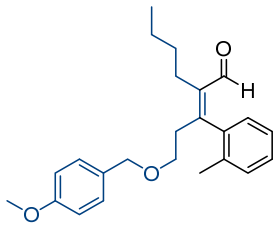

^{1}H NMR (500 MHz, $CDCl_3$) δ 9.24 (s, 1H), 7.27 – 7.12 (m, 5H), 6.98 (dd, *J* = 7.5, 1.3 Hz, 1H), 6.89 – 6.82 (m, 2H), 4.37 – 4.30 (m, 2H), 3.80 (s, 3H), 3.42 (td, *J* = 6.7, 1.0 Hz, 2H), 2.98 (dt, *J* = 14.0, 7.1 Hz, 1H), 2.75 (dt, *J* = 13.4, 6.5 Hz, 1H), 2.51 – 2.34 (m, 2H), 2.17 (s, 3H), 1.46 – 1.33 (m, 4H), 0.92 (t, *J* = 7.2 Hz, 3H). **^{13}C NMR** (126 MHz, $CDCl_3$) δ 194.09, 159.34, 157.98, 140.72, 137.88, 135.65, 130.34, 130.28, 129.34, 129.30, 128.05, 125.62, 113.90, 72.81, 67.10, 55.42, 35.90, 31.71, 25.01, 23.18, 19.77, 14.16. **HRMS** (ESI, m/z): $[M+Na]^+$ calcd. for $C_{24}H_{30}Na_1O_3$, 389.2087; found 389.2089. The regio- and stereochemistry of the product was determined by 2D-NMR analysis.

(*Z*)-9-formyl-10-(*o*-tolyl)dodec-9-en-1-yl benzoate (**47-β-Ar, major**). Colorless oil. 55% yield (56 mg as an inseparable mixture of regioisomers, **β-Ar**/α-Ar = 53:47)

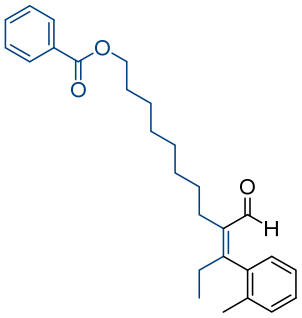

^{1}H NMR (400 MHz, $CDCl_3$) δ 9.24 (s, 1H, β-Ar), 8.06–8.03 (m, 2H), 7.56–7.53 (m, 1H), 7.45–7.41 (m, 2H), 7.24–7.16 (m, 3H), 7.01–7.00 (m, 1H), 4.32 (t, J = 6.68 Hz, 2H), 2.69–2.60 (m, 1H), 2.49–2.33 (m, 3H), 2.18 (s, 3H), 1.80–1.71 (m, 2H), 1.47–1.23 (m, 10H), 0.98 (t, J = 7.57 Hz, 3H). **^{13}C NMR** (151 MHz, $CDCl_3$) δ 194.27, 166.76, 162.98, 138.55, 138.22, 135.40, 132.87, 130.63, 130.20, 129.62, 129.21, 128.40, 127.83, 125.48, 65.19, 28.82, 28.76, 26.13, 24.88, 19.85, 11.96. **HRMS** (ESI, *m/z)*: $[M+Na]^+$ calcd. for $C_{27}H_{34}Na_1O_3$, 429.2400; found 429.2398. The regio- and stereochemistry of the product was determined by 2D-NMR analysis. Where assignments of C or H atoms within the isomers are ambiguous, no peak assignment is given.

Unassigned ^{13}C NMR shifts: 30.02, 29.93, 29.59, 29.48, 29.35, 29.34, 29.22 (four shifts from major and three from minor isomer).

(*Z*)-10-formyl-9-(*o*-tolyl)dodec-9-en-1-yl benzoate (**47-α-Ar, minor**).

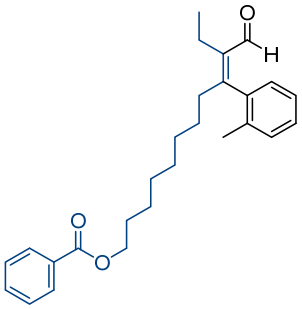

^{1}H NMR (400 MHz, $CDCl_3$) δ 9.22 (s, 1H, α-Ar), 8.06–8.03 (m, 2H), 7.56–7.53 (m, 1H), 7.45–7.41 (m, 2H), 7.24–7.16 (m, 3Hl), 7.01–7.00 (m, 1H), 4.30 (t, J = 6.67 Hz, 2H), 2.69–2.60 (m, 1H), 2.49–2.33 (m, 3H), 2.18 (s, 3H), 1.80–1.71 (m, 2H), 1.47–1.23 (m, 10H), 1.07 (t, J = 7.50 Hz, 3H). **^{13}C NMR** (151 MHz, $CDCl_3$) δ 194.05, 166.72, 161.54, 140.16, 138.53, 135.35, 132.90, 130.59, 130.26, 129.60, 129.15, 128.40, 127.84, 125.48, 65.09, 35.77, 28.75, 27.58, 26.05, 19.77, 18.27, 14.02. The regio- and stereochemistry of the product was determined by 2D-NMR analysis. Where assignments of C or H atoms within the isomers are ambiguous, no peak assignment is given.

Unassigned ^{13}C NMR shifts: 30.02, 29.93, 29.59, 29.48, 29.35, 29.34, 29.22 (four shifts from major and three from minor isomer).

(*Z*)-5-formyl-6-(*o*-tolyl)dec-5-en-1-yl benzoate (**48-β-Ar, major**). Colorless oil. 38% yield (36 mg).

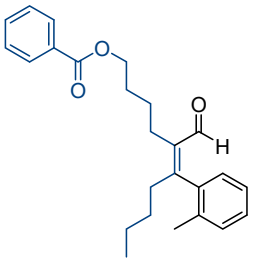

^{1}H NMR (400 MHz, $CDCl_3$) δ 9.24 (s, 1H), 8.06–8.05 (m, 2H), 7.56–7.54 (m, 1H), 7.45–7.42 (m, 2H), 7.25–7.16 (m, 3H), 7.01–7.00 (m, 1H), 4.38 (t, *J* = 6.53 Hz, 2H), 2.65–2.60 (m, 1H), 2.54–2.50 (m, 1H), 2.47–2.39 (m, 2H), 2.18 (s, 3H), 1.90–1.86 (m, 2H), 1.64–1.58 (m, 2H), 1.38–1.26 (m, 4H), 0.84 (t, *J* = 7.08 Hz). **^{13}C NMR** (151 MHz, $CDCl_3$) δ 194.15, 166.75, 162.47, 138.42, 138.33, 135.30, 132.95, 130.55, 130.30, 129.66, 129.16, 128.44, 127.93, 125.53, 64.86, 35.75, 29.72, 29.05, 26.03, 24.61, 23.20, 19.87, 13.94. **HRMS** (ESI, *m/z)*: $[M+Na]^+$ calcd. for $C_{25}H_{30}Na_1O_3$, 401.2087; found 401.2088. The regio- and stereochemistry of the product was determined by 2D-NMR analysis.

(*Z*)-6-formyl-5-(*o*-tolyl)dec-5-en-1-yl benzoate (**48-α-Ar, minor**). Colorless oil. 34% yield (32 mg).

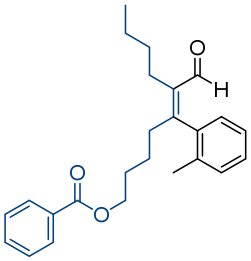

^{1}H NMR (400 MHz, $CDCl_3$) δ 9.24 (s, 1H), 7.98–7.96 (m, 2H), 7.57–7.54 (m, 1H), 7.44–7.41 (m, 2H), 7.24–7.20 (m, 2H), 7.17–7.14 (m, 1H), 7.02–7.00 (m, 1H) 4.29 (td, *J* = 6.54, 1.67 Hz, 2H), 2.75–2.70 (m, 1H), 2.52–2.42 (m, 2H), 2.37–2.33 (m, 1H), 2.19 (s, 3H), 1.85–1.75 (m, 2H), 1.60–1.47 (m, 2H), 1.44–1.35 (m, 4H), 0.93 (t, *J* = 7.12 Hz, 3H). **^{13}C NMR** (151 MHz, $CDCl_3$) δ 194.18, 166.64, 160.87, 139.31, 138.23, 135.36, 133.04, 130.39, 130.37, 129.62, 129.27, 128.46, 128.00, 125.59, 64.41, 35.22, 31.79, 29.01, 24.88, 24.02, 23.12, 19.86, 14.11. **HRMS** (ESI, *m/z)*: $[M+Na]^+$ calcd. for $C_{25}H_{30}Na_1O_3$, 401.2087; found 401.2088. The regio- and stereochemistry of the product was determined by 2D-NMR analysis.

Methyl (*E*)-2-formyl-3-mesityloct-2-enoate (**49**). Colorless oil. 39% yield (30 mg).

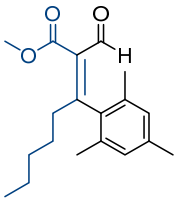

^{1}H NMR (500 MHz, $CDCl_3$) δ 9.10 (s, 1H), 6.90 (h, *J* = 0.6 Hz, 2H), 3.89 (s, 3H), 2.54 – 2.49 (m, 2H), 2.30 (s, 3H), 2.18 (s, 6H), 1.46 – 1.39 (m, 2H), 1.29 – 1.22 (m, 4H), 0.86 – 0.82 (m, 3H). **^{13}C NMR** (126 MHz, $CDCl_3$) δ 189.68, 166.66, 166.57, 138.18, 135.27, 134.96, 132.69, 128.85, 52.40, 37.86, 32.39, 27.28, 22.38, 21.12, 20.29, 14.02. **HRMS** (ESI, m/z): $[M+Na]^+$ calcd. for $C_{19}H_{26}Na_1O_3$, 325.1774; found 325.1773. The regio- and stereochemistry of the product was determined by 2D-NMR analysis and by analogy to previously reported literature[3].

(*Z*)-3-mesityl-2-methyl-3-phenylacrylaldehyde, A (**50-α-Ar**). Colorless oil. 39% yield (26 mg).

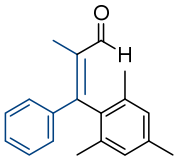

^{1}H NMR (600 MHz, $CDCl_3$) δ 9.40 (s, 1H), 7.37 – 7.28 (m, 3H), 7.27 – 7.22 (m, 2H), 6.90 (q, *J* = 0.8 Hz, 2H), 2.31 (s, 3H), 2.09 (s, 3H), 2.08 (s, 6H). **^{13}C NMR** (151 MHz, $CDCl_3$) δ 194.75, 157.75, 138.90, 137.89, 136.43, 135.38, 135.30, 129.66, 128.83, 128.71, 128.23, 21.18, 20.58, 13.10. **HRMS** (ESI, m/z): $[M+Na]^+$ calcd. for $C_{19}H_{20}Na_1O_1$, 287.1406; found 287.1404. The regio- and stereochemistry of the product was determined by 2D-NMR analysis.

(*Z*)-3-mesityl-2-phenylbut-2-enal, B (**50-β-Ar**). Colorless oil. 39% yield (26 mg).

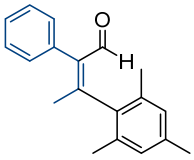

^{1}H NMR (600 MHz, $CDCl_3$) δ 9.46 (s, 1H), 7.48 – 7.41 (m, 2H), 7.40 – 7.34 (m, 1H), 7.24 – 7.19 (m, 2H), 6.95 (dq, *J* = 1.4, 0.7 Hz, 2H), 2.33 (s, 3H), 2.27 (s, 6H), 2.06 (s, 3H). **^{13}C NMR** (151 MHz, $CDCl_3$) δ 192.56, 160.20, 140.80, 137.54, 135.79, 134.68, 134.45, 129.95, 128.67, 128.45, 127.82, 23.30, 21.14, 19.73. **HRMS** (ESI, m/z): $[M+H]^+$ calcd. for $C_{19}H_{21}O_1$, 265.1587; found 265.1594. The regio- and stereochemistry of the product was determined by 2D-NMR analysis.

(*Z*)-2-(mesityl(phenyl)methylene)pentanal, A (**51-α-Ar, major**). Colorless oil. 45% yield (33 mg).

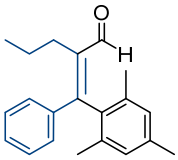

^{1}H NMR (500 MHz, $CDCl_3$) δ 9.36 (s, 1H), 7.36 – 7.30 (m, 3H), 7.25 – 7.22 (m, 2H), 6.89 (h, *J* = 0.6 Hz, 2H), 2.53 – 2.48 (m, 2H), 2.29 (s, 3H), 2.10 (s, 6H), 1.59 – 1.48 (m, 2H), 0.93 (t, *J* = 7.3 Hz, 3H). **^{13}C NMR** (126 MHz, $CDCl_3$) δ 194.78, 157.67, 140.30, 139.04, 137.82, 136.21, 135.59, 129.12, 128.77, 128.67, 128.29, 28.90, 22.92, 21.18, 20.63, 14.67. **HRMS** (ESI, m/z): $[M+Na]^+$

calcd. for $C_{21}H_{24}Na_1O_1$, 315.1719; found 315.1723. The regio- and stereochemistry of the product was determined by 2D-NMR analysis.

(*Z*)-3-mesityl-2-phenylhex-2-enal, B (**51-β-Ar, minor**). Colorless oil. 27% yield (19 mg).

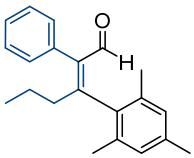

^{1}H NMR (500 MHz, $CDCl_3$) δ 9.42 (s, 1H), 7.46 – 7.41 (m, 2H), 7.39 – 7.34 (m, 1H), 7.21 – 7.18 (m, 2H), 6.94 (dd, *J* = 1.3, 0.7 Hz, 2H), 2.38 – 2.34 (m, 2H), 2.32 (s, 3H), 2.26 (s, 6H), 1.37 – 1.28 (m, 2H), 0.75 (t, *J* = 7.3 Hz, 3H). **^{13}C NMR** (126 MHz, $CDCl_3$) δ 193.23, 163.77, 140.81, 137.46, 135.27, 135.05, 134.32, 129.77, 128.74, 128.47, 127.76, 39.31, 21.25, 21.14, 20.48, 14.84. **HRMS** (ESI, m/z): $[M+Na]^+$ calcd. for $C_{21}H_{24}Na_1O_1$, 315.1719; found 315.1717. The regio- and stereochemistry of the product was determined by 2D-NMR analysis.

(*Z*)-2-(mesityl(phenyl)methylene)pent-4-enal (**52**). Pale yellow oil. 42% yield (31 mg).

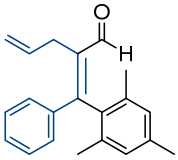

^{1}H NMR (500 MHz, $CDCl_3$) δ 9.39 (s, 1H), 7.35 – 7.29 (m, 5H), 6.91 (q, *J* = 0.7 Hz, 2H), 6.02 (ddt, *J* = 17.3, 10.2, 5.6 Hz, 1H), 5.12 (dq, *J* = 10.2, 1.7 Hz, 1H), 5.06 (dq, *J* = 17.3, 1.8 Hz, 1H), 3.30 (dt, *J* = 5.6, 1.8 Hz, 2H), 2.31 (s, 3H), 2.10 (s, 6H). **^{13}C NMR** (126 MHz, $CDCl_3$) δ 194.00, 159.01, 138.59, 138.03, 137.11, 136.50, 136.28, 135.28, 129.16, 129.12, 128.78, 128.28, 115.83, 31.28, 21.19, 20.59. **HRMS** (ESI, m/z): $[M+H]^+$ calcd. for $C_{21}H_{23}O_1$, 291.1743; found 291.1742. The regio- and stereochemistry of the product was determined by 2D-NMR analysis.

(*Z*)-*N*-(2-formyl-3-mesityl-3-phenylallyl)pivalamide (**53**). 24% yield (22 mg).

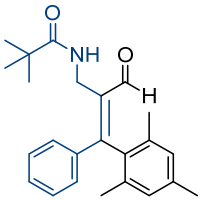

^{1}H NMR (500 MHz, $CDCl_3$) δ 9.31 (s, 1H), 7.38 – 7.34 (m, 3H), 7.27 – 7.24 (m, 2H), 6.90 (h, *J* = 0.7 Hz, 2H), 6.55 (s, 1H), 4.40 (d, *J* = 6.1 Hz, 2H), 2.30 (s, 3H), 2.06 (s, 6H), 1.13 (s, 9H). **^{13}C NMR** (126 MHz, $CDCl_3$) δ 195.52, 177.85, 161.46, 138.38, 137.80, 136.25, 135.49, 134.86, 129.75, 129.64, 128.87, 128.59, 38.87, 37.20, 27.62, 21.21, 20.51. **HRMS** (ESI, m/z): $[M+Na]^+$ calcd. for $C_{24}H_{29}N_1Na_1O_2$, 386.2090; found 386.2090. The regio- and stereochemistry of the product was determined by 2D-NMR analysis and X-ray crystallography.

(*E*)-3-mesityl-2-(trimethylsilyl)hex-2-enal (**54**). Colorless oil. 78% yield (56 mg).

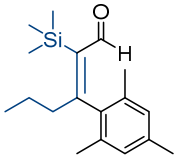

^{1}H NMR (500 MHz, $CDCl_3$) δ 9.32 (s, 1H), 6.86 (dq, *J* = 1.3, 0.6 Hz, 2H), 2.56 – 2.48 (m, 2H), 2.28 (s, 3H), 2.12 (s, 6H), 1.43 – 1.34 (m, 2H), 0.91 (t, *J* = 7.3 Hz, 3H), 0.31 (s, 9H). **^{13}C NMR** (126 MHz, $CDCl_3$) δ 199.41, 173.95, 140.44, 137.35, 136.98, 134.20, 128.54, 41.71, 22.19, 21.08, 20.40, 14.78, 1.28. **HRMS** (ESI, m/z): $[M+Na]^+$ calcd. for $C_{18}H_{28}Na_1O_1Si_1$, 311.1802; found 311.1802. The regio- and stereochemistry of the product was determined by 2D-NMR (including ^{1}H-^{29}Si HMBC) analysis.

(*E*)-3-cyclopropyl-3-mesityl-2-(trimethylsilyl)acrylaldehyde (**55**). Colorless oil. 97% yield (69 mg).

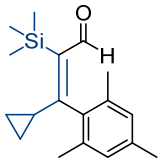

^{1}H NMR (600 MHz, $CDCl_3$) δ 9.23 (s, 1H), 6.81 (h, *J* = 0.6 Hz, 2H), 2.25 (s, 3H), 2.17 (tt, *J* = 8.1, 5.2 Hz, 1H), 2.09 (s, 6H), 0.89 – 0.86 (m, 2H), 0.37 – 0.34 (m, 2H), 0.35 (s, 9H). **^{13}C NMR** (151 MHz, $CDCl_3$) δ 198.47, 176.34, 139.67, 137.36, 135.32, 131.54, 128.18, 21.11, 20.17, 18.81, 8.80, 1.35. **HRMS** (ESI, m/z): $[M+Na]^+$ calcd. for $C_{18}H_{26}Na_1O_1Si_1$, 309.1645; found 309.1649. The regio- and stereochemistry of the product was determined by 2D-NMR analysis and by analogy to compound **54**.

(*E*)-3-mesityl-2-(triethylsilyl)oct-2-enal (**56**). Colorless oil. 56% yield (51 mg).

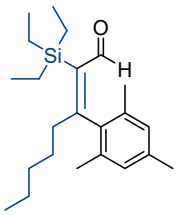

^{1}H NMR (500 MHz, $CDCl_3$) δ 9.35 (s, 1H), 6.86 (h, *J* = 0.7 Hz, 2H), 2.56 – 2.49 (m, 2H), 2.28 (s, 3H), 2.13 (s, 6H), 1.37 – 1.28 (m, 2H), 1.28 – 1.19 (m, 4H), 1.02 – 0.97 (m, 9H), 0.87 – 0.80 (m, 9H). **^{13}C NMR** (126 MHz, $CDCl_3$) δ 199.60, 174.56, 138.31, 137.49, 136.89, 134.08, 128.56, 39.47, 32.68, 28.13, 22.59, 21.08, 20.57, 14.13, 7.87, 4.73. **HRMS** (ESI, m/z): $[M+Na]^+$ calcd. for $C_{23}H_{38}Na_1O_1Si_1$, 381.2584; found 381.2580. The regio- and stereochemistry of the product was determined by 2D-NMR (including ^{1}H-^{29}Si HMBC) analysis.

(*E*)-3-mesityl-2-(triethylsilyl)-5-((triethylsilyl)oxy)pent-2-enal (**57**). Colorless oil. 55% yield (61 mg).

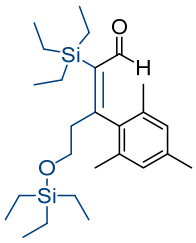

^{1}H NMR (500 MHz, $CDCl_3$) δ 9.35 (s, 1H), 6.85 (q, *J* = 0.7 Hz, 2H), 3.53 (dd, *J* = 7.6, 7.0 Hz, 2H), 2.84 (t, *J* = 7.3 Hz, 2H), 2.27 (s, 3H), 2.12 (s, 6H), 1.04 – 0.95 (m, 9H), 0.89 (t, *J* = 8.0 Hz, 9H), 0.89 – 0.82 (m, 6H), 0.52 (q, *J* = 8.0 Hz, 6H). **^{13}C NMR** (126 MHz, $CDCl_3$) δ 199.29, 170.13, 140.52, 137.11, 136.73, 134.16, 128.59, 60.80, 42.01, 21.07, 20.42, 7.84, 6.83, 4.75, 4.41. **HRMS** (ESI, m/z): $[M+Na]^+$ calcd. for $C_{26}H_{46}Na_1O_2Si_2$, 469.2929; found 469.2929. The regio- and stereochemistry of the product was determined by 2D-NMR (including ^{1}H-^{29}Si HMBC) analysis.

(*E*)-3-mesityl-3-phenyl-2-(trimethylsilyl)acrylaldehyde (**58**). Pale yellow solid. 70% yield (57 mg).

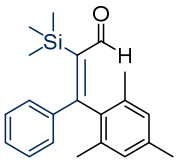

^{1}H NMR (500 MHz, $CDCl_3$) δ 9.48 (s, 1H), 7.35 – 7.28 (m, 3H), 7.21 – 7.17 (m, 2H), 6.88 (h, *J* = 0.6 Hz, 2H), 2.29 (s, 3H), 2.11 (s, 6H), 0.03 (s, 9H). **^{13}C NMR** (126 MHz, $CDCl_3$) δ 198.87, 172.24, 143.75, 141.49, 137.87, 137.63, 135.17, 129.52, 129.49, 128.81, 128.08, 21.17, 20.78, 1.04. **HRMS** (ESI, m/z): $[M+Na]^+$ calcd. for $C_{21}H_{26}Na_1O_1Si_1$, 345.1645; found 345.1644. The regio- and stereochemistry of the product was determined by 2D-NMR analysis and by analogy to related products.

(*E*)-3-mesityl-3-(4-methoxyphenyl)-2-(trimethylsilyl)acrylaldehyde (**59**). Yellow solid. 70% yield (62 mg).

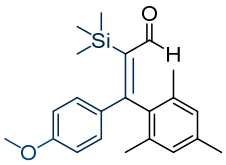

^{1}H NMR (500 MHz, $CDCl_3$) δ 9.76 (s, 1H), 7.09 – 7.05 (m, 2H), 6.86 (dd, *J* = 1.3, 0.7 Hz, 2H), 6.84 – 6.80 (m, 2H), 3.81 (s, 3H), 2.29 (s, 3H), 2.10 (s, 6H), -0.12 (s, 9H). **^{13}C NMR** (126 MHz, $CDCl_3$) δ 198.38, 168.64, 160.96, 142.33, 138.97, 137.64, 134.83, 132.59, 131.53, 128.50, 113.58, 55.49, 21.24, 20.28, -0.19. **HRMS** (ESI, m/z): $[M+Na]^+$ calcd. for $C_{22}H_{28}Na_1O_2Si_1$, 375.1751;

found 375.1752. The regio- and stereochemistry of the product was determined by 2D-NMR (including ^{1}H-^{29}Si HMBC) analysis.

(*E*)-4-(1-mesityl-3-oxo-2-(trimethylsilyl)prop-1-en-1-yl)benzonitrile (**60**). 74% yield (65 mg).

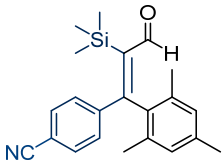

^{1}H NMR (400 MHz, $CDCl_3$) δ 9.48 (s, 1H), 7.63 – 7.59 (m, 2H), 7.32 – 7.28 (m, 2H), 6.90 (h, *J* = 0.6 Hz, 2H), 2.29 (s, 3H), 2.10 (s, 6H), 0.03 (s, 9H). **^{13}C NMR** (101 MHz, $CDCl_3$) δ 198.40, 168.84, 146.07, 145.91, 138.60, 136.43, 135.06, 131.89, 130.01, 129.12, 118.53, 112.93, 21.18, 20.83, 1.06. **HRMS** (ESI, m/z): $[M+Na]^+$ calcd. for $C_{22}H_{25}N_1Na_1O_1Si_1$, 370.1598; found 370.1598. The regio- and stereochemistry of the product was determined by 2D-NMR analysis and by analogy to related products.

(*E*)-3-mesityl-3-(4-(trifluoromethyl)phenyl)-2-(trimethylsilyl)acrylaldehyde (**61**). Yellow solid. 79% yield (77 mg).

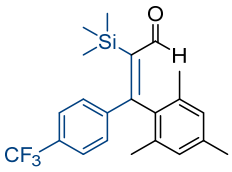

^{1}H NMR (400 MHz, $CDCl_3$) δ 9.49 (s, 1H), 7.61 – 7.53 (m, 2H), 7.35 – 7.27 (m, 2H), 6.90 (dd, *J* = 1.3, 0.7 Hz, 2H), 2.29 (s, 3H), 2.11 (s, 6H), 0.03 (s, 9H). ^{13}C NMR (151 MHz, $CDCl_3$) δ 198.57, 169.67, 145.42, 144.96 – 144.92 (m), 138.37, 136.88, 135.05, 131.27 (q, *J* = 32.7 Hz), 129.70, 129.04, 125.08 (q, *J* = 3.7 Hz), 124.01 (q, *J* = 272.2 Hz), 21.17, 20.81, 1.04. **^{19}F NMR** (376 MHz, $CDCl_3$) δ -62.66. **HRMS** (ESI, m/z): $[M+Na]^+$ calcd. for $C_{22}H_{25}F_3Na_1O_1Si_1$, 413.1519; found 413.1517. The regio- and stereochemistry of the product was determined by 2D-NMR (including ^{1}H-^{29}Si HMBC) analysis.

(*E*)-3-(1-mesityl-3-oxo-2-(trimethylsilyl)prop-1-en-1-yl)benzaldehyde (**62**). Pale yellow solid. 65% yield (57 mg).

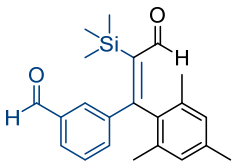

^{1}H NMR (500 MHz, $CDCl_3$) δ 10.00 (s, 1H), 9.49 (s, 1H), 7.86 (dt, *J* = 7.5, 1.5 Hz, 1H), 7.71 (td, *J* = 1.7, 0.6 Hz, 1H), 7.50 (t, *J* = 7.6 Hz, 1H), 7.44 (ddd, *J* = 7.7, 1.9, 1.3 Hz, 1H), 6.90 (q, *J* = 0.8 Hz, 2H), 2.29 (s, 3H), 2.12 (s, 6H), 0.03 (s, 9H). **^{13}C NMR** (151 MHz, $CDCl_3$) δ 198.58, 191.80, 169.82, 145.19, 142.44, 138.37, 136.85, 136.16, 135.11, 135.04, 130.78, 130.17, 129.05, 128.96, 21.18, 20.84, 1.10. **HRMS** (ESI, m/z): $[M+Na]^+$ calcd. for $C_{22}H_{26}Na_1O_2Si_1$, 373.1594; found 373.1590. The absolute configuration of the product was determined by 2D-NMR (including ^{1}H-^{29}Si HMBC) analysis and X-ray crystallography.

(*Z*)-3-mesityl-3-phenyl-2-(4,4,5,5-tetramethyl-1,3,2-dioxaborolan-2-yl)acrylaldehyde (**63**). Pale yellow solid. 41% yield (39 mg).

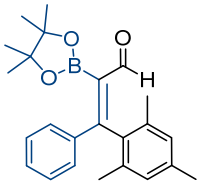

^{1}H NMR (500 MHz, $CDCl_3$) δ 9.38 (s, 1H), 7.38 – 7.33 (m, 3H), 7.32 – 7.28 (m, 2H), 6.91 (h, *J* = 0.7 Hz, 2H), 2.31 (s, 3H), 2.09 (s, 6H), 1.30 (s, 12H). **^{13}C NMR** (126 MHz, $CDCl_3$) δ 197.36, 167.81, 140.41, 138.05, 136.01, 135.13, 130.01, 128.58, 128.56, 128.54, 84.47, 24.89, 21.21, 20.51. **^{11}B NMR** (160 MHz, $CDCl_3$) δ 30.88. **HRMS** (ESI, m/z): $[M+Na]^+$ calcd. for $C_{24}H_{29}B_1Na_1O_3$, 399.2106; found 399.2109. The regio- and stereochemistry of the product was determined by 2D-NMR analysis.

(*Z*)-3-mesityl-2,3-diphenylacrylaldehyde (**64**). Pale yellow solid. 38% yield (31 mg).

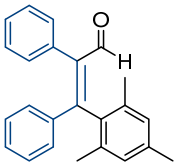

^{1}H NMR (500 MHz, $CDCl_3$) δ 9.56 (s, 1H), 7.32 – 7.26 (m, 3H), 7.17 – 7.14 (m, 3H), 7.10 – 7.06 (m, 2H), 6.98 – 6.95 (m, 4H), 2.34 (s, 3H), 2.19 (s, 6H). **^{13}C NMR** (126 MHz, $CDCl_3$) δ 193.53, 159.15, 139.96, 138.50, 138.36, 136.57, 135.39, 134.97, 131.06, 130.52, 128.96, 128.91, 128.41, 127.99, 127.78, 21.26, 20.46. **HRMS** (ESI, m/z): $[M+Na]^+$ calcd. for $C_{24}H_{22}Na_1O_1$, 349.1563; found 349.1562. The absolute configuration of the product was determined by 2D-NMR analysis and X-ray crystallography.

4. Hydroformylation of internal alkynes

General procedure

In a glovebox, a 4 mL screw-cap vial equipped with a stirring bar was charged with $[Pd(allyl)Cl]_2$ (2.5 mol%, 6.25 μmol, 2.29 mg) and DBFphos (4.0 mol%) and then PhCl (2 mL). The solution was stirred at room temperature for 10 min. To a pre-mixed solution were added hydrocinnamoyl chloride or butyryl chloride (1 equiv, 0.25 mmol), 5-decyne (2 equiv, 0.50 mmol) and *i*Pr$_3$SiH (1 equiv, 0.25 mmol). The reaction mixture was stirred at 120 °C for 12 h. The reaction was cooled to room temperature then quenched with sodium methoxide (1 equiv, 0.25 mmol, 0.05 mL of 5.4M solution in MeOH) and diluted with DCM (2 mL). The resulting solution was filtered through a celite/silica plug and concentrated under reduced pressure. The crude product was purified by column chromatography on silica gel (pentane/DCM). When employing BISBI (4.5 mol%) instead of DBFphos, the reaction also proceeded to form the desired hydroformylation product with a relatively decreased yield (10% lower, by GC analysis).

Supplementary Eq. 17.

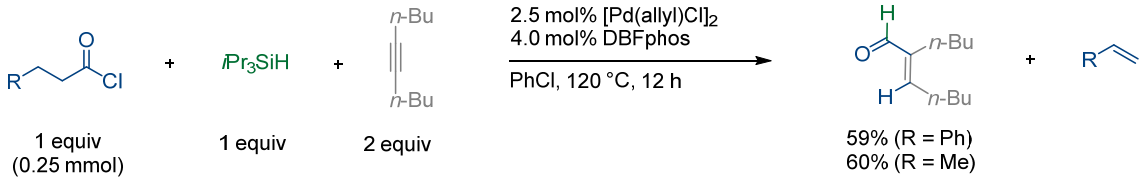

Supplementary Eq. 18.

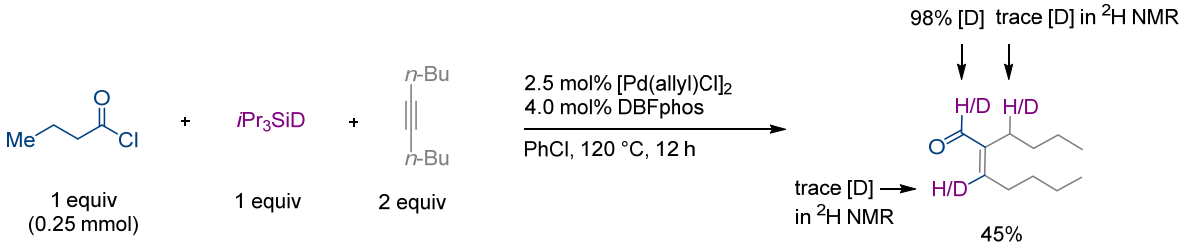

(*E*)-2-butylhept-2-enal (**65**). Colorless oil. 59% yield (25 mg, R= Ph in Supplementary Eq. 17), 60% yield (25 mg, R= Me in Supplementary Eq. 17).

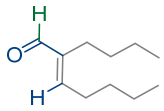

^{1}H NMR (600 MHz, $CDCl_3$) δ 9.36 (s, 1H), 6.44 (t, *J* = 7.4 Hz, 1H), 2.35 (q, *J* = 7.4 Hz, 2H), 2.26 – 2.20 (m, 2H), 1.52 – 1.46 (m, 2H), 1.42 – 1.35 (m, 2H), 1.34 – 1.29 (m, 4H), 0.94 (t, *J* = 7.3 Hz, 3H), 0.91 – 0.88 (m, 3H). **^{13}C NMR** (151 MHz, $CDCl_3$) δ 195.50, 155.46, 143.98, 31.10, 30.97, 28.78, 23.92, 22.91, 22.62, 14.05, 14.02. **HRMS** (ESI, m/z): $[M+Na]^+$ calcd. for $C_{11}H_{20}Na_1O_1$, 191.1406; found 191.1407. The regio- and stereochemistry of the product was determined by 2D-NMR analysis and by analogy to previously reported literature[4].

(*E*)-2-butylhept-2-enal-1-*d* (**68**). Colorless oil. 45% yield (19 mg, 98% [D]).

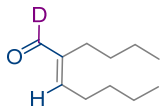

^{1}H NMR (600 MHz, $CDCl_3$) δ 6.44 (t, *J* = 7.4 Hz, 1H), 2.35 (q, *J* = 7.4 Hz, 2H), 2.25 – 2.21 (m, 2H), 1.51 – 1.46 (m, 2H), 1.42 – 1.35 (m, 2H), 1.33 – 1.29 (m, 4H), 0.94 (t, *J* = 7.3 Hz, 3H), 0.91 – 0.88 (m, 3H). **^{2}H NMR** (92 MHz, $CDCl_3$) δ 9.40. **^{13}C NMR** (151 MHz, $CDCl_3$) δ 195.19 (t, *J* = 26.4 Hz), 155.42, 143.91 (t, *J* = 3.3 Hz), 31.10, 30.97, 28.77, 23.87, 22.91, 22.62, 14.05, 14.02. **HRMS** (ESI, m/z): $[M+Na]^+$ calcd. for $C_{11}H_{19}D_1Na_1O_1$, 192.1469; found 192.1468. The regio- and stereochemistry of the product was determined by 2D-NMR and ^{2}H-NMR analysis and by analogy to compound **65**.

5. Carboacylation of internal alkynes

General procedure

In a glovebox, a 4 mL screw-cap vial equipped with a stirring bar was charged with [Pd(allyl)Cl]2 (2.5 mol%, 6.25 μmol, 2.29 mg) and DBFphos (4.0 mol%) and then PhCl (2 mL). The solution was stirred at room temperature for 10 min. To a pre-mixed solution were added *o*-Toluoyl chloride (1 equiv, 0.25 mmol), 4-octyne (2 equiv, 0.50 mmol) and tributylphenylstannane (nBu$_3$SnPh, 1 equiv, 0.25 mmol). The reaction mixture was stirred at 100 °C for 12 h. The reaction was cooled to room temperature then diluted with DCM (2 mL). The resulting solution was filtered through a celite/silica plug and concentrated under reduced pressure. The crude product was purified by column chromatography on silica gel (pentane/DCM). When employing BISBI (4.5 mol%) instead of DBFphos, the reaction also proceeded to form the desired carboacylation product with a relatively decreased yield (20% lower, by GC analysis).

Supplementary Eq. 19.

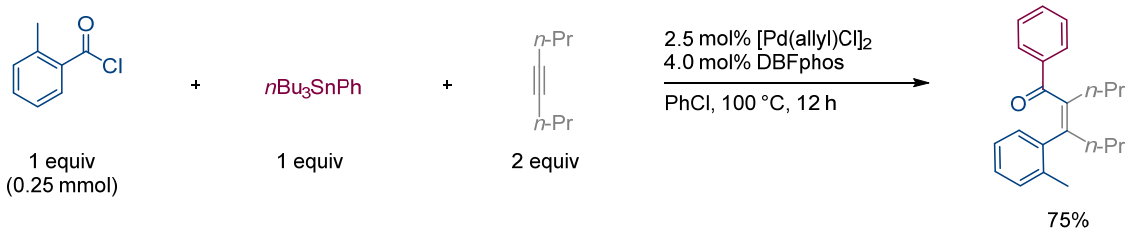

(*Z*)-1-phenyl-2-propyl-3-(*o*-tolyl)hex-2-en-1-one (**66**). Colorless oil. 75% yield (58 mg).

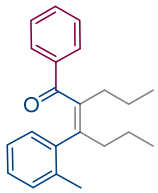

^{1}H NMR (400 MHz, $CDCl_3$) δ 7.59 – 7.55 (m, 2H), 7.35 – 7.30 (m, 1H), 7.25 – 7.19 (m, 2H), 6.92 – 6.85 (m, 2H), 6.83 – 6.76 (m, 2H), 2.63 – 2.46 (m, 3H), 2.32 – 2.24 (m, 1H), 2.18 (s, 3H), 1.59 – 1.47 (m, 2H), 1.44 – 1.30 (m, 2H), 1.01 (t, J = 7.3 Hz, 3H), 0.95 (t, J = 7.3 Hz, 3H). **^{13}C NMR** (101 MHz, $CDCl_3$) δ 201.19, 142.59, 140.54, 139.14, 138.48, 135.65, 132.12, 129.90, 129.88, 128.58, 127.87, 127.10, 124.84, 35.82, 32.80, 22.32, 21.39, 20.05, 14.50, 14.38. **HRMS** (ESI, m/z): $[M+H]^+$ calcd. for $C_{22}H_{27}O_1$, 307.2056; found 307.2059. The regio- and stereochemistry of the product was determined by 2D-NMR analysis and by analogy to previously reported literature[5].

6. Hydroacylation of internal alkynes

General procedure

In a glovebox, a 4 mL screw-cap vial equipped with a stirring bar was charged with [Pd(allyl)Cl]2 (2.5 mol%, 6.25 µmol, 2.29 mg) and DBFphos (4.0 mol%) and then PhCl (2 mL). The solution was stirred at room temperature for 10 min. To a pre-mixed solution were added 2-phenylpropionyl chloride (1 equiv, 0.25 mmol), 5-decyne (2 equiv, 0.50 mmol) and tributylphenylstannane (*n*Bu_3SnPh, 1 equiv, 0.25 mmol). The reaction mixture was stirred at 90 °C for 12 h. The reaction was cooled to room temperature then diluted with DCM (2 mL). The resulting solution was filtered through a celite/silica plug and concentrated under reduced pressure. The crude product was purified by column chromatography on silica gel (pentane/DCM).

Supplementary Eq. 20.

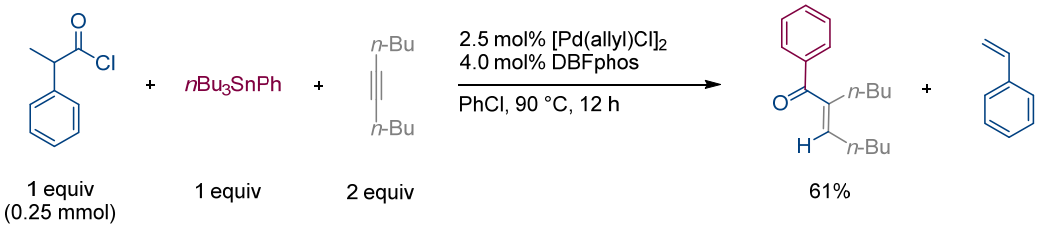

(*E*)-2-butyl-1-phenylhept-2-en-1-one (**67**). Colorless oil. 61% yield (37 mg).

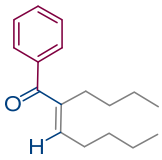

^{1}H NMR (400 MHz, $CDCl_3$) δ 7.70 – 7.61 (m, 2H), 7.53 – 7.47 (m, 1H), 7.44 – 7.37 (m, 2H), 6.18 (t, *J* = 7.4 Hz, 1H), 2.48 (t, *J* = 7.3 Hz, 2H), 2.28 (q, *J* = 7.3 Hz, 2H), 1.48 – 1.29 (m, 8H), 0.94 – 0.89 (m, 6H). **^{13}C NMR** (101 MHz, $CDCl_3$) δ 199.21, 145.94, 141.39, 139.25, 131.55, 129.52, 128.15, 31.38, 31.26, 28.73, 26.62, 22.98, 22.70, 14.15, 14.06. **HRMS** (ESI, m/z): $[M+Na]^+$ calcd. for $C_{17}H_{24}Na_1O_1$, 267.1719; found 267.1716. The regio- and stereochemistry of the product was determined by 2D-NMR analysis and by analogy to previously reported literature[6–8].

7. Syntheses of phosphine ligands

Synthesis of 1,4-bis(diphenylphosphaneyl)benzene (**L23**)

L23 was synthesized following the reported procedures[9]. ^{1}H-, ^{13}C- and ^{31}P-NMR data were consistent with the spectral data reported in literature[10,11].

Supplementary Eq. 21.

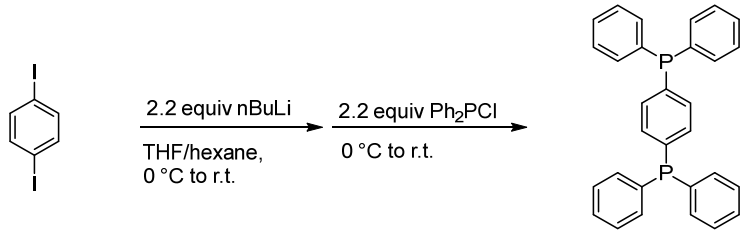

1,4-bis(diphenylphosphaneyl)benzene (**L23**). White solid.

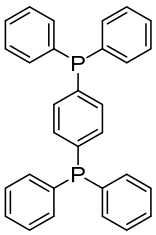

^{1}H NMR (400 MHz, $CDCl_3$) δ 7.36 – 7.28 (m, 20H), 7.25 – 7.22 (m, 4H). **^{13}C NMR** (101 MHz, $CDCl_3$) δ 137.99 (d, *J* = 12.3 Hz), 136.77 (d, *J* = 10.7 Hz), 133.87 (d, *J* = 20.0 Hz), 133.41 (dd, *J* = 19.4, 6.1 Hz), 128.89, 128.56 (dd, *J* = 3.7, 3.7 Hz). **^{31}P NMR** (162 MHz, $CDCl_3$) δ -5.79.

Synthesis of 4,6-bis(diphenylphosphaneyl)dibenzo[b,d]furan (**L07**)

L07 was synthesized following the reported procedures[12]. ^{1}H-, ^{13}C- and ^{31}P-NMR data were consistent with the spectral data reported in literature and the spectral data of a commercially supplied product.

Supplementary Eq. 22.

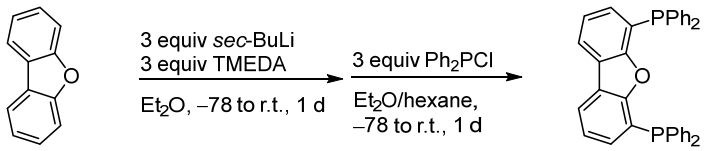

DBFphos (**L07**)
62% yield (4.7 g)

4,6-bis(diphenylphosphaneyl)dibenzo[b,d]furan (DBFphos, **L07**). White crystalline solid. 62% yield (4.7 g).

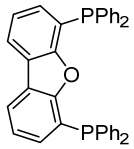

^{1}H NMR (500 MHz, $CDCl_3$) δ 7.86 (dd, *J* = 7.7, 1.3 Hz, 2H), 7.24 – 7.11 (m, 22H), 6.98 (ddd, *J* = 7.4, 6.2, 1.3 Hz, 2H). **^{13}C NMR** (126 MHz, $CDCl_3$) δ 158.06 (d, *J* = 13.7 Hz), 135.90 (d, *J* = 10.8 Hz), 134.00, 133.84, 132.18 (d, *J* = 8.7 Hz), 128.80, 128.51, 128.46, 123.65, 123.27, 123.24, 121.71, 121.59, 121.55. **^{31}P NMR** (202 MHz, $CDCl_3$) δ -16.95.

Synthesis of 6,8-bis(diphenylphosphaneyl)dinaphtho[2,1-b:1',2'-d]furan (**L08**)

L08 was synthesized in a similar manner as DBFphos (**L07**) by using dinaphtho[2,1-b:1',2'-d]furan (U-DNF) instead of dibenzo[b,d]furan[12]. U-DNF was synthesized following the reported procedures[13].

Supplementary Eq. 23.

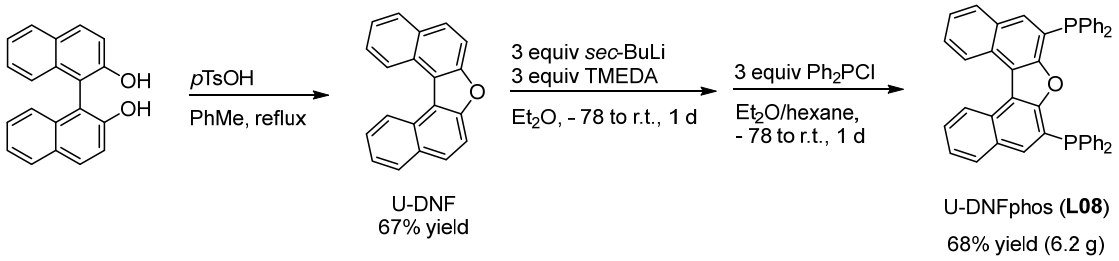

6,8-bis(diphenylphosphaneyl)dinaphtho[2,1-b:1',2'-d]furan (U-DNFphos, **L08**). White solid. 68% yield (6.2 g).

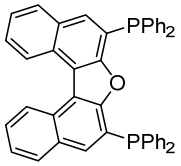

^{1}H NMR (500 MHz, $CDCl_3$) δ 9.04 (d, *J* = 8.5 Hz, 2H), 7.77 (d, *J* = 8.2 Hz, 2H), 7.64 (ddt, *J* = 8.2, 6.9, 1.2 Hz, 2H), 7.44 (ddt, *J* = 8.1, 7.0, 1.1 Hz, 2H), 7.38 (d, *J* = 5.8 Hz, 2H), 7.32 – 7.13 (m, 20H). **^{13}C NMR** (126 MHz, $CDCl_3$) δ 155.79 (d, *J* = 14.5 Hz), 135.64 (d, *J* = 10.8 Hz), 134.15, 133.99, 133.52 (d, *J* = 6.8 Hz), 131.44, 131.42, 129.82, 129.10, 128.98, 128.61, 128.55, 126.76, 125.47, 124.67, 123.33, 123.17, 118.88, 118.86, 118.85. **^{31}P NMR** (162 MHz, $CDCl_3$) δ -16.53. **HRMS** (ESI, m/z): $[M+Na]^+$ calcd. for $C_{44}H_{30}Na_1O_1P_2$ 659.1664; found 659.1663.

Synthesis of 3,3'-bis((diphenylphosphaneyl)methyl)-2,2'-binaphthalene (**L25**)

L25 was synthesized in a similar manner as **L24** by using 3,3'-bis(bromomethyl)-2,2'-binaphthalene instead of 2,2'-bis(bromomethyl)-1,1'-biphenyl[14,15]. 3,3'-bis(bromomethyl)-2,2'-binaphthalene was synthesized following the reported procedures[16–18]. In a glovebox, a 100 mL Schlenk flask equipped with a stirring bar was charged with diphenyl phosphane (10.00 mmol, 1.86g) and THF (10 mL) and then capped with a rubber septum and removed from the glovebox. To the stirred reaction mixture was added dropwise isopropyl magnesiumchloride (10.00 mmol, 5.00 mL, 2.0 M solution in THF) over 30 min at between −10 °C and 0 °C. The reaction mixture was stirred at 0 °C for 4 h. To the flask was added dropwise a THF solution of 3,3'-bis(bromomethyl)-2,2'-binaphthalene (3.07 mmol, 1.35 g) over 30 min at between −10 °C and 0 °C. The reaction mixture was stirred at 0 °C for 10 h thereafter quenched with anhydrous PhMe (10 mL), warmed up to room temperature and concentrated under reduced pressure. The resulting crude residue was dissolved in anhydrous DCM (50 mL) and washed with degassed water. The organic layer was concentrated under reduced pressure and the resulting residue was dissolved in anhydrous DCM then recrystallized with anhydrous isopropanol in a freezer. White solid. 84% yield (1.7 g).

Supplementary Eq. 24.

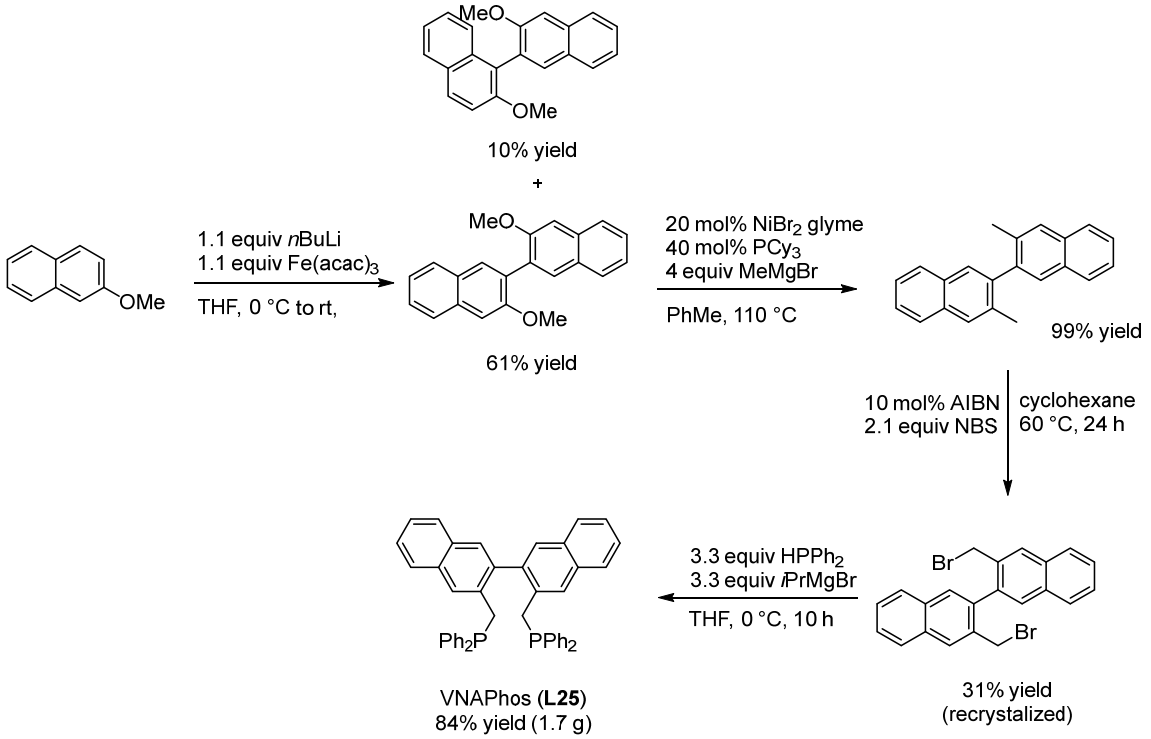

3,3'-bis((diphenylphosphaneyl)methyl)-2,2'-binaphthalene (VNAphos, **L25**). White solid. 84% yield (1.7 g).

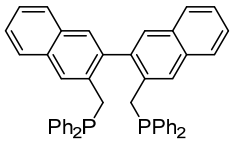

^{1}H NMR (400 MHz, $CDCl_3$) δ 7.65 – 7.55 (m, 4H), 7.50 (d, *J* = 2.6 Hz, 2H), 7.40 – 7.31 (m, 4H), 7.30 (s, 2H), 7.25 – 7.09 (m, 12H), 7.07 – 6.97 (m, 4H), 6.98 – 6.87 (m, 4H), 3.37 (dd, *J* = 13.6, 1.0 Hz, 2H), 3.22 (dd, *J* = 13.6, 2.4 Hz, 2H). **^{13}C NMR** (101 MHz, $CDCl_3$) δ 139.50 (d, *J* = 3.3 Hz), 138.43 (d, *J* = 15.3 Hz), 138.15 (d, *J* = 16.4 Hz), 134.35 (d, *J* = 8.6 Hz), 133.23 (d, *J* = 18.9 Hz), 132.97 (d, *J* = 18.4 Hz), 132.94, 131.82, 129.61, 128.78, 128.57, 128.55, 128.50, 128.45, 128.43, 128.33, 128.26, 127.93, 127.38, 125.95, 125.58, 33.67 (d, *J* = 16.2 Hz). **^{31}P NMR** (162 MHz, $CDCl_3$) δ -10.29. **HRMS** (ESI, m/z): $[M+Na]^+$ calcd. for $C_{46}H_{36}Na_1P_2$ 673.2184; found 673.2175.

8. Syntheses of acid chloride substrates

Acid chlorides were synthesized following the reported procedures[19] and used without further purification.

Supplementary Eq. 25.

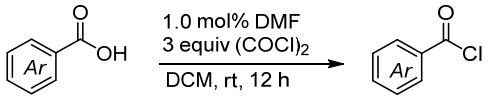

2-cyanobenzoyl chloride (**SAC-01**). Quantitative yield.

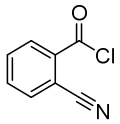

^{1}H NMR (400 MHz, $CDCl_3$) δ 8.42 – 8.34 (m, 1H), 7.91 – 7.86 (m, 1H), 7.83 – 7.80 (m, 2H). **^{13}C NMR** (101 MHz, $CDCl_3$) δ 165.73, 135.52, 135.00, 134.88, 134.09, 133.20, 116.56, 112.93.

2-methyl-6-(trifluoromethyl)nicotinoyl chloride (**SAC-02**). Quantitative yield.

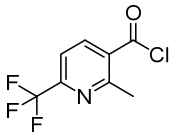

^{1}H NMR (400 MHz, $CDCl_3$) δ 8.65 – 8.59 (m, 1H), 7.71 (dd, *J* = 8.2, 0.7 Hz, 1H), 2.87 (s, 3H). **^{13}C NMR** (101 MHz, $CDCl_3$) δ 166.71, 161.00, 151.14 (d, *J* = 35.4 Hz), 142.57, 131.38, 120.80 (q, *J* = 274.9 Hz), 118.31 (q, *J* = 2.8 Hz), 25.04. **^{19}F NMR** (376 MHz, CDCl3) δ -68.62.

Benzoyl chloride-α-^{13}C (**SAC-03**). Quantitative yield.

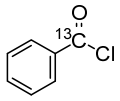

^{1}H NMR (400 MHz, $CDCl_3$) δ 8.17 – 8.10 (m, 2H), 7.73 – 7.66 (m, 1H), 7.56 – 7.50 (m, 2H). **^{13}C NMR** (101 MHz, $CDCl_3$) δ 168.63, 135.49 (d, *J* = 1.3 Hz), 131.60 (d, *J* = 3.4 Hz), 129.13 (d, *J* = 5.4 Hz).

4-(4,4,5,5-tetramethyl-1,3,2-dioxaborolan-2-yl)benzoyl chloride (**SAC-04**). Quantitative yield.

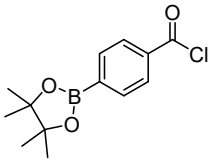

^{1}H NMR (400 MHz, $CDCl_3$) δ 8.19 – 8.03 (m, 2H), 8.00 – 7.83 (m, 2H), 1.36 (s, 12H). **^{13}C NMR** (101 MHz, $CDCl_3$) δ 168.85, 135.29, 135.26, 130.44, 84.67, 25.03.

4-(N,N-dipropylsulfamoyl)benzoyl chloride (**SAC-05**). Quantitative yield.

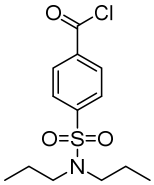

^{1}H NMR (400 MHz, $CDCl_3$) δ 8.28 – 8.20 (m, 2H), 7.99 – 7.90 (m, 2H), 3.16 – 3.08 (m, 4H), 1.62 – 1.50 (m, 4H), 0.88 (t, *J* = 7.4 Hz, 6H). **^{13}C NMR** (101 MHz, $CDCl_3$) δ 167.63, 146.64, 136.21, 131.99, 127.59, 50.08, 22.10, 11.29.

2-(3-cyano-4-isobutoxyphenyl)-4-methylthiazole-5-carbonyl chloride (**SAC-06**). Quantitative yield.

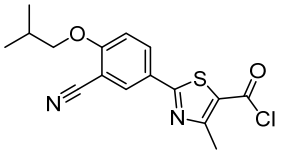

^{1}H NMR (400 MHz, $CDCl_3$) δ 8.23 (d, *J* = 2.3 Hz, 1H), 8.12 (dd, *J* = 8.9, 2.3 Hz, 1H), 7.04 (d, *J* = 8.9 Hz, 1H), 3.92 (d, *J* = 6.5 Hz, 2H), 2.74 (s, 3H), 2.31 – 2.13 (m, 1H), 1.10 (d, *J* = 6.7 Hz, 6H). **^{13}C NMR** (101 MHz, $CDCl_3$) δ 171.05, 164.36, 163.35, 158.28, 132.97, 132.59, 125.60, 116.12, 112.90, 103.45, 75.98, 28.30, 19.20, 18.64.

9. Syntheses of alkyne substrates

Synthesis of 1,8-diphenyloct-4-yne (**SAK-01**).

SAK-01 was synthesized according to a modified literature procedure[20] where the solution of lithiated alkyne was transferred to the bromide solution. ^{1}H- and ^{13}C-NMR data were consistent with the spectral data reported in literature[20].

Supplementary Eq. 26.

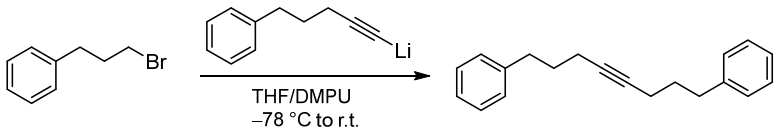

1,8-diphenyloct-4-yne (**SAK-01**). Colorless oil.

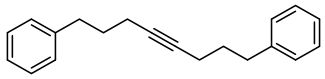

^{1}H NMR (400 MHz, $CDCl_3$) δ 7.33–7.19 (m, 10H), 2.76 (t, *J* = 7.62 Hz, 4H), 2.24–2.20 (tt, *J* = 7.04, 1.80 Hz, 4H), 1.88–1.81 (m, 4H). **^{13}C NMR** (101 MHz, $CDCl_3$) δ 142.0, 128.7, 128.5, 126.0, 80.5, 35.0, 30.9, 18.4.

Synthesis of 1,10-dichlorodec-5-yne (**SAK-02**).

SAK-02 was synthesized according to a literature procedure[21]. ^{1}H and ^{13}C NMR data were consistent with the spectral data reported in literature[21].

Supplementary Eq. 27.

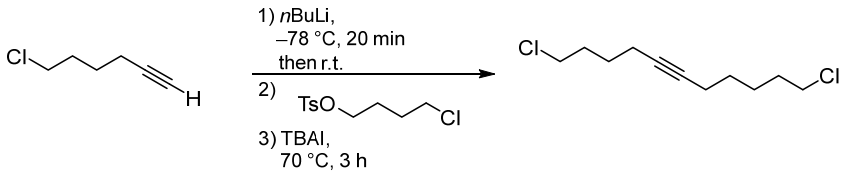

1,10-dichlorodec-5-yne (**SAK-02**). Colorless oil.

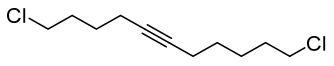

^{1}H NMR (400 MHz, $CDCl_3$) δ 3.58 (t, *J* = 6.60 Hz, 4H), 2.21–2.17 (tt, *J* = 6.99, 1.71 Hz, 4H), 1.92–1.85 (m, 4H), 1.67–1.60 (m, 4H). **^{13}C NMR** (101 MHz, $CDCl_3$) δ 80.1, 44.8, 31.7, 26.3, 18.2.

Synthesis of alkynes bearing an ester group (**SAK-03** to **SAK-08**).

General Procedure

The following esters were synthesized according to known literature procedures[6,19,22,23]. **Method A**: To a solution of alkynol (1.0 equiv, 5.0 mmol) in anhydrous DCM (10 mL) at 0 °C was added successively DMAP (10 mol%, 0.5 mmol, 61 mg), pyridine (3.0 equiv, 15.0 mmol, 1.2 mL) and acid chloride (2 equiv, 10.0 mmol). The solution was allowed to warm to room temperature and stir for 1 h before removing volatiles under reduced pressure, after which the crude material was purified by flash column chromatography to obtain the corresponding ester. **Method B**: To a solution of alkynol (1.0 equiv, 5.00 mmol) in DCM at 0 °C was added successively Et_3N (1.5 equiv, 0.75 mmol, 1.05 mL), DMAP (2 mol%, 0.10 mmol, 12 mg). After cooling the solution to 0 °C, acid chloride (1.5 equiv, 7.50 mmol) was added dropwise before allowing the reaction to warm to ambient temperature for 12 h. The crude mixture was then diluted with DCM (10 mL) and quenched with H_2O (10 mL) and then extracted with DCM (3 x 10 mL). The combined the organic phases washed with a saturated aqueous solution of $NaHCO_3$ (10 mL) then brine (10 mL) then dried over $MgSO_4$, filtered and concentrated under reduced pressure. The crude material was purified by flash column chromatography to give the corresponding ester. **Method C**: To a stirred suspension of sodium hydride (2 equiv, 10.0 mmol, 400 mg of the 60% dispersion slurry) in THF (10 mL), was added alkynol (1 equiv, 5.0 mmol) as a solution in THF (1.3 mL) at ambient temperature. After 2 h, *N,N*-diethylcarbamoyl chloride (2 equiv, 10.0 mmol, 1.27 mL) in THF (2 mL) was added dropwise. After 8 h, the reaction mixture was quenched with a saturated aqueous solution of NH_4Cl (10 mL) and extracted with Et_2O (3 × 15 mL). The combined organic phases were dried over $MgSO_4$, filtered and concentrated under reduced pressure. The crude material was then purified by flash column chromatography to give the alkynyl carbamate.

Supplementary Eq. 28.

hept-2-yn-1-yl benzoate (**SAK-03**). Colorless oil. 60% yield (0.65 g, Method A).

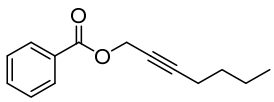

^{1}H NMR (400 MHz, $CDCl_3$) δ 8.09–8.06 (m, 2H), 7.59–7.55 (m, 1H), 7.46–7.42 (m, 2H), 4.92 (t, *J* = 2.2 Hz, 2H), 2.27–2.22 (tt, *J* = 7.10, 2.22 Hz, 2H), 1.54–1.48 (m, 2H), 1.46–1.37 (m, 2H), 0.91

(t, J = 7.25, 3H). **^{13}C NMR** (101 MHz, $CDCl_3$) δ 166.2, 133.3, 130.0, 129.9, 128.5, 88.0, 74.1, 53.5, 30.6, 22.1, 18.6, 13.7. **HRMS** (ESI, m/z):$[M+Na]^+$ calcd. for $C_{14}H_{16}O_2Na$ 239.1043; found 239.1043.

oct-3-yn-1-yl benzoate (**SAK-04**). Colorless oil. 91% yield (1.04 g, Method A).

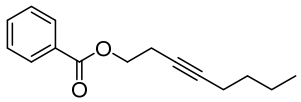

^{1}H NMR (400 MHz, $CDCl_3$) δ 8.08–8.05 (m, 2H), 7.58–7.54 (m, 1H), 7.47–7.42 (m, 2H), 4.40–4.37 (t, J = 6.99 Hz, 2H), 2.65–2.60 (m, 2H), 2.18–2.13 (m, 2H), 1.49–1.34 (m, 4H), 0.90–0.86 (t, J = 7.2 Hz, 3H). **^{13}C NMR** (101 MHz, $CDCl_3$) δ 166.5, 133.1, 130.3, 129.8, 128.5, 82.3, 75.6, 63.5, 31.1, 22.0, 19.5, 18.5, 13.7. **HRMS** (ESI, m/z): $[M+Na]^+$ calcd. for $C_{15}H_{18}O_2Na$; 253.199, found 253.1197.

oct-3-yn-1-yl butyrate (**SAK-05**). Colorless oil. 69% yield (0.67 g, Method B).

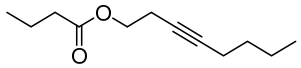

^{1}H NMR (400 MHz, $CDCl_3$) δ 4.13 (t, J = 6.97 Hz, 2H), 2.50–2.45 (m, 2H), 2.30 (t, J = 7.33 Hz, 2H), 2.16–2.11 (m, 2H), 1.70–1.61 (m, 2H), 1.49–1.34 (m, 4H), 0.95 (t, J = 7.41 Hz, 3H), 0.90 (t, J = 7.20 Hz, 3H). **^{13}C NMR** (101 MHz, $CDCl_3$) δ 173.6, 82.1, 75.7, 62.8, 36.3, 31.1, 22.0, 19.4, 18.6, 18.5, 13.8, 13.7. **HRMS** (ESI, m/z): $[M+Na]^+$ calcd. for $C_{12}H_{20}O_2Na$ 219.1356; found 219.1356.

oct-3-yn-1-yl diethylcarbamate (**SAK-06**). Pale yellow oil. 70% yield (0.79 g, Method C).

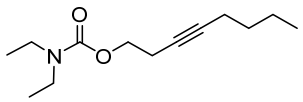

^{1}H NMR (400 MHz, $CDCl_3$) δ 4.15–4.11 (t, J = 6.82 Hz, 2H), 3.27 (br, 4H), 2.50–2.45 (m, 2H), 2.16–2.11 (m, 2H), 1.49–1.34 (m, 4H), 1.14–1.10 (t, J = 7.11 Hz, 6H), 0.91–0.88 (t, J = 7.14 Hz, 3H). **^{13}C NMR** (101 MHz, $CDCl_3$) δ 155.84, 81.79, 76.20, 63.58, 41.99, 31.16, 22.01, 19.90, 18.52, 13.75, 13.75. **HRMS** (ESI, m/z): $[M+Na]^+$ calcd. for $C_{13}H_{23}O_2NNa$ 248.1621; found 248.1622.

dodec-9-yn-1-yl benzoate (**SAK-07**). Colorless oil. 70% yield (0.60 g, Method B).

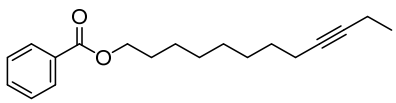

^{1}H NMR (400 MHz, $CDCl_3$) δ 8.06–8.03 (m, 2H), 7.58–7.53 (m, 1H), 7.46 (m, 2H), 4.34 (t, J = 6.67 Hz, 2H), 2.19–2.11 (m, 4H), 1.80–1.73 (m, 2H), 1.51–1.29 (m, 10H), 1.11 (t, J = 7.43 Hz, 3H). **^{13}C NMR** (101 MHz, $CDCl_3$) δ 166.9, 132.9, 130.7, 129.7, 128.5, 81.8, 79.6, 65.3, 29.3, 29.2,

29.2, 29.9, 28.9, 18.9, 14.5, 12.6. **HRMS** (ESI, m/z): $[M+Na]^+$ calcd. for $C_{19}H_{26}O_2Na$ 309.1825; found 309.1828.

dec-5-yn-1-yl benzoate (**SAK-08**). Colorless oil. 93% yield (1.19g, Method B).

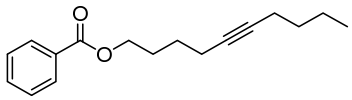

^{1}H NMR (400 MHz, $CDCl_3$) δ 8.06–8.03 (m, 2H), 7.58–7.53 (m, 1H), 7.46–7.42 (m, 2H), 4.34 (t, *J* = 6.45 Hz, 2H), 2.27–2.22 (m, 2H), 2.17–2.12 (m, 2H), 1.92–1.85 (m, 2H), 1.69–1.61 (m, 2H), 1.50–1.34 (m, 4H), 0.90 (t, *J* = 7.21 Hz, 3H). **^{13}C NMR** (101 MHz, $CDCl_3$) δ 166.8, 133.0, 130.6, 129.7, 128.5, 81.0, 79.5, 64.8, 31.3, 28.0, 25.8, 22.1, 18.6, 18.6, 13.8. The spectra were consistent with the literature[24].

Synthesis of methoxy-4-((oct-3-yn-1-yloxy)methyl)benzene (**SAK-09**)

SAK-09 was synthesised according to literature precedent[25]. ^{1}H and ^{13}C NMR data were consistent with the spectral data reported in literature[25].

Supplementary Eq. 29.

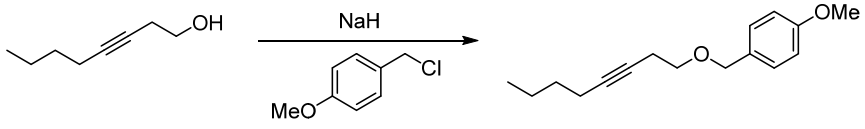

methoxy-4-((oct-3-yn-1-yloxy)methyl)benzene (**SAK-09**).

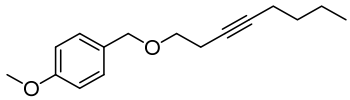

^{1}H NMR (400 MHz, $CDCl_3$) δ 7.31–7.28 (m, 2H), 6.91–6.89 (m, 2H), 4.50 (s, 2H), 3.83 (s, 3H), 3.55 (t, *J* = 7.16 Hz, 2H), 2.50–2.45 (m, 2H), 2.19–2.15 (m, 2H) 1.52–1.39 (m, 4H), 0.92 (t, *J* = 7.19, 3H). **^{13}C NMR** (101 MHz, $CDCl_3$) δ 159.3, 130.5, 129.4, 113.9, 81.6, 76.8, 72.7, 68.8, 55.4, 31.2, 22.1, 30.3, 18.6, 13.8.

Synethesis of *N*-(3-phenylprop-2-yn-1-yl)pivalamide (**SAK-10**)

SAK-10 was made according to a literature procedure[26]. The spectra are consistent with reported ones[27].

Supplementary Eq. 30.

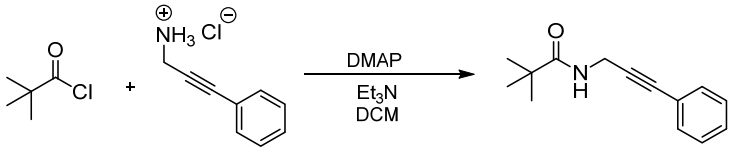

N-(3-phenylprop-2-yn-1-yl)pivalamide (**SAK-10**). 92% yield (0.60 g).

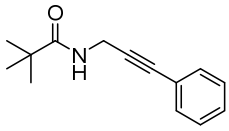

^{1}H NMR (400 MHz, $CDCl_3$) δ 7.45–7.40 (m, 2H), 7.33–7.28 (m, 3H), 5.83 (br, 1H), 4.28–4.26 (d, *J* = 4.97 Hz, 2H), 1.23 (s, 9H). **^{13}C NMR** (101 MHz, $CDCl_3$) δ 178.2, 131.9, 128.6, 128.5, 122.7, 85.1, 83.6, 38.9, 30.5, 27.6.

10. Additional control and kinetic experiments

10.1. Control reaction using o-tolualdehyde

Supplementary Eq. 31. Control reaction using o-tolualdehyde instead of *o*-toluoyl chloride.

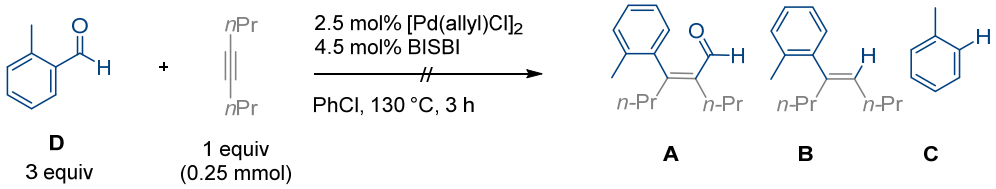

Supplementary Table 15. Control reaction using o-tolualdehyde instead of *o*-toluoyl chloride.

				Yield[a] (%)
entry	A	B	C	D
1	n.d.	n.d.	n.d.	253
2[b,c]	n.d.	n.d.	n.d.	249
3[d]	n.d.	n.d.	n.d.	280
4[d,e]	n.d.	n.d.	n.d.	245

[a]The GC yields are based on the moles of a limiting reagent, 4-octyne (0.25 mmol, 1 equiv.). [b]*i*Pr$_3$SiH (3 equiv.) was added. [c]PhH was observed presumably from reduction of PhCl. [d]*i*Pr$_3$SiCl (3 equiv.) was added. [e]TDMPP (10.0 mol%) was used instead of BISBI (4.5 mol%).

10.2. Mercury poisoning test

The reaction in presence of Hg was performed following the reported procedures[28,29]. In a glovebox, a 4 mL screw-cap vial equipped with a stirring bar was charged with $[Pd(allyl)Cl]_2$ (2.5 mol%, 6.25 μmol, 2.29 mg) and TDMPP (10.0 mol%) or BISBI (4.5 mol%) and then PhCl (2 mL). The solution was stirred at room temperature for 10 min. To a pre-mixed solution were added *o*-toluoyl chloride (3 equiv, 0.75 mmol), 4-octyne (1.0 equiv, 0.25 mmol) and *i*Pr$_3$SiH (3 equiv, 0.75 mmol). Metallic Hg (78 equiv, 19.4 mmol, 3.9 g, 1,560 equiv vs. Pd) was added to the reaction mixture. The reaction mixture was stirred at 130 °C for 3 h. The reaction was cooled to room temperature then diluted with DCM (2 mL) and *n*-dodecane was added as an internal standard. The resulting solution was filtered through a celite/silica plug and the filtrate was analyzed by GC/FID and GC/MS.

Supplementary Eq. 32. Mercury poisoning test.

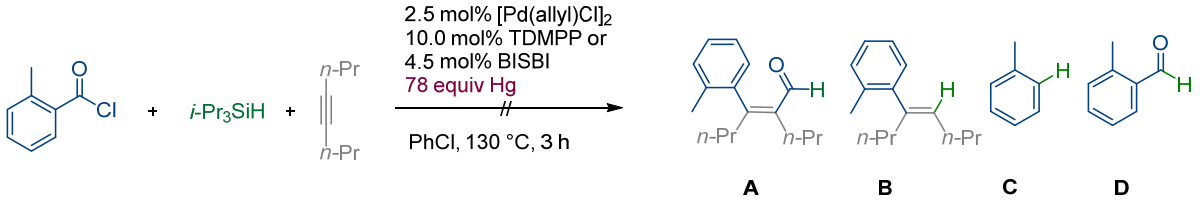

Supplementary Table 16. Mercury poisoning test[b].

						Yield[a] (%)
entry	P ligand	A	B	C	D	*i*Pr$_3$SiH (unreacted)
1	TDMPP	n.d.	n.d.	trace	trace	255
2	BISBI	n.d.	n.d.	trace	trace	246

[a]The GC yields are based on the moles of a limiting reagent, 4-octyne (0.25 mmol, 1 equiv.). [b]The result may suggest that Pd nanoparticles are presumably forming during the reaciton, however, it may also indicate that the reaction is incompatible with Hg as observed in other reactions[29].

10.3. Crossover experiment using benzoyl chloride-α-^{13}C and unlabeled *p*-toluoyl chloride

Supplementary Eq. 33. Crossover experiment, TDMPP.

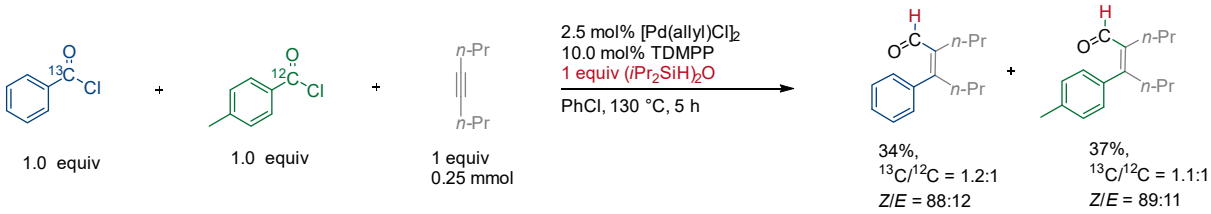

Supplementary Eq. 34. Crossover experiment, BISBI.

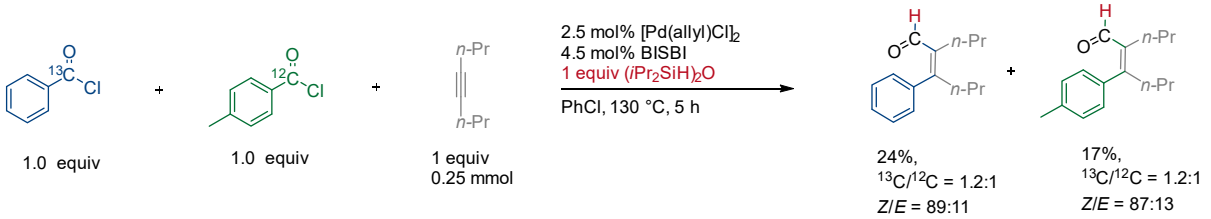

Supplementary Fig. 12. Crossover experiment using benzoyl chloride-α-^{13}C and unlabeled *p*-toluoyl chloride.

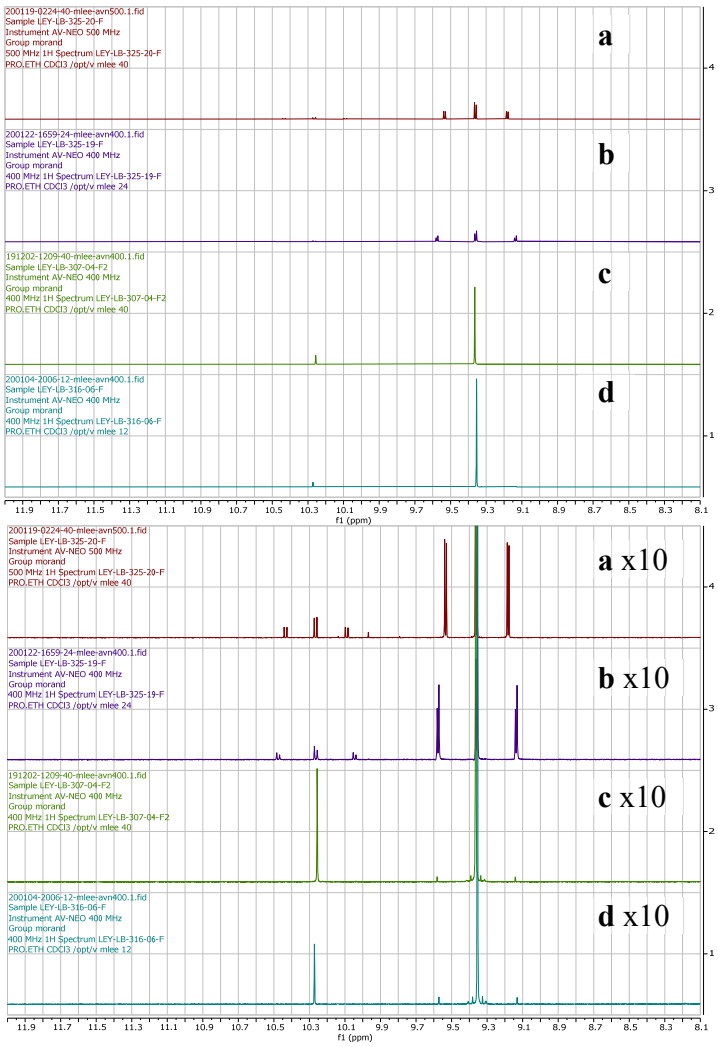

a, ^{1}H NMR spectrum of an isolated mixture of α,β-unsaturated aldehydes from Supplementary Eq. 33 (TDMPP).
b, ^{1}H NMR spectrum of an isolated mixture of α,β-unsaturated aldehydes from Supplementary Eq. 34 (BISBI).
c, ^{1}H NMR spectrum of **18**, *p*-MePh (*Z* isomer, δH of C**H**O= 9.36 ppm; *E* isomer, δH of C**H**O= 10.26 ppm).
d, ^{1}H NMR spectrum of **19**, Ph (*Z* isomer, δH of C**H**O= 9.35 ppm, *E* isomer, δH of C**H**O= 10.27 ppm).

10.4. Kinetic experiments using D-labeled and unlabeled silanes

General procedure

In a glovebox, a 4 mL screw-cap vial equipped with a stirring bar was charged with [Pd(allyl)Cl]2 (2.5 mol%, 6.25 μmol, 2.29 mg) and TDMPP (10.0 mol%) then PhCl (2 mL). The solution was stirred at room temperature for 10 min. To a pre-mixed solution were added o-toluoyl chloride (3 equiv, 0.75 mmol), 4-octyne (1.0 equiv, 0.25 mmol) and a triisopropylsilane-*d* (iPr3SiD, 3 equiv, 0.75 mmol). The reaction mixture was stirred at 120 °C for the indicated time (0.5 to 6.0 h). The reaction was cooled to room temperature then quenched with sodium methoxide (3 equiv, 0.75 mmol, 0.14 mL of 5.4M solution in MeOH) and diluted with DCM (2 mL) and *n*-dodecane was added as an internal standard. The resulting solution was filtered through a celite/silica plug and the filtrate was analyzed by GC/FID and GC/MS. For o-toluoyl chloride and *i*Pr$_3$SiCl, their GC yields were determined using the corresponding ester and silylether, respectively.

Supplementary Eq. 35. Kinetic experiments using unlabeled silane.

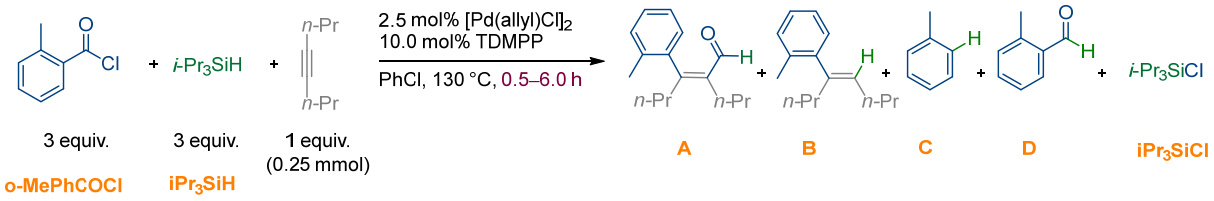

Supplementary Eq. 36. Kinetic experiments using D-labeled silane.

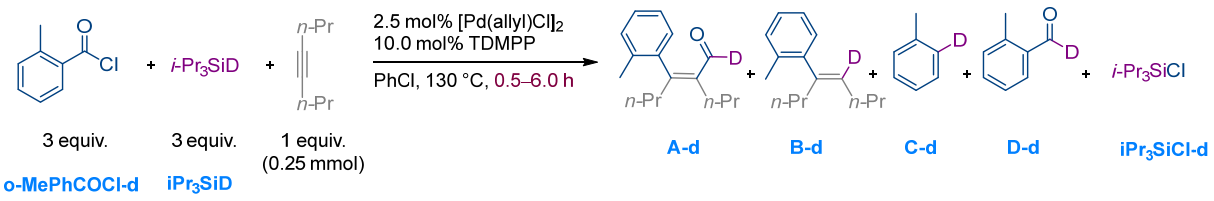

Supplementary Fig. 13. Kinetic experiments using D-labeled and unlabeled silanes (Supplementary Eq. 35 and 36). **a,** A desired product, **A**. **b,** A side product by decarbonylative hydroarylation, **B**. **c,** A side product by reductive decarbonylation, **C**. **d,** A side product by Rosenmund type reduction, **D**. The GC yields are based on the moles of a limiting reagent, 4-octyne (0.25 mmol, 1 equiv.).

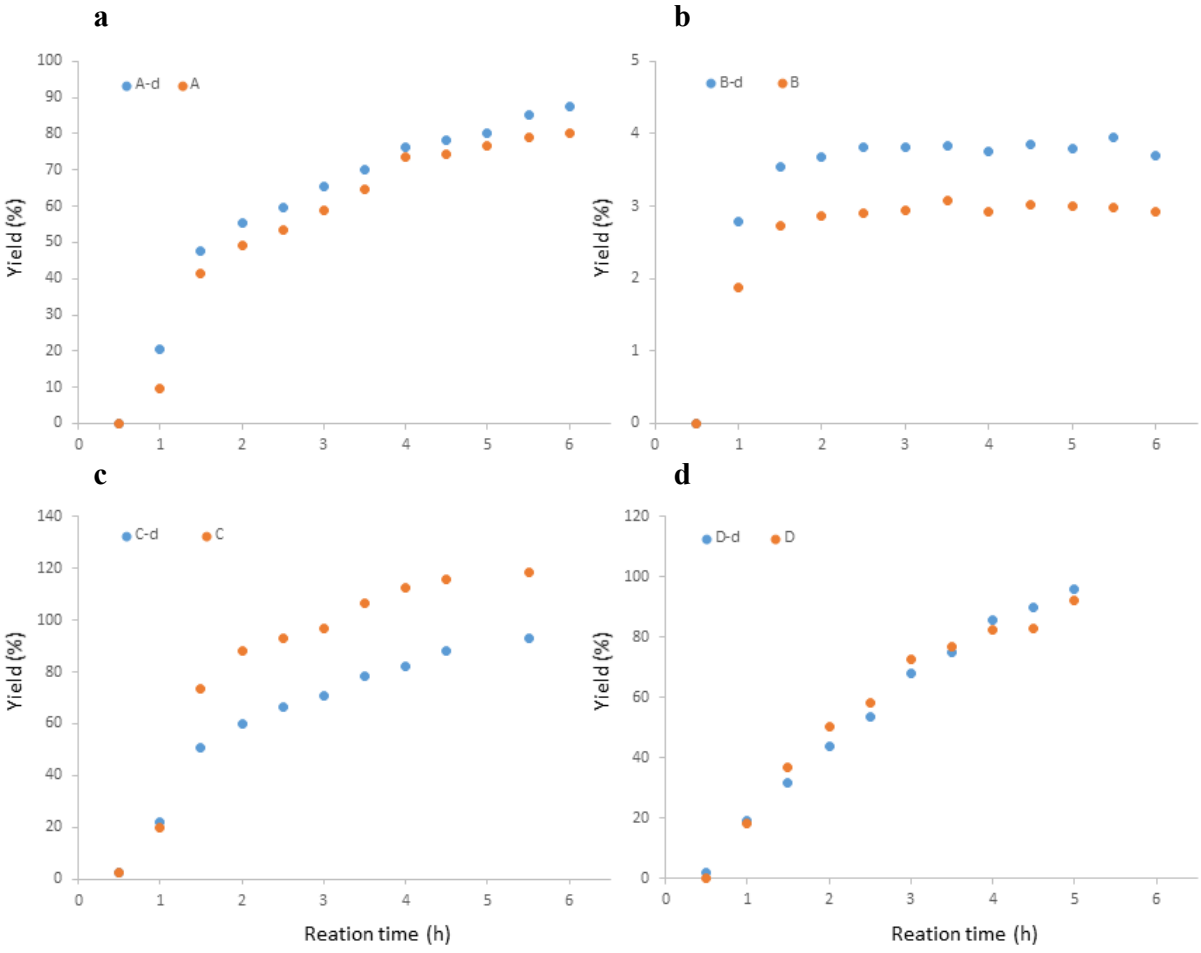

Supplementary Fig. 14. Kinetic experiments using D-labeled and unlabeled silanes (Supplementary Eq. 35 and 36). **a,** Overall yields of **A**, **B**, **C** and **D**. **b,** A by-product, ***i*Pr$_3$SiCl**. **c,** Unconverted ***o*-MePhCOCl**. **d,** Unconverted ***i*Pr$_3$Si-D/H**. GC yields of the unconverted ***o*-MePhCOCl** and the ***i*Pr$_3$SiCl** by-product are referred on the corresponding methyl ester and the *i*Pr$_3$SiOMe after quenching with NaOMe, and all yields are based on the moles of a limiting reagent, 4-octyne (0.25 mmol, 1 equiv.).

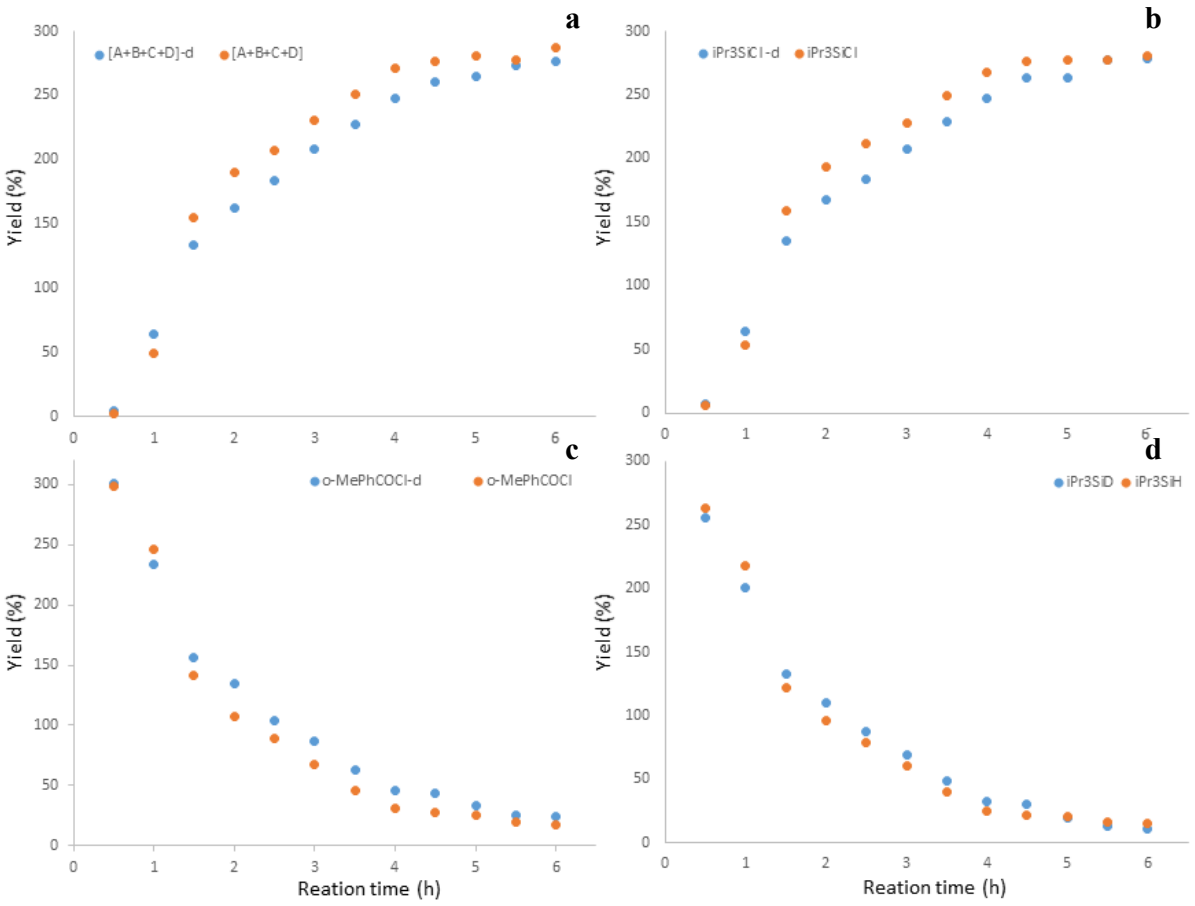

Synthesis of triisopropylsilane-*d* (*i*Pr$_3$SiD).

A deuterated triisopropyl silane was synthesized following the reported procedure[30]. ^{1}H and ^{13}C NMR data were consistent with the spectral data reported in literature[30].

Supplementary Eq. 37.

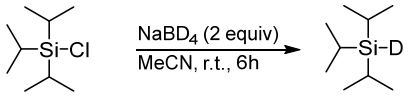

Triisopropylsilane-*d* (*i*Pr$_3$SiD). Colorless oil.

^{1}H NMR (400 MHz, $CDCl_3$) δ 1.06 (s, 21H). **^{13}C NMR** (101 MHz, $CDCl_3$) δ 19.5, 10.3.

10.5. Closed system vs. Open system

Supplementary Eq. 38. Comparison between closed and open system.

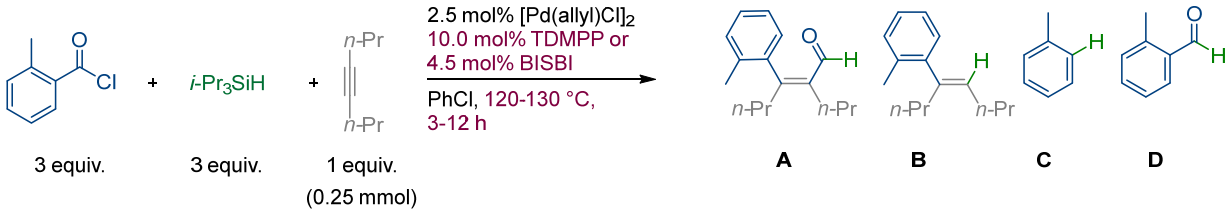

Supplementary Table 17. Comparison between closed and open system. **a,** TDMPP, 130 °C, 3 h. **b,** BISBI, 130 °C, 3 h. **c,** BISBI, 120 °C, 12 h.

a						Yield (%)[a,b]
entry	**TDMPP, 130 °C, 3 h**	A	B	C	D	A+B+C+D
1	Closed system	83 (80)	3	111	63	260
2	Open (connected to an oil bubbler)	93 (82)	9	148	26	275
3	Open (w/ N_2 balloon)	87	15	141	23	266
b						
entry	**BISBI, 130 °C, 3 h**	A	B	C	D	A+B+C+D
1	Closed system	65 (65)	1	162	43	271
2	Open (connected to oil bubbler)	41	19	187	10	257
3	Open (w/ N_2 balloon)	35	22	200	9	265
c						
entry	**BISBI, 120 °C, 12 h**	A	B	C	D	A+B+C+D
1	Closed system	62	1	159	47	269
2	Open (connected to oil bubbler)	62	5	166	13	245
3	Open (w/ N_2 balloon)	57	7	152	11	227

[a]Yields of isolated product given in parentheses. [b]The GC yields are based on the moles of a limiting reagent, 4-octyne (0.25 mmol, 1 equiv.).

11. Large scale experiment

Supplementary Eq. 39. Large scale experiment under open system.

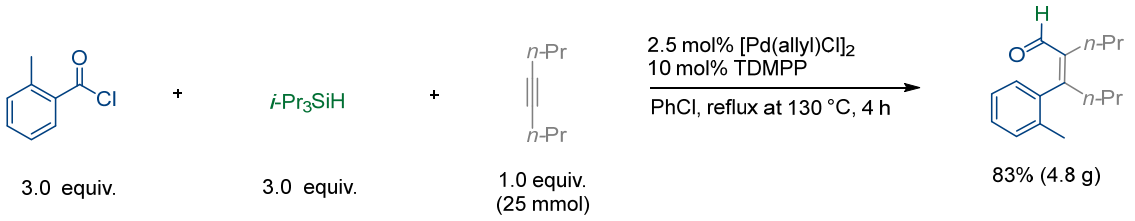

In a glovebox, a 500 mL Schlenk flask equipped with a stirring bar was charged with $[Pd(allyl)Cl]_2$ (2.5 mol%, 0.625 mmol, 0.229 g) and TDMPP (10.0 mol%, 2.5 mmol, 1.106 g) or BISBI (4.5 mol%) and then PhCl (200 mL). The solution was stirred at room temperature for 20 min. To a pre-mixed solution were added o-toluoyl chloride (3 equiv, 75 mmol, 9.78 mL), 4-octyne (1.0 equiv, 25 mmol, 3.67 mL) and *i*Pr_3SiH (3 equiv, 75 mmol, 15.36 mL). The flask was capped with a rubber septum, and was removed from the glovebox. The septum on top of the flask was pierced by a needle connected to an oil bubbler-attached manifolder under weak N_2 flow, for releasing the pressure. The reaction mixture was refluxed at 130 °C for 4 h under oil bath. The reaction was cooled to room temperature then quenched with sodium methoxide (3 equiv, 75 mmol, 13.89 mL of 5.4 M solution in MeOH) and diluted with DCM (100 mL). The resulting solution was filtered through a column packed with celite and silica (height 5 cm) and washed with DCM (100 mL) twice. The filtrate was concentrated under reduced pressure and purified by column chromatography on silica gel (pentane/DCM = 3:1). Pale yellow oil. 83% yield (4.8 g). Besides the desired product, a side product (**B**, Supplementary Table 17) was isolated as an inseparable mixture with unidentified impurities. 5% yield (257 mg).

(*Z*)-2-propyl-3-(*o*-tolyl)hex-2-enal (**1**, **A**)**.** Colorless oil. 65% yield (38 mg, BISBI). 80% yield (46 mg, TDMPP), 82% yield (47 mg, TDMPP, open), **83% yield (4.8 g, TDMPP, 25 mmol scale).**

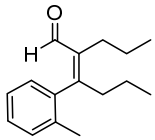

^{1}H NMR (600 MHz, $CDCl_3$) δ 9.24 (s, 1H), 7.25 – 7.20 (m, 2H), 7.19 – 7.15 (m, 1H), 7.00 (dd, *J* = 7.5, 1.4 Hz, 1H), 2.61 (ddd, *J* = 13.1, 10.6, 5.9 Hz, 1H), 2.47 – 2.29 (m, 3H), 2.19 (s, 3H), 1.53 – 1.29 (m, 4H), 0.99 (t, *J* = 7.4 Hz, 3H), 0.94 (t, *J* = 7.3 Hz, 3H). **^{13}C NMR** (151 MHz, $CDCl_3$) δ 194.42, 161.98, 138.86, 138.65, 135.38, 130.30, 129.28, 127.87, 125.50, 37.97, 27.00, 22.78, 20.97, 19.89, 14.62, 14.45. **HRMS** (EI, m/z): $[M-H]^+$ calcd. for $C_{16}H_{21}O_1$, 229.1587; found 229.1593. The stereochemistry of the product was determined by 2D-NMR analysis.

(*E*)-1-methyl-2-(oct-4-en-4-yl)benzene (**B**). Colorless oil. 5% yield (257 mg, TDMPP, 25 mmol scale).

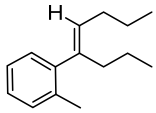

^{1}H NMR (400 MHz, $CDCl_3$) δ 7.19 – 7.09 (m, 3H), 7.06 – 7.02 (m, 1H), 5.24 (tt, *J* = 7.3, 0.9 Hz, 1H), 2.35 – 2.28 (m, 2H), 2.27 (s, 3H), 2.21 – 2.10 (m, 2H), 1.45 (h, *J* = 7.4 Hz, 2H), 1.35 – 1.21 (m, 2H), 0.96 (t, *J* = 7.4 Hz, 3H), 0.87 (t, *J* = 7.3 Hz, 3H). **^{13}C NMR** (101 MHz, $CDCl_3$) δ 144.80, 140.69, 135.41, 130.03, 129.90, 129.17, 126.36, 125.30, 33.97, 30.25, 23.17, 21.51, 14.36, 14.06. ^{1}H- and ^{13}C-NMR data were consistent with the spectral data reported in literature[31].

12. X-ray structure analysis

(*Z*)-3-(9-oxo-9H-fluoren-4-yl)-2-propylhex-2-enal (**10**).

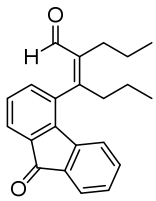

Experimental procedure

Single crystals of $C_{22}H_{22}O_2$ (**10**) [bm131219_1_1]. A suitable crystal was selected on a XtaLAB Synergy, Dualflex, Pilatus 300K diffractometer. The crystal was kept at 100.0(1) K during data collection. Using Olex2[32], the structure was solved with the SHELXT[33] structure solution program using Intrinsic Phasing and refined with the SHELXL[34] refinement package using Least Squares minimisation.

Crystal structure determination of **10** [bm131219_1_1]

Crystal Data for $C_{22}H_{22}O_2$ (M =318.39 g/mol): triclinic, space group P-1 (no. 2), a = 9.3396(3) Å, b = 10.0026(4) Å, c = 10.6386(4) Å, α = 72.702(3)°, β = 66.204(3)°, γ = 74.286(3)°, V = 855.20(6) Å^3, Z = 2, T = 100.0(1) K, μ(Cu Kα) = 0.608 mm^{-1}, *Dcalc* = 1.236 g/cm^3, 20980 reflections measured (9.3° ≤ 2Θ ≤ 159.778°), 3627 unique (R_{int} = 0.0404, R_{sigma} = 0.0245) which were used in all calculations. The final R_1 was 0.0392 (I > 2σ(I)) and wR_2 was 0.1050 (all data).

(*Z*)-3-mesityl-2,4-dimethylpent-2-enal, B (**36-α-Ar, minor**).

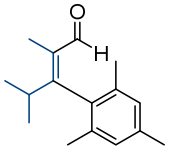

Experimental

Single crystals of $C_{16}H_{22}O$ (**36-α-Ar, minor**) [bm020420_1_1]. A suitable crystal was selected on a Bruker APEX-II CCD diffractometer. The crystal was kept at 100.02 K during data collection. Using Olex2[32], the structure was solved with the SHELXT[33] structure solution program using Intrinsic Phasing and refined with the SHELXL[34] refinement package using Least Squares minimisation.

Crystal structure determination of **36-α-Ar** [bm020420_1_1]

Crystal Data for $C_{16}H_{22}O$ (M =230.33 g/mol): orthorhombic, space group $P2_12_12_1$ (no. 19), a = 7.0391(9) Å, b = 8.7047(11) Å, c = 22.051(3) Å, V = 1351.2(3) Å^3, Z = 4, T = 100.02 K, μ(MoKα) = 0.068 mm^{-1}, *Dcalc* = 1.132 g/cm^3, 24518 reflections measured ($3.694° \leq 2\Theta \leq 56.63°$), 3360 unique ($R_{int}$ = 0.0442, R_{sigma} = 0.0269) which were used in all calculations. The final R_1 was 0.0733 ($I > 2\sigma(I)$) and wR_2 was 0.2386 (all data).

(*Z*)-*N*-(2-formyl-3-mesityl-3-phenylallyl)pivalamide (**53**).

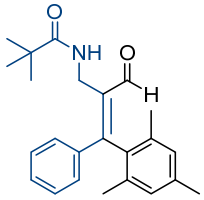

Experimental

Single crystals of $C_{24}H_{29}NO_2$ (**53**) [bm010420_2_1]. A suitable crystal was selected on a Bruker/Nonius Kappa Apex2 diffractometer. The crystal was kept at 100.0(1) K during data collection. Using Olex2[32], the structure was solved with the SHELXT[33] structure solution program using Intrinsic Phasing and refined with the SHELXL[34] refinement package using Least Squares minimisation.

Crystal structure determination of **53** [bm010420_2_1]

Crystal Data for $C_{24}H_{29}NO_2$ (M =363.48 g/mol): monoclinic, space group $P2_1/c$ (no. 14), a = 20.9789(18) Å, b = 11.8894(11) Å, c = 8.6763(9) Å, β = 97.691(4)°, V = 2144.6(4) Å^3, Z = 4, T = 100.0(1) K, μ(MoKα) = 0.071 mm^{-1}, *Dcalc* = 1.126 g/cm^3, 18548 reflections measured (5.878° ≤ 2Θ ≤ 54.98°), 4889 unique (R_{int} = 0.0665, R_{sigma} = 0.0840) which were used in all calculations. The final R_1 was 0.0570 (I > 2σ(I)) and wR_2 was 0.1551 (all data).

(*E*)-3-(1-mesityl-3-oxo-2-(trimethylsilyl)prop-1-en-1-yl)benzaldehyde (**62**).

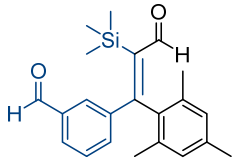

Experimental procedure

Single crystals of $C_{22}H_{26}O_2Si$ (**62**) [bm140320_1_1]. A suitable crystal was selected on a Bruker APEX-II Duo (Mo) diffractometer. The crystal was kept at 100.0(1) K during data collection. Using Olex2[32], the structure was solved with the SHELXT[33] structure solution program using Intrinsic Phasing and refined with the SHELXL[34] refinement package using Least Squares minimisation.

Crystal structure determination of **62** [bm140320_1_1]

Crystal Data for $C_{22}H_{26}O_2Si$ (M =350.52 g/mol): monoclinic, space group $P2_1/c$ (no. 14), a = 9.1023(7) Å, b = 17.6579(15) Å, c = 12.0789(9) Å, β = 94.953(2)°, V = 1934.2(3) Å^3, Z = 4, T = 100.0(1) K, μ(MoKα) = 0.133 mm^{-1}, *Dcalc* = 1.204 g/cm^3, 23843 reflections measured (4.096° ≤ 2Θ ≤ 61.082°), 5913 unique (R_{int} = 0.0559, R_{sigma} = 0.0529) which were used in all calculations. The final R_1 was 0.0467 (I > 2σ(I)) and wR_2 was 0.1216 (all data).

(*Z*)-3-mesityl-2,3-diphenylacrylaldehyde (**64**).

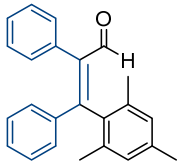

Experimental procedure

Single crystals of $C_{24}H_{22}O$ (**64**) [bm130320_1_1]. A suitable crystal was selected on a Bruker APEX-II Duo (Mo) diffractometer. The crystal was kept at 100.0(1) K during data collection. Using Olex2[32], the structure was solved with the SHELXT[33] structure solution program using Intrinsic Phasing and refined with the SHELXL[34] refinement package using Least Squares minimisation.

Crystal structure determination of **64** [bm130320_1_1]

Crystal Data for $C_{24}H_{22}O$ (M =326.41 g/mol): triclinic, space group P-1 (no. 2), a = 8.337(7) Å, b = 9.731(9) Å, c = 11.818(11) Å, α = 103.49(2)°, β = 98.52(2)°, γ = 101.66(2)°, V = 893.6(14) Å^3, Z = 2, T = 100.0(1) K, μ(MoKα) = 0.072 mm^{-1}, $Dcalc$ = 1.213 g/cm^3, 21193 reflections measured (3.622° ≤ 2Θ ≤ 61.596°), 5556 unique (R_{int} = 0.0460, R_{sigma} = 0.0463) which were used in all calculations. The final R_1 was 0.0483 (I > 2σ(I)) and wR_2 was 0.1241 (all data).

6,8-bis(diphenylphosphaneyl)dinaphtho[2,1-b:1',2'-d]furan (U-DNFphos, **L08**).

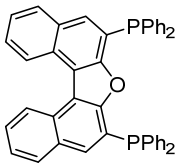

Experimental procedure

Single crystals of $C_{44}H_{30}OP_2$ (**L08**) [bm270819_2_1]. A suitable crystal was selected on a XtaLAB Synergy, Dualflex, Pilatus 300K diffractometer. The crystal was kept at 100.0(1) K during data collection. Using Olex2[32], the structure was solved with the ShelXS[35] structure solution program using Direct Methods and refined with the ShelXL[34] refinement package using Least Squares minimisation.

Crystal structure determination of **L08** [bm270819_2_1]

Crystal Data for $C_{44}H_{30}OP_2$ (M =636.62 g/mol): monoclinic, space group $P2_1/c$ (no. 14), a = 10.65063(7) Å, b = 19.02946(12) Å, c = 16.01500(10) Å, β = 91.6925(6)°, V = 3244.44(4) Å^3, Z = 4, T = 100.0(1) K, μ(CuKα) = 1.484 mm^{-1}, $Dcalc$ = 1.303 g/cm^3, 50422 reflections measured (7.216° ≤ 2Θ ≤ 159.248°), 6969 unique (R_{int} = 0.0373, R_{sigma} = 0.0178) which were used in all calculations. The final R_1 was 0.0324 (I > 2σ(I)) and wR_2 was 0.0878 (all data).

[(TDMPP-*O,P*)Pd(Cl)(o-toluoyl)] (**69**).

Procedure for acquisition for a single crystal of [(TDMPP-*O,P*)Pd(Cl)(o-toluoyl)] (**69**)

In a glovebox, a 4 mL screw-cap vial equipped with a stirring bar was charged with $[Pd(allyl)Cl]_2$ (6.25 μmol, 2.29 mg) and TDMPP (0.025 mmol) then PhCl (1 mL). The solution was stirred at room temperature for 10 min. To a pre-mixed solution were added o-toluoyl chloride (0.50 mmol) and triisopropylsilane (0.50 mmol). The reaction mixture was stirred at room temperature for 30 min. Single crystals suitable for X-ray diffraction were obtained by slow diffusion of pentane into the resulting solution.

Experimental procedure

Single crystals of $C_{32}H_{34}ClO_7PPd$ (**69**) [bm021219_1_1]. A suitable crystal was selected on a XtaLAB Synergy, Dualflex, Pilatus 300K diffractometer. The crystal was kept at 100.0(1) K during data collection. Using Olex2[32], the structure was solved with the SHELXT[33] structure solution program using Intrinsic Phasing and refined with the SHELXL[34] refinement package using Least Squares minimisation.

Crystal structure determination of **69** [bm021219_1_1]

Crystal Data for $C_{32}H_{34}ClO_7PPd$ (M =703.41 g/mol): triclinic, space group P-1 (no. 2), a = 10.9494(2) Å, b = 11.1621(2) Å, c = 13.2564(2) Å, α = 76.4930(10)°, β = 88.4080(10)°, γ = 76.7110(10)°, V = 1532.60(5) Å^3, Z = 2, T = 100.0(1) K, μ(Cu Kα) = 6.570 mm^{-1}, *Dcalc* = 1.524 g/cm^3, 41654 reflections measured (6.86° ≤ 2Θ ≤ 159.482°), 6482 unique (R_{int} = 0.0464, R_{sigma} = 0.0276) which were used in all calculations. The final R_1 was 0.0319 (I > 2σ(I)) and wR_2 was 0.0898 (all data).

(*Z*)-3-(9-oxo-9H-fluoren-4-yl)-2-propylhex-2-enal (**10**).

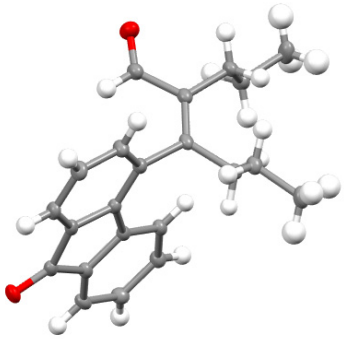

Supplementary Fig. 15. X-ray structure of compound **10**. Thermal ellipsoids are drawn at the 50% probability level.

Supplementary Table 18. Crystal data and structure refinement for compound **10**.

Crystal data and structure refinement for compound **10** (307-08, bm131219_1_1).	
Identification code	bm131219_1_1
Empirical formula	$C_{22}H_{22}O_2$
Formula weight	318.39
Temperature/K	100.0(1)
Crystal system	triclinic
Space group	P-1
a/Å	9.3396(3)
b/Å	10.0026(4)
c/Å	10.6386(4)
α/°	72.702(3)
β/°	66.204(3)
γ/°	74.286(3)
Volume/Å^3	855.20(6)
Z	2
ρ_{calc}g/cm^3	1.236
μ/mm^{-1}	0.608
F(000)	340.0
Crystal size/mm^3	0.268 × 0.175 × 0.108
Radiation	Cu Kα (λ = 1.54184)
2Θ range for data collection/°	9.3 to 159.778
Index ranges	-11 ≤ h ≤ 11, -12 ≤ k ≤ 12, -13 ≤ l ≤ 13
Reflections collected	20980
Independent reflections	3627 [R_{int} = 0.0404, R_{sigma} = 0.0245]
Data/restraints/parameters	3627/0/219
Goodness-of-fit on F^2	1.088
Final R indexes [I>=2σ (I)]	R_1 = 0.0392, wR_2 = 0.0982
Final R indexes [all data]	R_1 = 0.0471, wR_2 = 0.1050
Largest diff. peak/hole / e Å^{-3}	0.24/-0.24

(*Z*)-3-mesityl-2,4-dimethylpent-2-enal, B (**36-α-Ar, minor**).

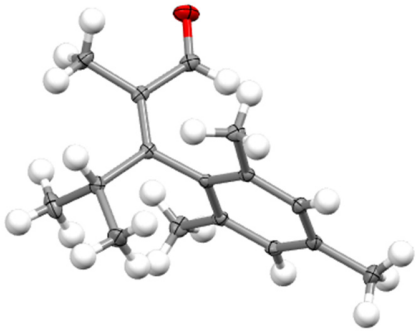

Supplementary Fig. 16. X-ray structure of compound **36-α-Ar**. Thermal ellipsoids are drawn at the 50% probability level.

Supplementary Table 19. Crystal data and structure refinement for compound **36-α-Ar**.

Crystal data and structure refinement for compound **36-α-Ar** (bm020420_1_1).	
Identification code	bm020420_1_1
Empirical formula	$C_{16}H_{22}O$
Formula weight	230.33
Temperature/K	100.02
Crystal system	orthorhombic
Space group	$P2_12_12_1$
a/Å	7.0391(9)
b/Å	8.7047(11)
c/Å	22.051(3)
α/°	90
β/°	90
γ/°	90
Volume/Å^3	1351.2(3)
Z	4
ρ_{calc}g/cm^3	1.132
μ/mm^{-1}	0.068
F(000)	504.0
Crystal size/mm^3	0.2 × 0.08 × 0.05
Radiation	MoKα (λ = 0.71073)
2Θ range for data collection/°	3.694 to 56.63
Index ranges	$-9 \le h \le 9$, $-11 \le k \le 11$, $-29 \le l \le 29$
Reflections collected	24518
Independent reflections	3360 [R_{int} = 0.0442, R_{sigma} = 0.0269]
Data/restraints/parameters	3360/0/154
Goodness-of-fit on F^2	1.926
Final R indexes [I>=2σ (I)]	R_1 = 0.0733, wR_2 = 0.2326
Final R indexes [all data]	R_1 = 0.0808, wR_2 = 0.2386
Largest diff. peak/hole / e Å^{-3}	0.66/-0.32
Flack parameter	-0.4(6)

(*Z*)-*N*-(2-formyl-3-mesityl-3-phenylallyl)pivalamide (**53**).

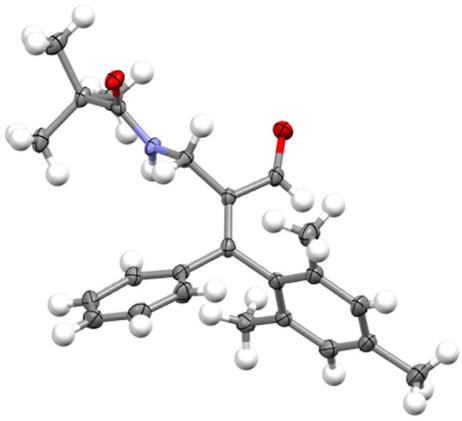

Supplementary Fig. 17. X-ray structure of compound **53**. Thermal ellipsoids are drawn at the 50% probability level.

Supplementary Table 20. Crystal data and structure refinement for compound **53**.

Crystal data and structure refinement for **53** (bm010420_2_1).

Identification code	bm010420_2_1
Empirical formula	$C_{24}H_{29}NO_2$
Formula weight	363.48
Temperature/K	100.0(1)
Crystal system	monoclinic
Space group	$P2_1/c$
a/Å	20.9789(18)
b/Å	11.8894(11)
c/Å	8.6763(9)
α/°	90
β/°	97.691(4)
γ/°	90
Volume/Å^3	2144.6(4)
Z	4
ρ_{calc}g/cm^3	1.126
μ/mm^{-1}	0.071
F(000)	784.0
Crystal size/mm^3	0.14 × 0.09 × 0.03
Radiation	MoKα (λ = 0.71073)
2Θ range for data collection/°	5.878 to 54.98
Index ranges	-24 ≤ h ≤ 27, -15 ≤ k ≤ 15, -10 ≤ l ≤ 11
Reflections collected	18548
Independent reflections	4889 [R_{int} = 0.0665, R_{sigma} = 0.0840]
Data/restraints/parameters	4889/1/253
Goodness-of-fit on F^2	1.021
Final R indexes [I>=2σ (I)]	R_1 = 0.0570, wR_2 = 0.1346
Final R indexes [all data]	R_1 = 0.1148, wR_2 = 0.1551
Largest diff. peak/hole / e Å^{-3}	0.29/-0.24

(*E*)-3-(1-mesityl-3-oxo-2-(trimethylsilyl)prop-1-en-1-yl)benzaldehyde (**62**).

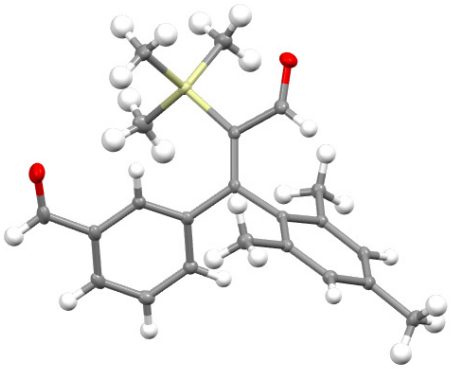

Supplementary Fig. 18. X-ray structure of compound **62**. Thermal ellipsoids are drawn at the 50% probability level.

Supplementary Table 21. Crystal data and structure refinement for compound **62**.

Crystal data and structure refinement for compound **62** (328-11, bm140320_1_1).

Identification code	bm140320_1_1
Empirical formula	$C_{22}H_{26}O_2Si$
Formula weight	350.52
Temperature/K	100.0(1)
Crystal system	monoclinic
Space group	$P2_1/c$
a/Å	9.1023(7)
b/Å	17.6579(15)
c/Å	12.0789(9)
α/°	90
β/°	94.953(2)
γ/°	90
Volume/Å^3	1934.2(3)
Z	4
ρ_{calc}g/cm^3	1.204
μ/mm^{-1}	0.133
F(000)	752.0
Crystal size/mm^3	0.16 × 0.14 × 0.1
Radiation	MoKα (λ = 0.71073)
2Θ range for data collection/°	4.096 to 61.082
Index ranges	$-12 \leq h \leq 12$, $-25 \leq k \leq 25$, $-15 \leq l \leq 17$
Reflections collected	23843
Independent reflections	5913 [R_{int} = 0.0559, R_{sigma} = 0.0529]
Data/restraints/parameters	5913/0/232
Goodness-of-fit on F^2	1.016
Final R indexes [I>=2σ (I)]	R_1 = 0.0467, wR_2 = 0.1082
Final R indexes [all data]	R_1 = 0.0767, wR_2 = 0.1216
Largest diff. peak/hole / e Å^{-3}	0.50/-0.26

(Z)-3-mesityl-2,3-diphenylacrylaldehyde (**64**).

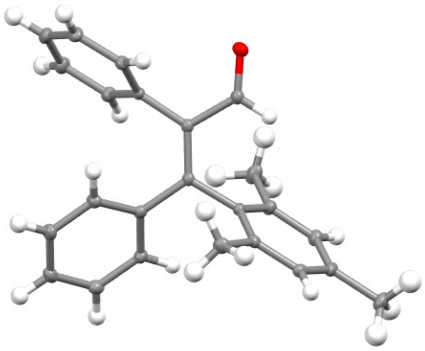

Supplementary Fig. 19. X-ray structure of compound **64**. Thermal ellipsoids are drawn at the 50% probability level.

Supplementary Table 22. Crystal data and structure refinement for compound **64**.

Crystal data and structure refinement for compound **64** (320-04, bm130320_1_1).

Identification code	bm130320_1_1
Empirical formula	$C_{24}H_{22}O$
Formula weight	326.41
Temperature/K	100.0(1)
Crystal system	triclinic
Space group	P-1
a/Å	8.337(7)
b/Å	9.731(9)
c/Å	11.818(11)
α/°	103.49(2)
β/°	98.52(2)
γ/°	101.66(2)
Volume/Å^3	893.6(14)
Z	2
ρ_{calc}g/cm^3	1.213
μ/mm^{-1}	0.072
F(000)	348.0
Crystal size/mm^3	0.16 × 0.12 × 0.06
Radiation	MoKα (λ = 0.71073)
2Θ range for data collection/°	3.622 to 61.596
Index ranges	-11 ≤ h ≤ 11, -14 ≤ k ≤ 14, -16 ≤ l ≤ 17
Reflections collected	21193
Independent reflections	5556 [R_{int} = 0.0460, R_{sigma} = 0.0463]
Data/restraints/parameters	5556/0/229
Goodness-of-fit on F^2	1.029
Final R indexes [I>=2σ (I)]	R_1 = 0.0483, wR_2 = 0.1114
Final R indexes [all data]	R_1 = 0.0753, wR_2 = 0.1241
Largest diff. peak/hole / e Å^{-3}	0.40/-0.23

6,8-bis(diphenylphosphaneyl)dinaphtho[2,1-b:1',2'-d]furan (U-DNFphos, **L08**).

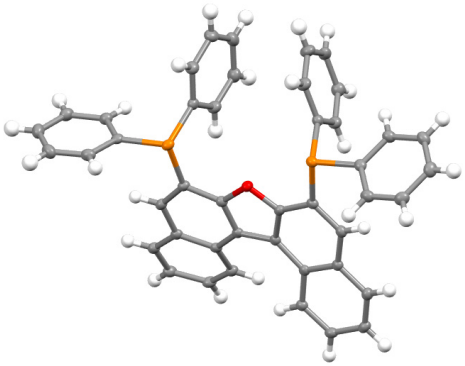

Supplementary Fig. 20. X-ray structure of compound **L08**. Thermal ellipsoids are drawn at the 50% probability level.

Supplementary Table 23. Crystal data and structure refinement for compound **L08**.

Crystal data and structure refinement for compound **L08** (bm270819_2_1).

Identification code	bm270819_2_1
Empirical formula	$C_{44}H_{30}OP_2$
Formula weight	636.62
Temperature/K	100.0(1)
Crystal system	monoclinic
Space group	$P2_1/c$
a/Å	10.65063(7)
b/Å	19.02946(12)
c/Å	16.01500(10)
α/°	90
β/°	91.6925(6)
γ/°	90
Volume/Å^3	3244.44(4)
Z	4
ρ_{calc}g/cm^3	1.303
μ/mm^{-1}	1.484
F(000)	1328.0
Crystal size/mm^3	0.115 × 0.087 × 0.027
Radiation	CuKα (λ = 1.54184)
2Θ range for data collection/°	7.216 to 159.248
Index ranges	$-12 \le h \le 13$, $-24 \le k \le 24$, $-20 \le l \le 18$
Reflections collected	50422
Independent reflections	6969 [R_{int} = 0.0373, R_{sigma} = 0.0178]
Data/restraints/parameters	6969/0/424
Goodness-of-fit on F^2	1.048
Final R indexes [I>=2σ (I)]	R_1 = 0.0324, wR_2 = 0.0855
Final R indexes [all data]	R_1 = 0.0362, wR_2 = 0.0878
Largest diff. peak/hole / e Å^{-3}	0.31/-0.32

[(TDMPP-*O,P*)Pd(Cl)(o-toluoyl)] (**69**).

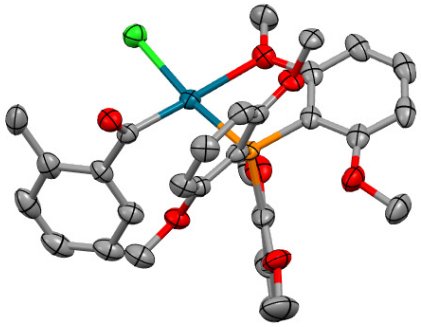

Supplementary Fig. 21. X-ray structure of compound **69**. Thermal ellipsoids are drawn at the 50% probability level, hydrogen atoms are omitted for clarity.

Supplementary Table 24. Crystal data and structure refinement for compound **69**.

Crystal data and structure refinement for compound **69** (bm021219_1_1).

Identification code	bm021219_1_1
Empirical formula	$C_{32}H_{34}ClO_7PPd$
Formula weight	703.41
Temperature/K	100.0(1)
Crystal system	triclinic
Space group	P-1
a/Å	10.9494(2)
b/Å	11.1621(2)
c/Å	13.2564(2)
α/°	76.4930(10)
β/°	88.4080(10)
γ/°	76.7110(10)
Volume/Å^3	1532.60(5)
Z	2
ρ_{calc}g/cm^3	1.524
μ/mm^{-1}	6.570
F(000)	720.0
Crystal size/mm^3	0.127 × 0.098 × 0.07
Radiation	Cu Kα (λ = 1.54184)
2Θ range for data collection/°	6.86 to 159.482
Index ranges	-13 ≤ h ≤ 13, -14 ≤ k ≤ 14, -16 ≤ l ≤ 16
Reflections collected	41654
Independent reflections	6482 [R_{int} = 0.0464, R_{sigma} = 0.0276]
Data/restraints/parameters	6482/126/386
Goodness-of-fit on F^2	1.085
Final R indexes [I>=2σ (I)]	R_1 = 0.0319, wR_2 = 0.0856
Final R indexes [all data]	R_1 = 0.0374, wR_2 = 0.0898
Largest diff. peak/hole / e Å^{-3}	0.70/-0.65

13. NMR spectra

13.1. Carboformylation

(*Z*)-2-propyl-3-(*o*-tolyl)hex-2-enal (**1**).

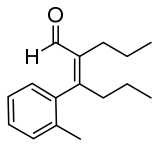

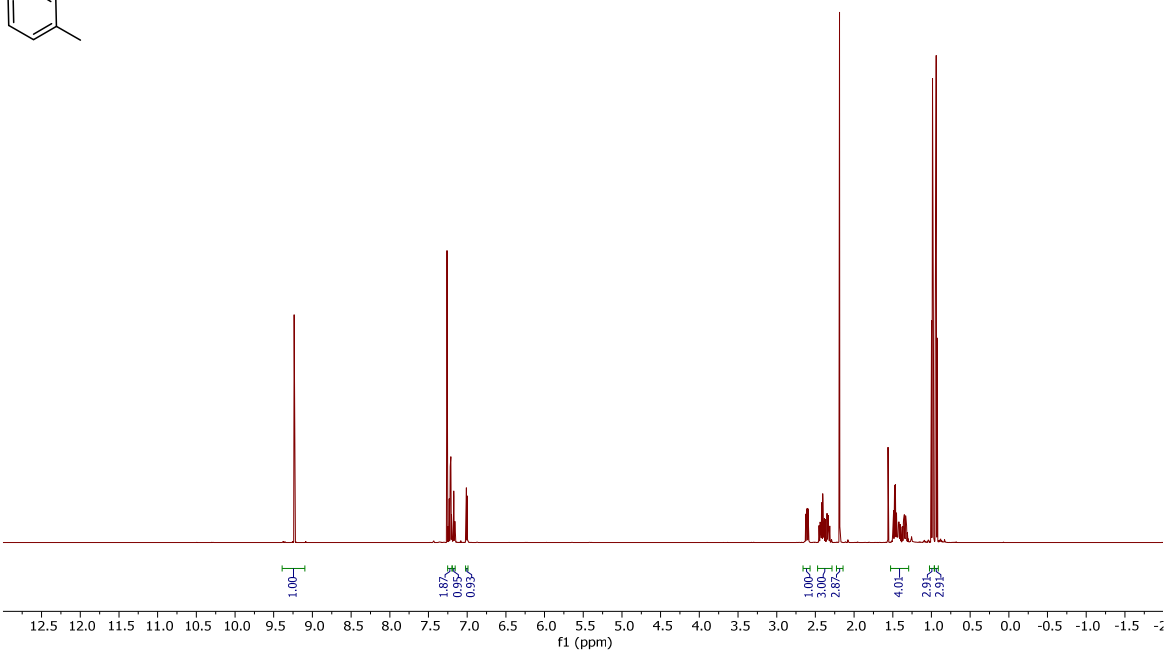

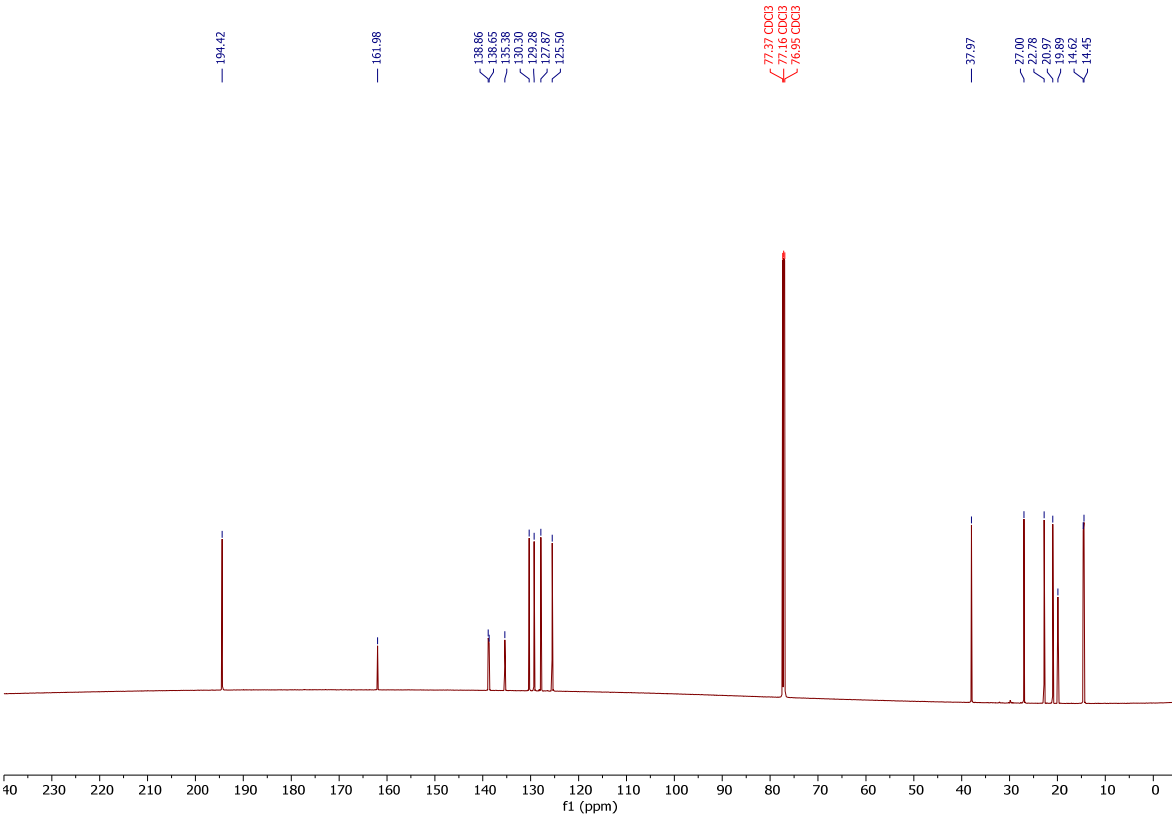

NOESY

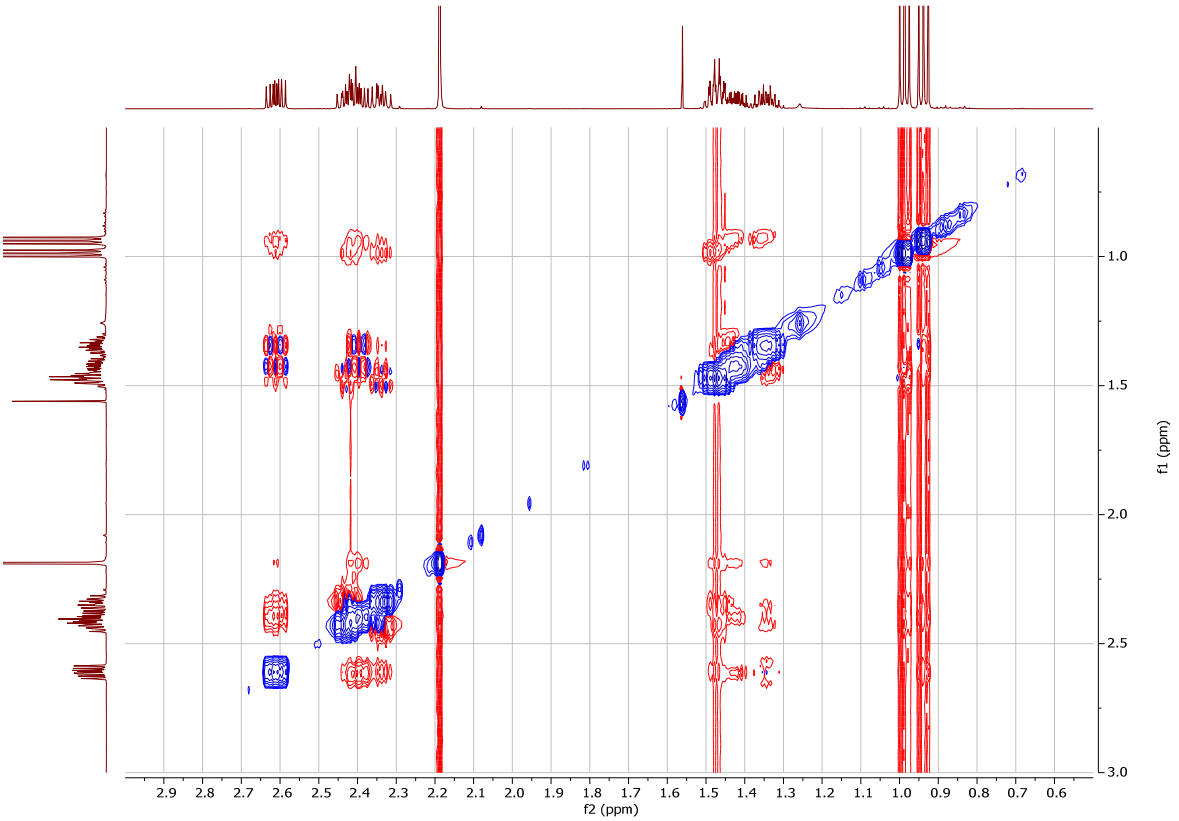
2.9 2.8 2.7 2.6 2.5 2.4 2.3 2.2 2.1 2.0 1.9 1.8 1.7 1.6 1.5 1.4 1.3 1.2 1.1 1.0 0.9 0.8 0.7 0.6
f2 (ppm)
1.0
1.5
2.0
2.5
3.0
f1 (ppm)

(*Z*)-2-propyl-3-(*o*-tolyl)hex-2-enal-1-*d* (**2**).

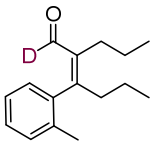

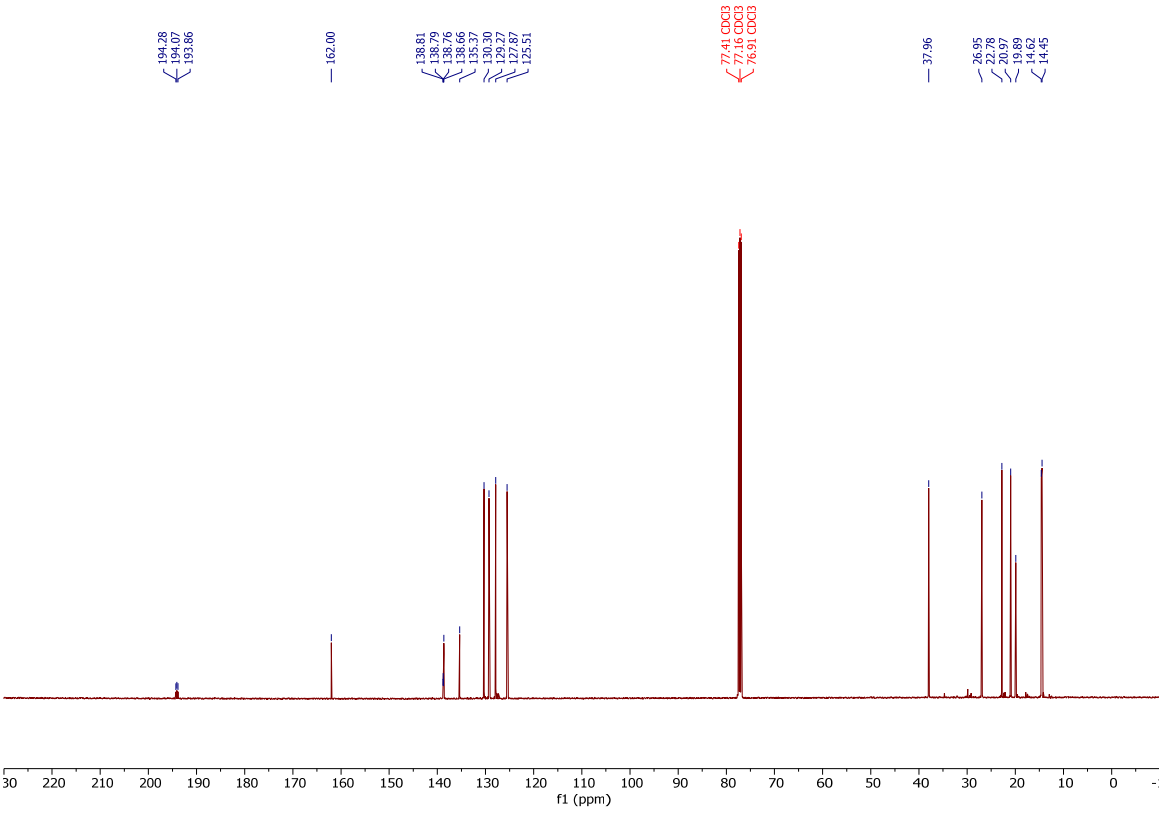

NOESY

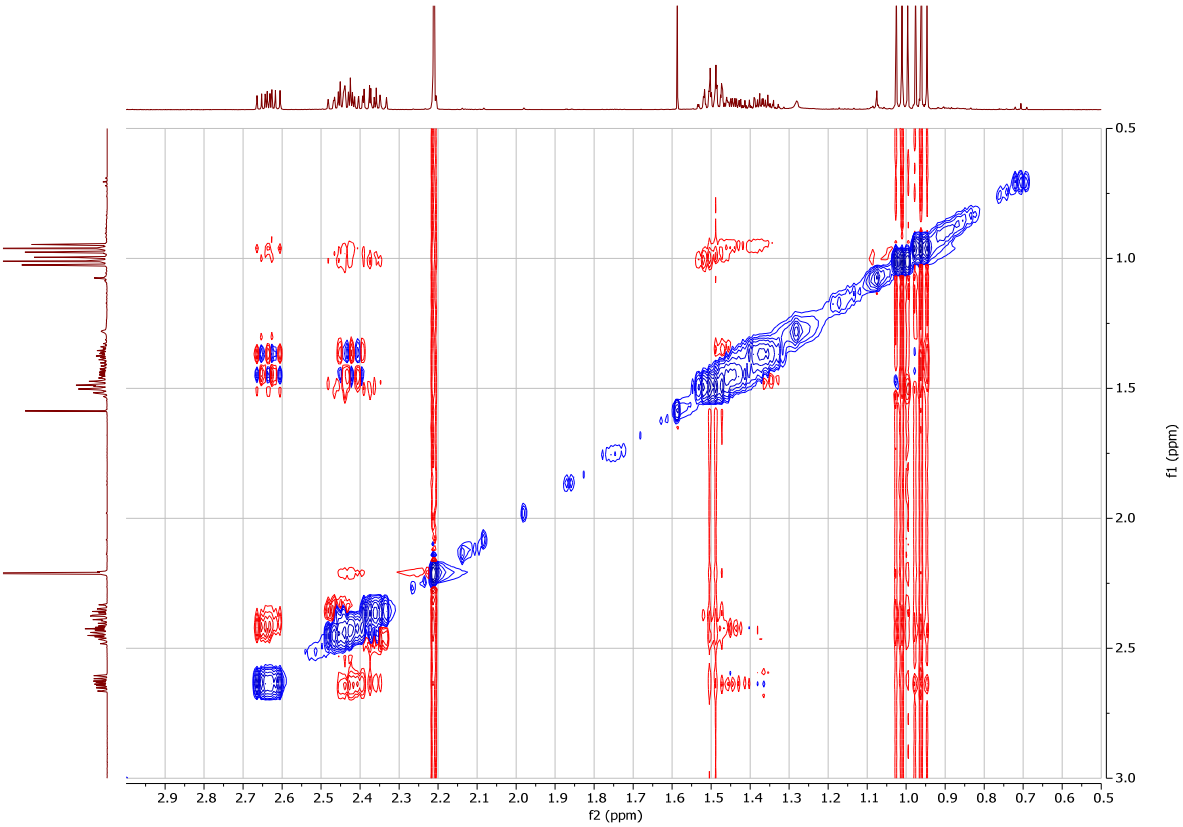
0.5
1.0
1.5
2.0
2.5
3.0
f1 (ppm)
2.9 2.8 2.7 2.6 2.5 2.4 2.3 2.2 2.1 2.0 1.9 1.8 1.7 1.6 1.5 1.4 1.3 1.2 1.1 1.0 0.9 0.8 0.7 0.6 0.5
f2 (ppm)

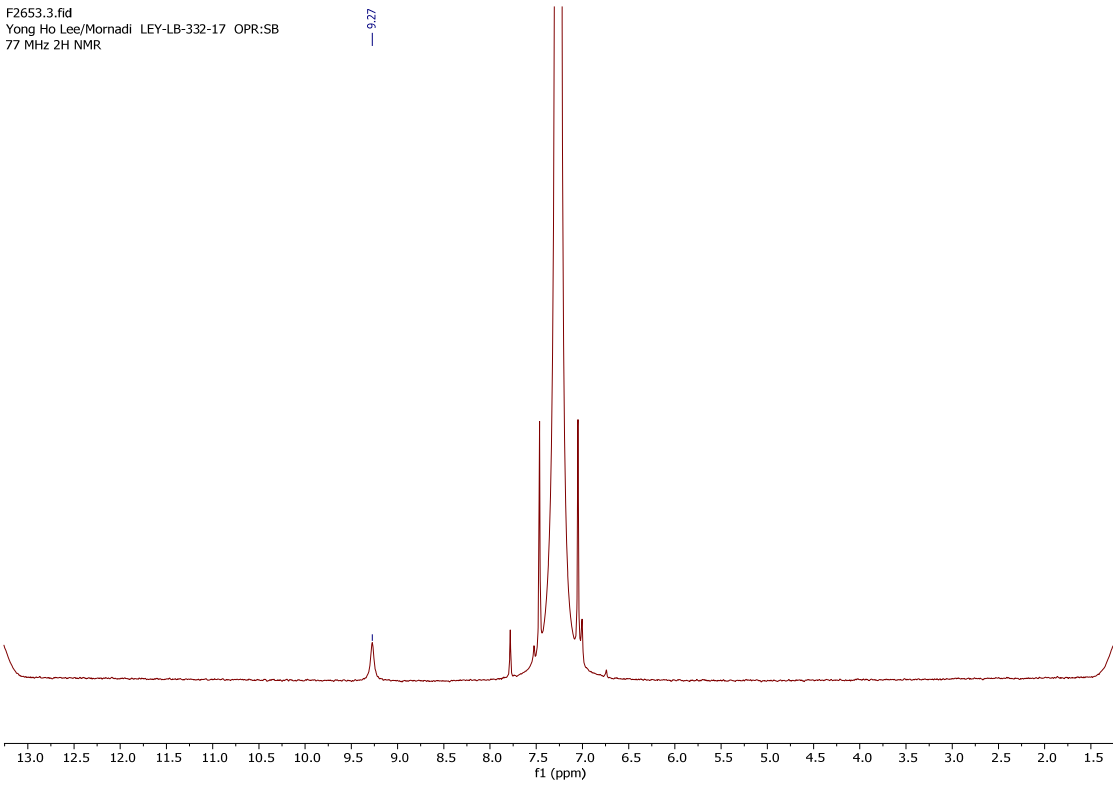
F2653.3.fid
Yong Ho Lee/Mornadi LEY-LB-332-17 OPR:SB
77 MHz 2H NMR
9.27
13.0 12.5 12.0 11.5 11.0 10.5 10.0 9.5 9.0 8.5 8.0 7.5 7.0 6.5 6.0 5.5 5.0 4.5 4.0 3.5 3.0 2.5 2.0 1.5
f1 (ppm)

(*Z*)-3-(2-ethoxyphenyl)-2-propylhex-2-enal (**3**).

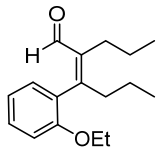

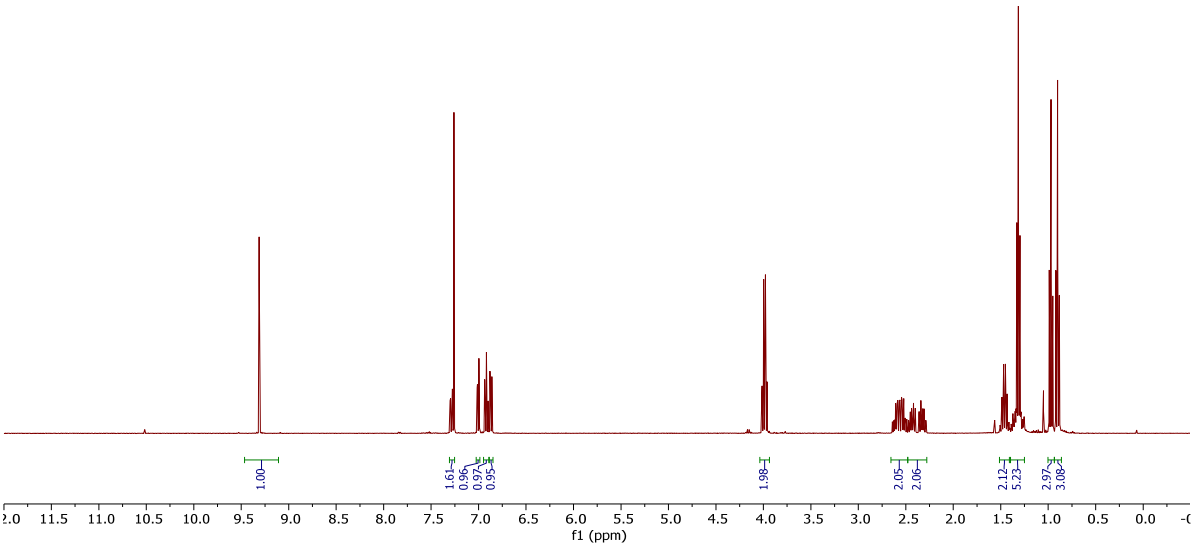

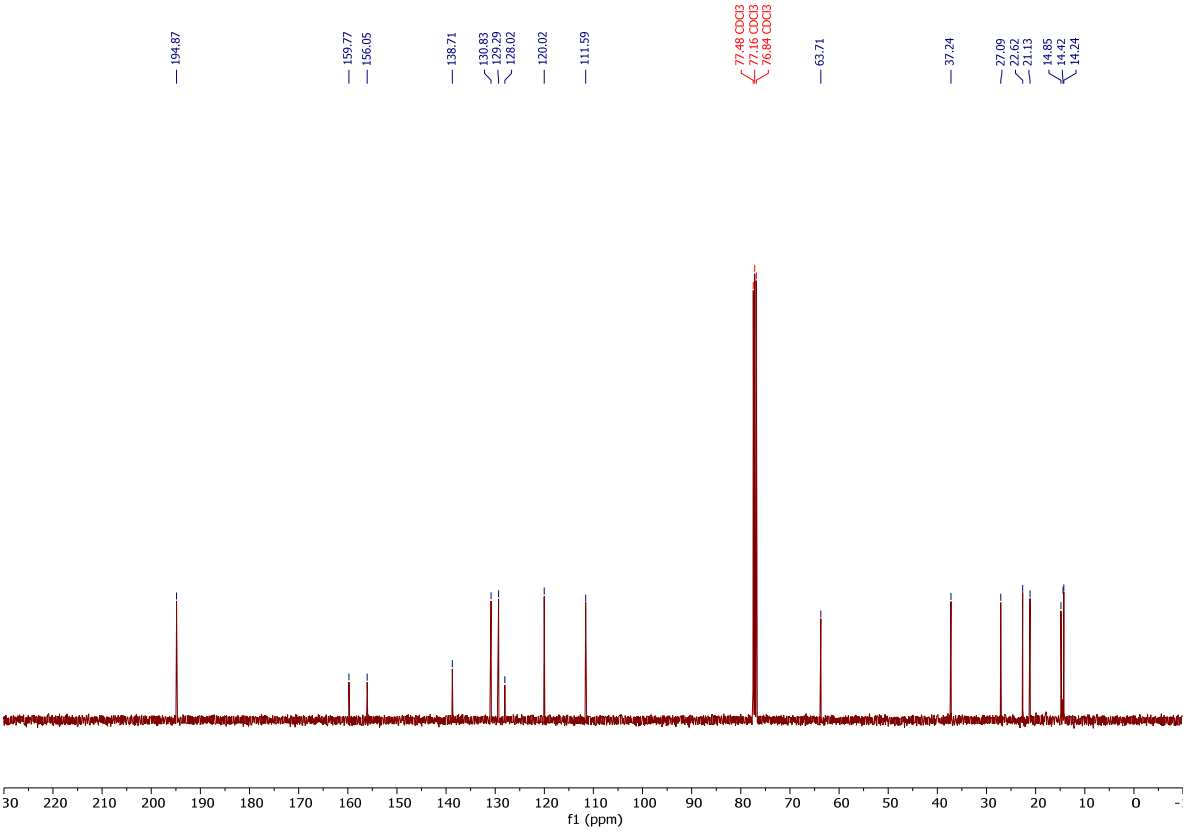

NOESY

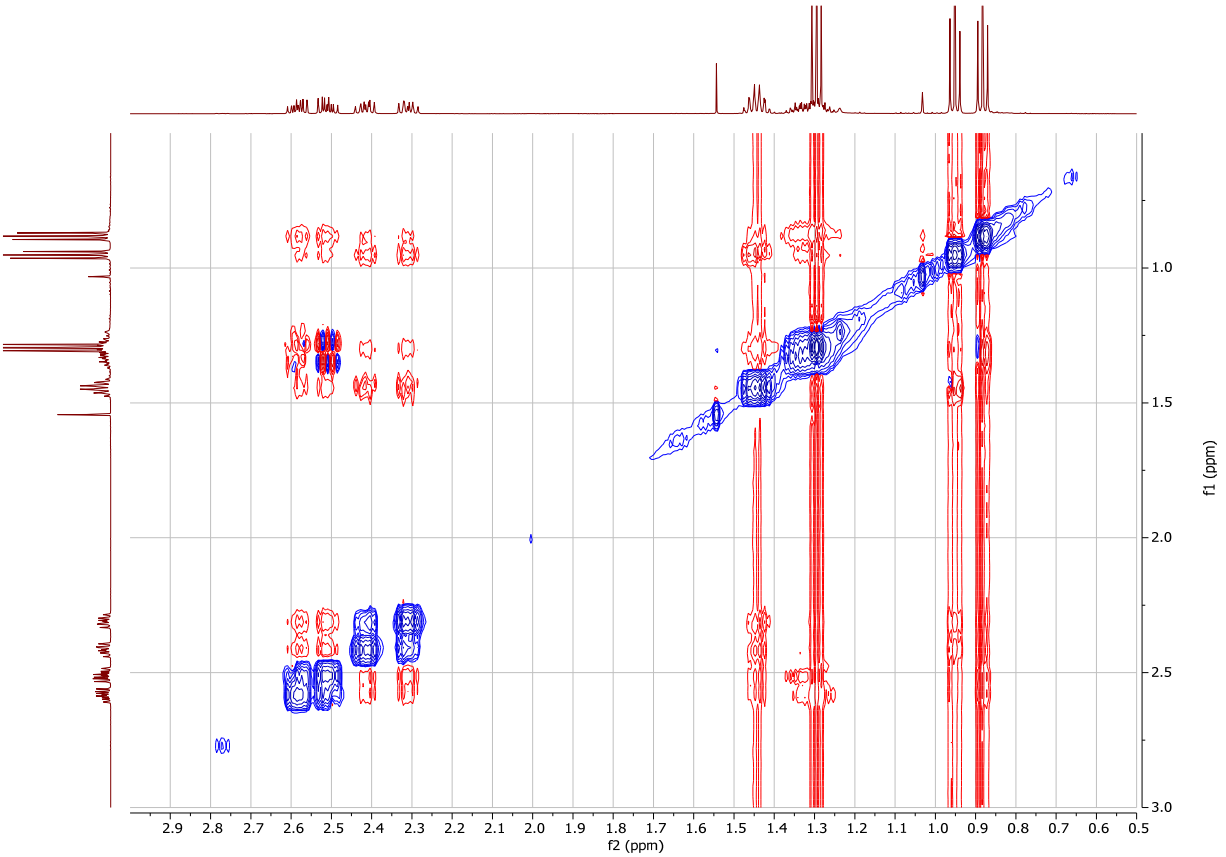
f1 (ppm)
1.0
1.5
2.0
2.5
3.0
2.9 2.8 2.7 2.6 2.5 2.4 2.3 2.2 2.1 2.0 1.9 1.8 1.7 1.6 1.5 1.4 1.3 1.2 1.1 1.0 0.9 0.8 0.7 0.6 0.5
f2 (ppm)

(*Z*)-2-(5-formyloct-4-en-4-yl)phenyl acetate (**4**).

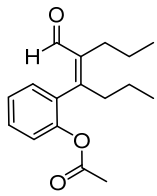

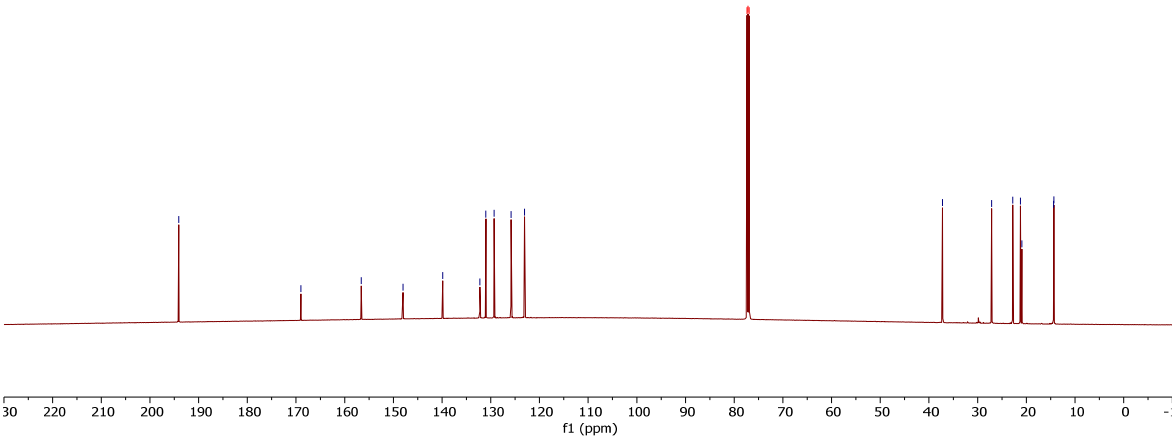

NOESY

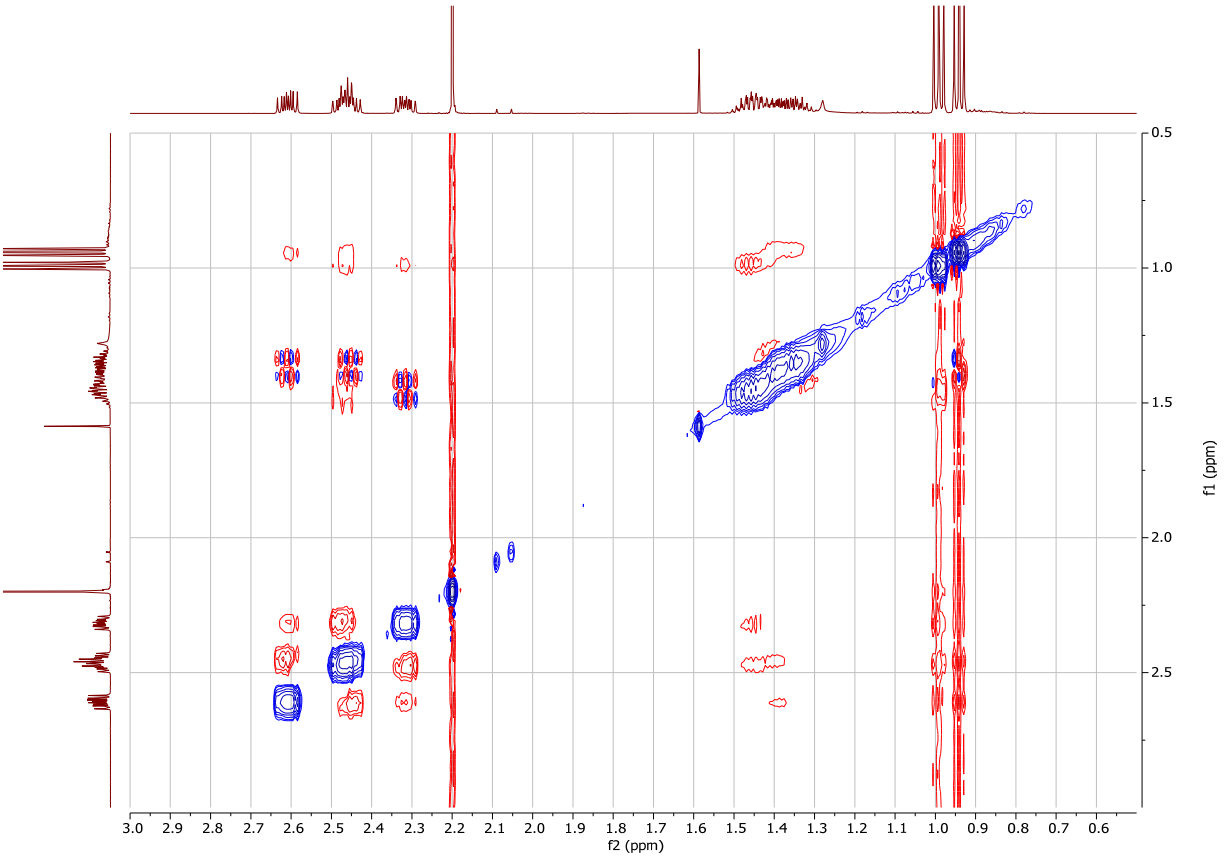
0.5
1.0
1.5
2.0
2.5
f1 (ppm)
3.0 2.9 2.8 2.7 2.6 2.5 2.4 2.3 2.2 2.1 2.0 1.9 1.8 1.7 1.6 1.5 1.4 1.3 1.2 1.1 1.0 0.9 0.8 0.7 0.6
f2 (ppm)

(*Z*)-2-propyl-3-(2-(trifluoromethoxy)phenyl)hex-2-enal (**5**).

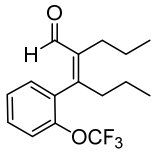

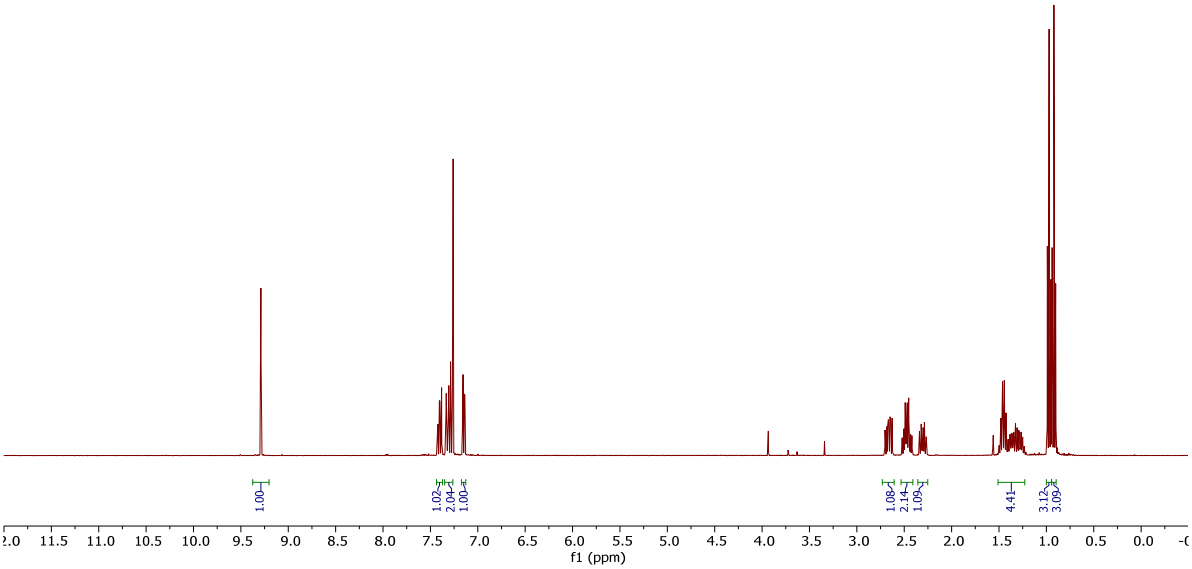

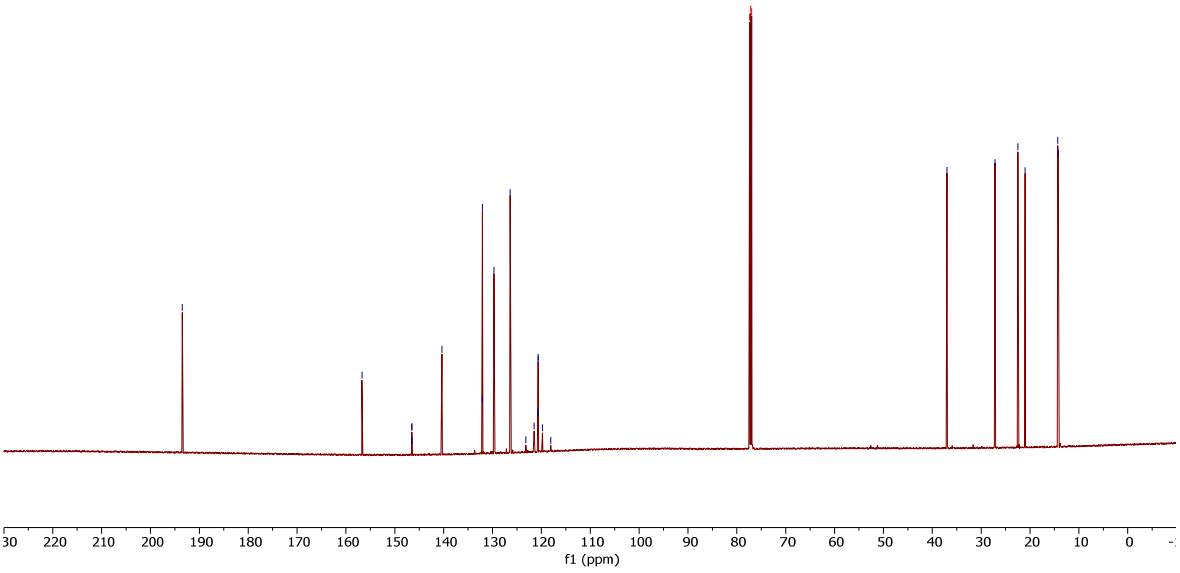

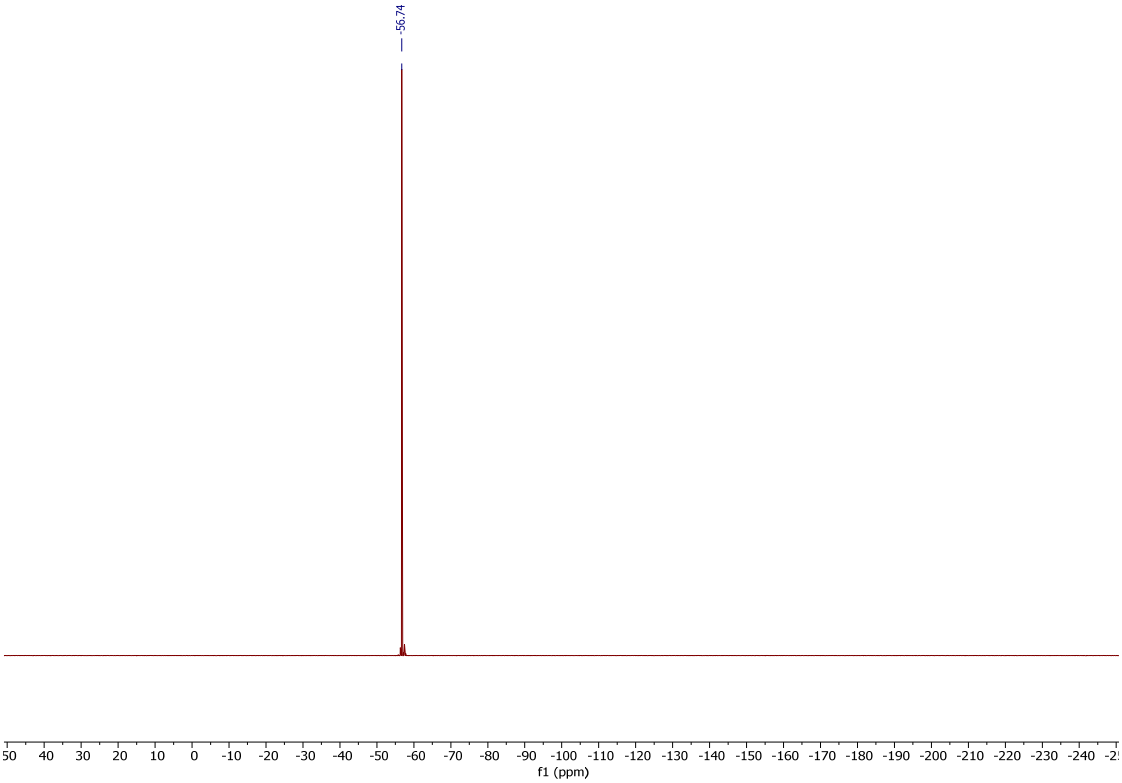
-56.74
50 40 30 20 10 0 -10 -20 -30 -40 -50 -60 -70 -80 -90 -100 -110 -120 -130 -140 -150 -160 -170 -180 -190 -200 -210 -220 -230 -240
f1 (ppm)

NOESY

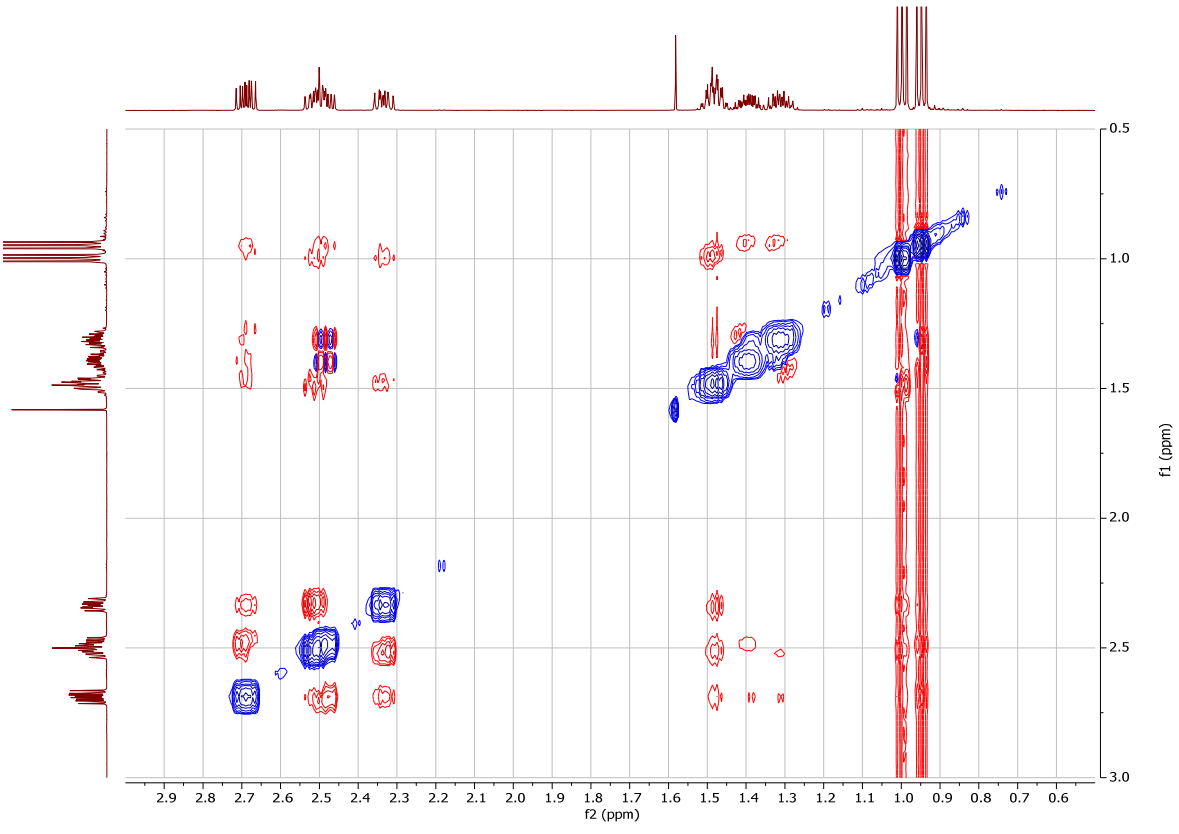
0.5
1.0
1.5
2.0
2.5
3.0
f1 (ppm)
2.9 2.8 2.7 2.6 2.5 2.4 2.3 2.2 2.1 2.0 1.9 1.8 1.7 1.6 1.5 1.4 1.3 1.2 1.1 1.0 0.9 0.8 0.7 0.6
f2 (ppm)

(*Z*)-2-(5-formyloct-4-en-4-yl)benzonitrile (**6-*Z***).

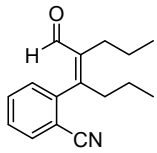

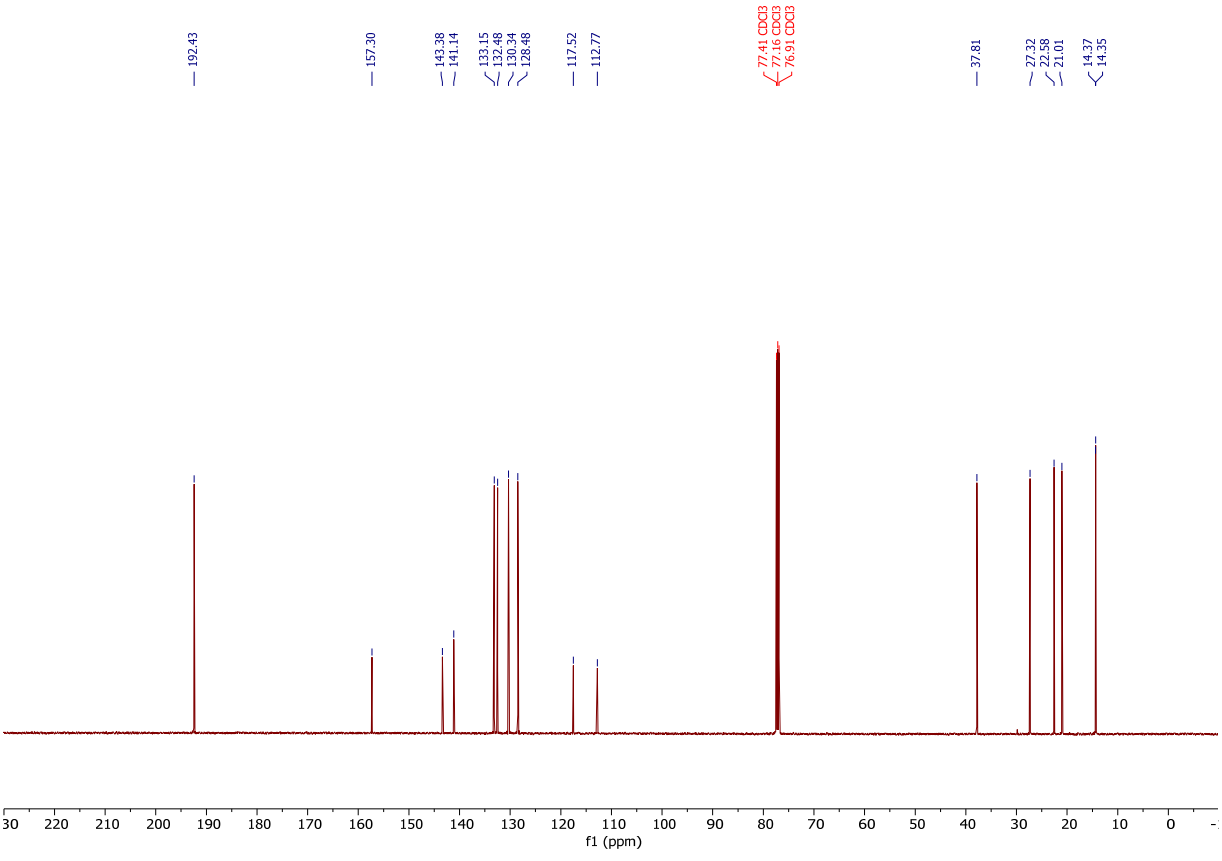

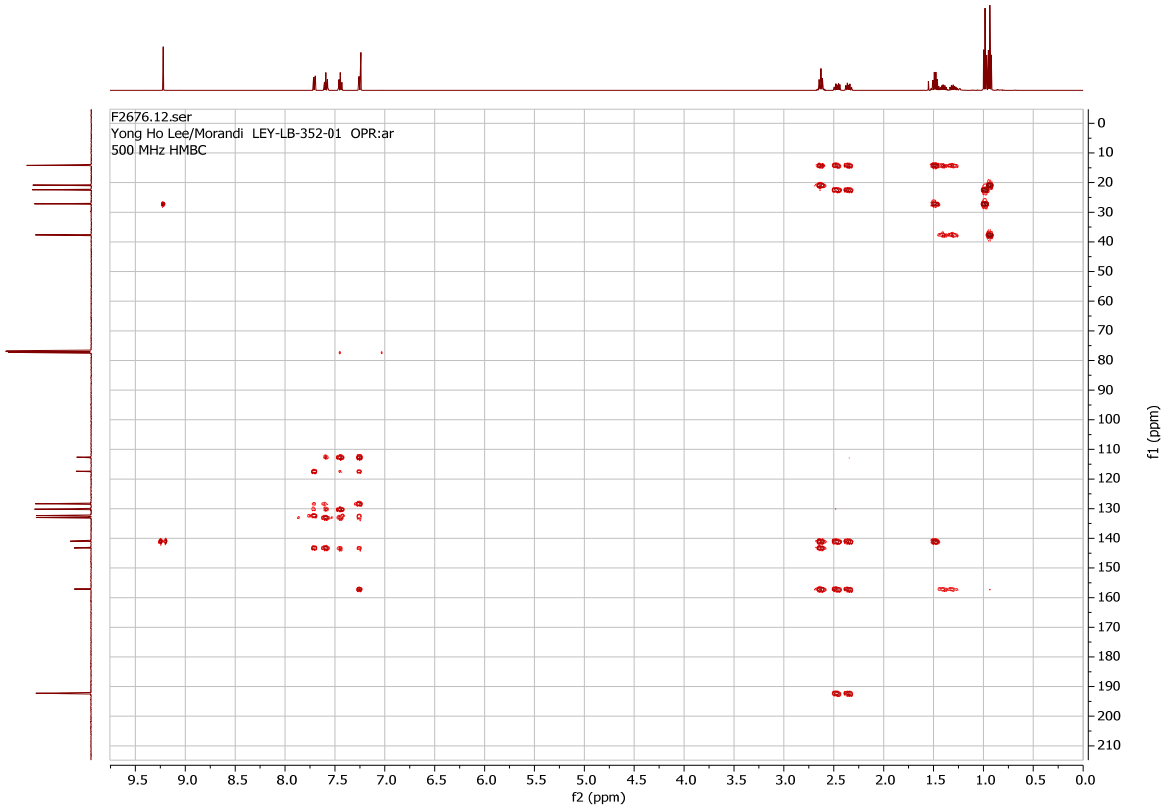
F2676.12.ser
Yong Ho Lee/Morandi LEY-LB-352-01 OPR:ar
500 MHz HMBC
f2 (ppm)
f1 (ppm)

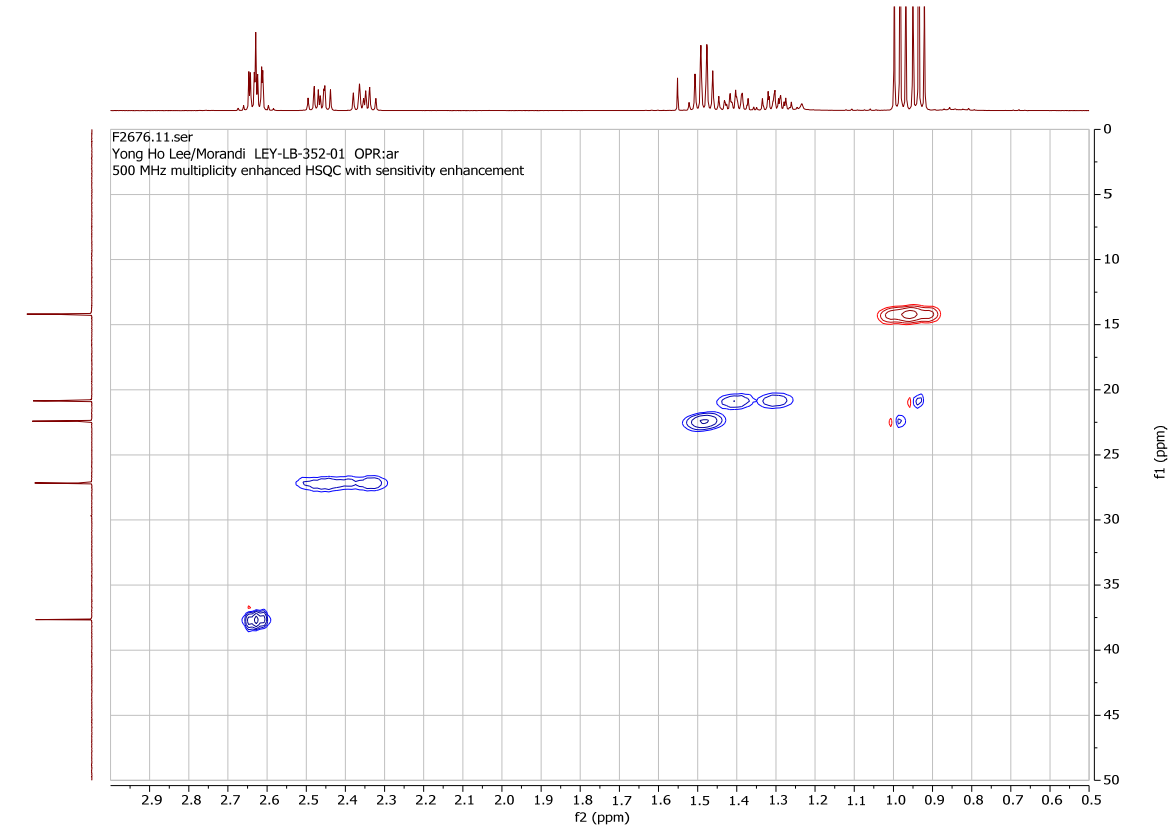
F2676.11.ser
Yong Ho Lee/Morandi LEY-LB-352-01 OPR:ar
500 MHz multiplicity enhanced HSQC with sensitivity enhancement
f2 (ppm)
f1 (ppm)

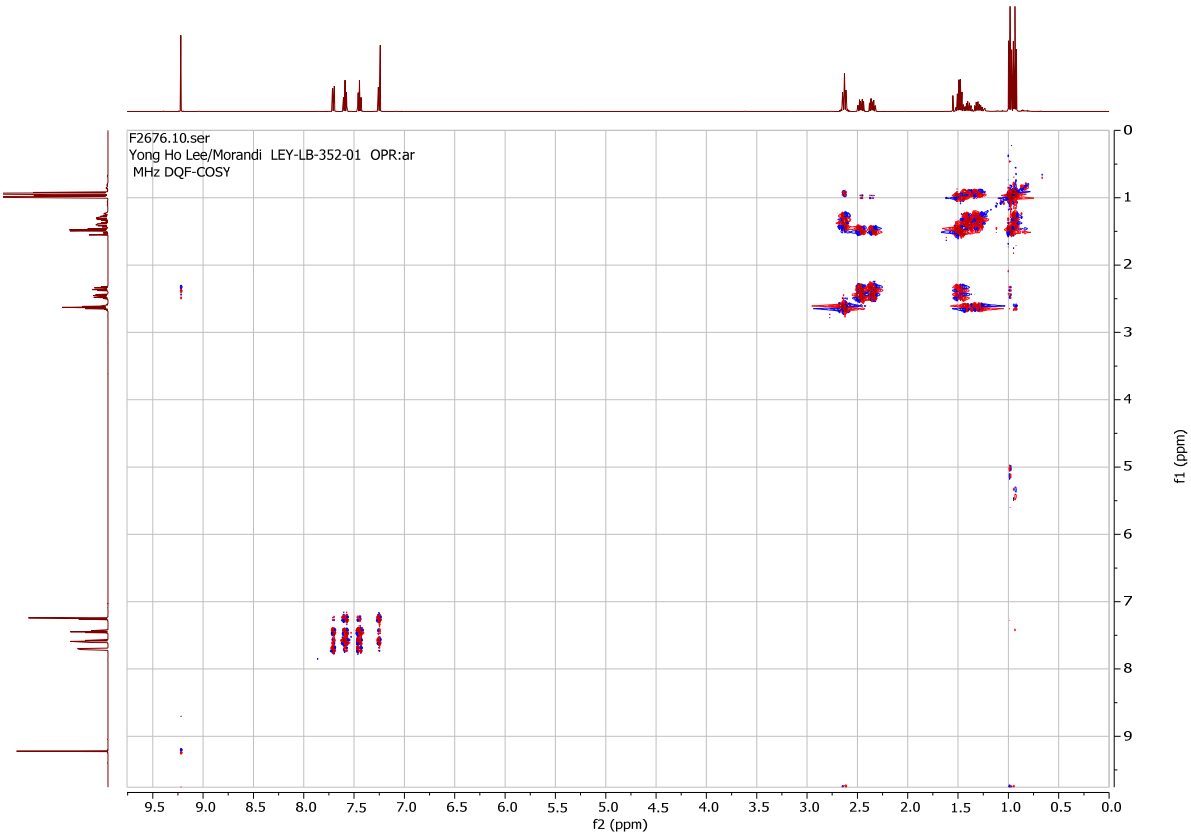
F2676.10.ser
Yong Ho Lee/Morandi LEY-LB-352-01 OPR:ar
MHz DQF-COSY
f2 (ppm)
f1 (ppm)

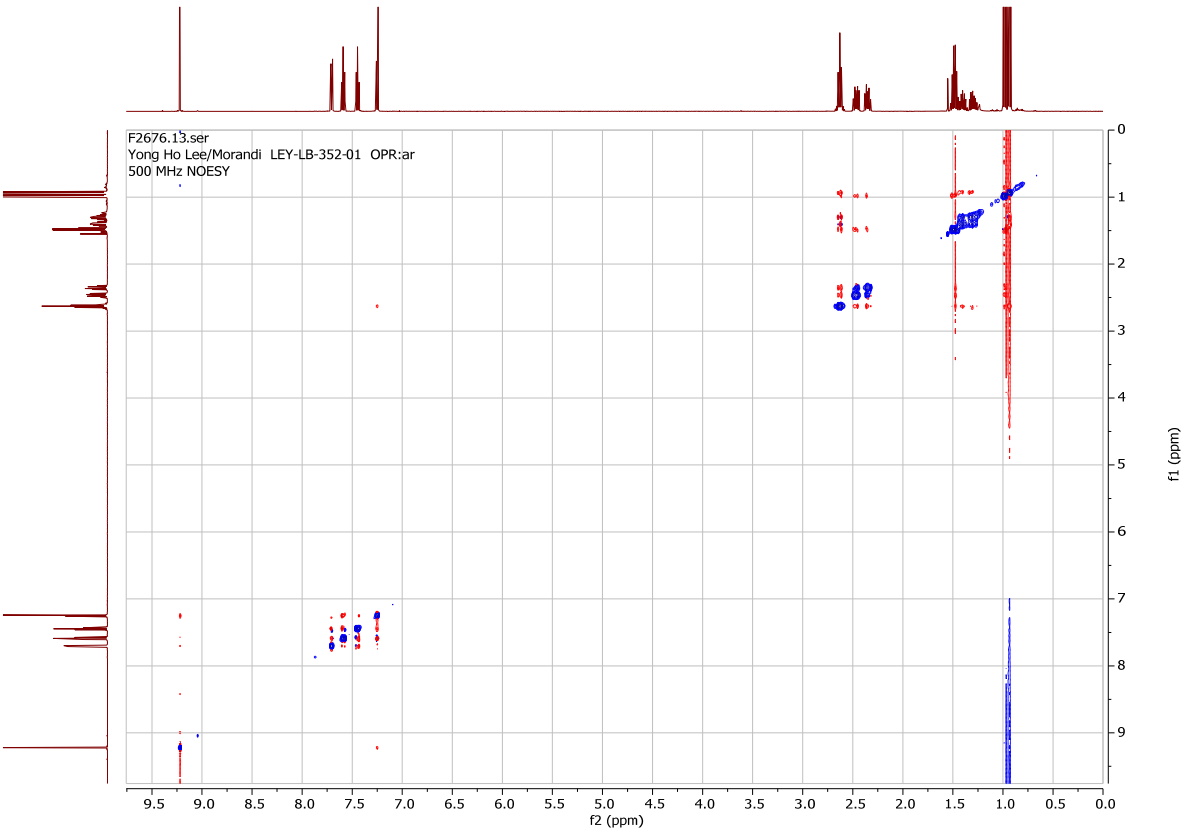
F2676.13.ser
Yong Ho Lee/Morandi LEY-LB-352-01 OPR:ar
500 MHz NOESY
f2 (ppm)
f1 (ppm)

(*E*)-2-(5-formyloct-4-en-4-yl)benzonitrile (**6-*E***).

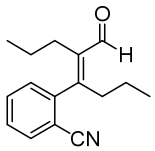

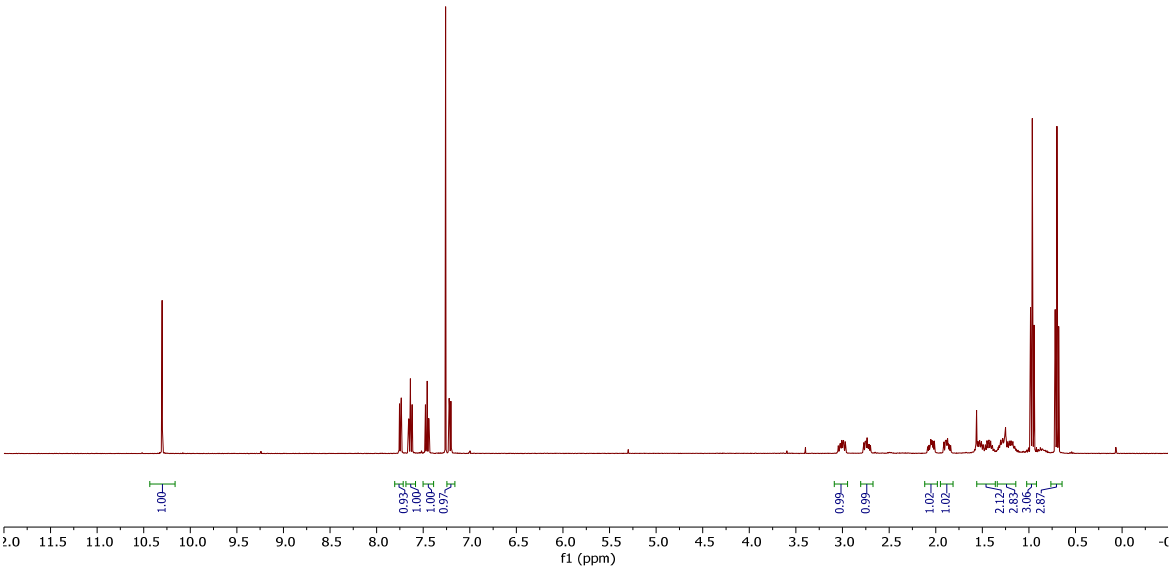

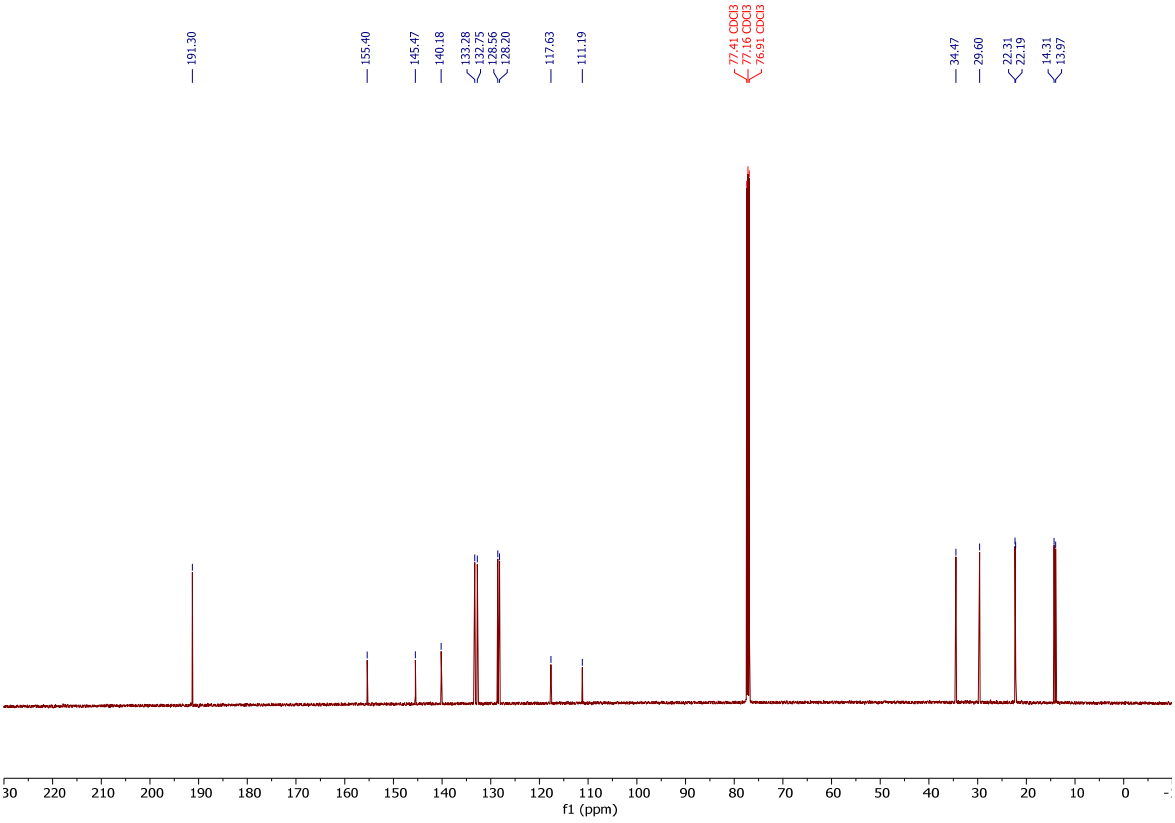

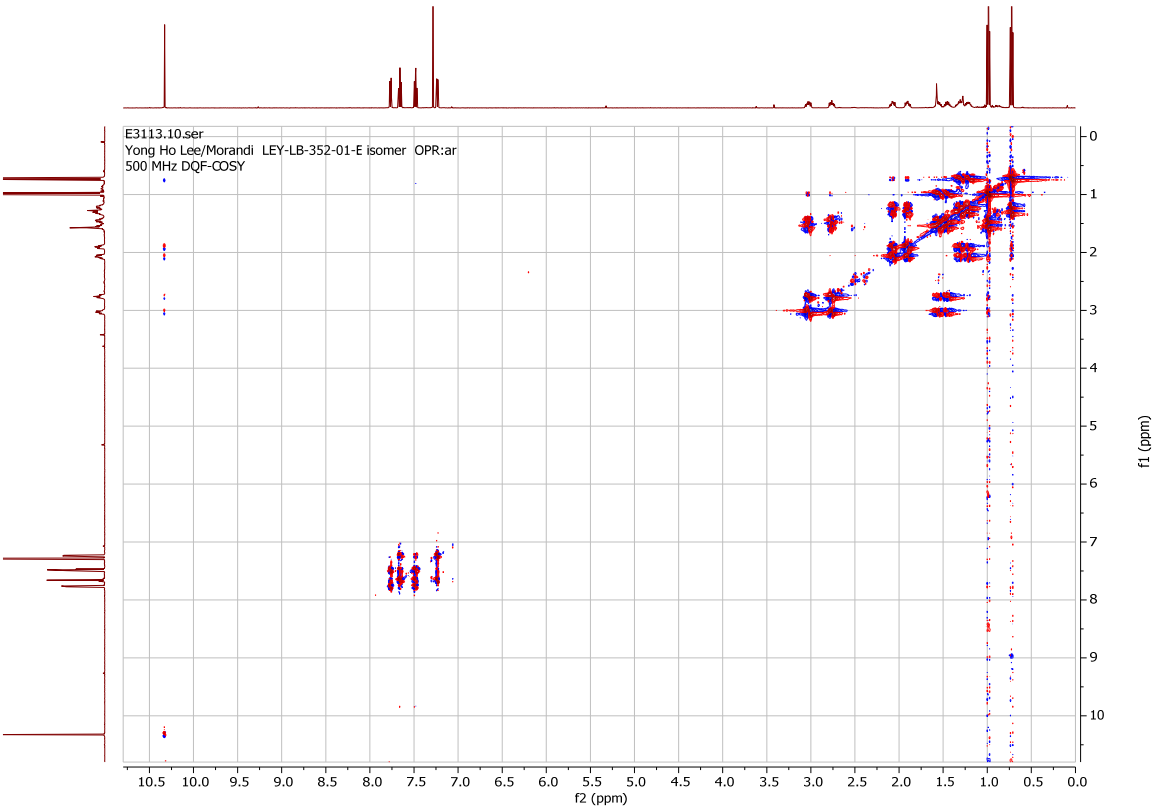
E3113.10.ser
Yong Ho Lee/Morandi LEY-LB-352-01-E isomer OPR:ar
500 MHz DQF-COSY
f2 (ppm)
f1 (ppm)

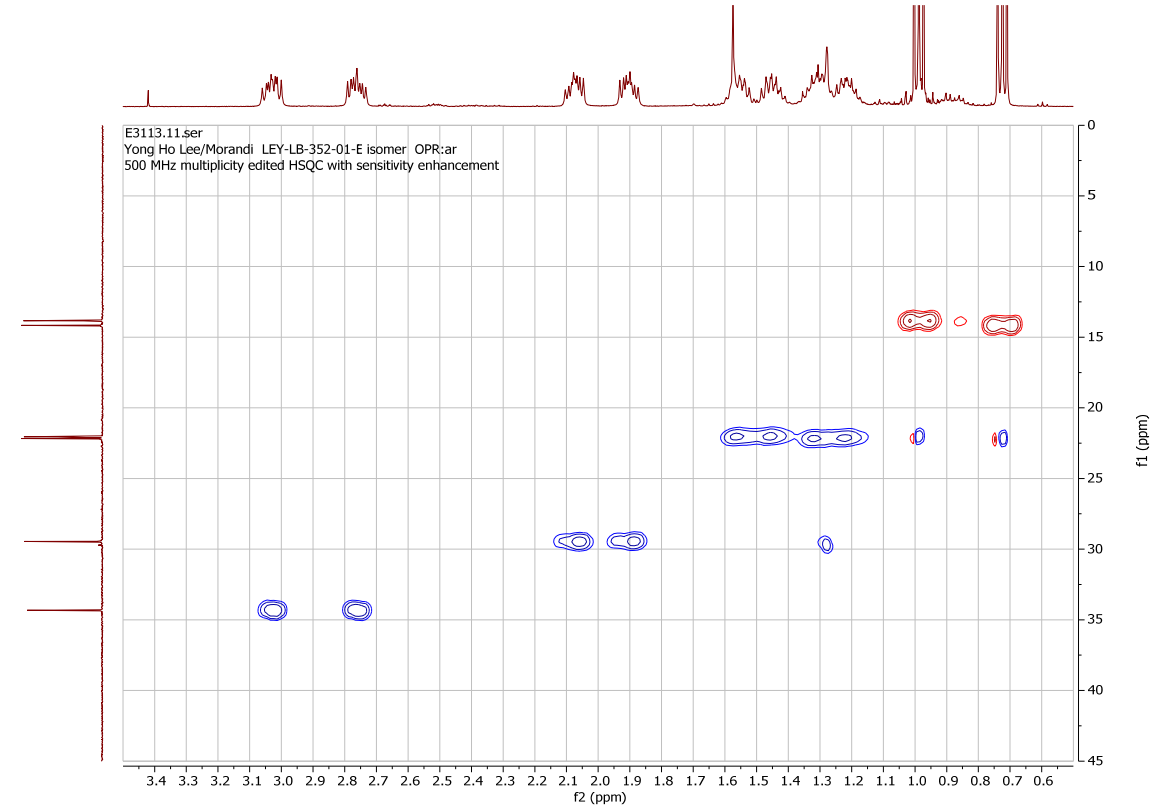
E3113.11.ser
Yong Ho Lee/Morandi LEY-LB-352-01-E isomer OPR:ar
500 MHz multiplicity edited HSQC with sensitivity enhancement
f2 (ppm)
f1 (ppm)

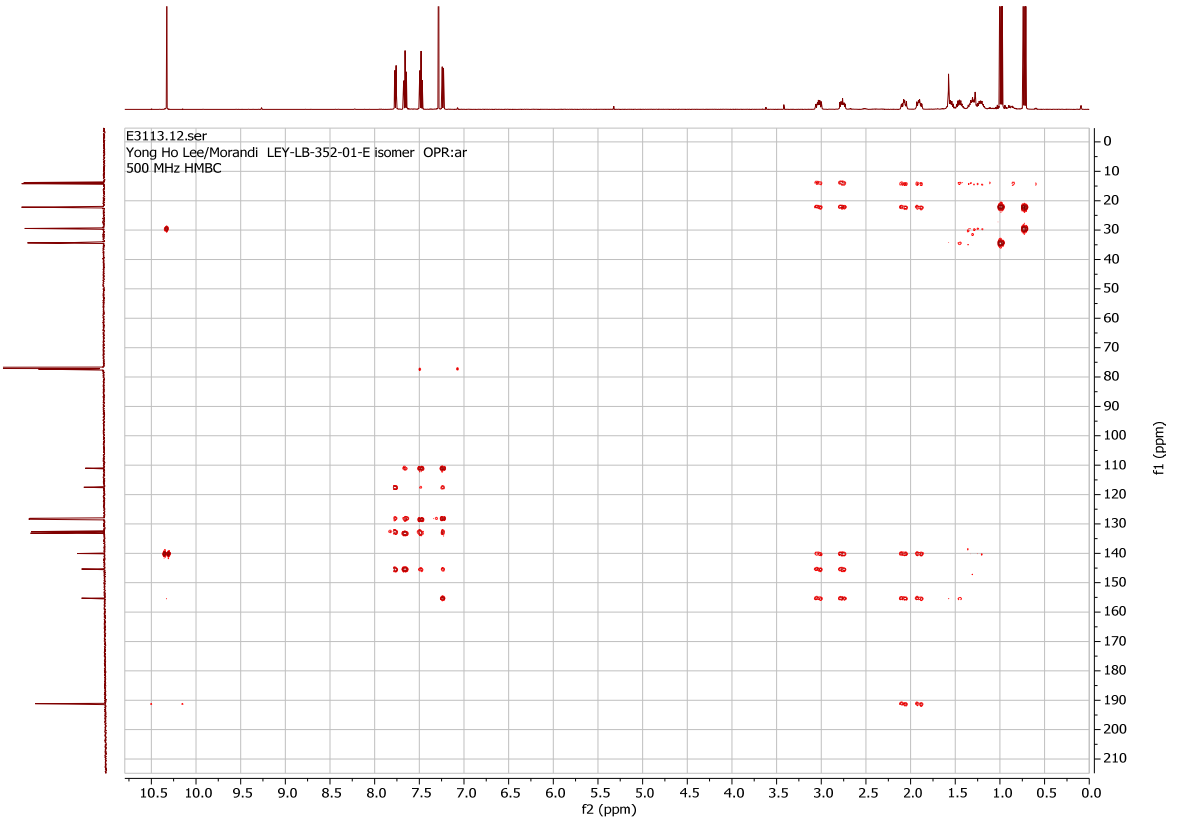
E3113.12.ser
Yong Ho Lee/Morandi LEY-LB-352-01-E isomer OPR:ar
500 MHz HMBC
f2 (ppm)
f1 (ppm)

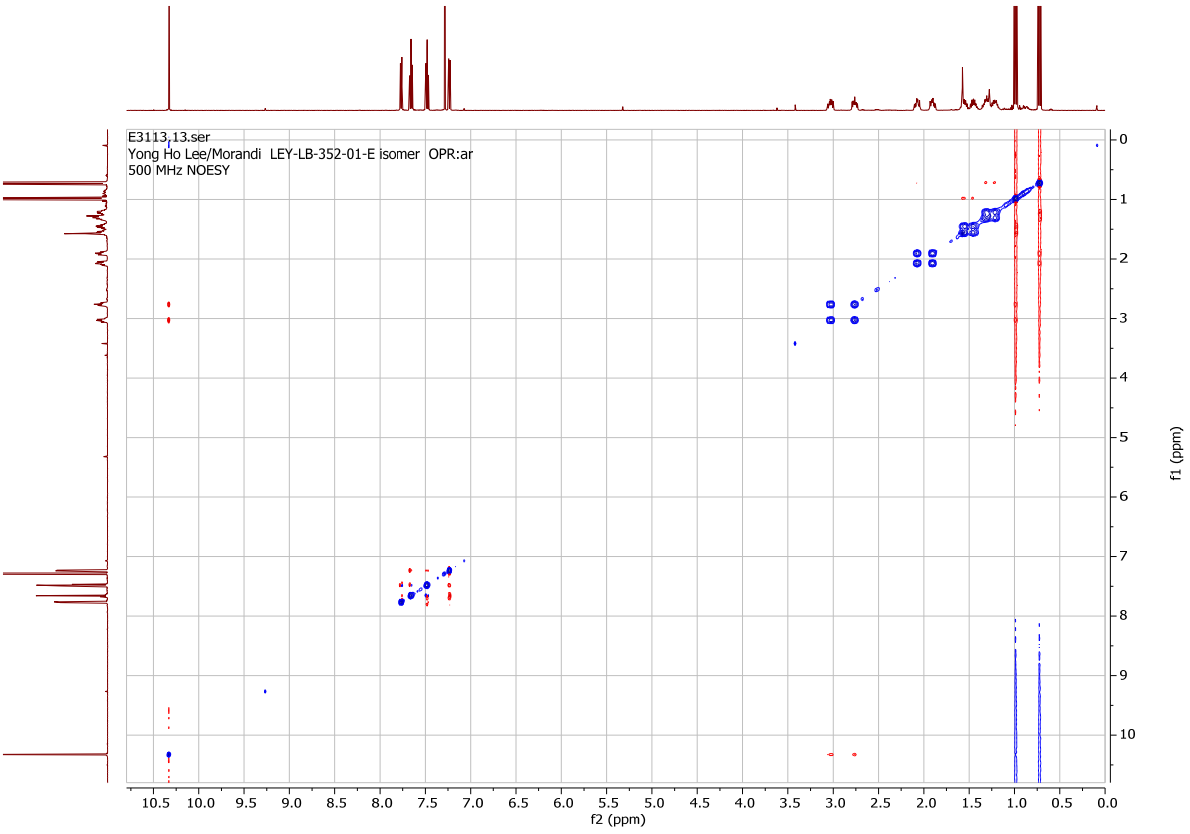
E3113.13.ser
Yong Ho Lee/Morandi LEY-LB-352-01-E isomer OPR:ar
500 MHz NOESY
f2 (ppm)
f1 (ppm)

(*Z*)-2-propyl-3-(2-(trifluoromethyl)phenyl)hex-2-enal (**7**).

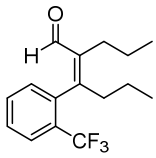

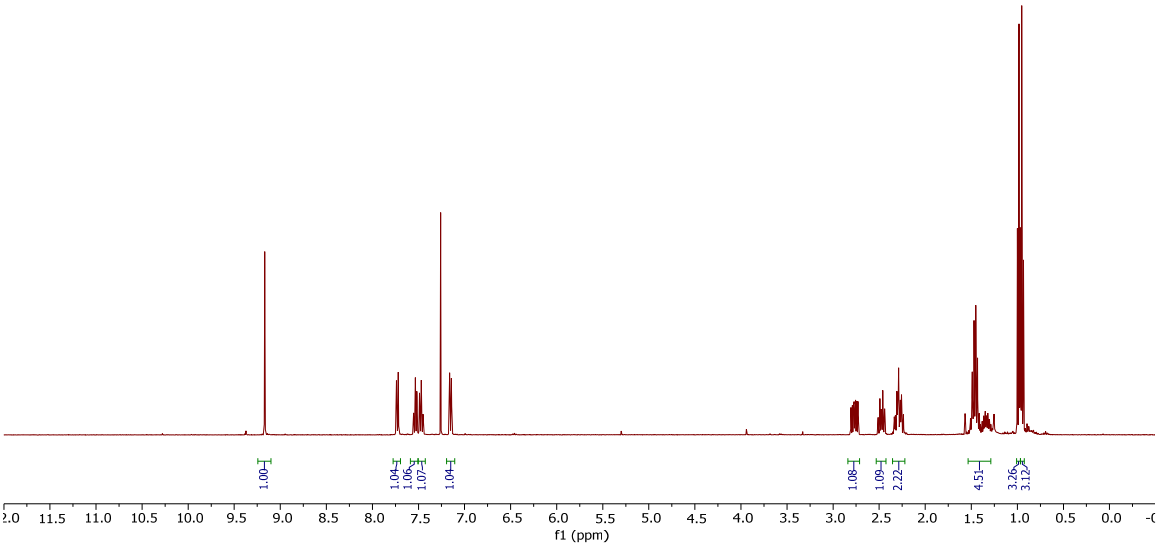

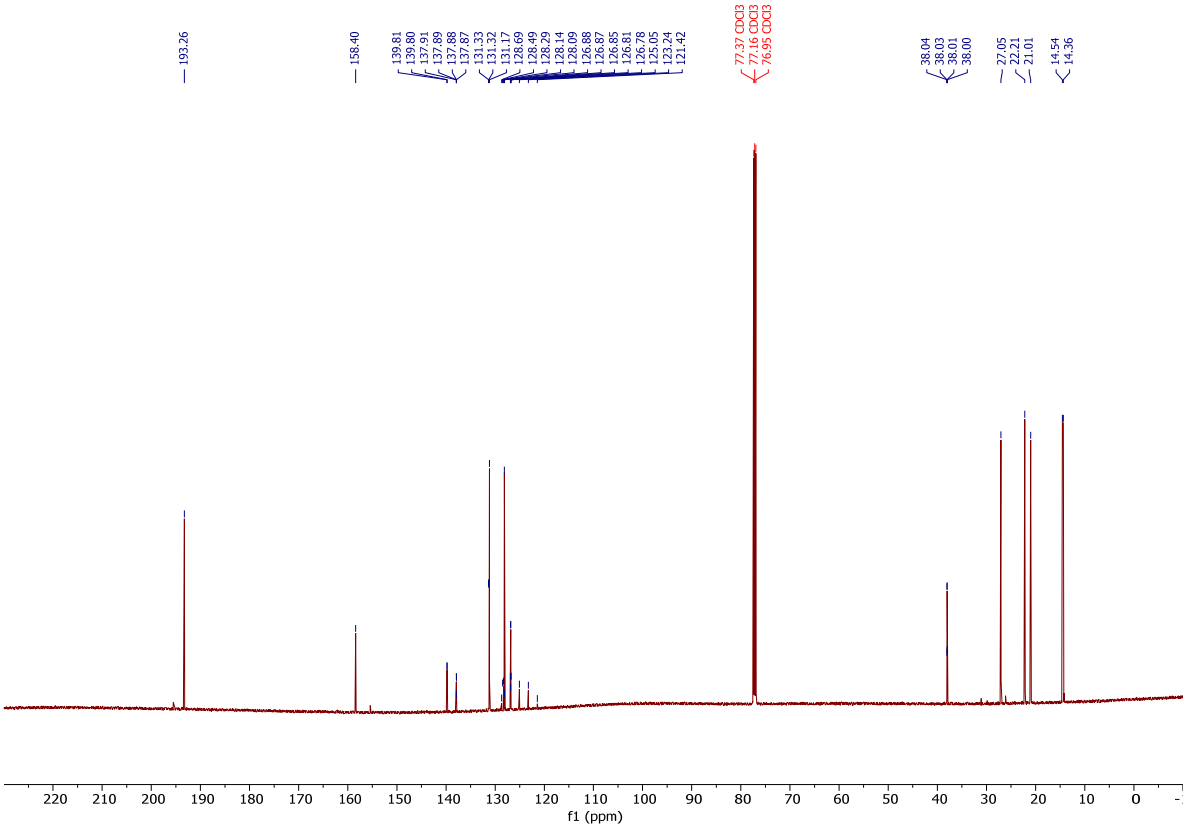

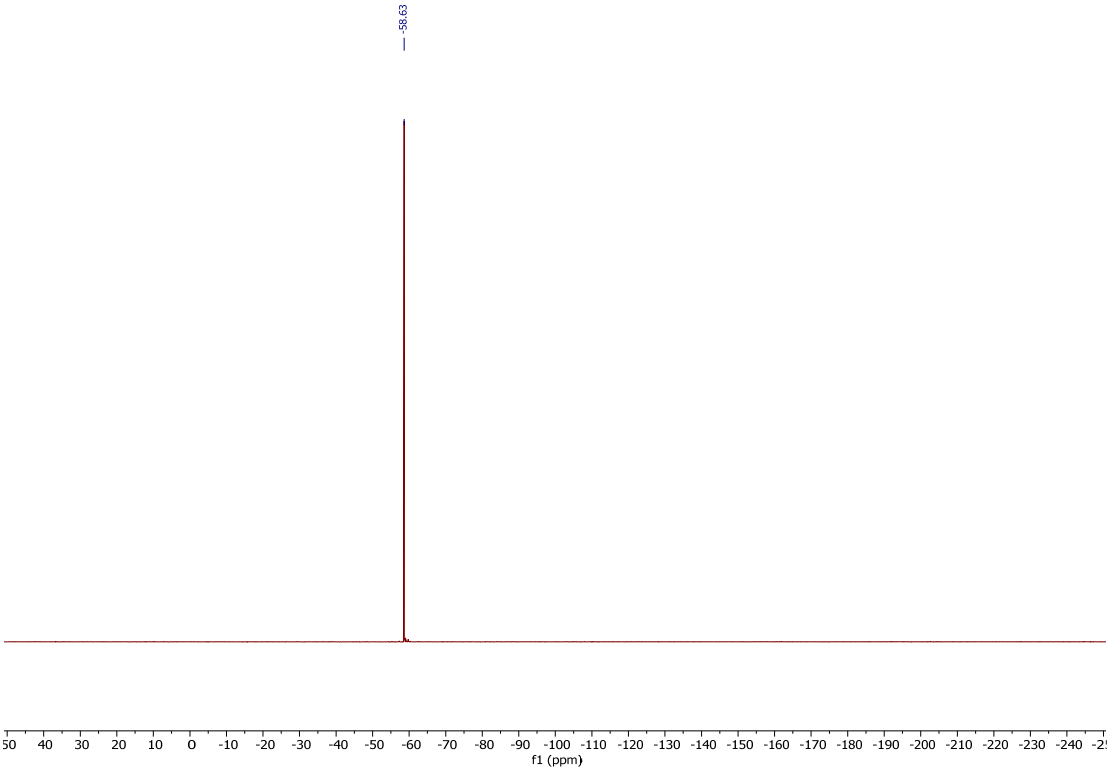

NOESY

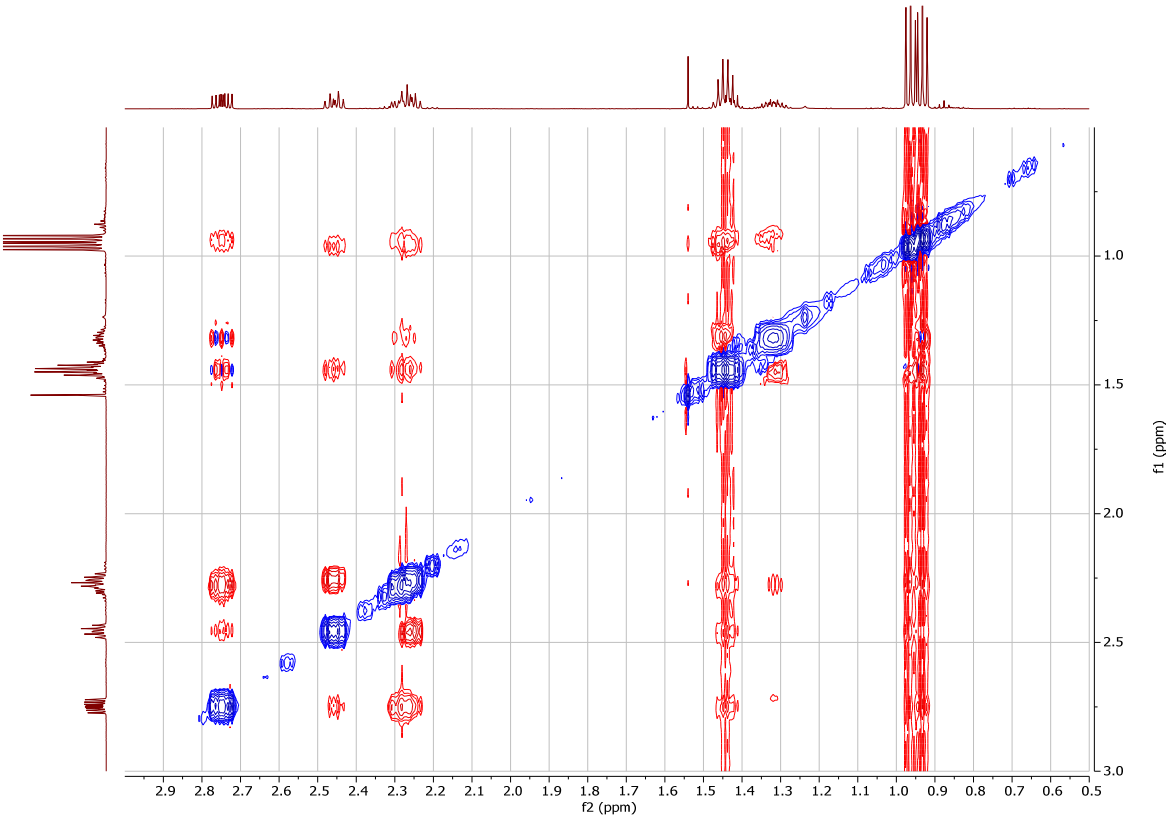

(*Z*)-3-(2,4-dichlorophenyl)-2-propylhex-2-enal (**8**).

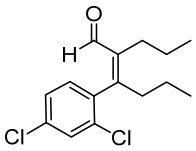

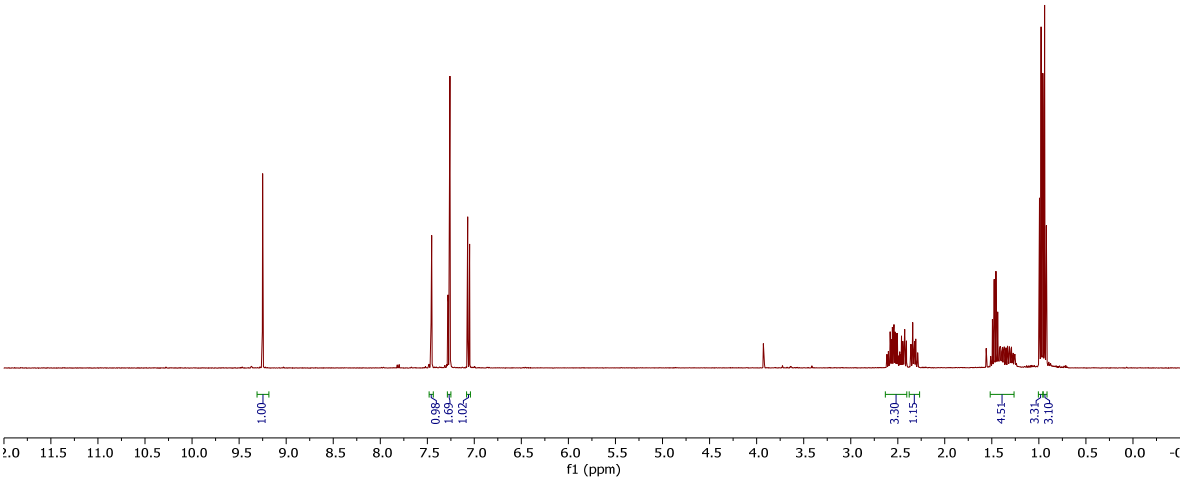

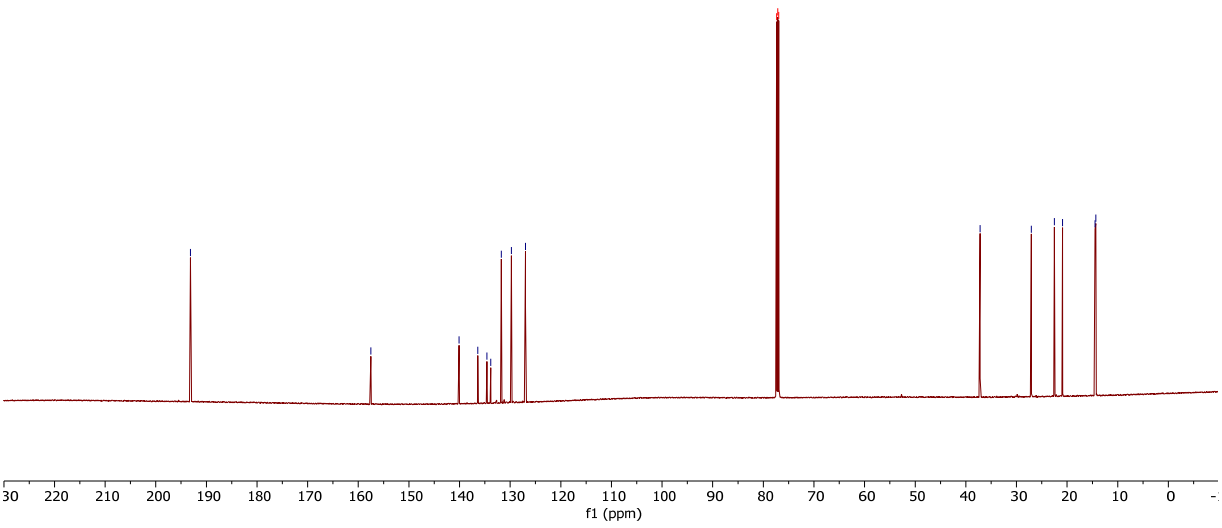

NOESY

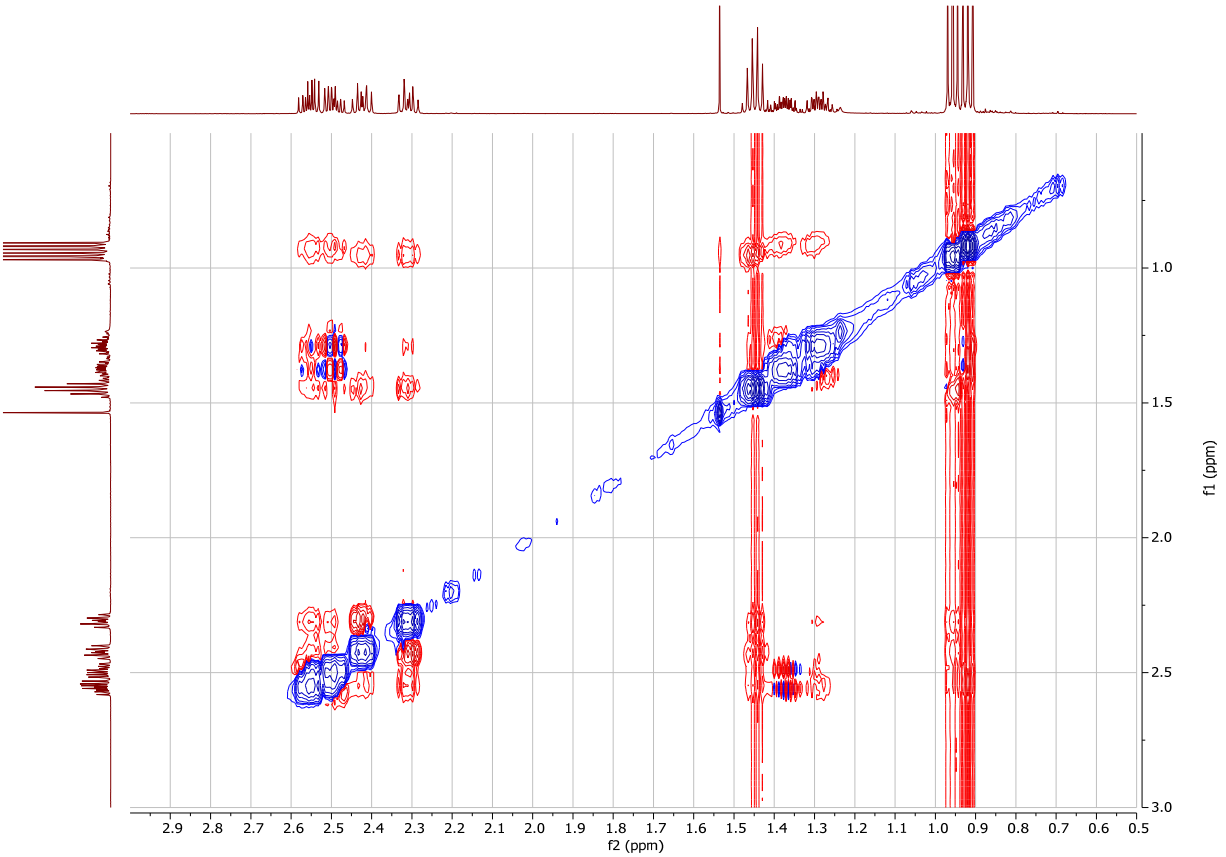
1.0
1.5
2.0
2.5
3.0
f1 (ppm)
2.9 2.8 2.7 2.6 2.5 2.4 2.3 2.2 2.1 2.0 1.9 1.8 1.7 1.6 1.5 1.4 1.3 1.2 1.1 1.0 0.9 0.8 0.7 0.6 0.5
f2 (ppm)

(*Z*)-3-(naphthalen-1-yl)-2-propylhex-2-enal (**9**).

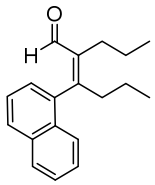

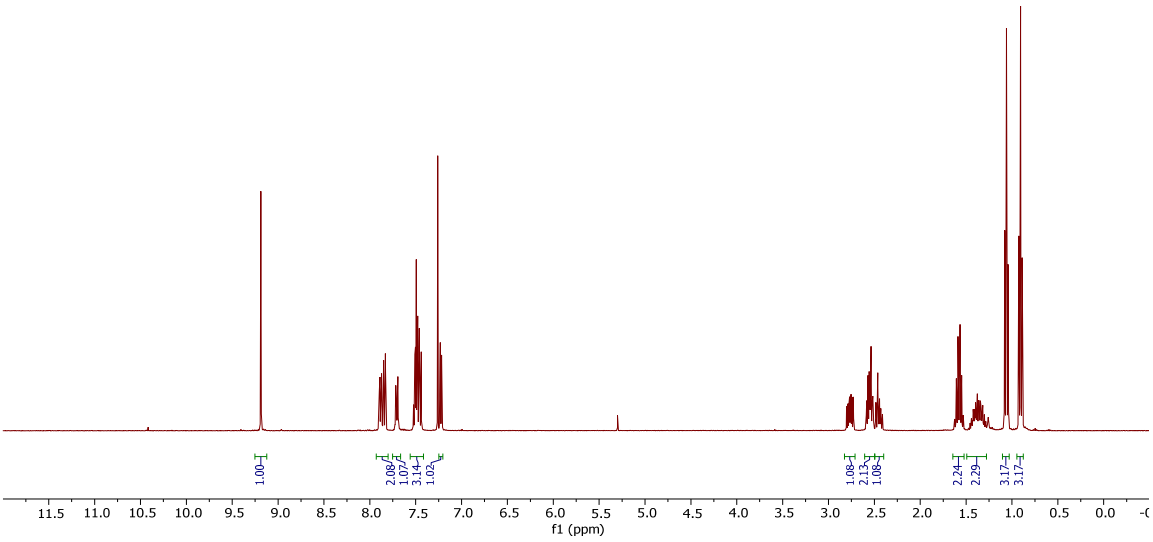

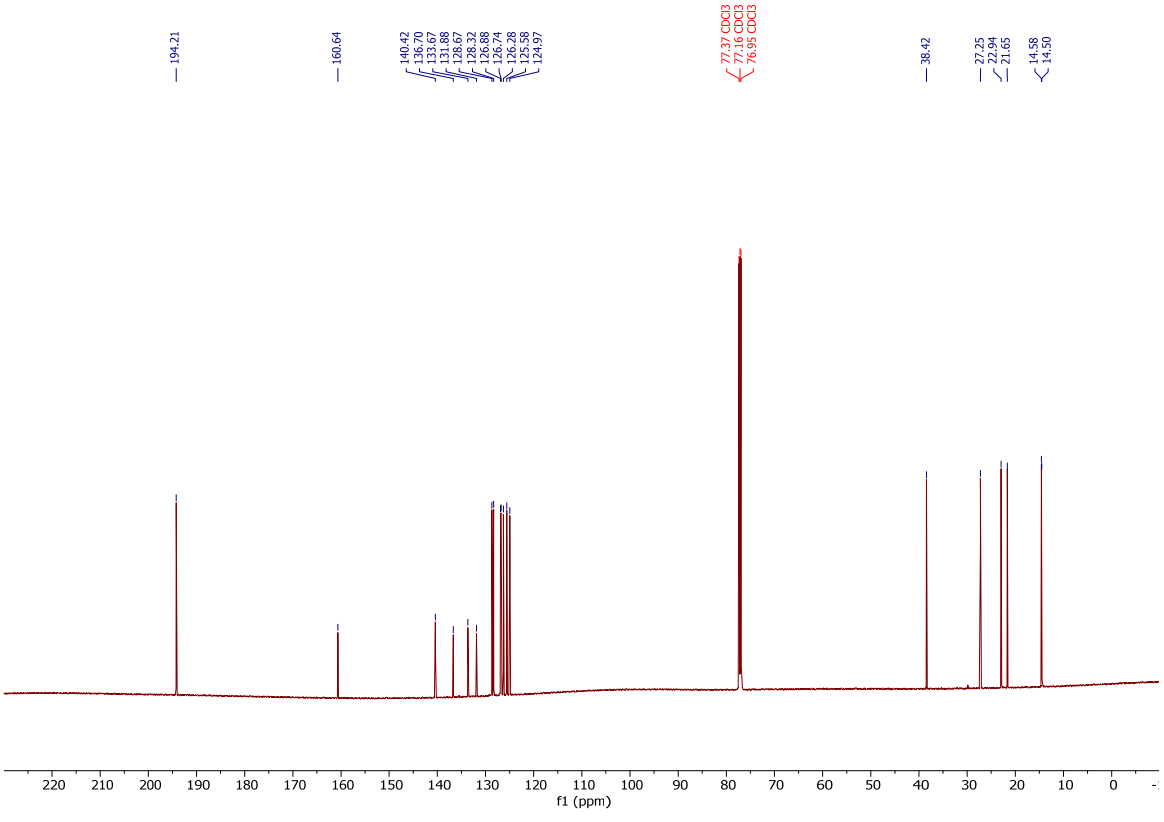

NOESY

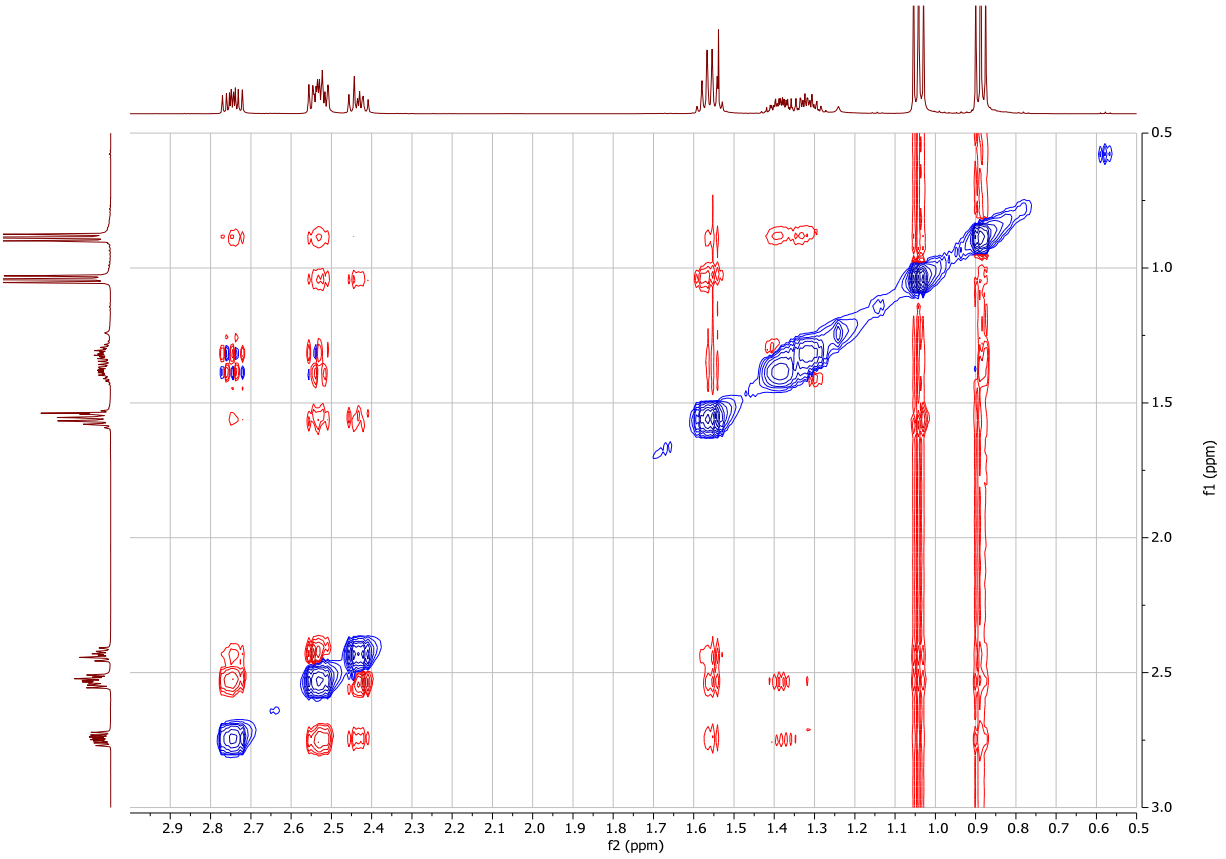

(*Z*)-3-(9-oxo-9H-fluoren-4-yl)-2-propylhex-2-enal (**10**).

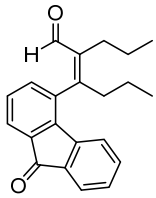

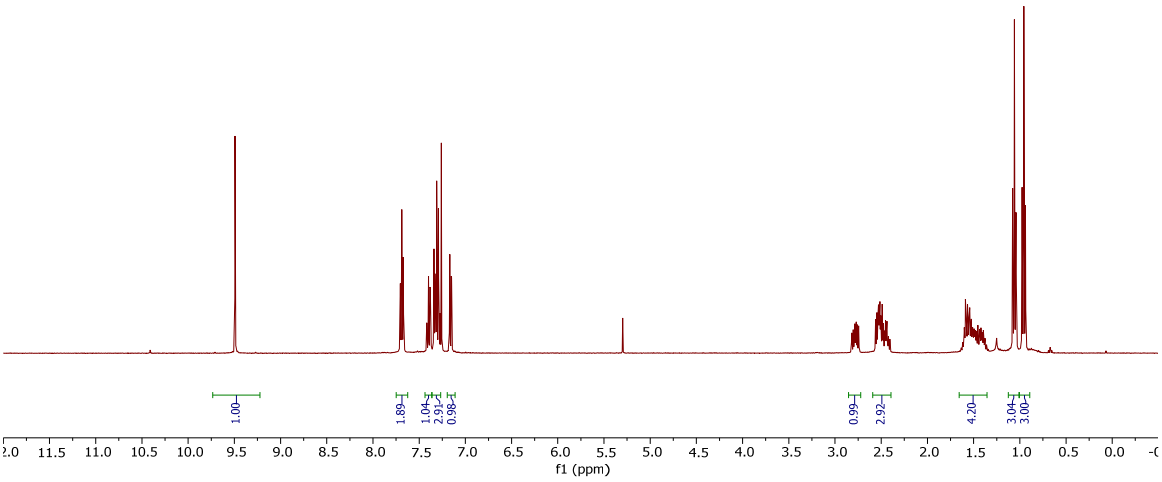

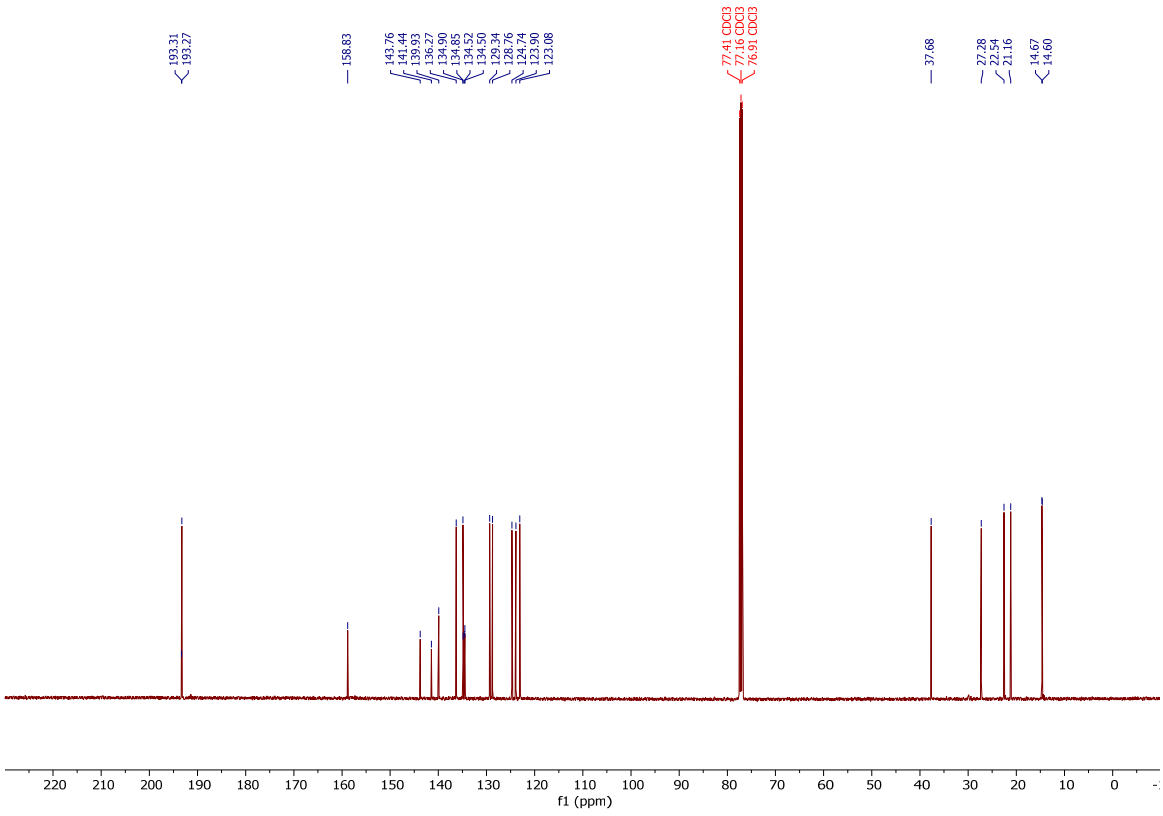

NOESY

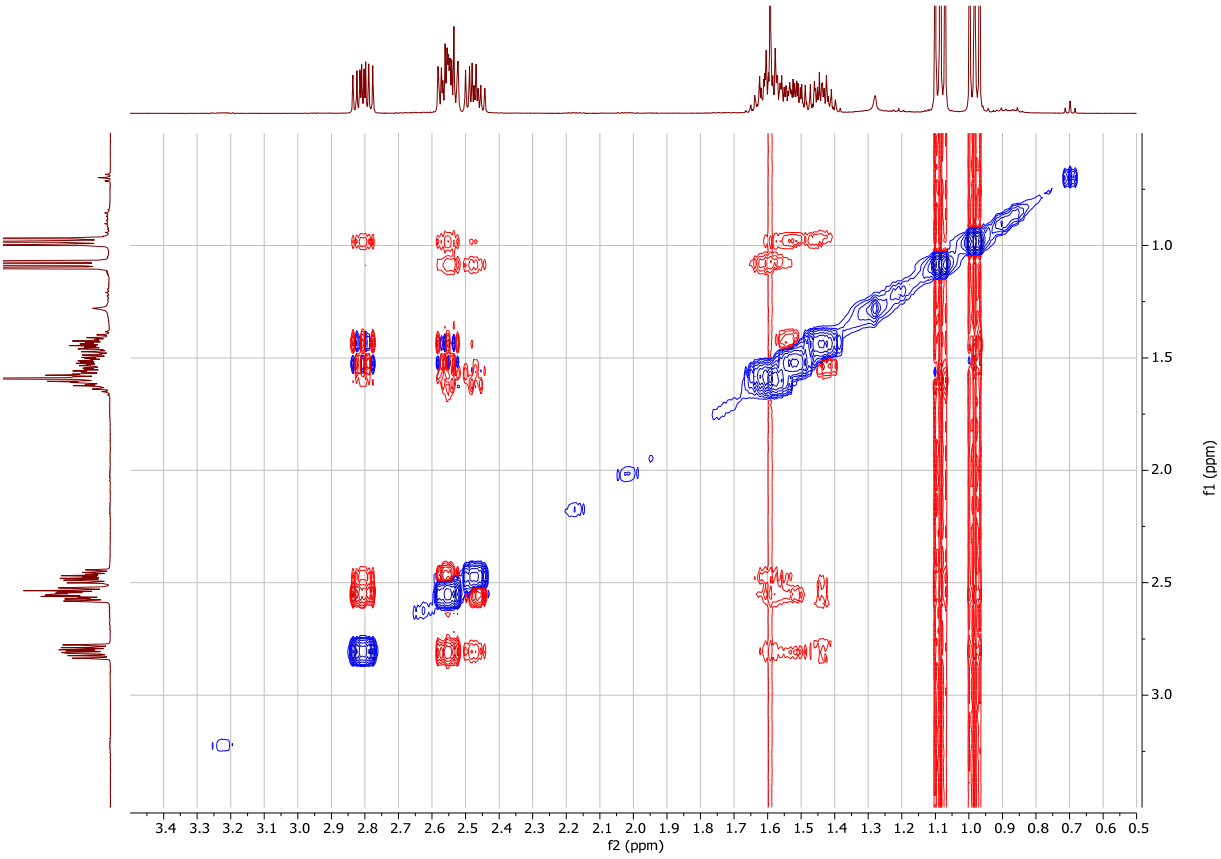
1.0
1.5
2.0
2.5
3.0
f1 (ppm)
3.4 3.3 3.2 3.1 3.0 2.9 2.8 2.7 2.6 2.5 2.4 2.3 2.2 2.1 2.0 1.9 1.8 1.7 1.6 1.5 1.4 1.3 1.2 1.1 1.0 0.9 0.8 0.7 0.6 0.5
f2 (ppm)

(*Z*)-3-(3-methylthiophen-2-yl)-2-propylhex-2-enal (**11**)

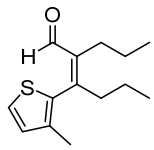

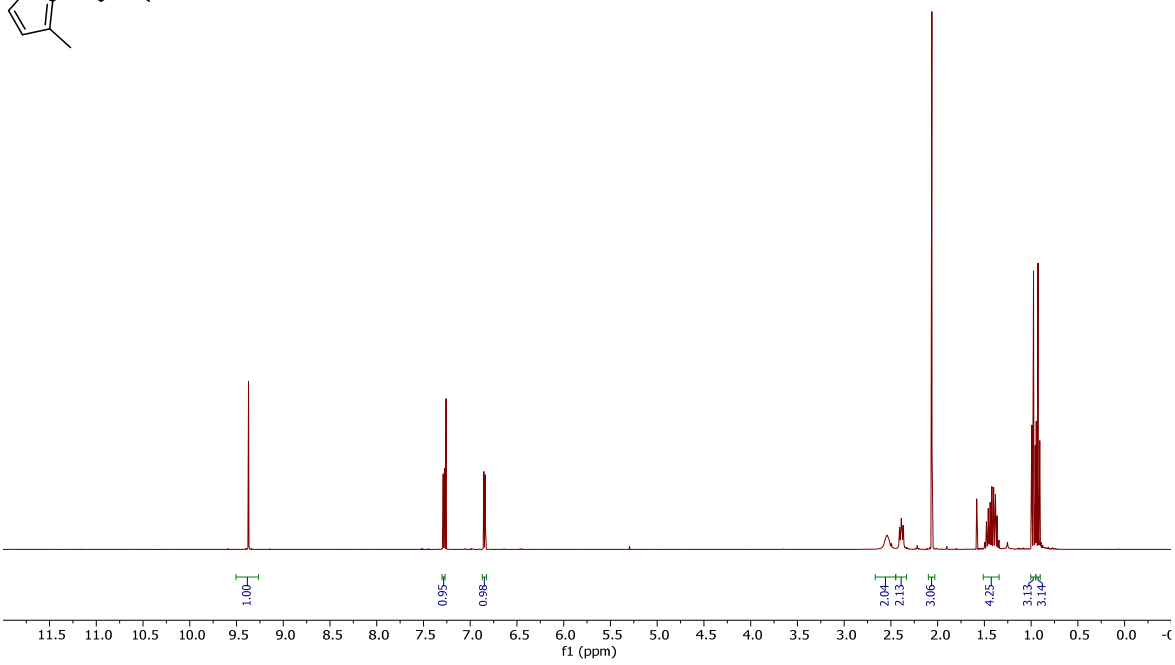

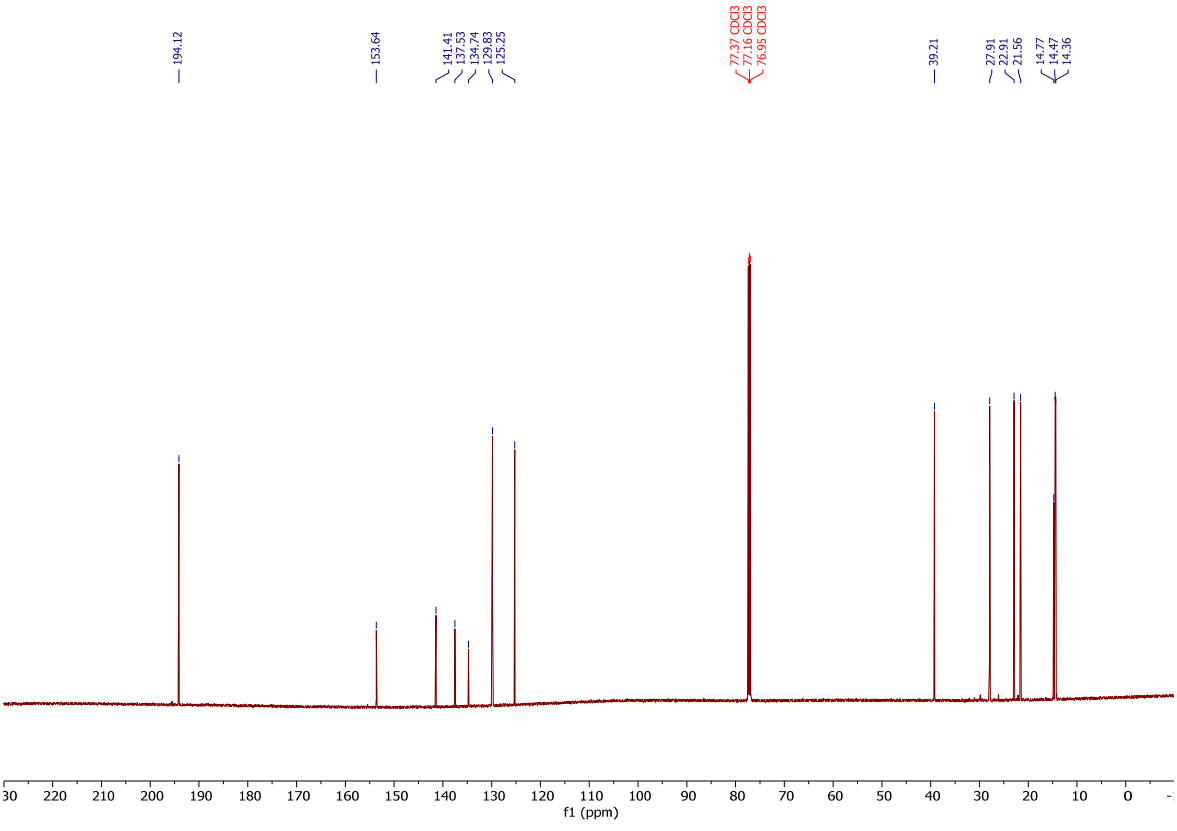

NOESY

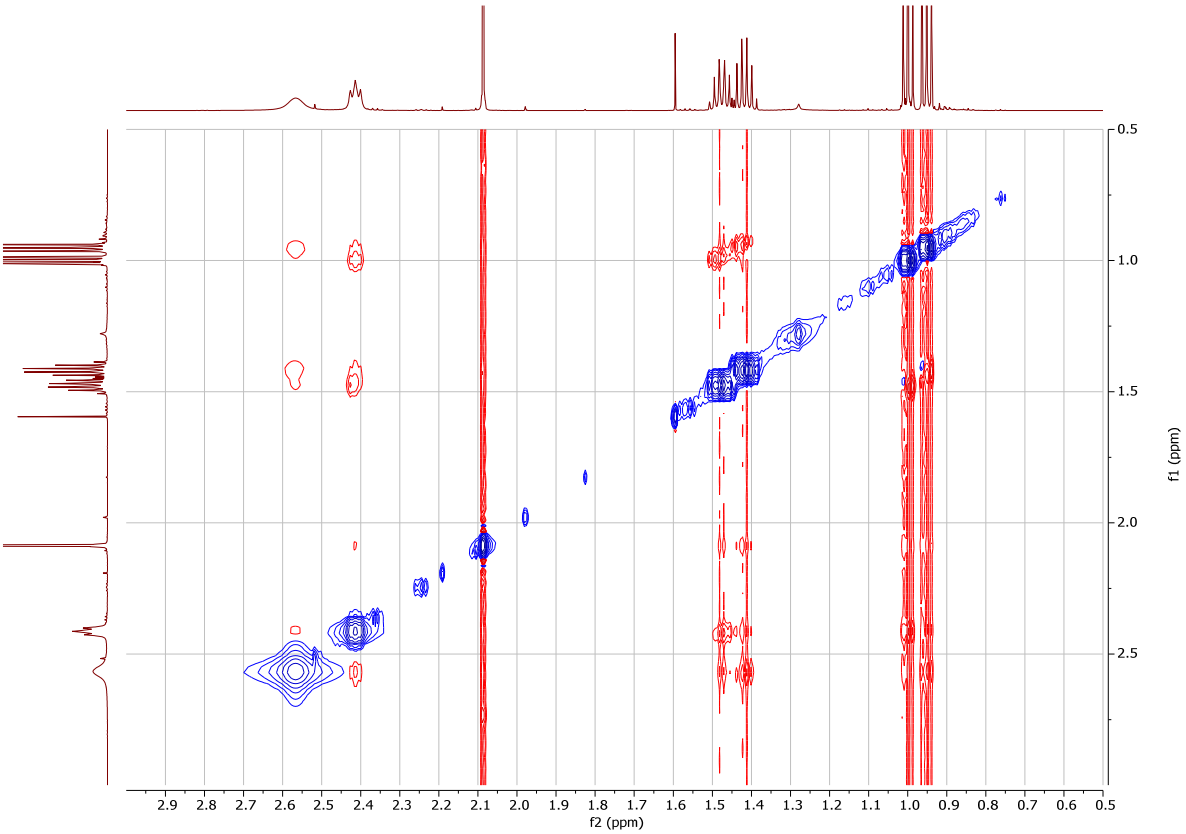
0.5
1.0
1.5
2.0
2.5
f1 (ppm)
2.9 2.8 2.7 2.6 2.5 2.4 2.3 2.2 2.1 2.0 1.9 1.8 1.7 1.6 1.5 1.4 1.3 1.2 1.1 1.0 0.9 0.8 0.7 0.6 0.5
f2 (ppm)

(*Z*)-3-(3-methylbenzofuran-2-yl)-2-propylhex-2-enal (**12**).

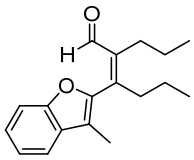

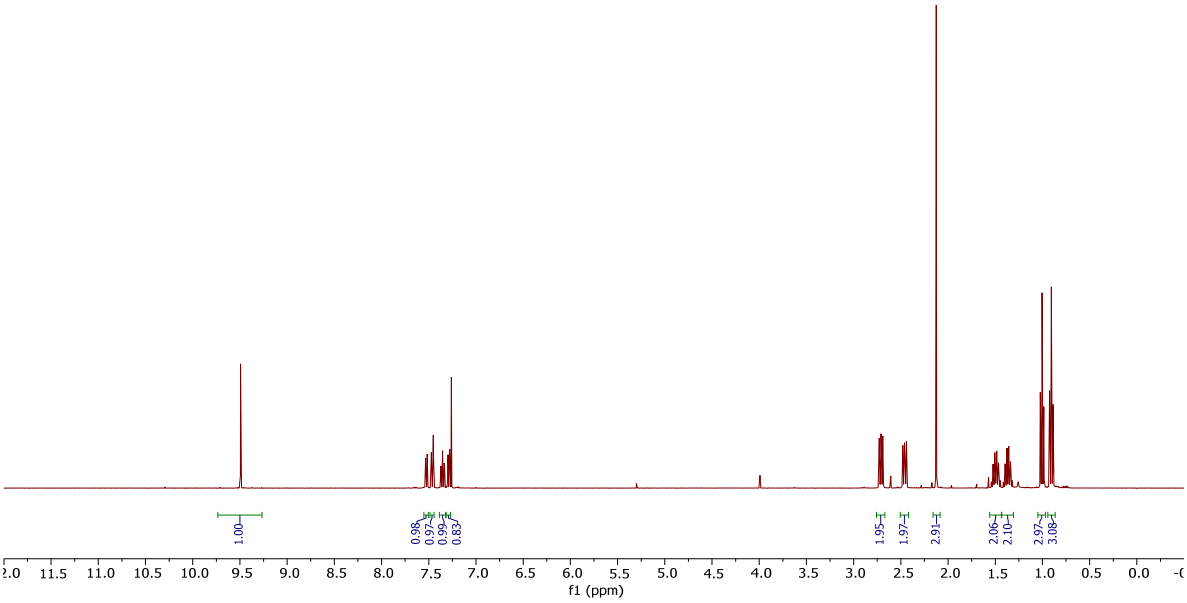

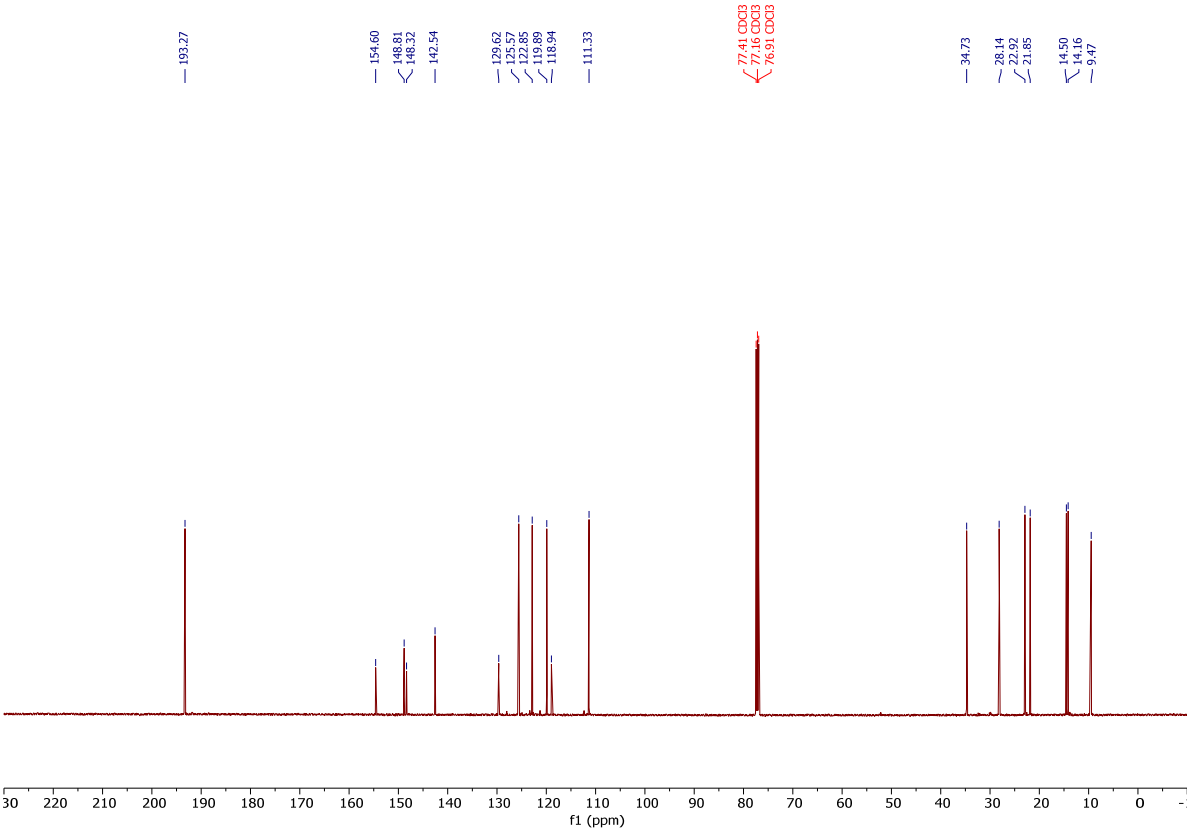

NOESY

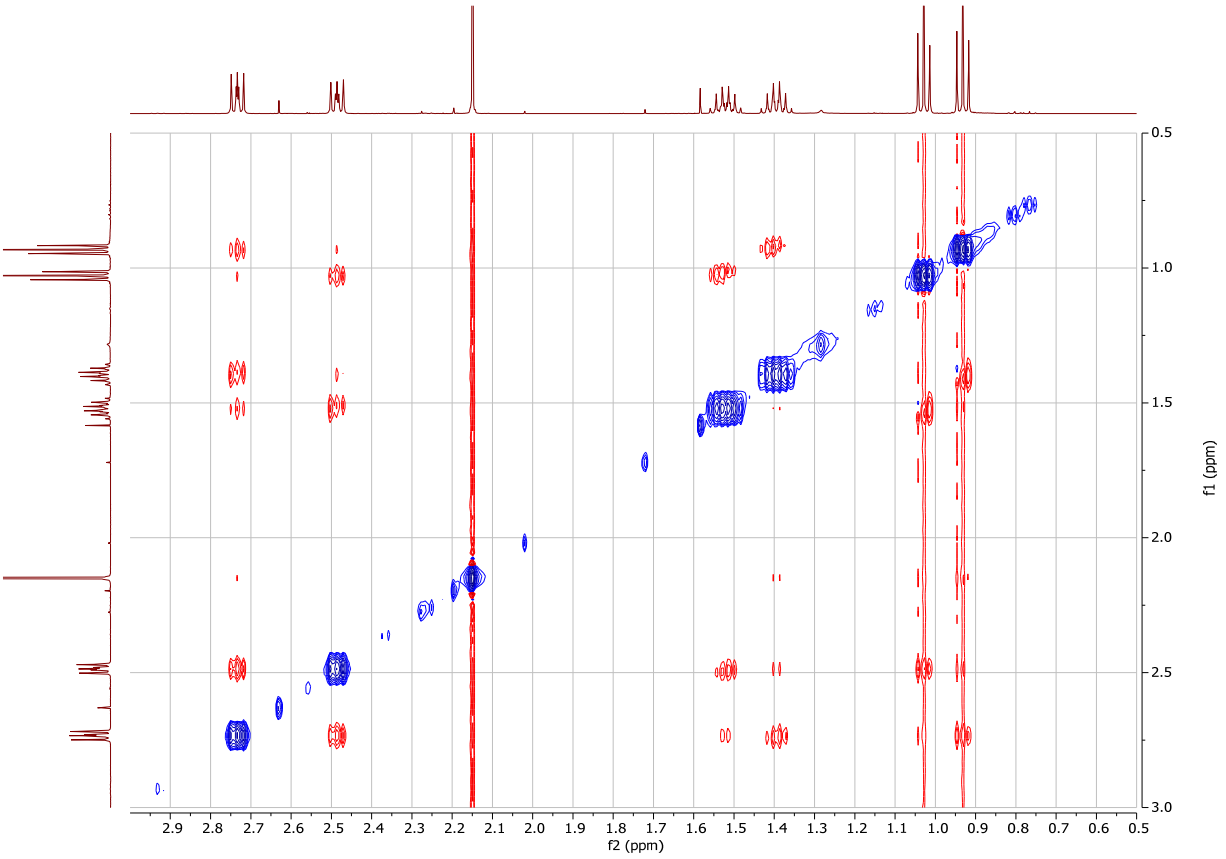

(*Z*)-3-(2-methyl-6-(trifluoromethyl)pyridin-3-yl)-2-propylhex-2-enal (**13**).

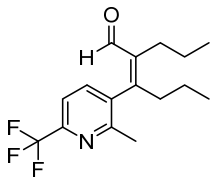

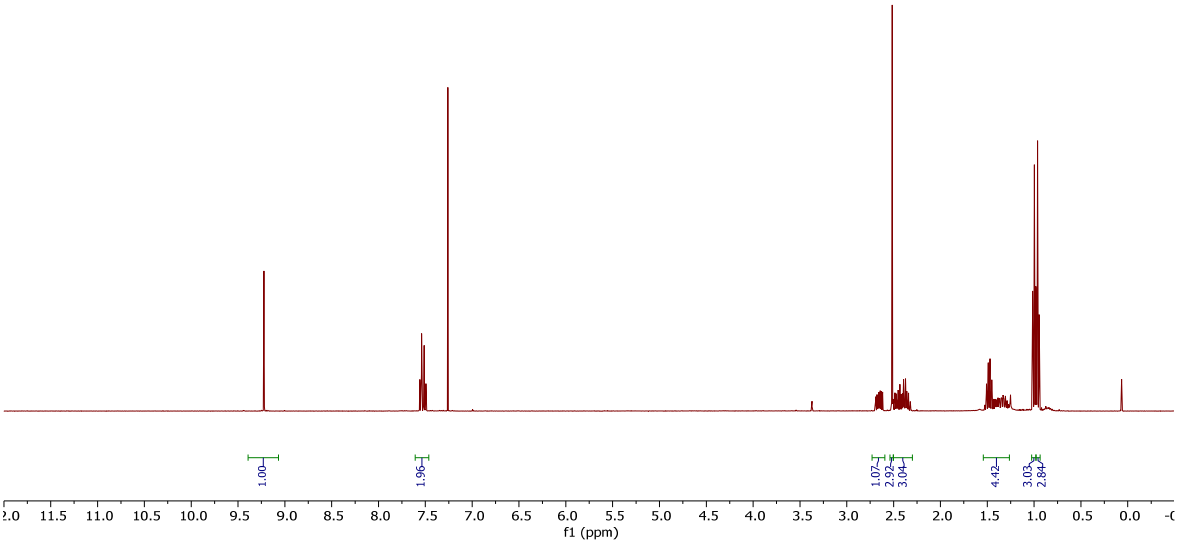

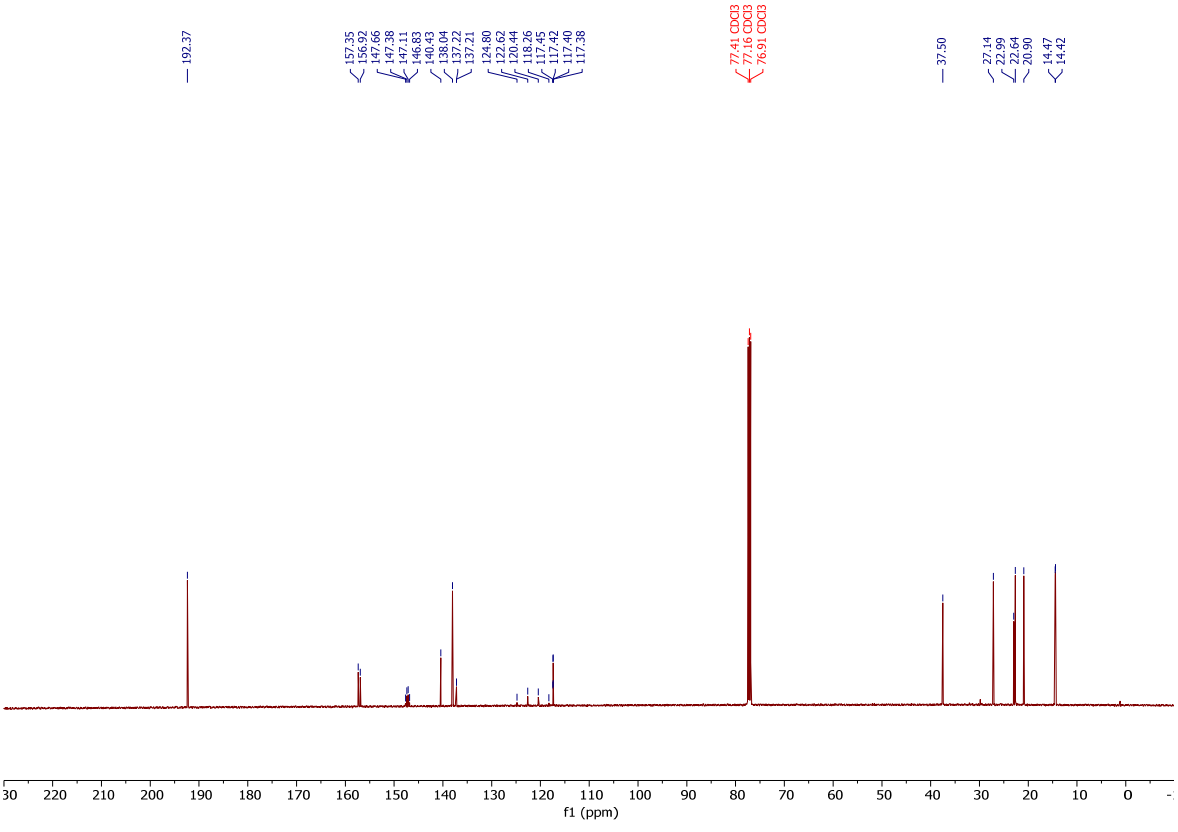

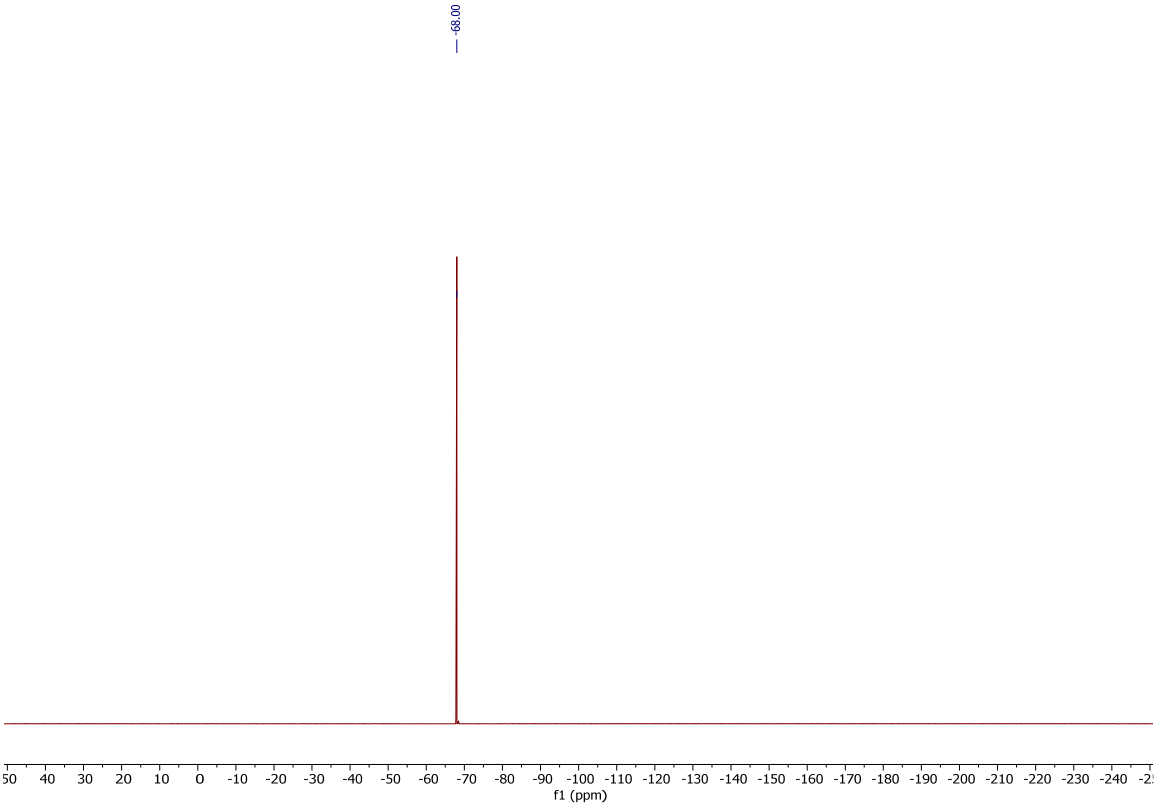
-68.00
50 40 30 20 10 0 -10 -20 -30 -40 -50 -60 -70 -80 -90 -100 -110 -120 -130 -140 -150 -160 -170 -180 -190 -200 -210 -220 -230 -240
f1 (ppm)

NOESY

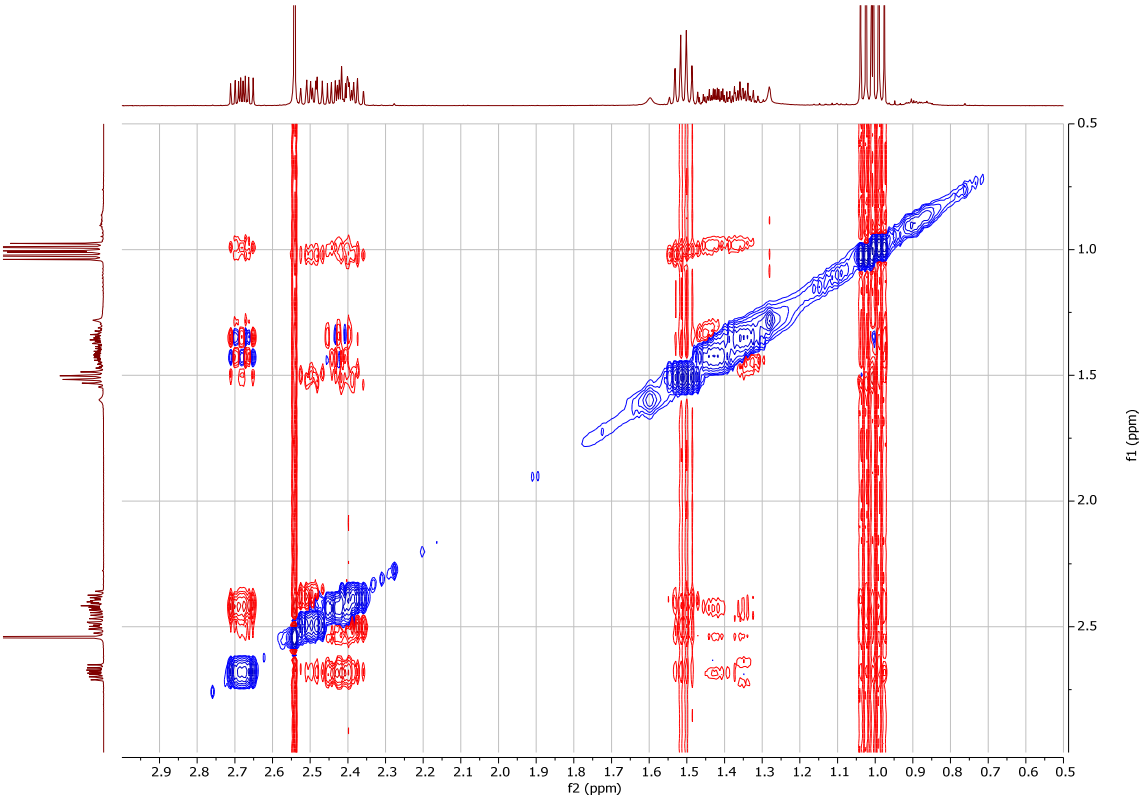
0.5
1.0
1.5
2.0
2.5
f1 (ppm)
2.9 2.8 2.7 2.6 2.5 2.4 2.3 2.2 2.1 2.0 1.9 1.8 1.7 1.6 1.5 1.4 1.3 1.2 1.1 1.0 0.9 0.8 0.7 0.6 0.5
f2 (ppm)

(*Z*)-3-mesityl-2-propylhex-2-enal (**14**)

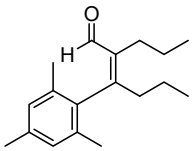

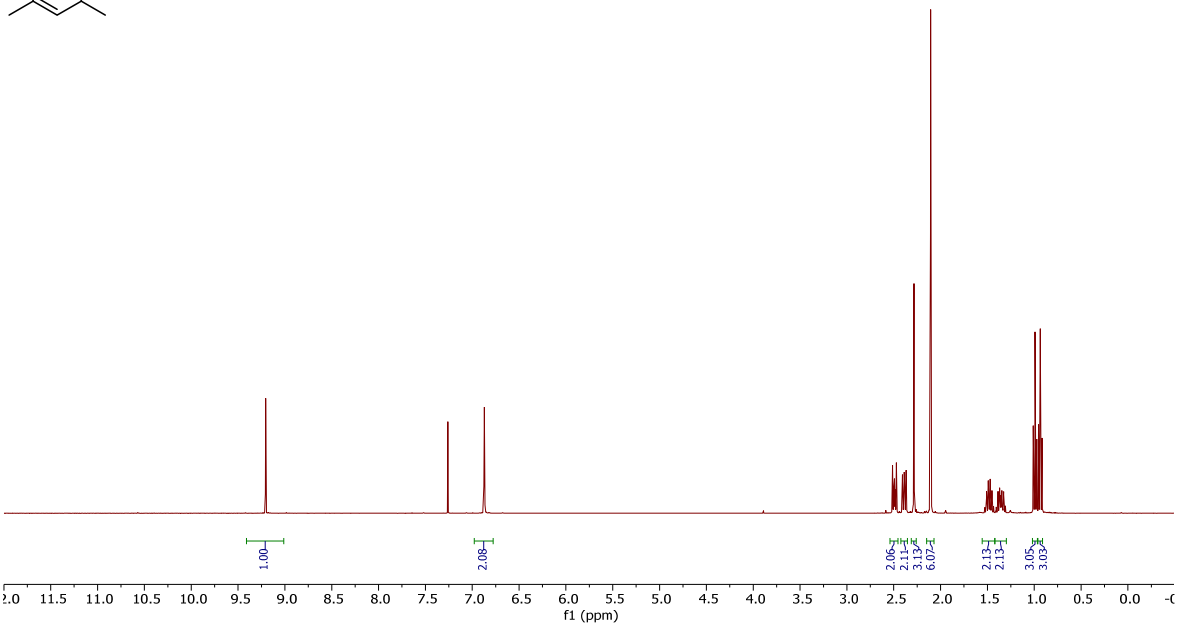

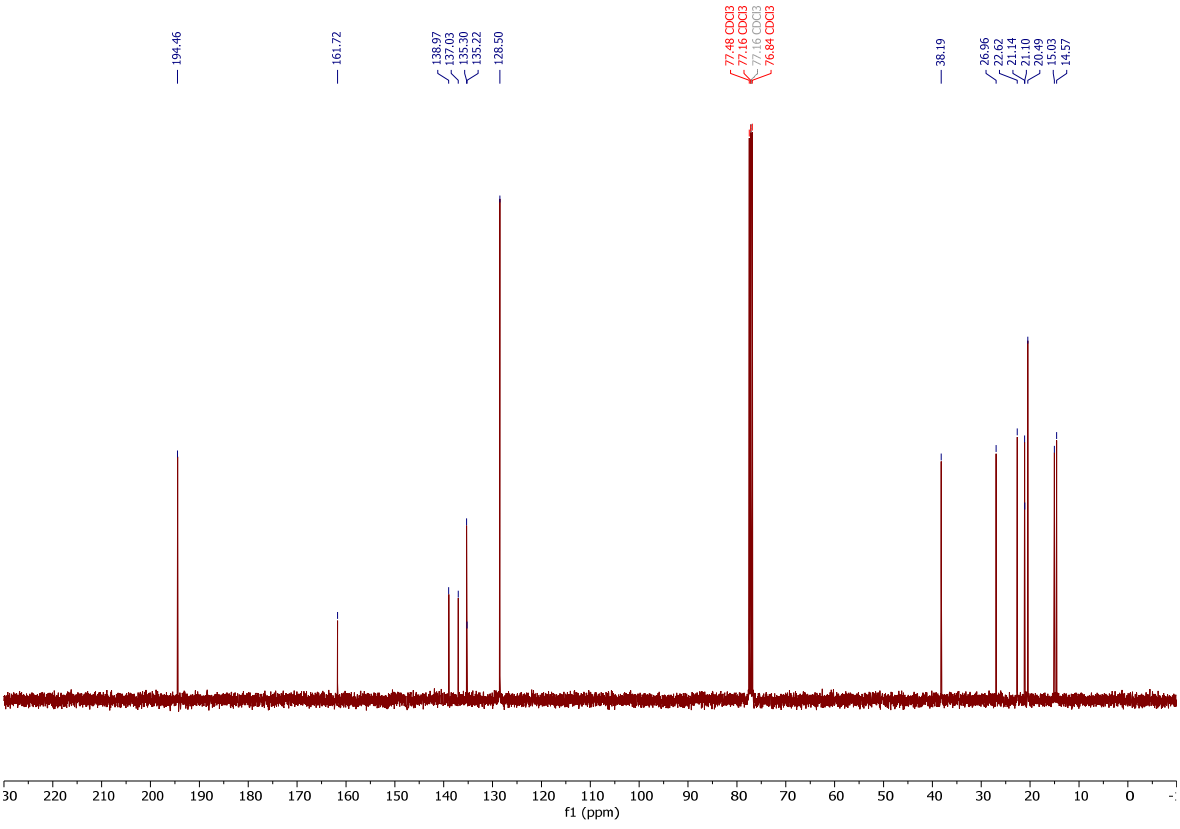

NOESY

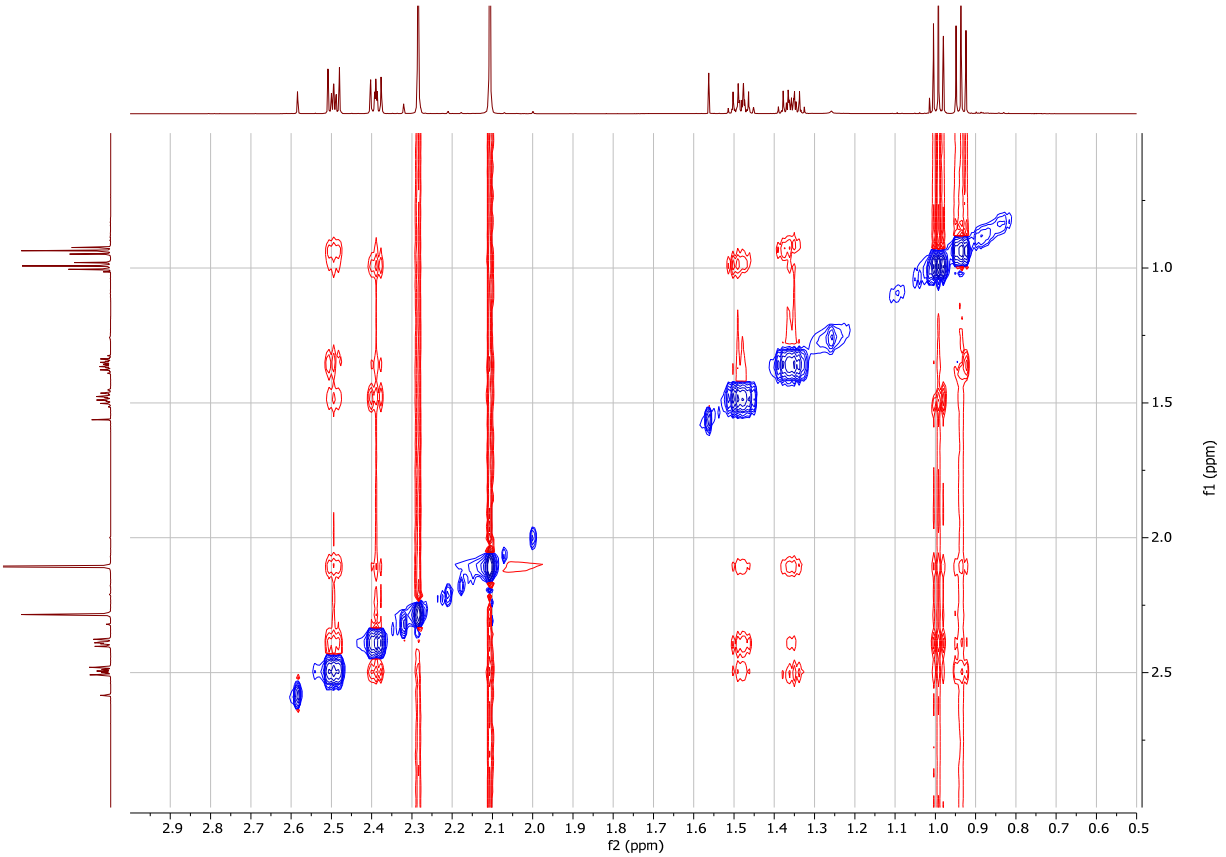
2.9 2.8 2.7 2.6 2.5 2.4 2.3 2.2 2.1 2.0 1.9 1.8 1.7 1.6 1.5 1.4 1.3 1.2 1.1 1.0 0.9 0.8 0.7 0.6 0.5
f2 (ppm)
1.0
1.5
2.0
2.5
f1 (ppm)

(*Z*)-3-(2,6-dichlorophenyl)-2-propylhex-2-enal (**15**).

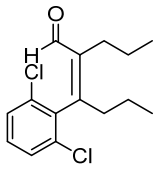

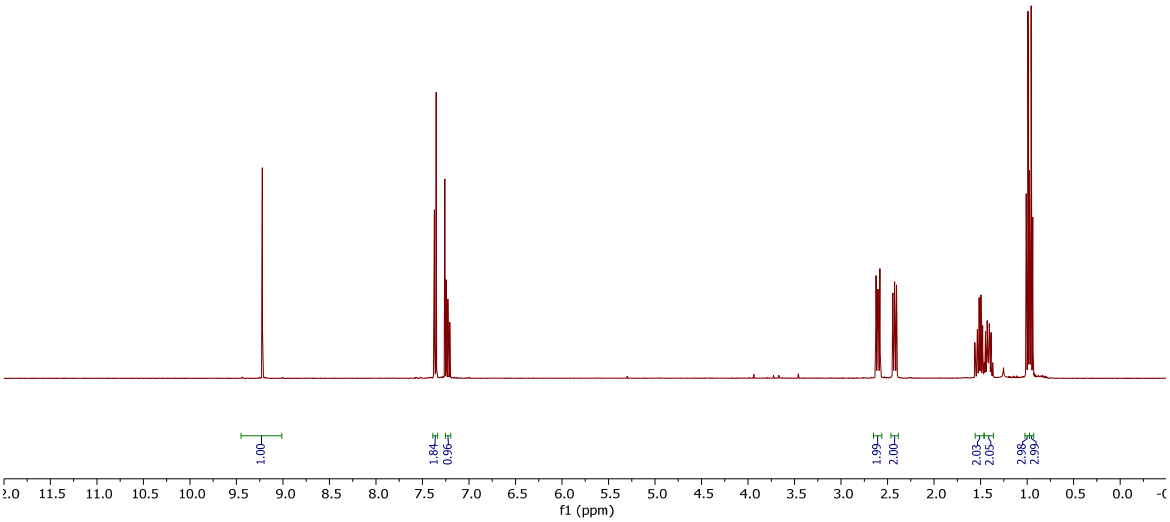

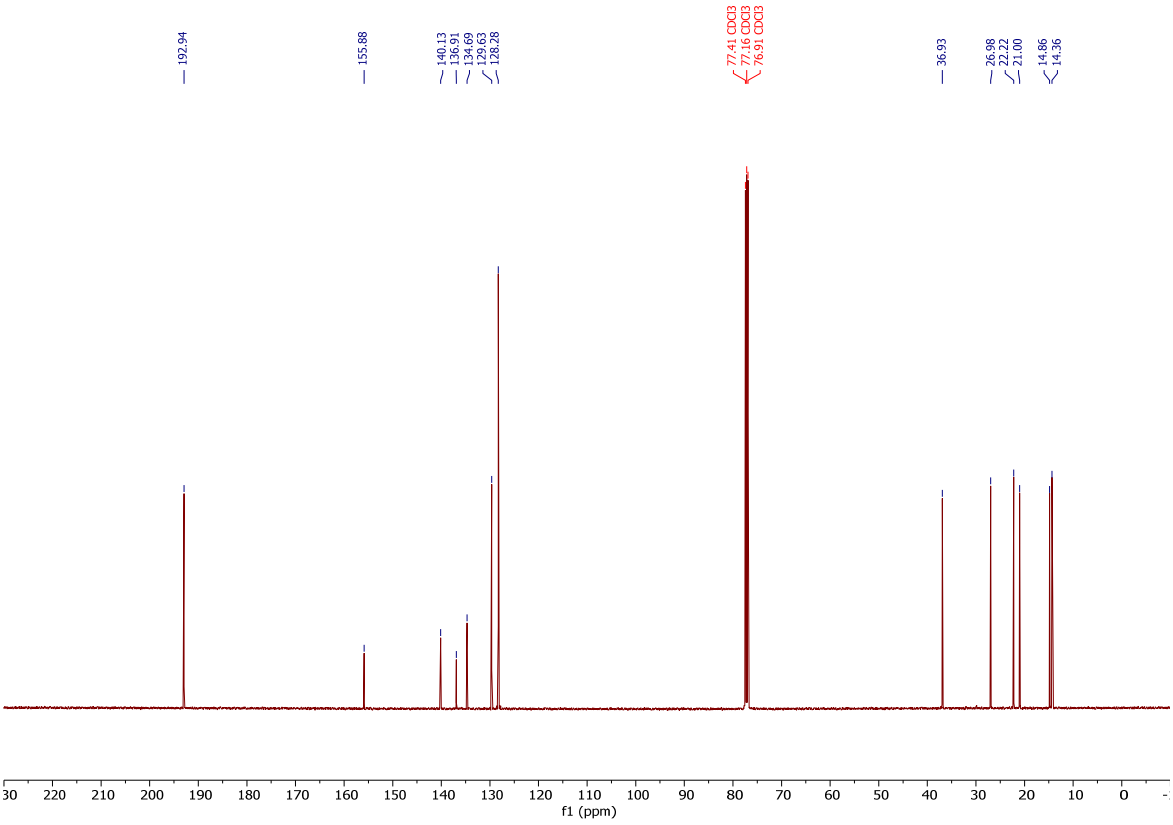

NOESY

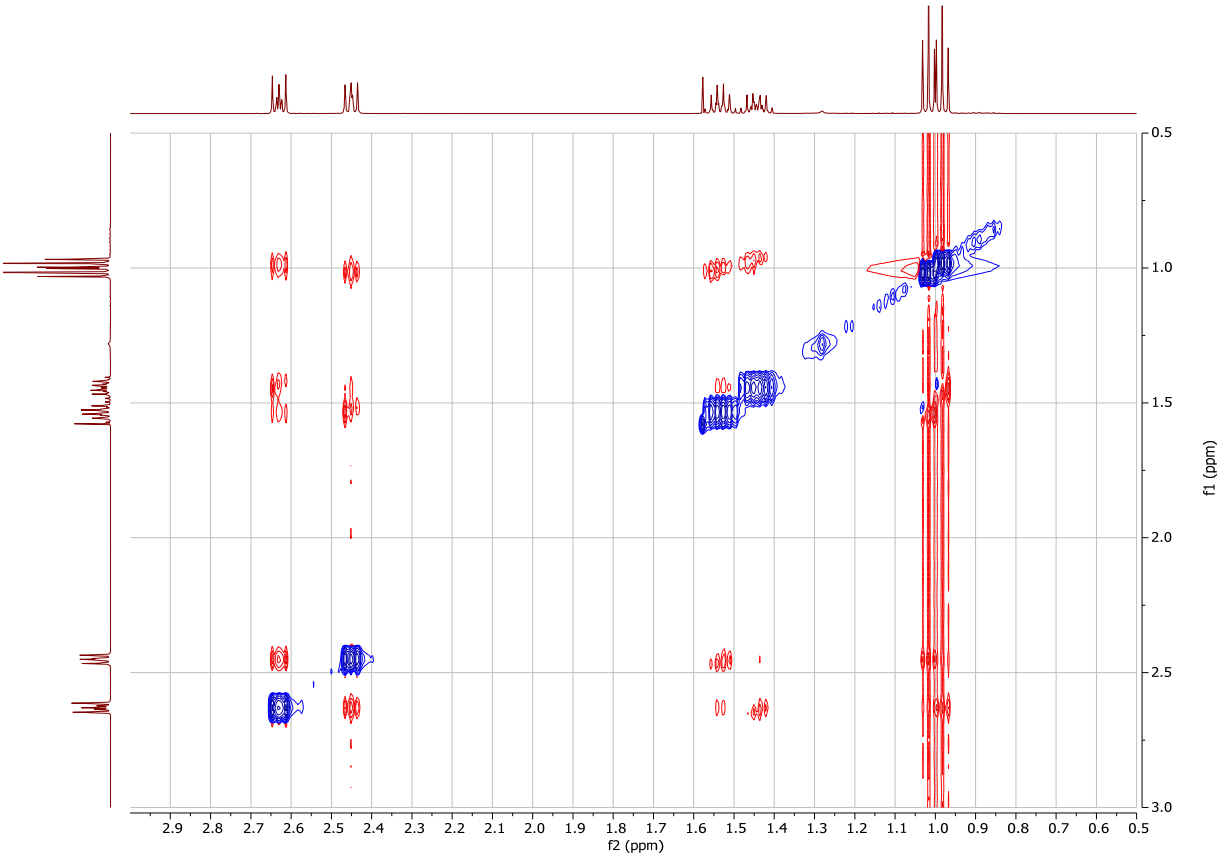
0.5
1.0
1.5
2.0
2.5
3.0
f1 (ppm)
2.9 2.8 2.7 2.6 2.5 2.4 2.3 2.2 2.1 2.0 1.9 1.8 1.7 1.6 1.5 1.4 1.3 1.2 1.1 1.0 0.9 0.8 0.7 0.6 0.5
f2 (ppm)

(*Z*)-3-(5-methyl-3-phenylisoxazol-4-yl)-2-propylhex-2-enal (**16**).

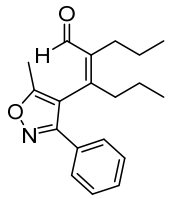

NOESY

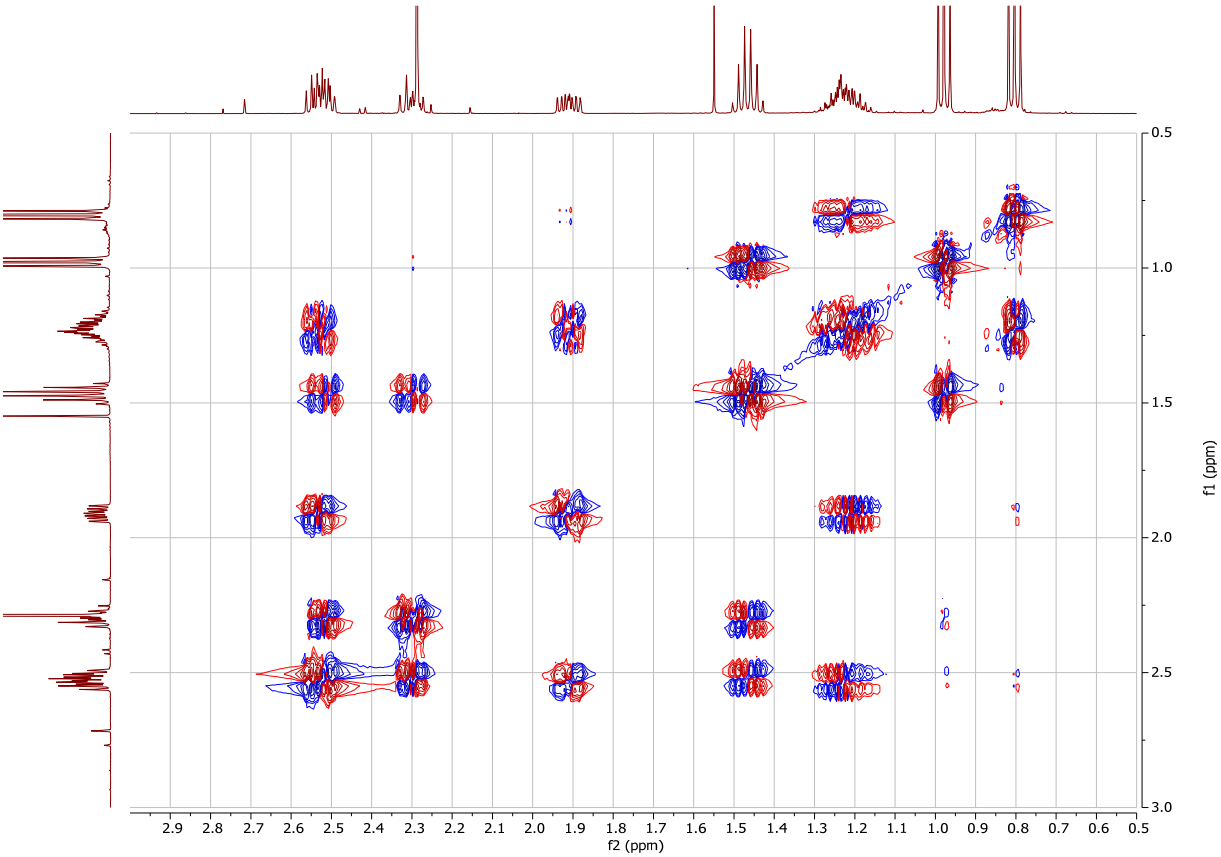

(*Z*)-3-(2,6-difluorophenyl)-2-propylhex-2-enal (**17**).

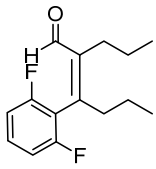

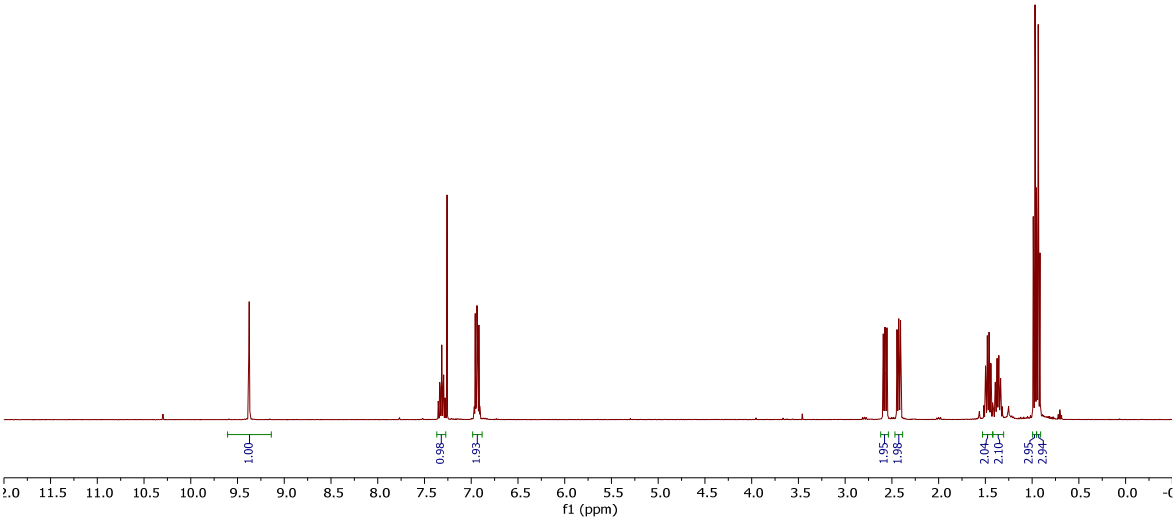

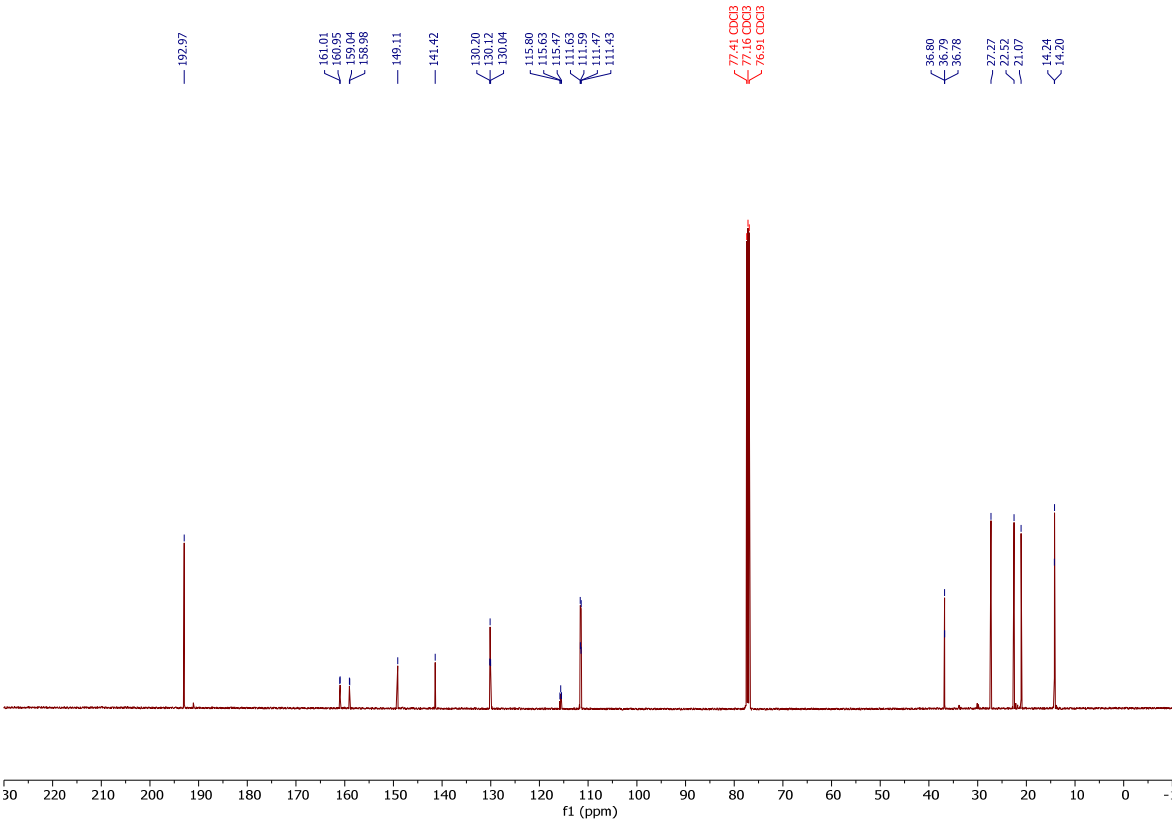

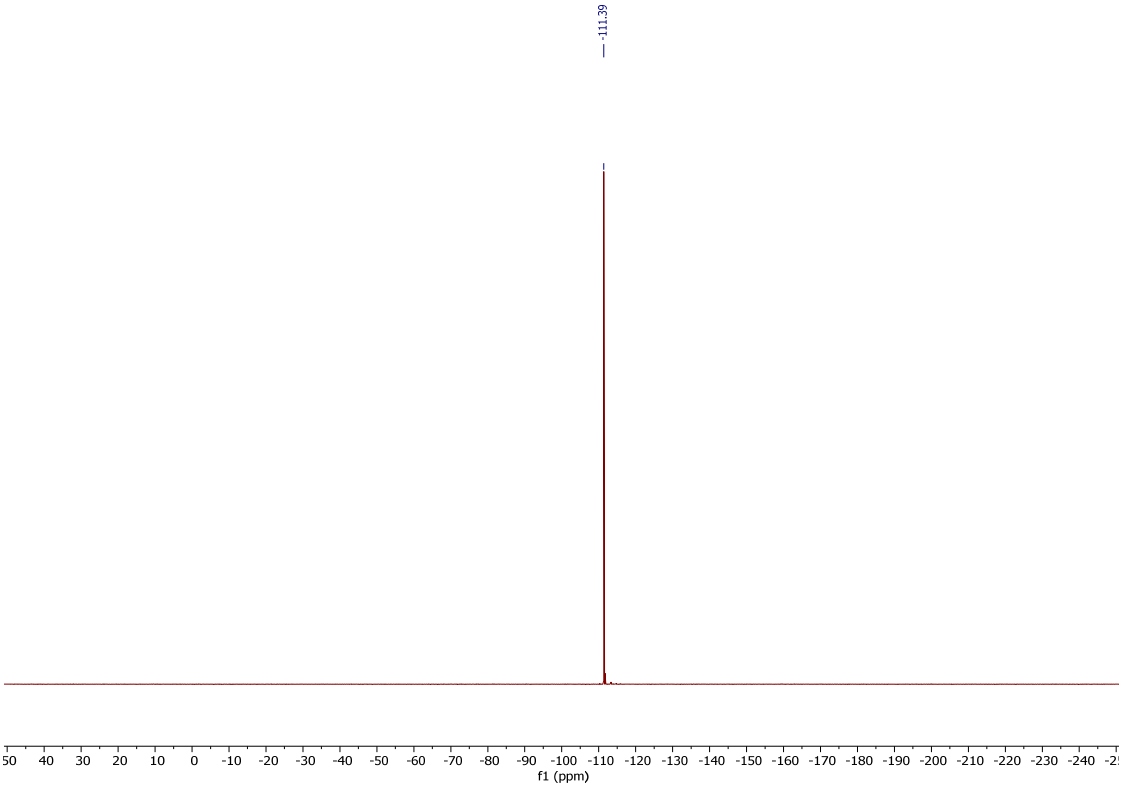
-111.39
50 40 30 20 10 0 -10 -20 -30 -40 -50 -60 -70 -80 -90 -100 -110 -120 -130 -140 -150 -160 -170 -180 -190 -200 -210 -220 -230 -240
f1 (ppm)

NOESY

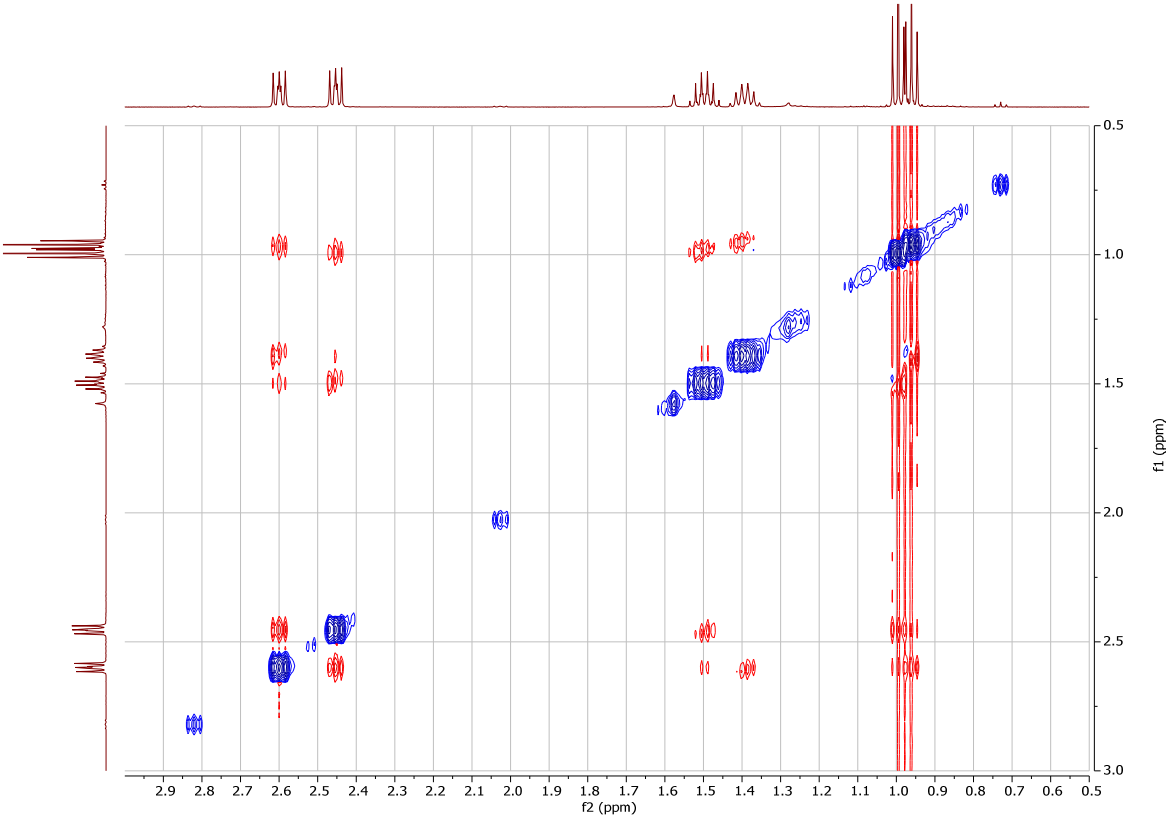
0.5
1.0
1.5
2.0
2.5
3.0
f1 (ppm)
2.9 2.8 2.7 2.6 2.5 2.4 2.3 2.2 2.1 2.0 1.9 1.8 1.7 1.6 1.5 1.4 1.3 1.2 1.1 1.0 0.9 0.8 0.7 0.6 0.5
f2 (ppm)

(*Z*)-2-propyl-3-(*p*-tolyl)hex-2-enal (**18**).

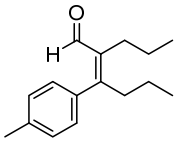

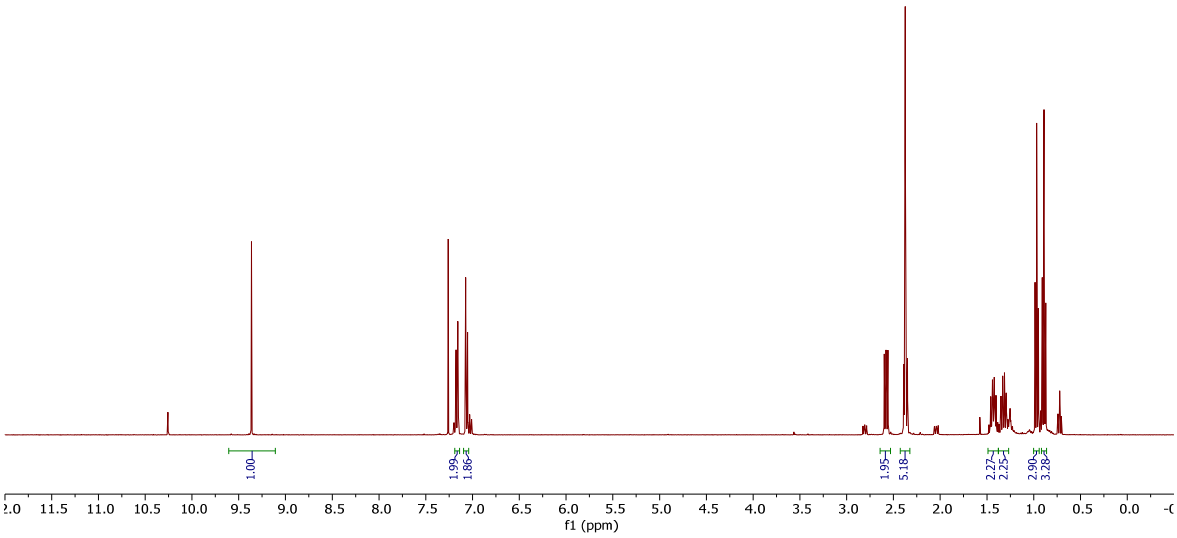

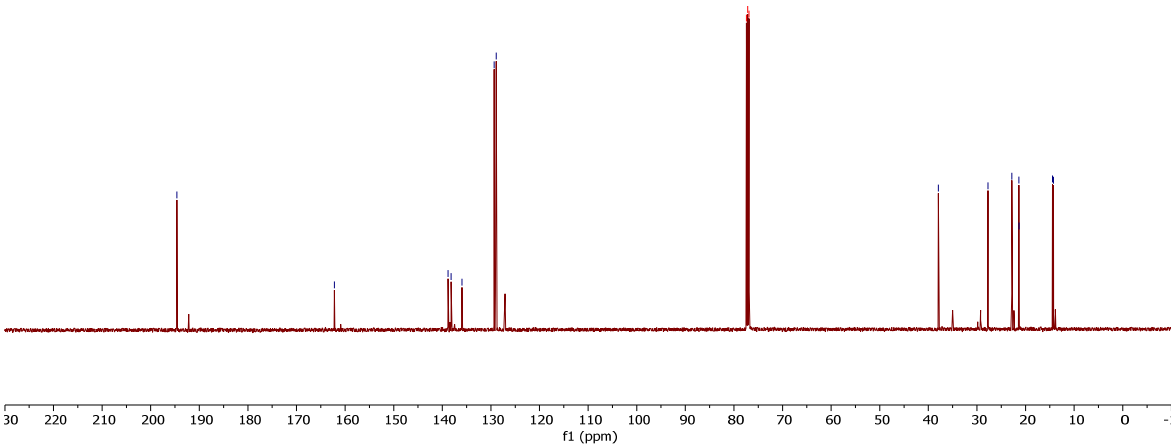

NOESY

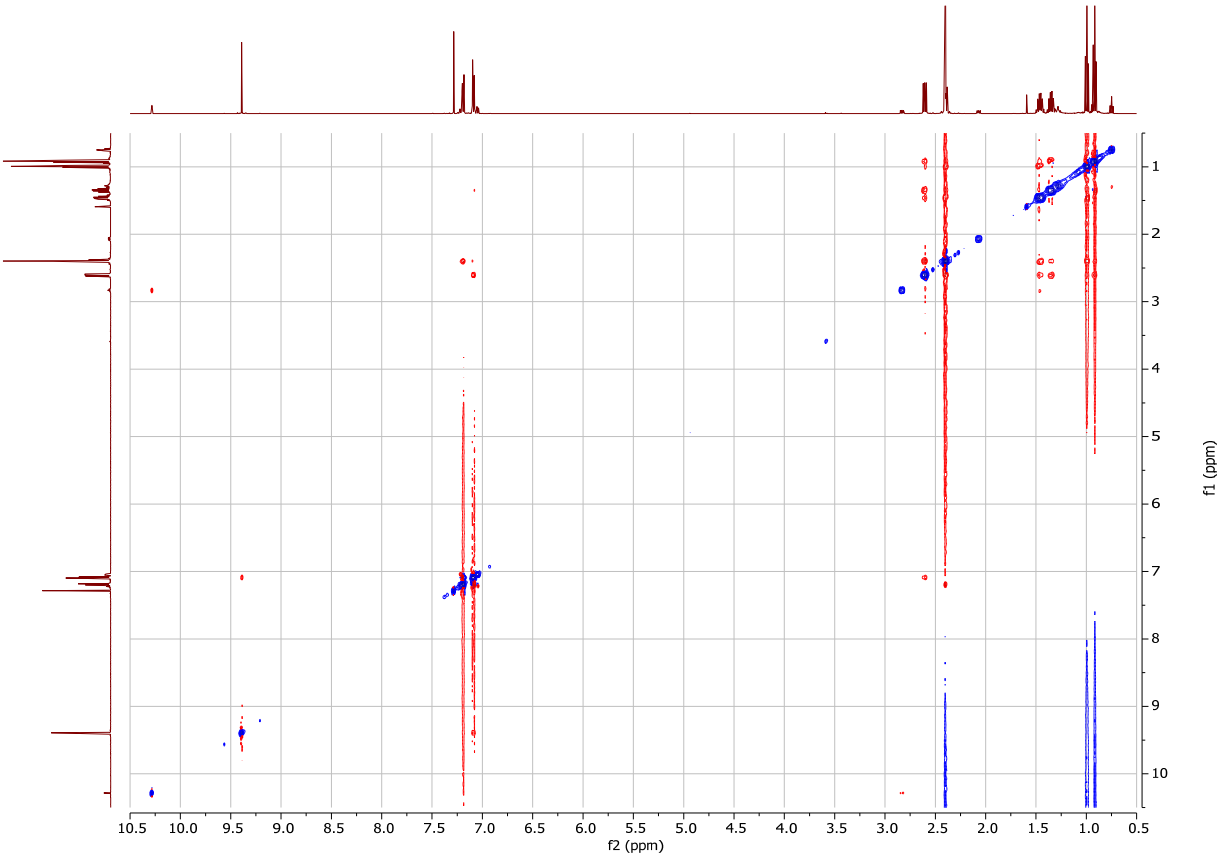

(*Z*)-3-phenyl-2-propylhex-2-enal (**19**).

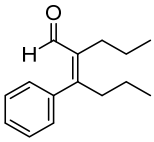

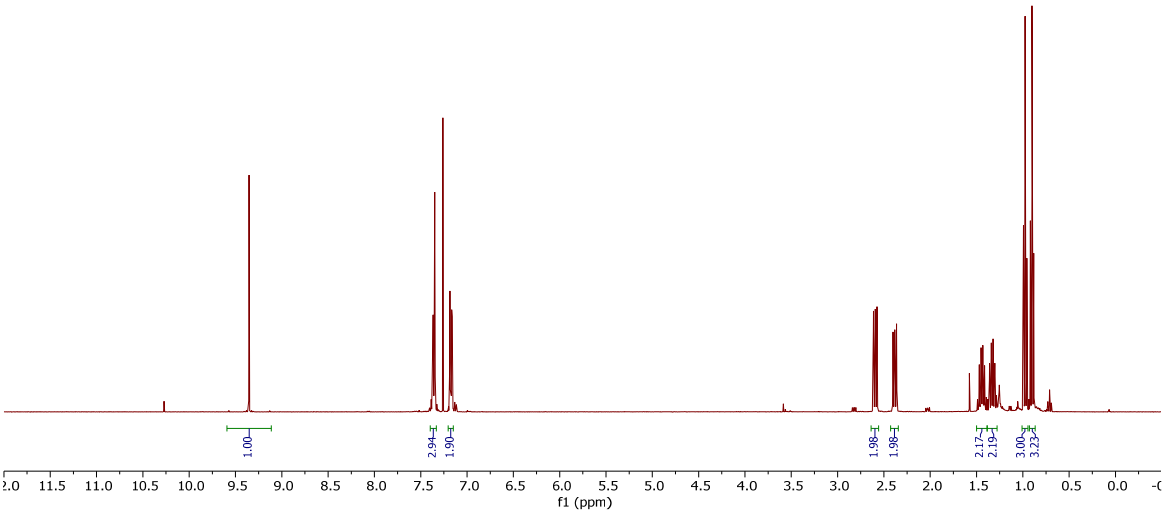

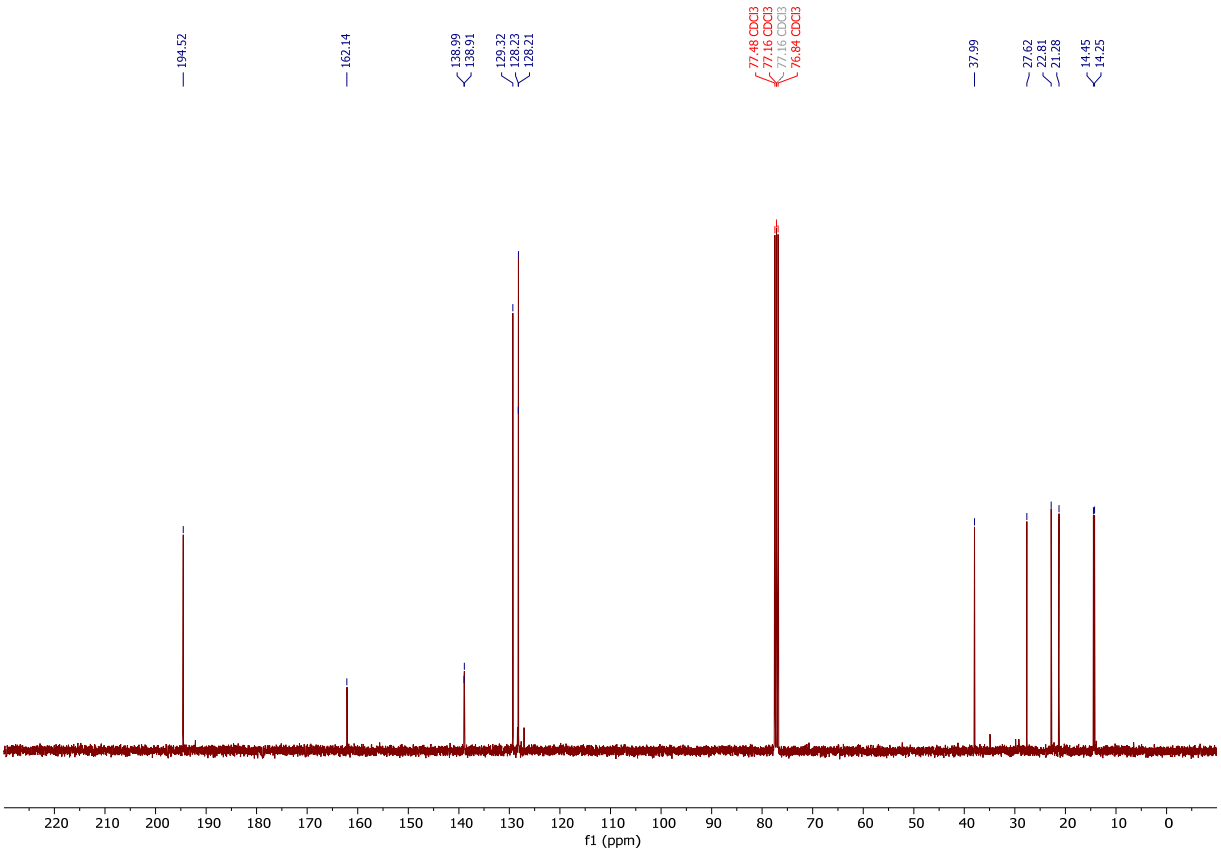

NOESY

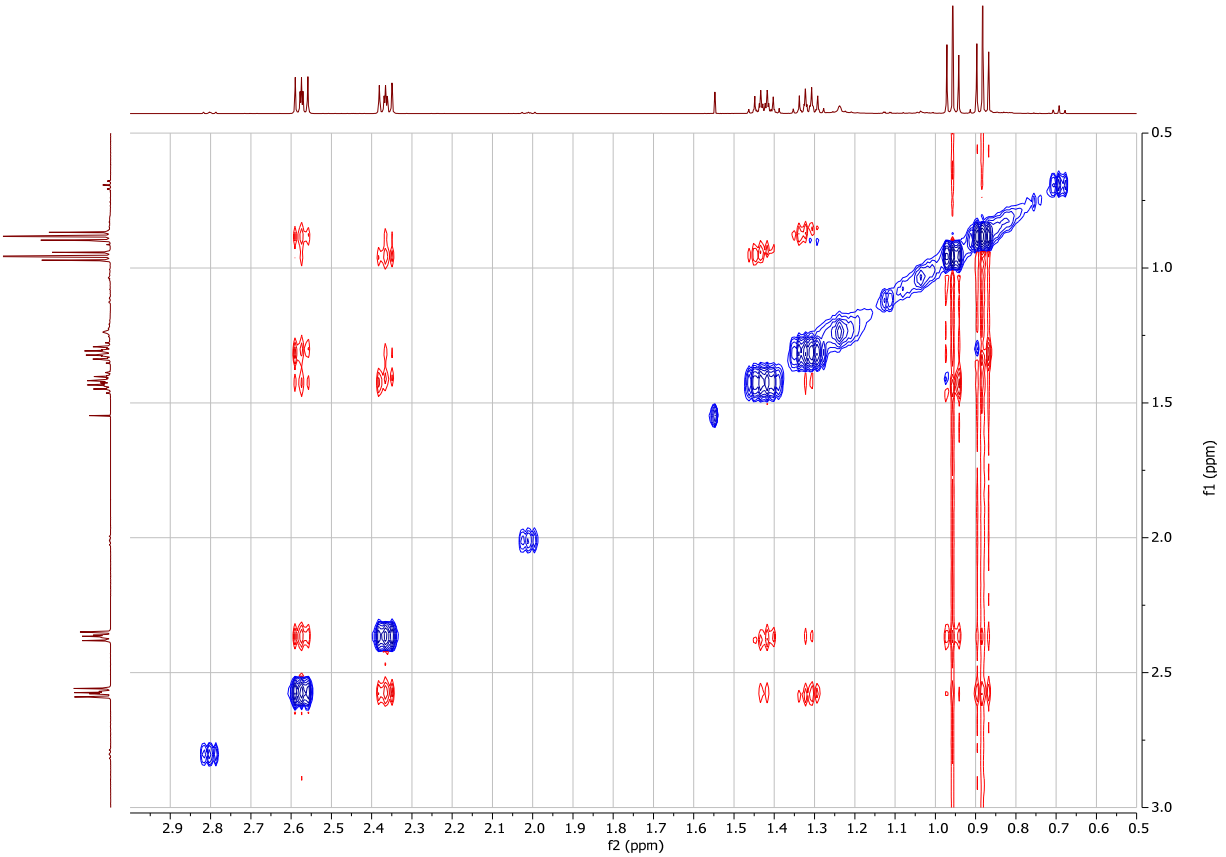

(*Z*)-3-phenyl-2-propylhex-2-enal-1-13C (**20**).

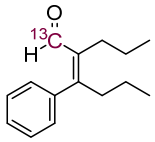

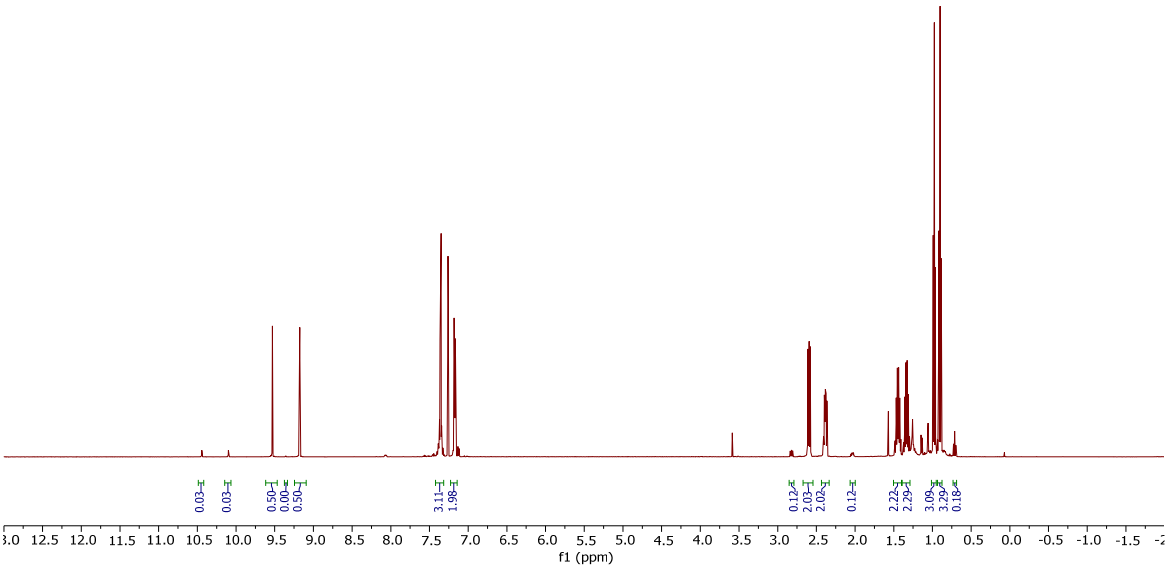

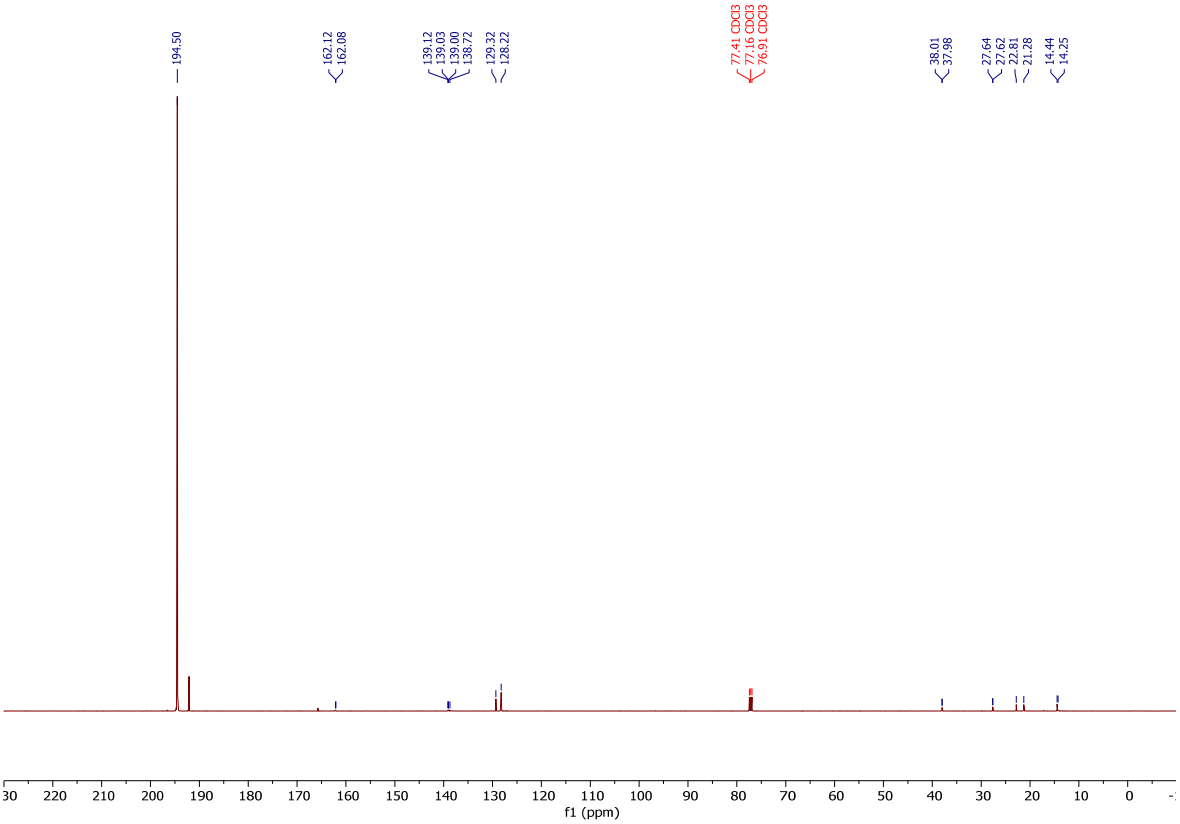

NOESY

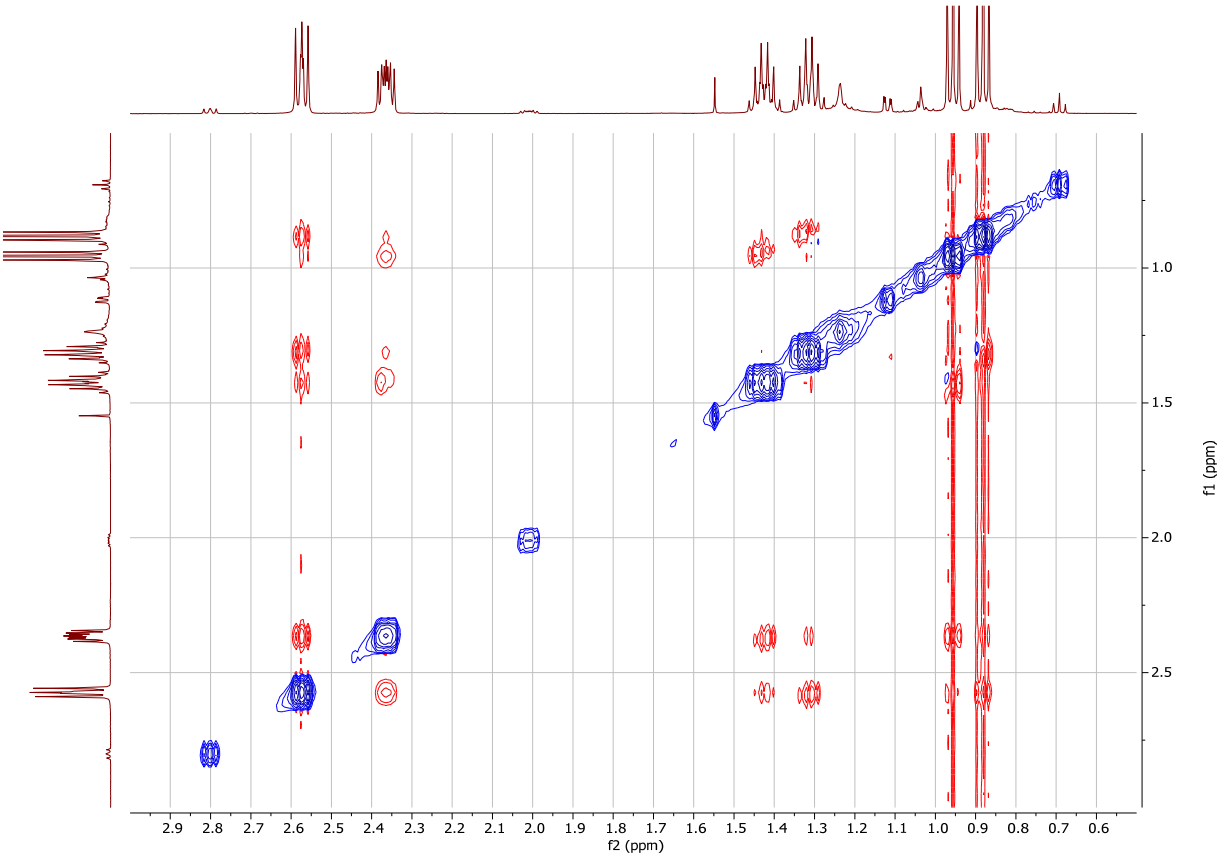
2.9 2.8 2.7 2.6 2.5 2.4 2.3 2.2 2.1 2.0 1.9 1.8 1.7 1.6 1.5 1.4 1.3 1.2 1.1 1.0 0.9 0.8 0.7 0.6
f2 (ppm)
1.0
1.5
2.0
2.5
f1 (ppm)

(*Z*)-3-(4-methoxyphenyl)-2-propylhex-2-enal (**21**).

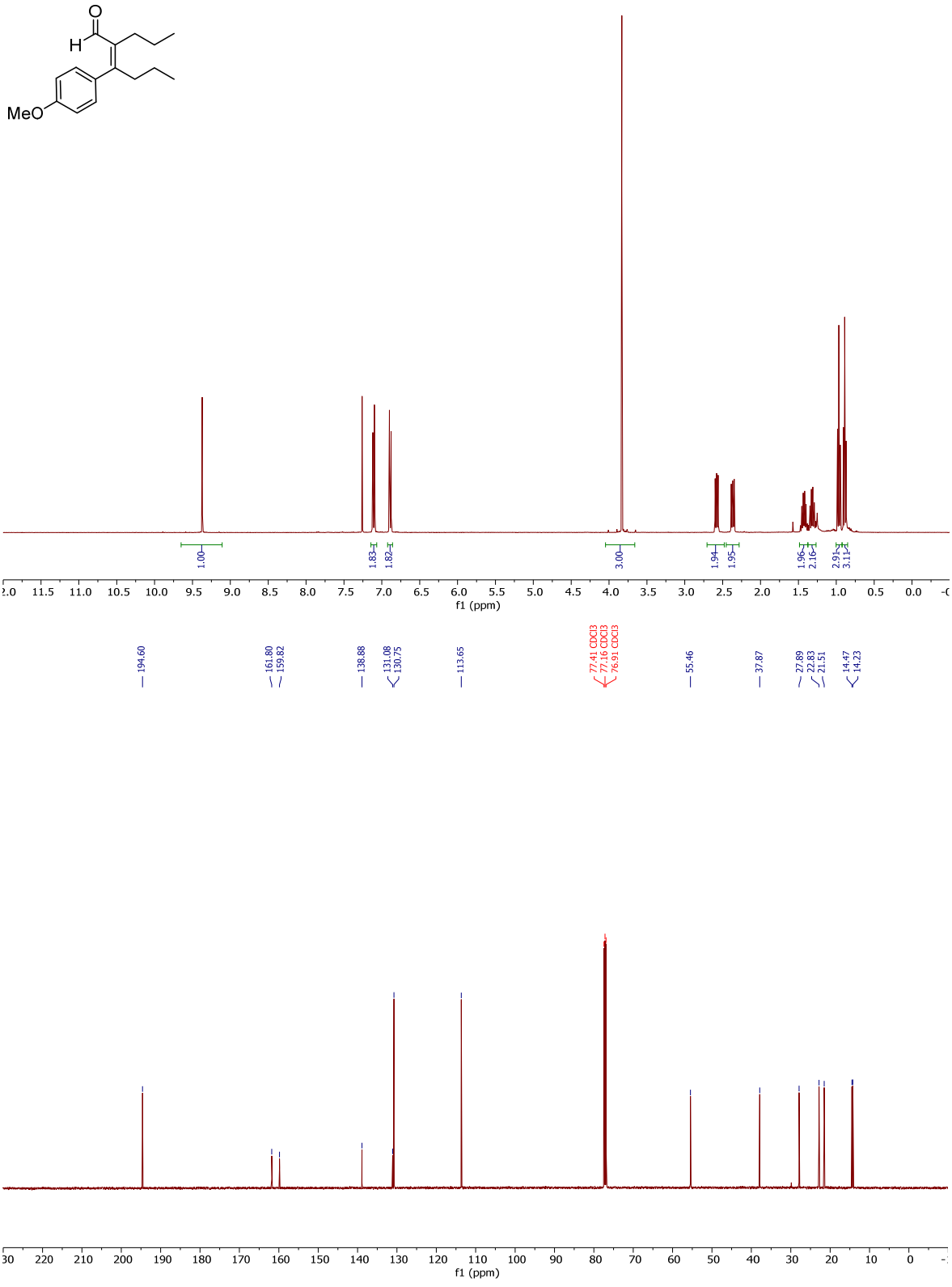

NOESY

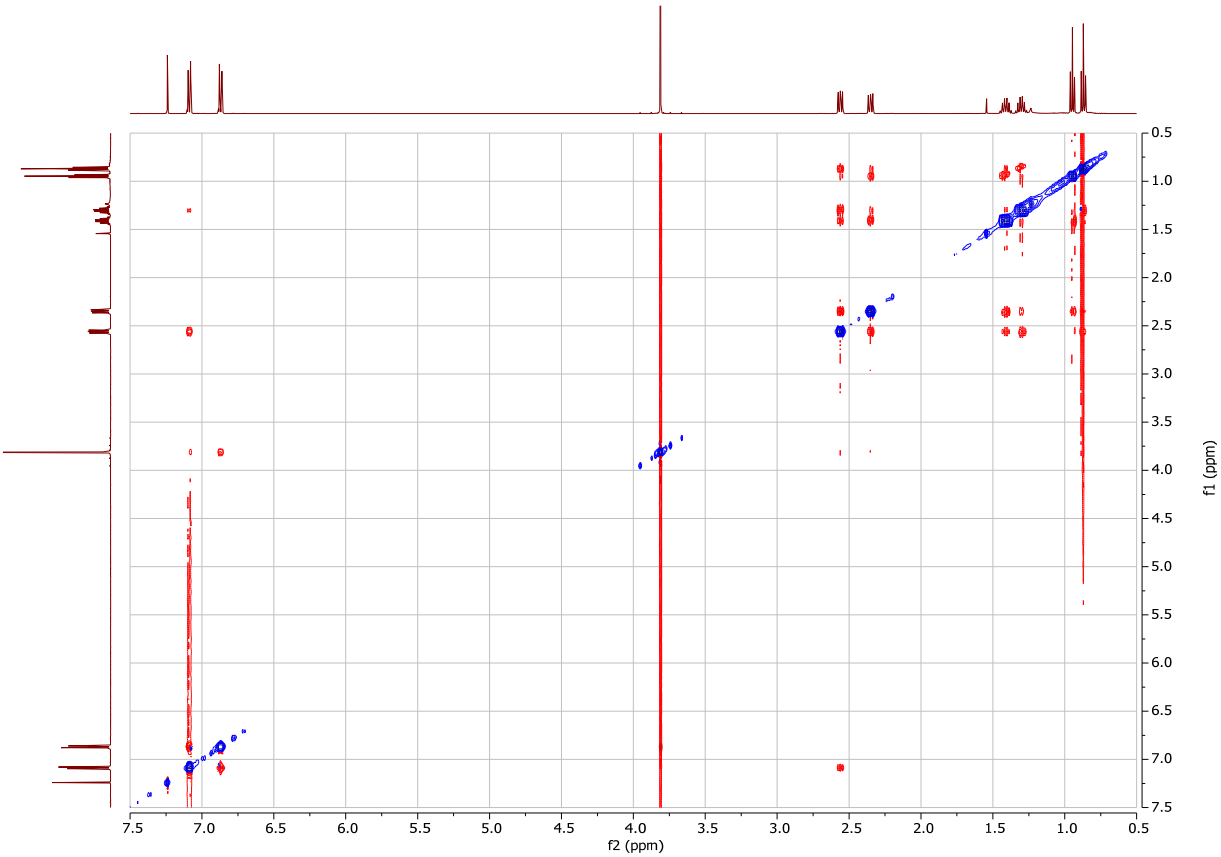

(*Z*)-3-(4-(benzyloxy)phenyl)-2-propylhex-2-enal (**22**).

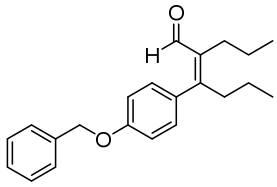

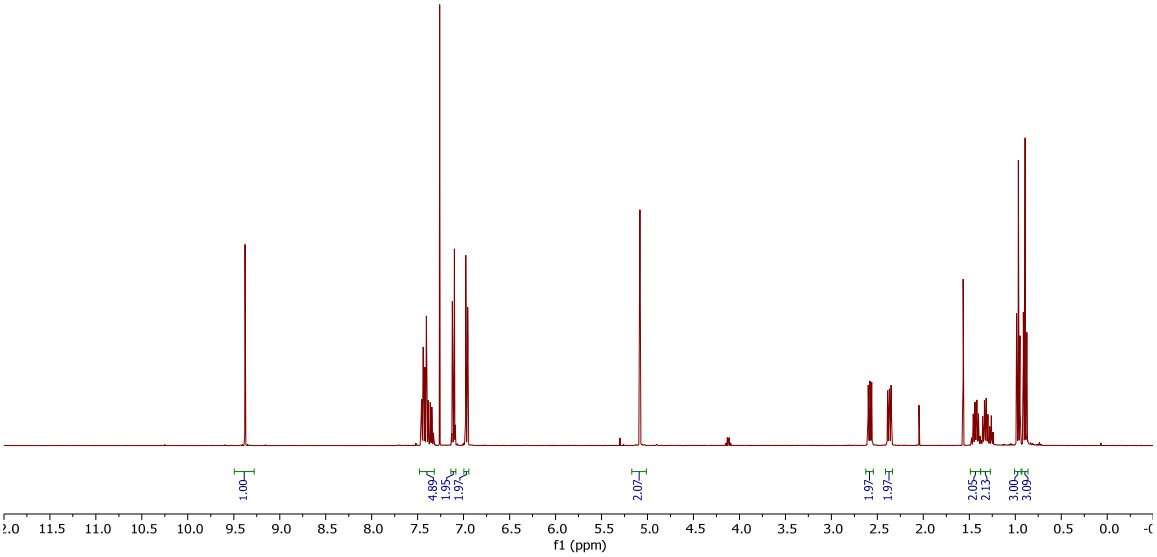

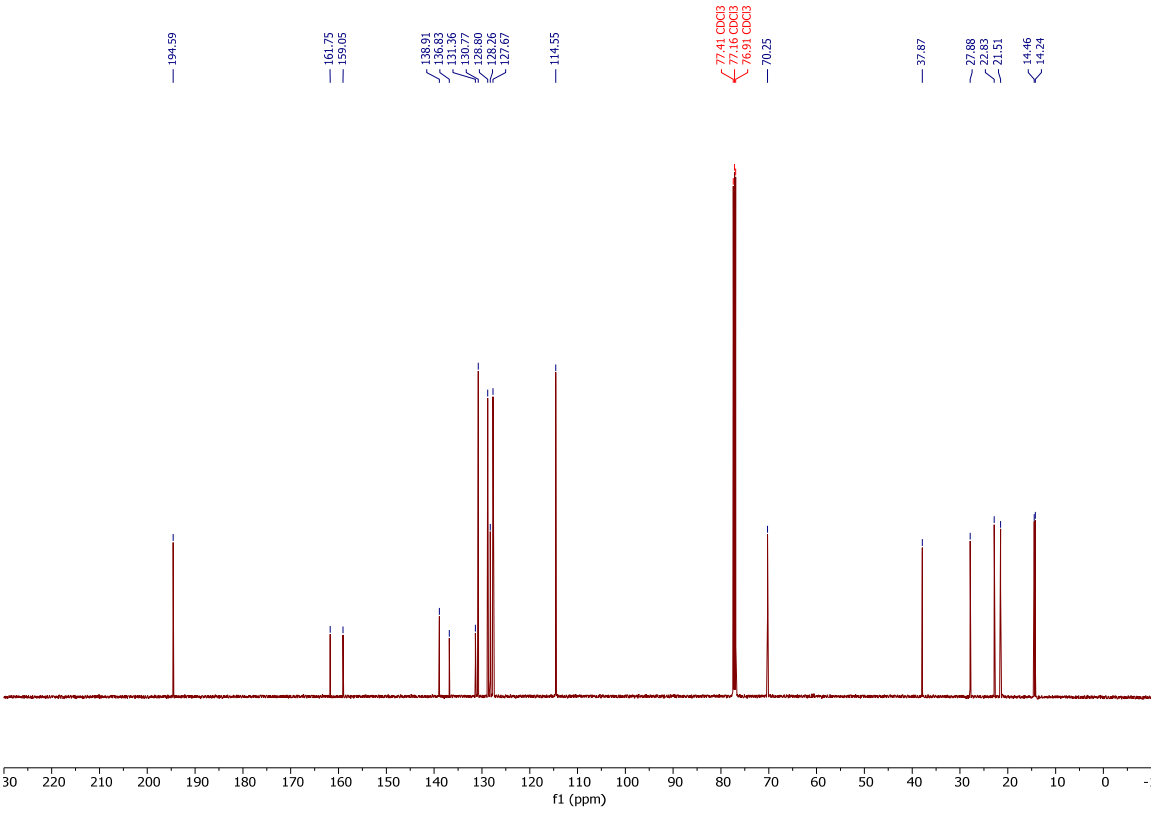

NOESY

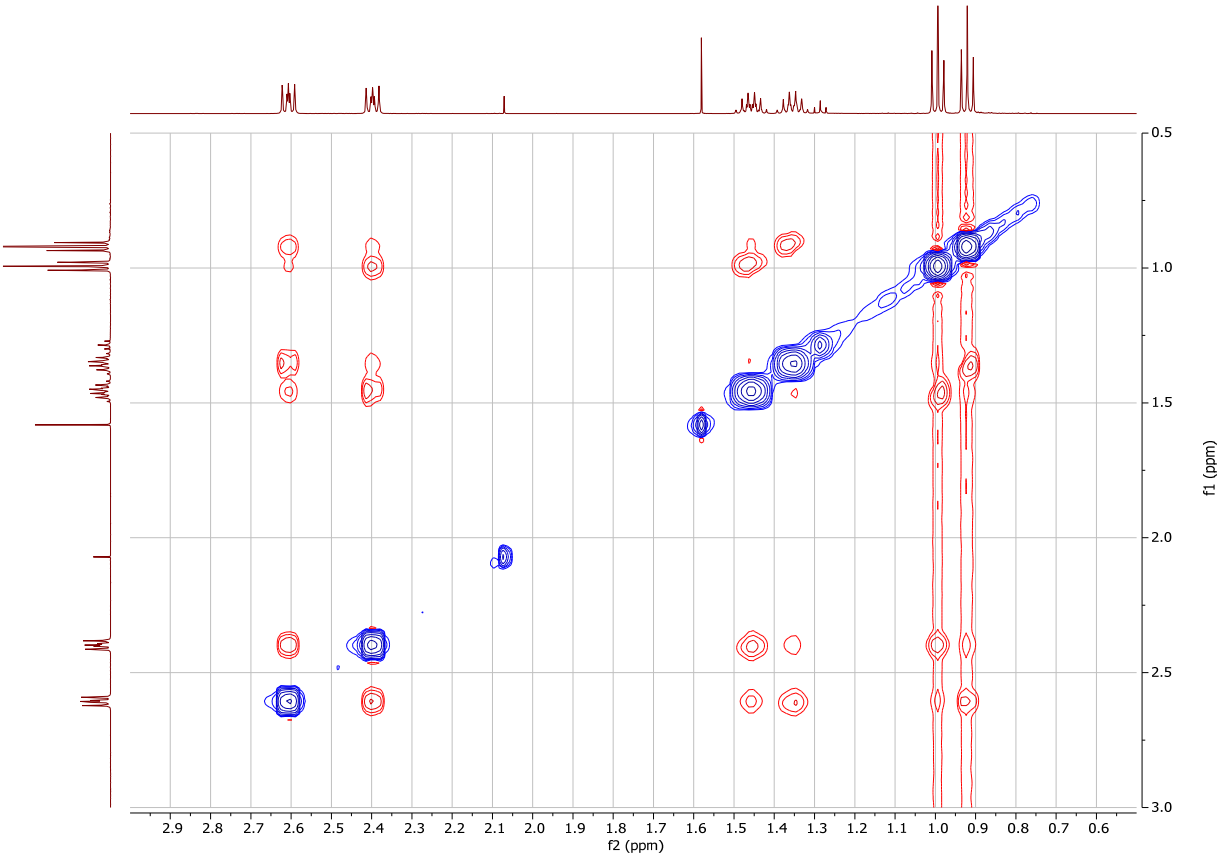
0.5
1.0
1.5
2.0
2.5
3.0
f1 (ppm)
2.9 2.8 2.7 2.6 2.5 2.4 2.3 2.2 2.1 2.0 1.9 1.8 1.7 1.6 1.5 1.4 1.3 1.2 1.1 1.0 0.9 0.8 0.7 0.6
f2 (ppm)

(*Z*)-2-propyl-3-(4-(4,4,5,5-tetramethyl-1,3,2-dioxaborolan-2-yl)phenyl)hex-2-enal (**23**).

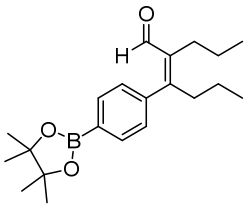

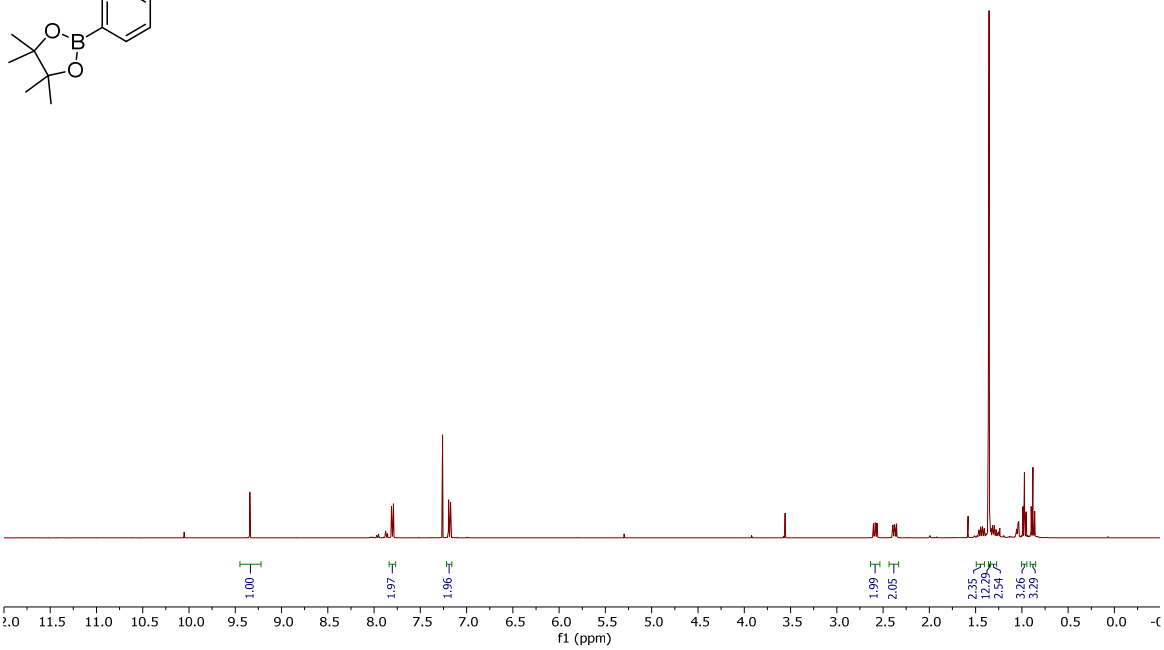

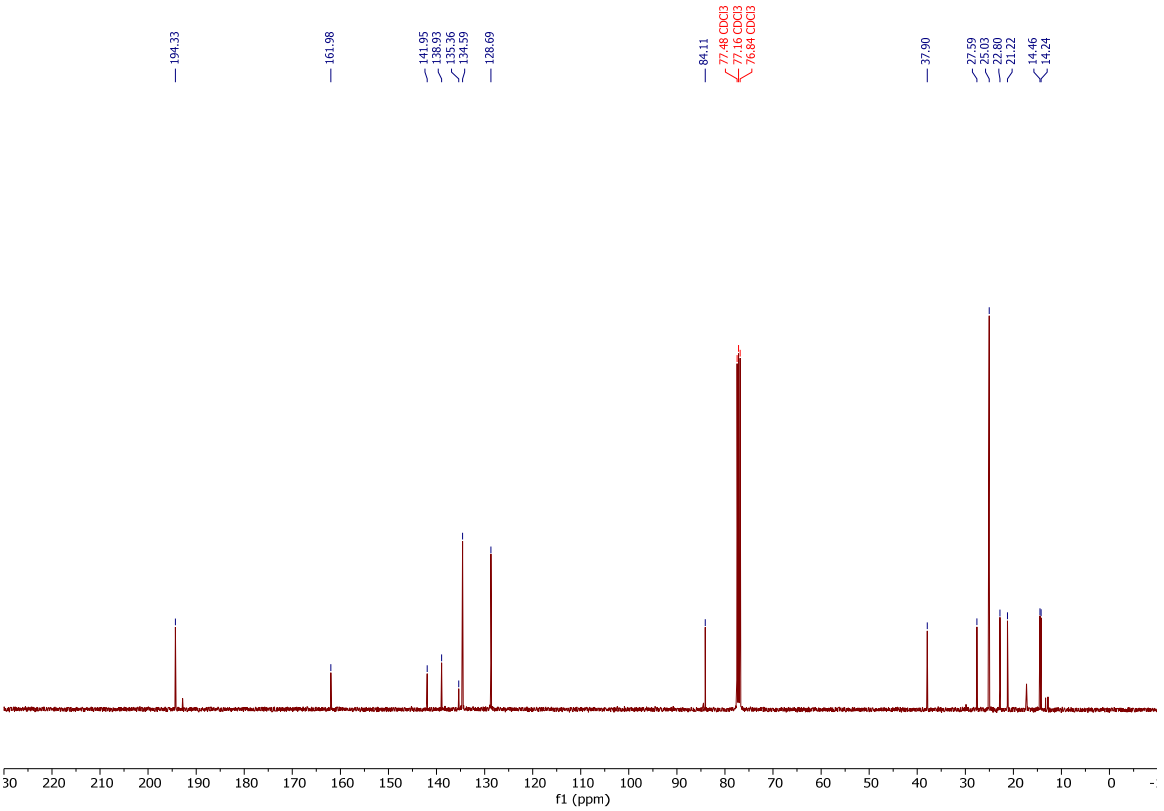

Methyl (*Z*)-3-(5-formyloct-4-en-4-yl)benzoate (**24**).

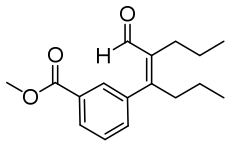

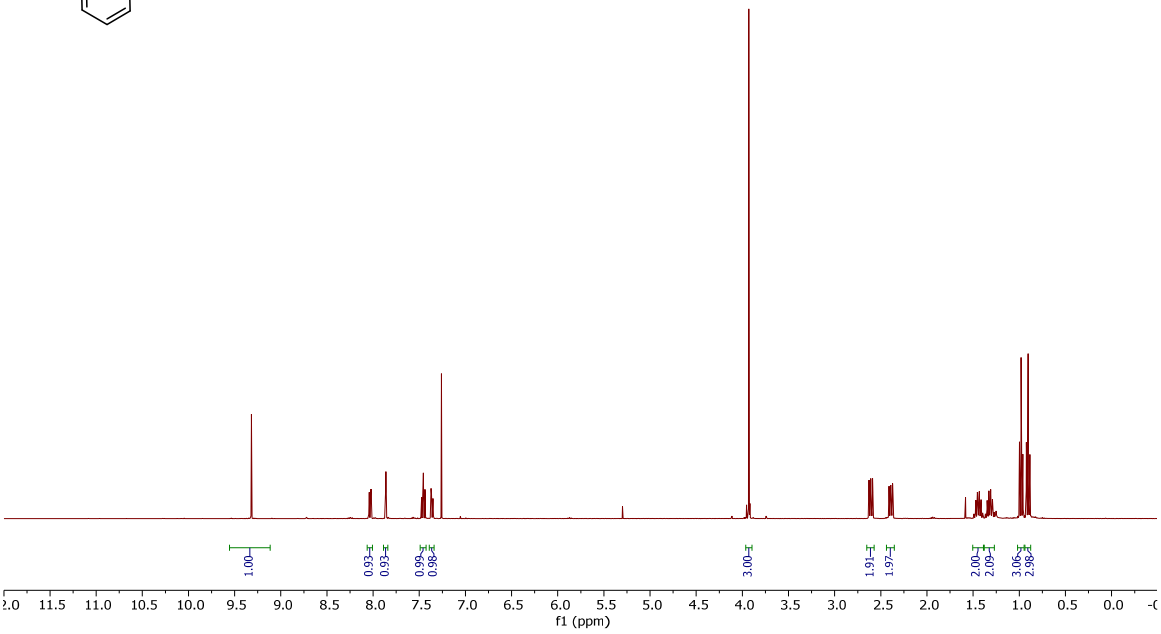

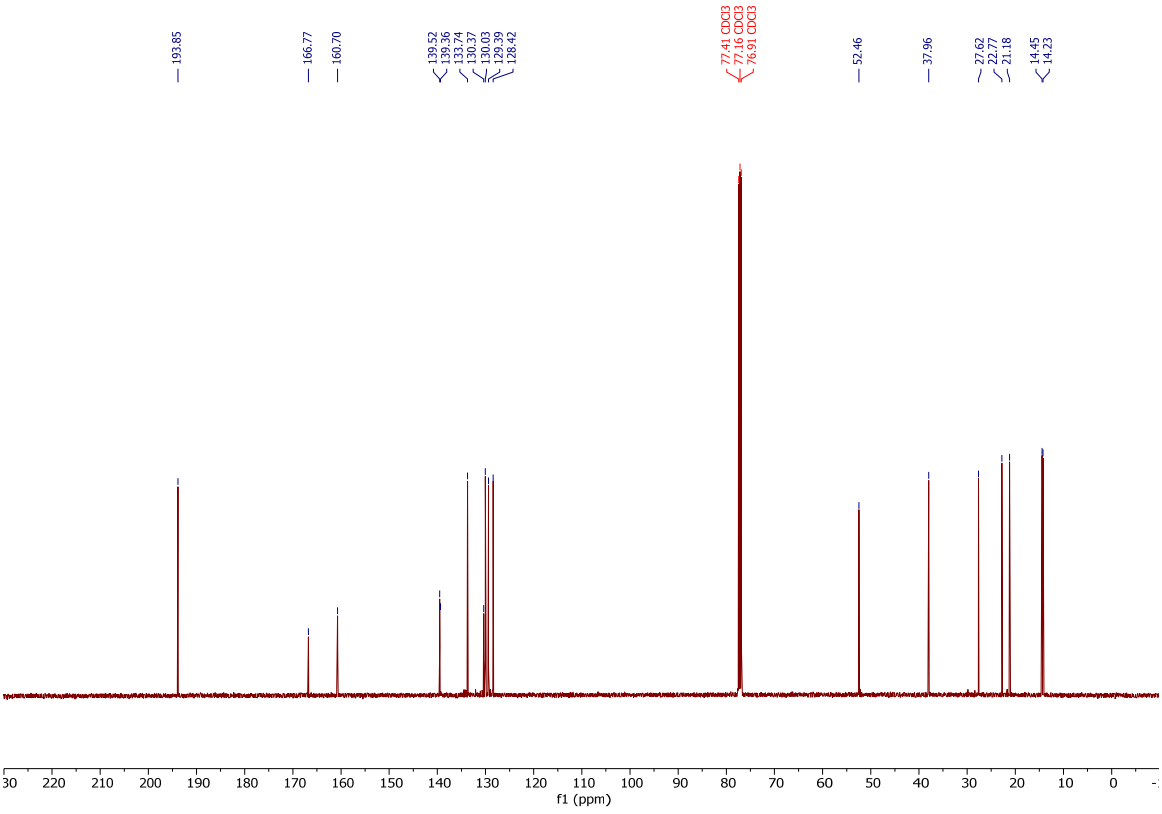

NOESY

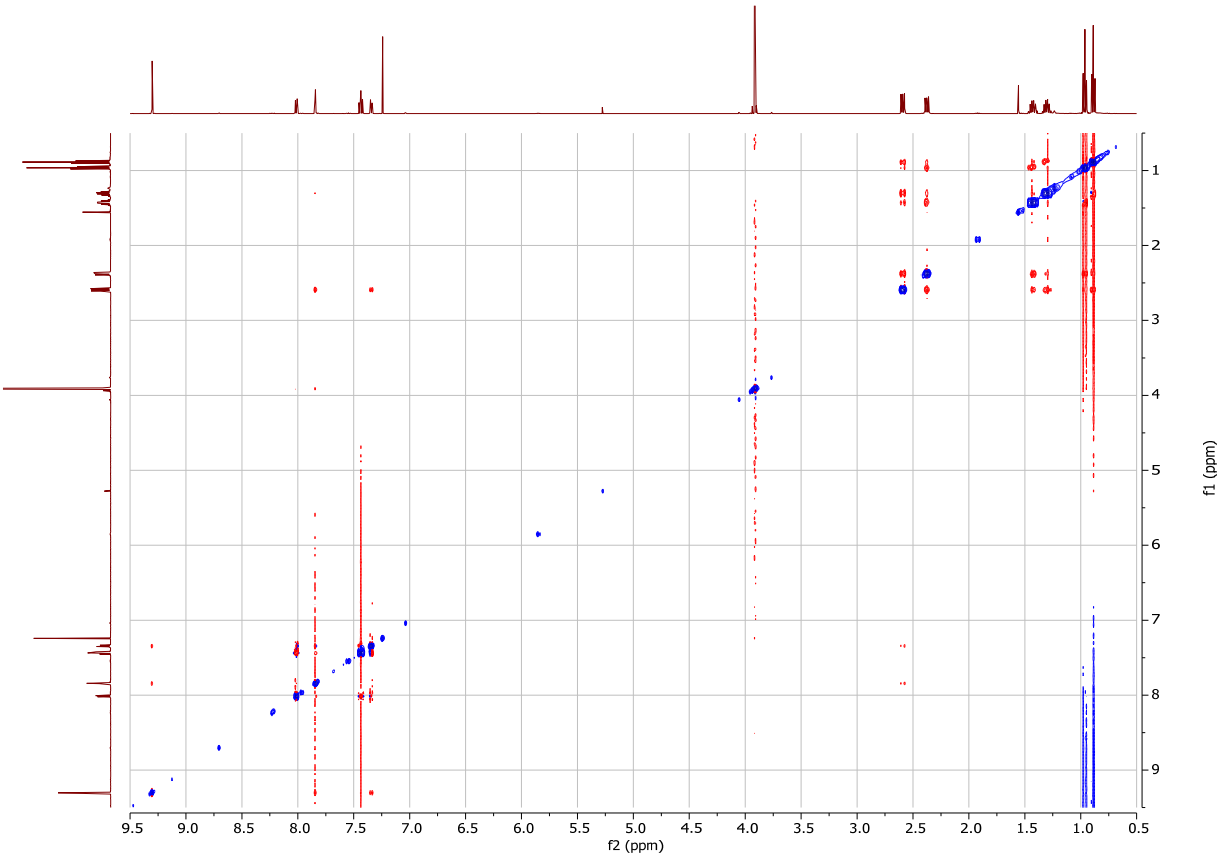

(*Z*)-3-(3-bromophenyl)-2-propylhex-2-enal (**25**).

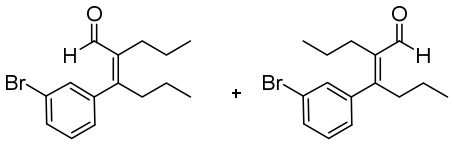

E isomer, minor
Z/*E* = 79:21

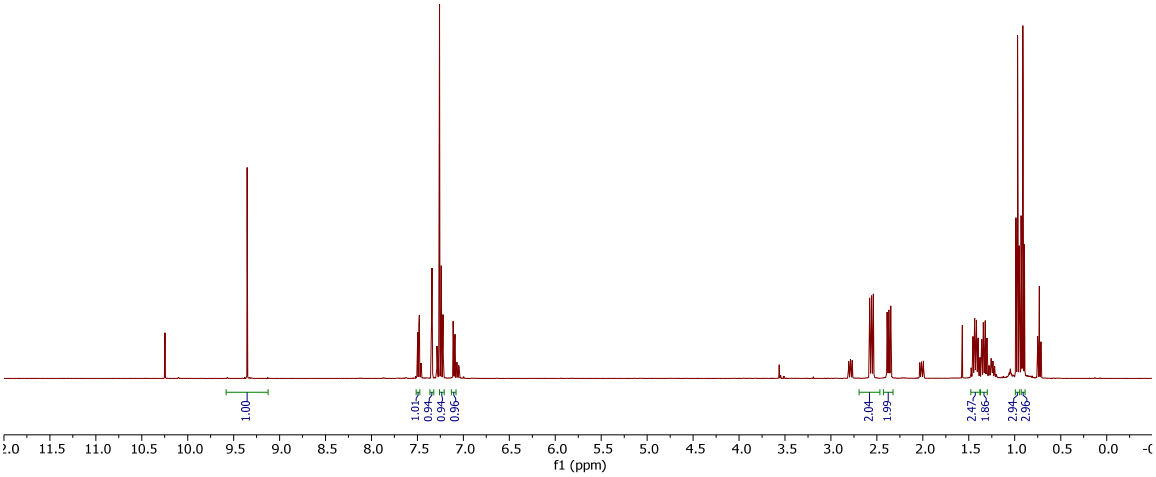

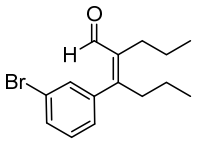

Z isomer, major
Z/*E* = **79**:21

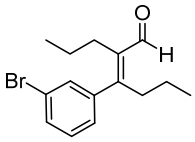

E isomer, minor
Z/*E* = 79:**21**

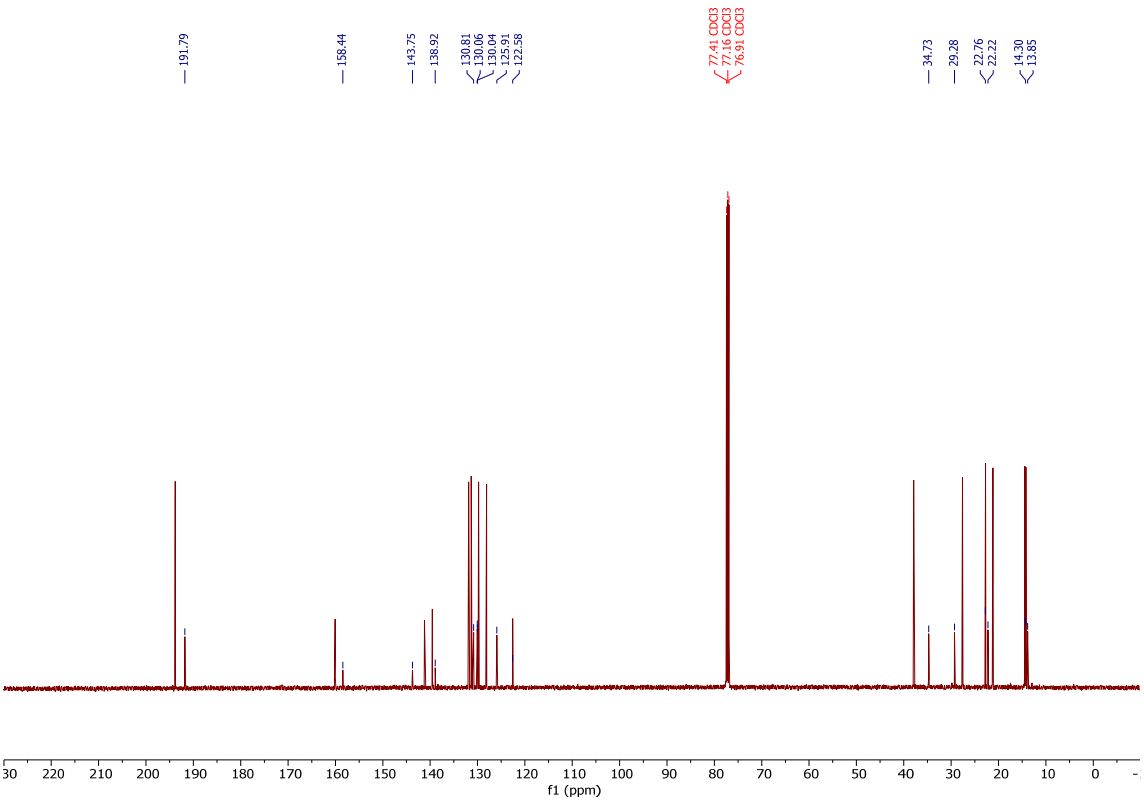

NOESY

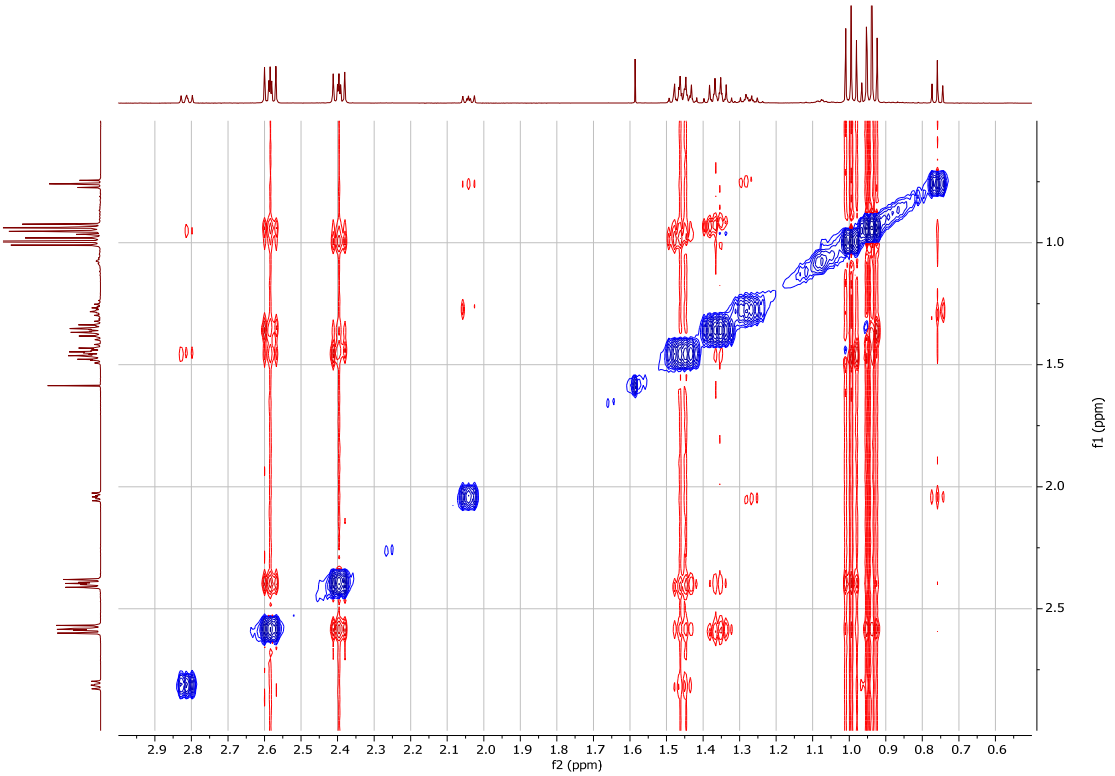
f2 (ppm)
f1 (ppm)

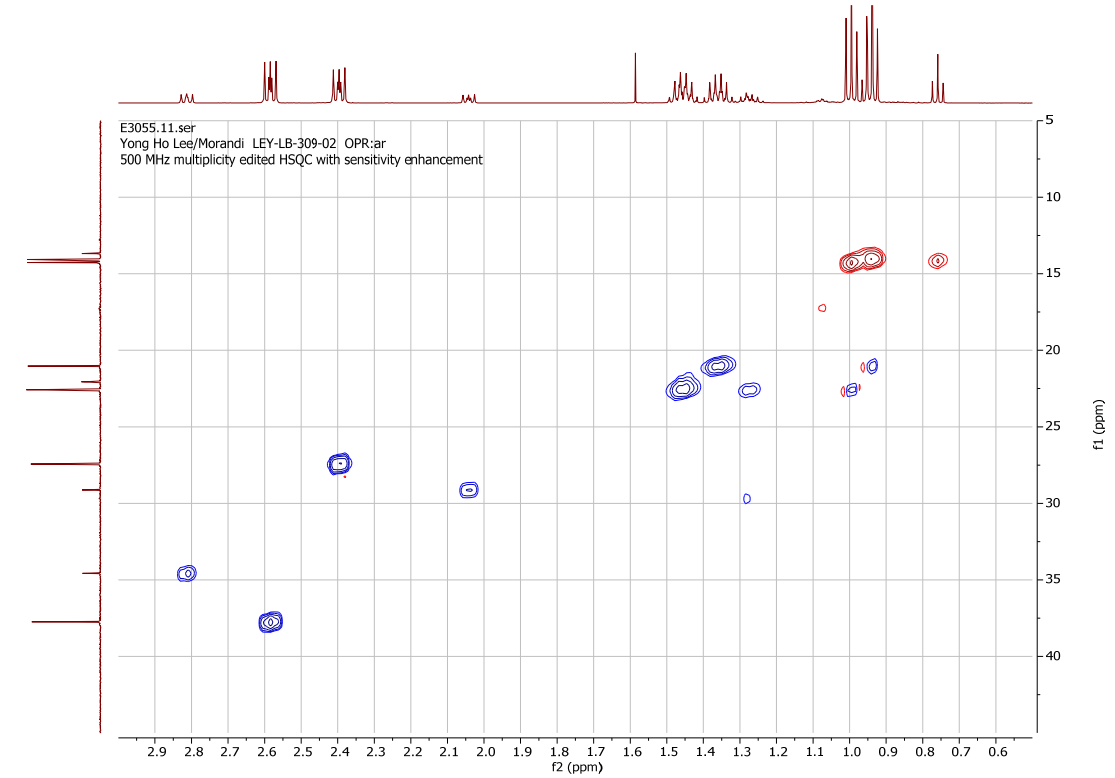
E3055.11.ser
Yong Ho Lee/Morandi LEY-LB-309-02 OPR:ar
500 MHz multiplicity edited HSQC with sensitivity enhancement
f2 (ppm)
f1 (ppm)

(*Z*)-4-(5-formyloct-4-en-4-yl)benzonitrile (**26**).

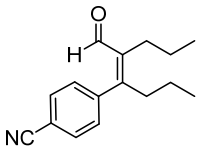

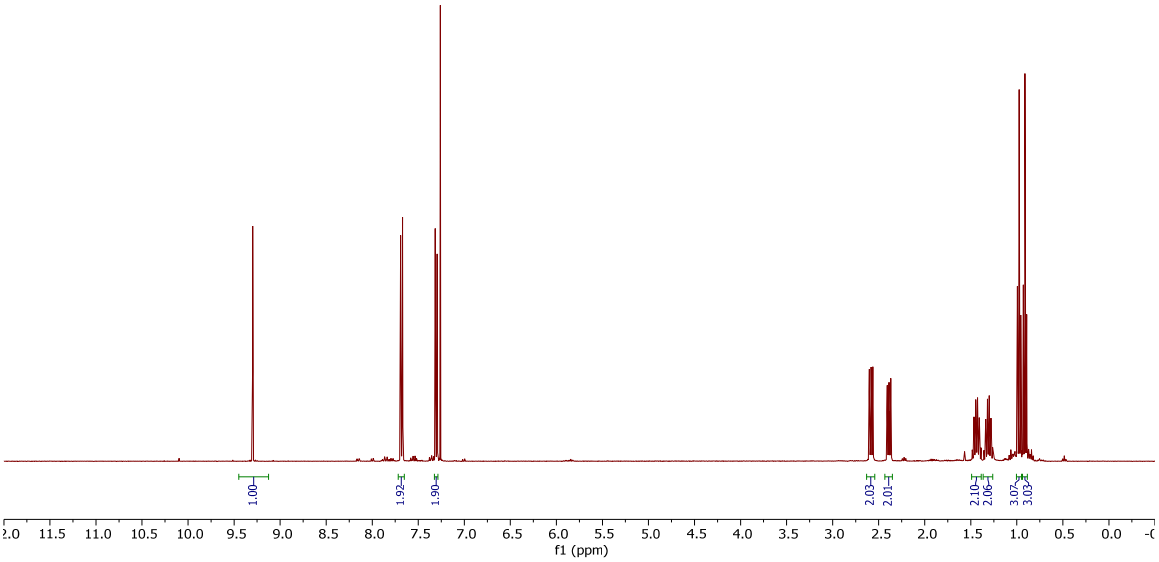

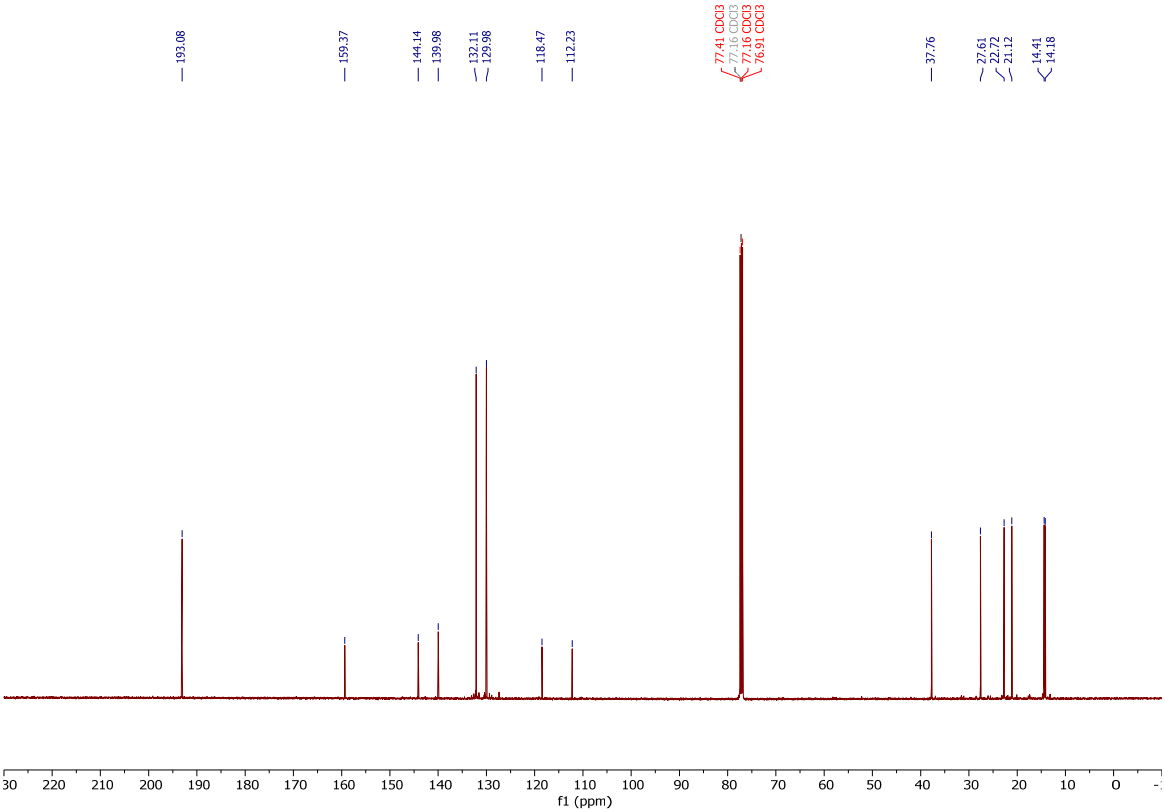

NOESY

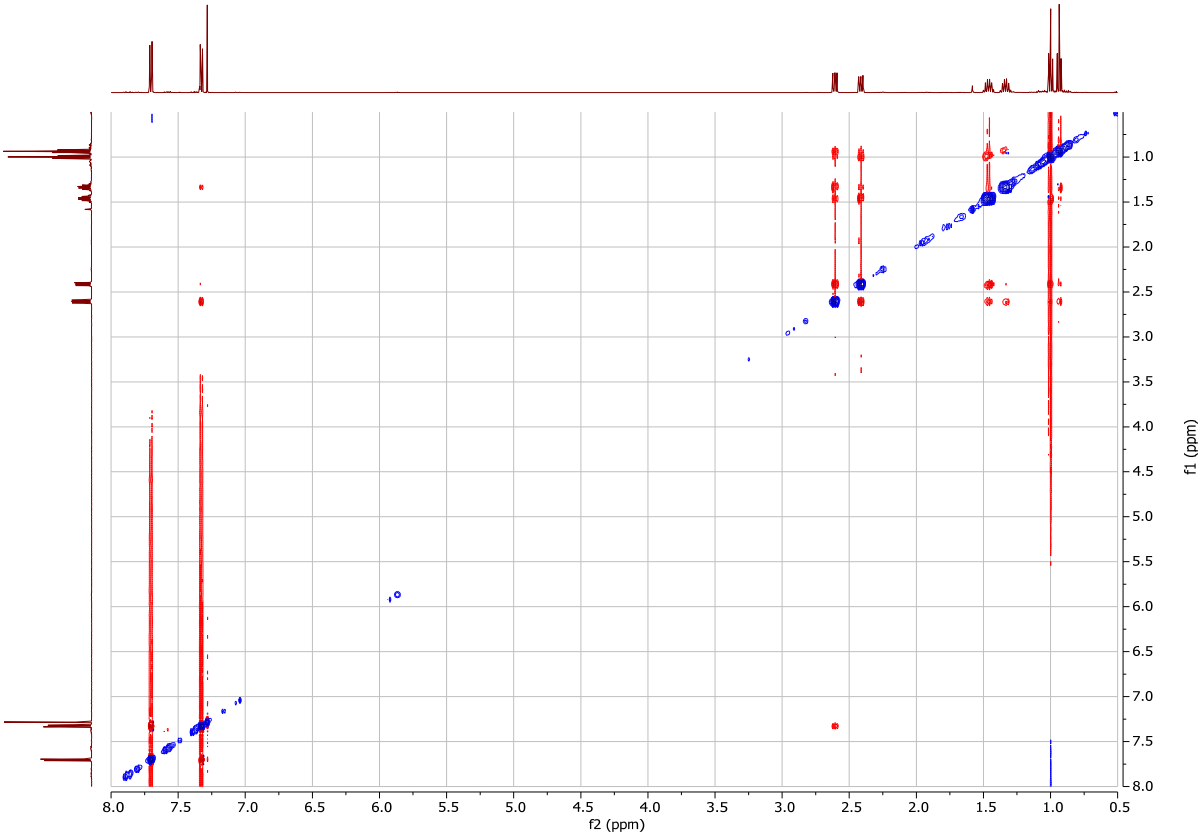

(*Z*)-3-(4-fluorophenyl)-2-propylhex-2-enal (**27**).

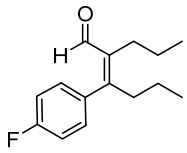

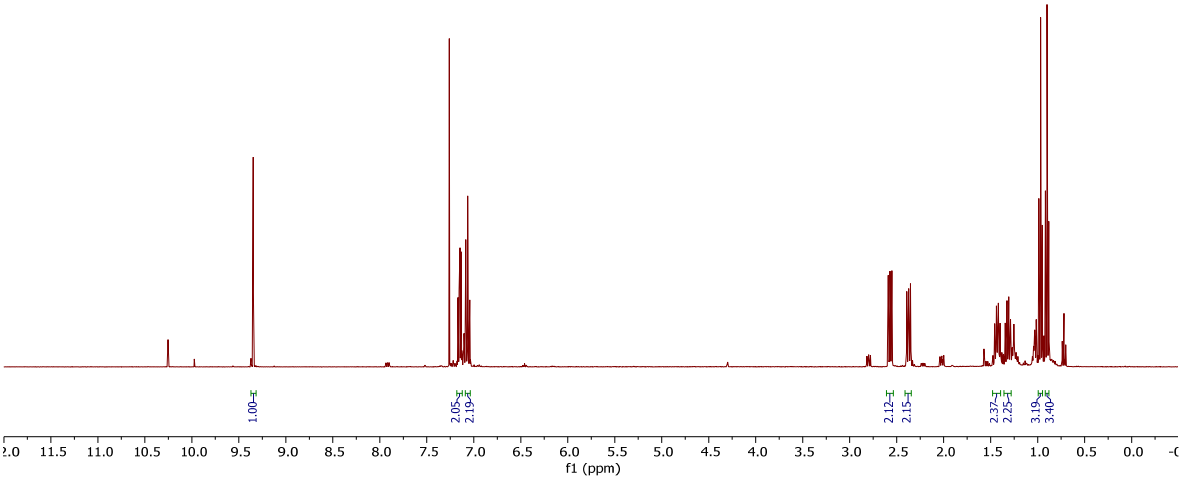

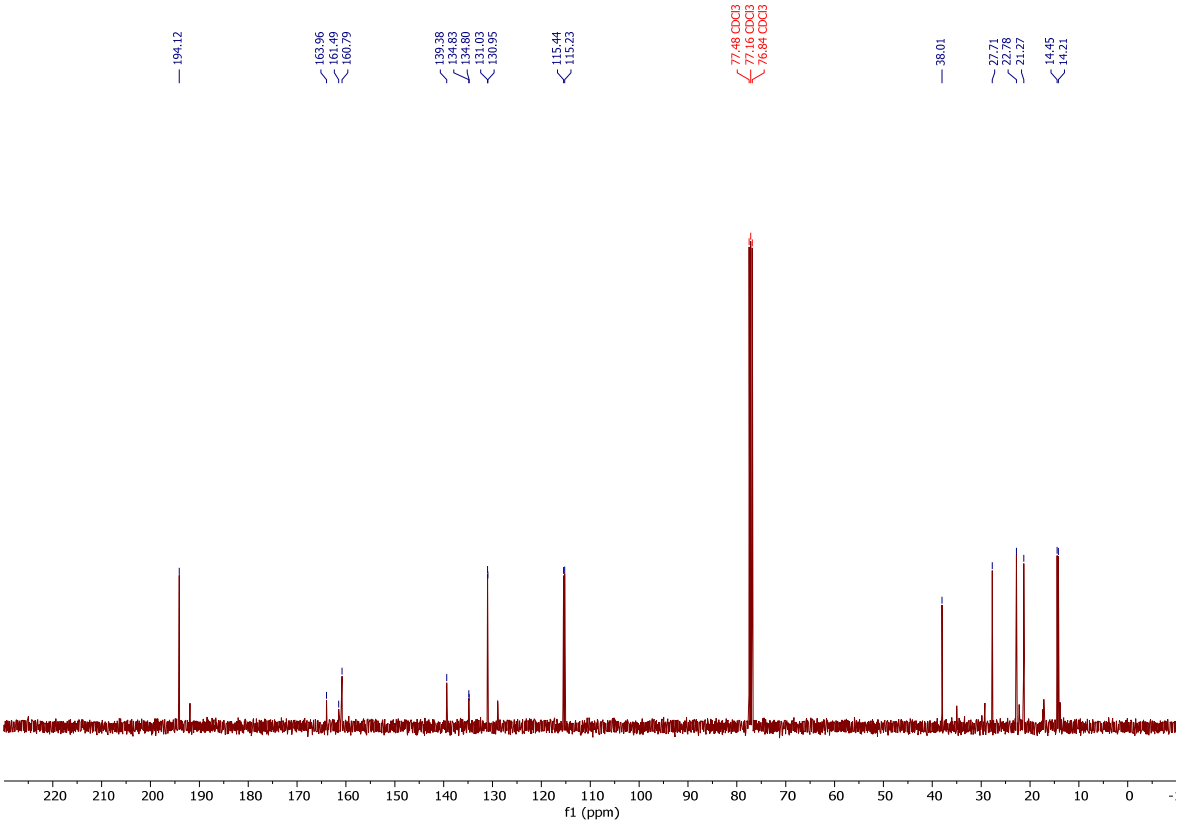

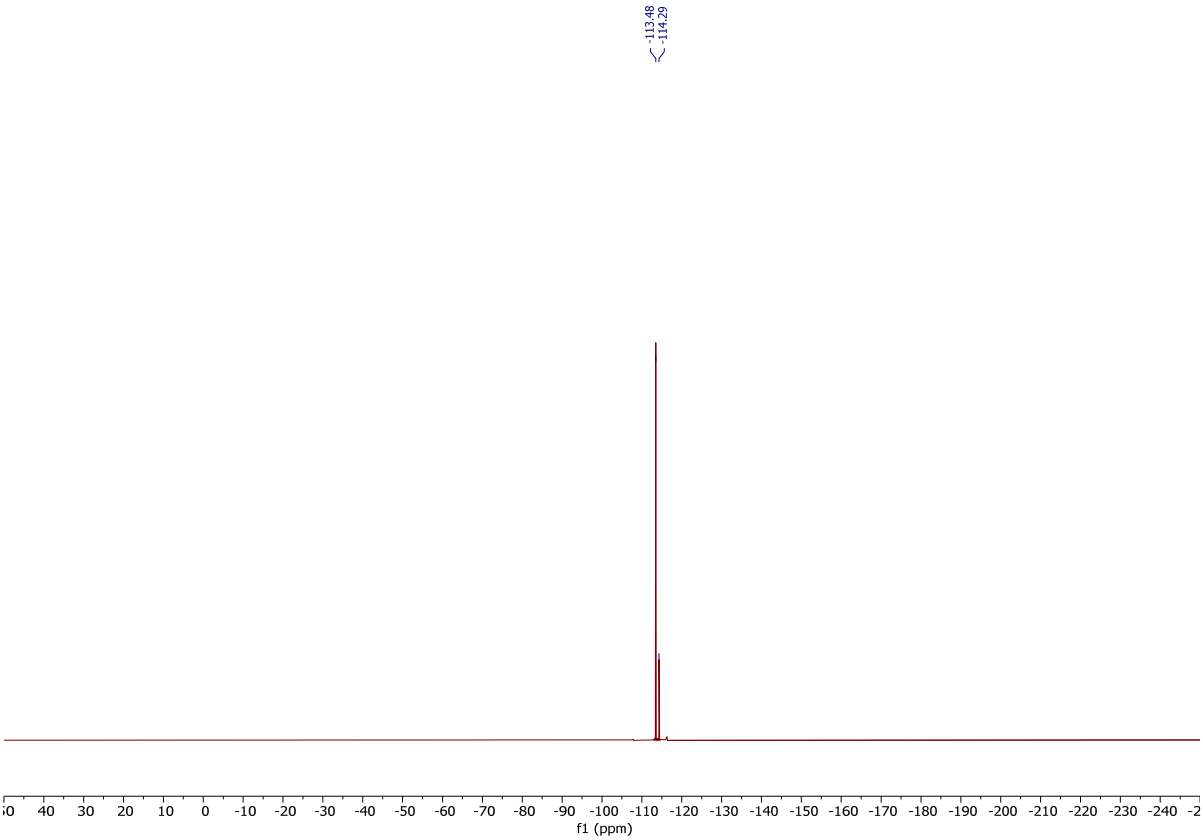
-113.48
-114.29
60 40 30 20 10 0 -10 -20 -30 -40 -50 -60 -70 -80 -90 -100 -110 -120 -130 -140 -150 -160 -170 -180 -190 -200 -210 -220 -230 -240 -2
f1 (ppm)

(*Z*)-3-(3,5-bis(trifluoromethyl)phenyl)-2-propylhex-2-enal (**28-*Z***).

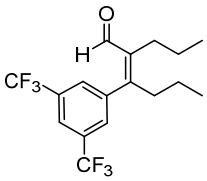

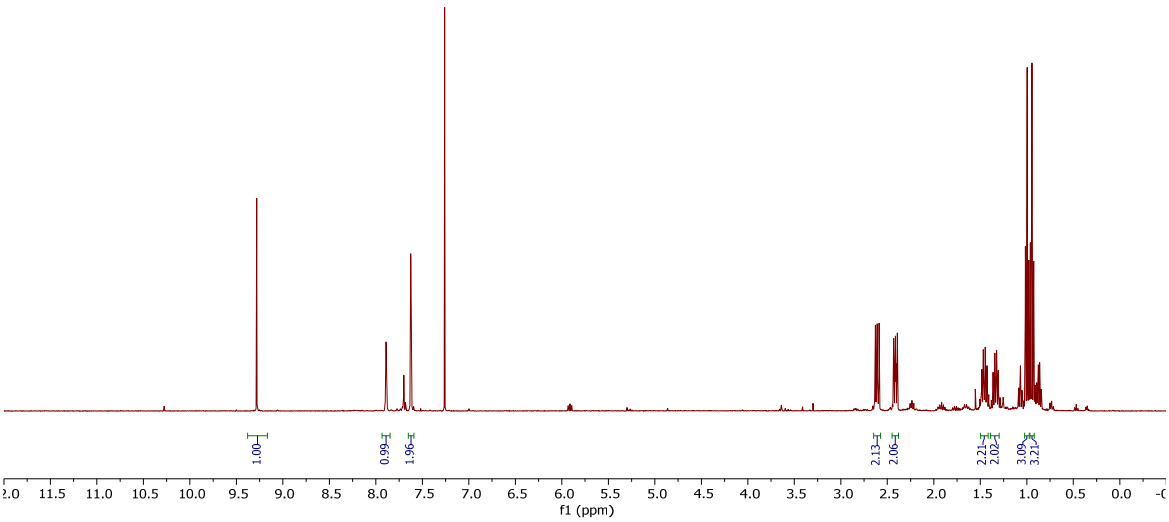

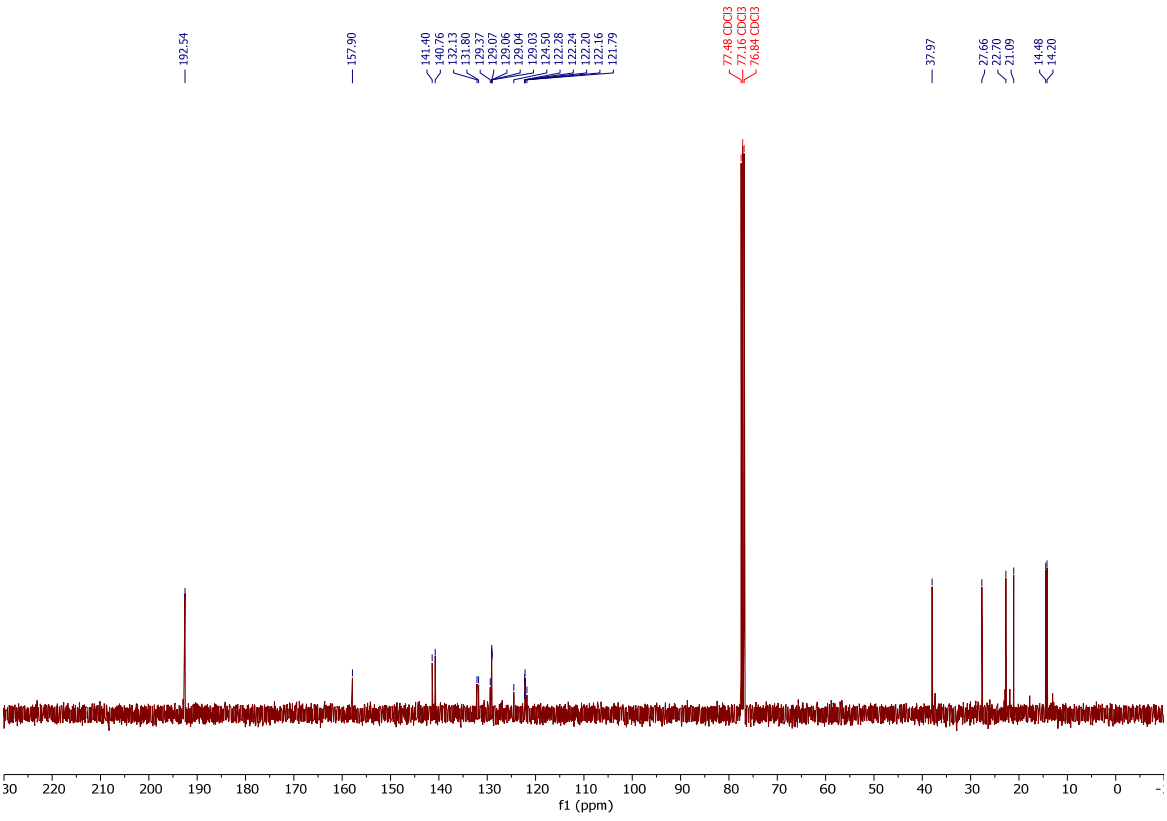

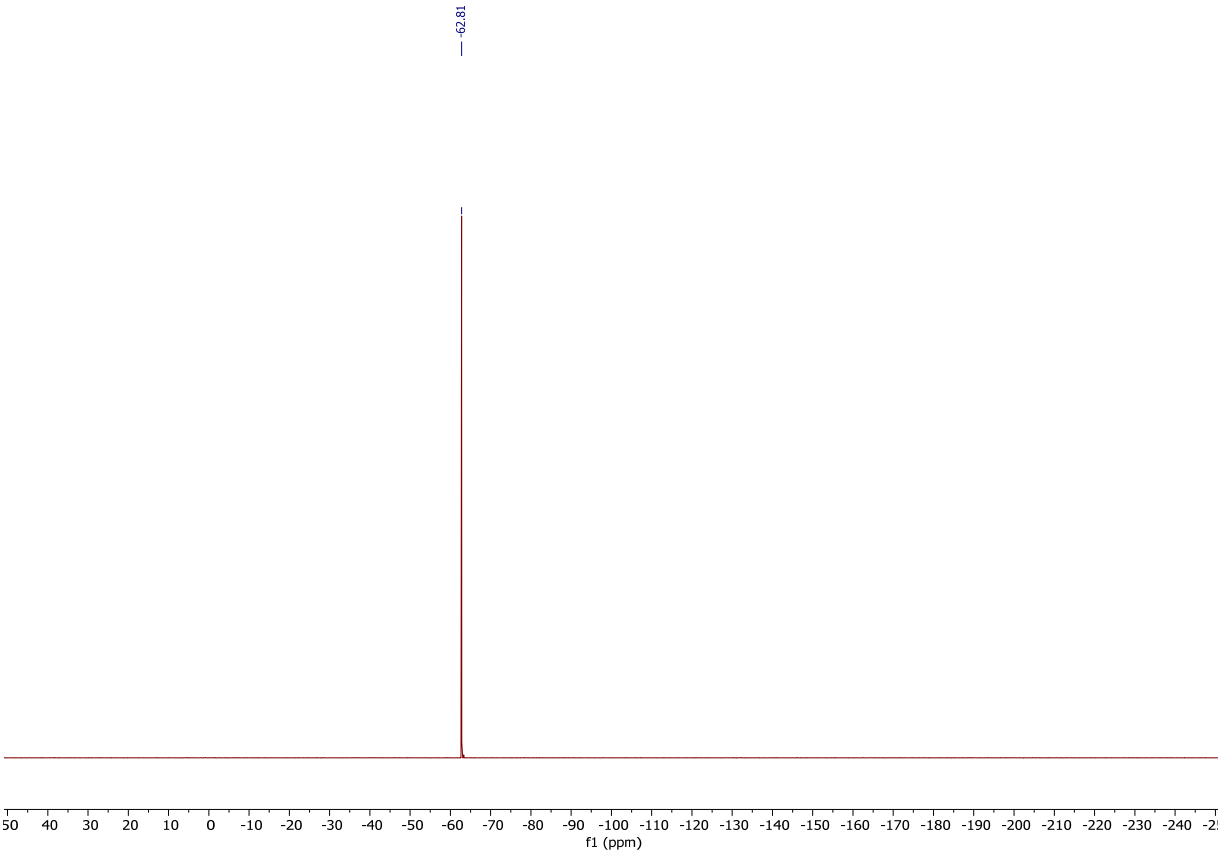
-62.81
50 40 30 20 10 0 -10 -20 -30 -40 -50 -60 -70 -80 -90 -100 -110 -120 -130 -140 -150 -160 -170 -180 -190 -200 -210 -220 -230 -240
f1 (ppm)

(*E*)-3-(3,5-bis(trifluoromethyl)phenyl)-2-propylhex-2-enal (**28-*E***).

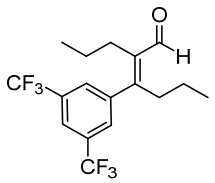

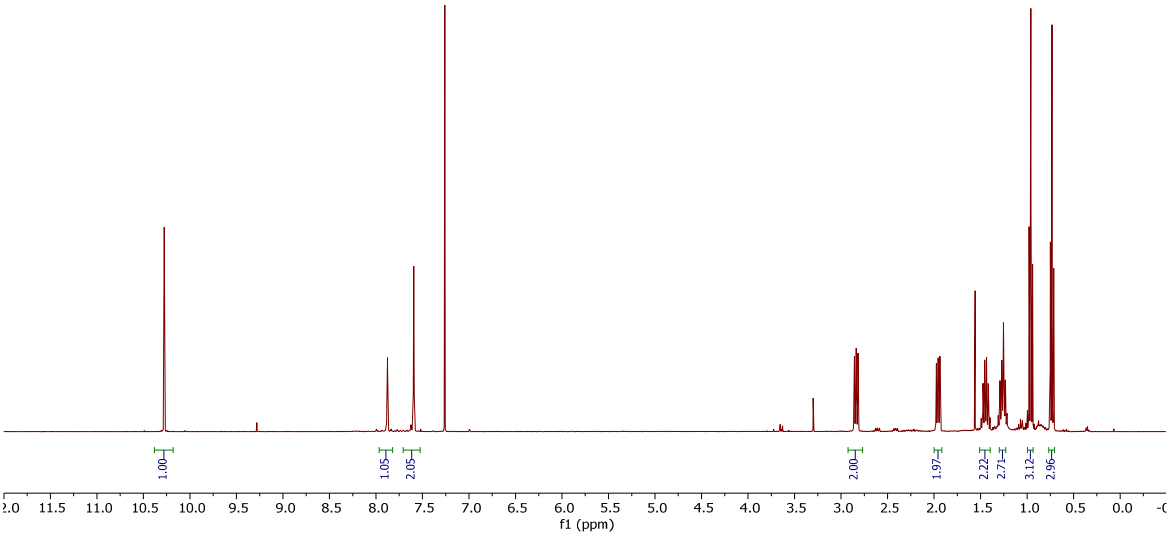

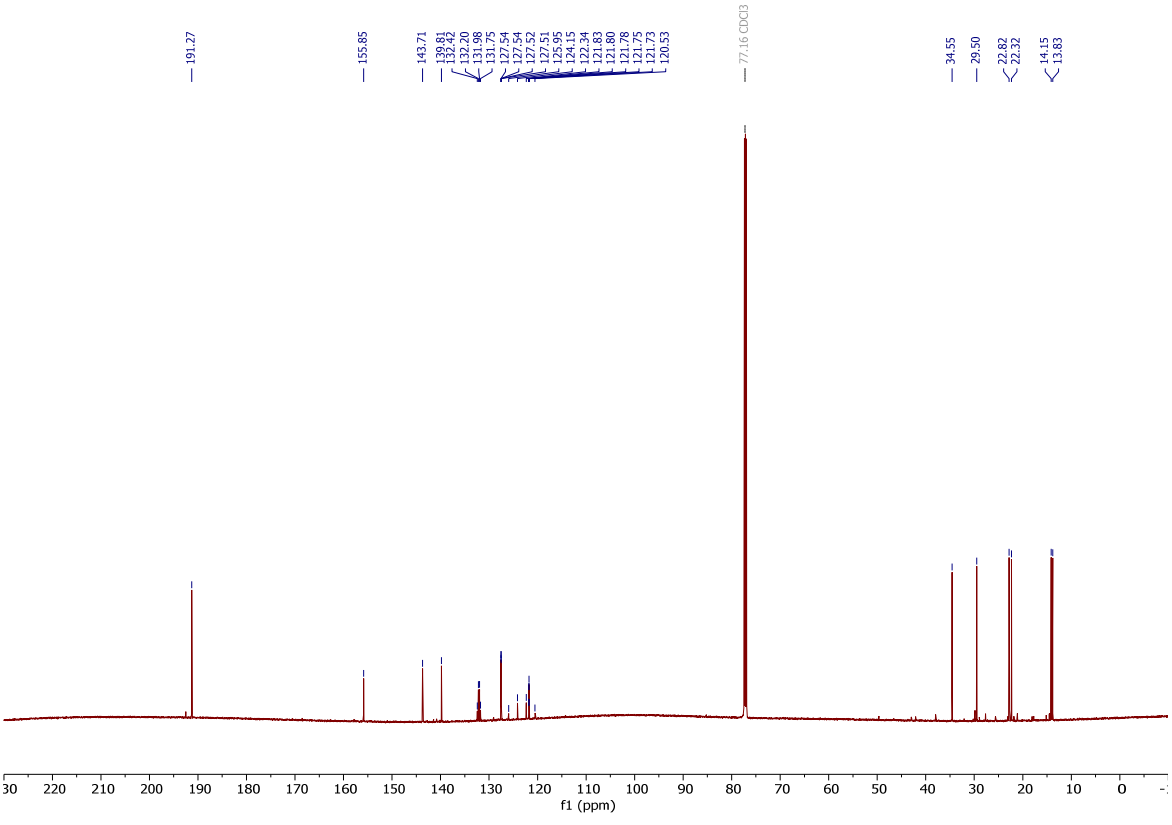

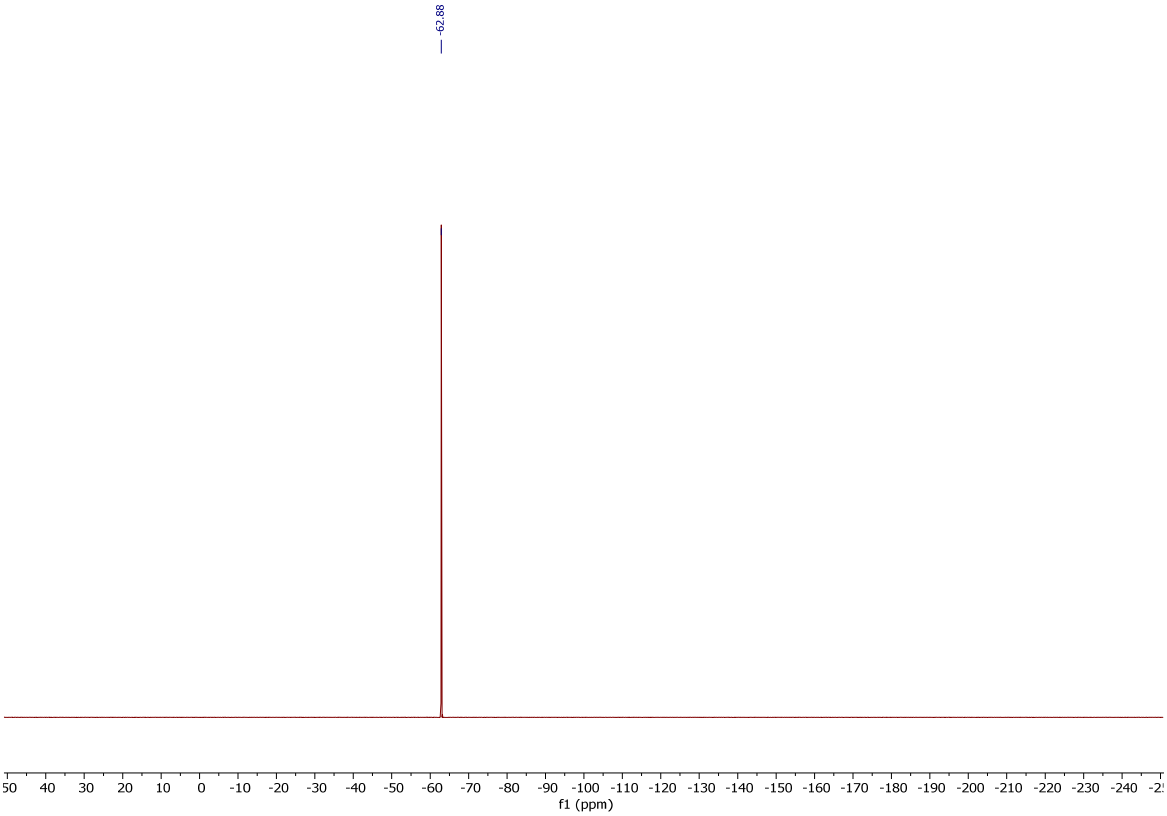
-62.86
f1 (ppm)

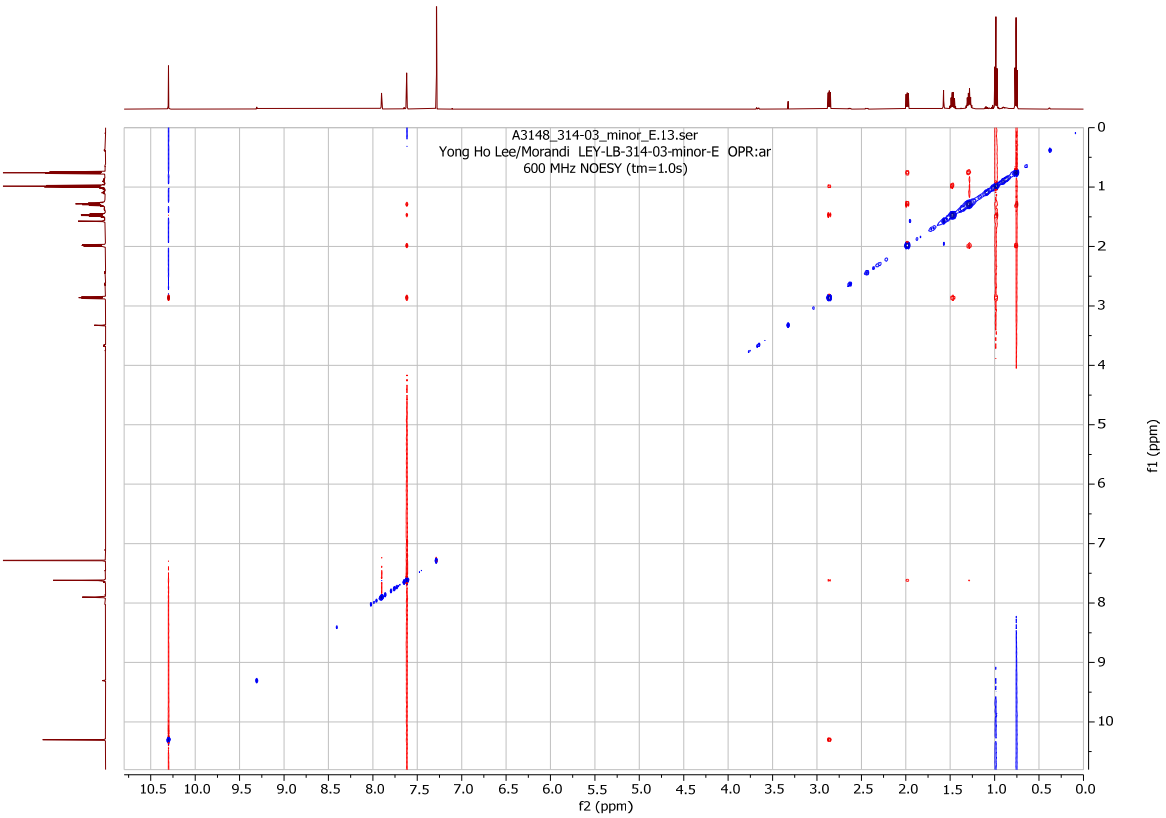
A3148_314-03_minor_E.13.ser
Yong Ho Lee/Morandi LEY-LB-314-03-minor-E OPR:ar
600 MHz NOESY (tm=1.0s)
f2 (ppm)
f1 (ppm)

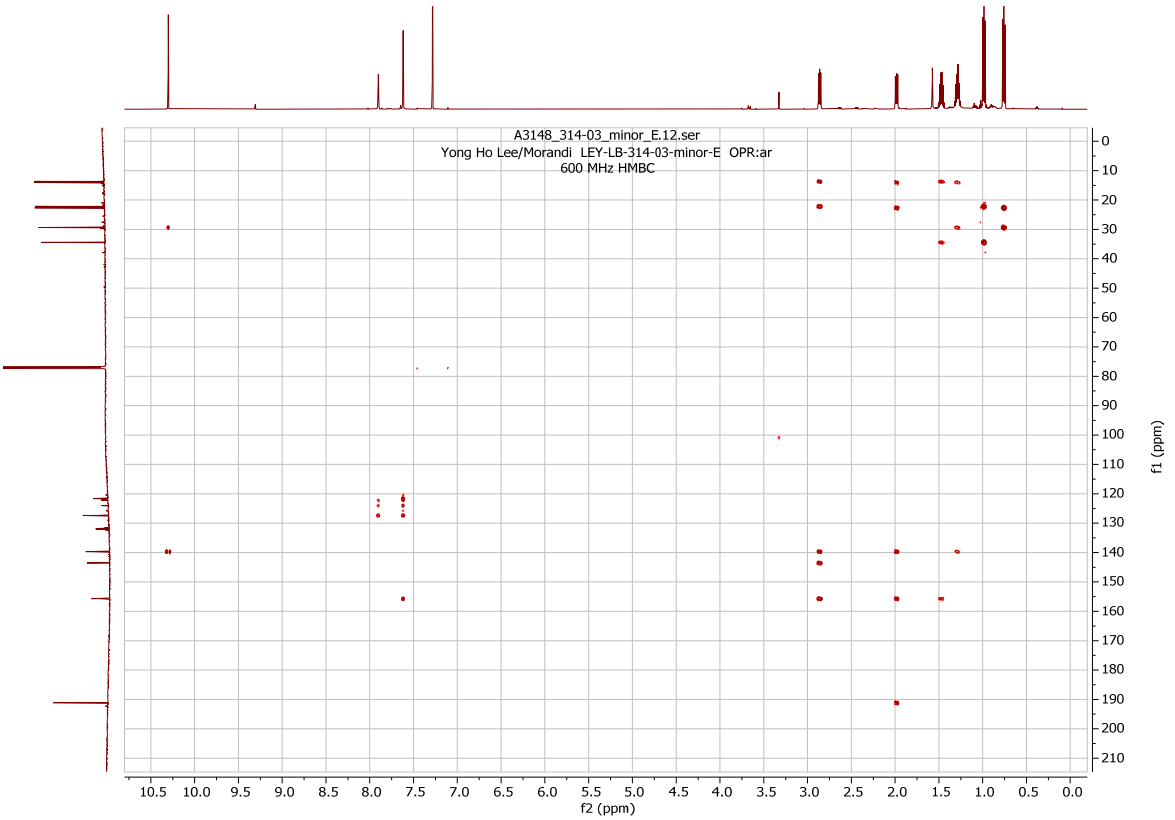
A3148_314-03_minor_E.12.ser
Yong Ho Lee/Morandi LEY-LB-314-03-minor-E OPR:ar
600 MHz HMBC
f2 (ppm)
f1 (ppm)

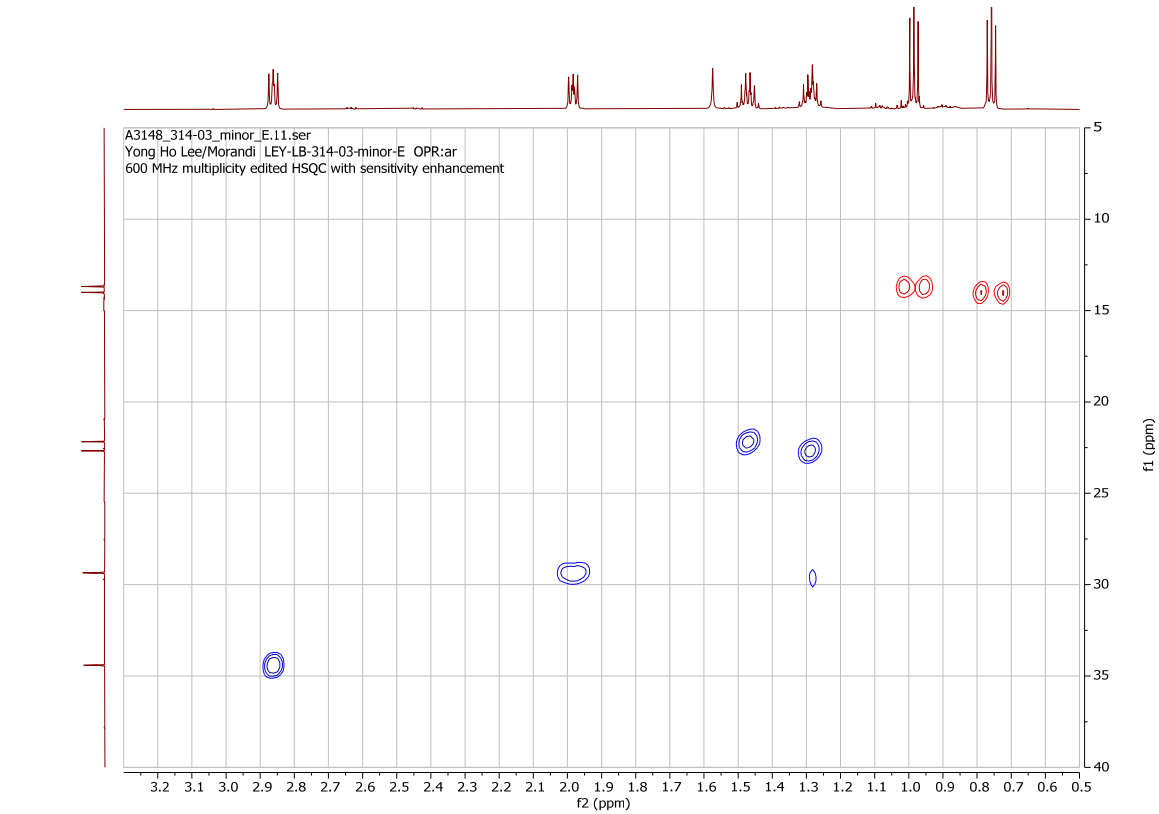
A3148_314-03_minor_E.11.ser
Yong Ho Lee/Morandi LEY-LB-314-03-minor-E OPR:ar
600 MHz multiplicity edited HSQC with sensitivity enhancement
f2 (ppm)
f1 (ppm)

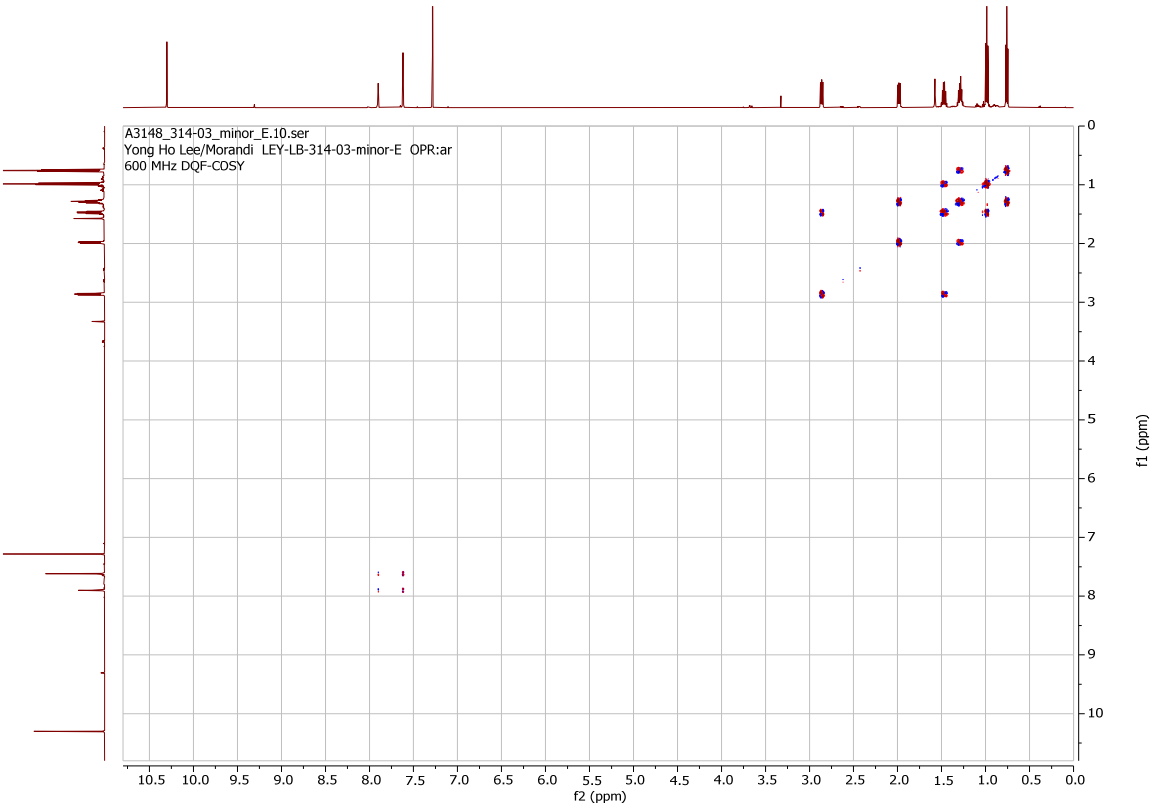
A3148_314-03_minor_E.10.ser
Yong Ho Lee/Morandi LEY-LB-314-03-minor-E OPR:ar
600 MHz DQF-COSY
f2 (ppm)
f1 (ppm)

(*Z*)-4-(5-formyloct-4-en-4-yl)-*N*,*N*-dipropylbenzenesulfonamide (**29**).

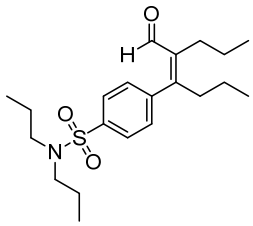

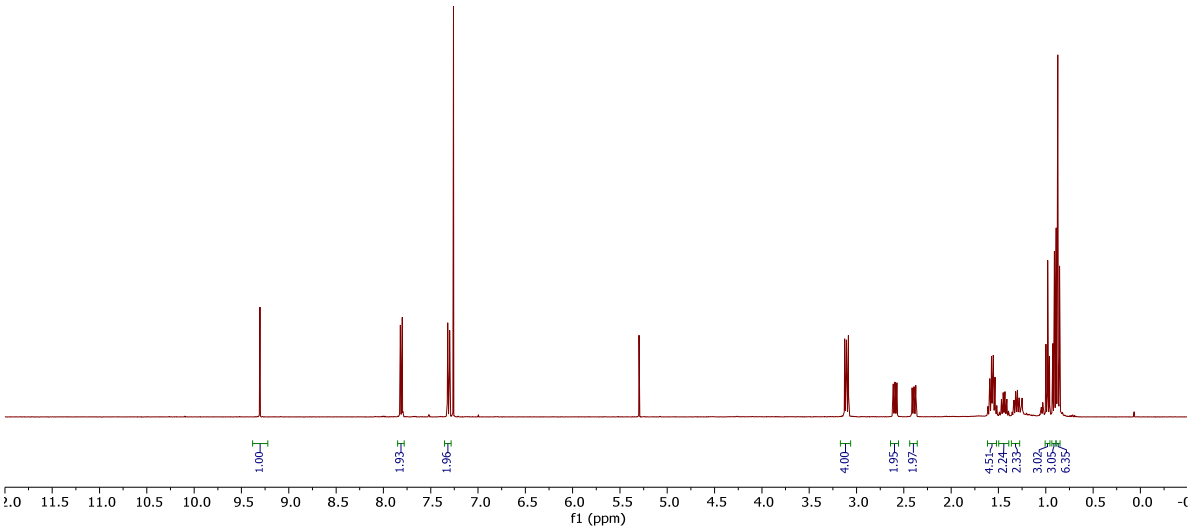

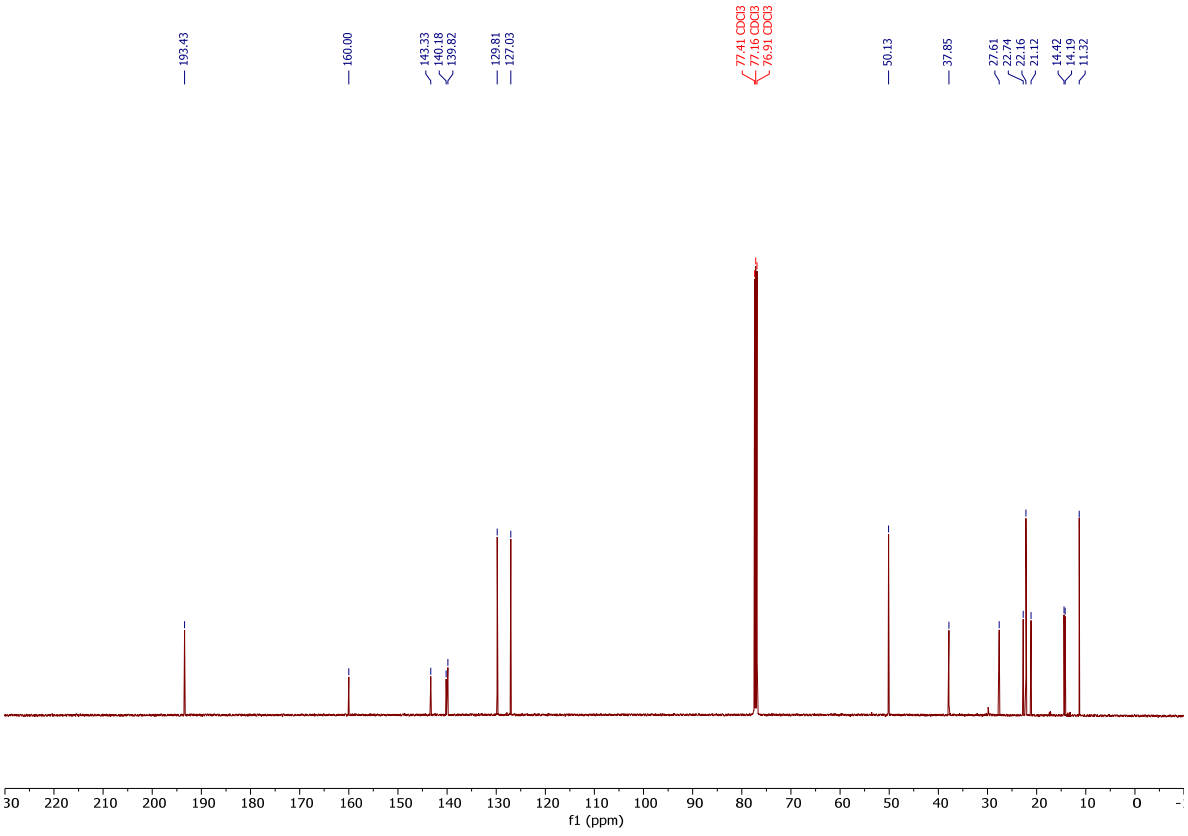

NOESY

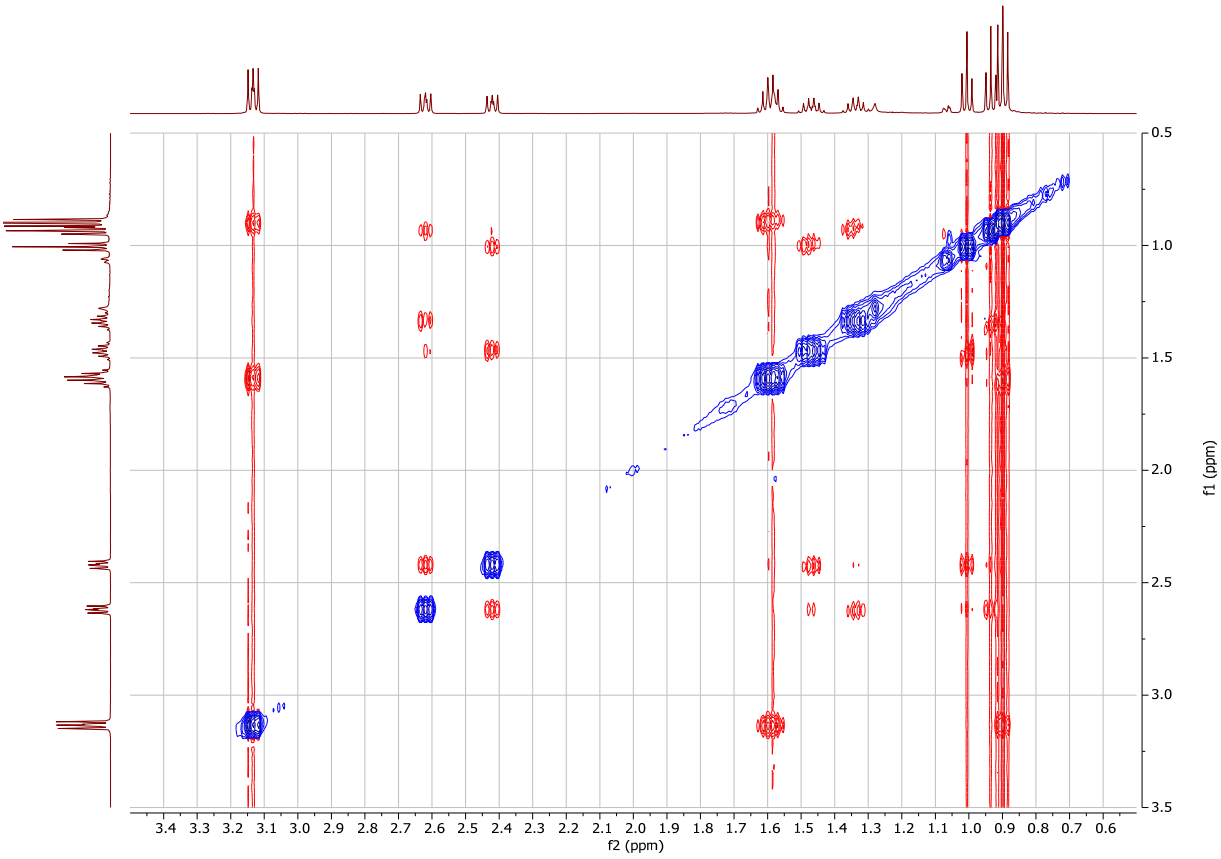
0.5
1.0
1.5
2.0
2.5
3.0
3.5
f1 (ppm)
3.4 3.3 3.2 3.1 3.0 2.9 2.8 2.7 2.6 2.5 2.4 2.3 2.2 2.1 2.0 1.9 1.8 1.7 1.6 1.5 1.4 1.3 1.2 1.1 1.0 0.9 0.8 0.7 0.6
f2 (ppm)

(*Z*)-5-(5-(5-formyloct-4-en-4-yl)-4-methylthiazol-2-yl)-2-isobutoxybenzonitrile (**30**).

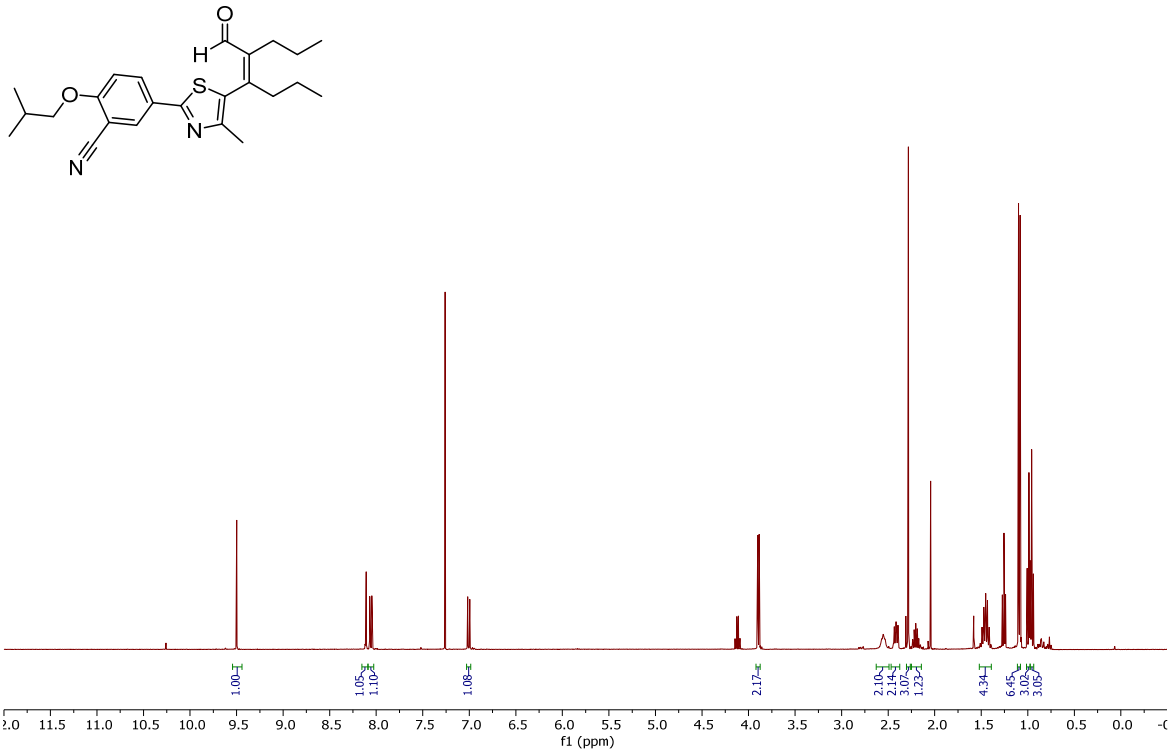

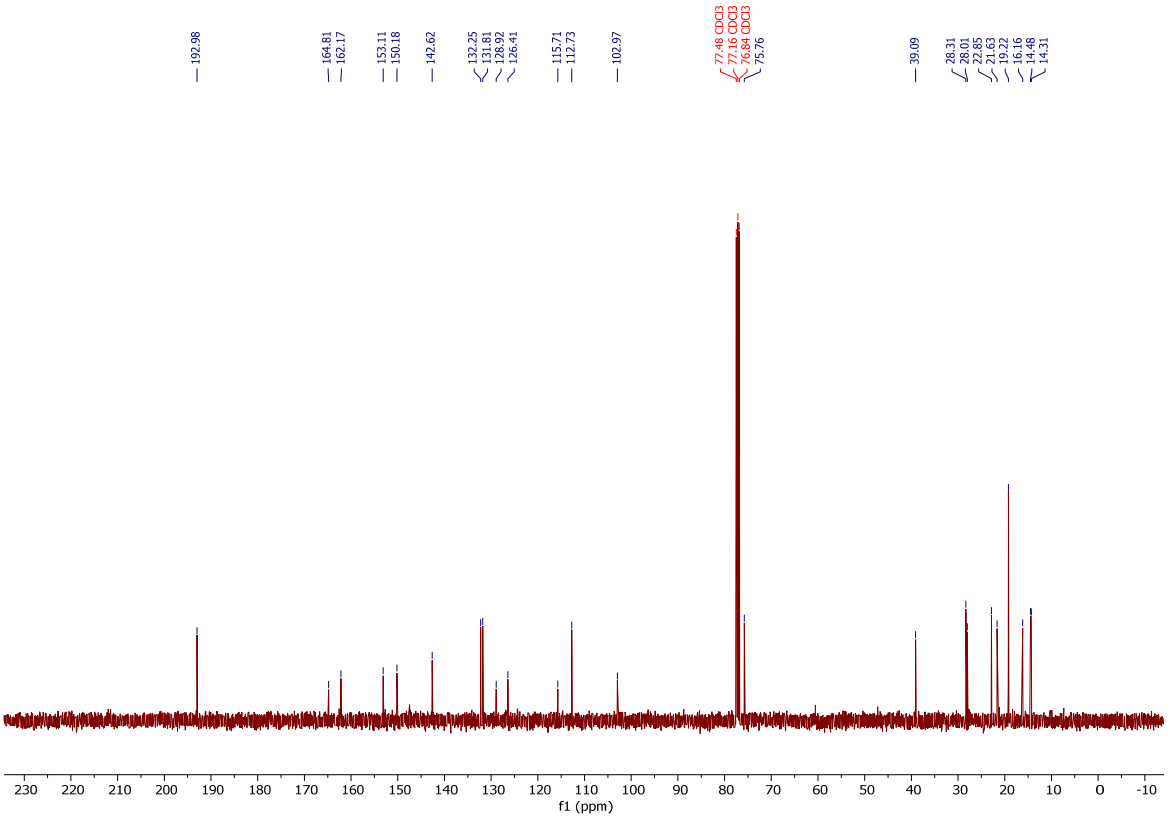

NOESY

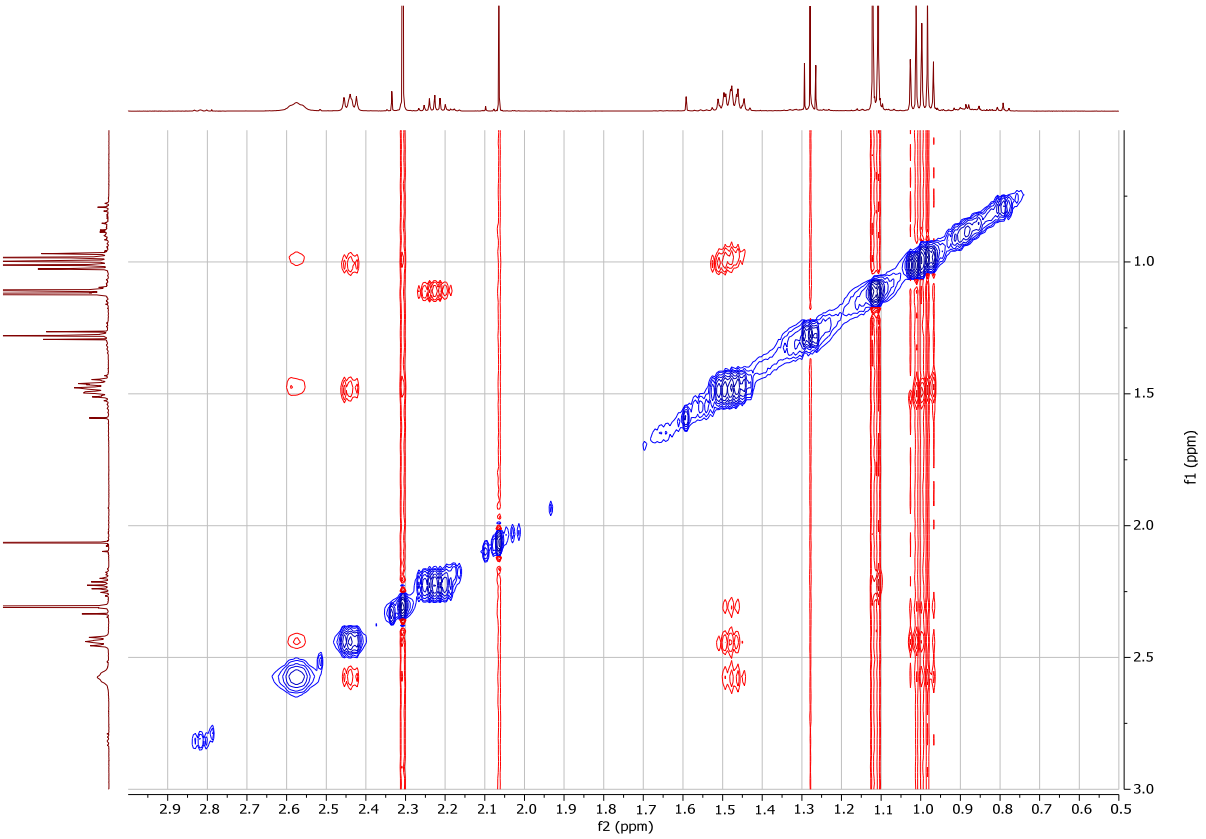
2.9 2.8 2.7 2.6 2.5 2.4 2.3 2.2 2.1 2.0 1.9 1.8 1.7 1.6 1.5 1.4 1.3 1.2 1.1 1.0 0.9 0.8 0.7 0.6 0.5
f2 (ppm)
1.0
1.5
2.0
2.5
3.0
f1 (ppm)

(*Z*)-2-heptyl-3-(*o*-tolyl)dec-2-enal (**31**).

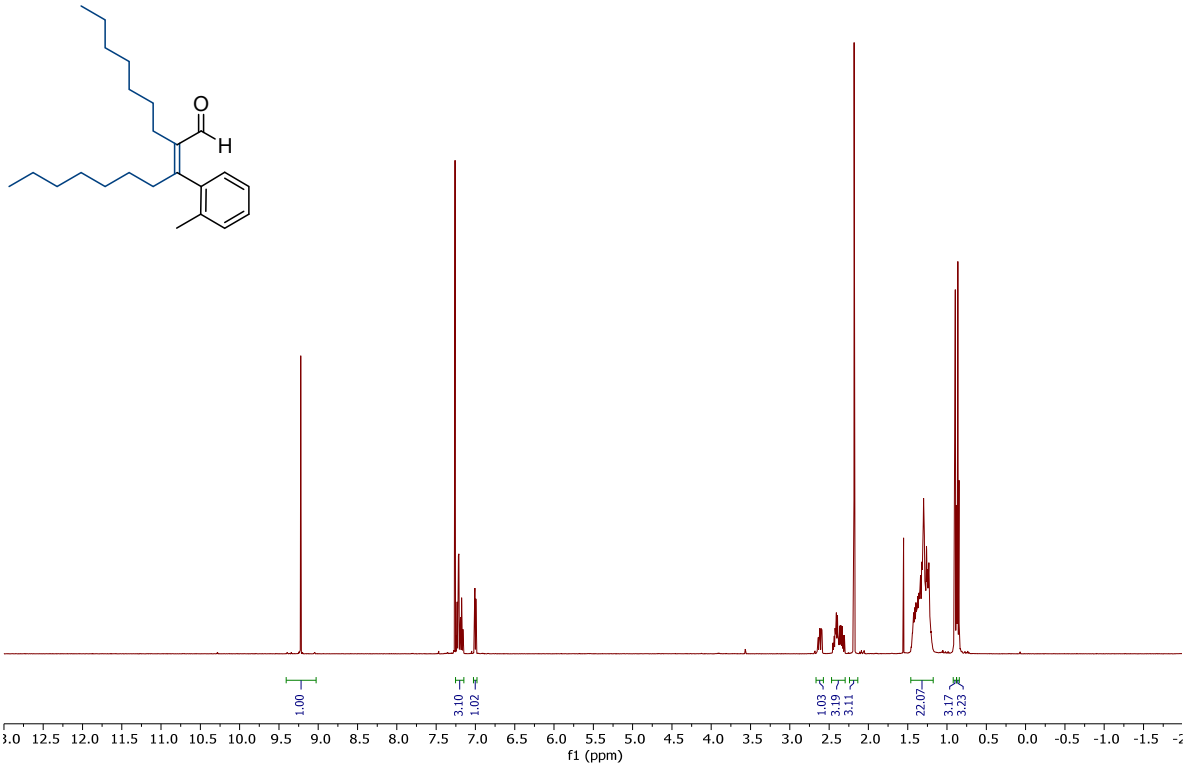

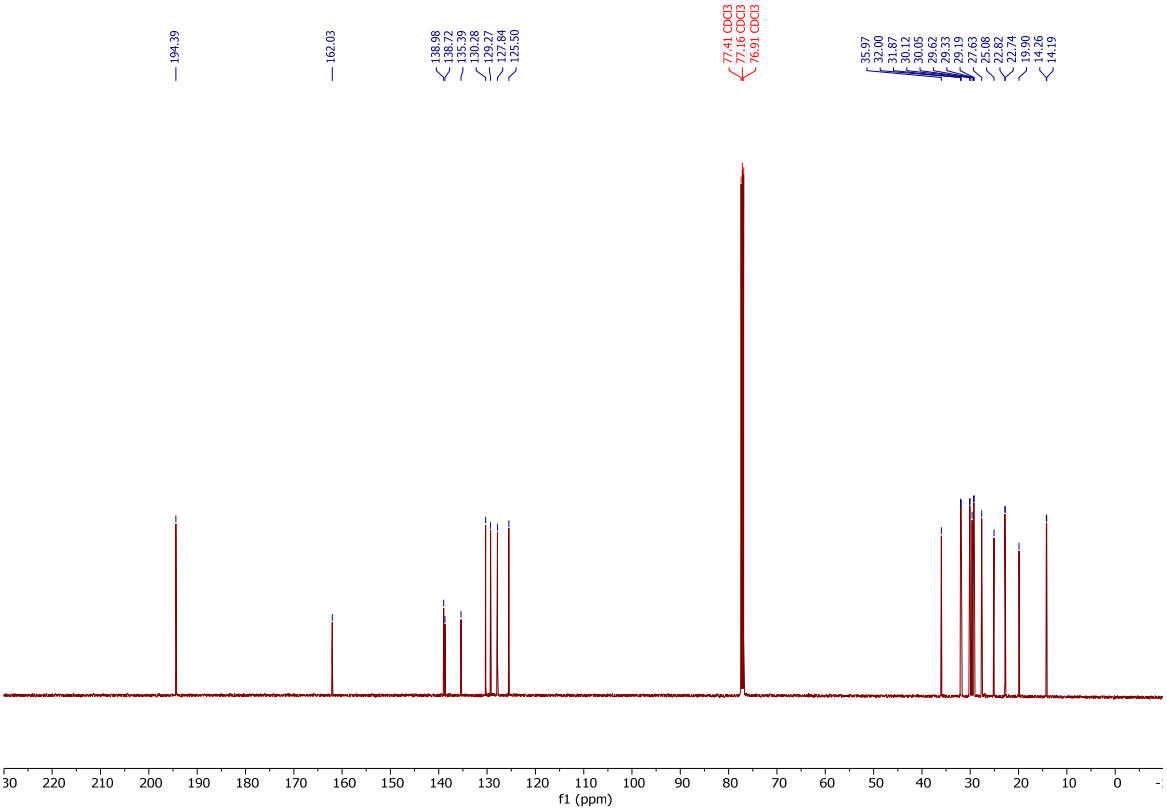

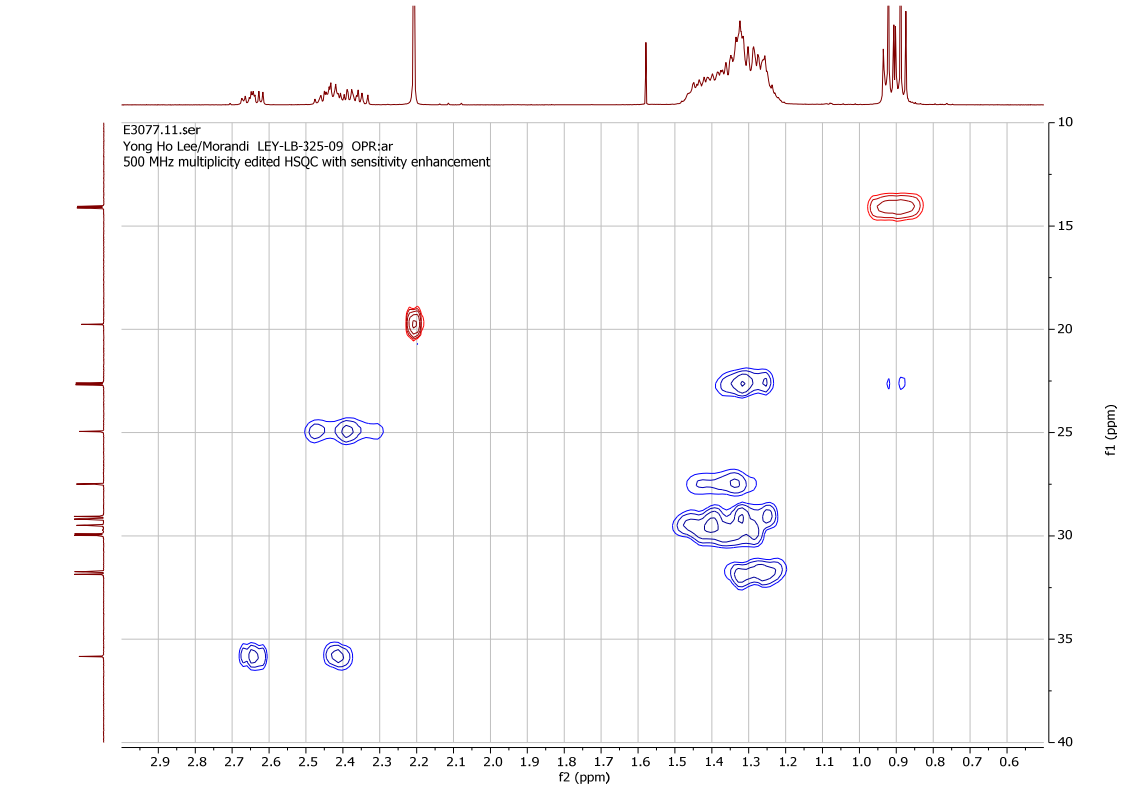
E3077.11.ser
Yong Ho Lee/Morandi LEY-LB-325-09 OPR:ar
500 MHz multiplicity edited HSQC with sensitivity enhancement
f2 (ppm)
f1 (ppm)

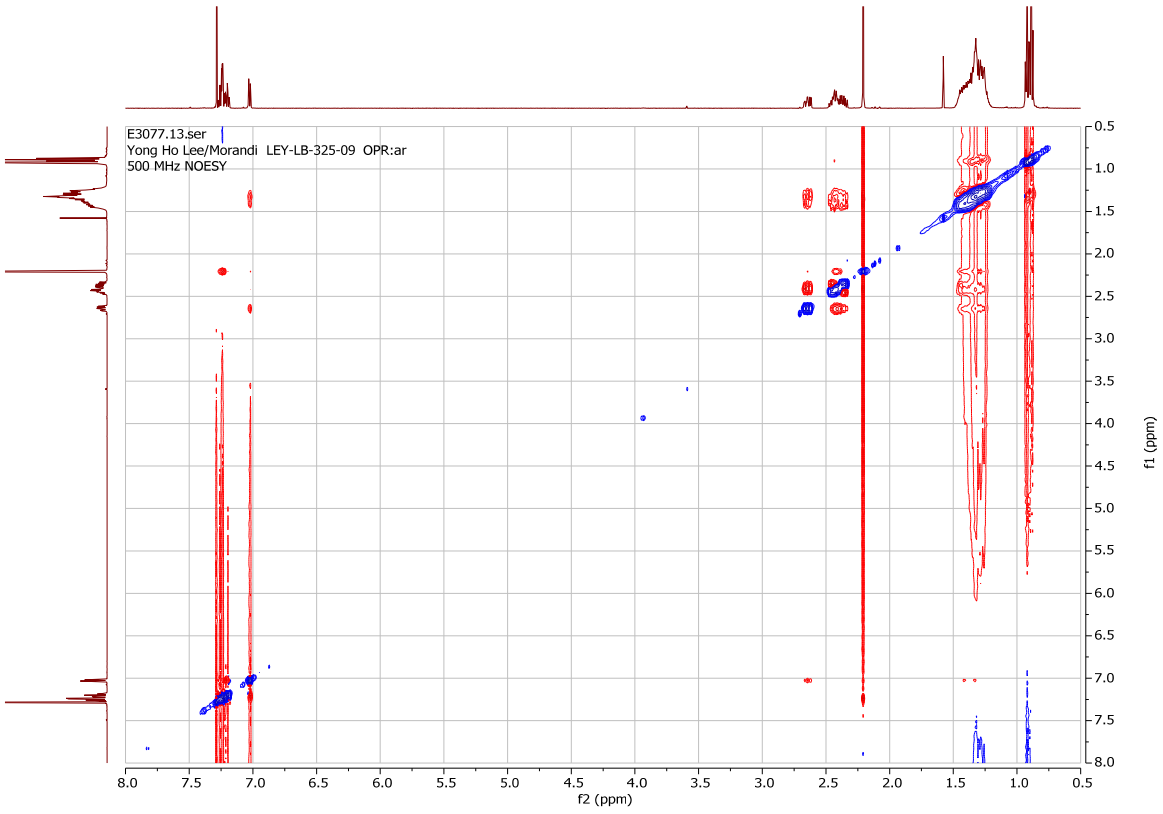
E3077.13.ser
Yong Ho Lee/Morandi LEY-LB-325-09 OPR:ar
500 MHz NOESY
f2 (ppm)
f1 (ppm)

(*Z*)-2-heptyl-3-(*p*-tolyl)dec-2-enal (**32**).

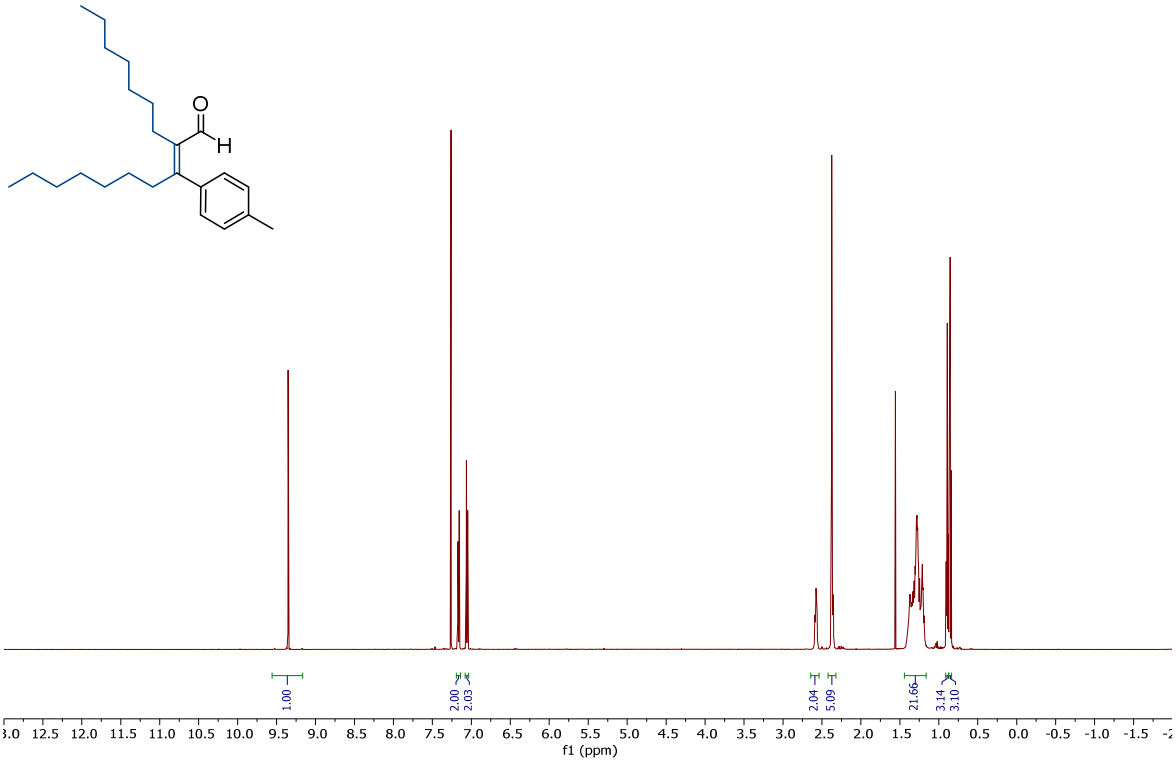

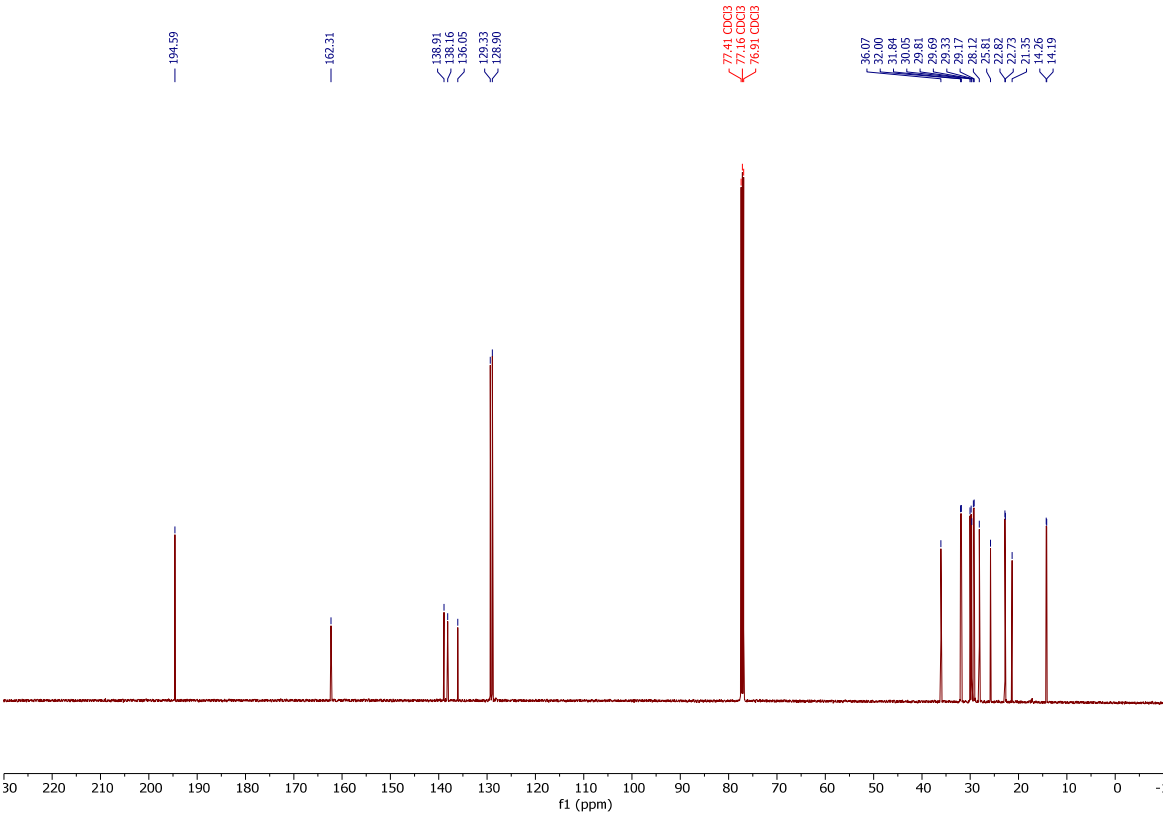

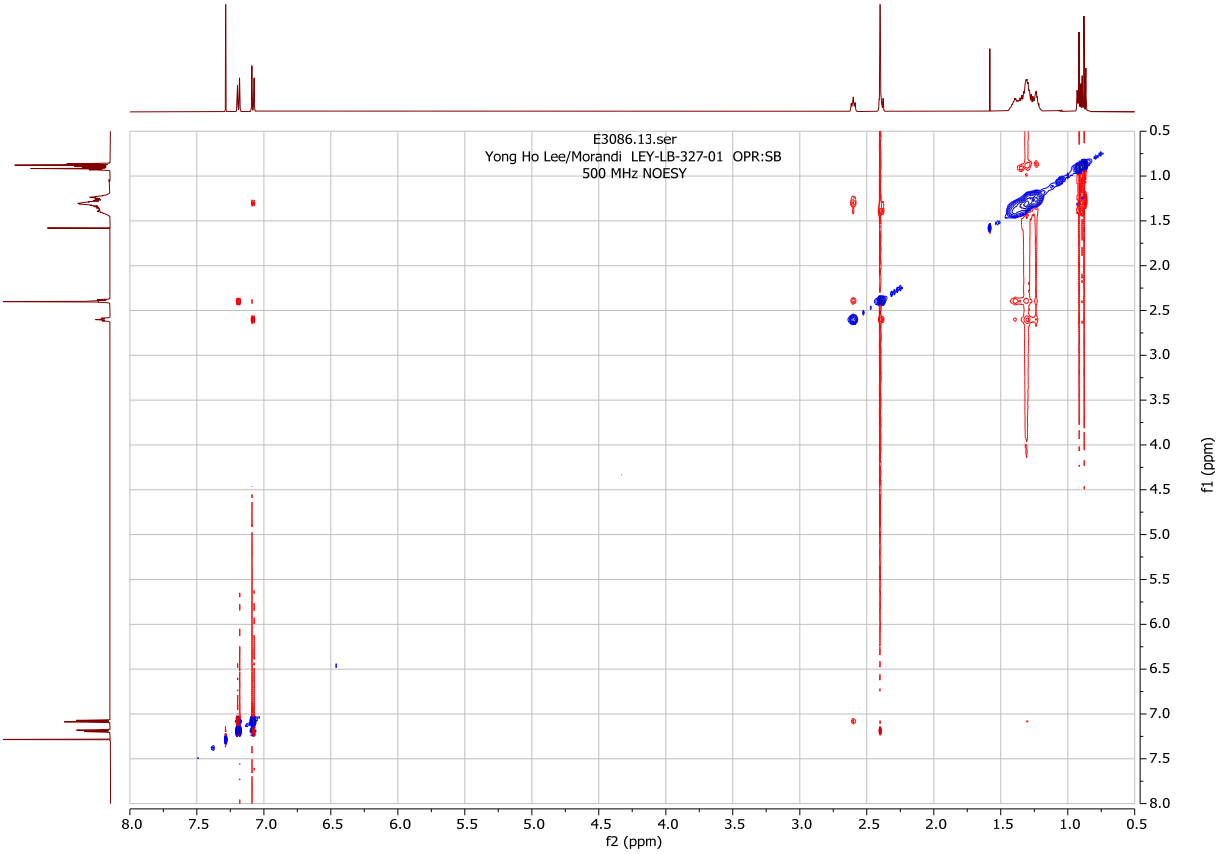
E3086.13.ser
Yong Ho Lee/Morandi LEY-LB-327-01 OPR:SB
500 MHz NOESY
f2 (ppm)
f1 (ppm)

(*Z*)-6-phenyl-2-(3-phenylpropyl)-3-(*o*-tolyl)hex-2-enal (**33**).

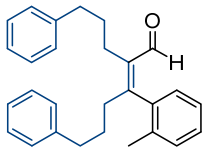

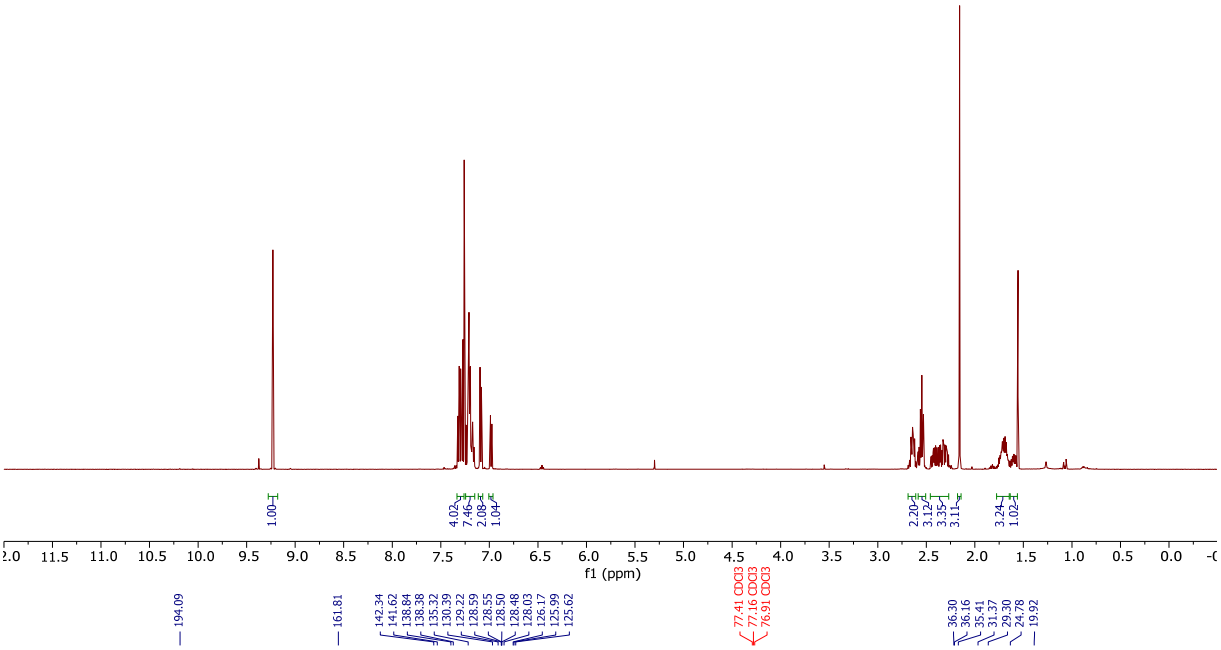

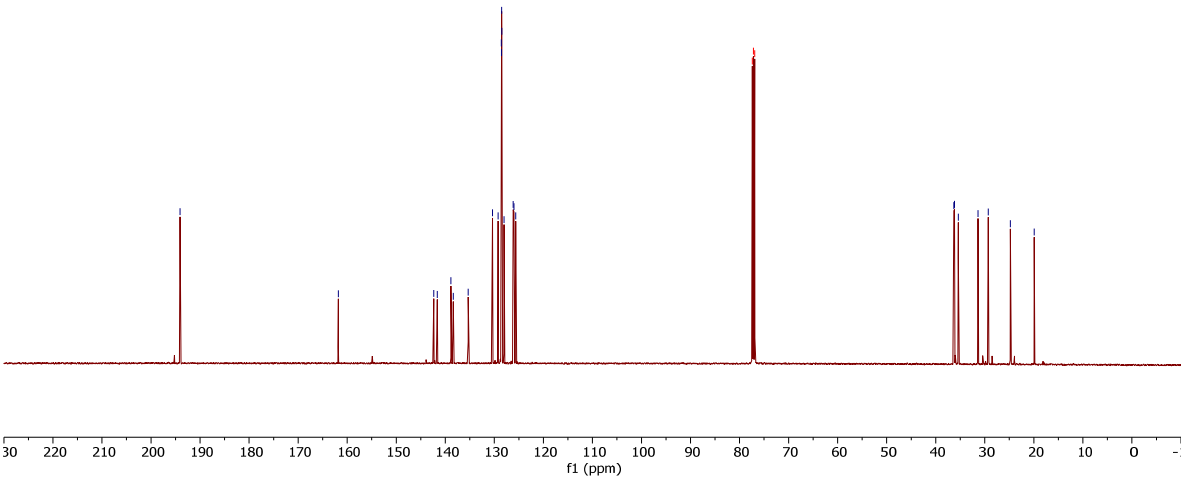

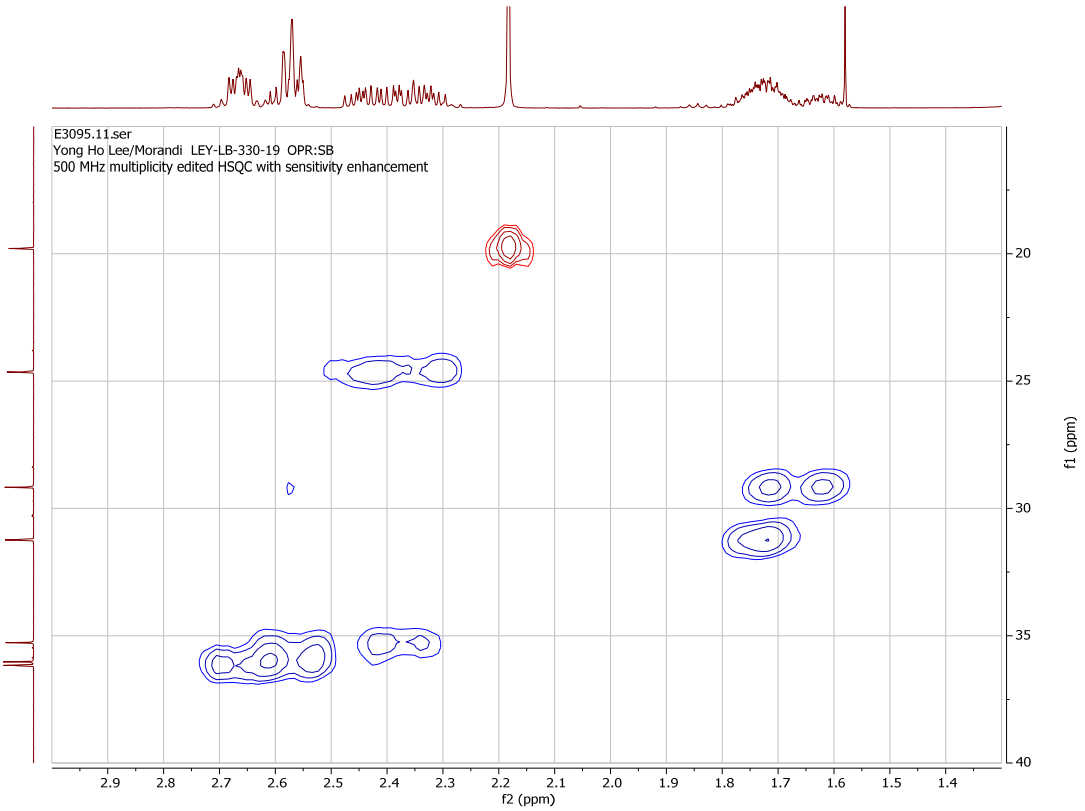
E3095.11.ser
Yong Ho Lee/Morandi LEY-LB-330-19 OPR:SB
500 MHz multiplicity edited HSQC with sensitivity enhancement
f2 (ppm)
f1 (ppm)

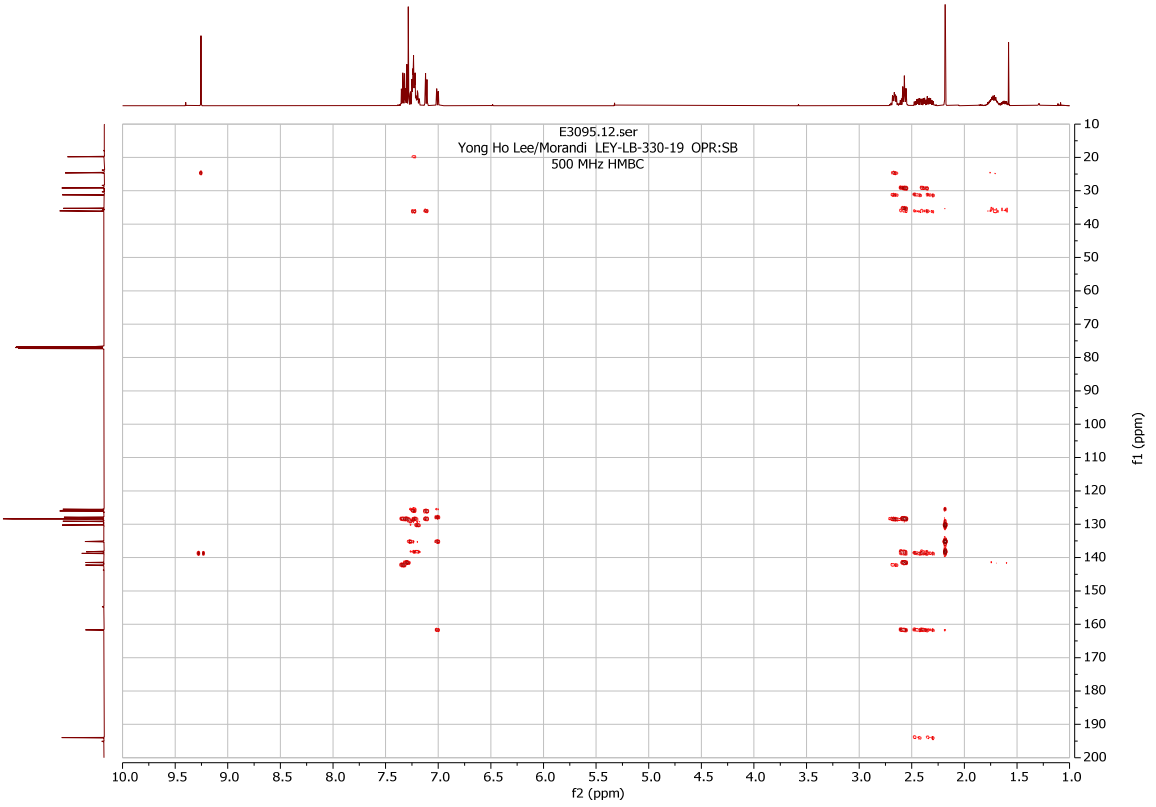
E3095.12.ser
Yong Ho Lee/Morandi LEY-LB-330-19 OPR:SB
500 MHz HMBC
f2 (ppm)
f1 (ppm)

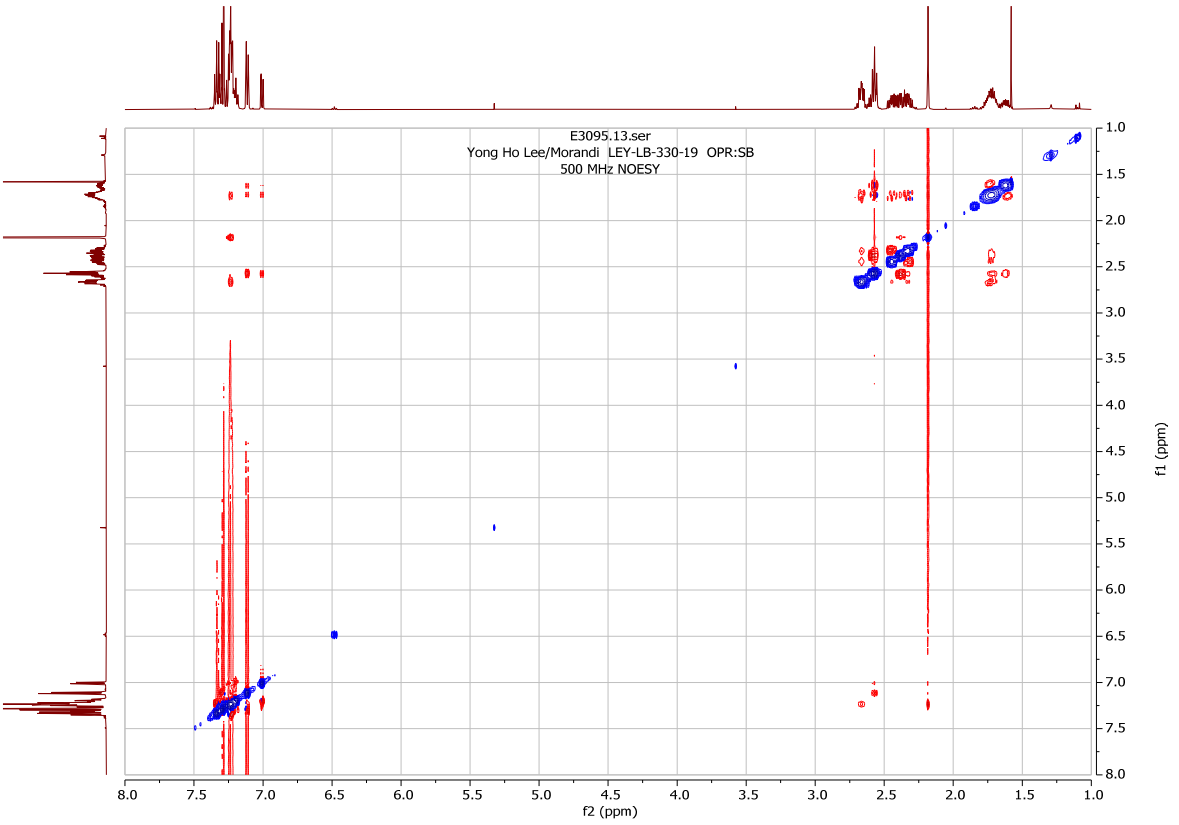
E3095.13.ser
Yong Ho Lee/Morandi LEY-LB-330-19 OPR:SB
500 MHz NOESY
f2 (ppm)
f1 (ppm)

(*Z*)-7-chloro-2-(4-chlorobutyl)-3-(*o*-tolyl)hept-2-enal (**34**).

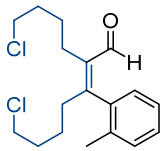

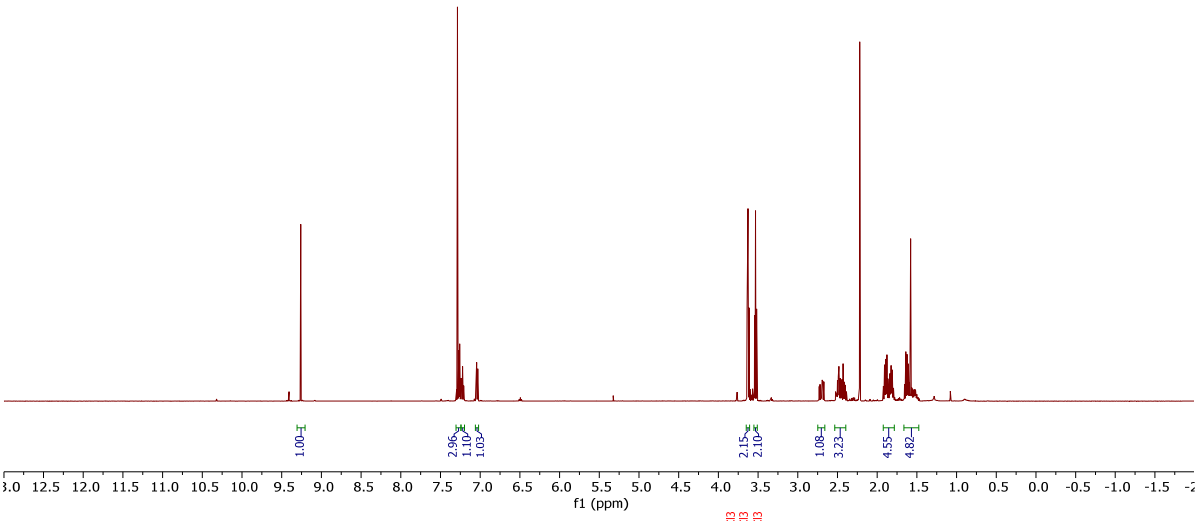

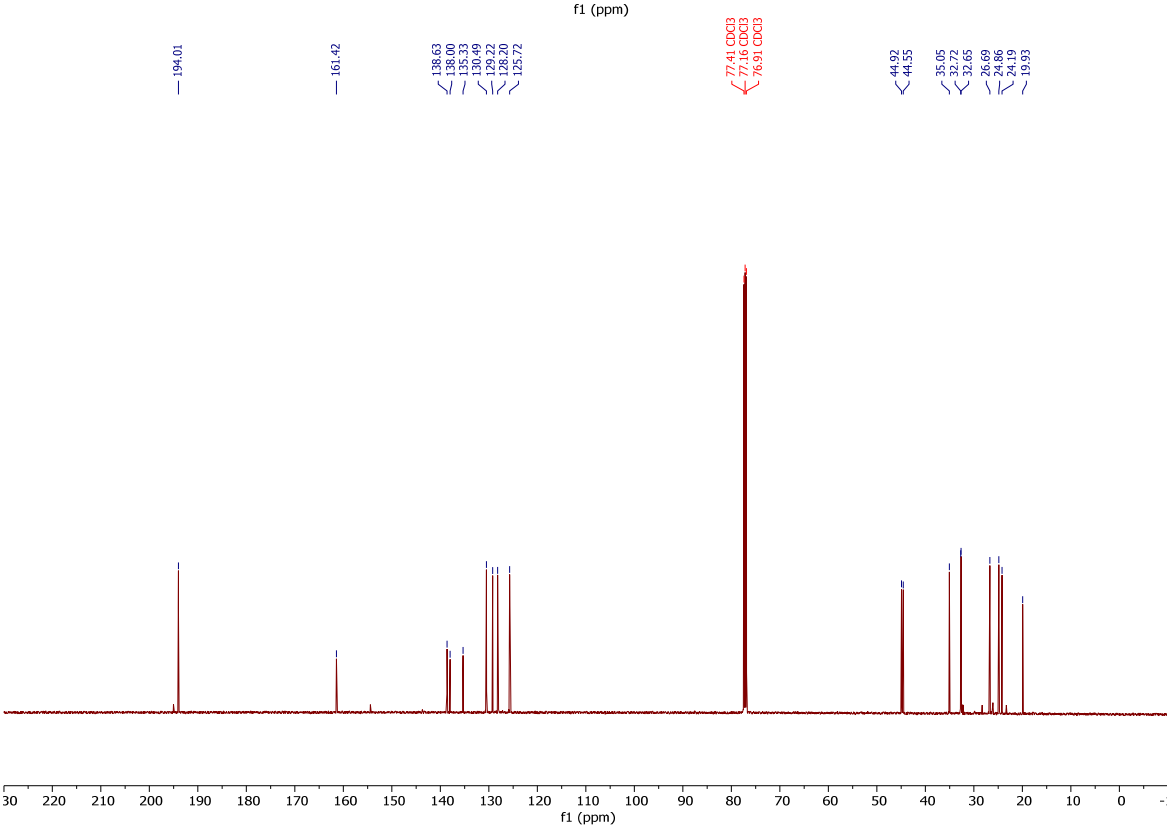

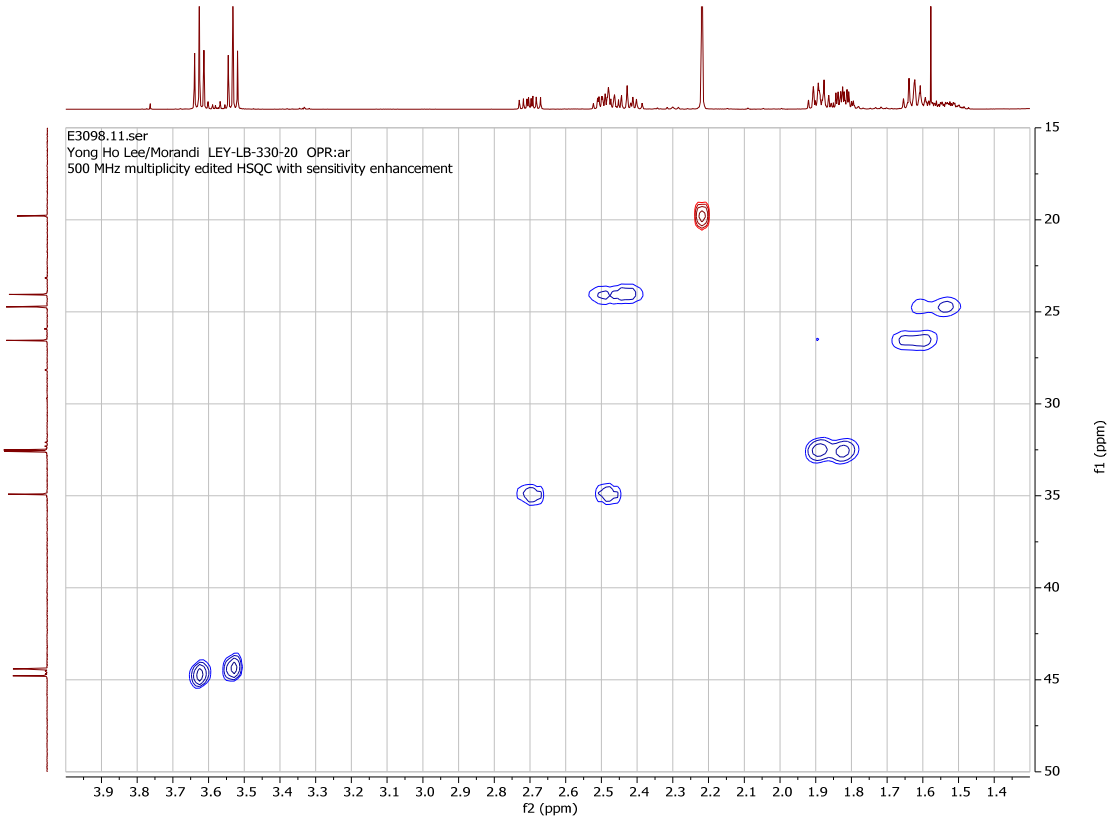
E3098.11.ser
Yong Ho Lee/Morandi LEY-LB-330-20 OPR:ar
500 MHz multiplicity edited HSQC with sensitivity enhancement
f2 (ppm)
f1 (ppm)

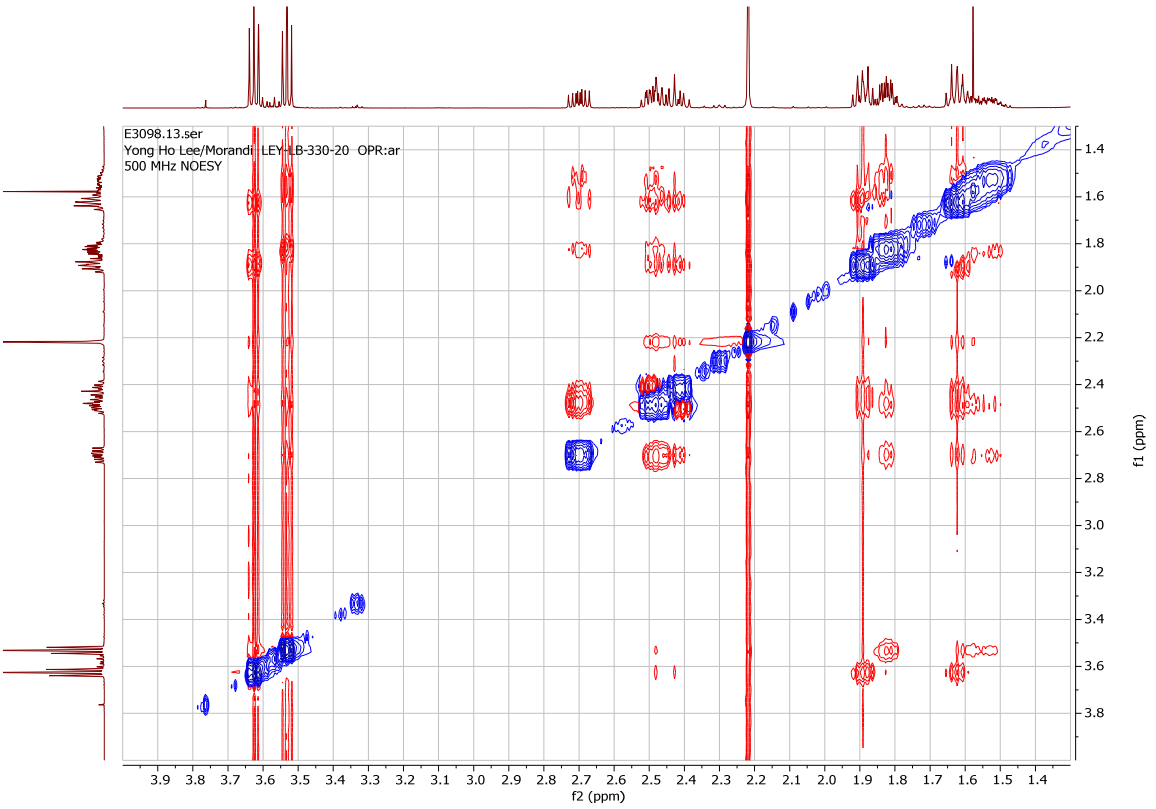
E3098.13.ser
Yong Ho Lee/Morandi LEY-LB-330-20 OPR:ar
500 MHz NOESY
f2 (ppm)
f1 (ppm)

(*Z*)-2-(*tert*-butyl)-3-mesitylbut-2-enal (**35**).

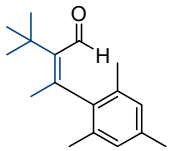

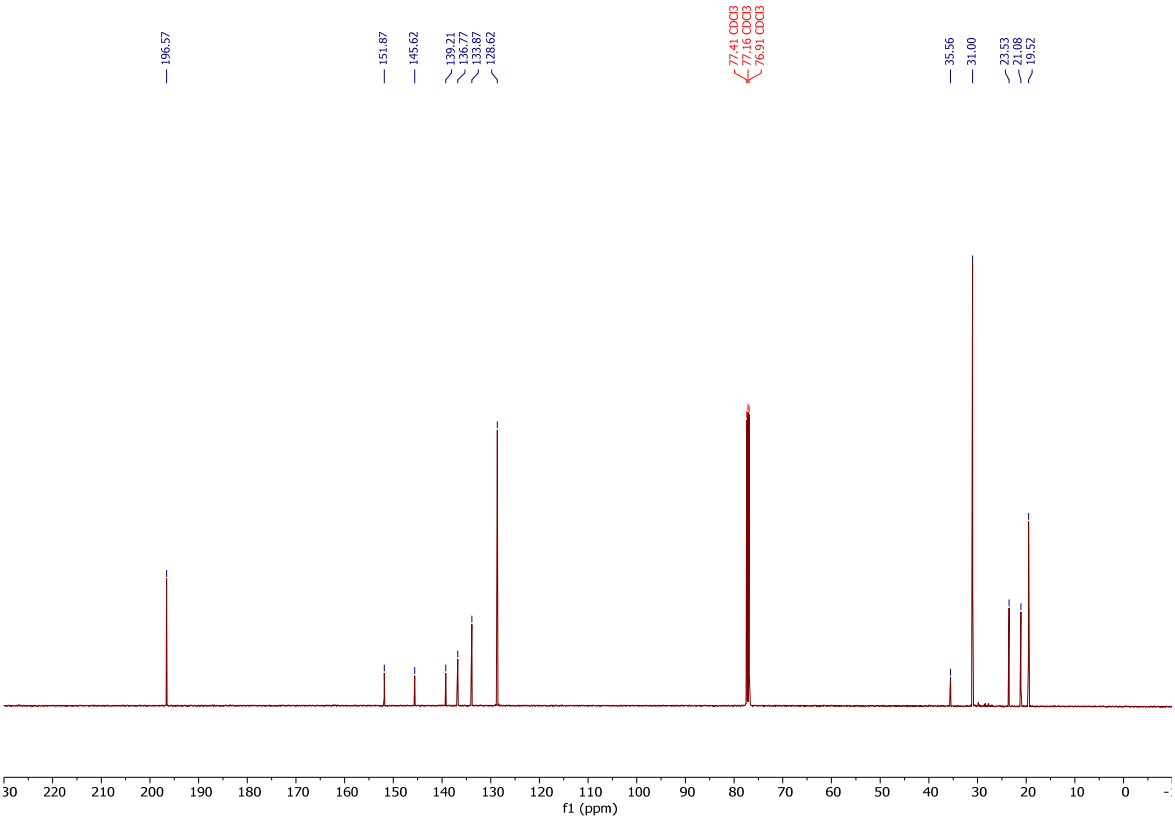

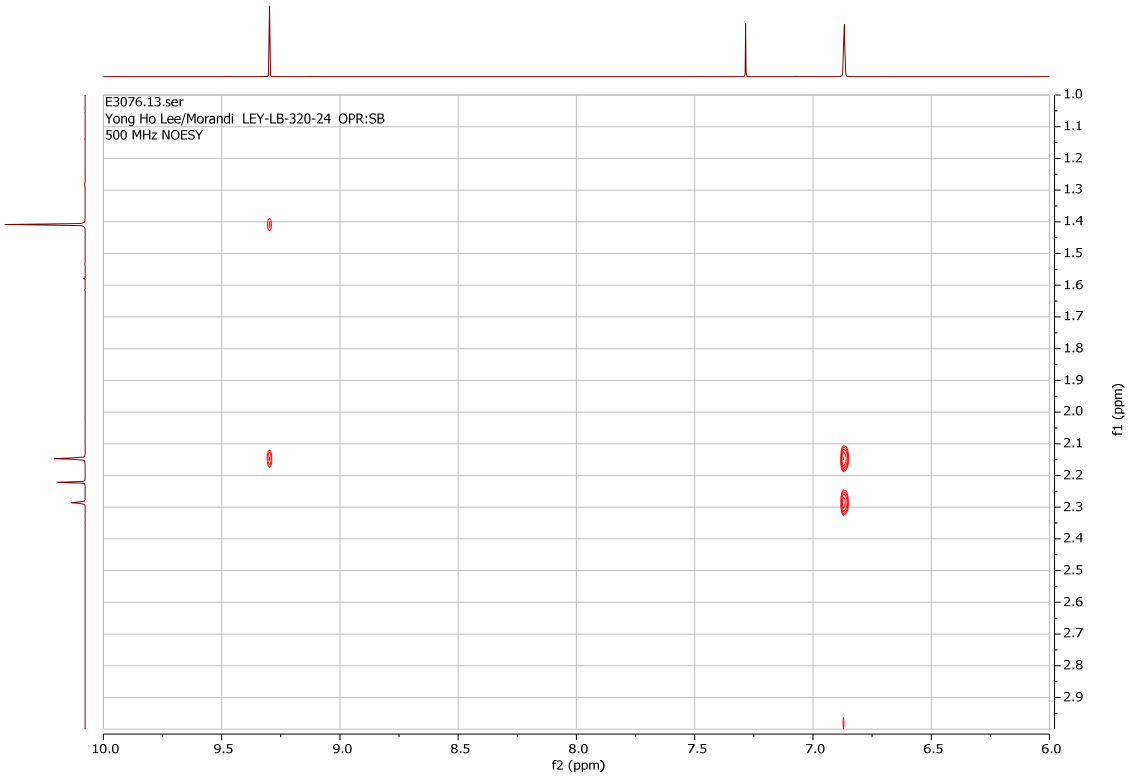
E3076.13.ser
Yong Ho Lee/Morandi LEY-LB-320-24 OPR:SB
500 MHz NOESY
f2 (ppm)
f1 (ppm)

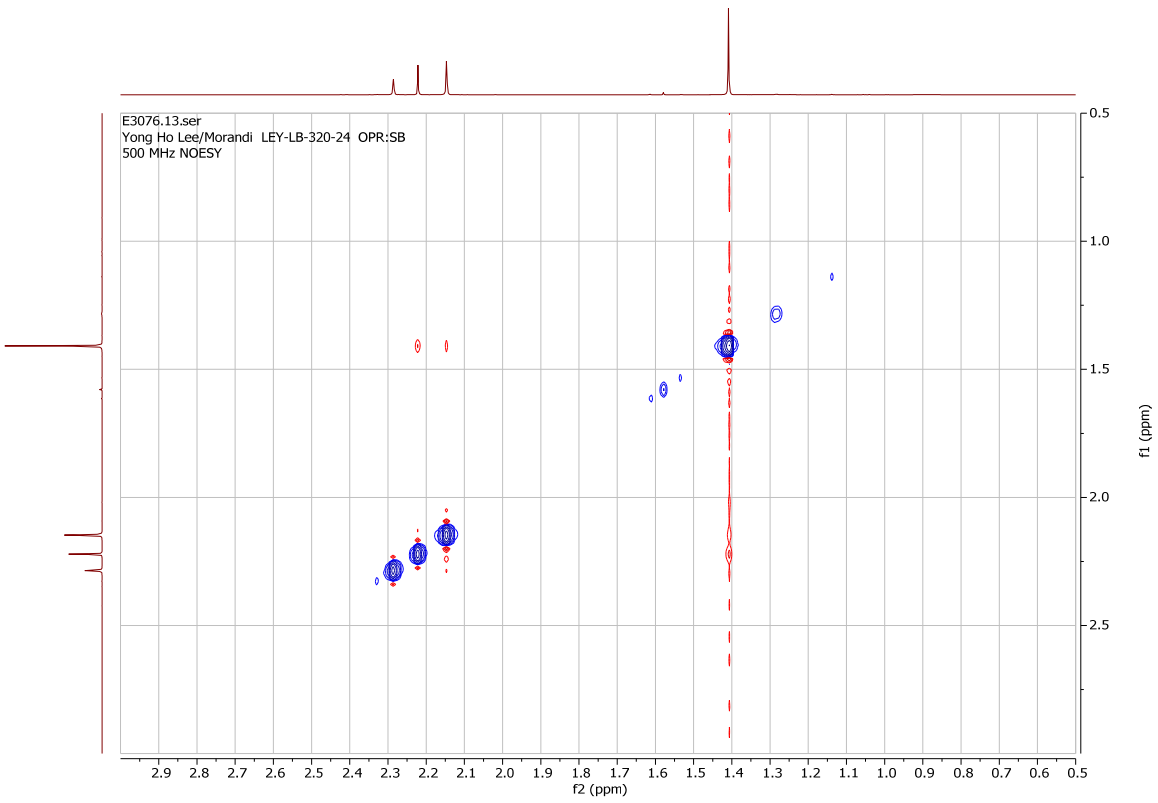
E3076.13.ser
Yong Ho Lee/Morandi LEY-LB-320-24 OPR:SB
500 MHz NOESY
f2 (ppm)
f1 (ppm)

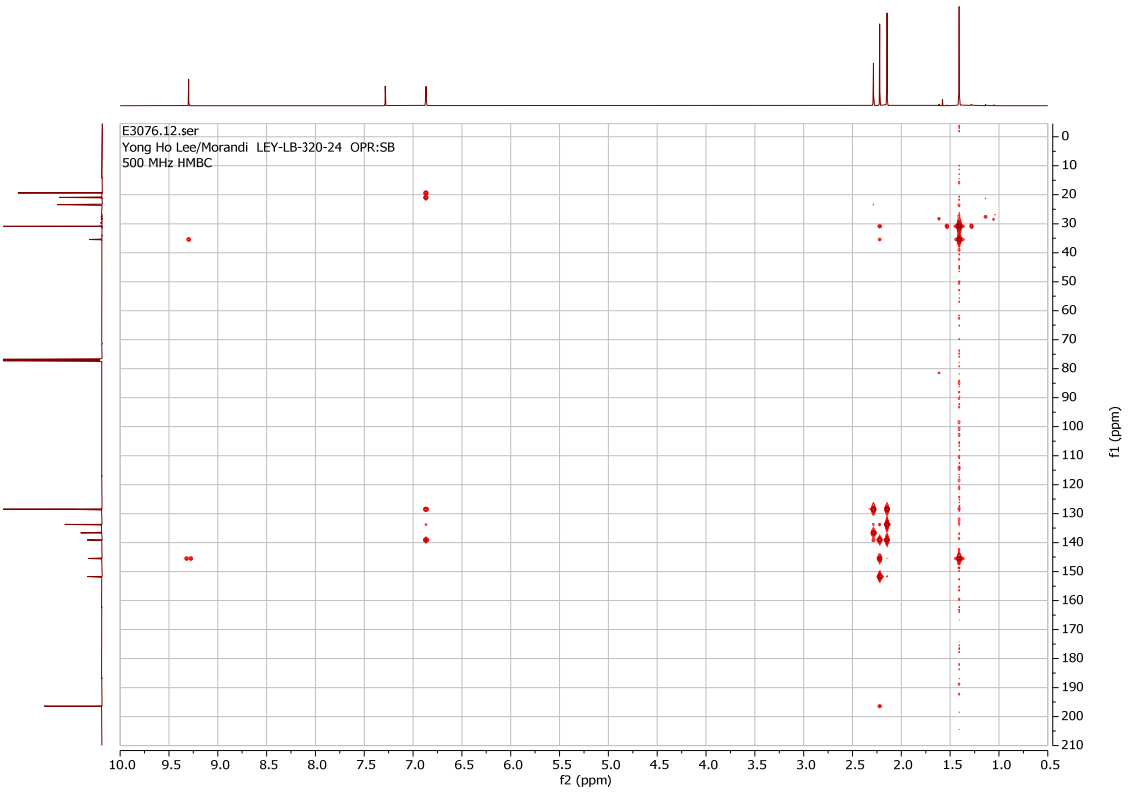
E3076.12.ser
Yong Ho Lee/Morandi LEY-LB-320-24 OPR:SB
500 MHz HMBC
f2 (ppm)
f1 (ppm)

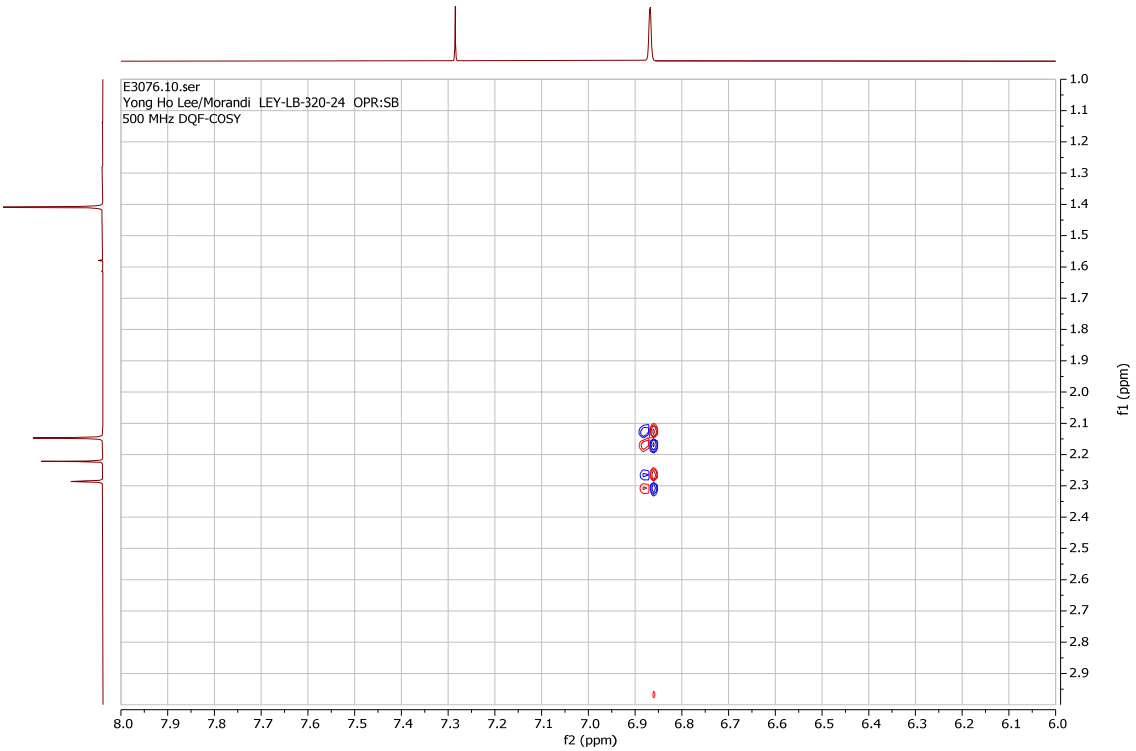
E3076.10.ser
Yong Ho Lee/Morandi LEY-LB-320-24 OPR:SB
500 MHz DQF-COSY
f2 (ppm)
f1 (ppm)

(*Z*)-2-isopropyl-3-mesitylbut-2-enal (**36-β-Ar, major**).

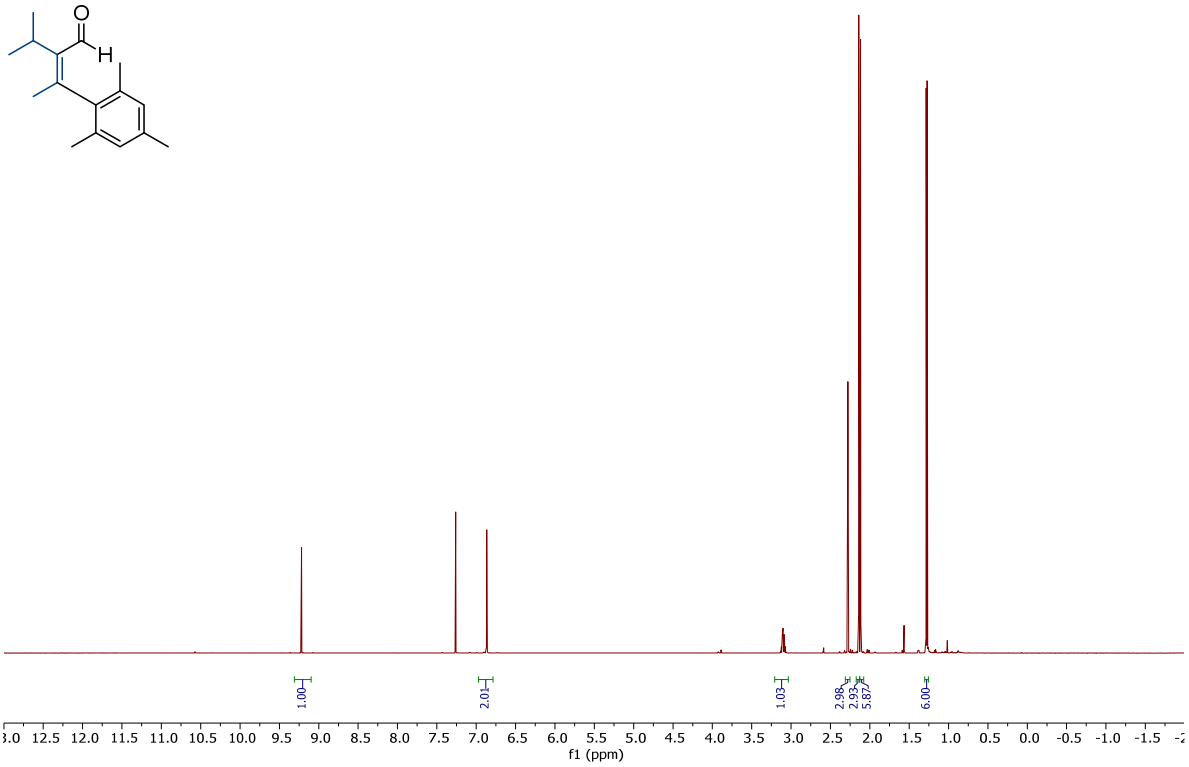

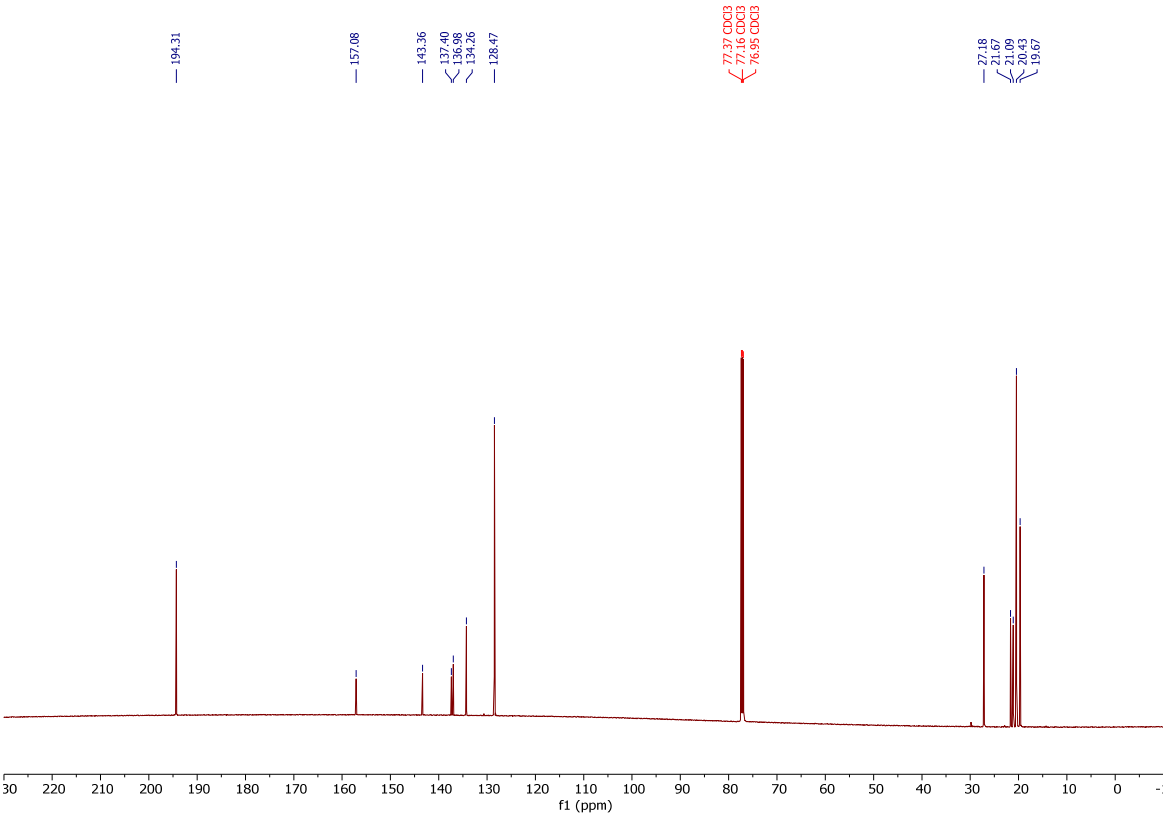

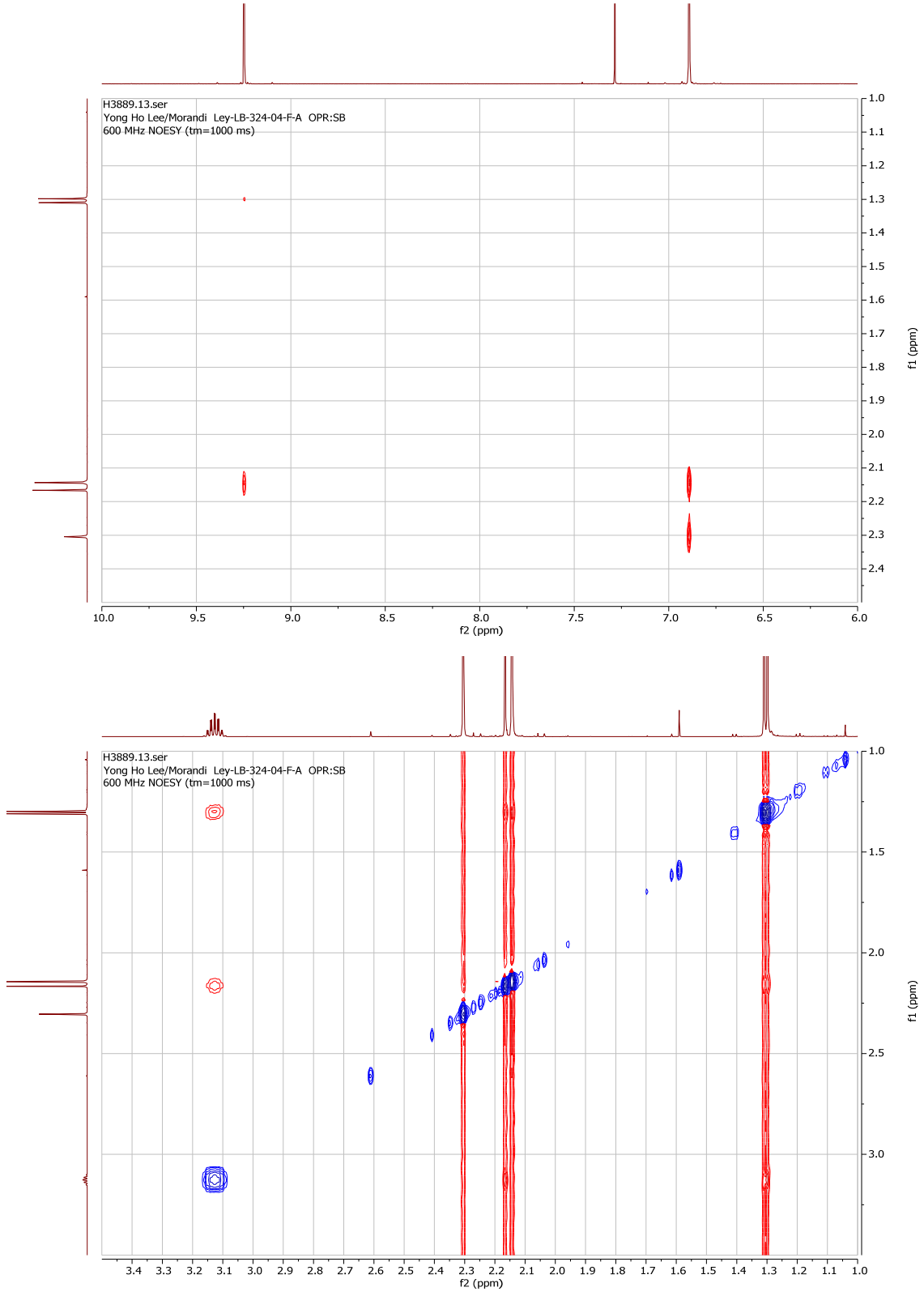
H3889.13.ser
Yong Ho Lee/Morandi Ley-LB-324-04-F-A OPR:SB
600 MHz NOESY (tm=1000 ms)
f2 (ppm)
f1 (ppm)
H3889.13.ser
Yong Ho Lee/Morandi Ley-LB-324-04-F-A OPR:SB
600 MHz NOESY (tm=1000 ms)
f2 (ppm)
f1 (ppm)

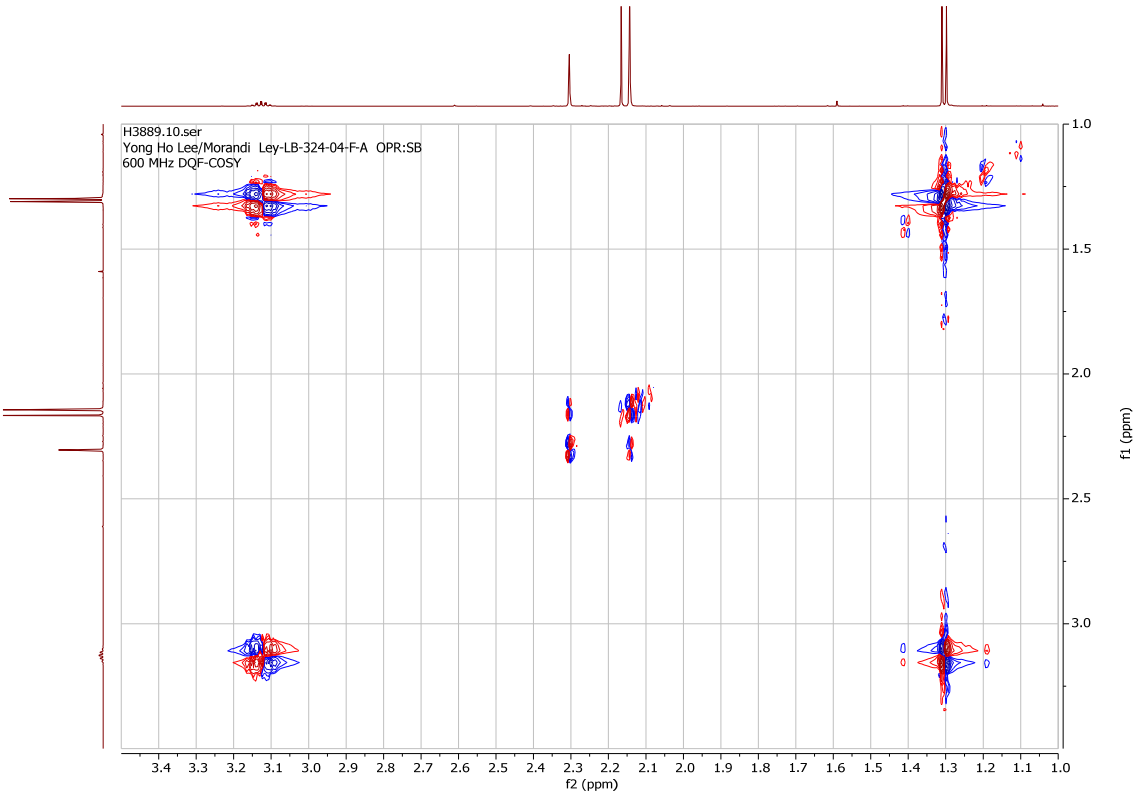
H3889.10.ser
Yong Ho Lee/Morandi Ley-LB-324-04-F-A OPR:SB
600 MHz DQF-COSY
f2 (ppm)
f1 (ppm)

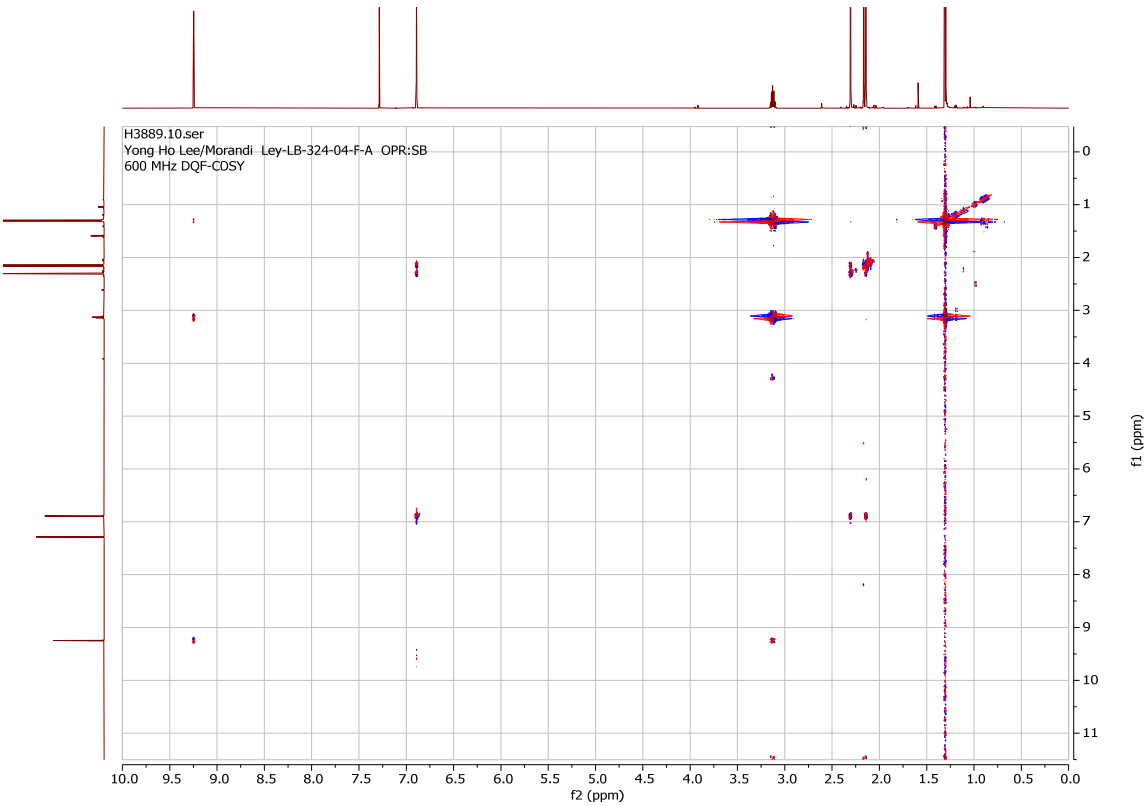
H3889.10.ser
Yong Ho Lee/Morandi Ley-LB-324-04-F-A OPR:SB
600 MHz DQF-COSY
f2 (ppm)
f1 (ppm)

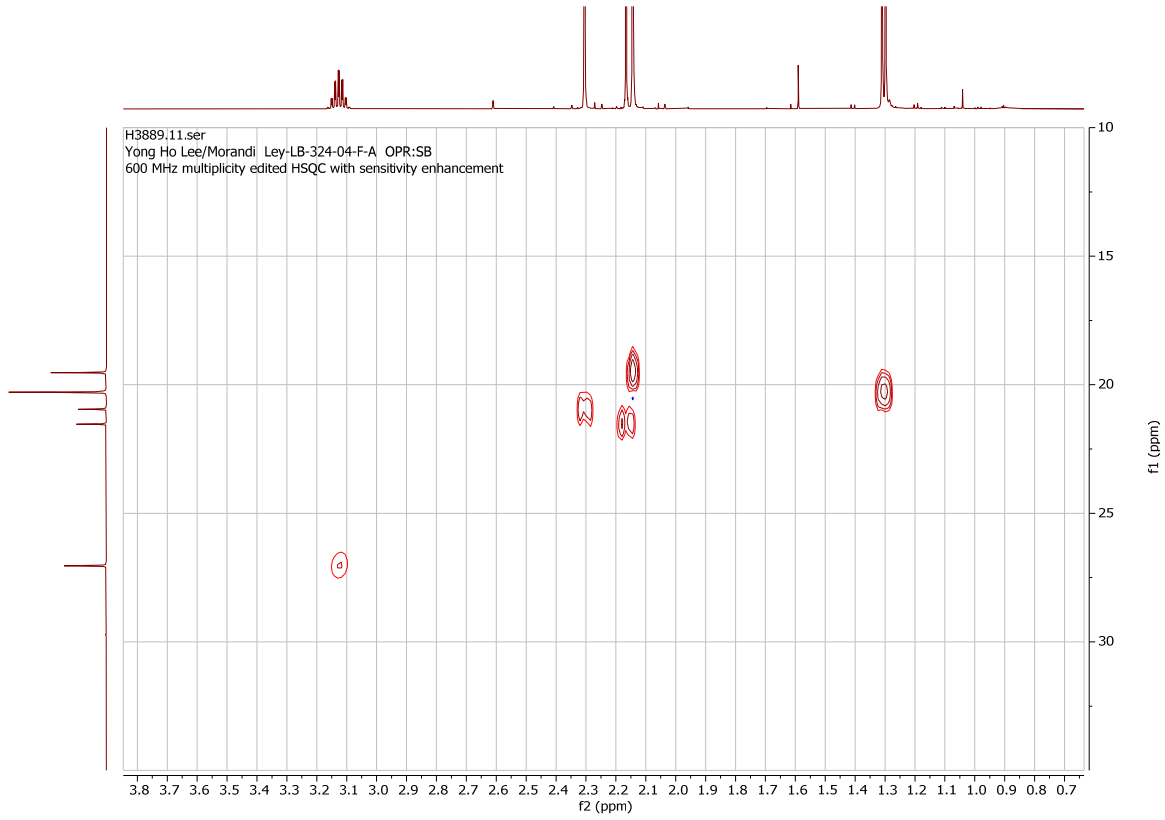
H3889.11.ser
Yong Ho Lee/Morandi Ley-LB-324-04-F-A OPR:SB
600 MHz multiplicity edited HSQC with sensitivity enhancement
f2 (ppm)
f1 (ppm)

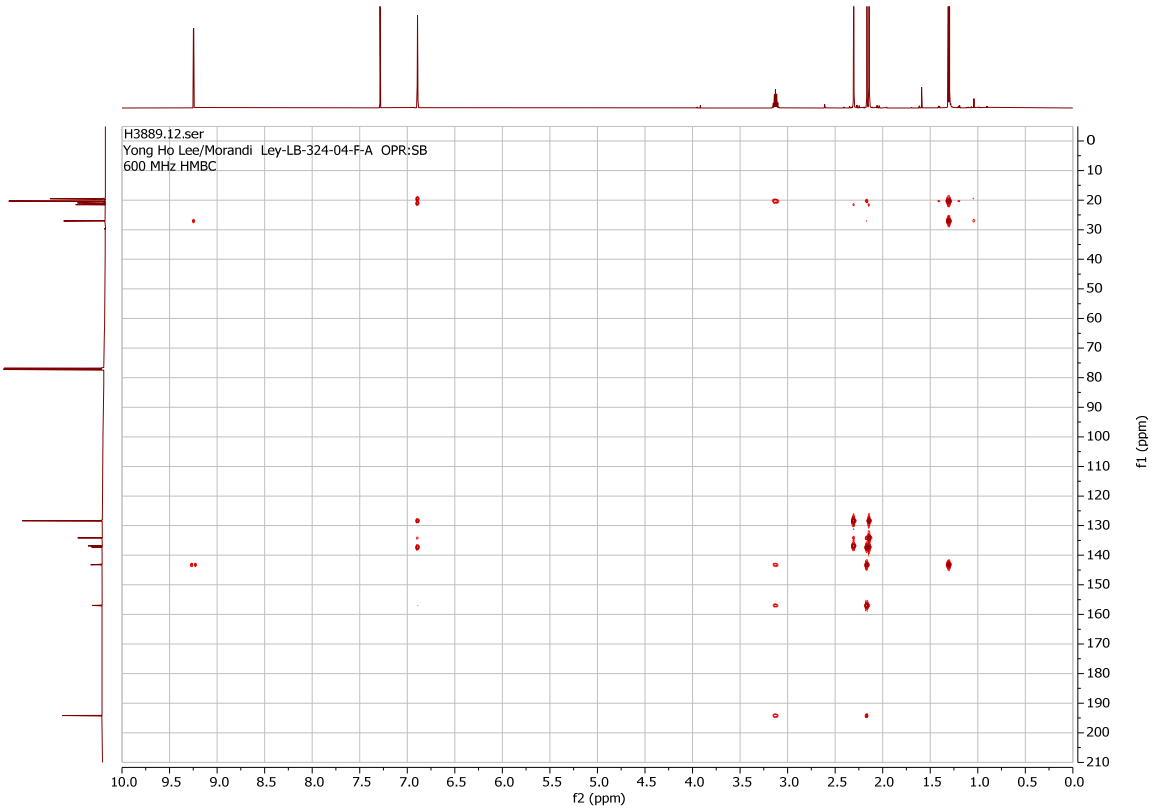
H3889.12.ser
Yong Ho Lee/Morandi Ley-LB-324-04-F-A OPR:SB
600 MHz HMBC
f2 (ppm)
f1 (ppm)

(*Z*)-3-mesityl-2,4-dimethylpent-2-enal (**36-α-Ar, minor**).

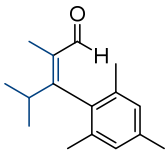

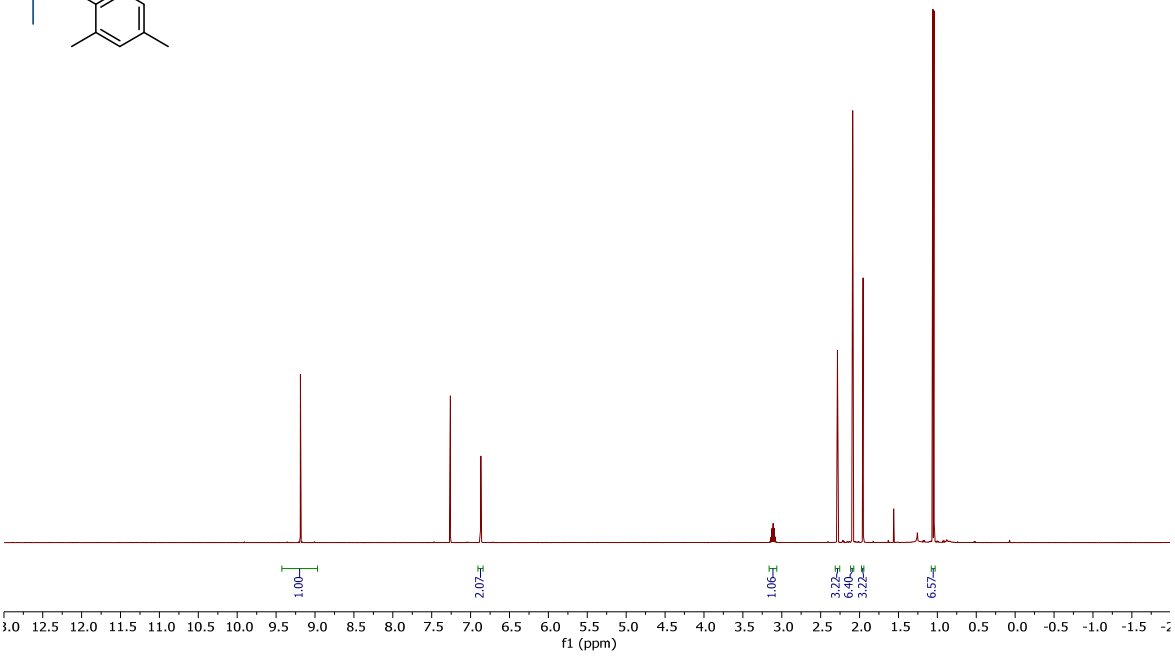

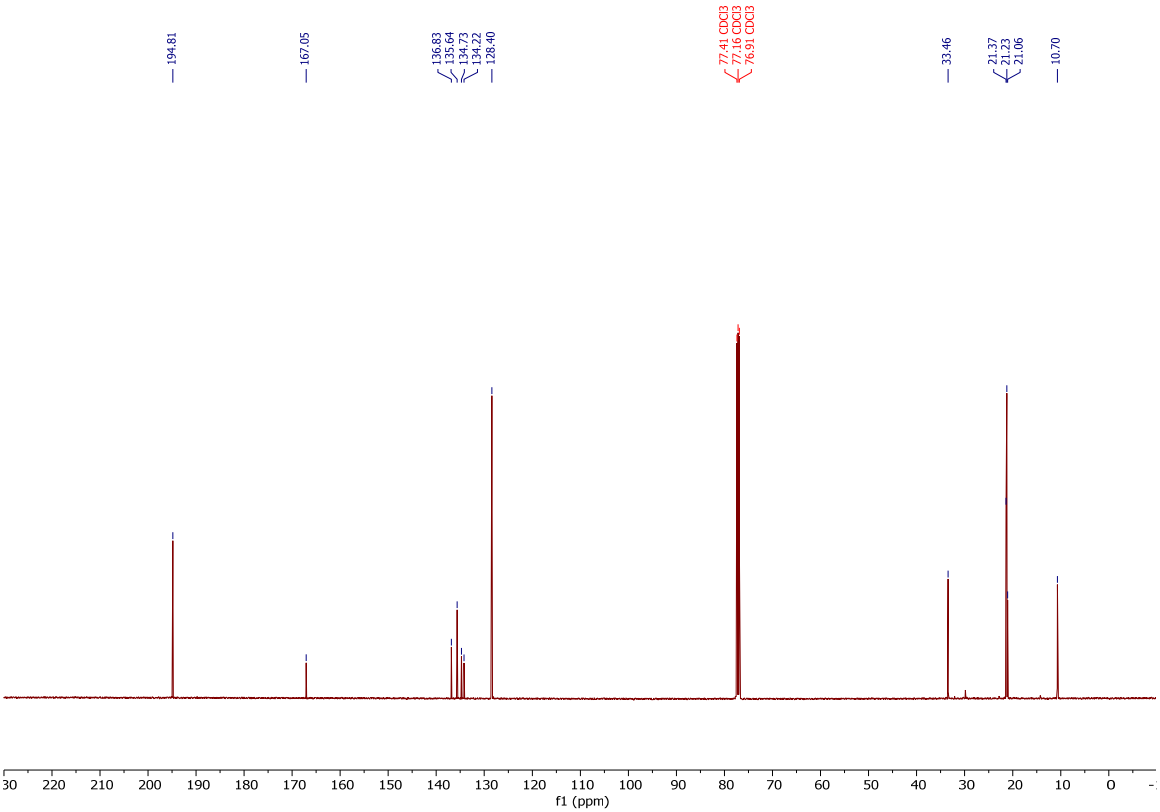

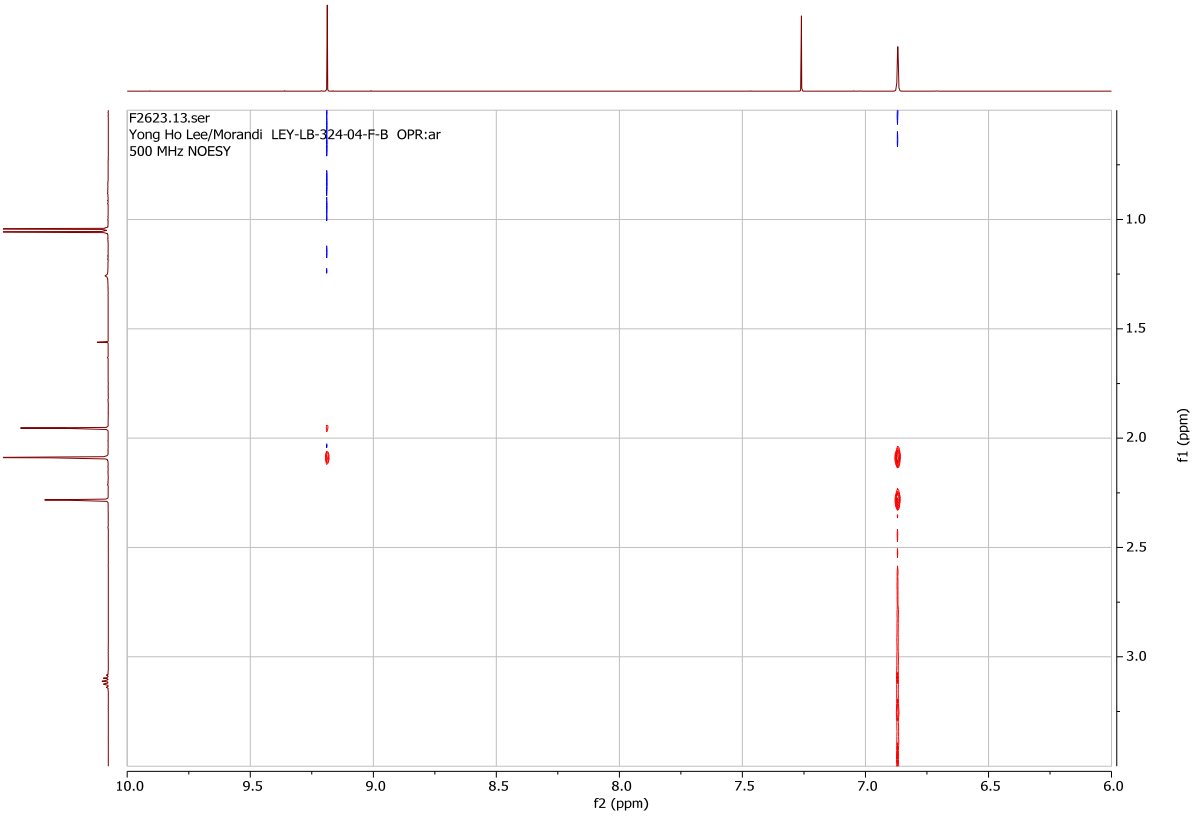
F2623.13.ser
Yong Ho Lee/Morandi LEY-LB-324-04-F-B OPR:ar
500 MHz NOESY
1.0
1.5
2.0
2.5
3.0
f1 (ppm)
10.0
9.5
9.0
8.5
8.0
7.5
7.0
6.5
6.0
f2 (ppm)

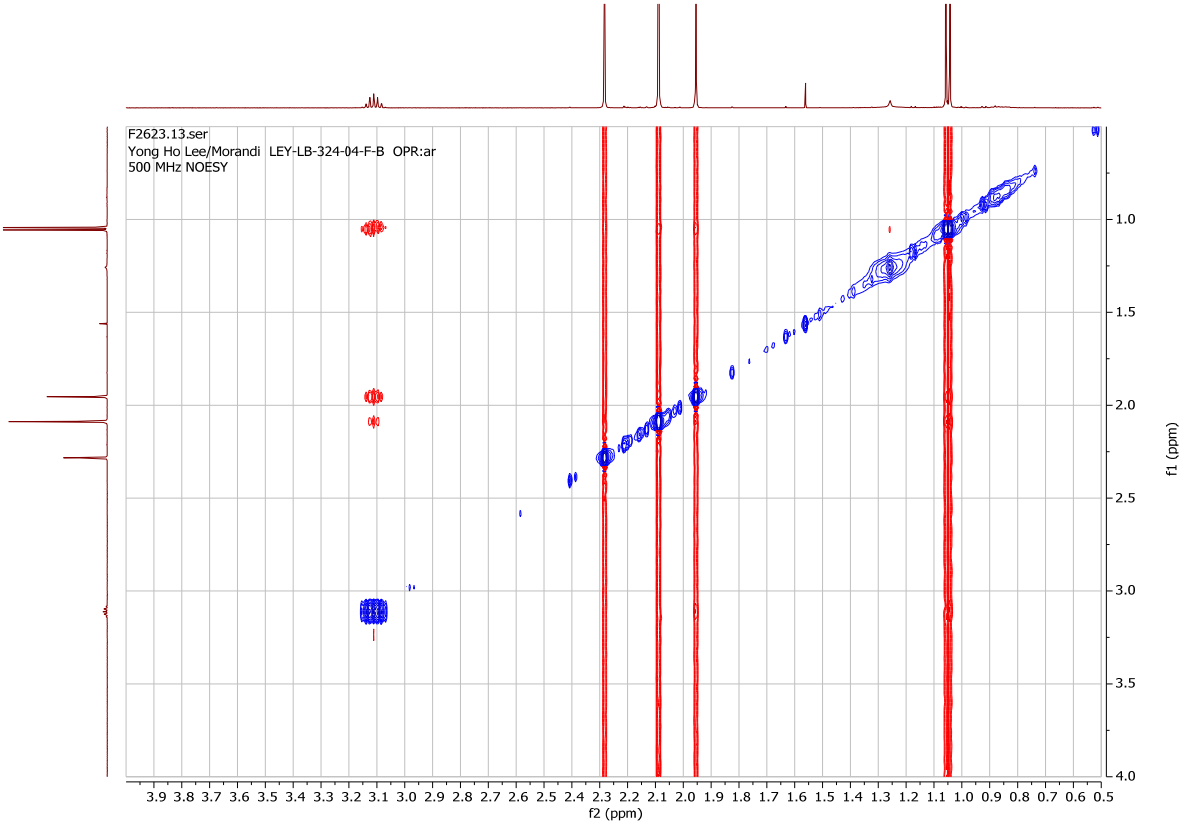
F2623.13.ser
Yong Ho Lee/Morandi LEY-LB-324-04-F-B OPR:ar
500 MHz NOESY
1.0
1.5
2.0
2.5
3.0
3.5
4.0
f1 (ppm)
3.9 3.8 3.7 3.6 3.5 3.4 3.3 3.2 3.1 3.0 2.9 2.8 2.7 2.6 2.5 2.4 2.3 2.2 2.1 2.0 1.9 1.8 1.7 1.6 1.5 1.4 1.3 1.2 1.1 1.0 0.9 0.8 0.7 0.6 0.5
f2 (ppm)

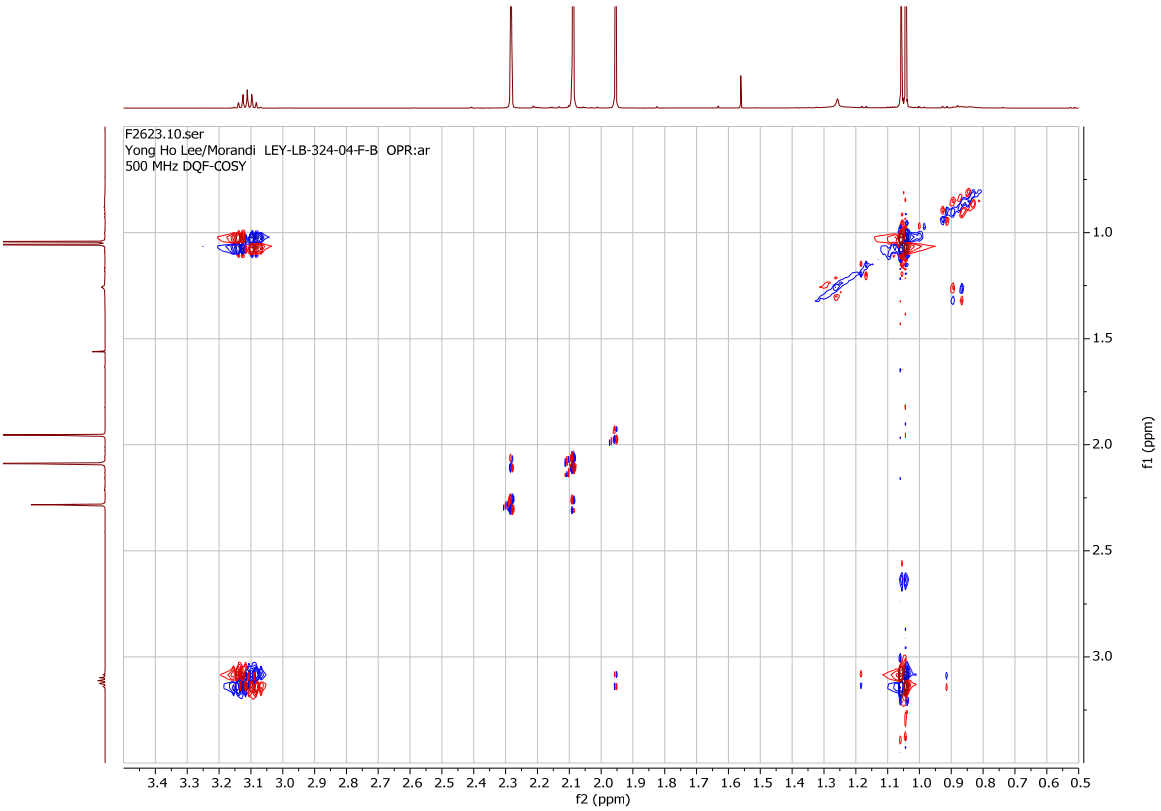
F2623.10.ser
Yong Ho Lee/Morandi LEY-LB-324-04-F-B OPR:ar
500 MHz DQF-COSY
f2 (ppm)
f1 (ppm)

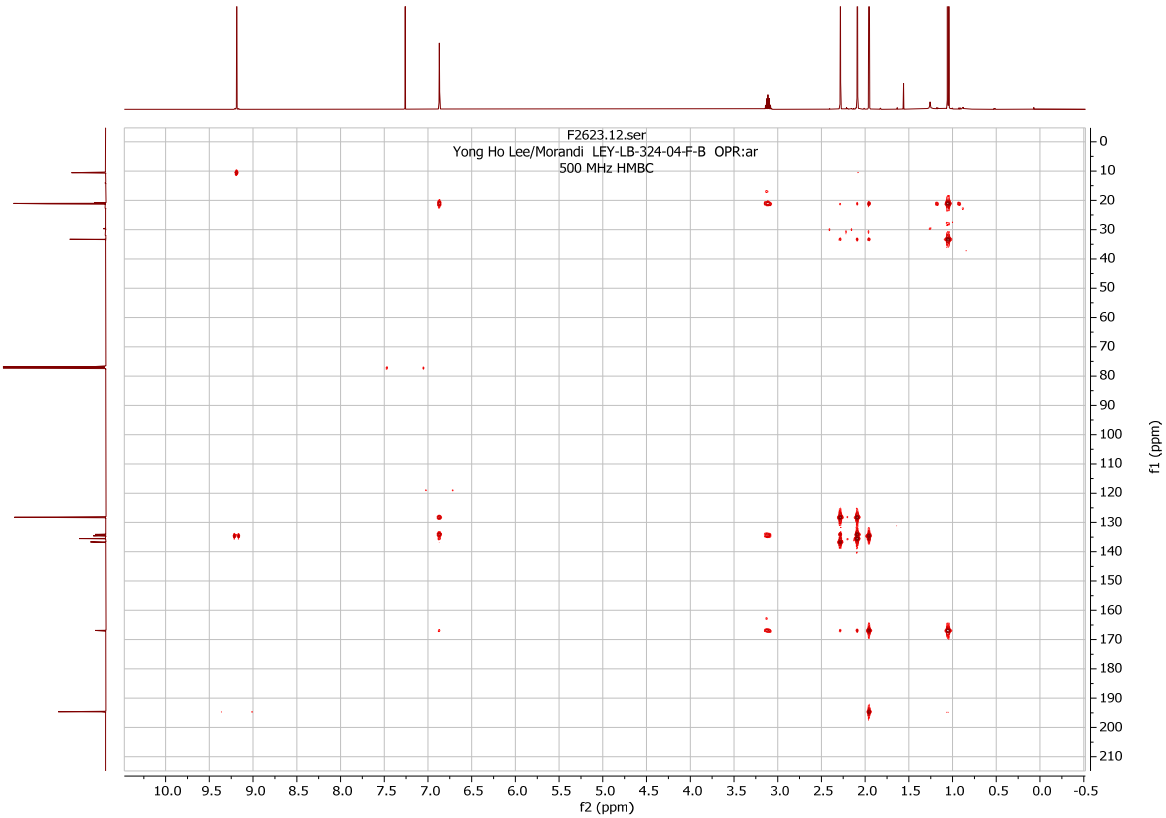
F2623.12.ser
Yong Ho Lee/Morandi LEY-LB-324-04-F-B OPR:ar
500 MHz HMBC
f2 (ppm)
f1 (ppm)

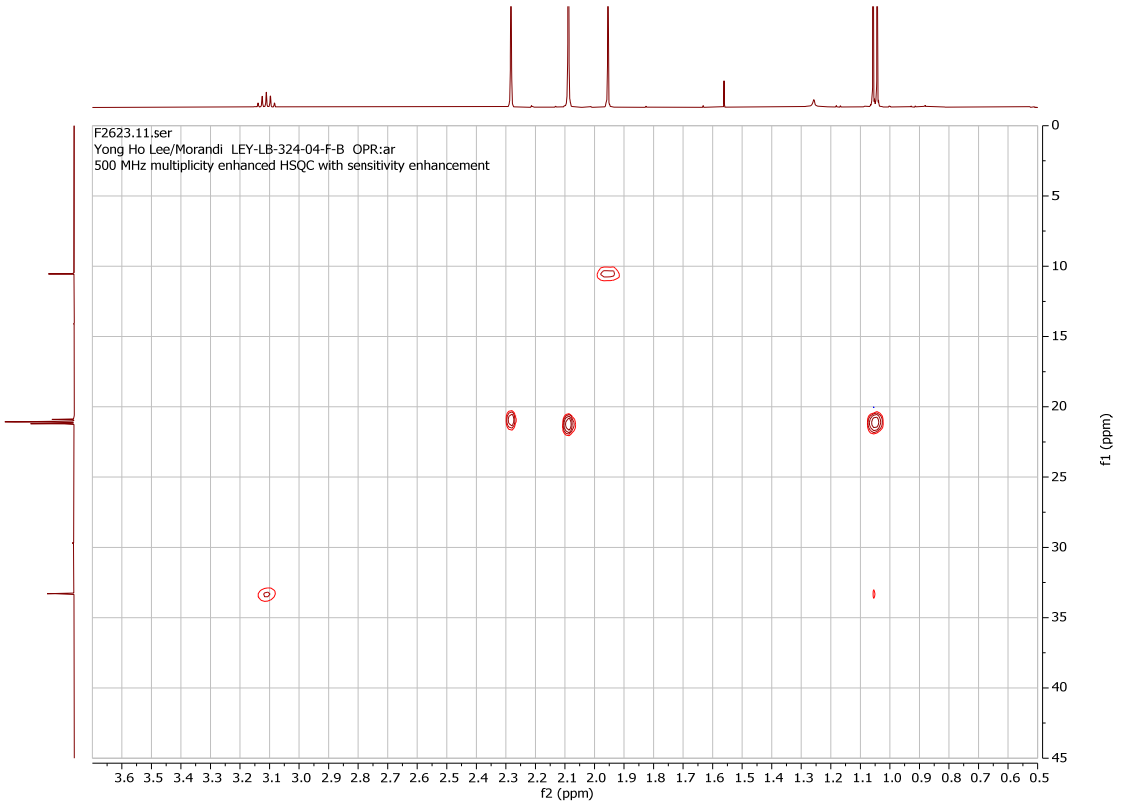
F2623.11.ser
Yong Ho Lee/Morandi LEY-LB-324-04-F-B OPR:ar
500 MHz multiplicity enhanced HSQC with sensitivity enhancement
f1 (ppm)
f2 (ppm)

(*Z*)-2-isopropyl-3-(*o*-tolyl)but-2-enal (**37-β-Ar, major**).

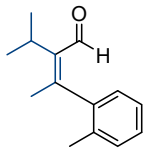

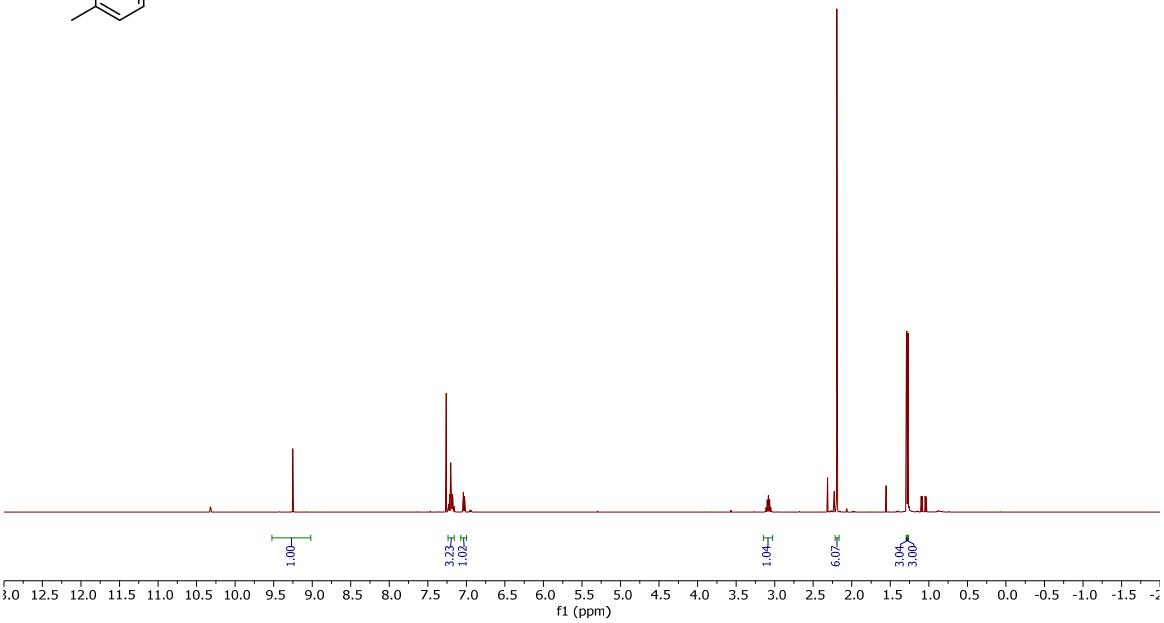

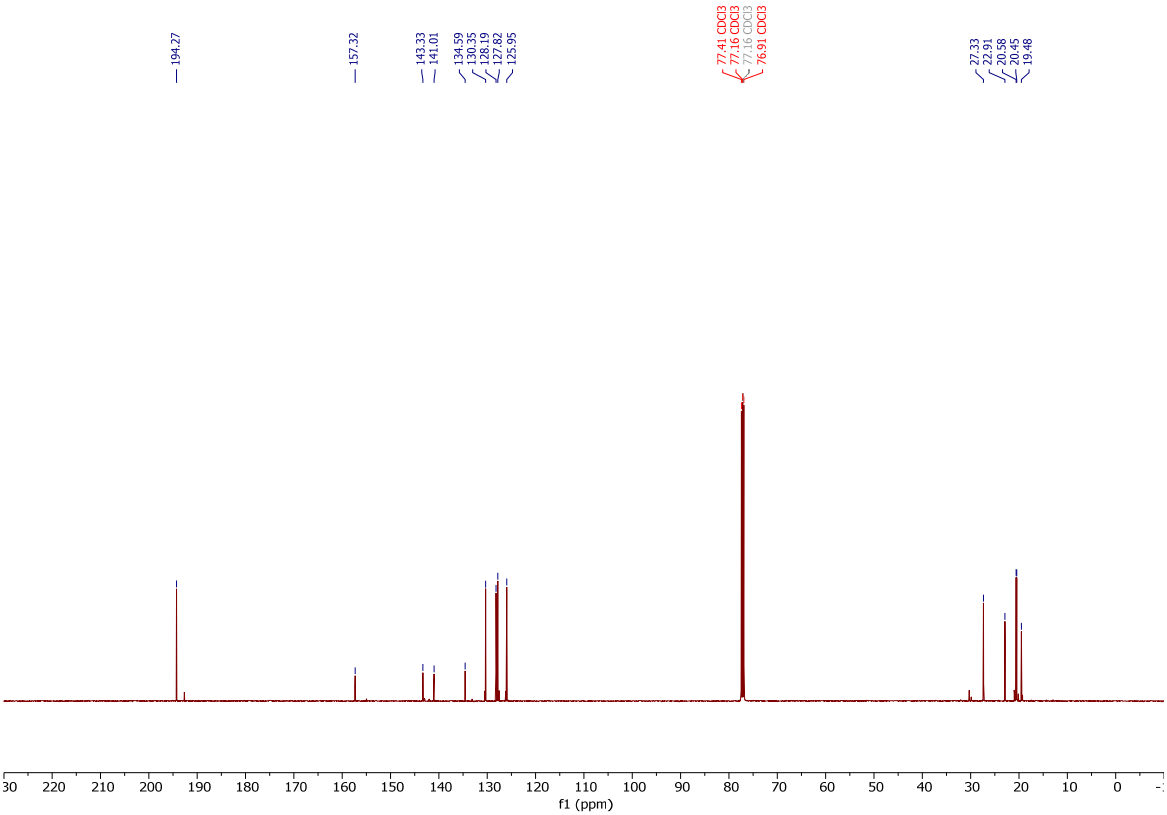

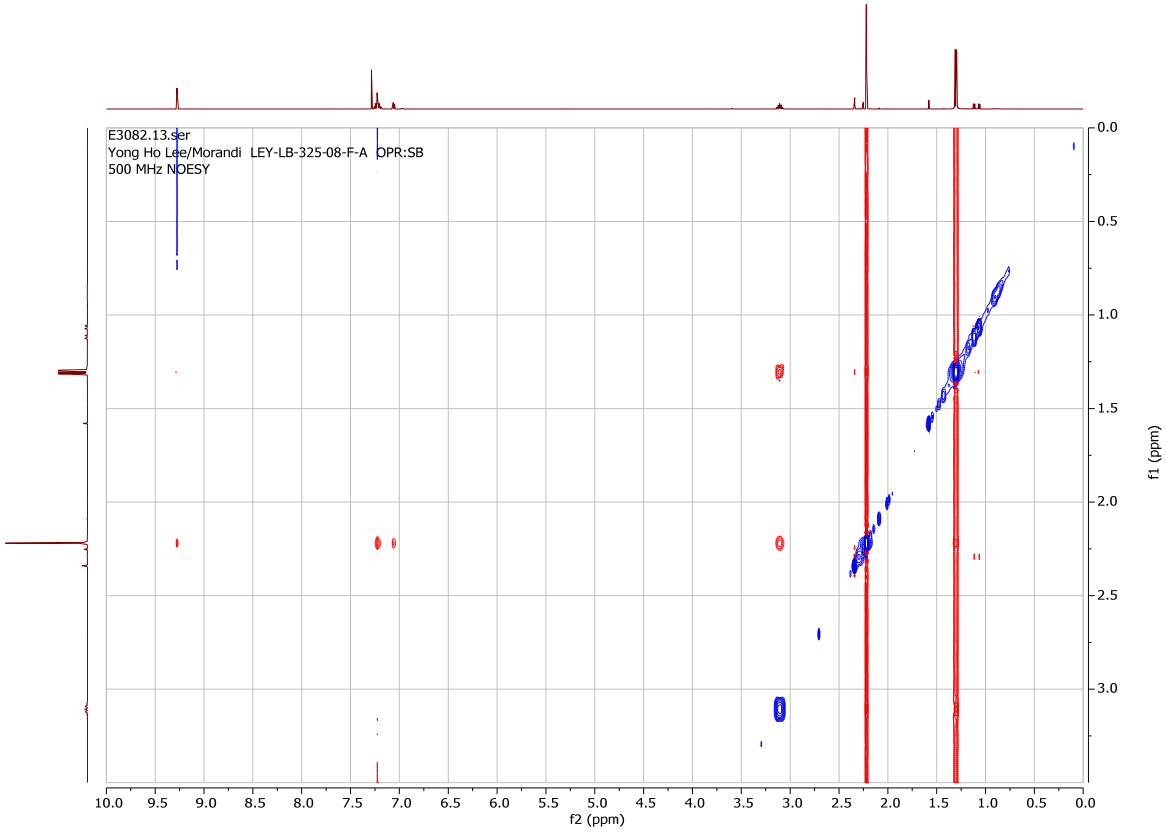
E3082.13.ser
Yong Ho Lee/Morandi LEY-LB-325-08-F-A OPR:SB
500 MHz NOESY
f2 (ppm)
f1 (ppm)

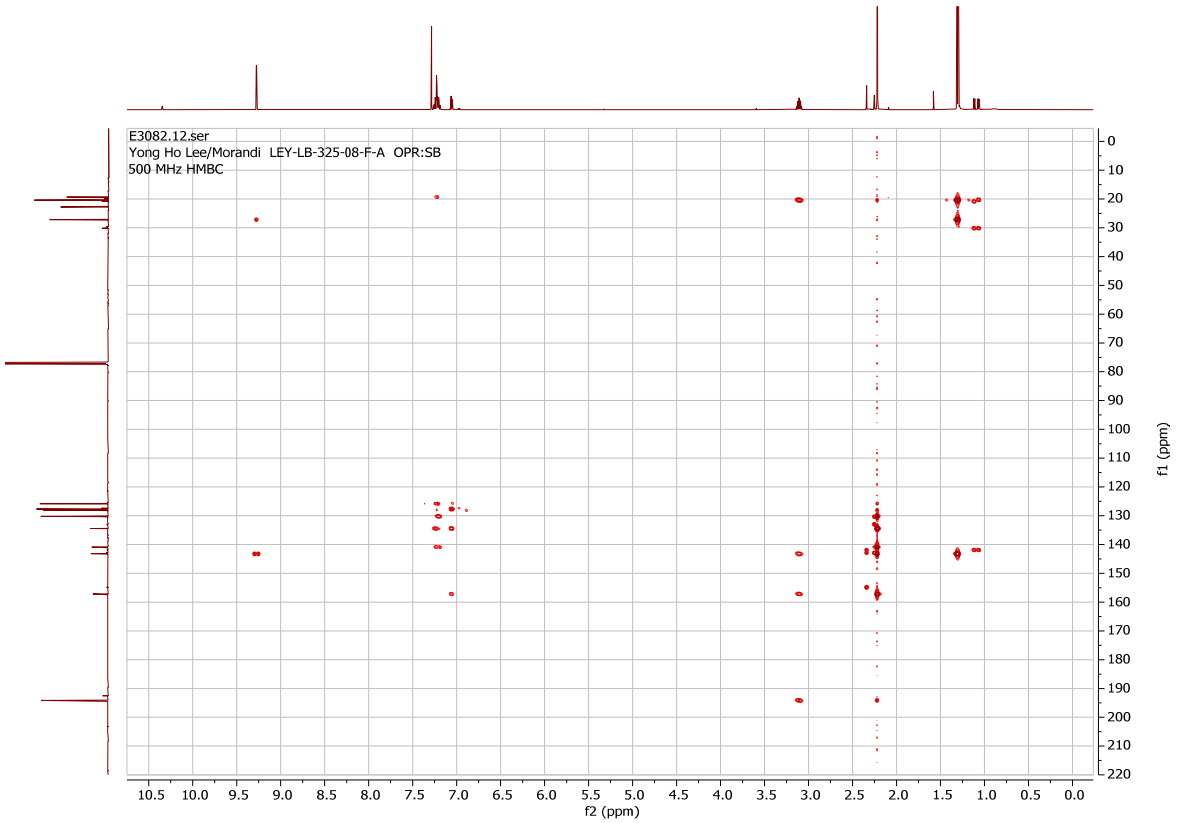
E3082.12.ser
Yong Ho Lee/Morandi LEY-LB-325-08-F-A OPR:SB
500 MHz HMBC
f2 (ppm)
f1 (ppm)

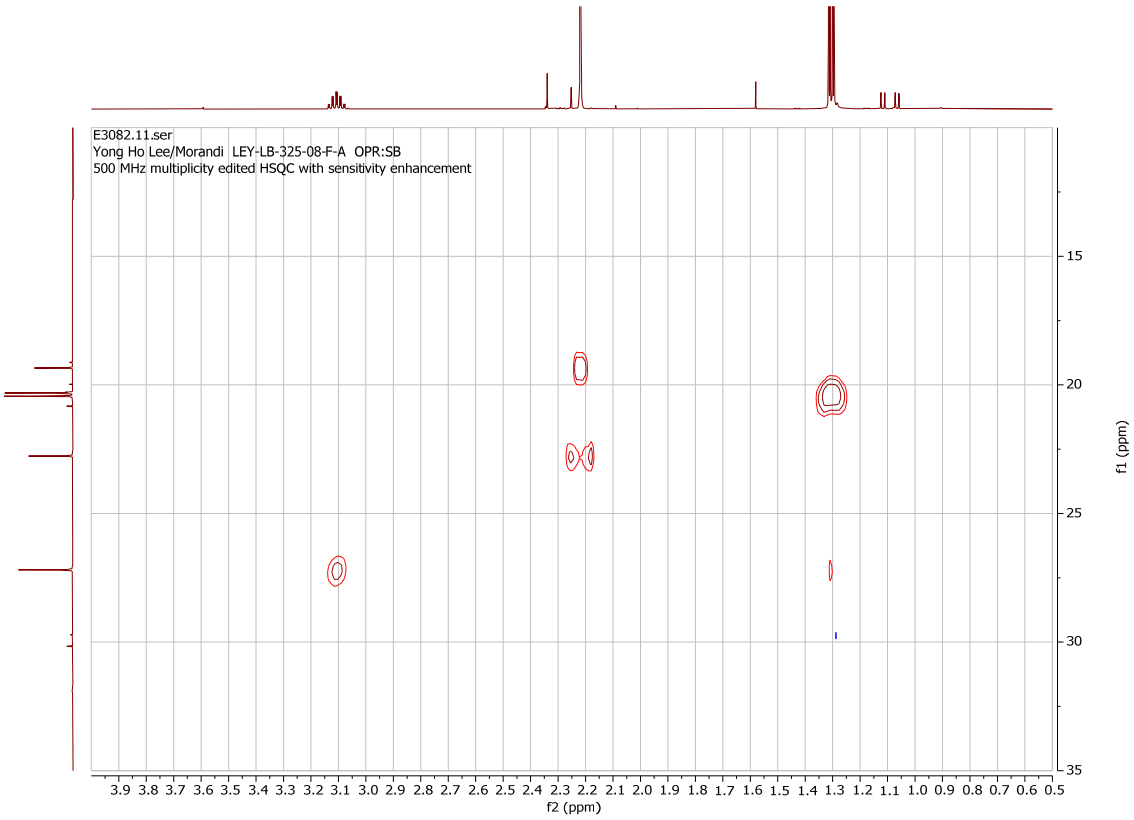
E3082.11.ser
Yong Ho Lee/Morandi LEY-LB-325-08-F-A OPR:SB
500 MHz multiplicity edited HSQC with sensitivity enhancement
15
20
25
30
35
f1 (ppm)
3.9 3.8 3.7 3.6 3.5 3.4 3.3 3.2 3.1 3.0 2.9 2.8 2.7 2.6 2.5 2.4 2.3 2.2 2.1 2.0 1.9 1.8 1.7 1.6 1.5 1.4 1.3 1.2 1.1 1.0 0.9 0.8 0.7 0.6 0.5
f2 (ppm)

(*Z*)-2,4-dimethyl-3-(*o*-tolyl)pent-2-enal (**37-α-Ar, minor**).

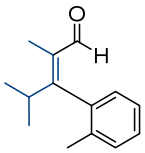

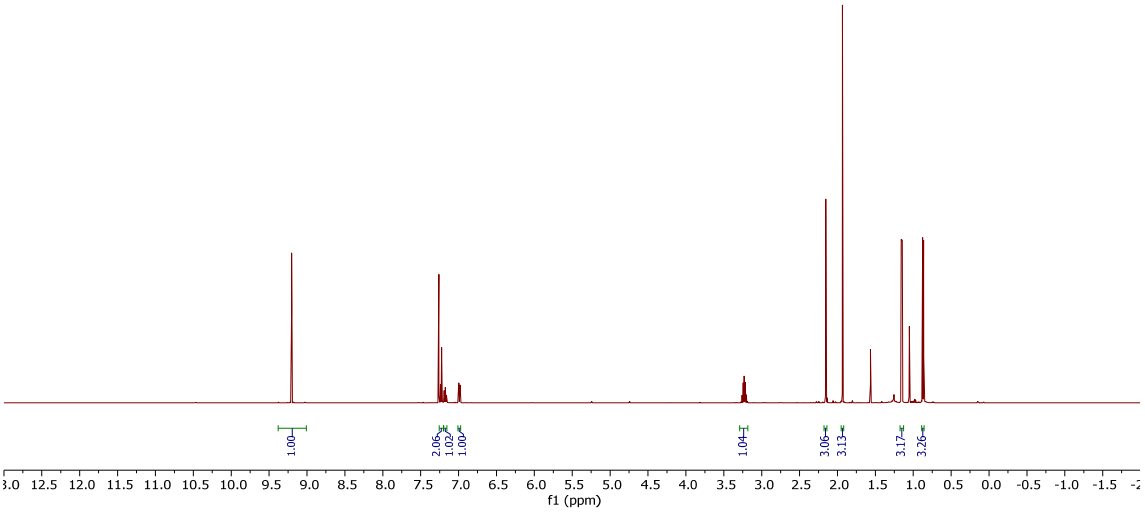

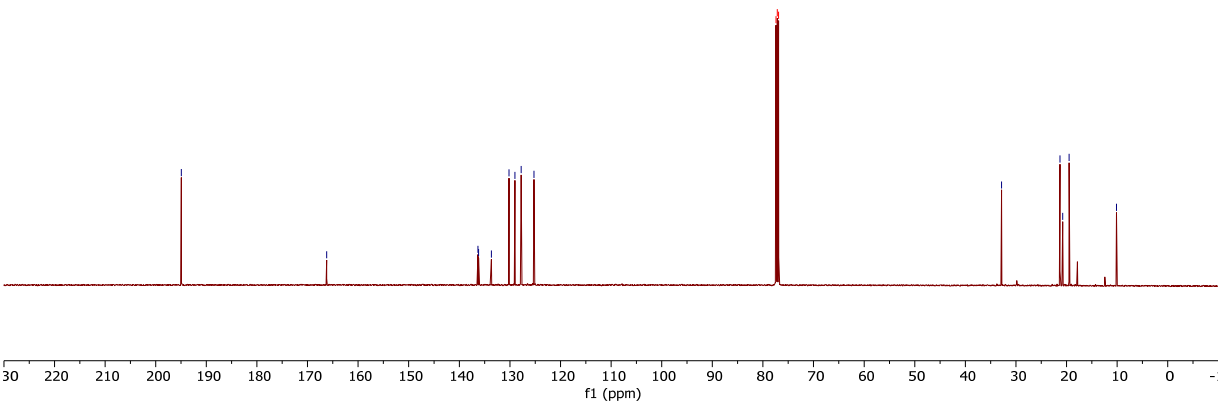

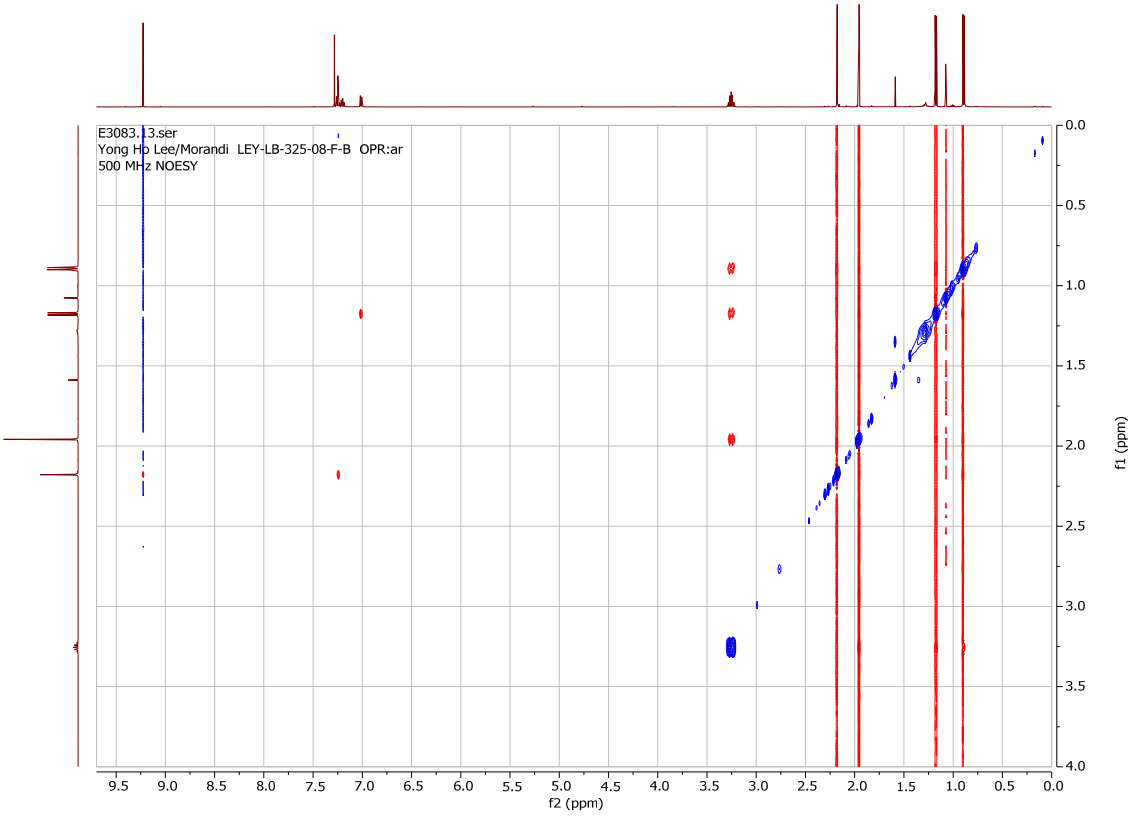
E3083.13.ser
Yong Ho Lee/Morandi LEY-LB-325-08-F-B OPR:ar
500 MHz NOESY
f2 (ppm)
f1 (ppm)

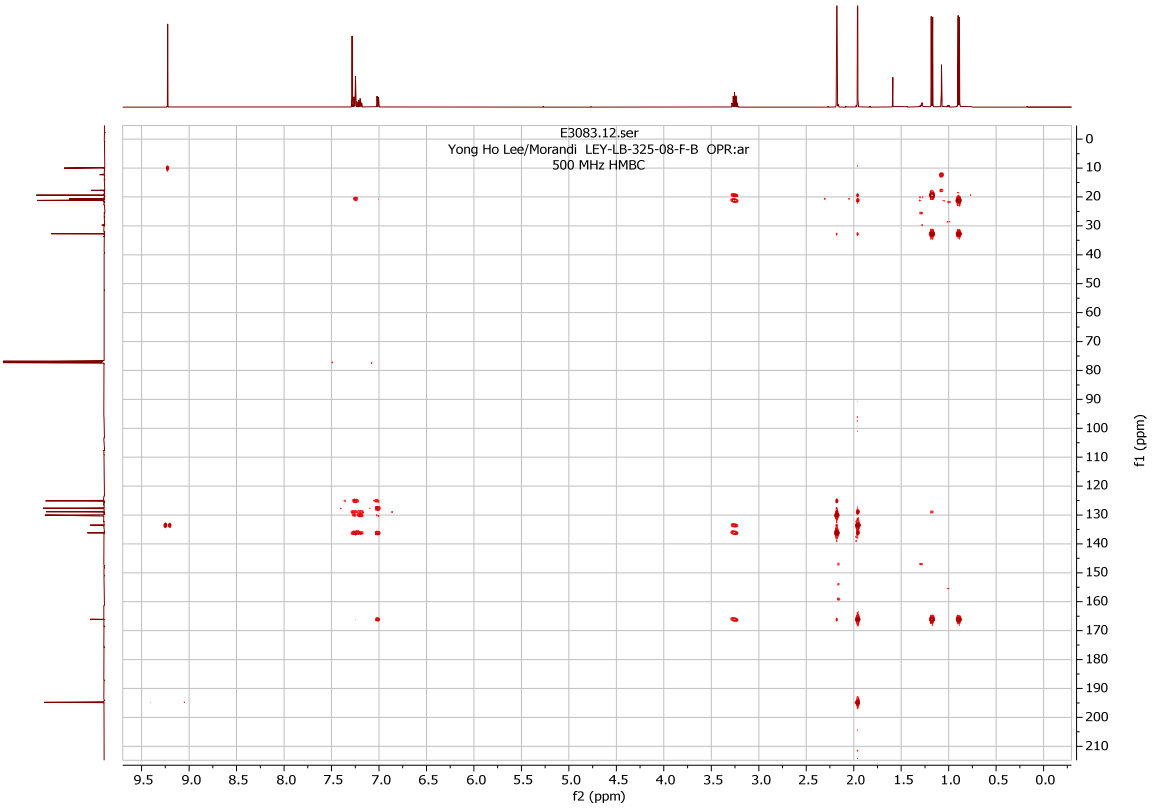
E3083.12.ser
Yong Ho Lee/Morandi LEY-LB-325-08-F-B OPR:ar
500 MHz HMBC
f2 (ppm)
f1 (ppm)

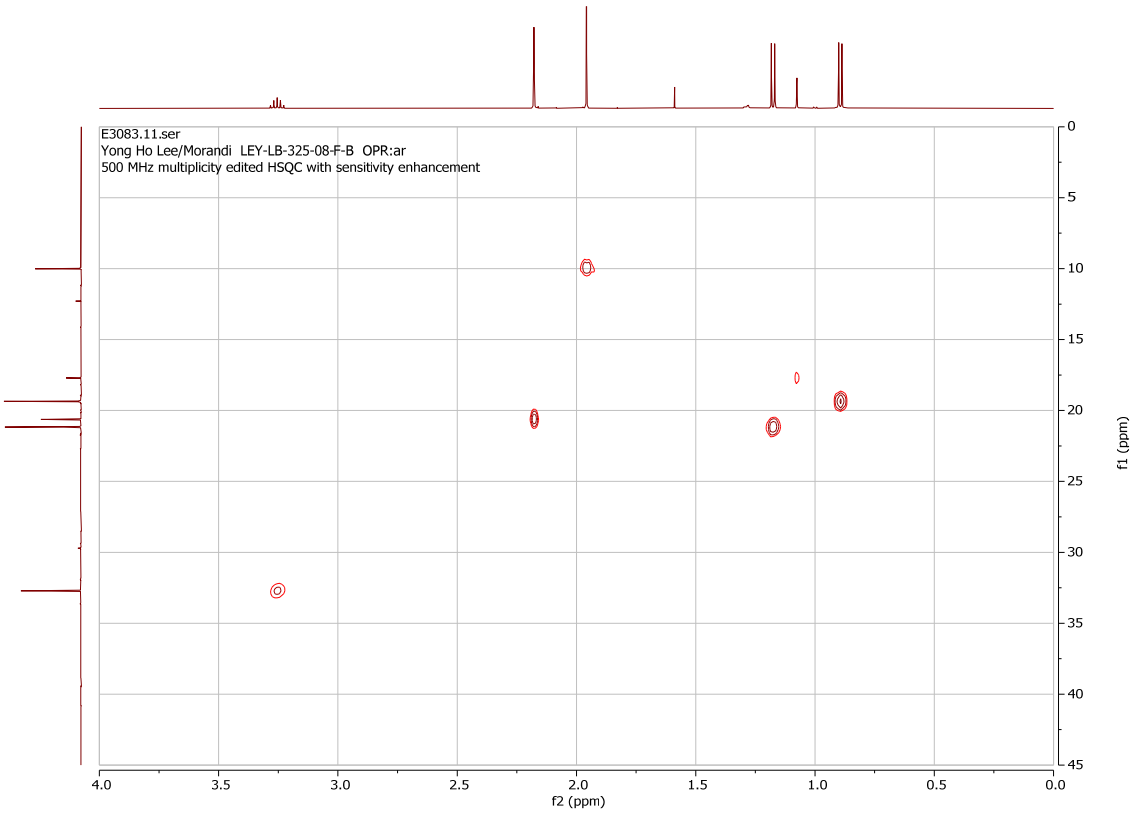
E3083.11.ser
Yong Ho Lee/Morandi LEY-LB-325-08-F-B OPR:ar
500 MHz multiplicity edited HSQC with sensitivity enhancement
f2 (ppm)
f1 (ppm)

(*Z*)-2-(1-mesitylethylidene)heptanal (**38-β-Ar, major**).

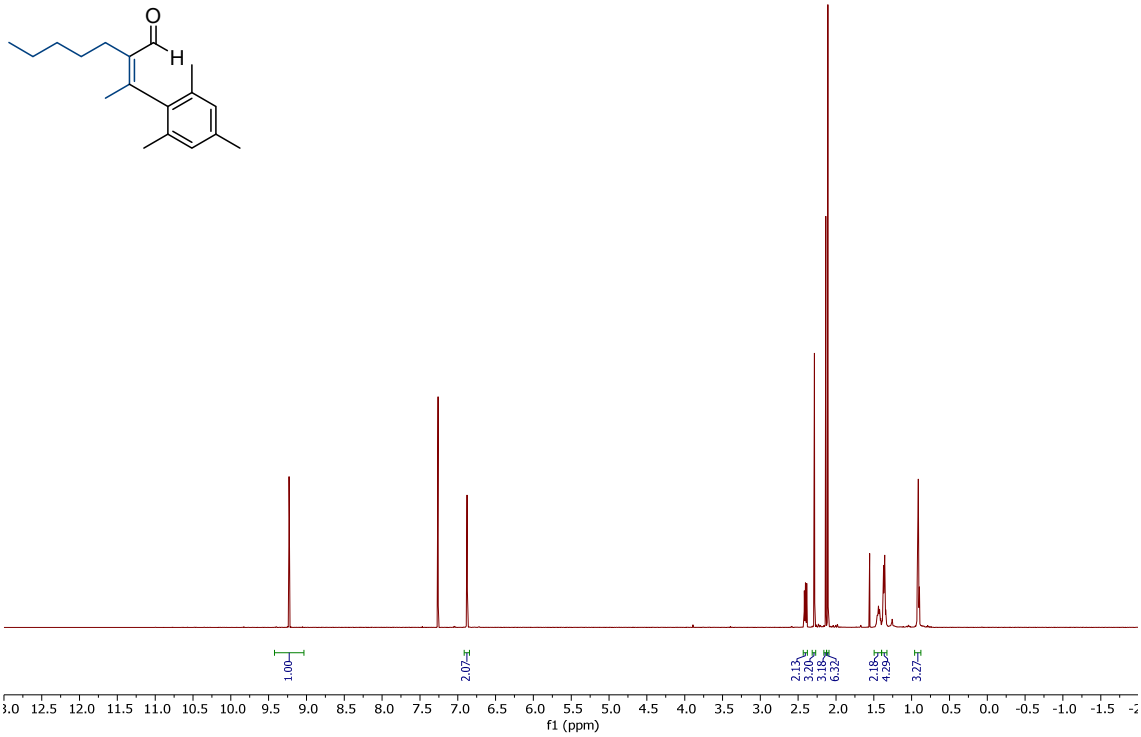

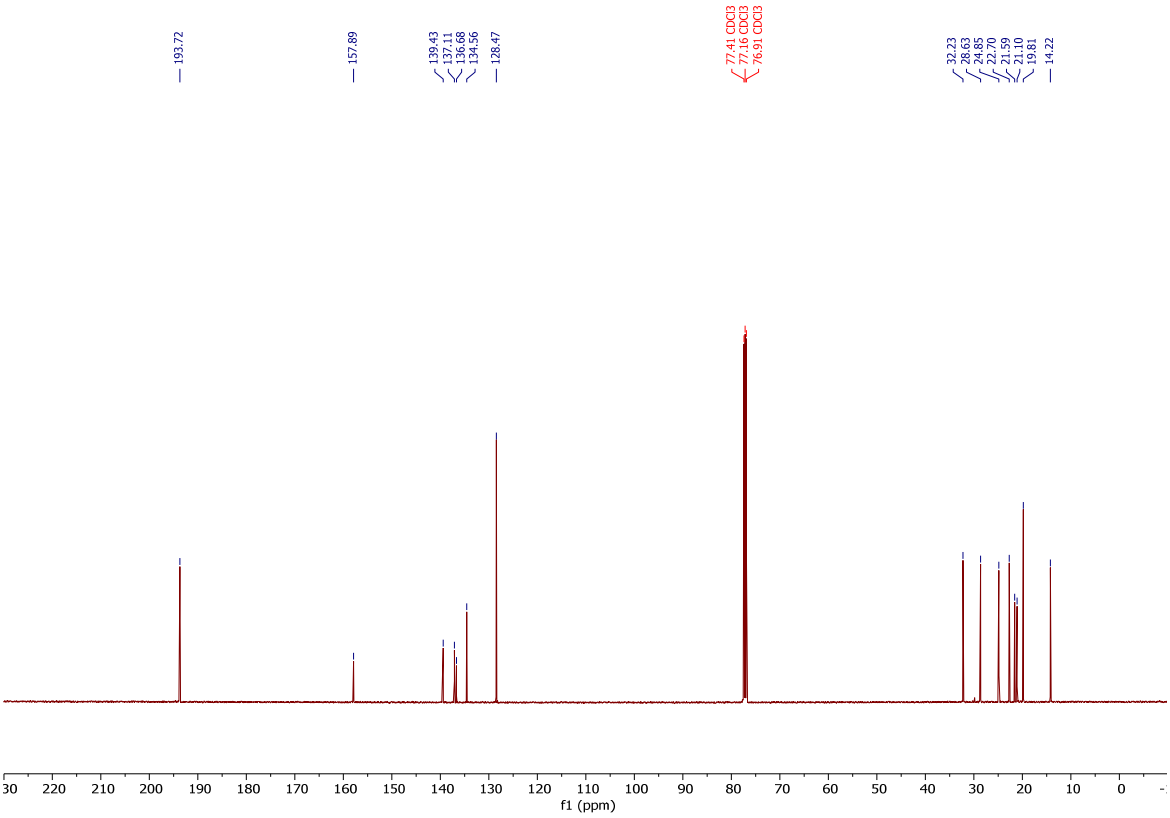

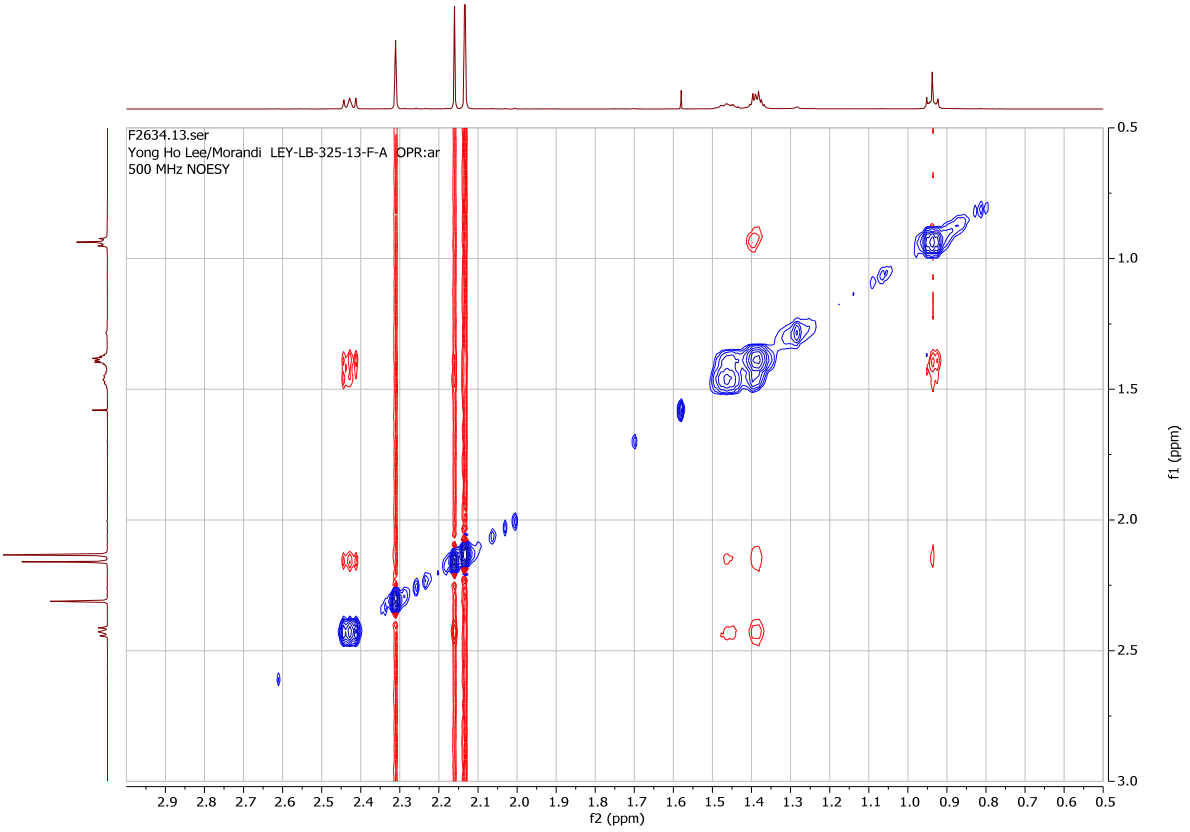
F2634.13.ser
Yong Ho Lee/Morandi LEY-LB-325-13-F-A OPR:ar
500 MHz NOESY
f1 (ppm)
f2 (ppm)

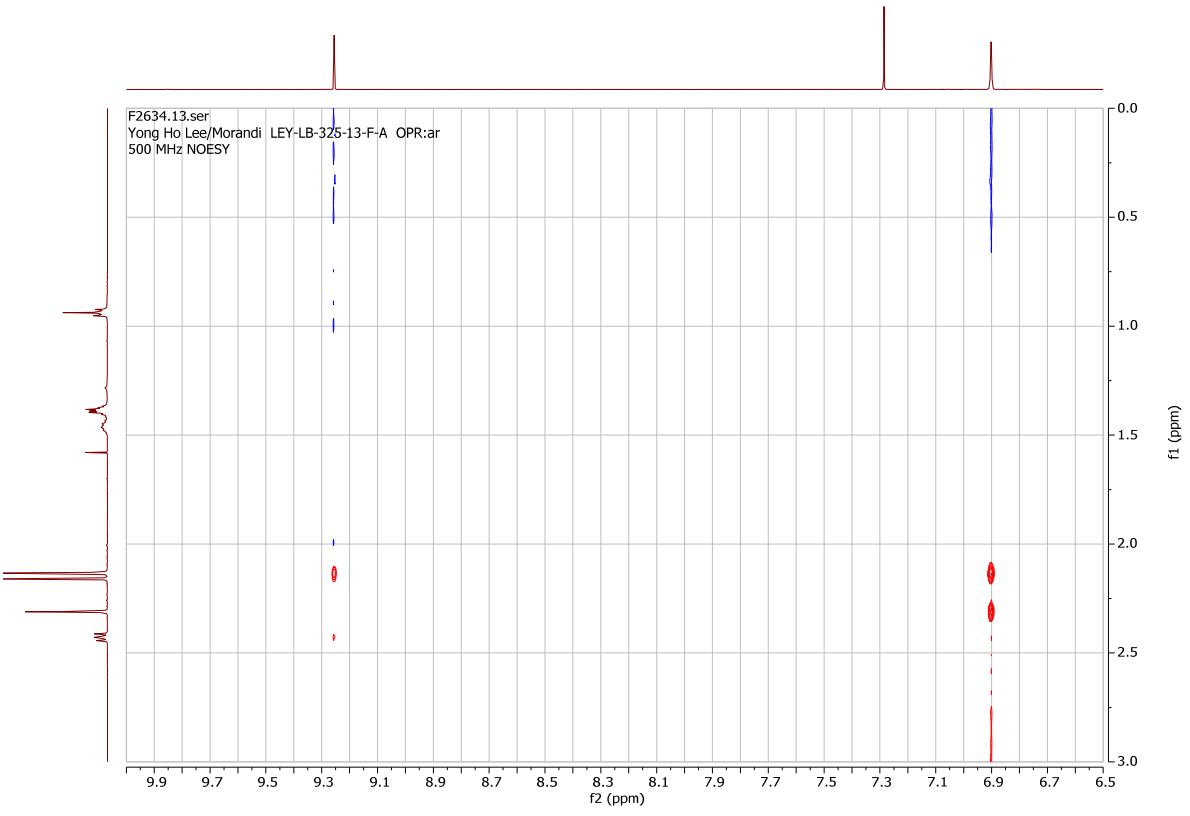
F2634.13.ser
Yong Ho Lee/Morandi LEY-LB-325-13-F-A OPR:ar
500 MHz NOESY
f1 (ppm)
f2 (ppm)

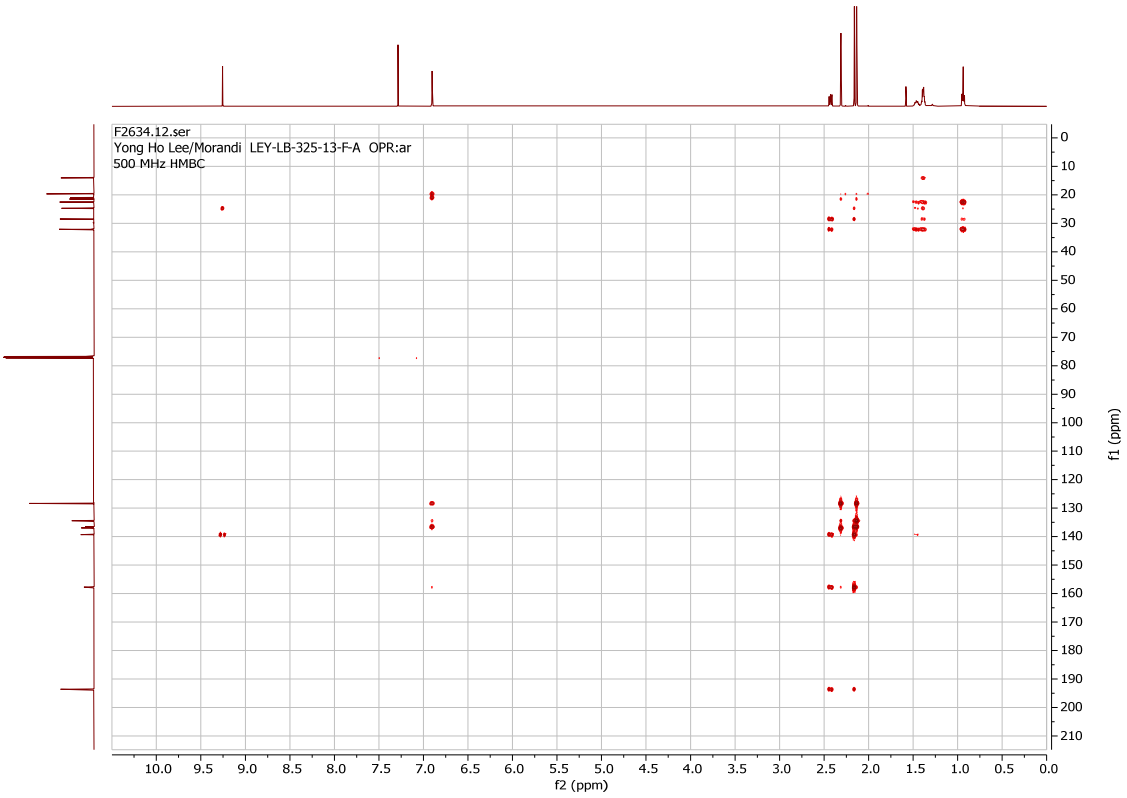
F2634.12.ser
Yong Ho Lee/Morandi LEY-LB-325-13-F-A OPR:ar
500 MHz HMBC
f2 (ppm)
f1 (ppm)

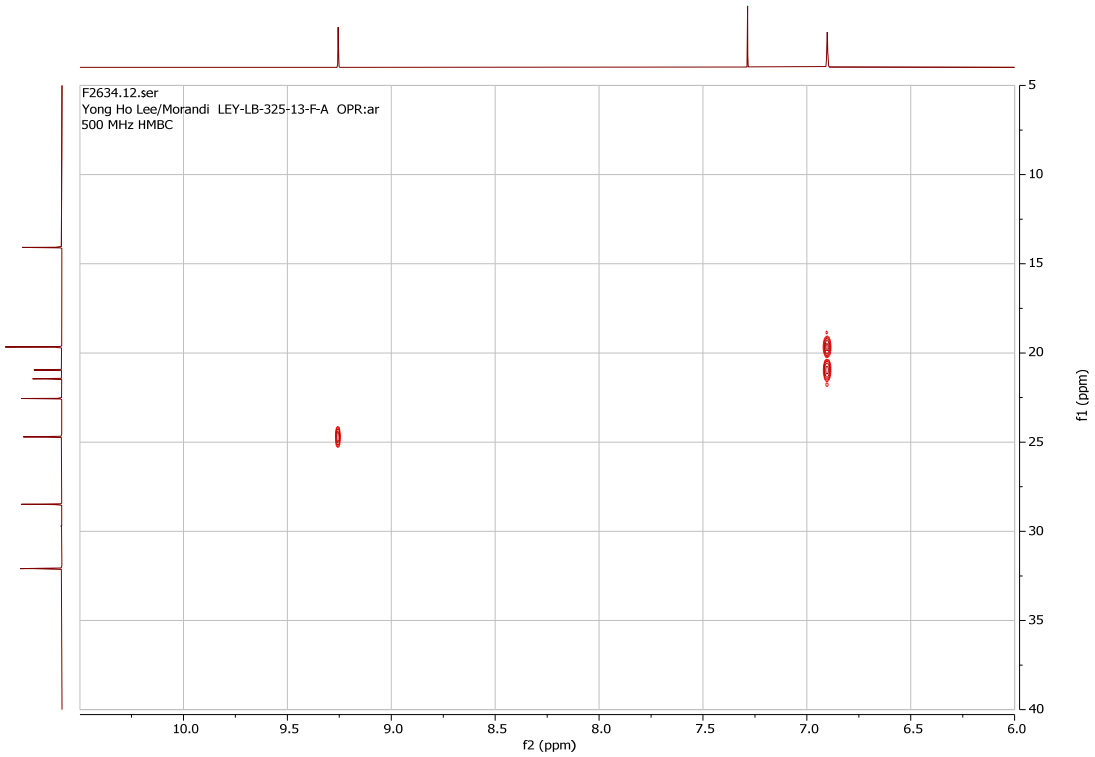
F2634.12.ser
Yong Ho Lee/Morandi LEY-LB-325-13-F-A OPR:ar
500 MHz HMBC
f2 (ppm)
f1 (ppm)

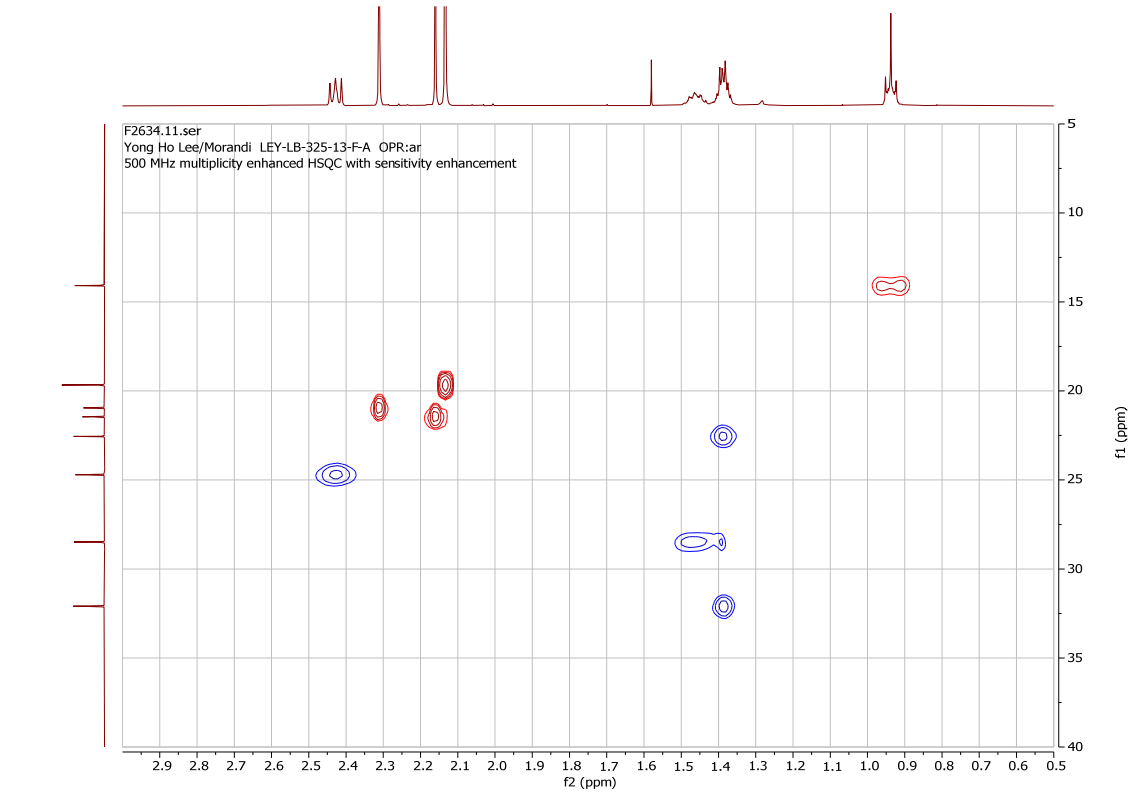
F2634.11.ser
Yong Ho Lee/Morandi LEY-LB-325-13-F-A OPR:ar
500 MHz multiplicity enhanced HSQC with sensitivity enhancement
f2 (ppm)
f1 (ppm)

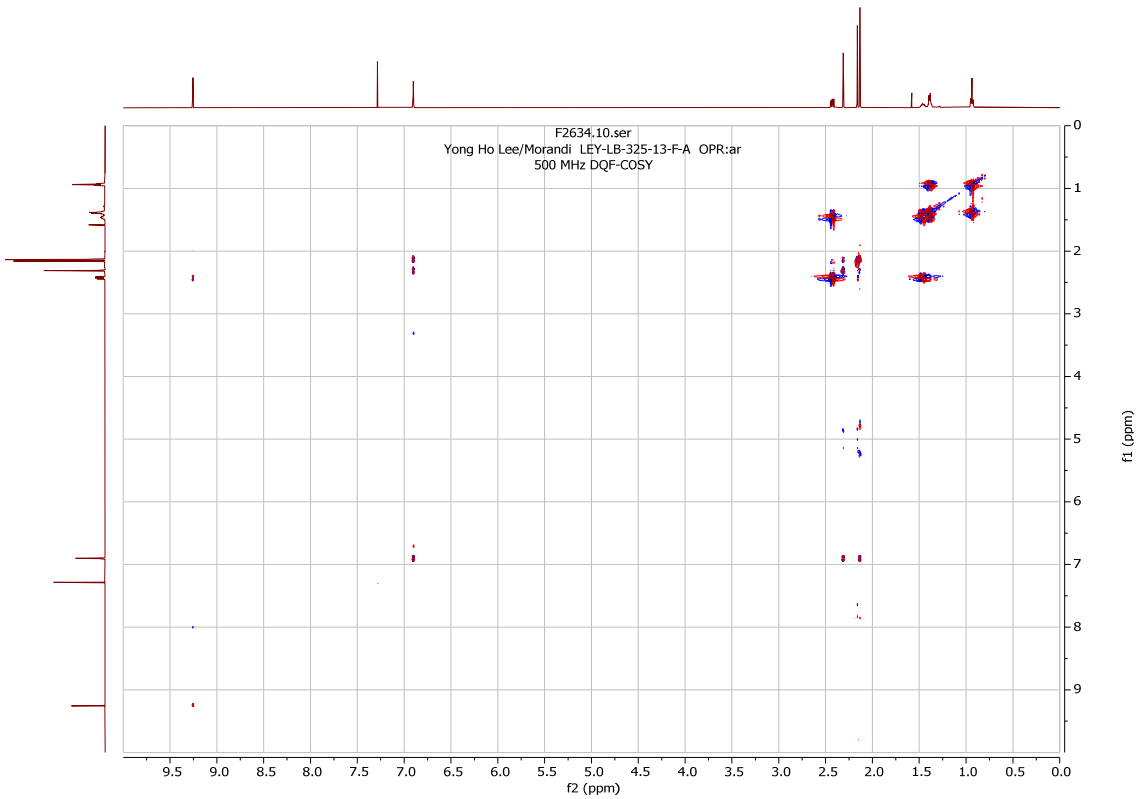
F2634.10.ser
Yong Ho Lee/Morandi LEY-LB-325-13-F-A OPR:ar
500 MHz DQF-COSY
f2 (ppm)
f1 (ppm)

(*Z*)-3-mesityl-2-methyloct-2-enal (**38-α-Ar, minor**).

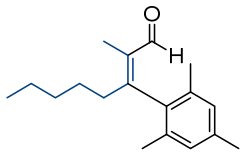

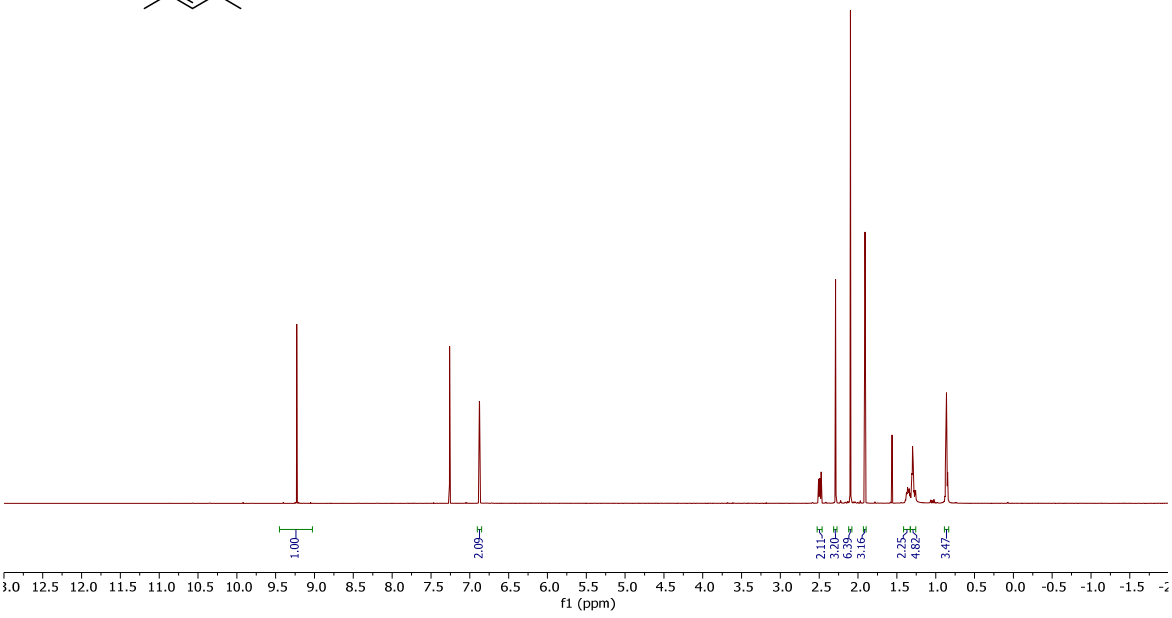

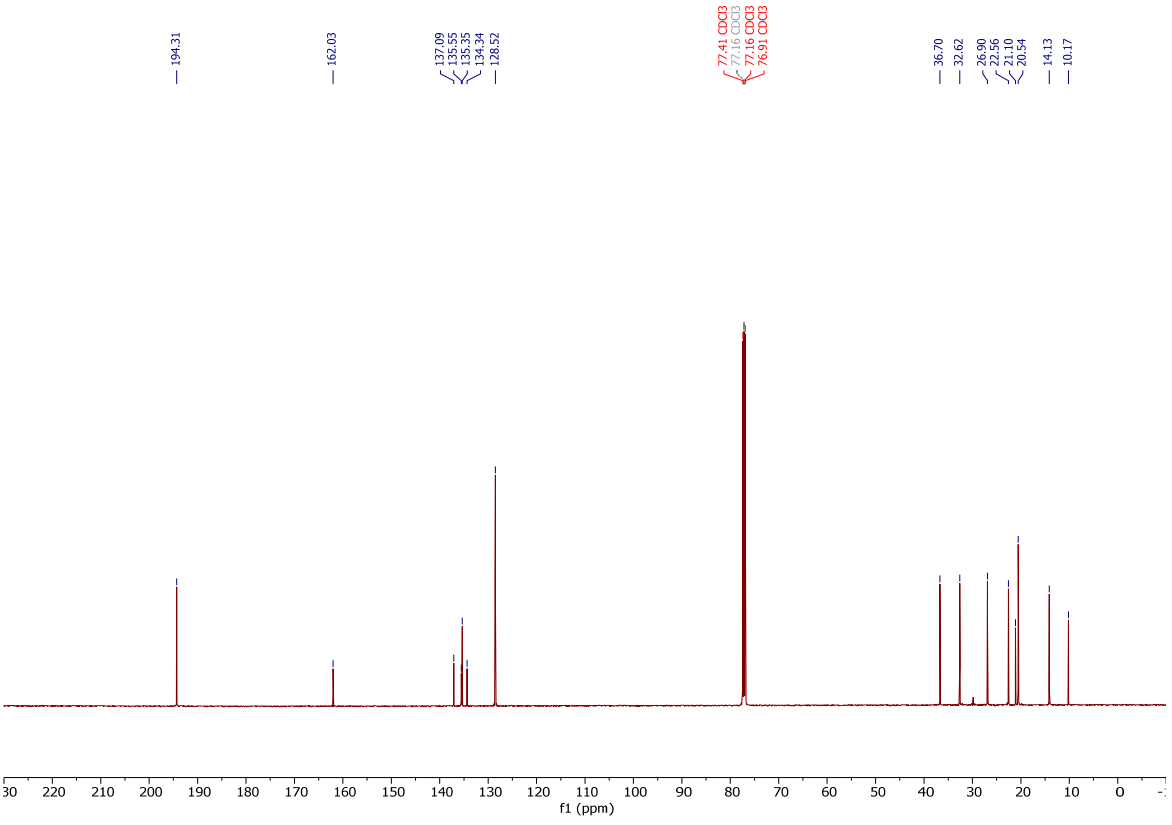

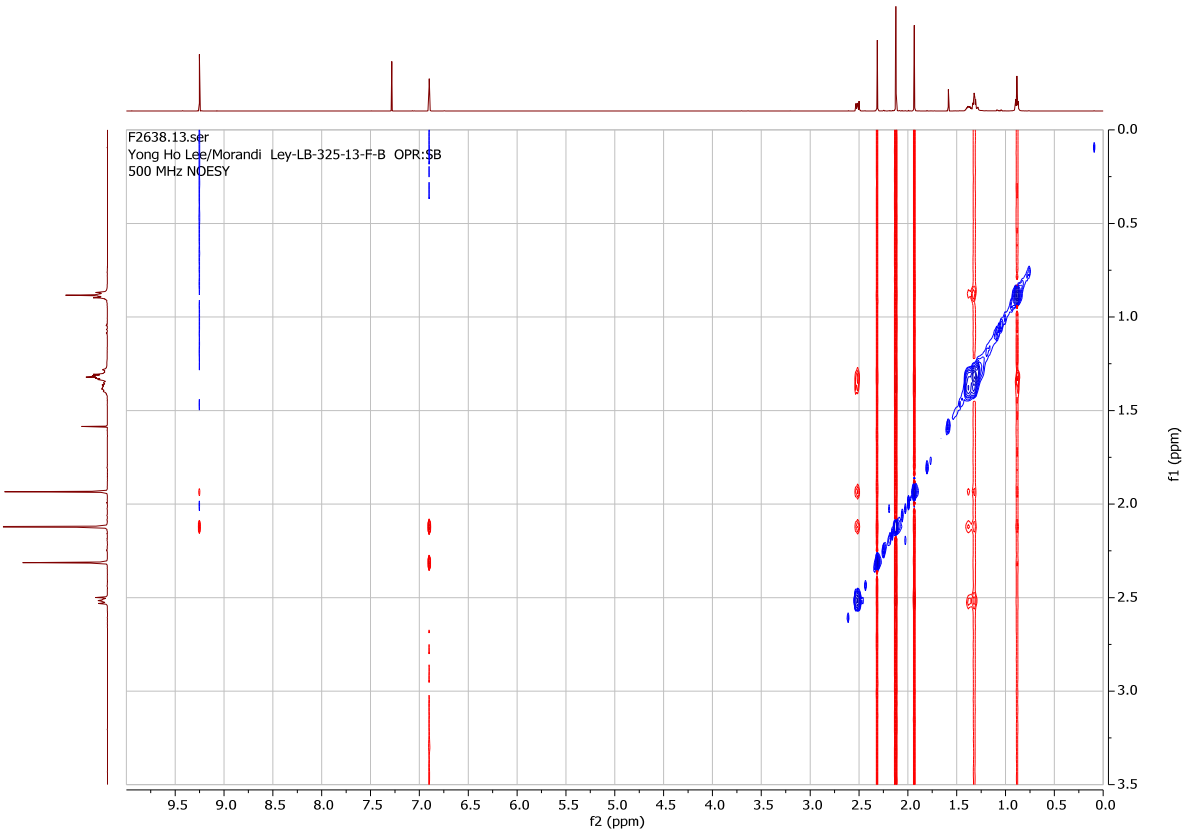
F2638.13.ser
Yong Ho Lee/Morandi Ley-LB-325-13-F-B OPR:SB
500 MHz NOESY
f2 (ppm)
f1 (ppm)

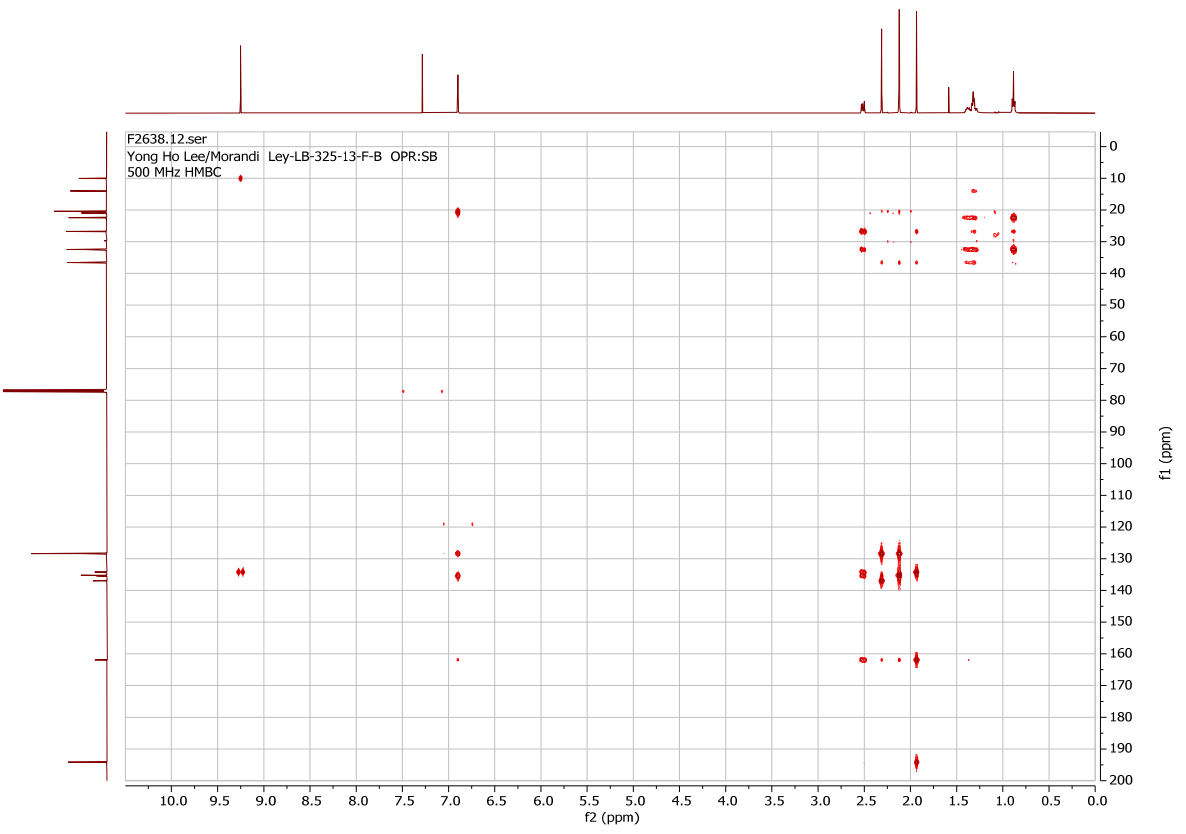
F2638.12.ser
Yong Ho Lee/Morandi Ley-LB-325-13-F-B OPR:SB
500 MHz HMBC
f2 (ppm)
f1 (ppm)

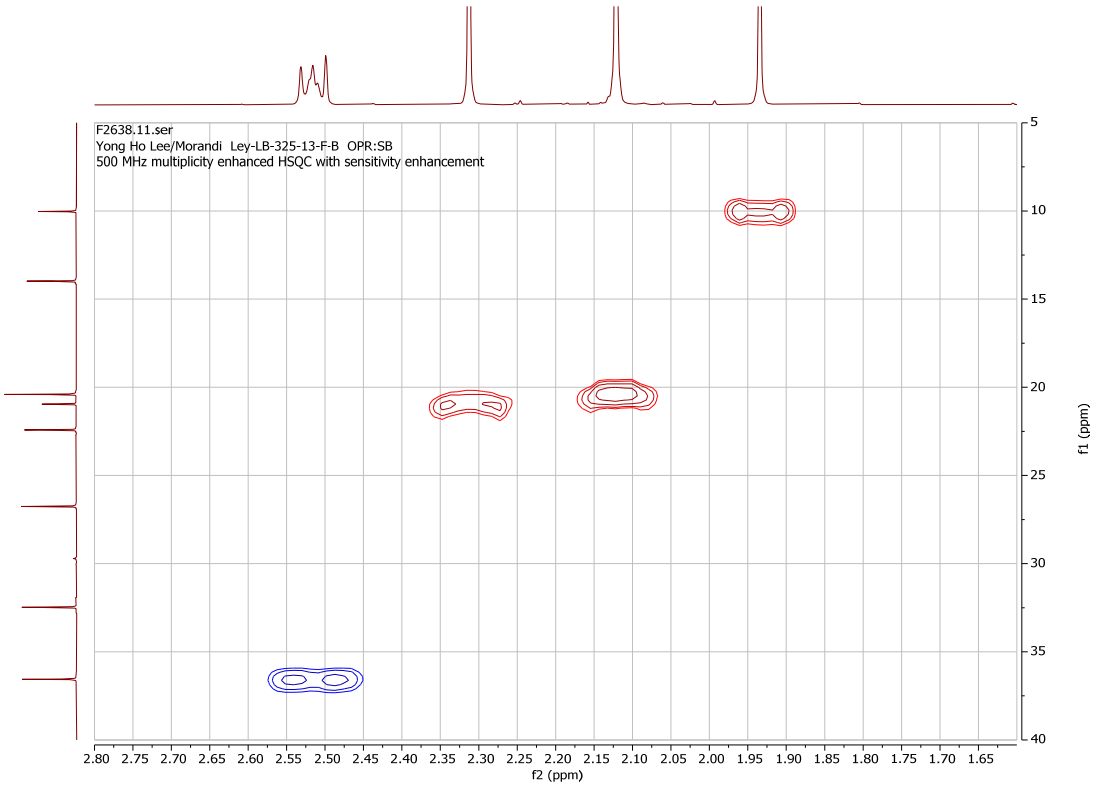
F2638.11.ser
Yong Ho Lee/Morandi Ley-LB-325-13-F-B OPR:SB
500 MHz multiplicity enhanced HSQC with sensitivity enhancement
f2 (ppm)
f1 (ppm)

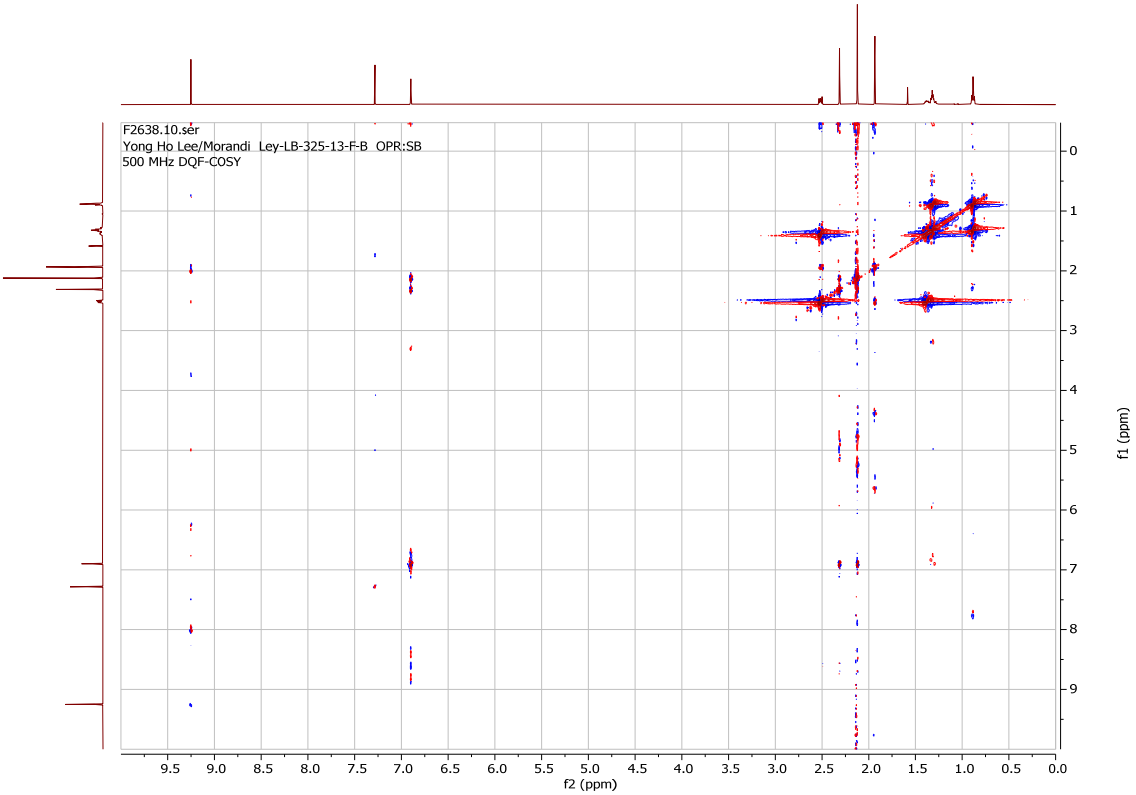
F2638.10.ser
Yong Ho Lee/Morandi Ley-LB-325-13-F-B OPR:SB
500 MHz DQF-COSY
f2 (ppm)
f1 (ppm)

(*Z*)-2-(1-(*o*-tolyl)ethylidene)heptanal (**39-β-Ar, major**).

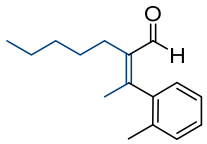

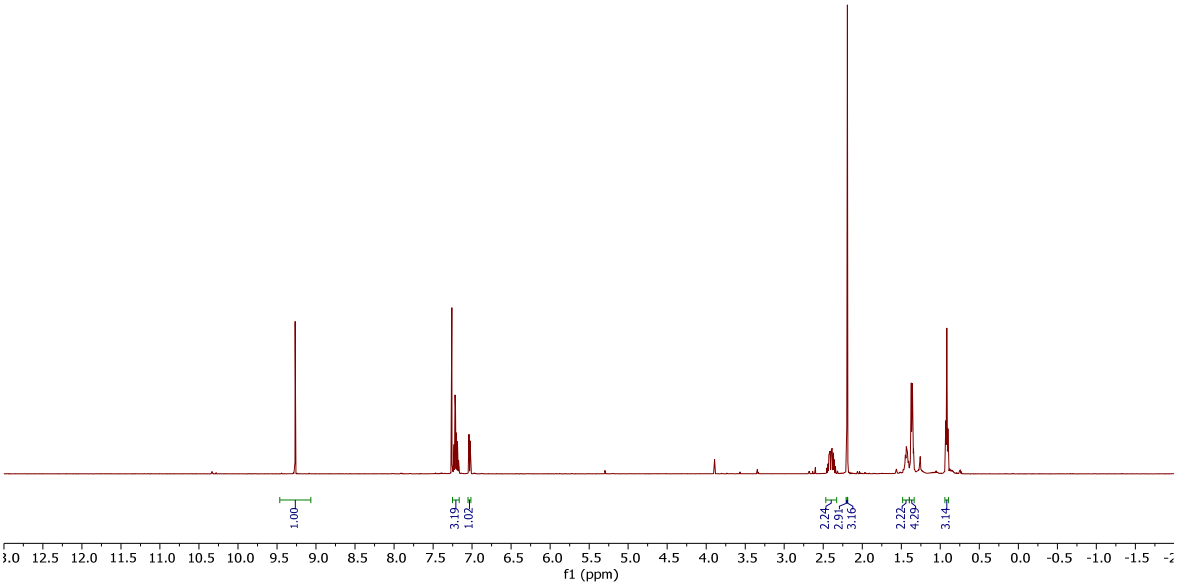

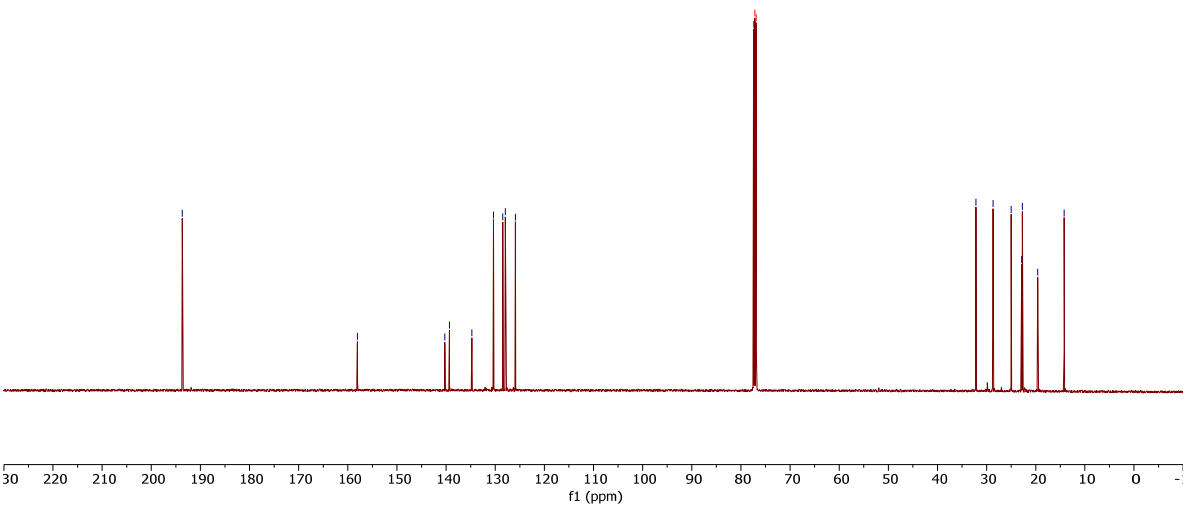

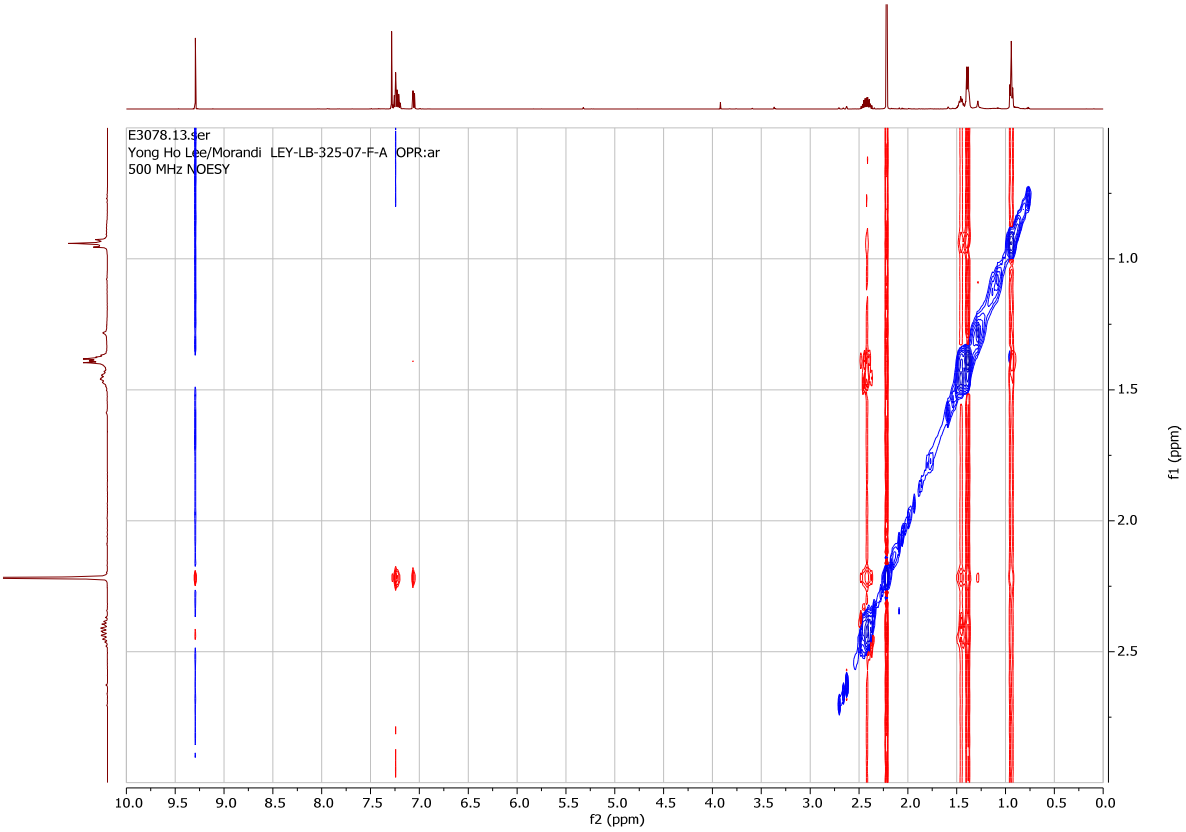
E3078.13.ser
Yong Ho Lee/Morandi LEY-LB-325-07-F-A OPR:ar
500 MHz NOESY
f2 (ppm)
f1 (ppm)

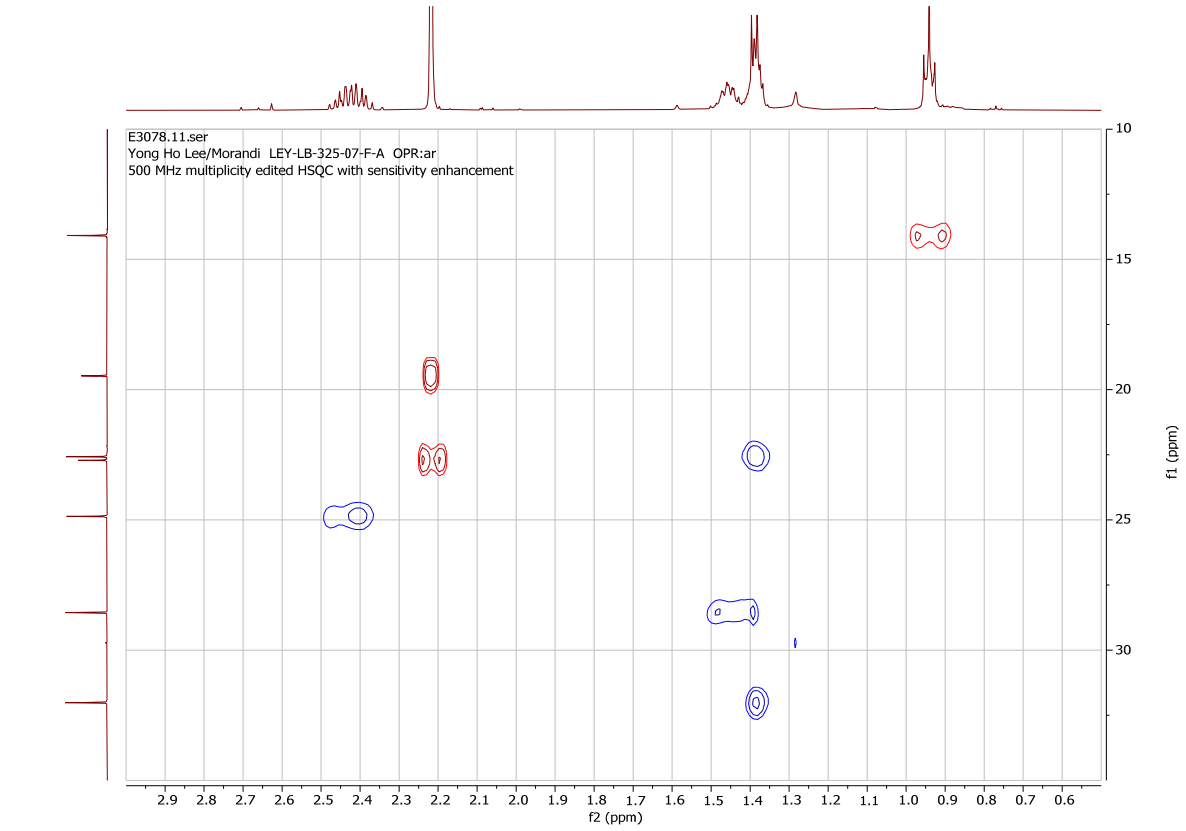
E3078.11.ser
Yong Ho Lee/Morandi LEY-LB-325-07-F-A OPR:ar
500 MHz multiplicity edited HSQC with sensitivity enhancement
f2 (ppm)
f1 (ppm)

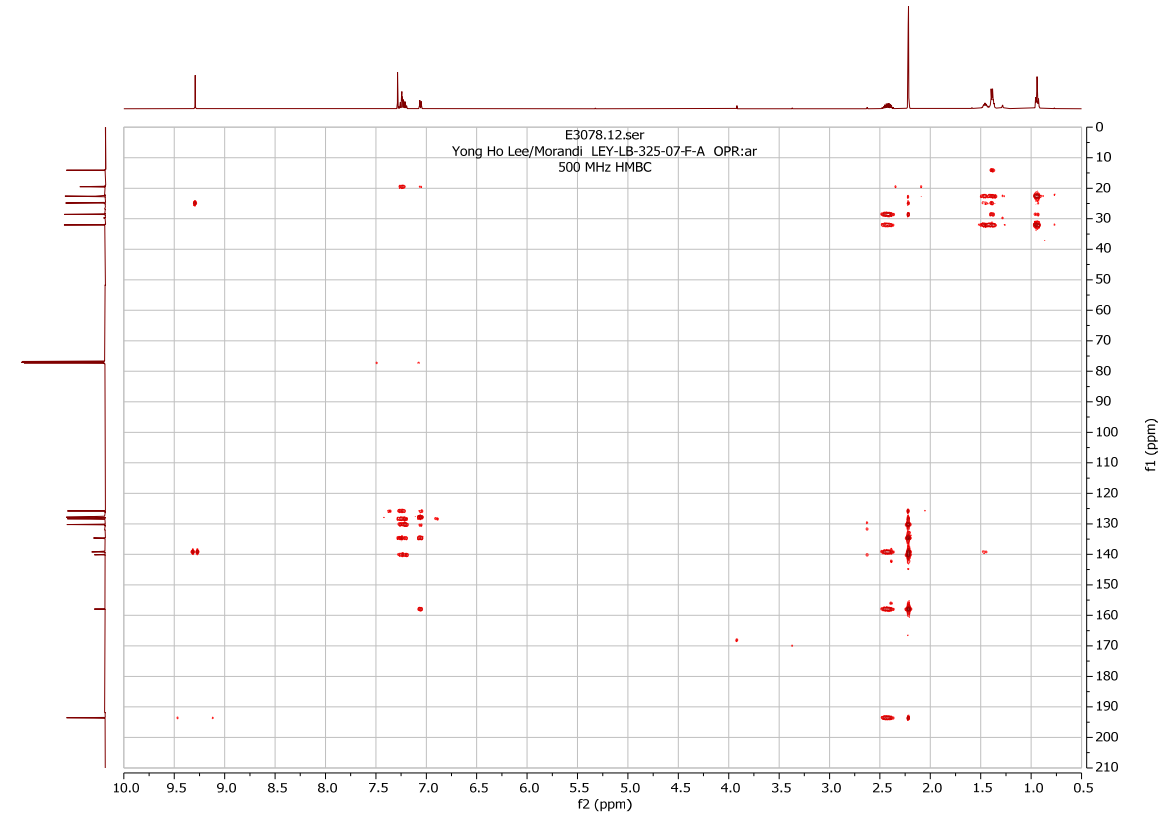
E3078.12.ser
Yong Ho Lee/Morandi LEY-LB-325-07-F-A OPR:ar
500 MHz HMBC
f2 (ppm)
f1 (ppm)

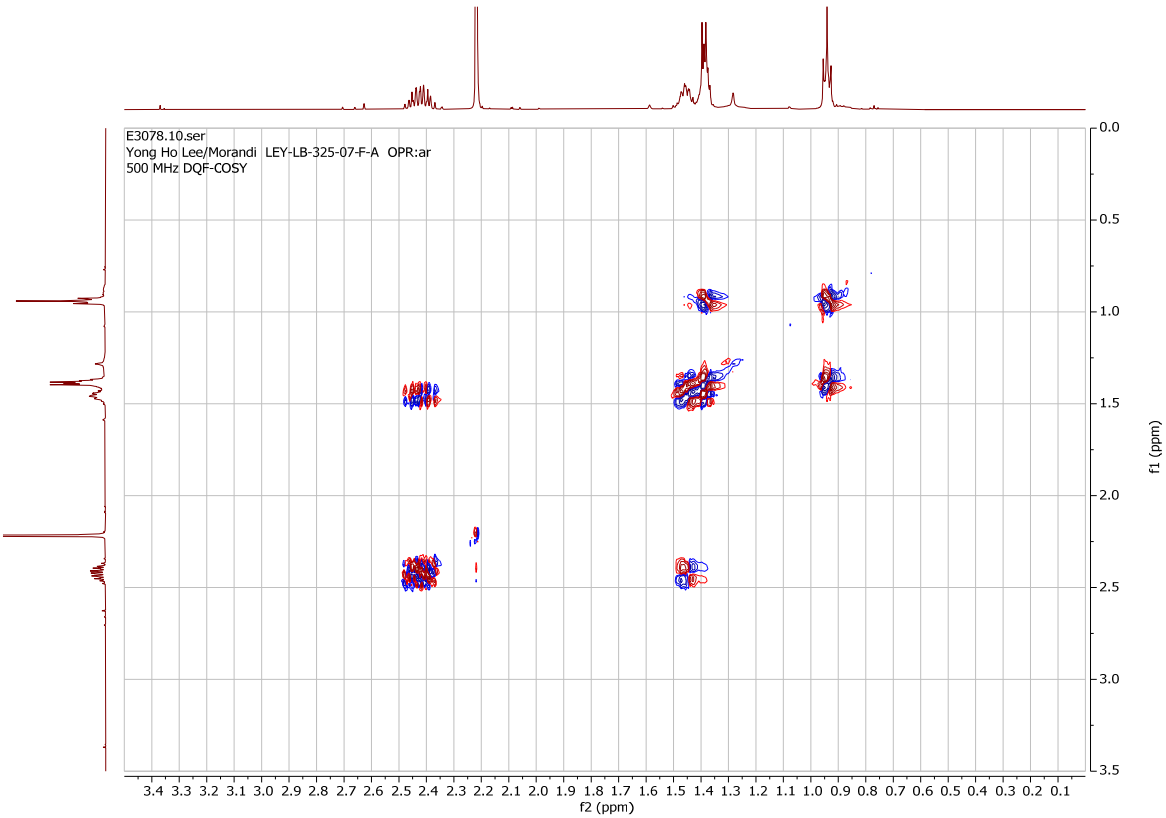
E3078.10.ser
Yong Ho Lee/Morandi LEY-LB-325-07-F-A OPR:ar
500 MHz DQF-COSY
f2 (ppm)
f1 (ppm)

(*Z*)-2-methyl-3-(*o*-tolyl)oct-2-enal (**39-α-Ar, minor**).

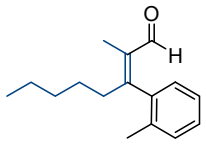

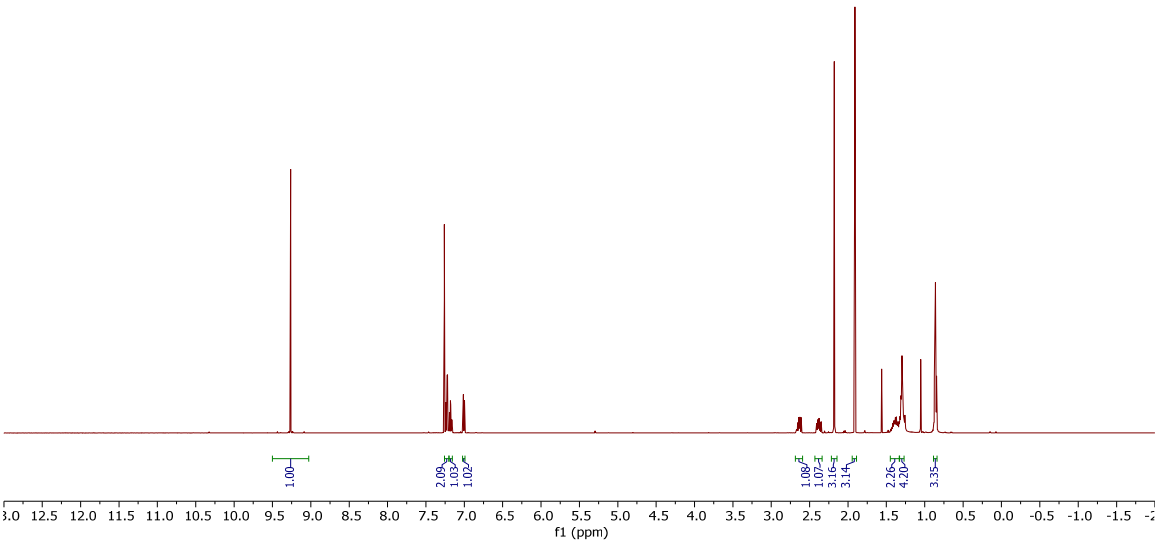

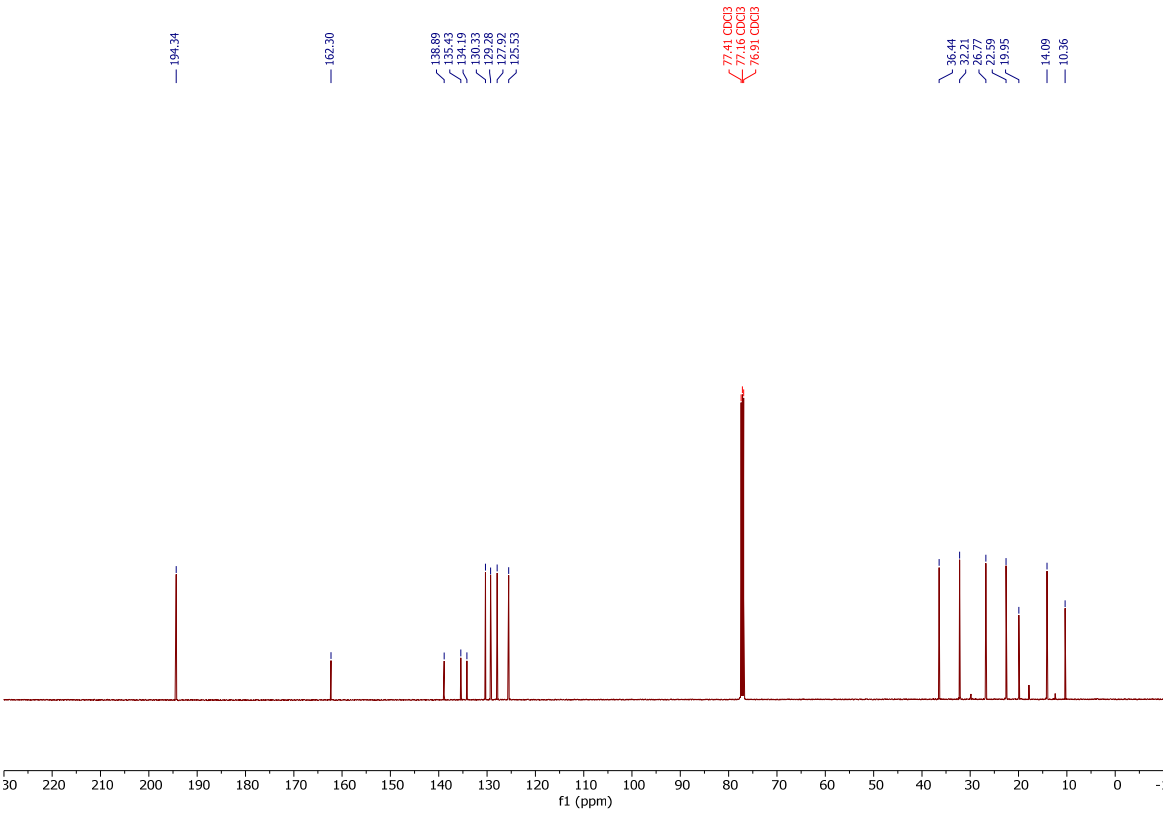

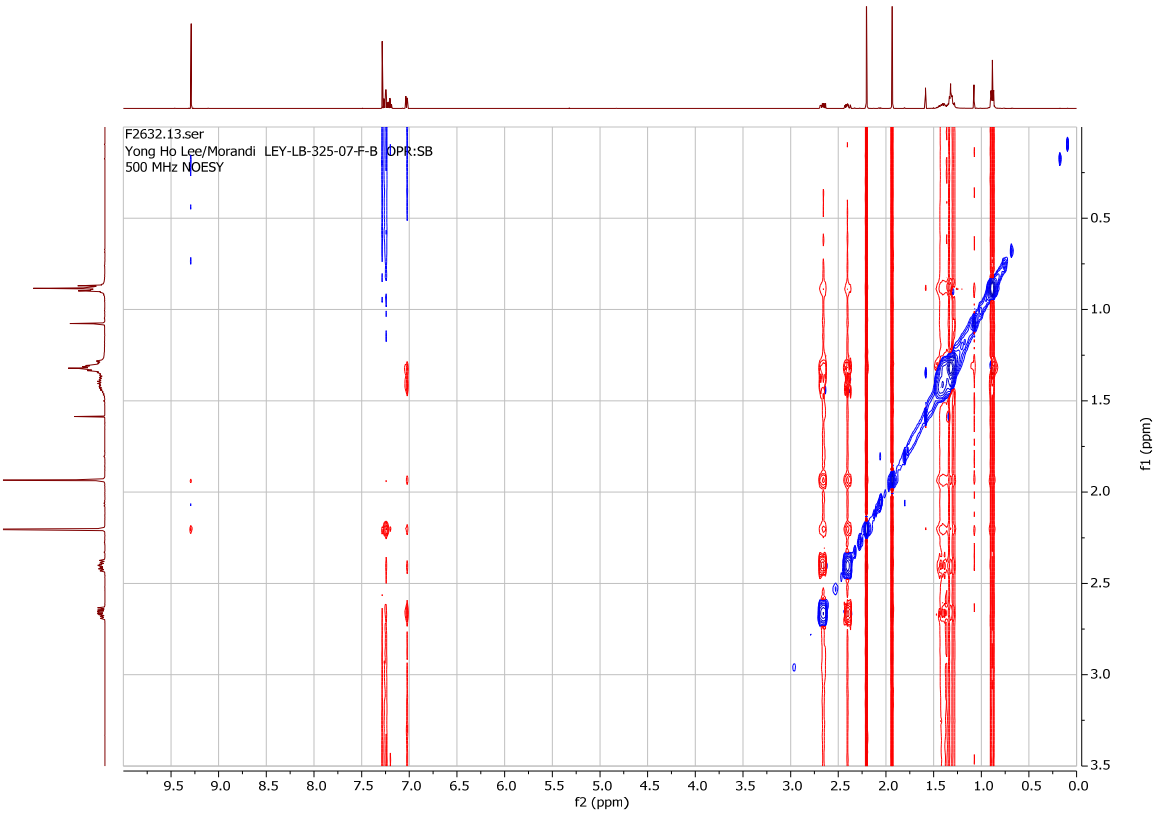
F2632.13.ser
Yong Ho Lee/Morandi LEY-LB-325-07-F-B OPR:SB
500 MHz NOESY
f2 (ppm)
f1 (ppm)

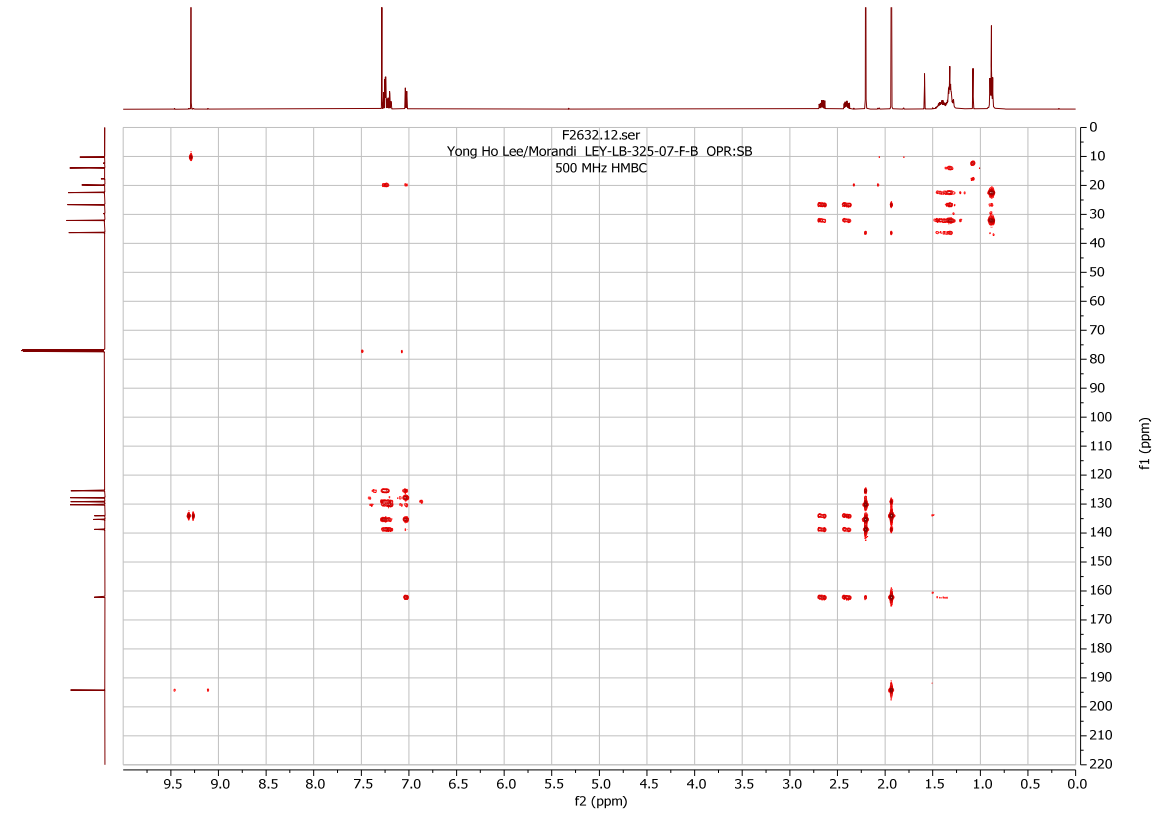
F2632.12.ser
Yong Ho Lee/Morandi LEY-LB-325-07-F-B OPR:SB
500 MHz HMBC
f2 (ppm)
f1 (ppm)

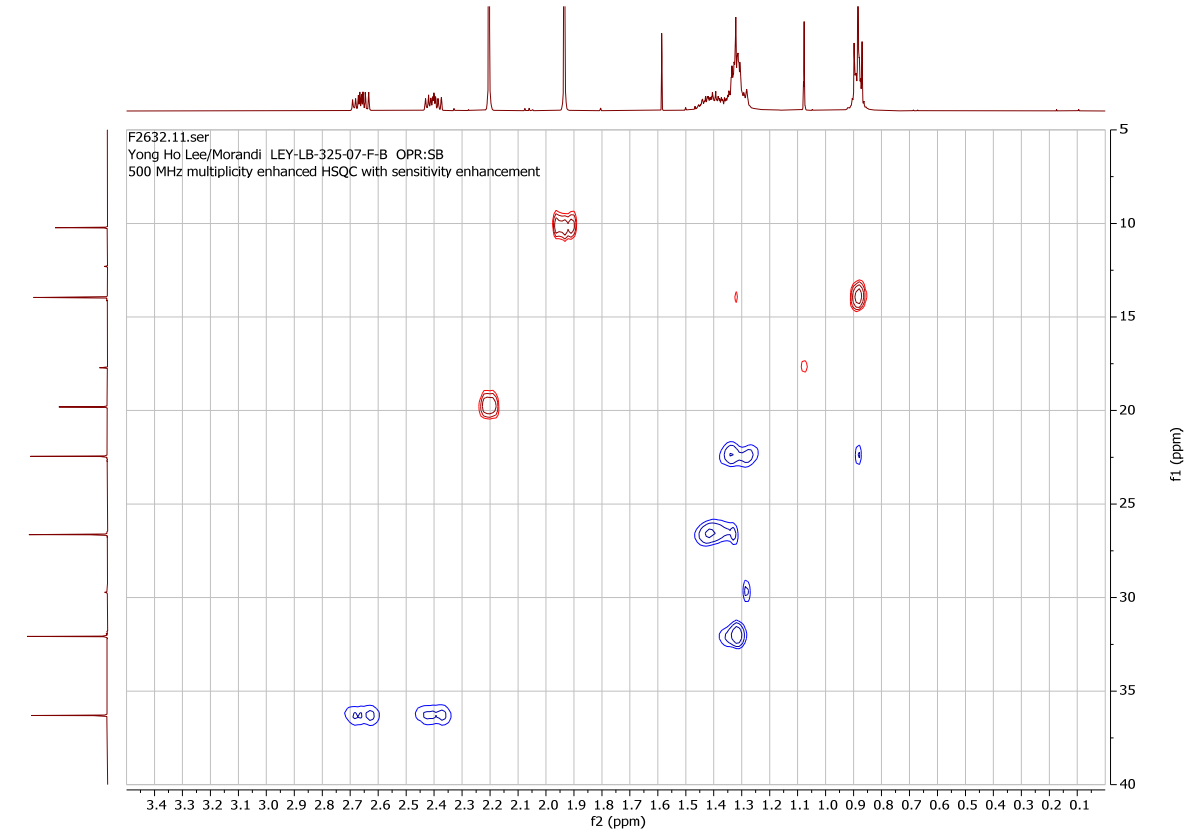
F2632.11.ser
Yong Ho Lee/Morandi LEY-LB-325-07-F-B OPR:SB
500 MHz multiplicity enhanced HSQC with sensitivity enhancement
f1 (ppm)
f2 (ppm)

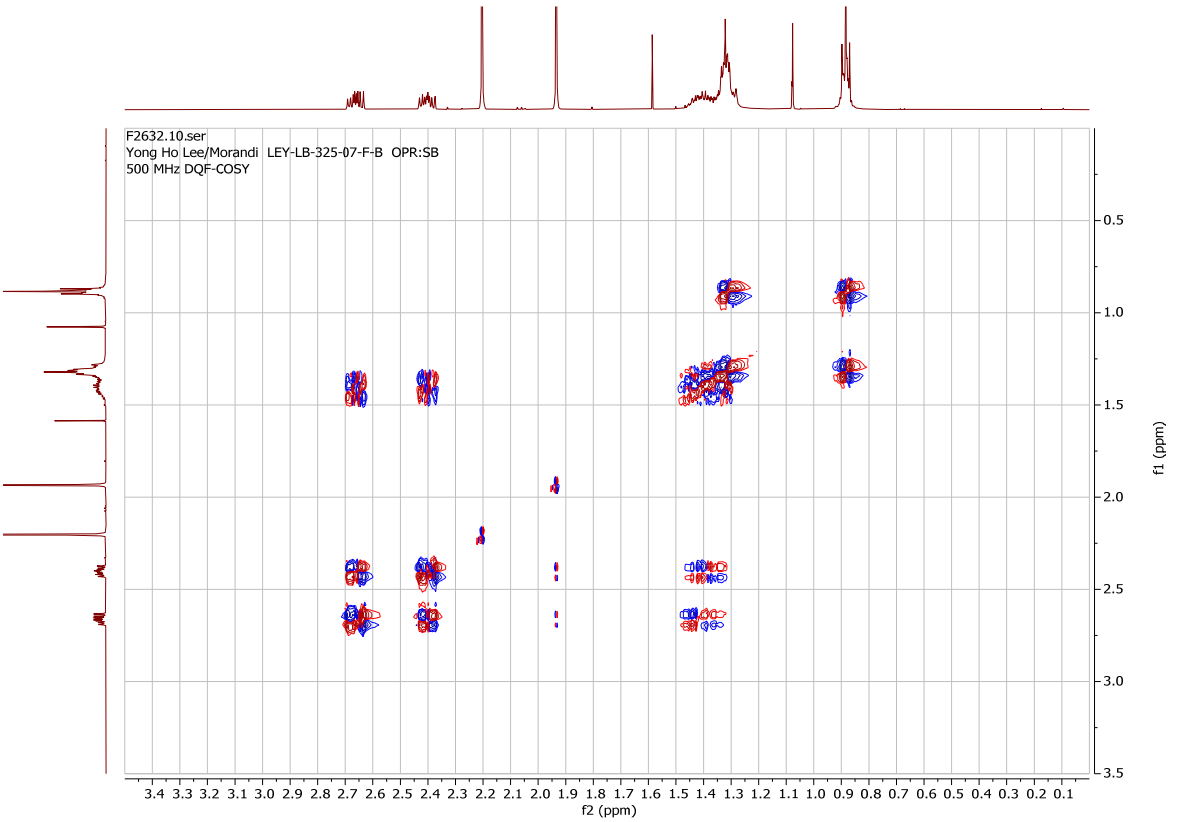
F2632.10.ser
Yong Ho Lee/Morandi LEY-LB-325-07-F-B OPR:SB
500 MHz DQF-COSY
f1 (ppm)
f2 (ppm)

(*Z*)-2-((1,3-dioxoisoindolin-2-yl)methyl)-3-(o-tolyl)but-2-enal, B (**40-β-Ar, major**).

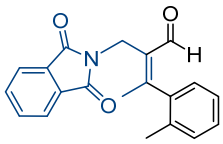

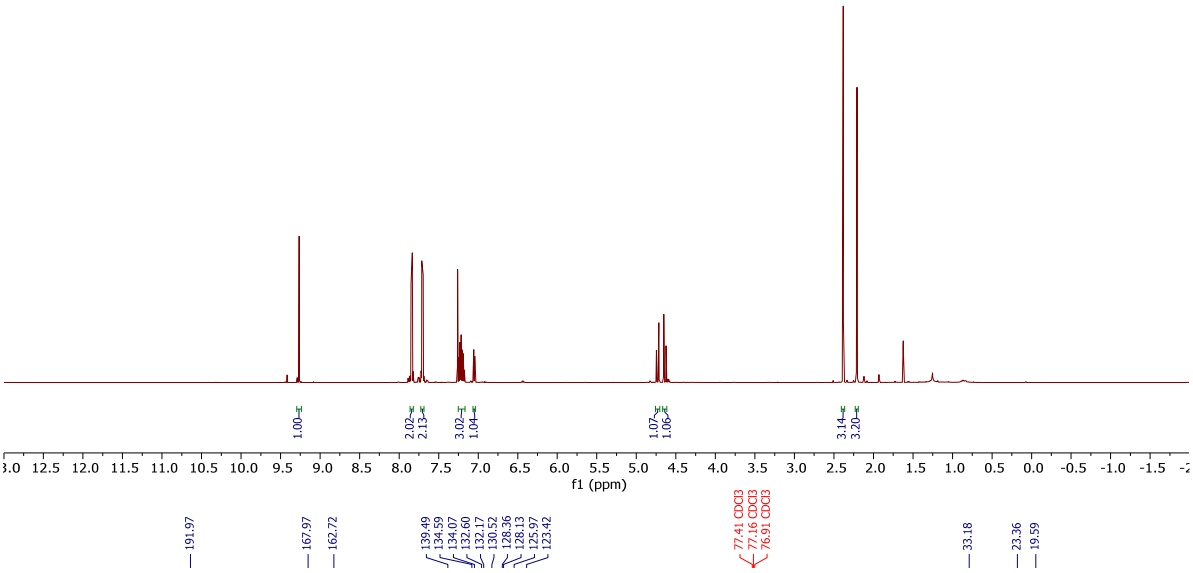

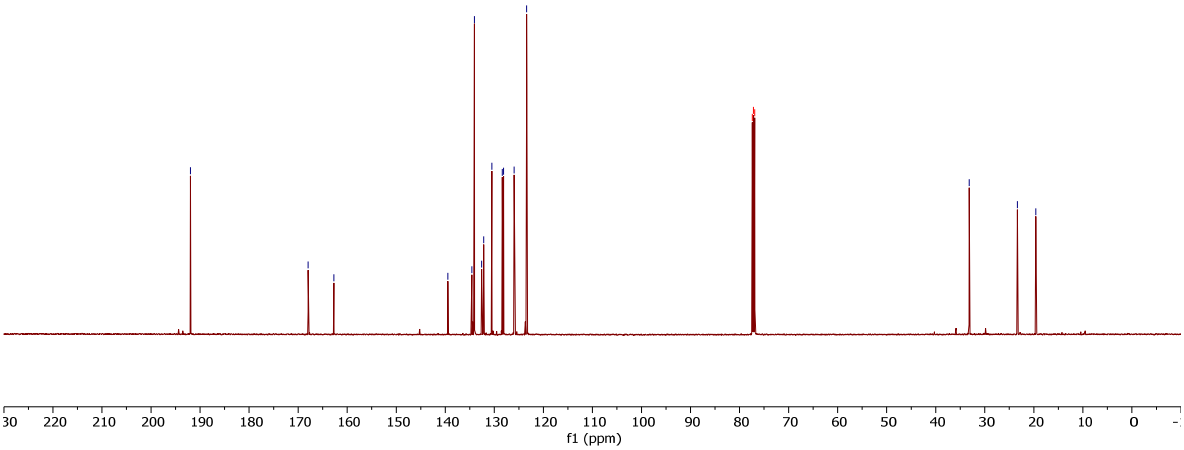

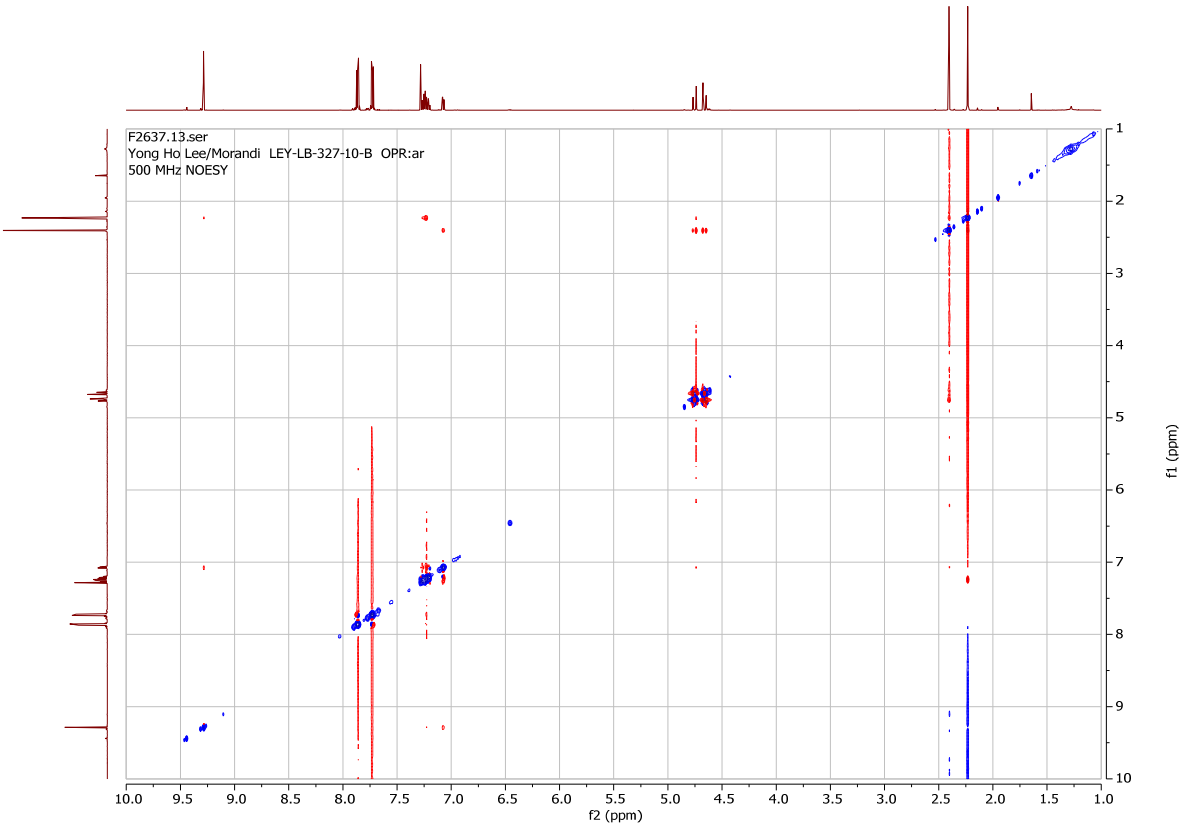
F2637.13.ser
Yong Ho Lee/Morandi LEY-LB-327-10-B OPR:ar
500 MHz NOESY
f2 (ppm)
f1 (ppm)

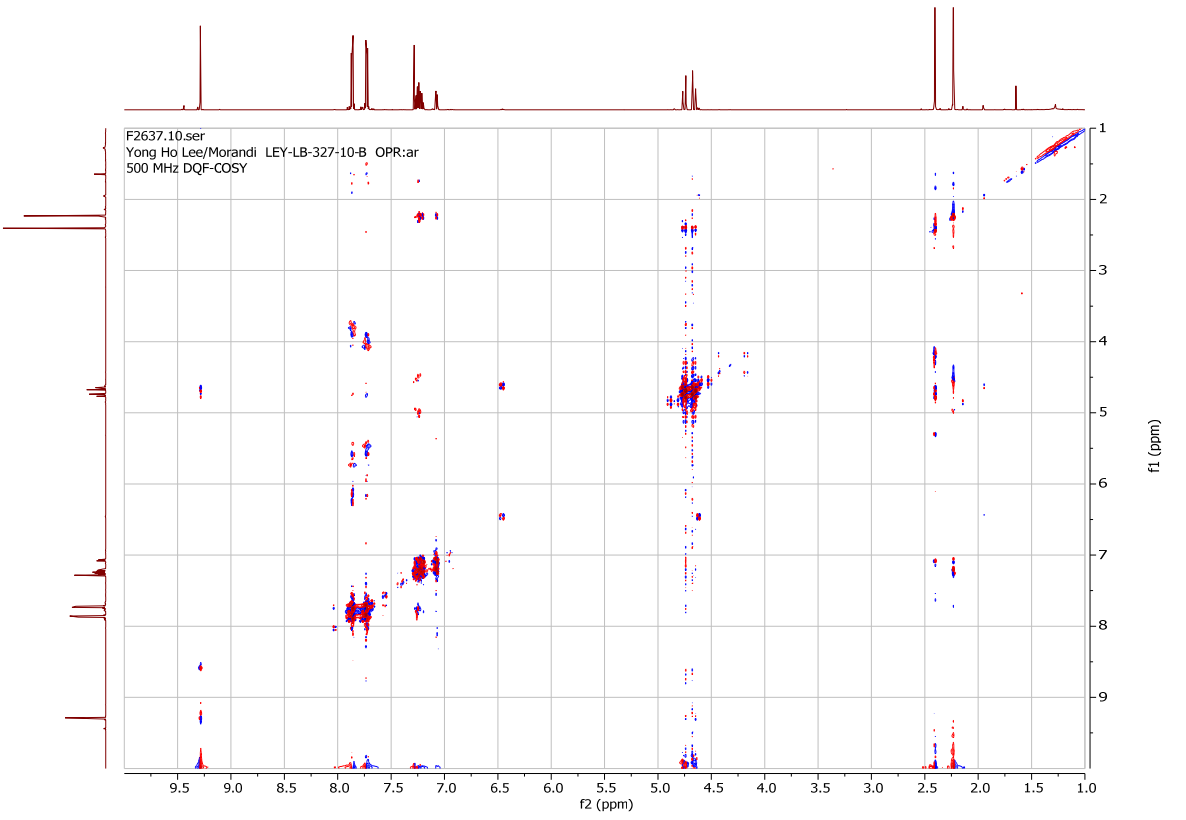
F2637.10.ser
Yong Ho Lee/Morandi LEY-LB-327-10-B OPR:ar
500 MHz DQF-COSY
f2 (ppm)
f1 (ppm)

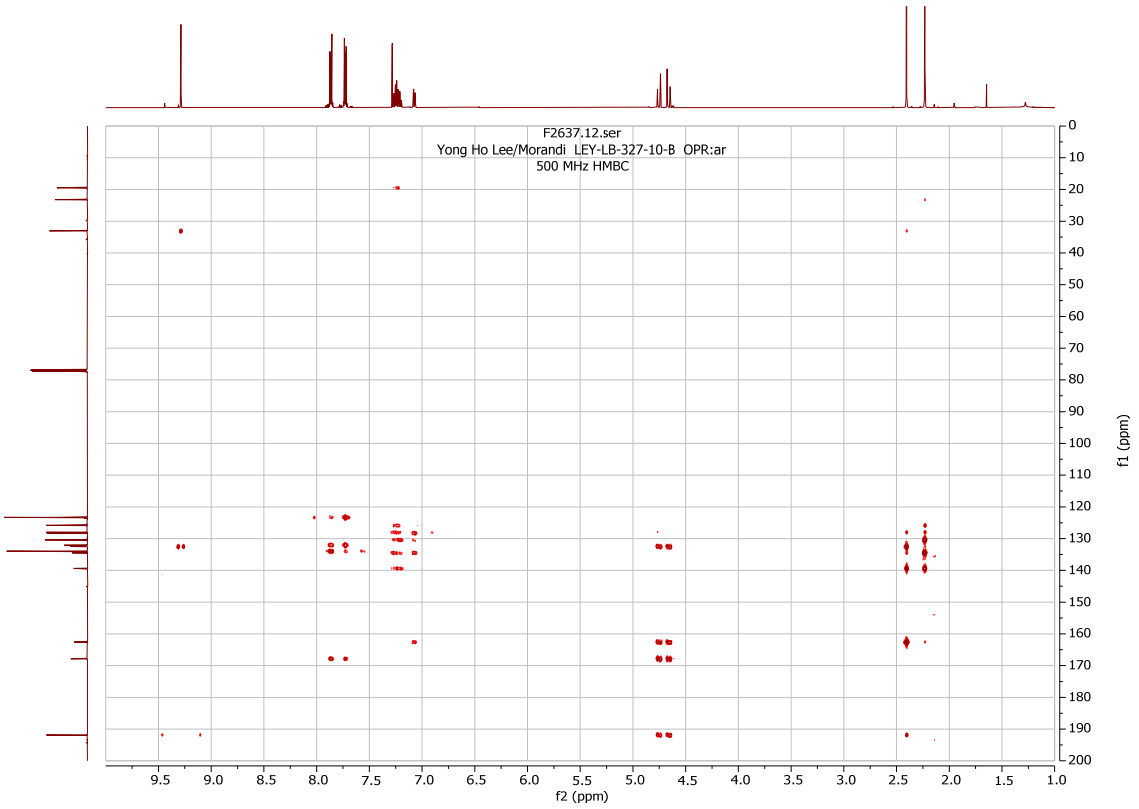
F2637.12.ser
Yong Ho Lee/Morandi LEY-LB-327-10-B OPR:ar
500 MHz HMBC
f2 (ppm)
f1 (ppm)

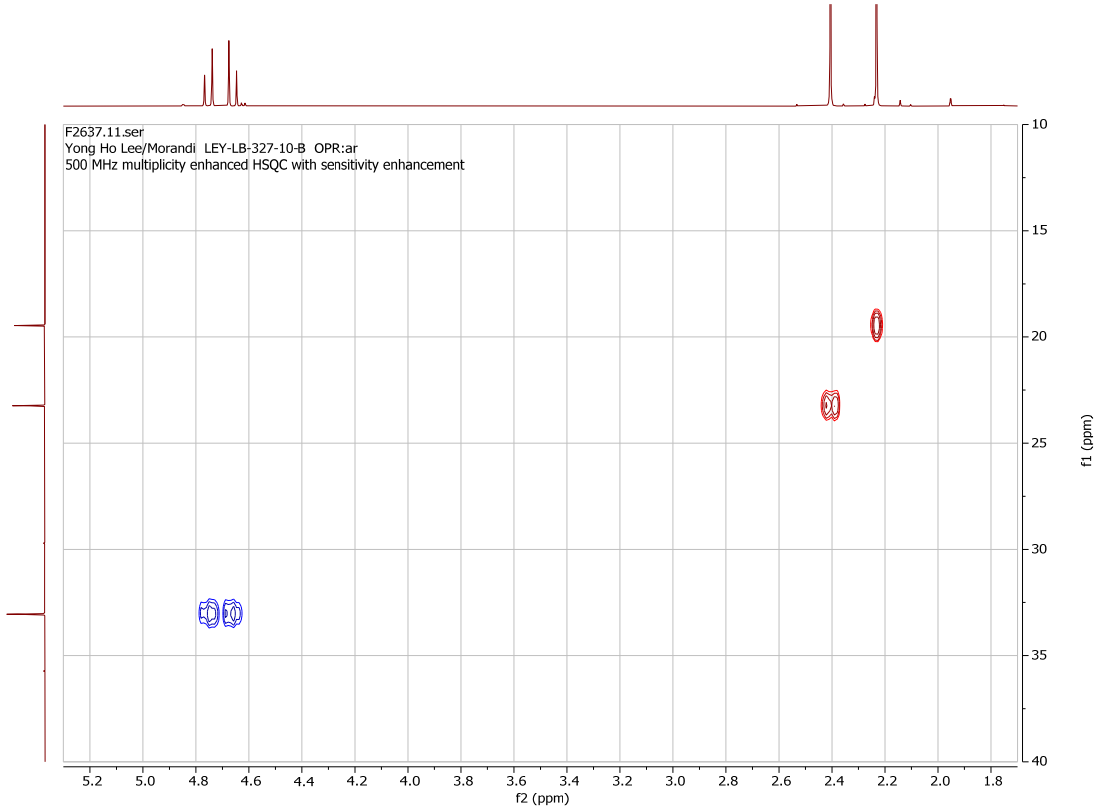
F2637.11.ser
Yong Ho Lee/Morandi LEY-LB-327-10-B OPR:ar
500 MHz multiplicity enhanced HSQC with sensitivity enhancement
f2 (ppm)
f1 (ppm)

(*E*)-4-(1,3-dioxoisoindolin-2-yl)-2-methyl-3-(*o*-tolyl)but-2-enal, A (**40-α-Ar, minor**).

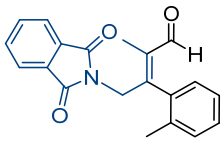

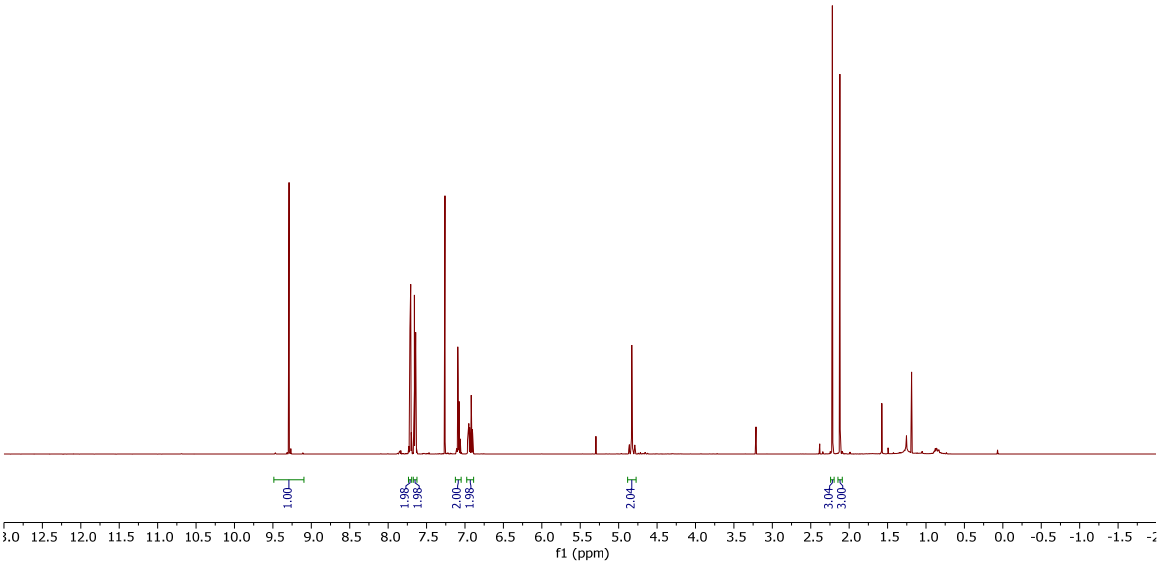

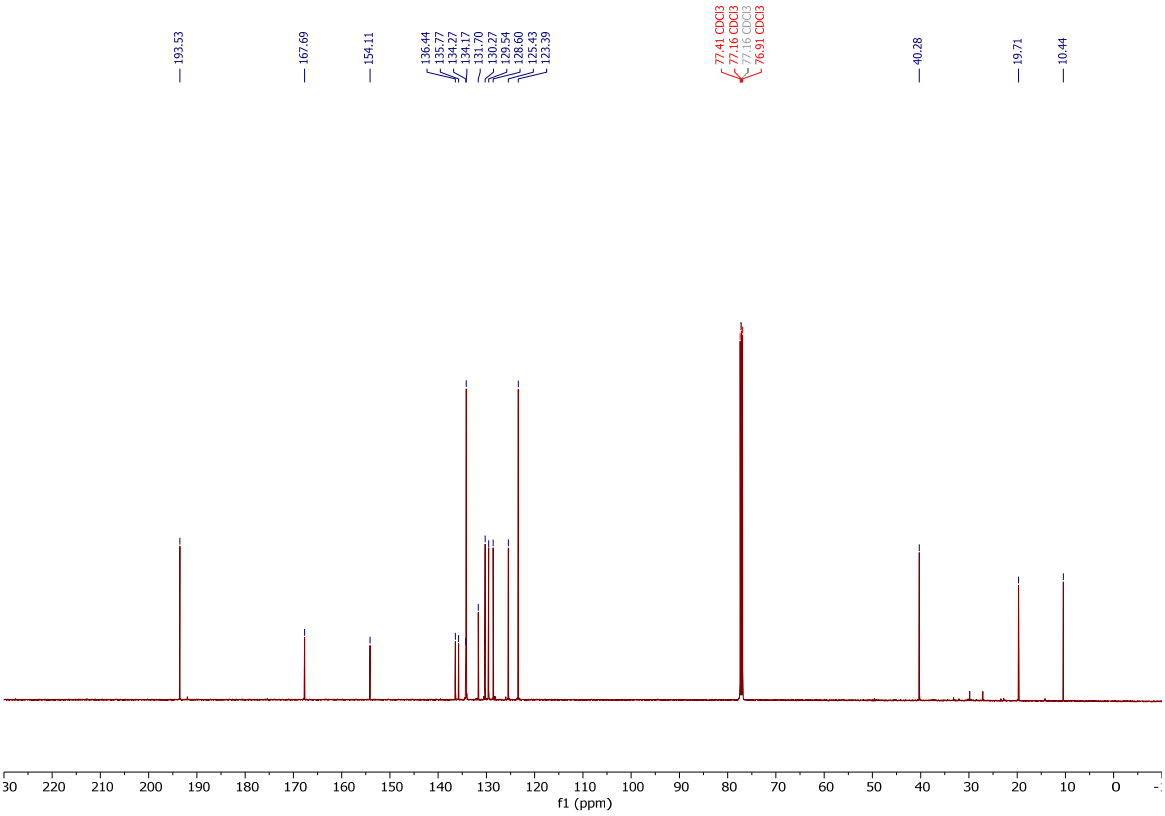

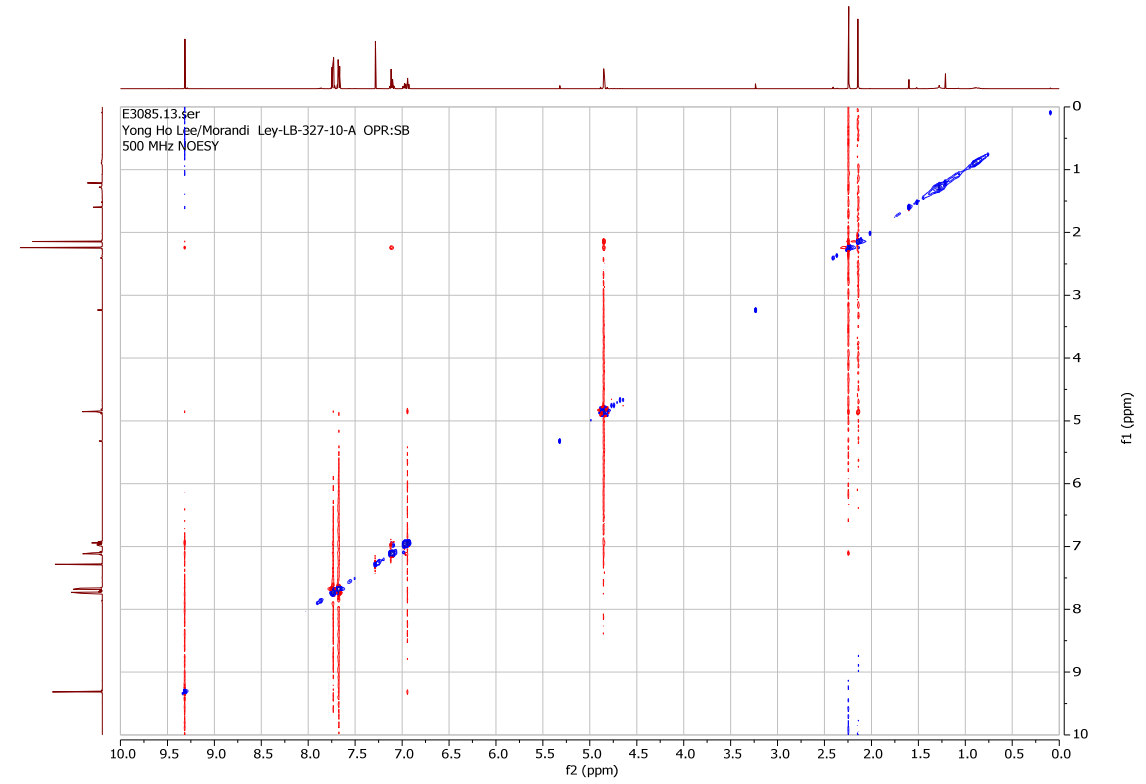
E3085.13.ser
Yong Ho Lee/Morandi Ley-LB-327-10-A OPR:SB
500 MHz NOESY
f2 (ppm)
f1 (ppm)

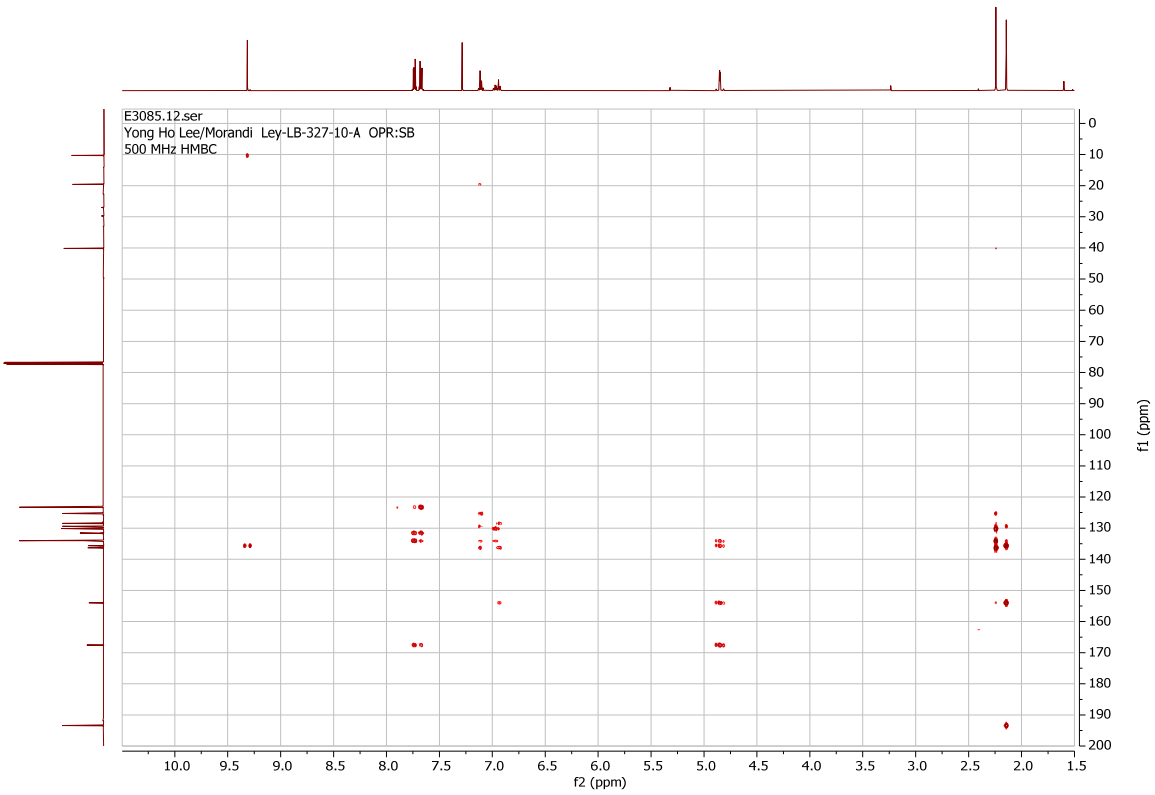
E3085.12.ser
Yong Ho Lee/Morandi Ley-LB-327-10-A OPR:SB
500 MHz HMBC
f2 (ppm)
f1 (ppm)

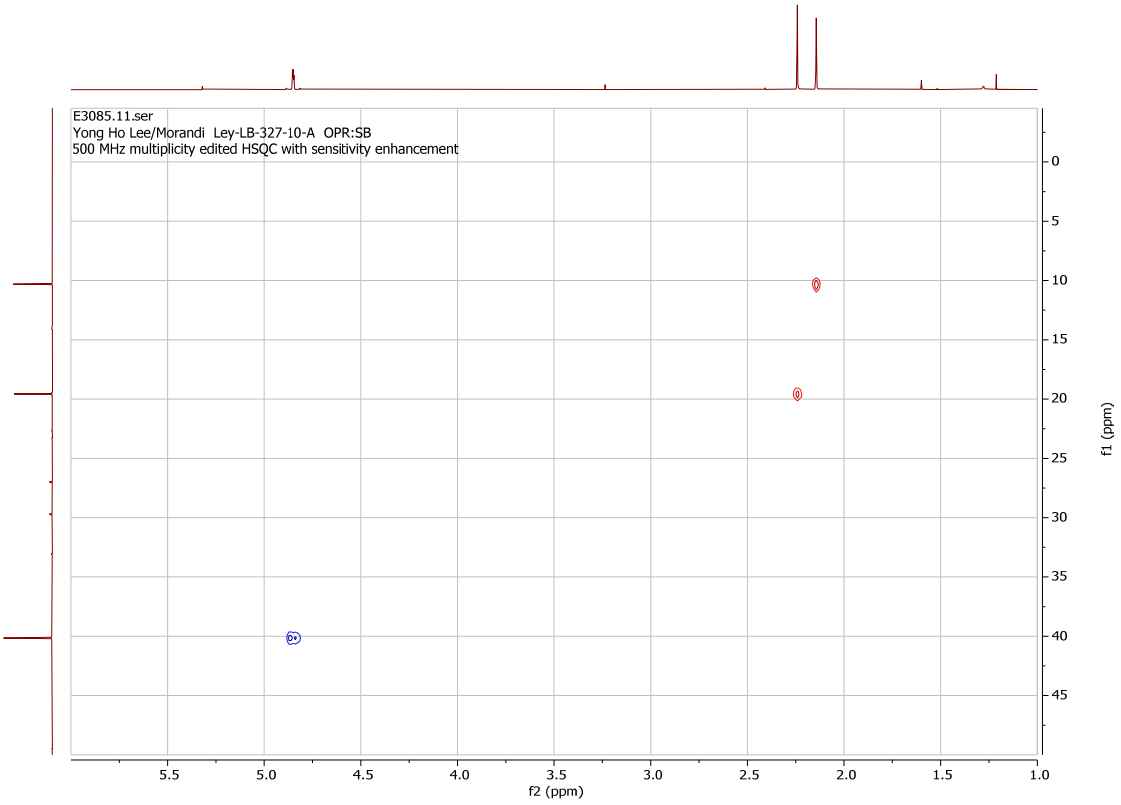
E3085.11.ser
Yong Ho Lee/Morandi Ley-LB-327-10-A OPR:SB
500 MHz multiplicity edited HSQC with sensitivity enhancement
f2 (ppm)
f1 (ppm)

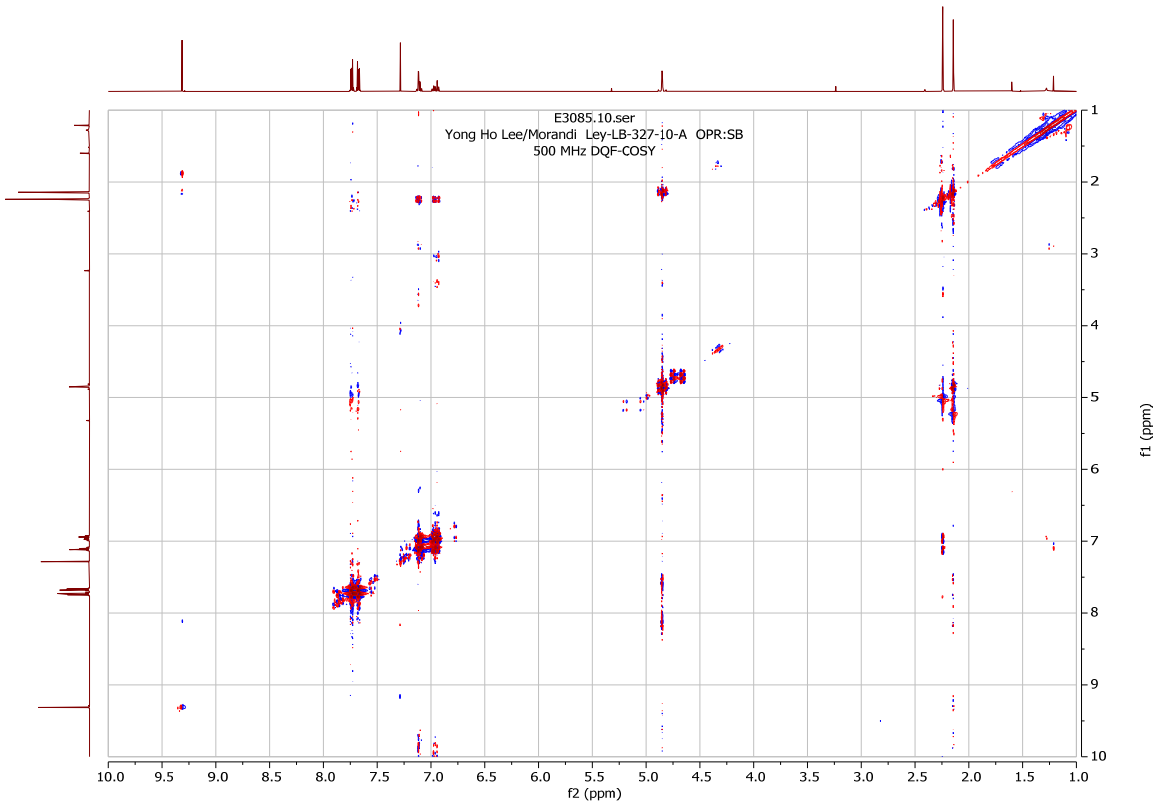
E3085.10.ser
Yong Ho Lee/Morandi Ley-LB-327-10-A OPR:SB
500 MHz DQF-COSY
f2 (ppm)
f1 (ppm)

(*Z*)-2-formyl-3-(*o*-tolyl)hept-2-en-1-yl benzoate, B (**41-β-Ar, major**).

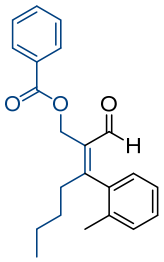

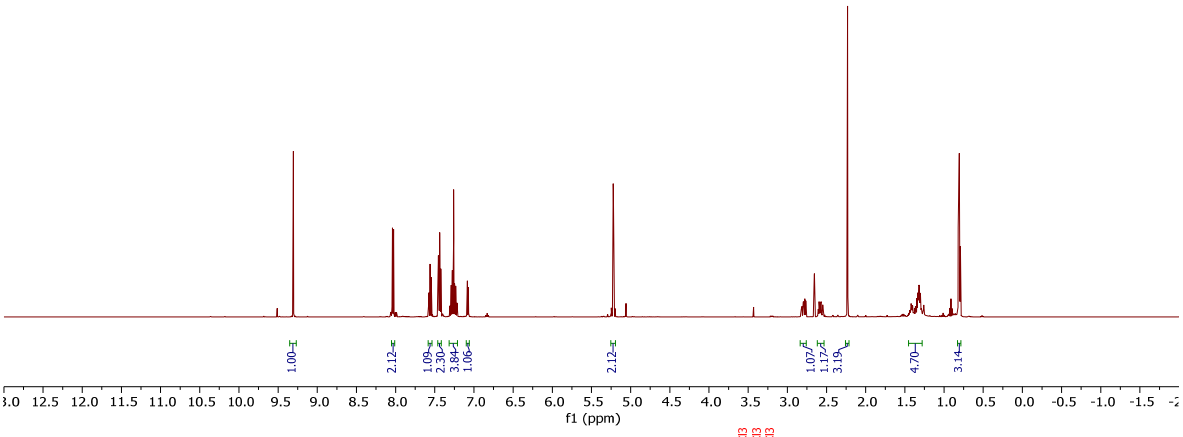

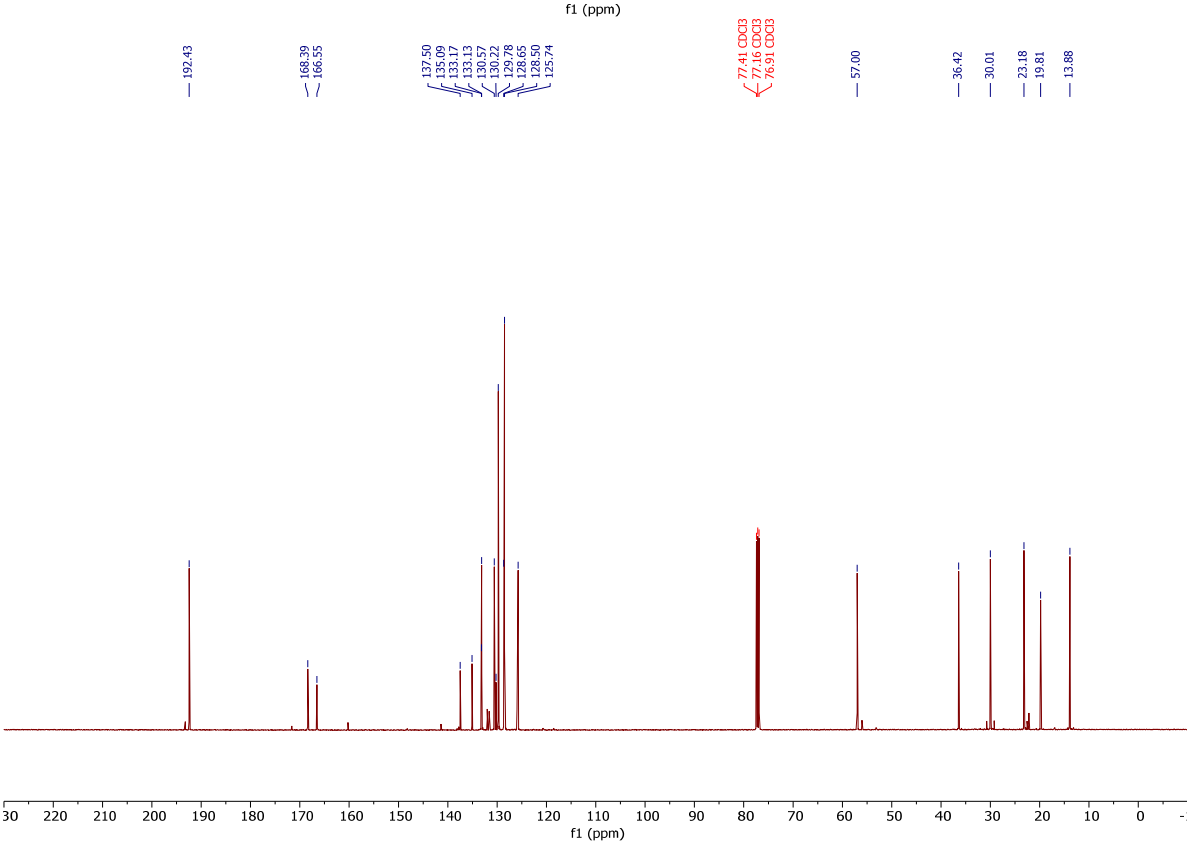

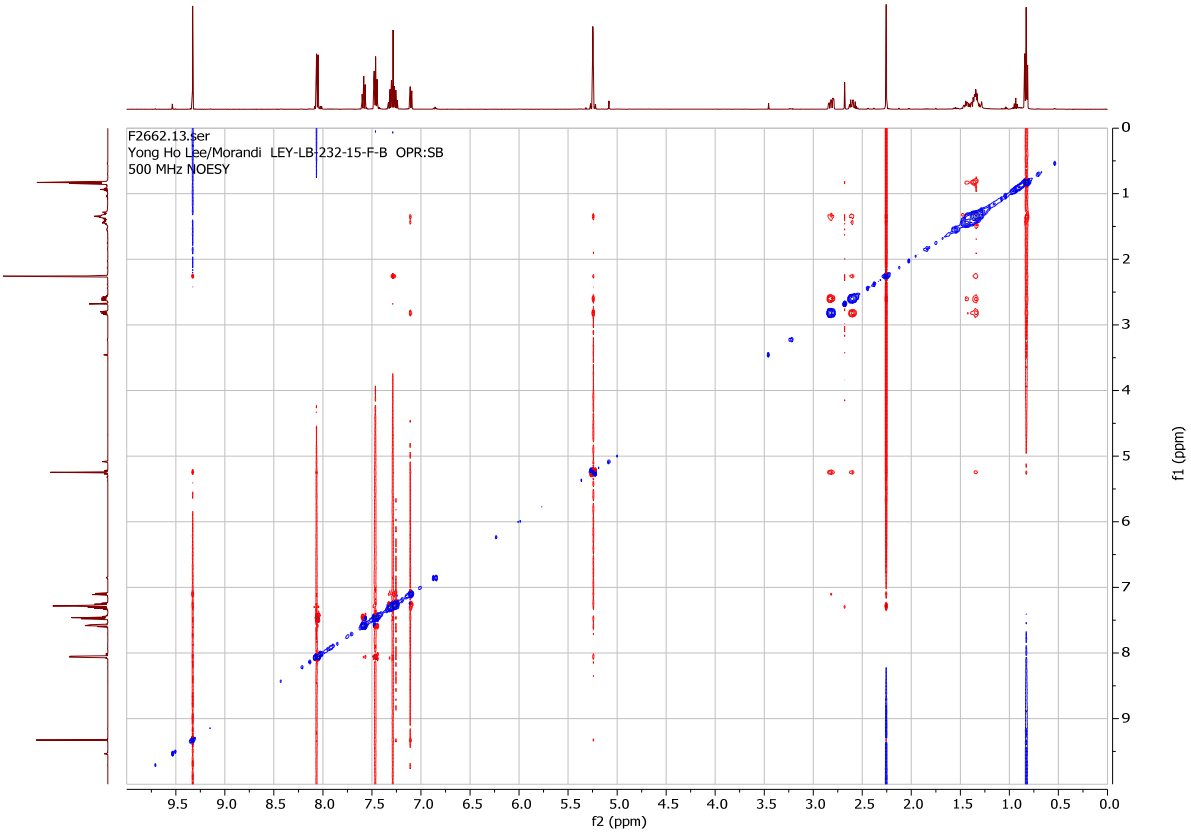
F2662.13.ser
Yong Ho Lee/Morandi LEY-LB-232-15-F-B OPR:SB
500 MHz NOESY
f2 (ppm)
f1 (ppm)

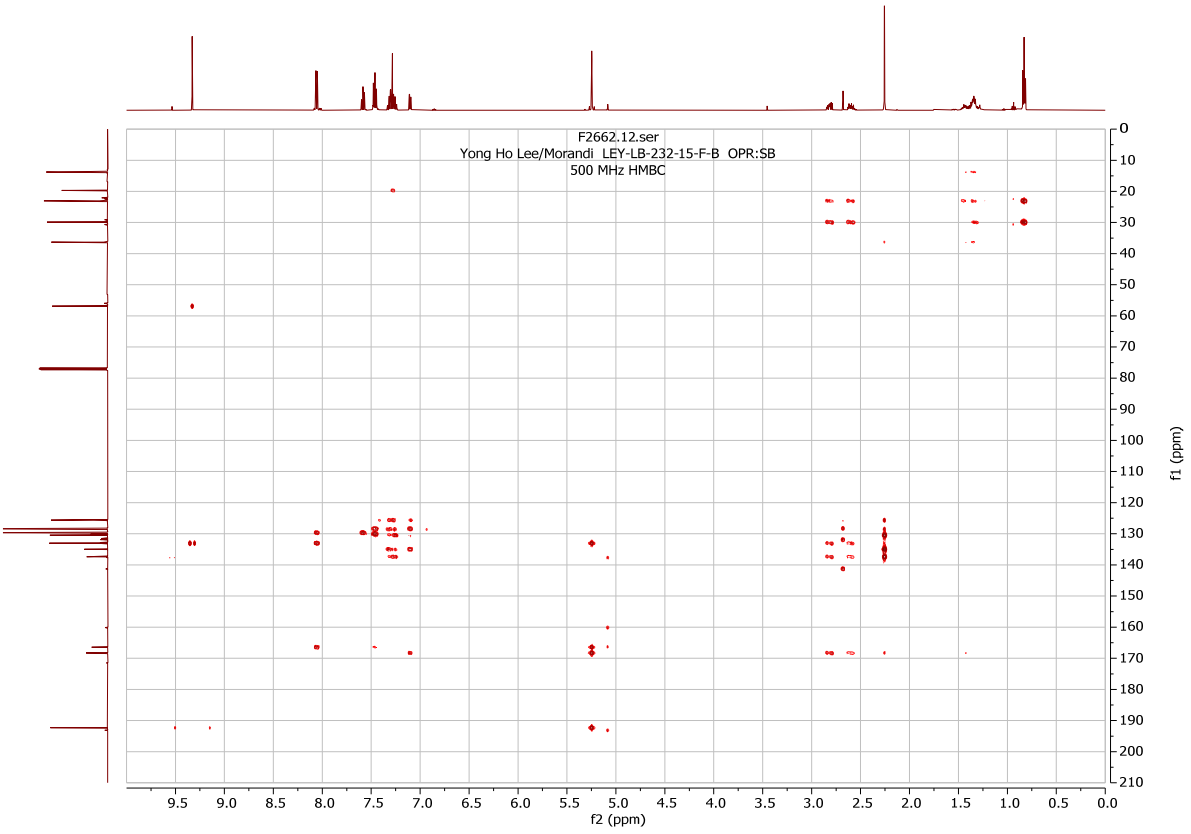
F2662.12.ser
Yong Ho Lee/Morandi LEY-LB-232-15-F-B OPR:SB
500 MHz HMBC
f2 (ppm)
f1 (ppm)

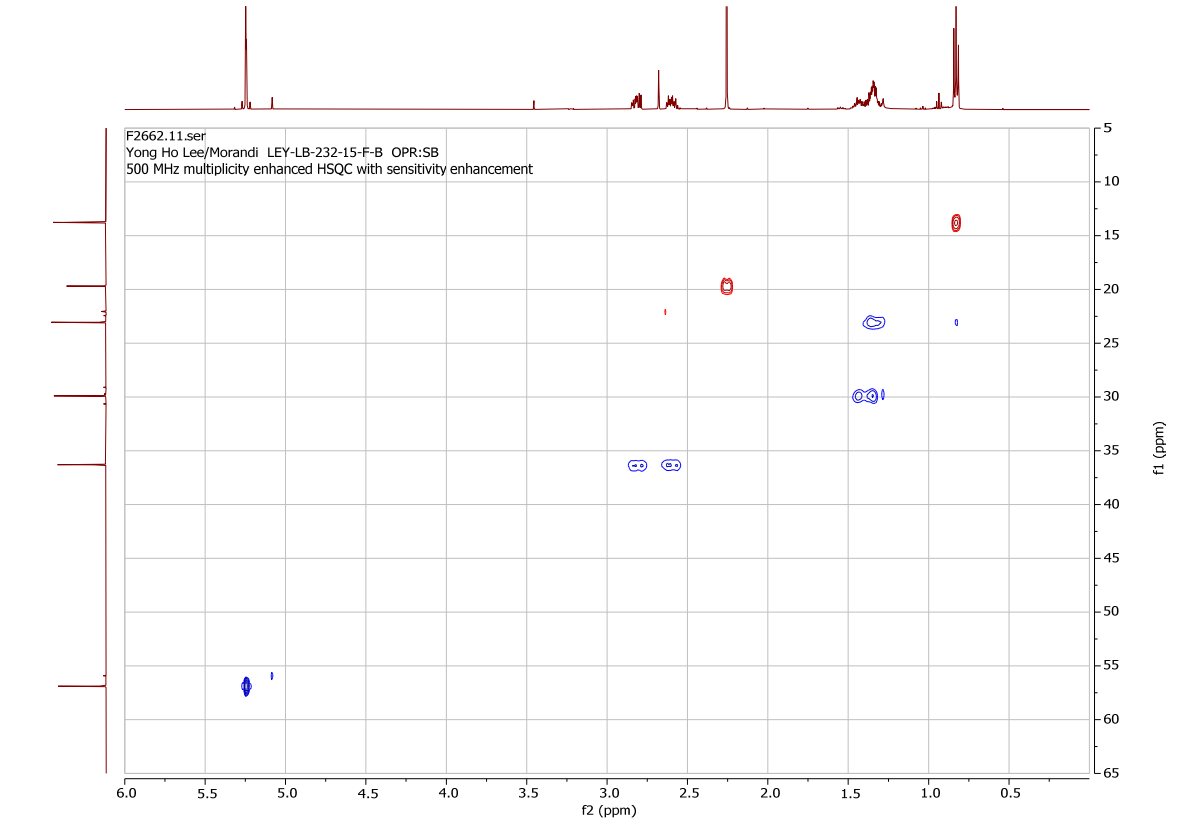
F2662.11.ser
Yong Ho Lee/Morandi LEY-LB-232-15-F-B OPR:SB
500 MHz multiplicity enhanced HSQC with sensitivity enhancement
f2 (ppm)
f1 (ppm)

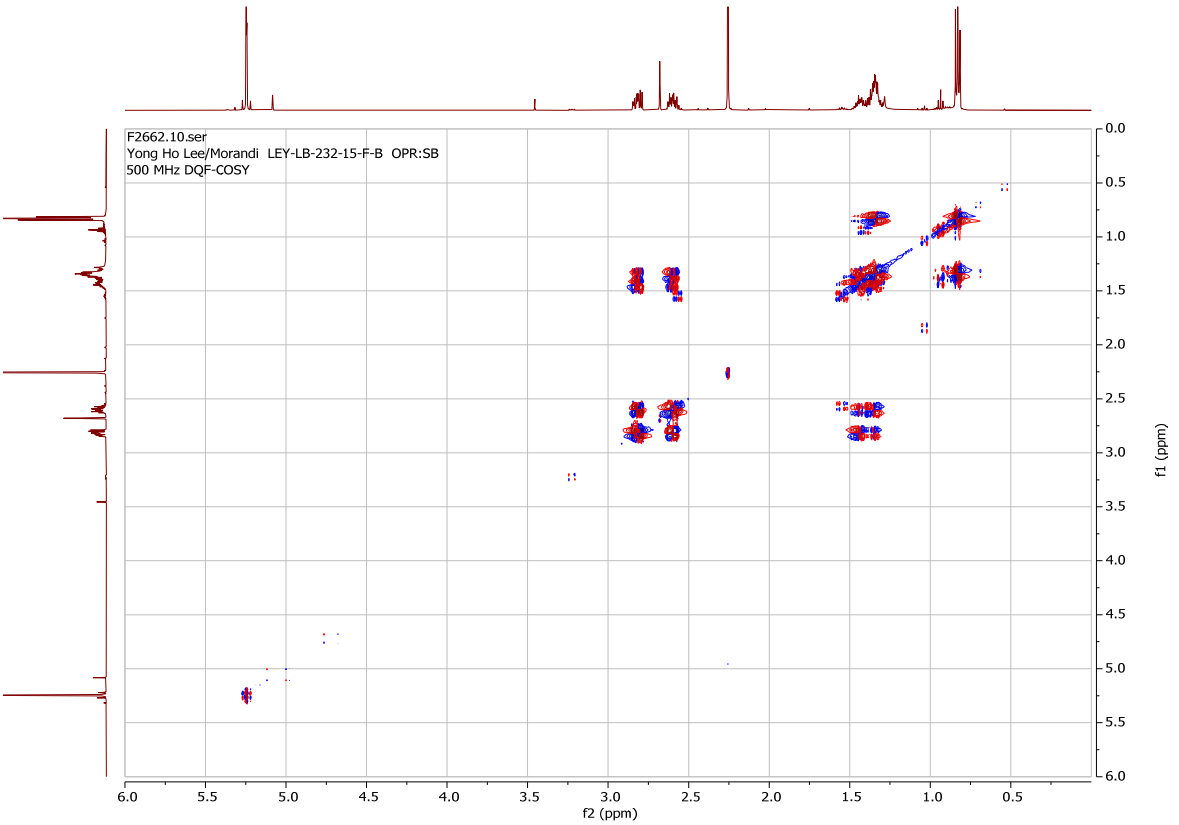
F2662.10.ser
Yong Ho Lee/Morandi LEY-LB-232-15-F-B OPR:SB
500 MHz DQF-COSY
f2 (ppm)
f1 (ppm)

(*E*)-3-formyl-2-(*o*-tolyl)hept-2-en-1-yl benzoate, A (**41-α-Ar, minor**).

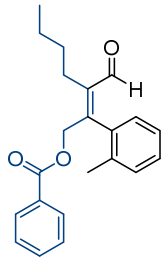

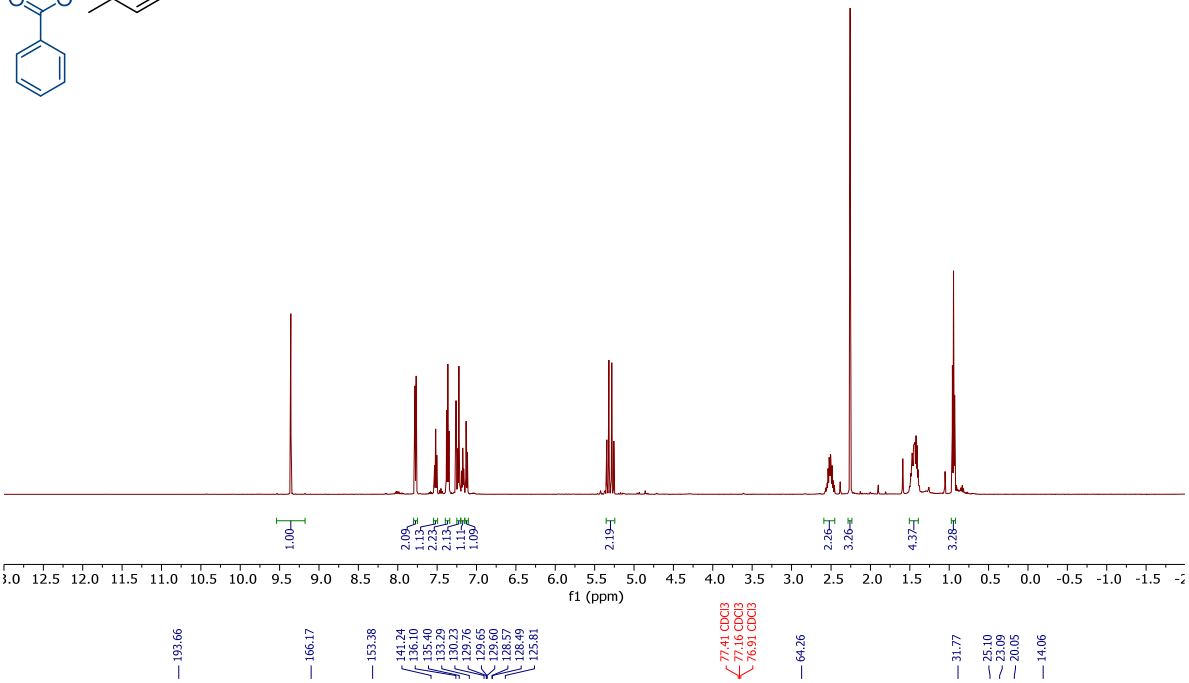

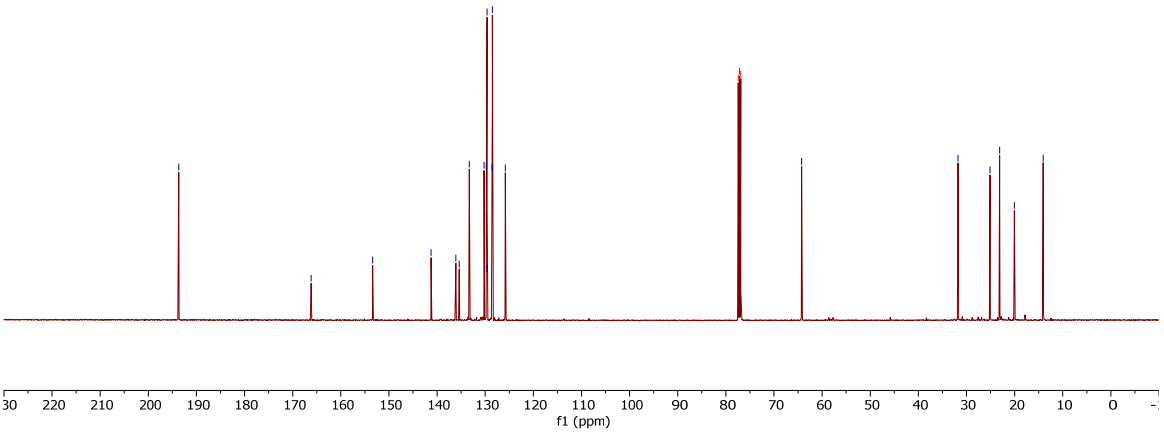

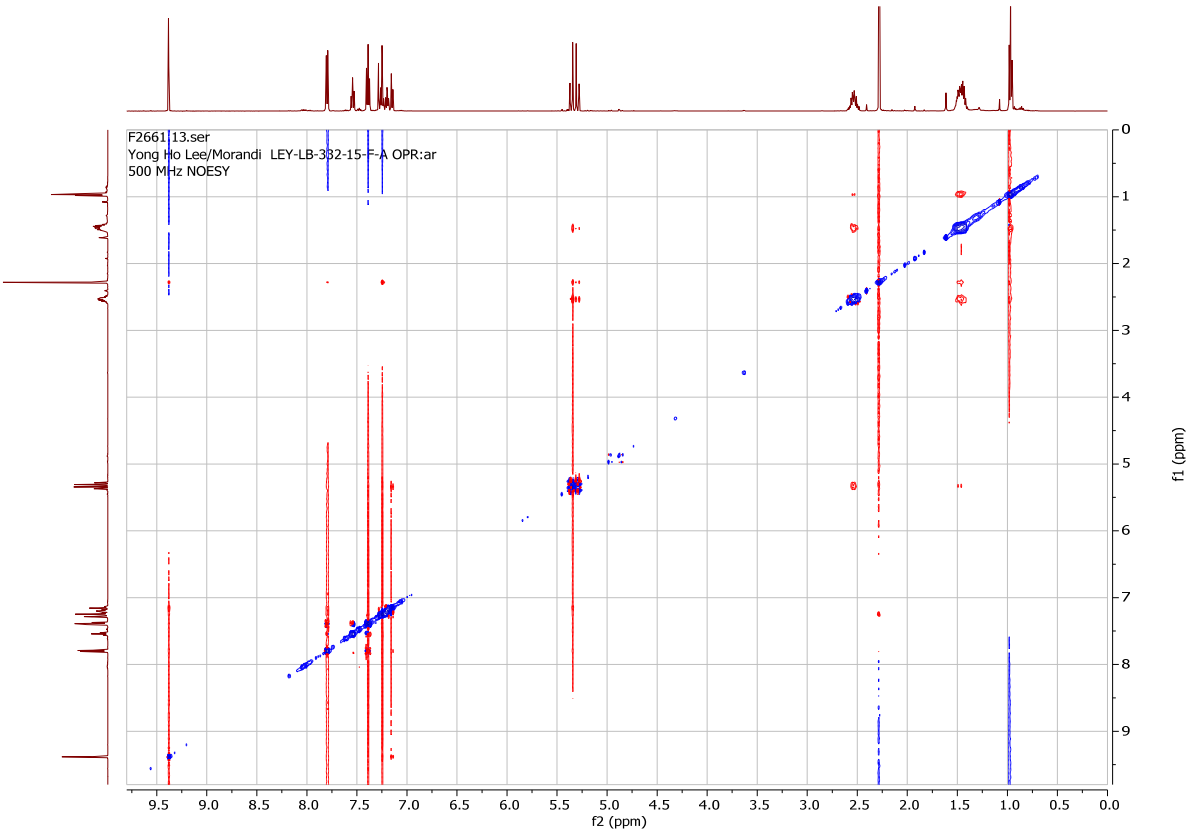
F2661.13.ser
Yong Ho Lee/Morandi LEY-LB-332-15-F-A OPR:ar
500 MHz NOESY
f2 (ppm)
f1 (ppm)

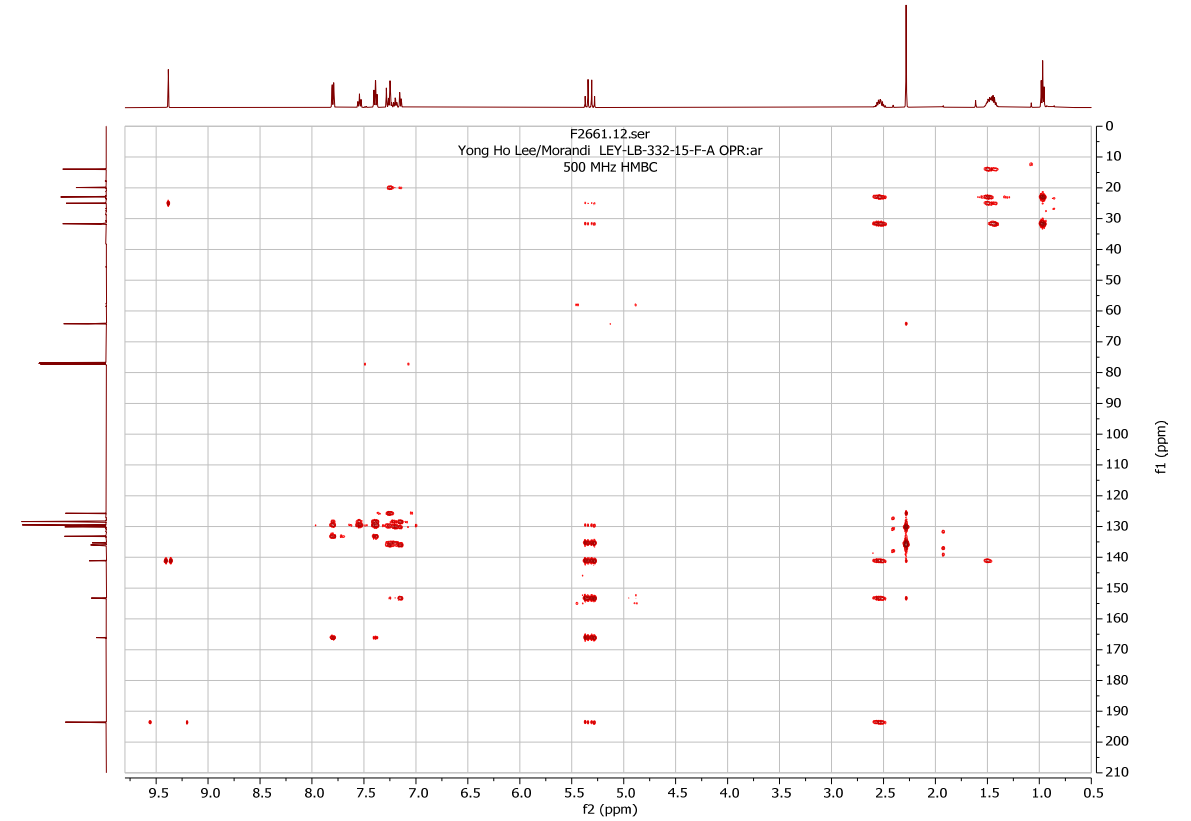
F2661.12.ser
Yong Ho Lee/Morandi LEY-LB-332-15-F-A OPR:ar
500 MHz HMBC
f2 (ppm)
f1 (ppm)

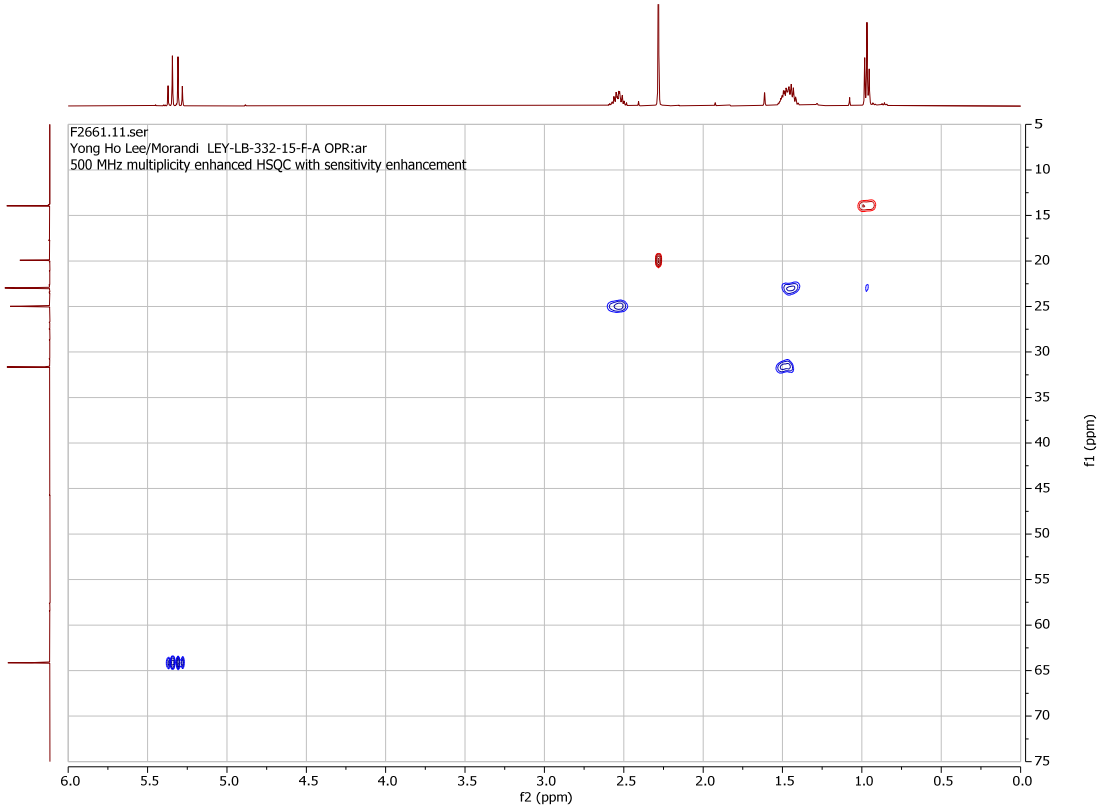
F2661.11.ser
Yong Ho Lee/Morandi LEY-LB-332-15-F-A OPR:ar
500 MHz multiplicity enhanced HSQC with sensitivity enhancement
f2 (ppm)
f1 (ppm)

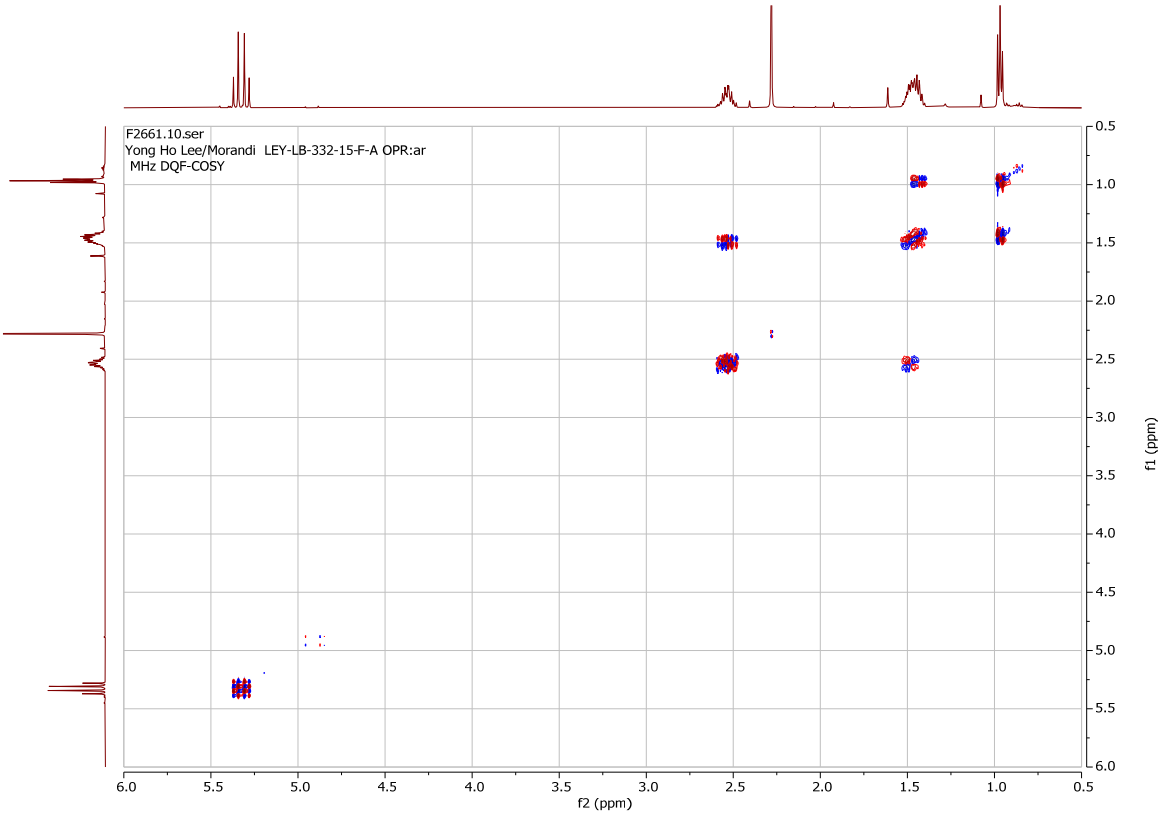
F2661.10.ser
Yong Ho Lee/Morandi LEY-LB-332-15-F-A OPR:ar
MHz DQF-COSY
f2 (ppm)
f1 (ppm)

(*Z*)-3-formyl-4-mesityloct-3-en-1-yl benzoate, B (**42-β-Ar, major**).

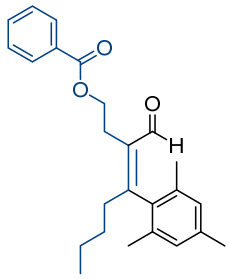

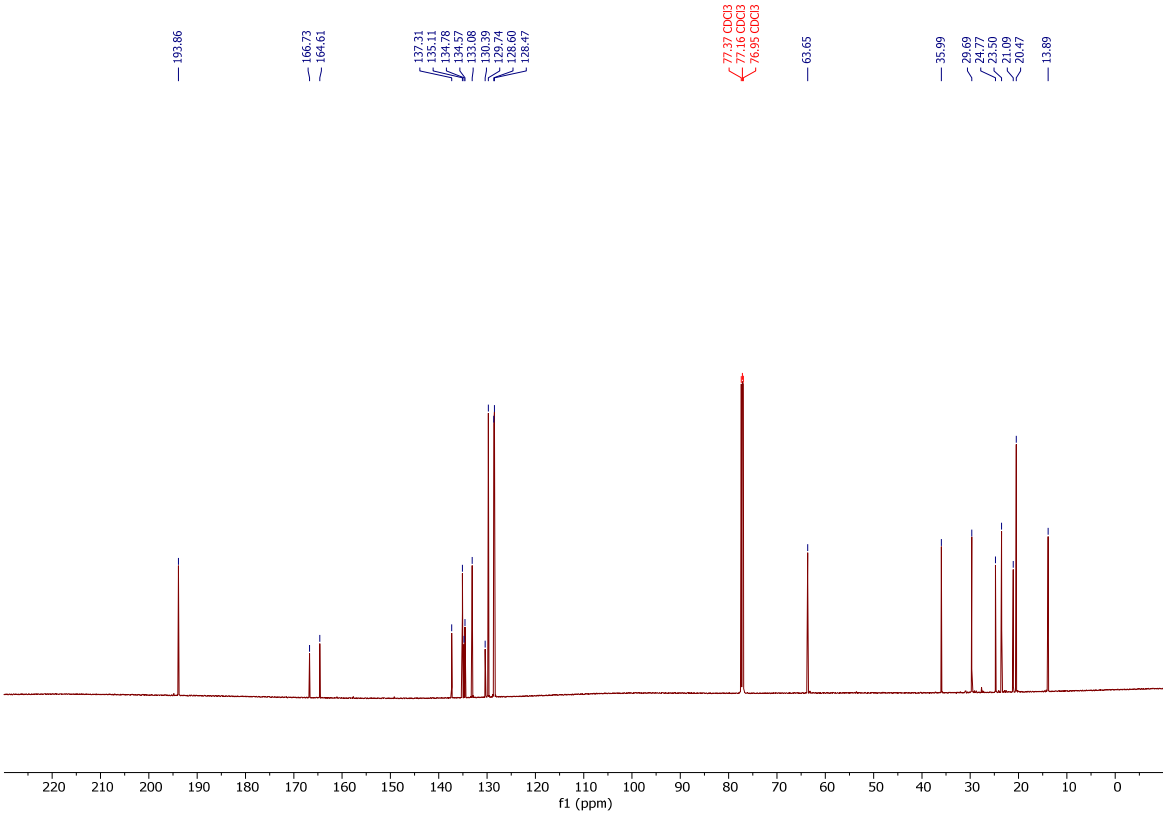

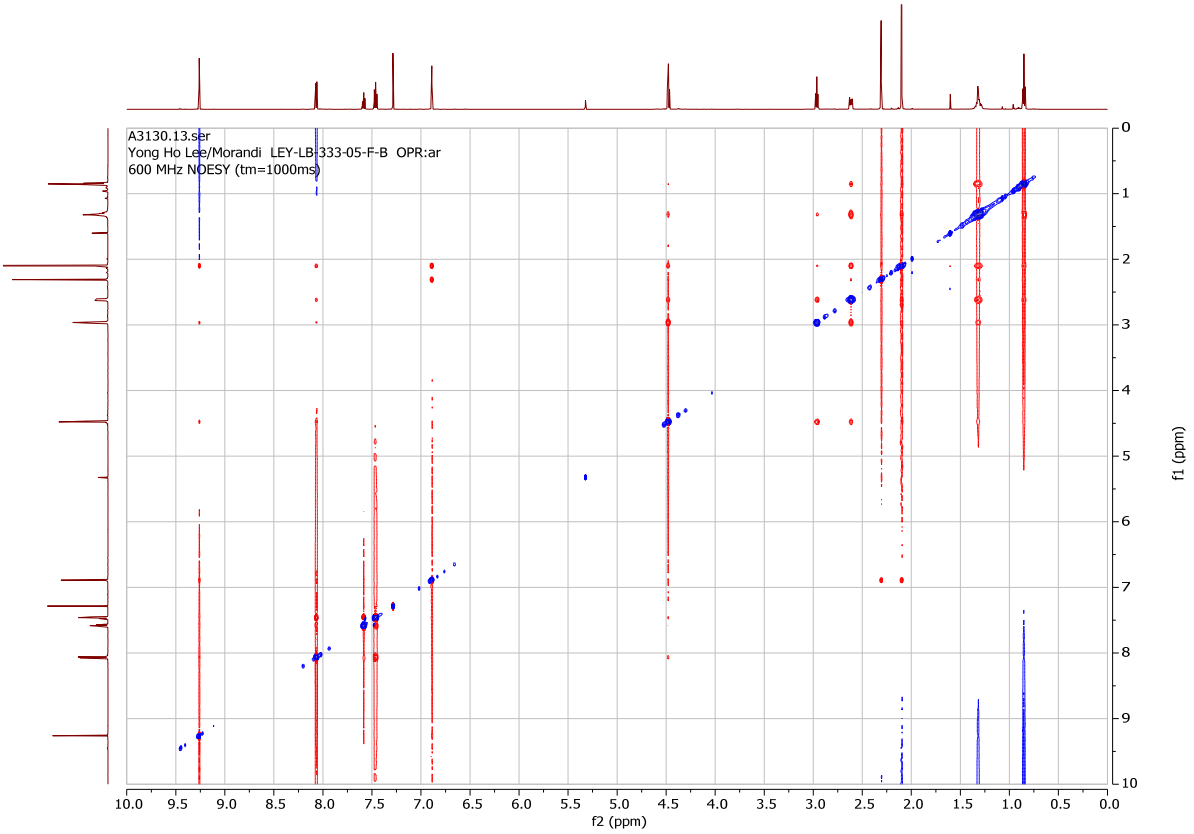
A3130.13.ser
Yong Ho Lee/Morandi LEY-LB-333-05-F-B OPR:ar
600 MHz NOESY (tm=1000ms)
f2 (ppm)
f1 (ppm)

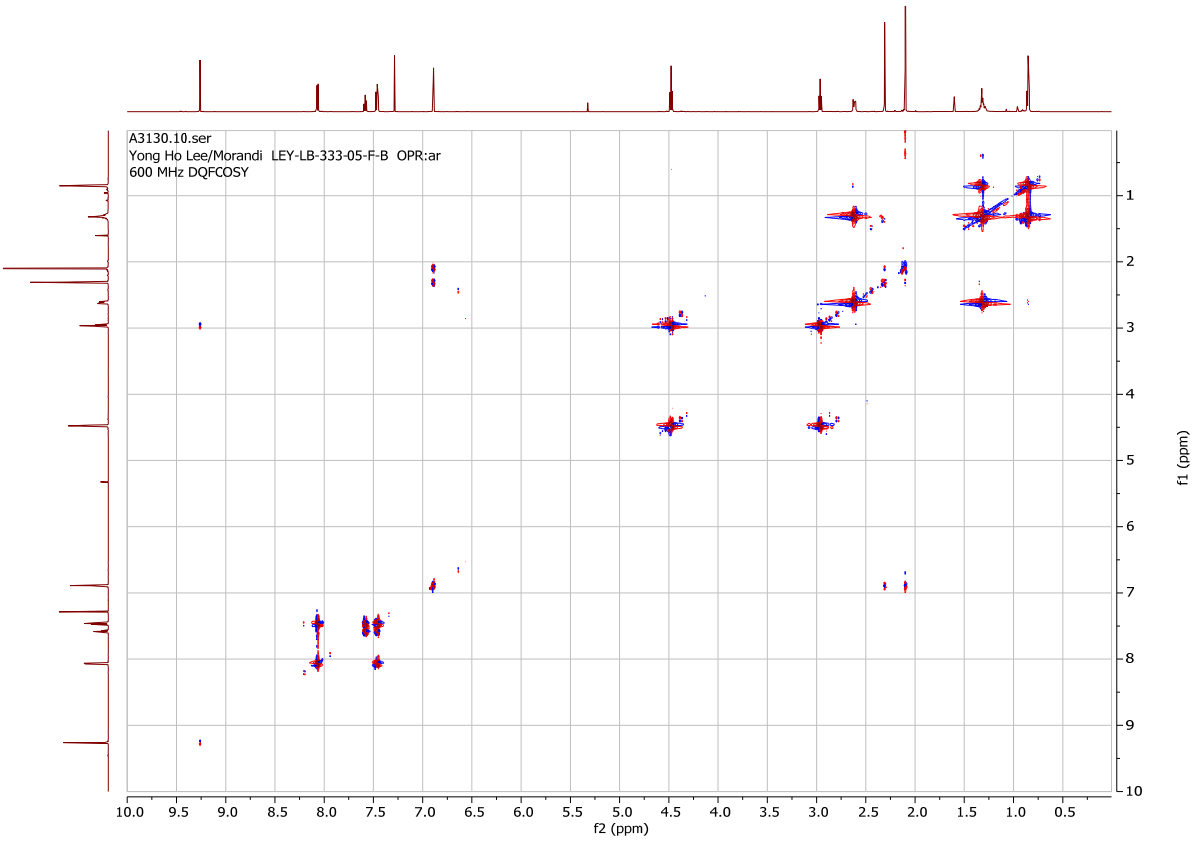
A3130.10.ser
Yong Ho Lee/Morandi LEY-LB-333-05-F-B OPR:ar
600 MHz DQFCOSY
f2 (ppm)
f1 (ppm)

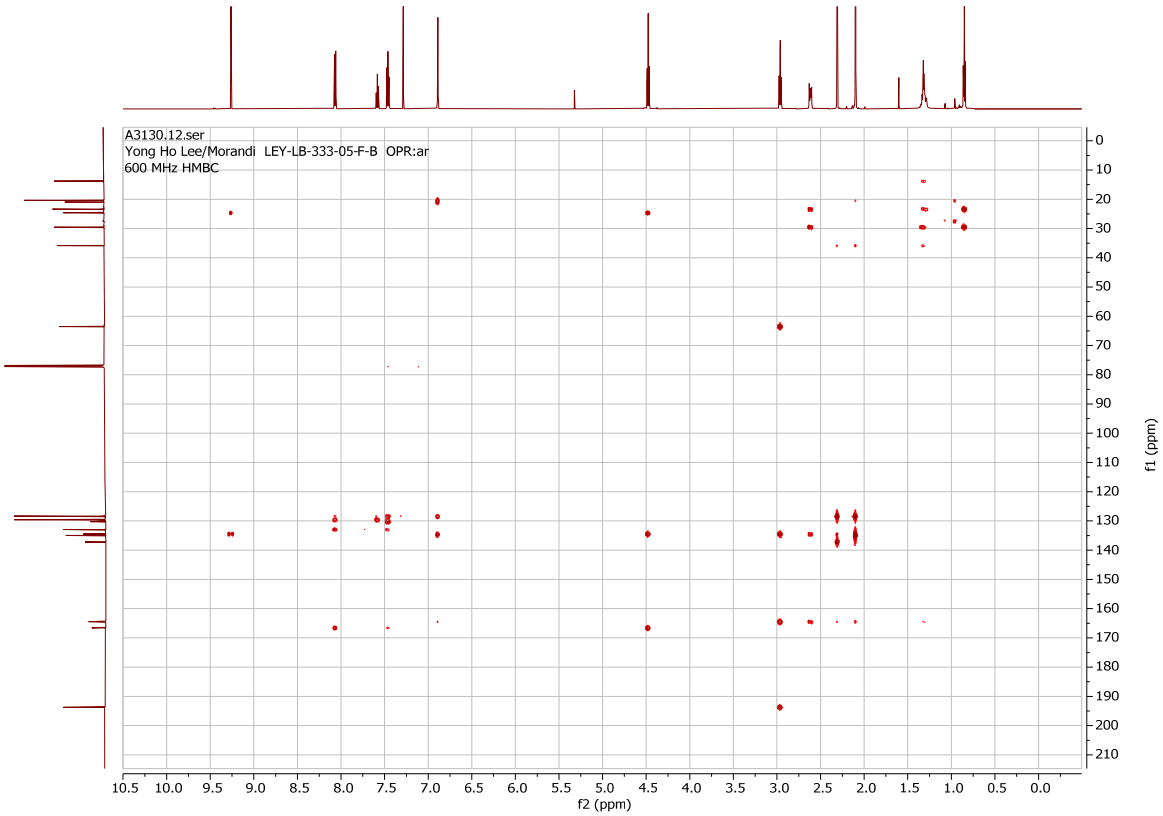
A3130.12.ser
Yong Ho Lee/Morandi LEY-LB-333-05-F-B OPR:ar
600 MHz HMBC
f2 (ppm)
f1 (ppm)

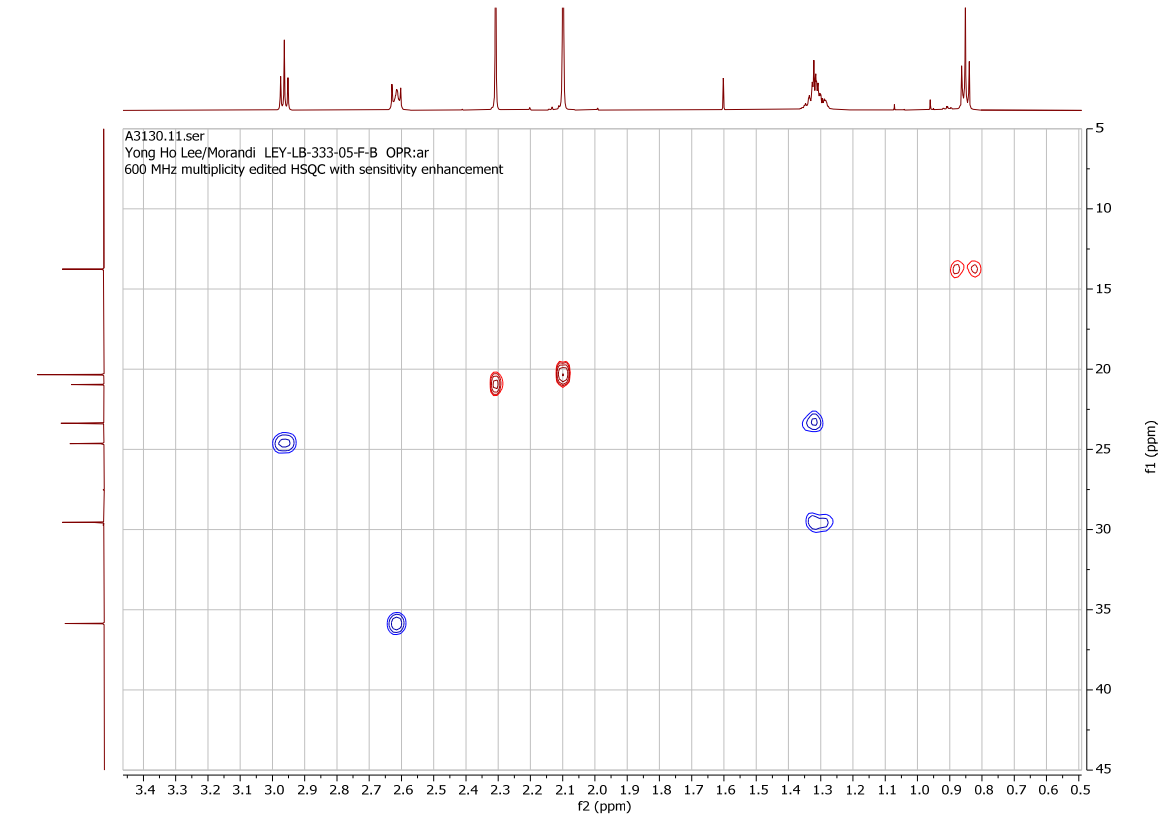
A3130.11.ser
Yong Ho Lee/Morandi LEY-LB-333-05-F-B OPR:ar
600 MHz multiplicity edited HSQC with sensitivity enhancement
f2 (ppm)
f1 (ppm)

(*Z*)-4-formyl-3-mesityloct-3-en-1-yl benzoate, A (**42-α-Ar, minor**).

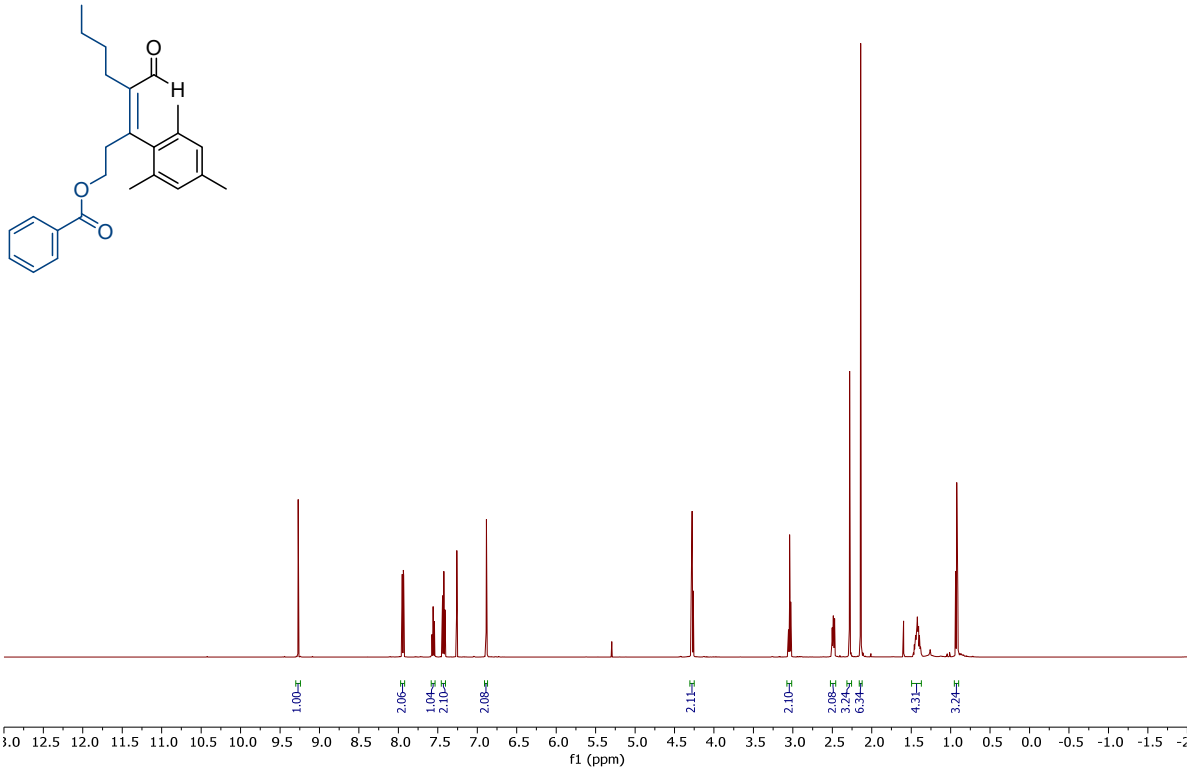

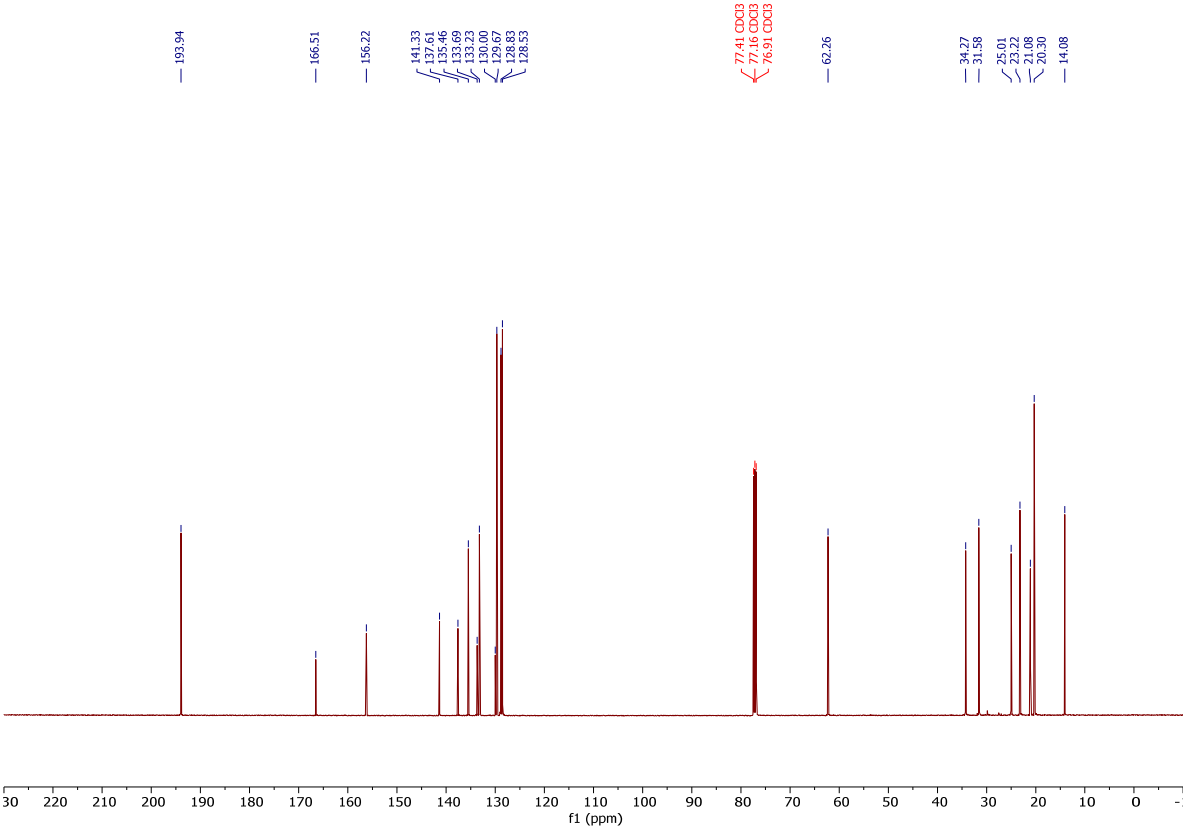

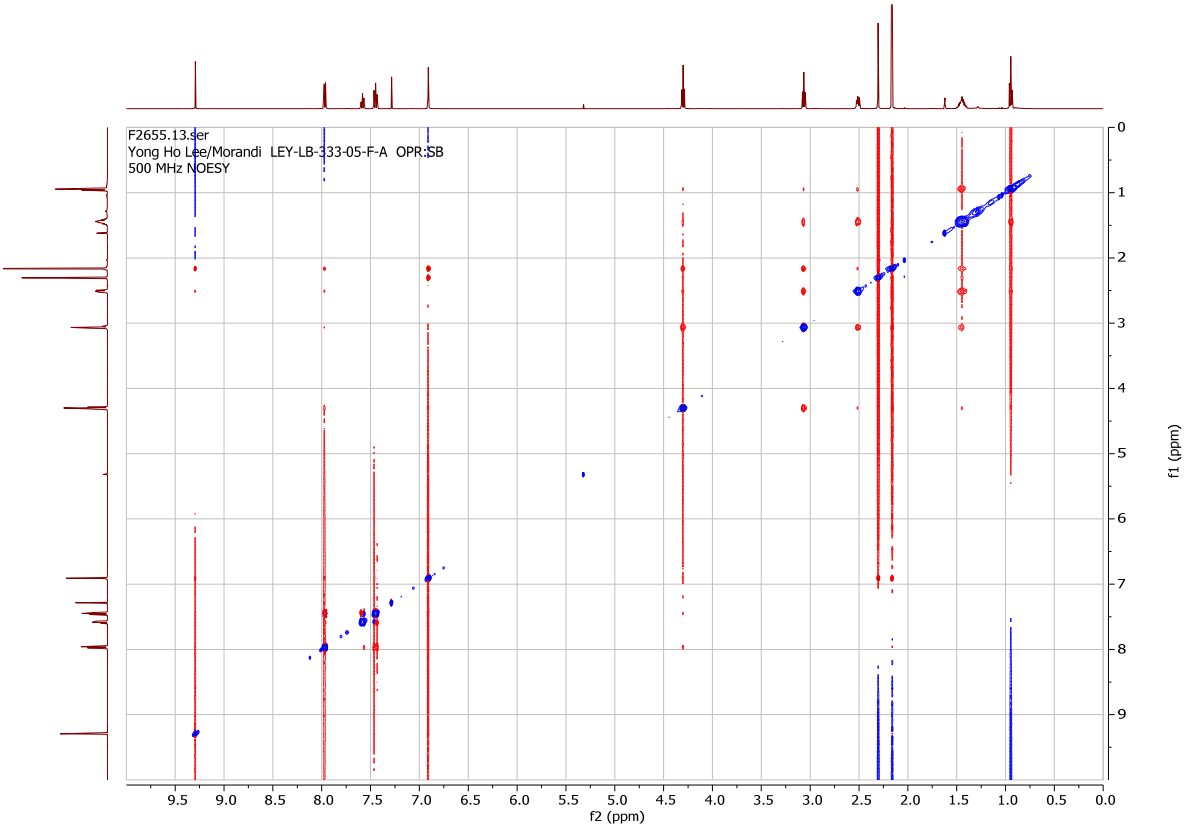
F2655.13.ser
Yong Ho Lee/Morandi LEY-LB-333-05-F-A OPR:SB
500 MHz NOESY
f2 (ppm)
f1 (ppm)

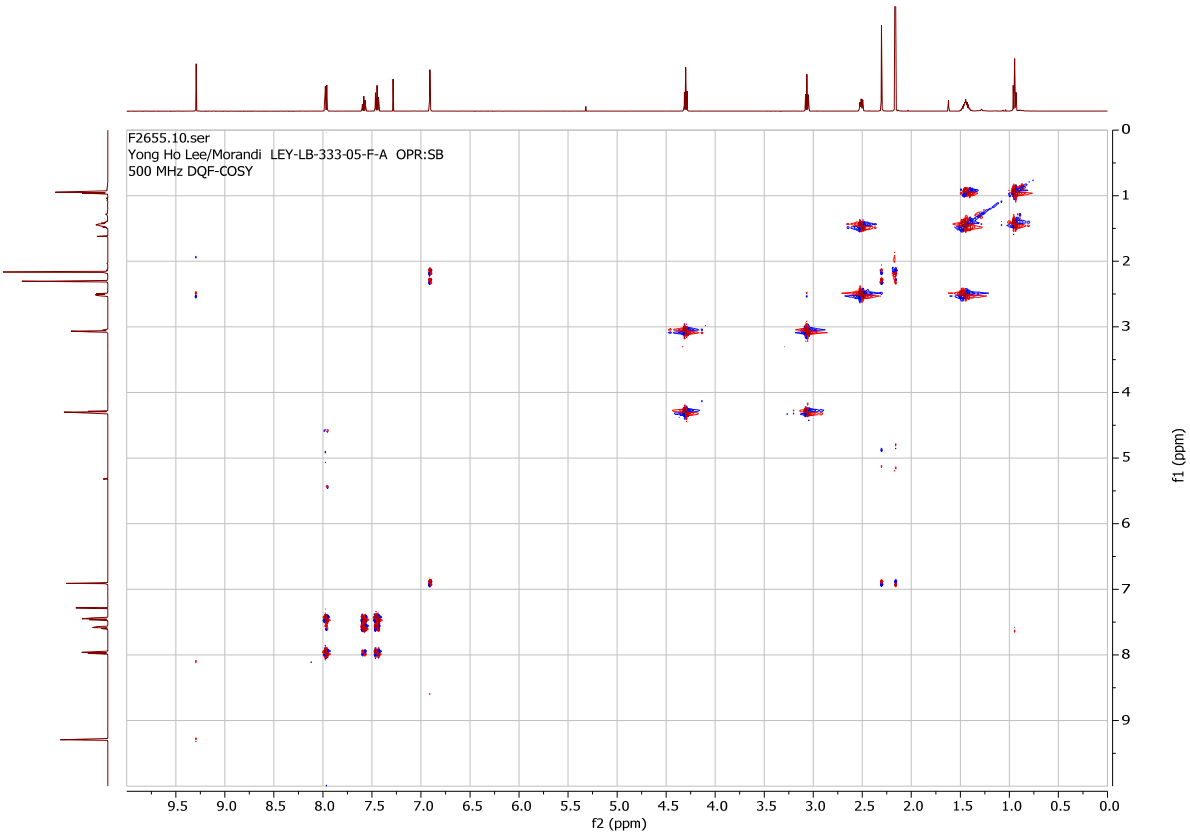
F2655.10.ser
Yong Ho Lee/Morandi LEY-LB-333-05-F-A OPR:SB
500 MHz DQF-COSY
f2 (ppm)
f1 (ppm)

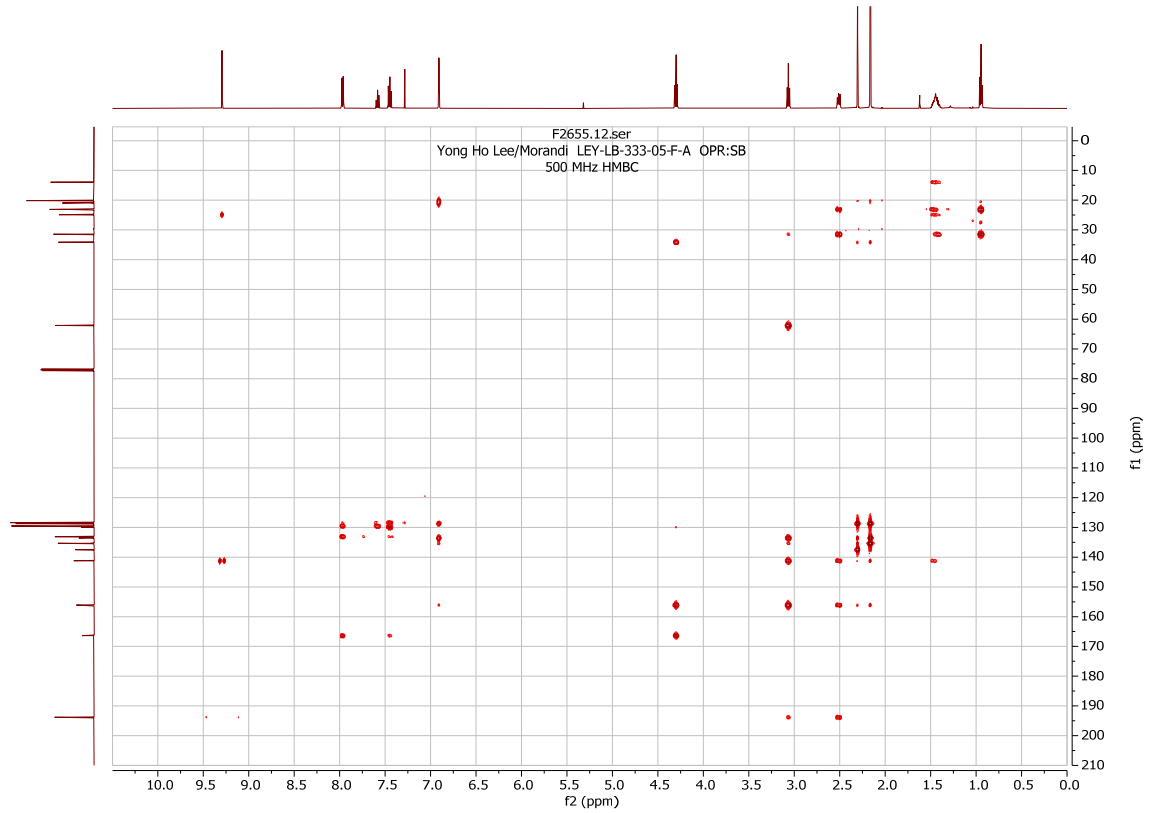
F2655.12.ser
Yong Ho Lee/Morandi LEY-LB-333-05-F-A OPR:SB
500 MHz HMBC
f2 (ppm)
f1 (ppm)

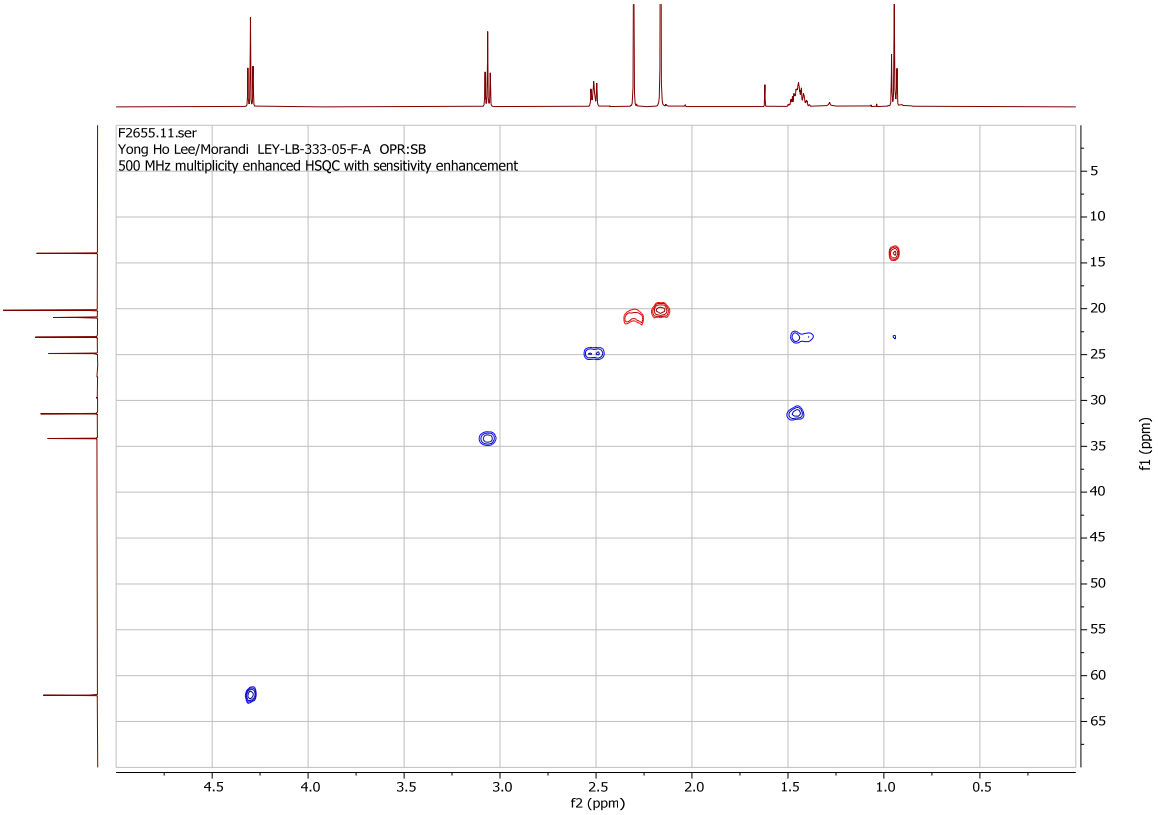
F2655.11.ser
Yong Ho Lee/Morandi LEY-LB-333-05-F-A OPR:SB
500 MHz multiplicity enhanced HSQC with sensitivity enhancement
f2 (ppm)
f1 (ppm)

(*Z*)-3-formyl-4-(*o*-tolyl)oct-3-en-1-yl benzoate, B (**43-β-Ar, major**).

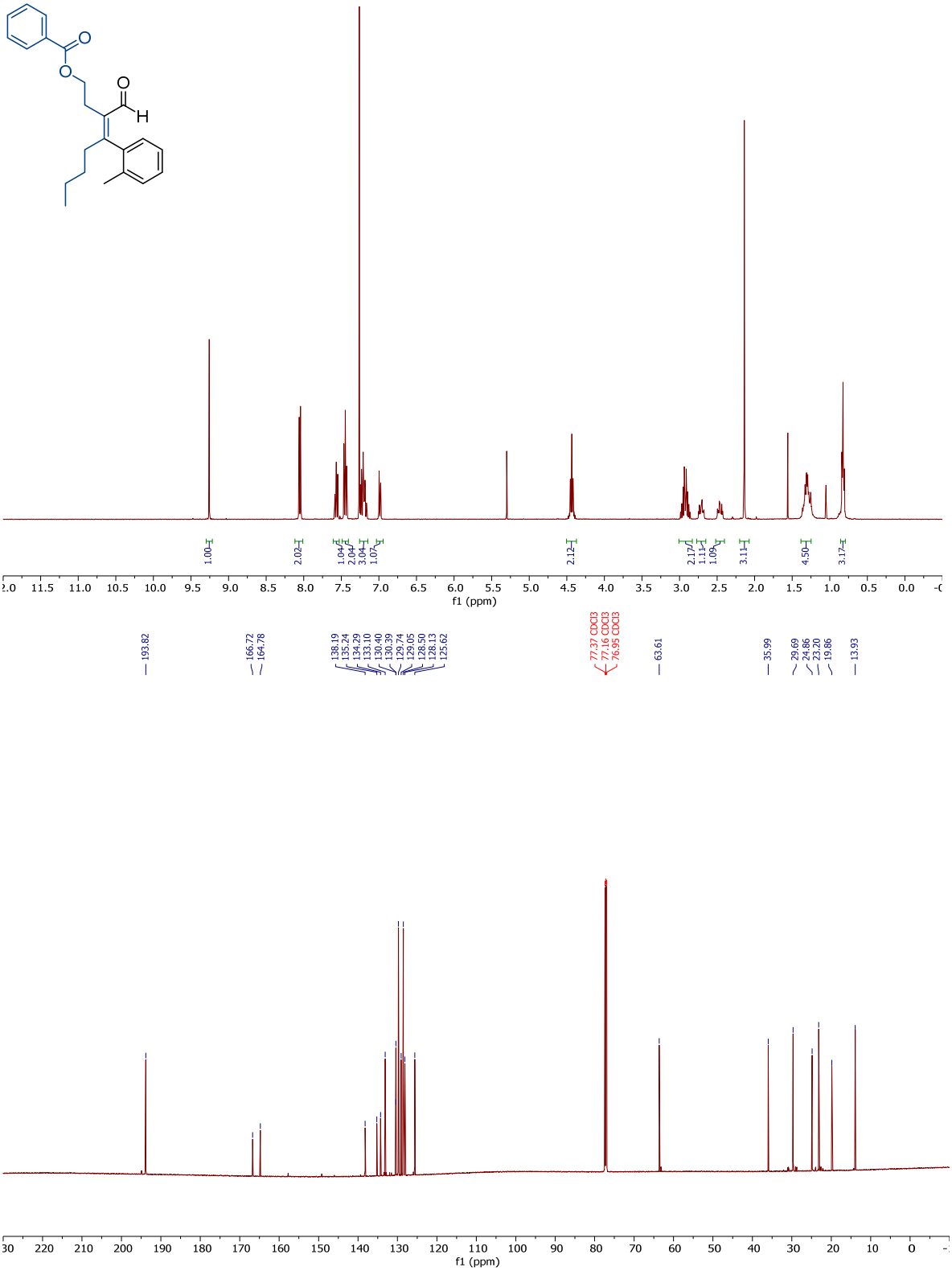

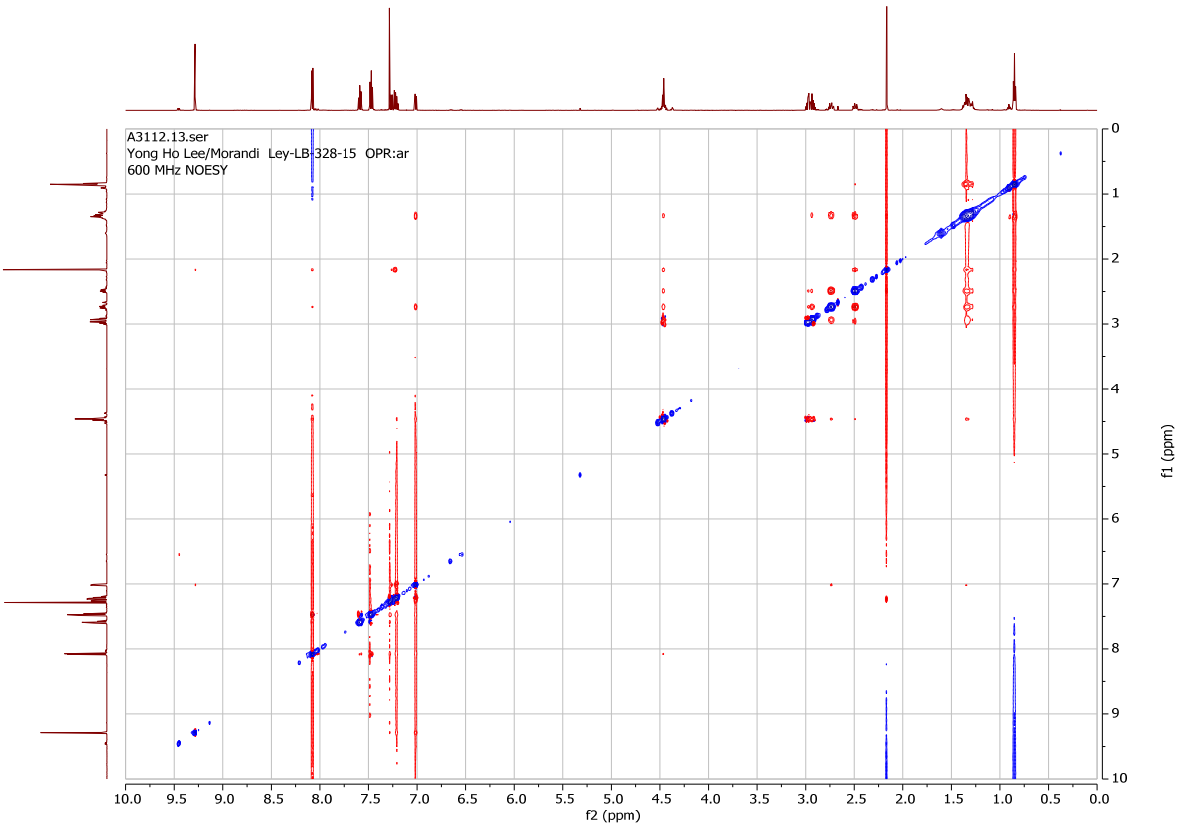
A3112.13.ser
Yong Ho Lee/Morandi Ley-LB-328-15 OPR:ar
600 MHz NOESY
f2 (ppm)
f1 (ppm)

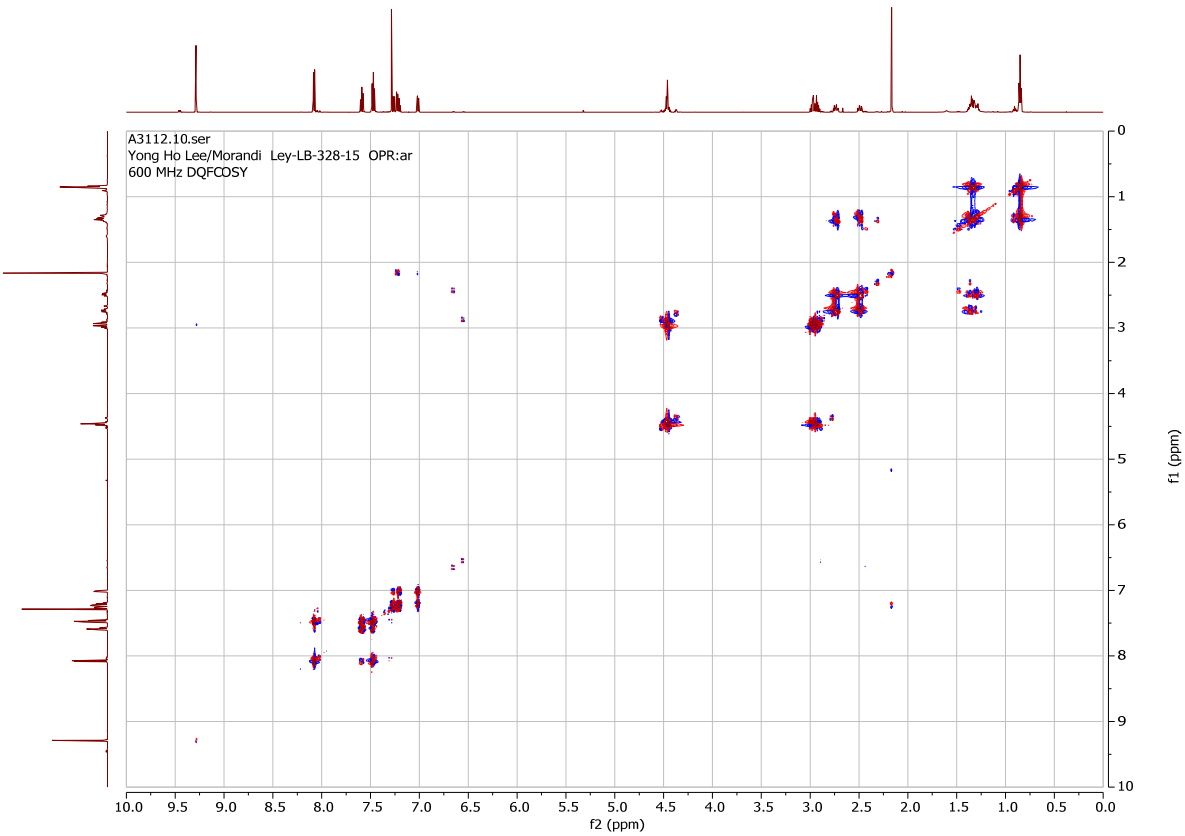
A3112.10.ser
Yong Ho Lee/Morandi Ley-LB-328-15 OPR:ar
600 MHz DQFCOSY
f2 (ppm)
f1 (ppm)

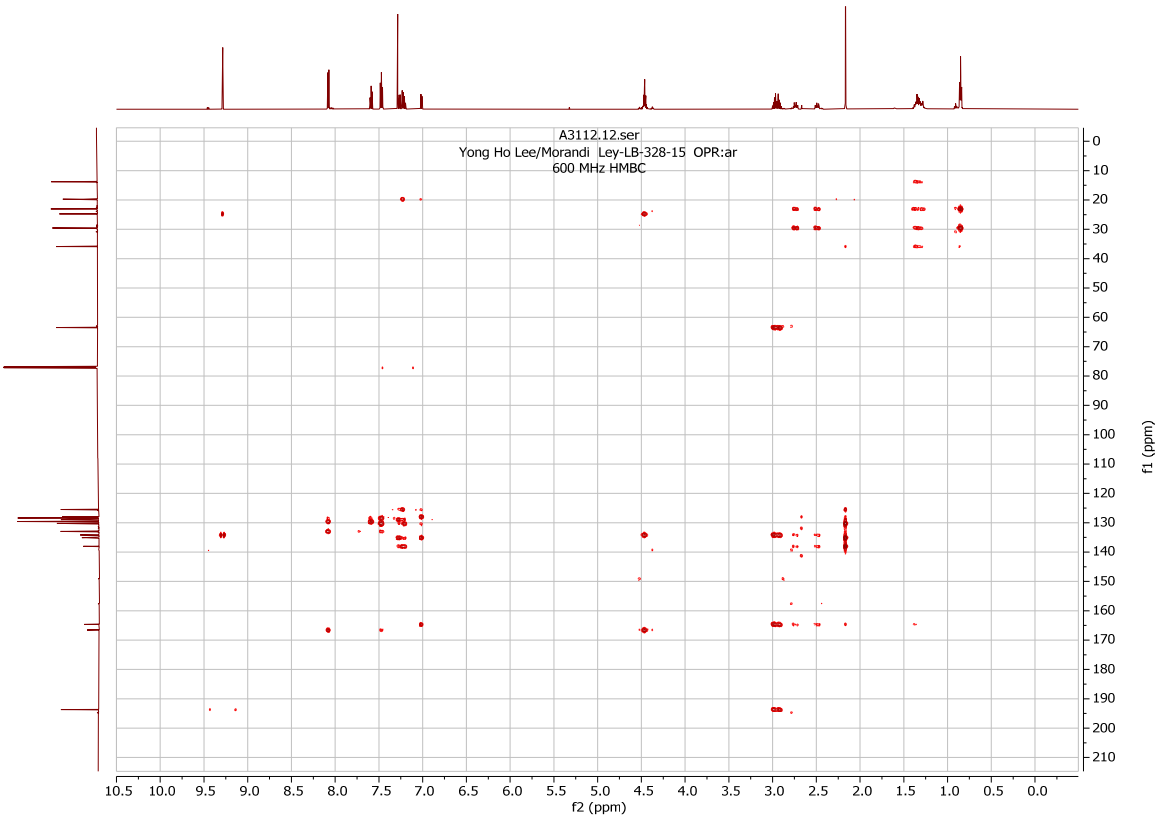
A3112.12.ser
Yong Ho Lee/Morandi Ley-LB-328-15 OPR:ar
600 MHz HMBC
f2 (ppm)
f1 (ppm)

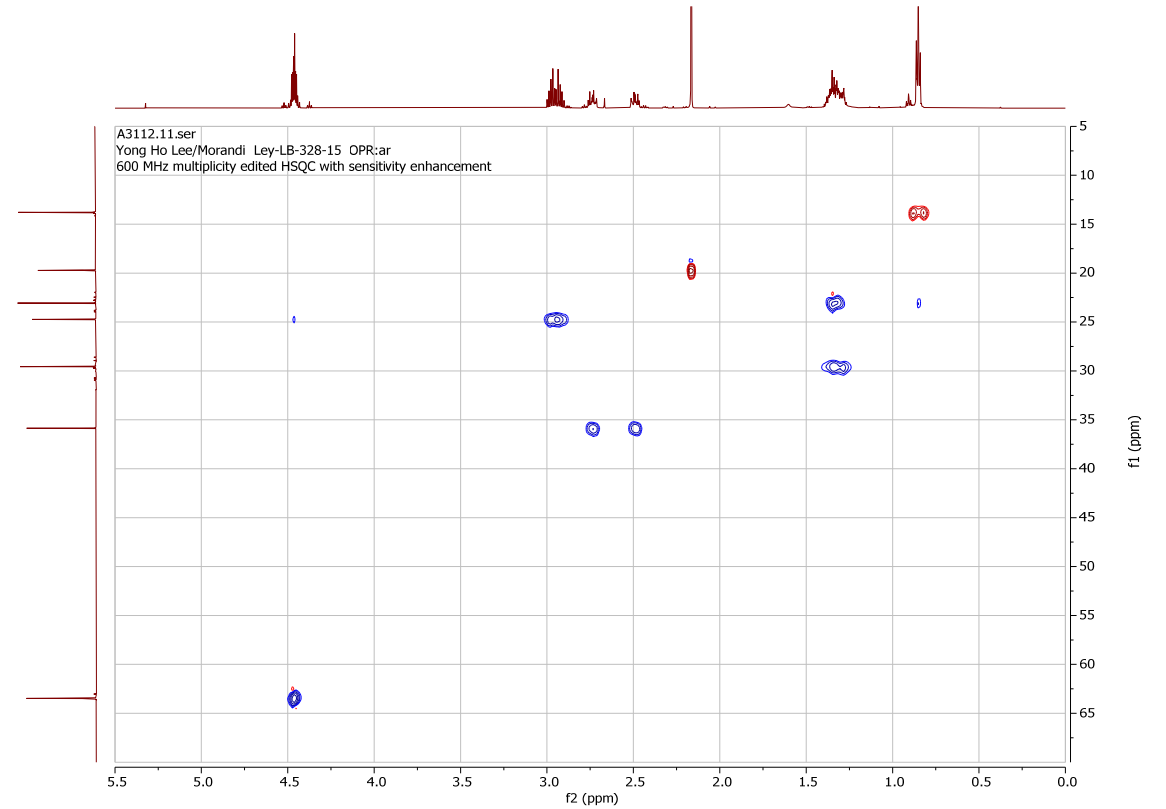
A3112.11.ser
Yong Ho Lee/Morandi Ley-LB-328-15 OPR:ar
600 MHz multiplicity edited HSQC with sensitivity enhancement
f2 (ppm)
f1 (ppm)

(*Z*)-4-formyl-3-(*o*-tolyl)oct-3-en-1-yl benzoate, A (**43-α-Ar, minor**).

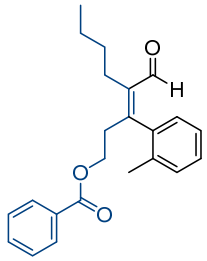

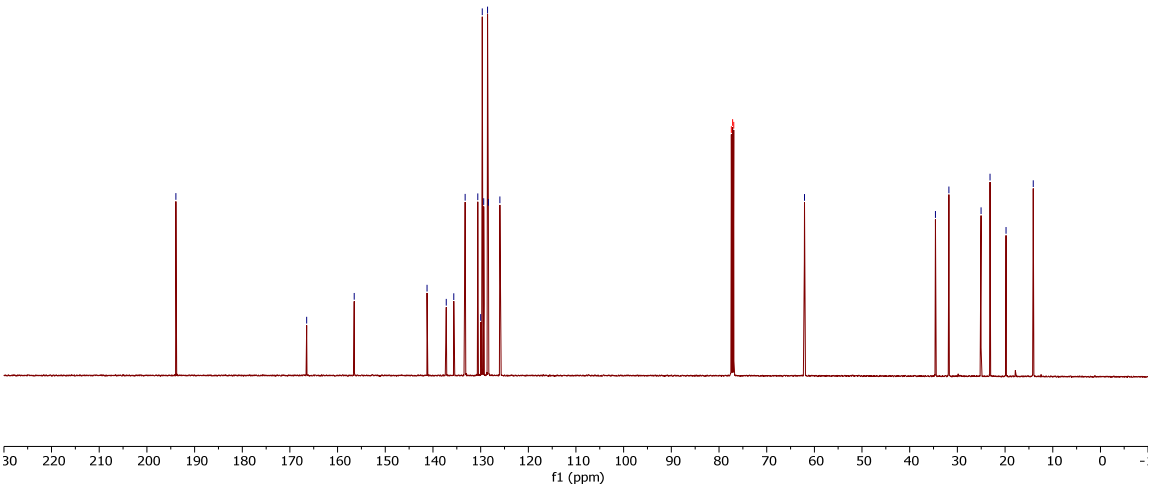

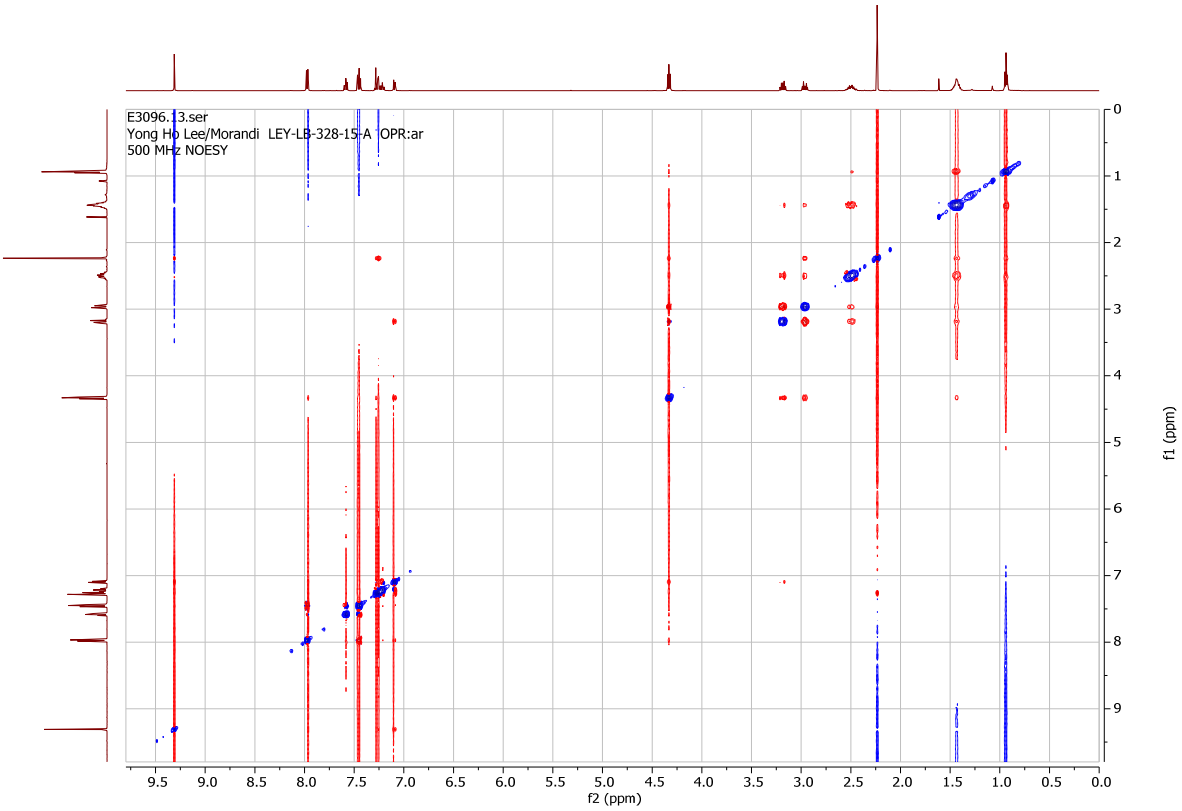
E3096.13.ser
Yong Ho Lee/Morandi LEY-LB-328-15-A OPR:ar
500 MHz NOESY
f2 (ppm)
f1 (ppm)

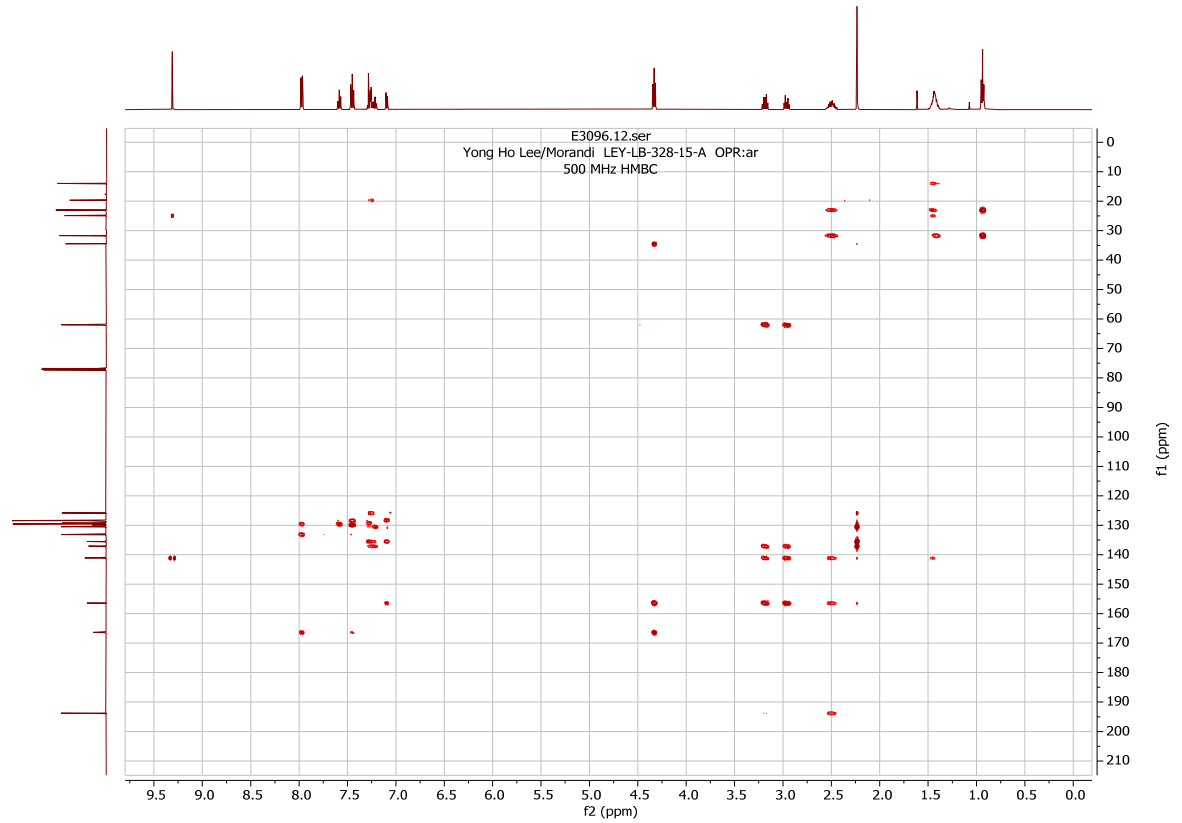
E3096.12.ser
Yong Ho Lee/Morandi LEY-LB-328-15-A OPR:ar
500 MHz HMBC
f2 (ppm)
f1 (ppm)

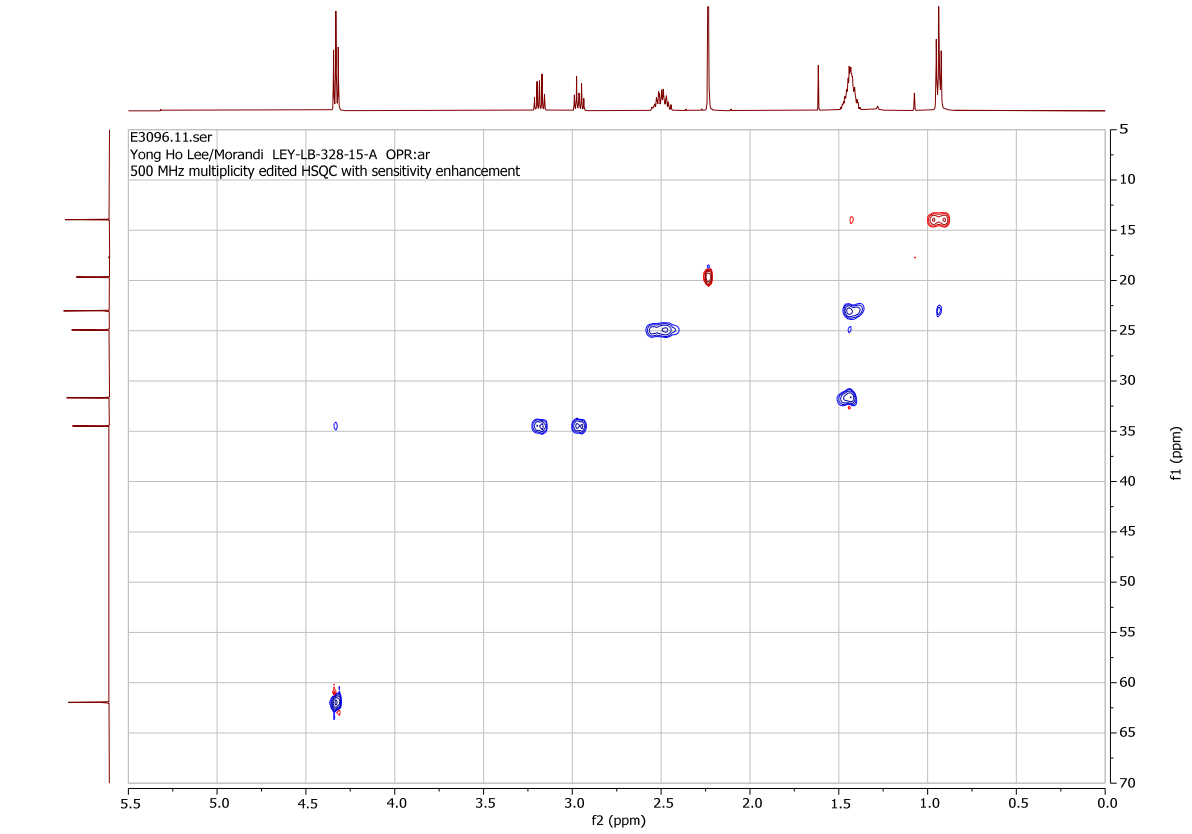
E3096.11.ser
Yong Ho Lee/Morandi LEY-LB-328-15-A OPR:ar
500 MHz multiplicity edited HSQC with sensitivity enhancement
f2 (ppm)
f1 (ppm)

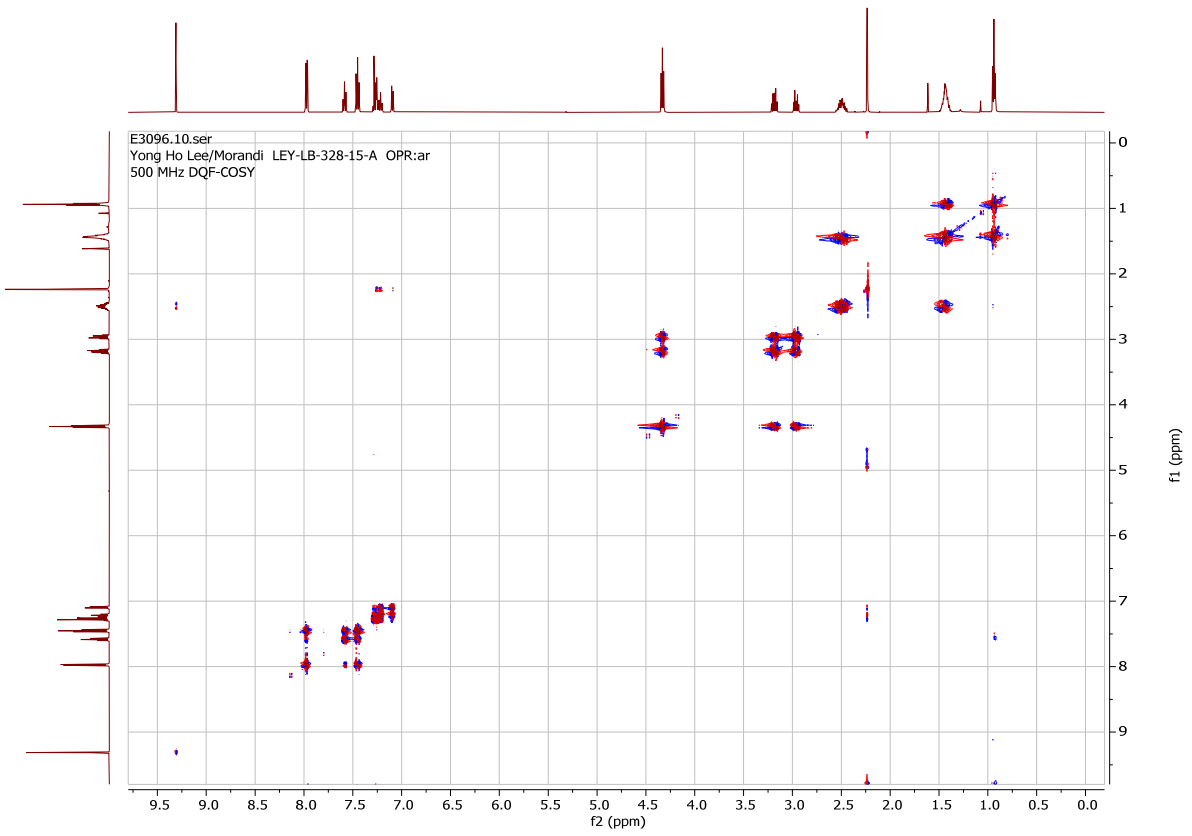
E3096.10.ser
Yong Ho Lee/Morandi LEY-LB-328-15-A OPR:ar
500 MHz DQF-COSY
f2 (ppm)
f1 (ppm)

(*Z*)-3-formyl-4-(*o*-tolyl)oct-3-en-1-yl butyrate, B (**44-β-Ar, major**).

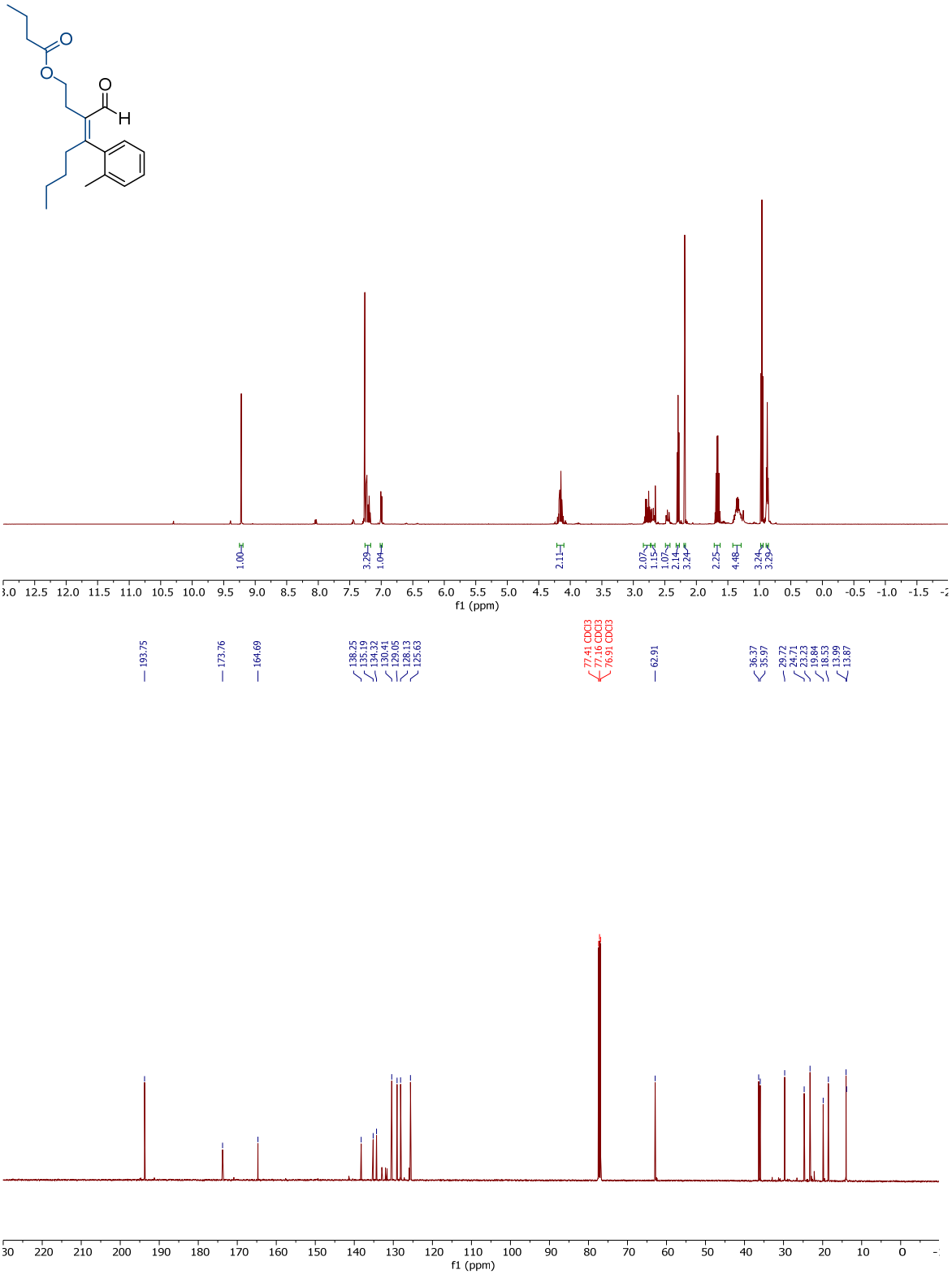

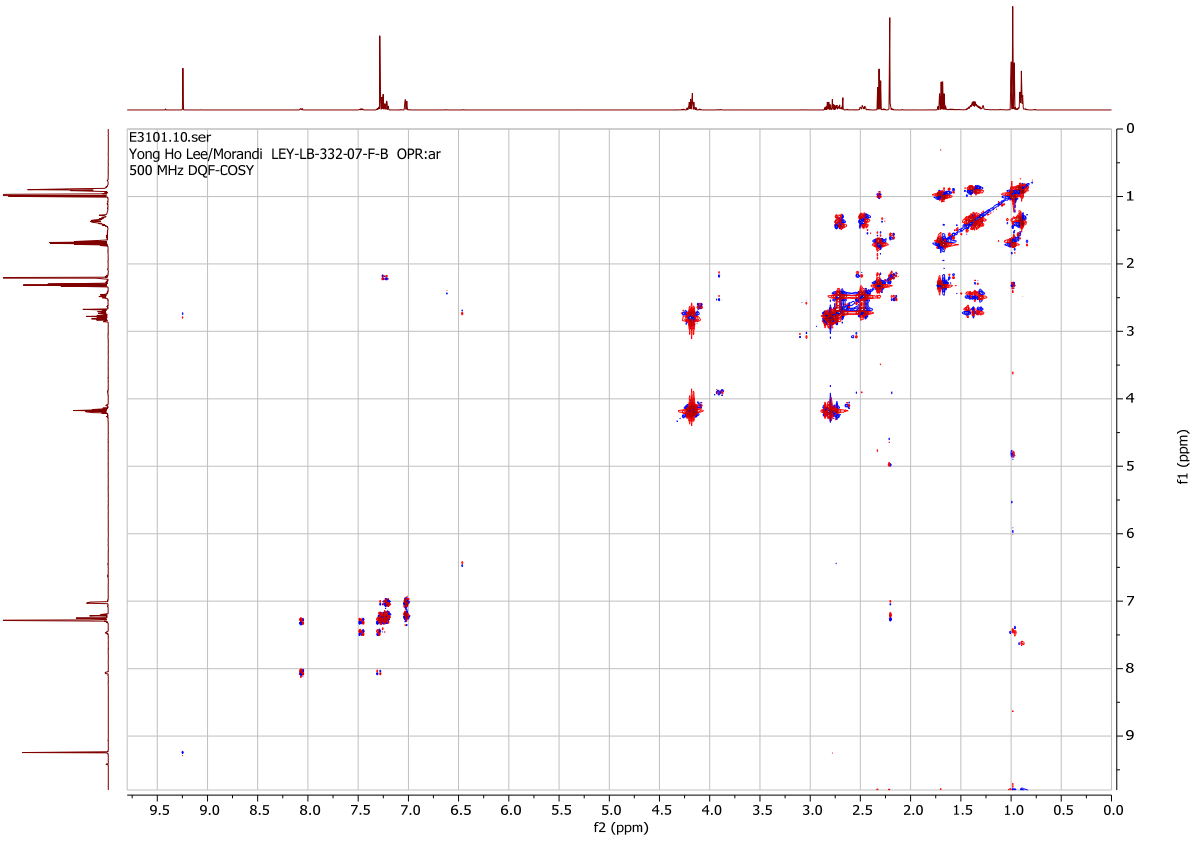
E3101.10.ser
Yong Ho Lee/Morandi LEY-LB-332-07-F-B OPR:ar
500 MHz DQF-COSY
f2 (ppm)
f1 (ppm)

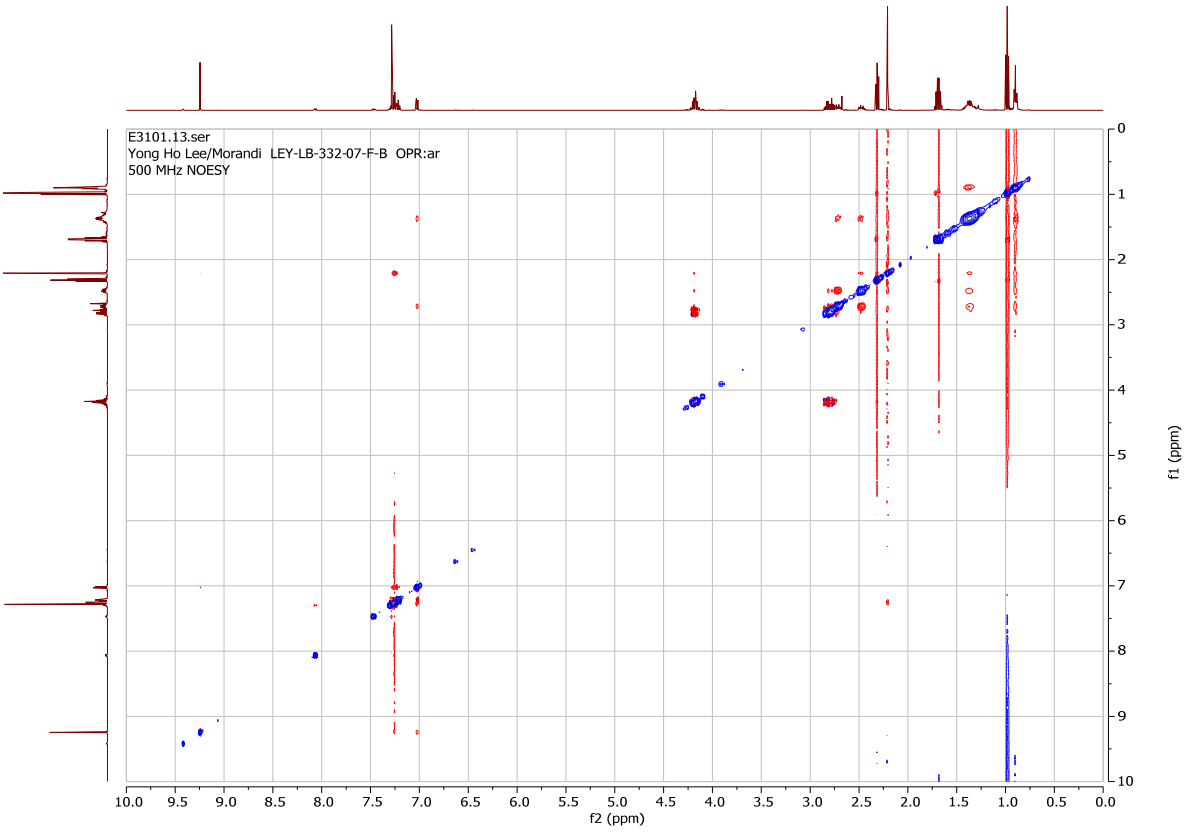
E3101.13.ser
Yong Ho Lee/Morandi LEY-LB-332-07-F-B OPR:ar
500 MHz NOESY
f2 (ppm)
f1 (ppm)

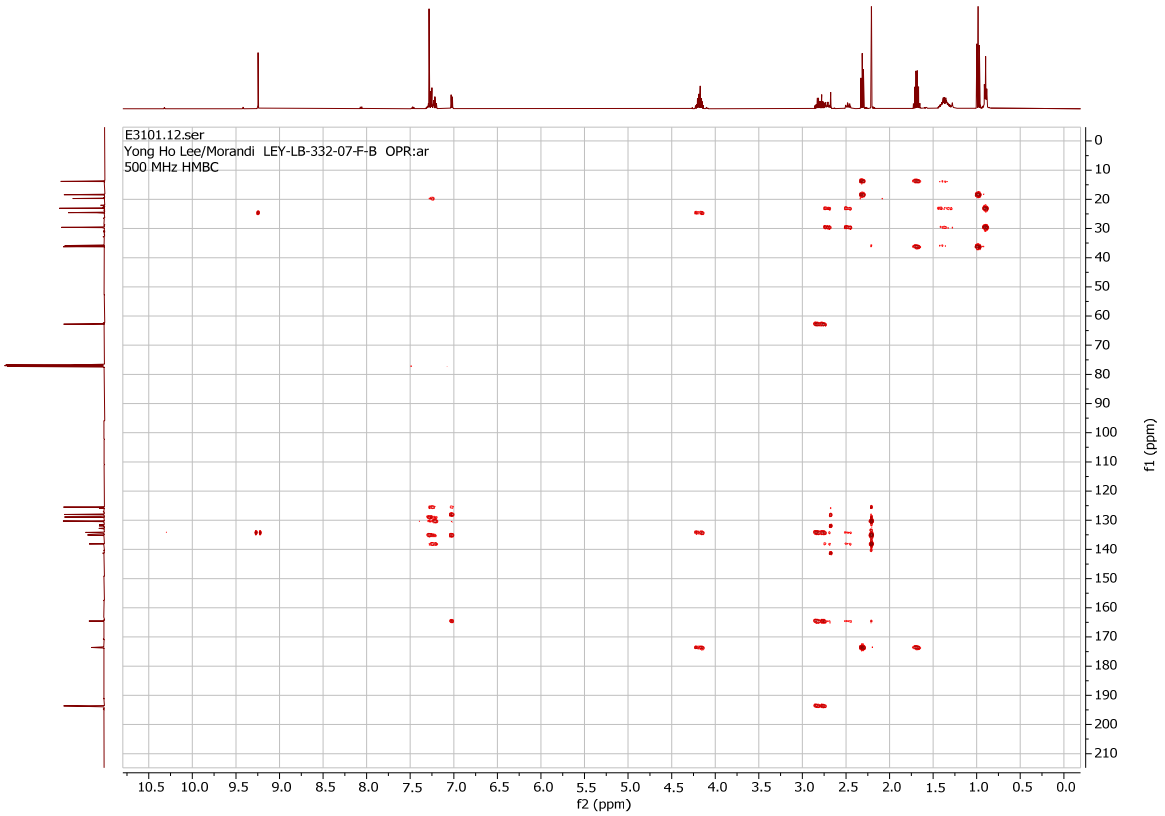
E3101.12.ser
Yong Ho Lee/Morandi LEY-LB-332-07-F-B OPR:ar
500 MHz HMBC
f2 (ppm)
f1 (ppm)

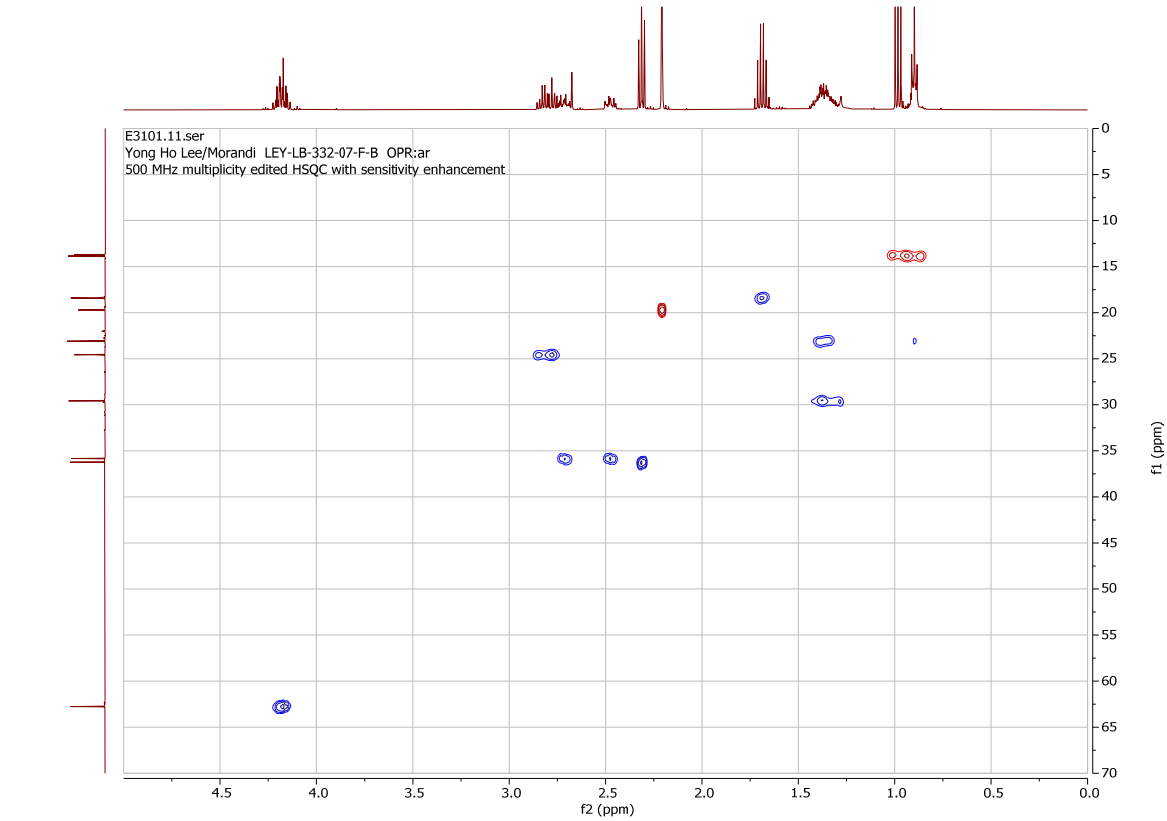
E3101.11.ser
Yong Ho Lee/Morandi LEY-LB-332-07-F-B OPR:ar
500 MHz multiplicity edited HSQC with sensitivity enhancement
f2 (ppm)
f1 (ppm)

(*Z*)-4-formyl-3-(*o*-tolyl)oct-3-en-1-yl butyrate, A (**44-α-Ar, minor**).

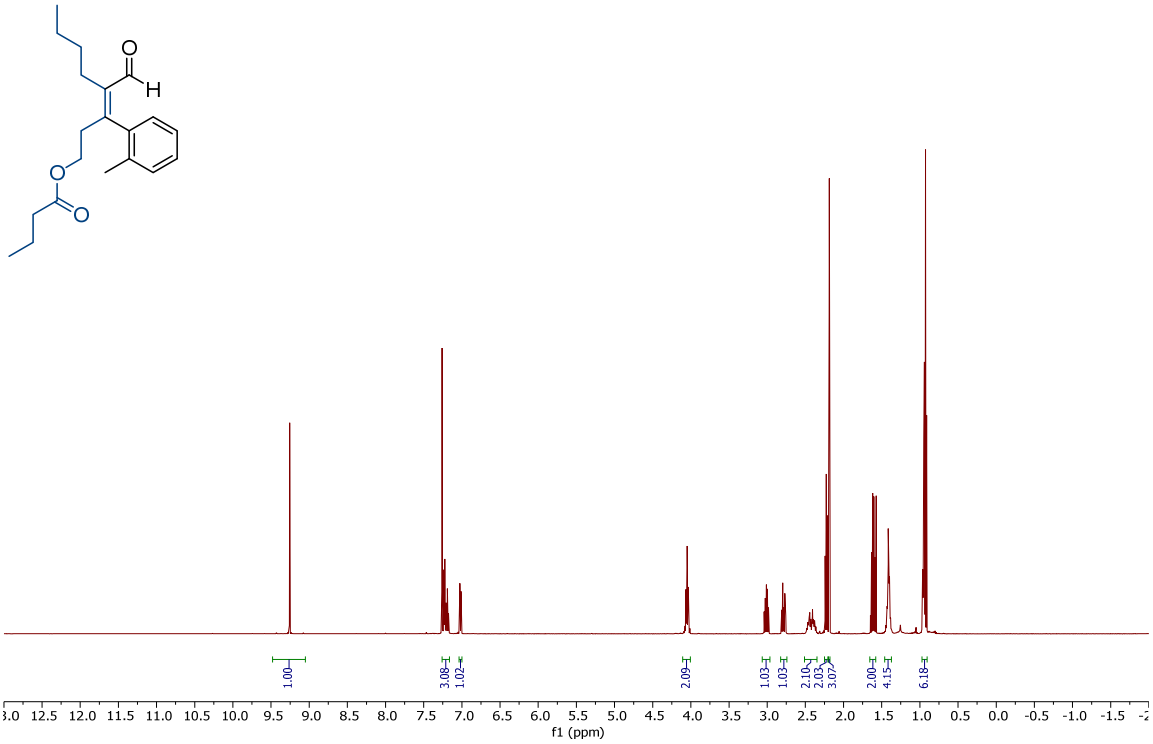

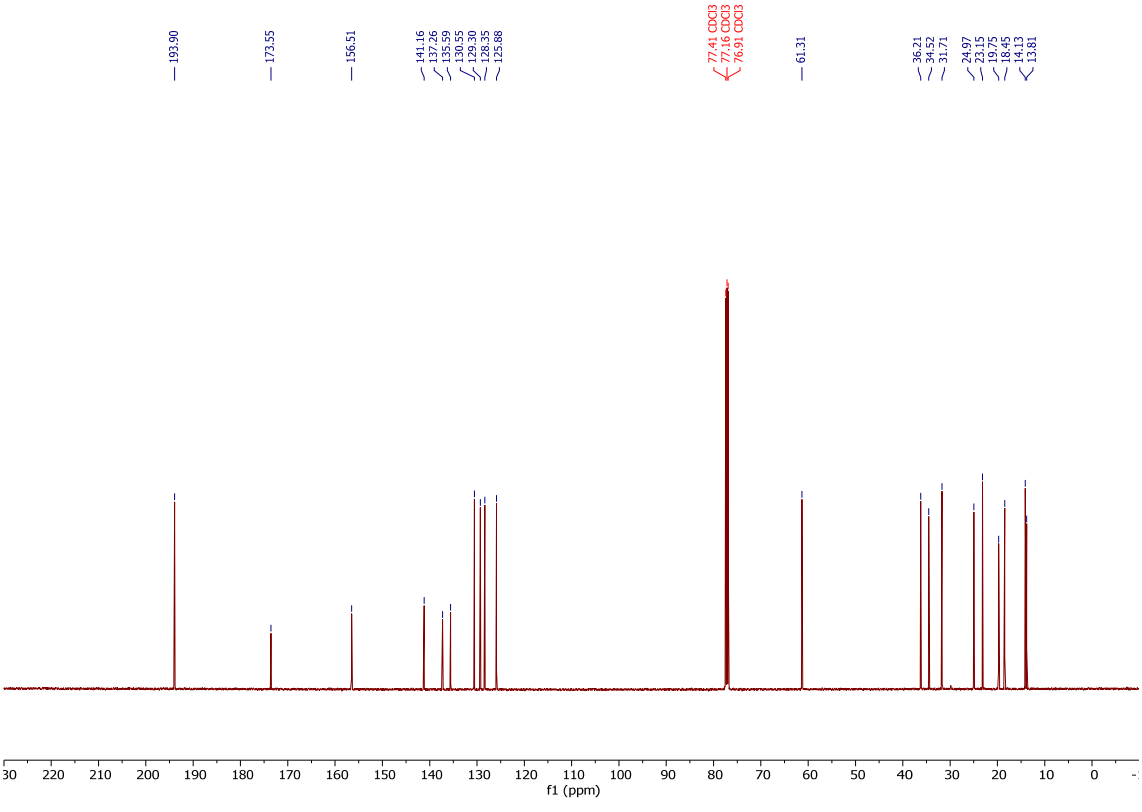

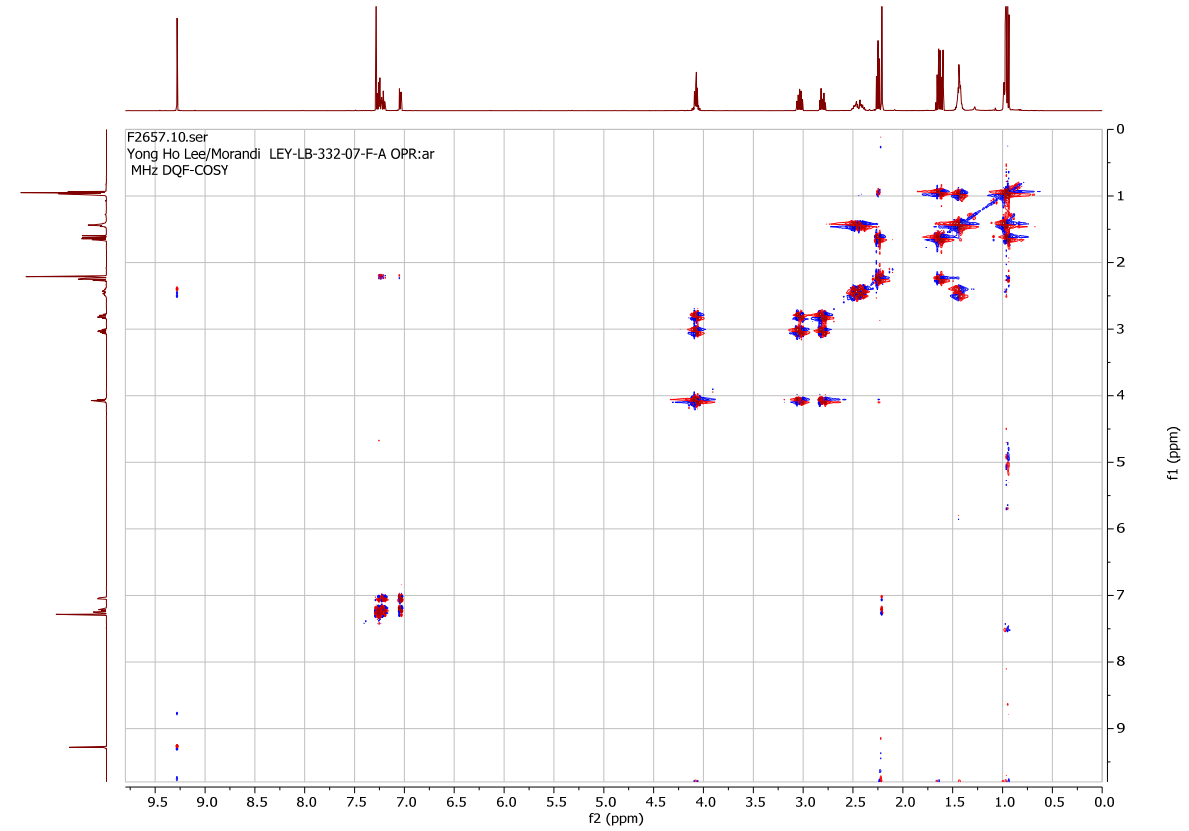
F2657.10.ser
Yong Ho Lee/Morandi LEY-LB-332-07-F-A OPR:ar
MHz DQF-COSY
f2 (ppm)
f1 (ppm)

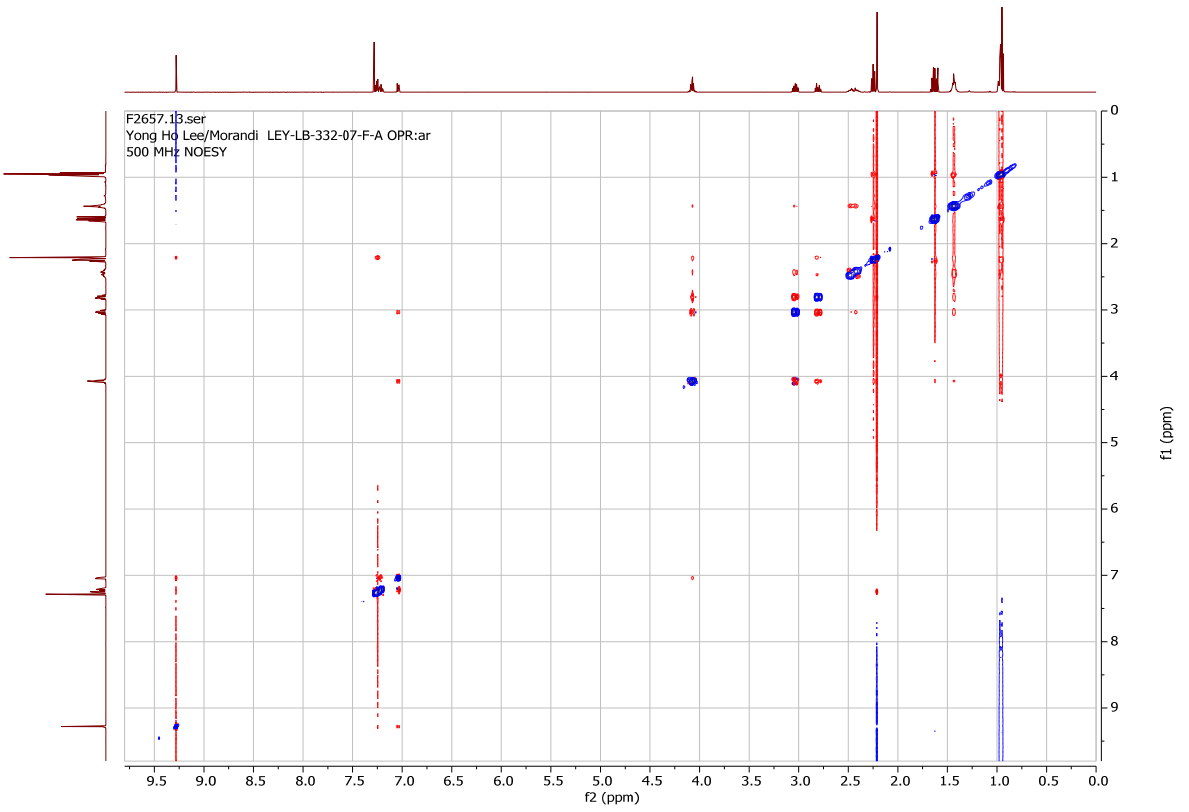
F2657.13.ser
Yong Ho Lee/Morandi LEY-LB-332-07-F-A OPR:ar
500 MHz NOESY
f2 (ppm)
f1 (ppm)

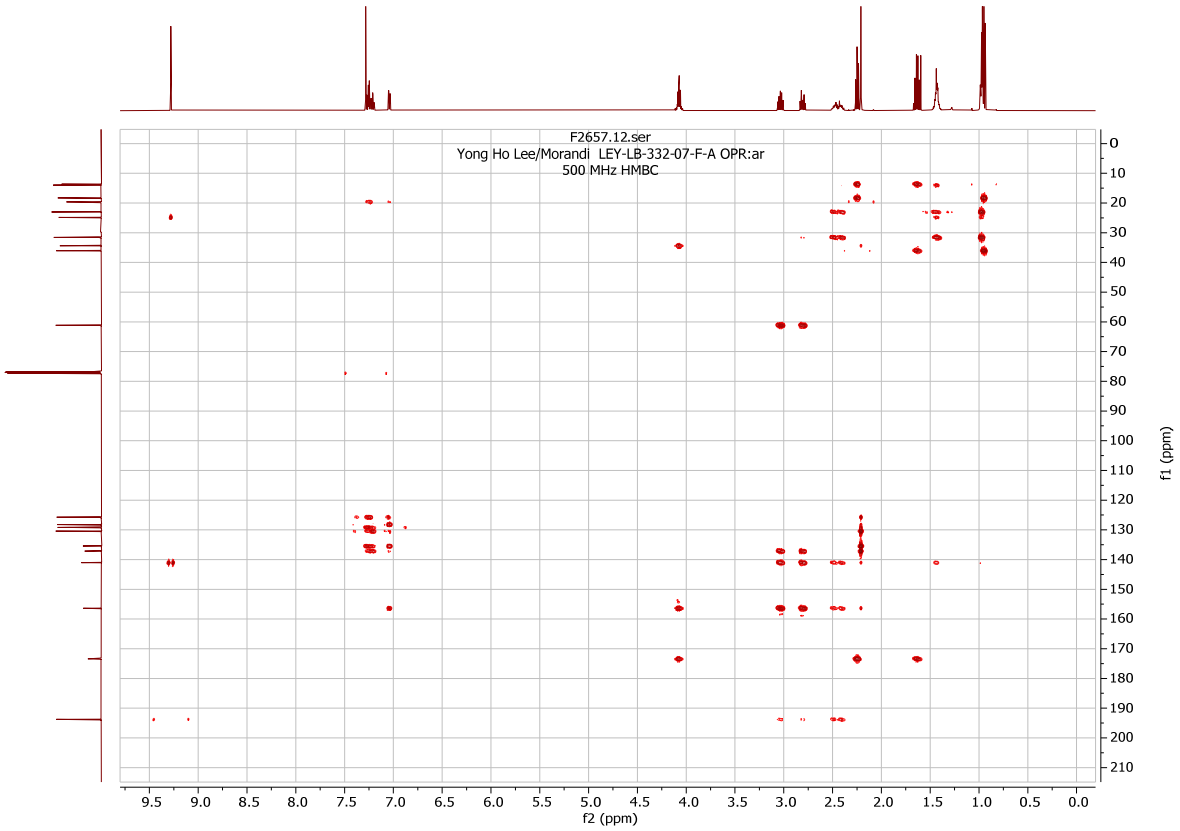
F2657.12.ser
Yong Ho Lee/Morandi LEY-LB-332-07-F-A OPR:ar
500 MHz HMBC
f2 (ppm)
f1 (ppm)

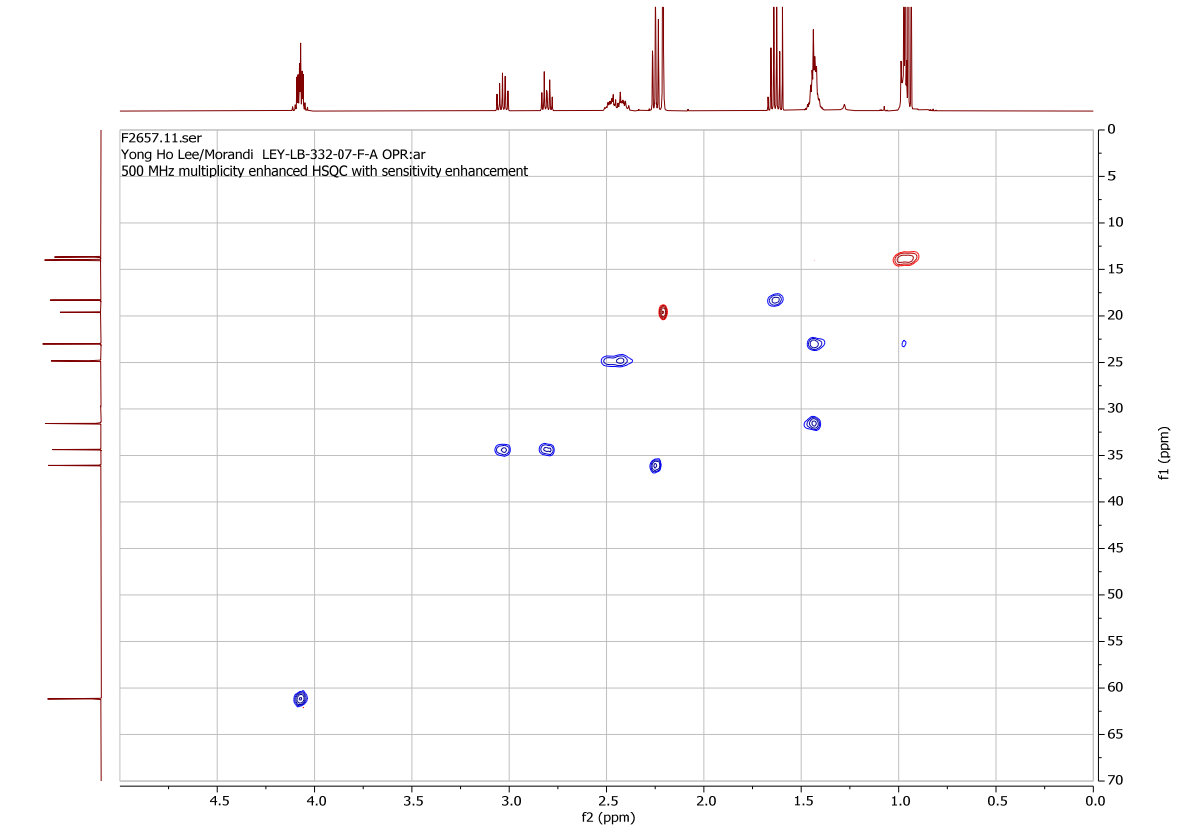
F2657.11.ser
Yong Ho Lee/Morandi LEY-LB-332-07-F-A OPR:ar
500 MHz multiplicity enhanced HSQC with sensitivity enhancement
f2 (ppm)
f1 (ppm)

(*Z*)-3-formyl-4-(*o*-tolyl)oct-3-en-1-yl diethylcarbamate, A, (**45-β-Ar, major**, an inseparable mixture of regioisomers, **β-Ar**/α-Ar = 66:34).

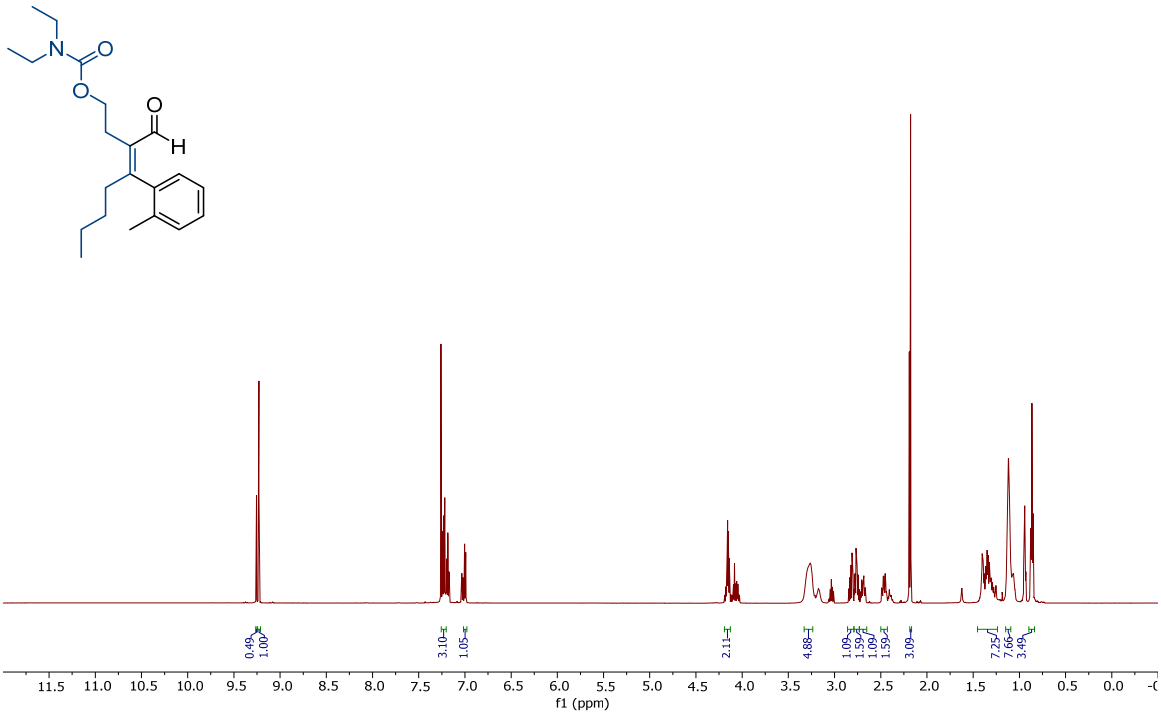

(*Z*)-4-formyl-3-(*o*-tolyl)oct-3-en-1-yl diethylcarbamate, B (**45-α-Ar, minor**, an inseparable mixture of regioisomers, β-Ar/**α-Ar** = 66:34).

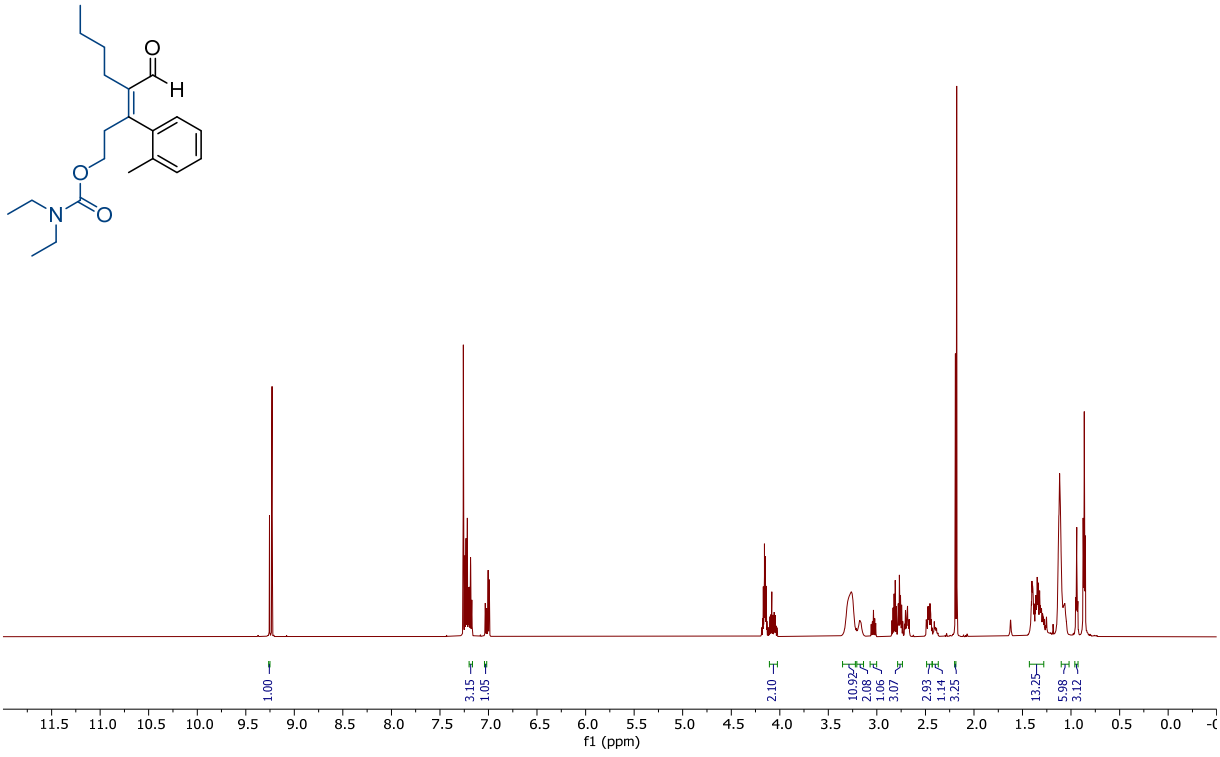

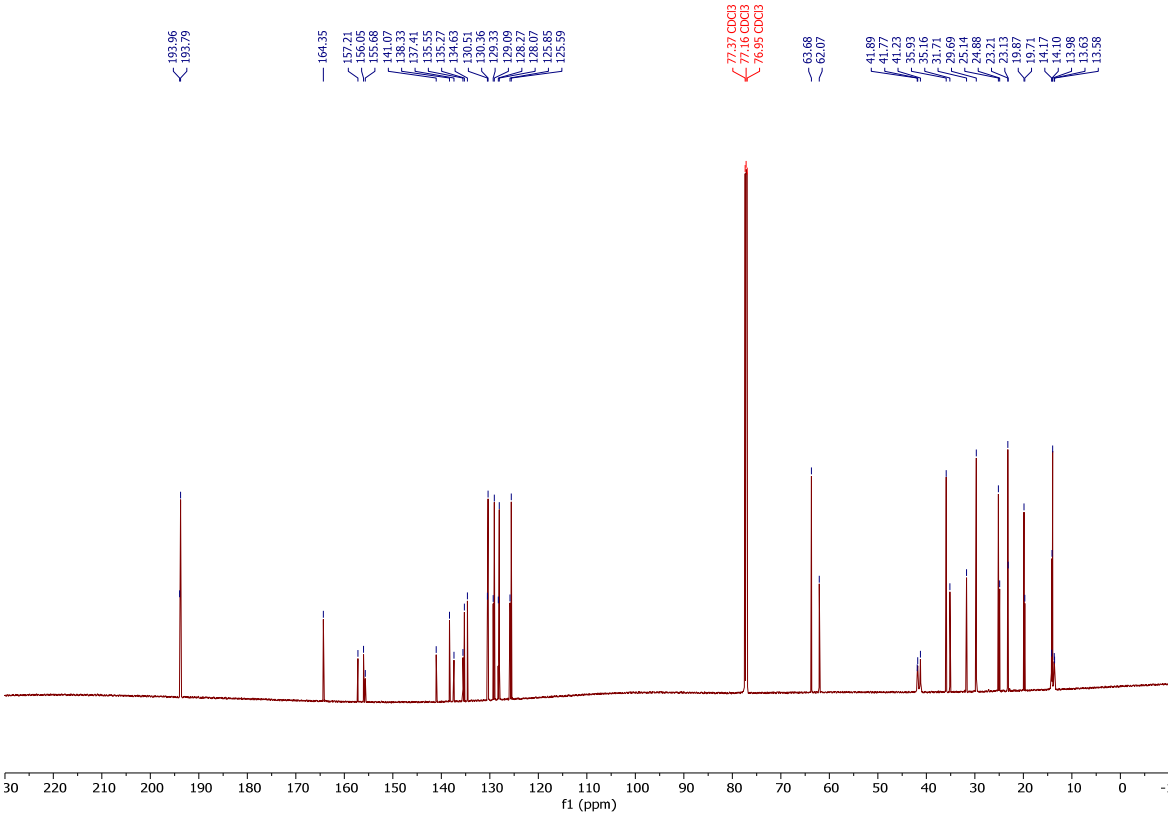
193.96
193.79
164.35
157.21
156.05
155.68
141.07
138.33
137.41
135.55
135.27
134.63
130.51
130.36
129.33
129.09
128.27
128.07
125.85
125.59
77.37 CDCl3
77.16 CDCl3
76.95 CDCl3
63.68
62.07
41.89
41.77
41.23
35.93
35.16
31.71
29.69
25.14
24.88
23.21
23.13
19.87
19.71
14.17
14.10
13.98
13.63
13.58
f1 (ppm)

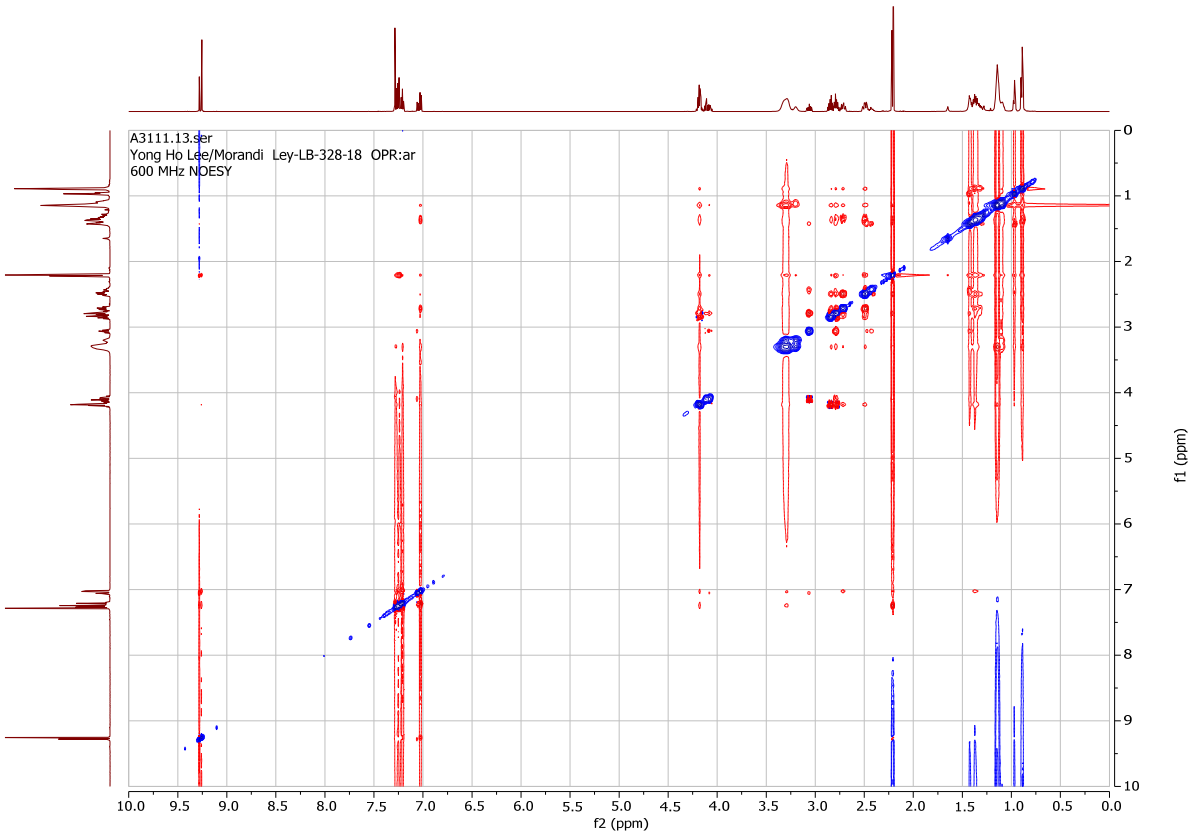
A3111.13.ser
Yong Ho Lee/Morandi Ley-LB-328-18 OPR:ar
600 MHz NOESY
f2 (ppm)
f1 (ppm)

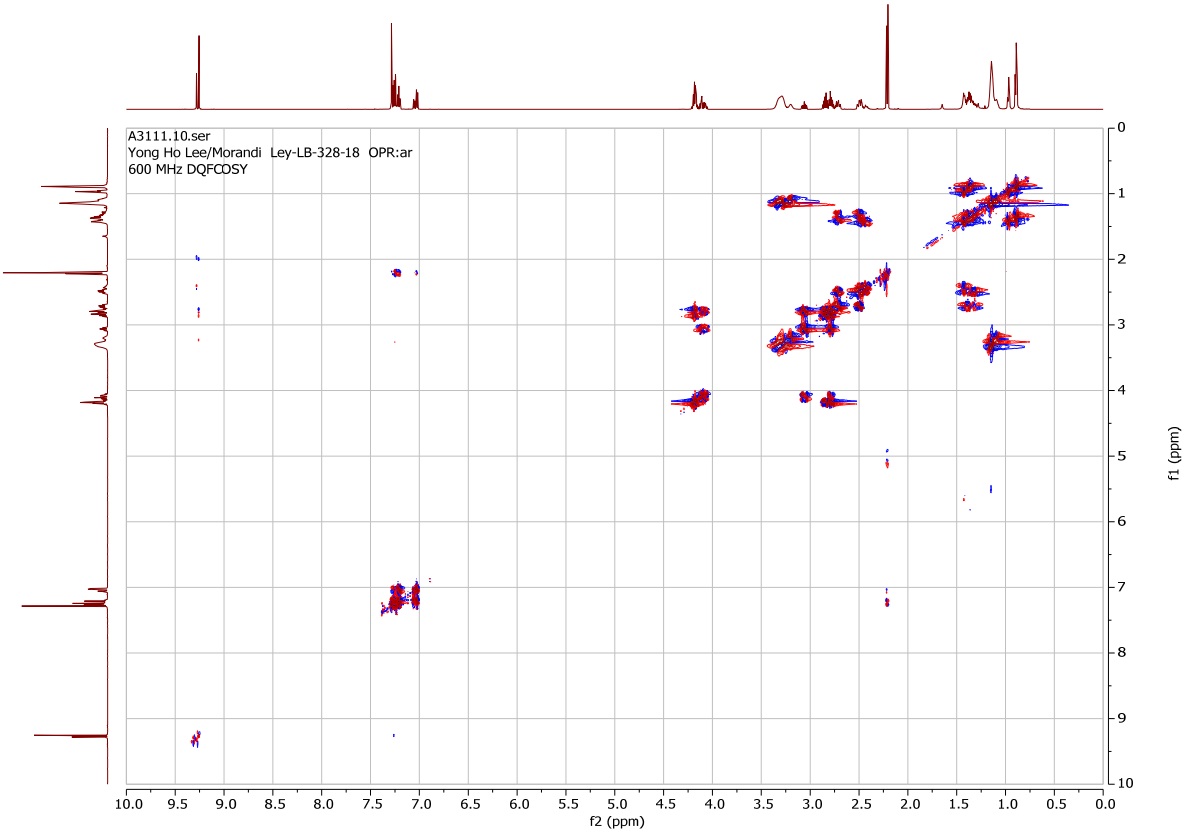
A3111.10.ser
Yong Ho Lee/Morandi Ley-LB-328-18 OPR:ar
600 MHz DQFCOSY
f2 (ppm)
f1 (ppm)

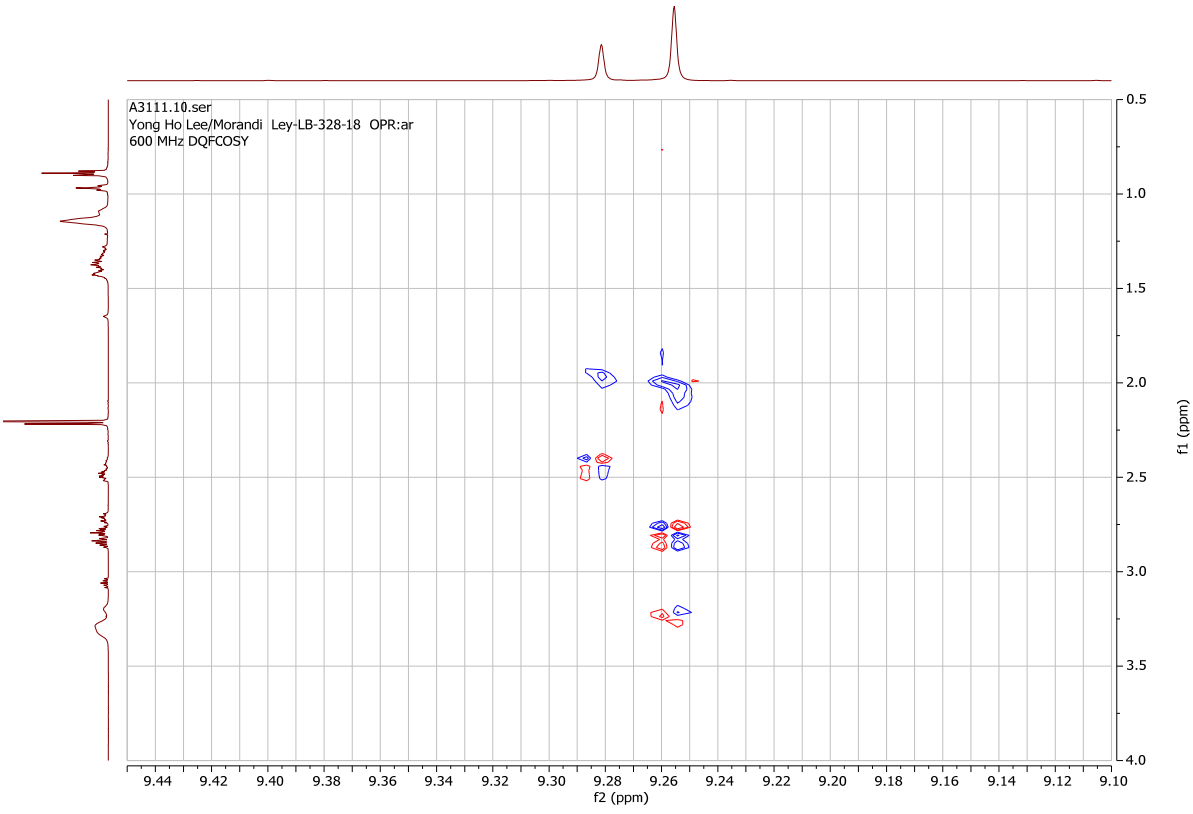
A3111.10.ser
Yong Ho Lee/Morandi Ley-LB-328-18 OPR:ar
600 MHz DQFCOSY
f2 (ppm)
f1 (ppm)

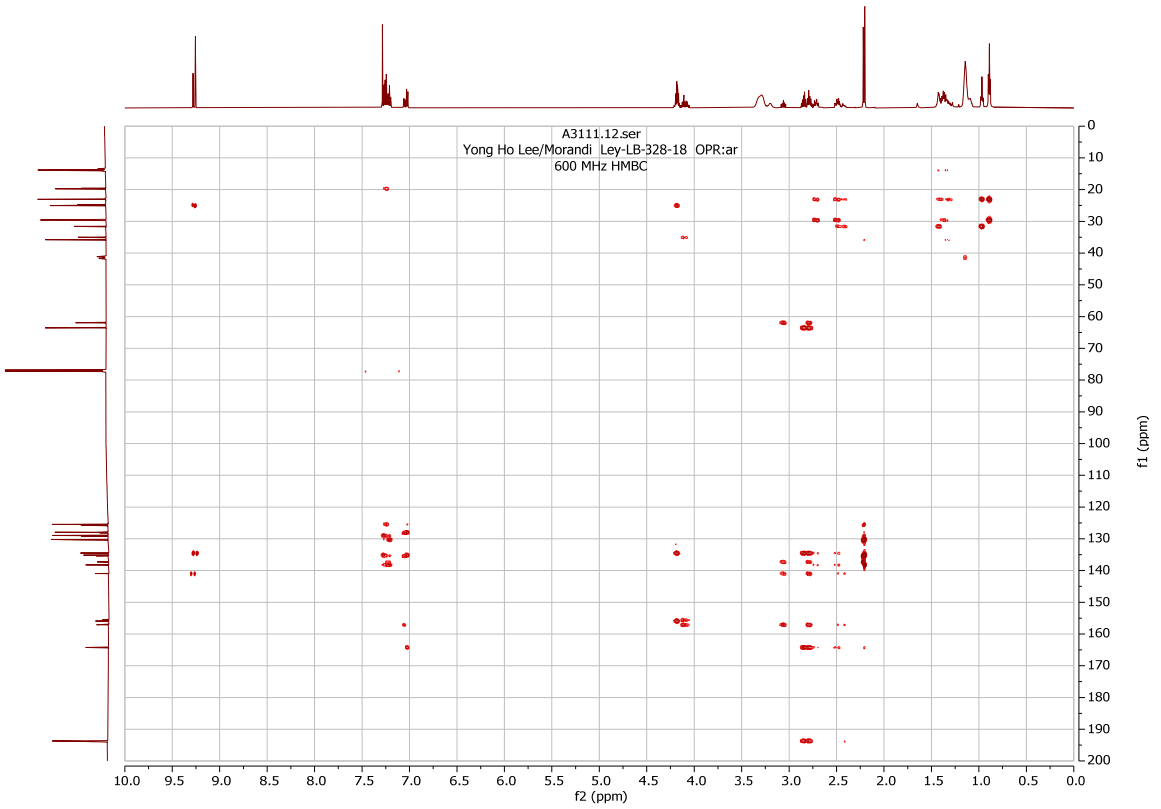
A3111.12.ser
Yong Ho Lee/Morandi Ley-LB-328-18 OPR:ar
600 MHz HMBC
f2 (ppm)
f1 (ppm)

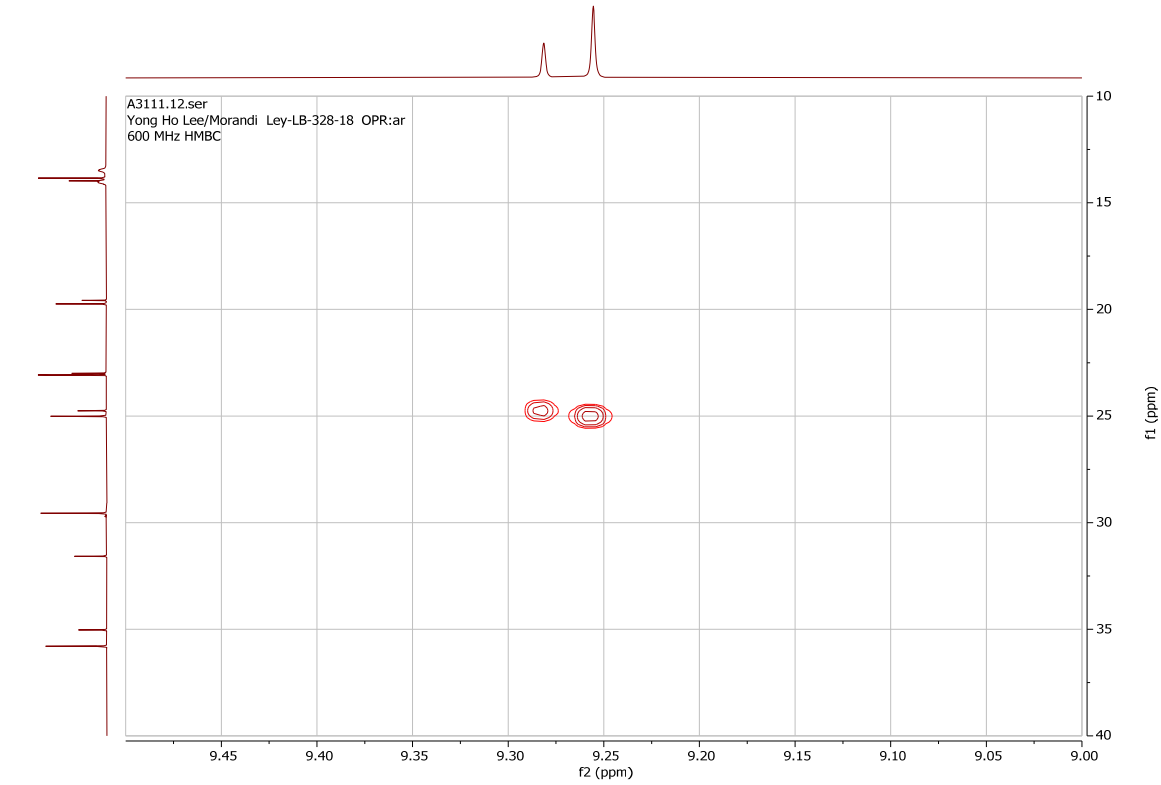
A3111.12.ser
Yong Ho Lee/Morandi Ley-LB-328-18 OPR:ar
600 MHz HMBC
f2 (ppm)
f1 (ppm)

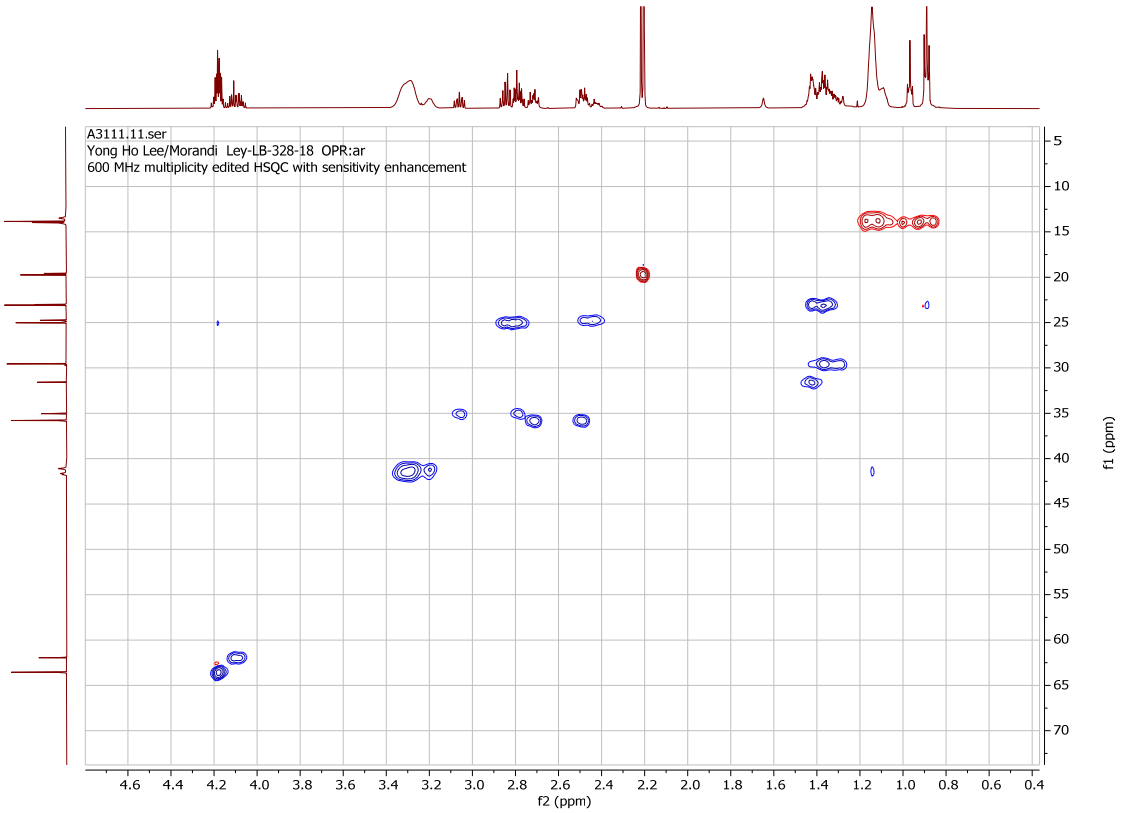
A3111.11.ser
Yong Ho Lee/Morandi Ley-LB-328-18 OPR:ar
600 MHz multiplicity edited HSQC with sensitivity enhancement
f2 (ppm)
f1 (ppm)

(*Z*)-2-(2-((4-methoxybenzyl)oxy)ethyl)-3-(*o*-tolyl)hept-2-enal, B (**46-β-Ar, major**).

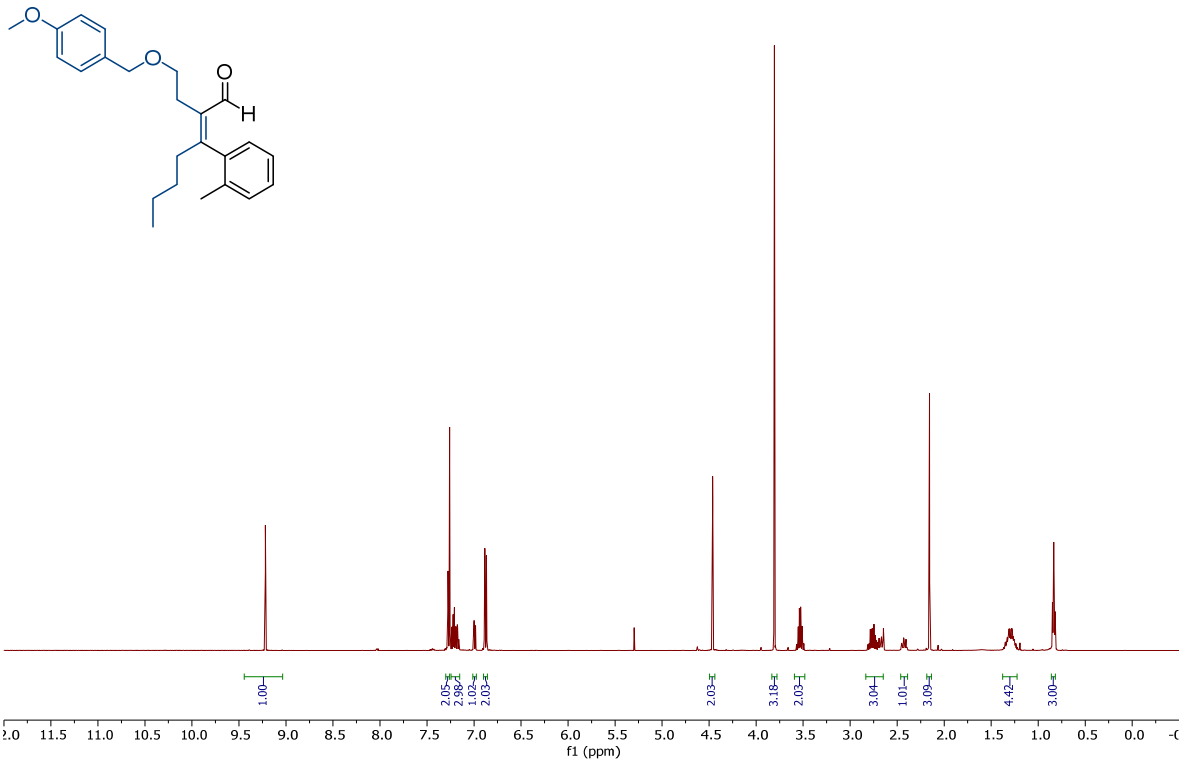

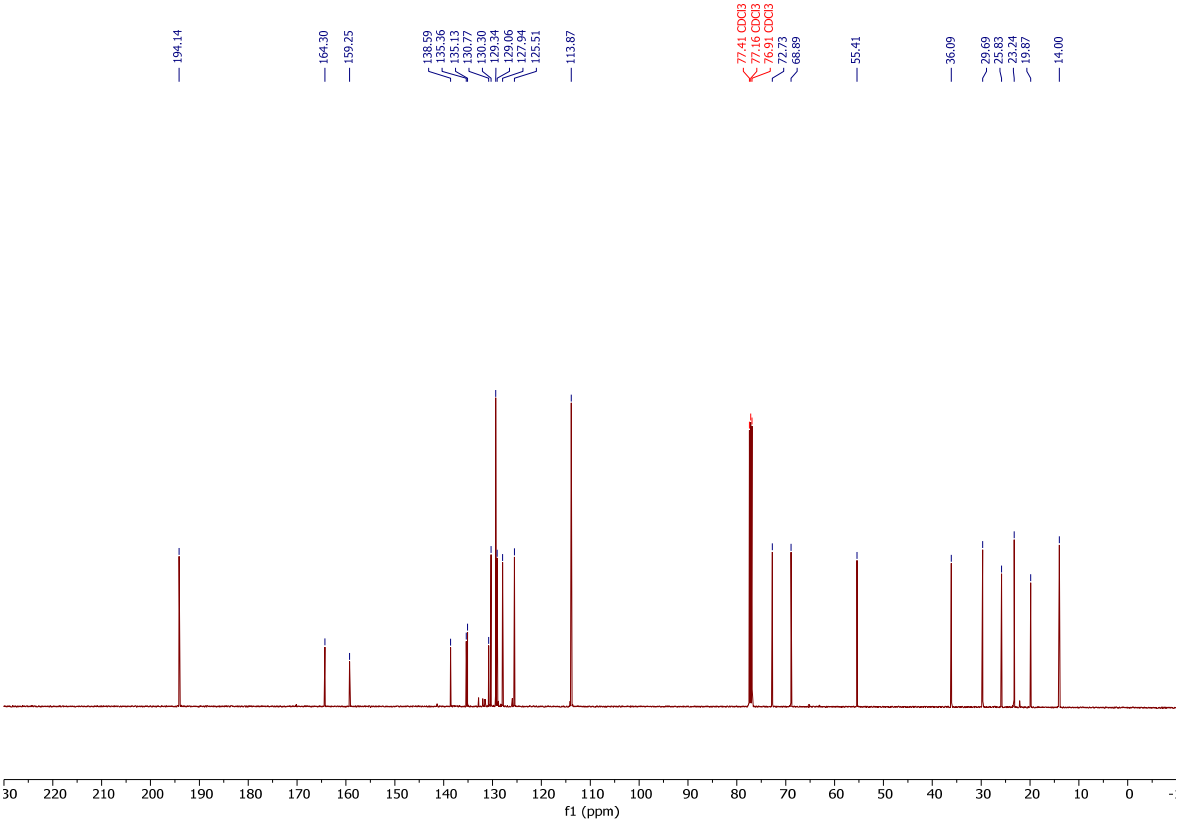

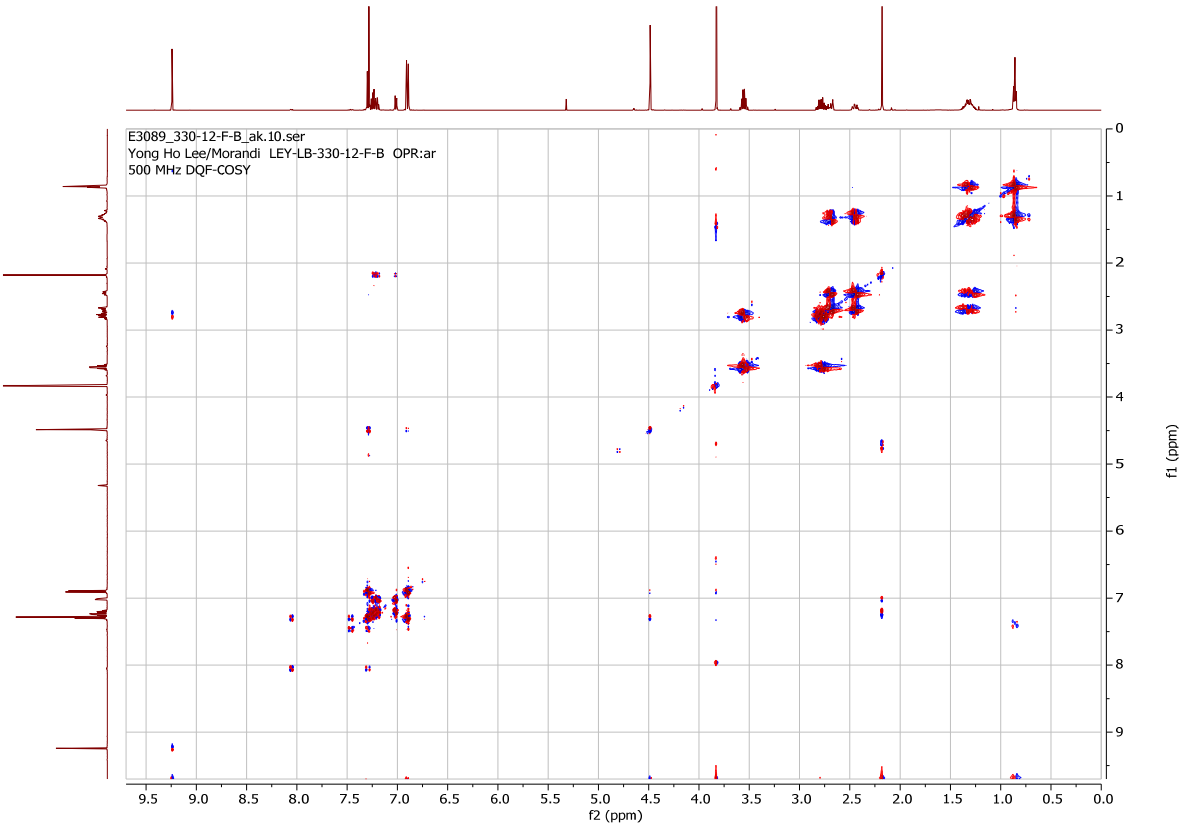
E3089_330-12-F-B_ak.10.ser
Yong Ho Lee/Morandi LEY-LB-330-12-F-B OPR:ar
500 MHz DQF-COSY
f2 (ppm)
f1 (ppm)

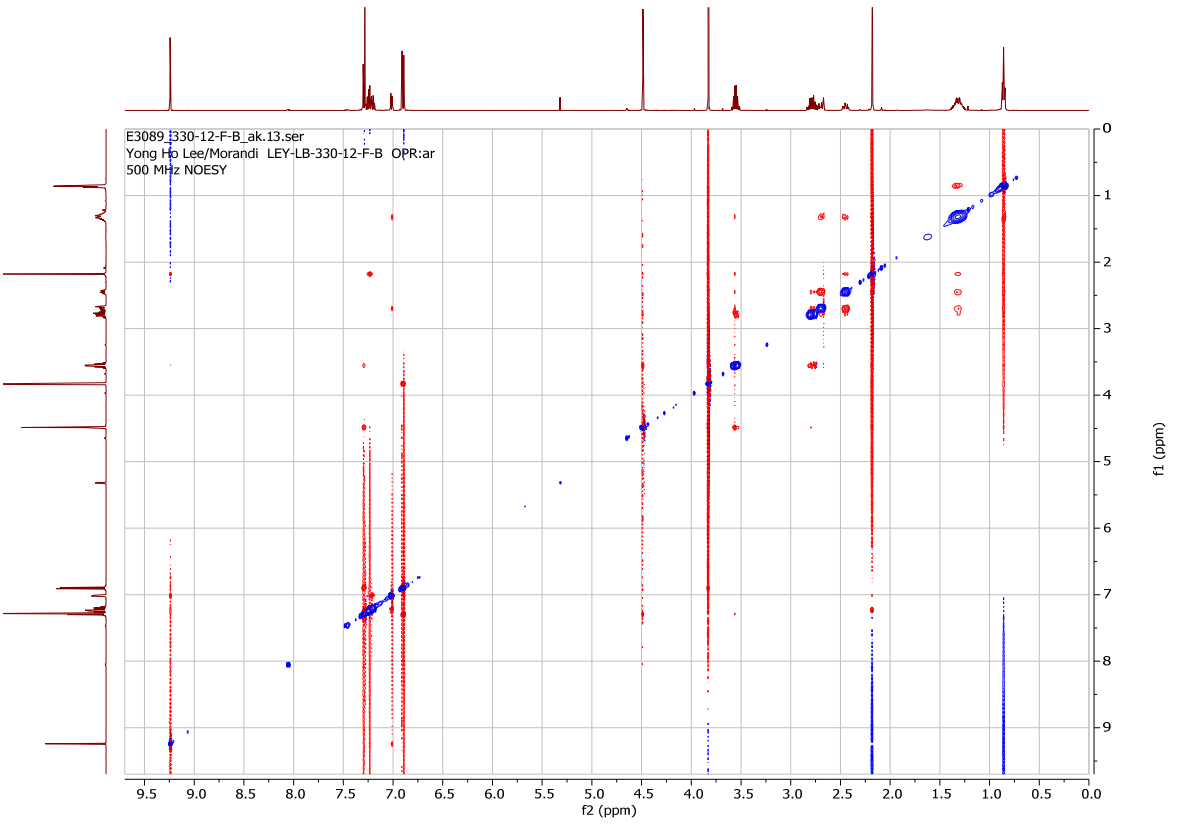
E3089_330-12-F-B_ak.13.ser
Yong Ho Lee/Morandi LEY-LB-330-12-F-B OPR:ar
500 MHz NOESY
f2 (ppm)
f1 (ppm)

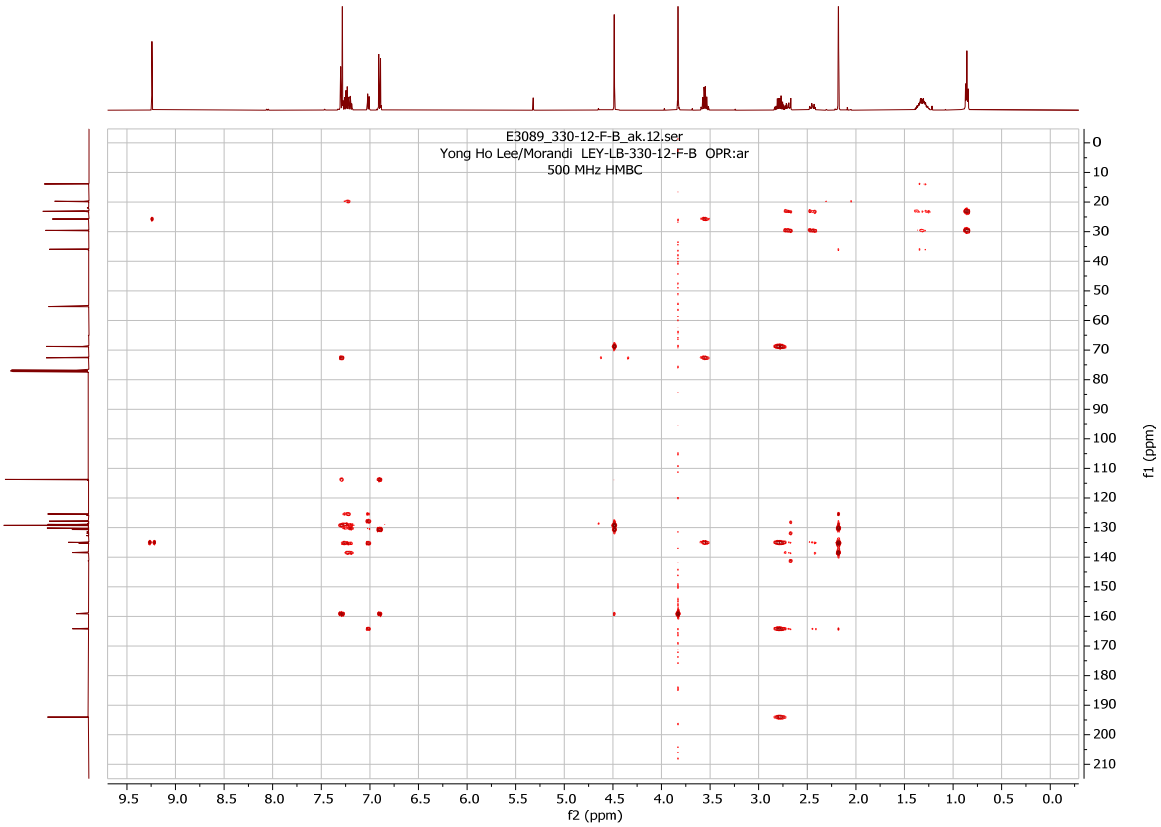
E3089_330-12-F-B_ak.12.ser
Yong Ho Lee/Morandi LEY-LB-330-12-F-B OPR:ar
500 MHz HMBC
f2 (ppm)
f1 (ppm)

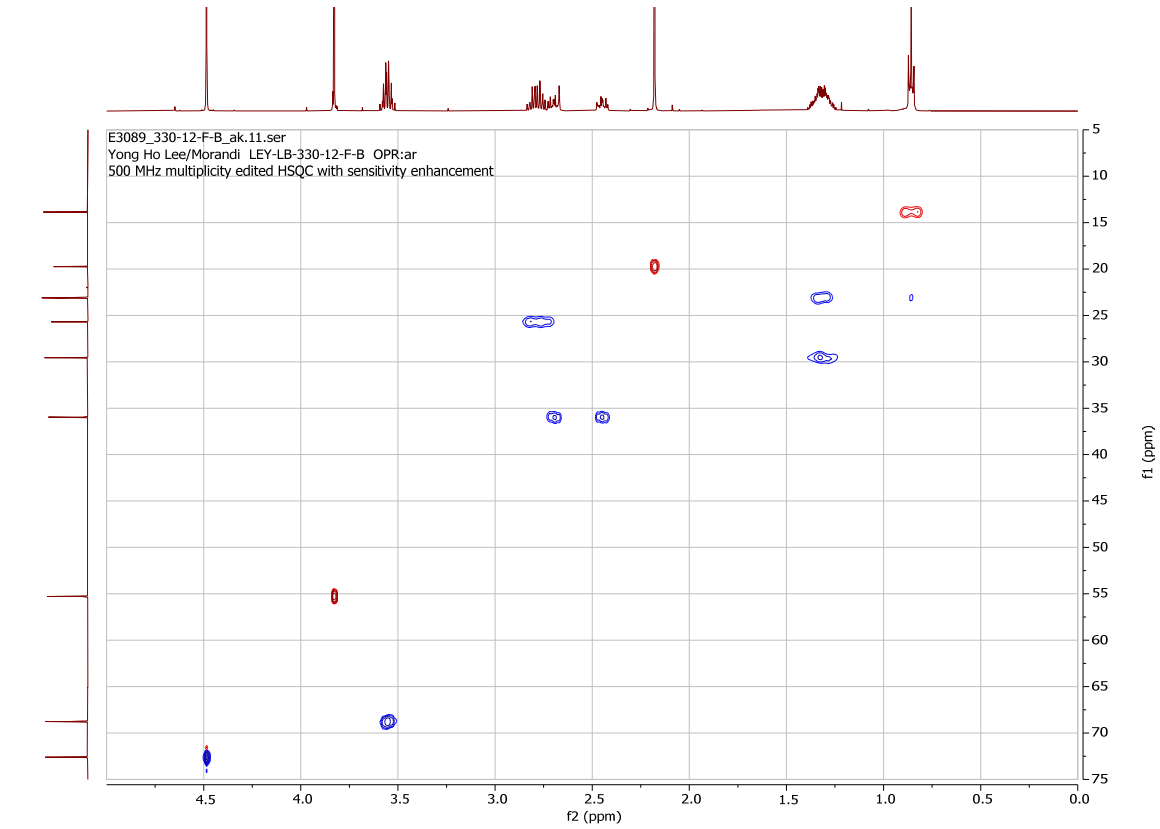
E3089_330-12-F-B_ak.11.ser
Yong Ho Lee/Morandi LEY-LB-330-12-F-B OPR:ar
500 MHz multiplicity edited HSQC with sensitivity enhancement
f2 (ppm)
f1 (ppm)

(*Z*)-2-(3-((4-methoxybenzyl)oxy)-1-(*o*-tolyl)propylidene)hexanal, A (**46-α-Ar, minor**).

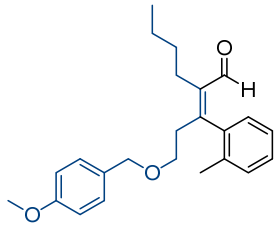

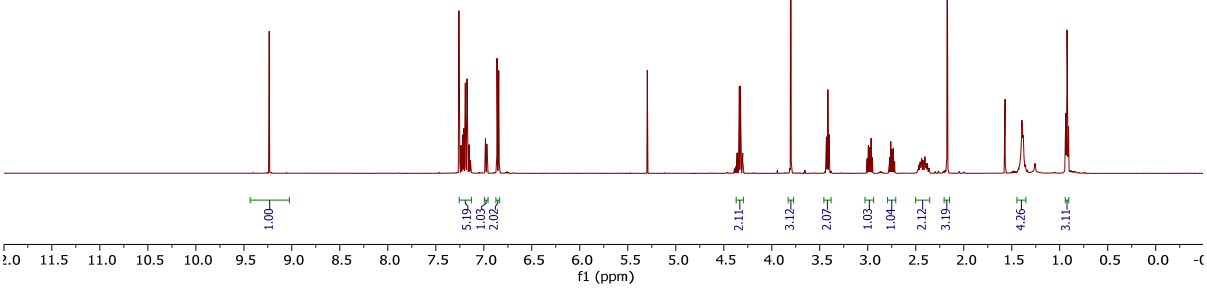

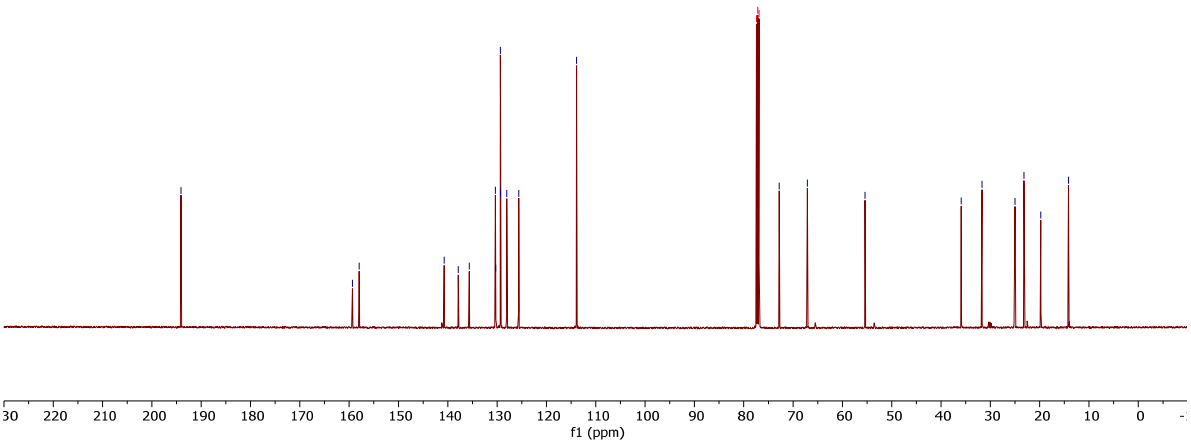

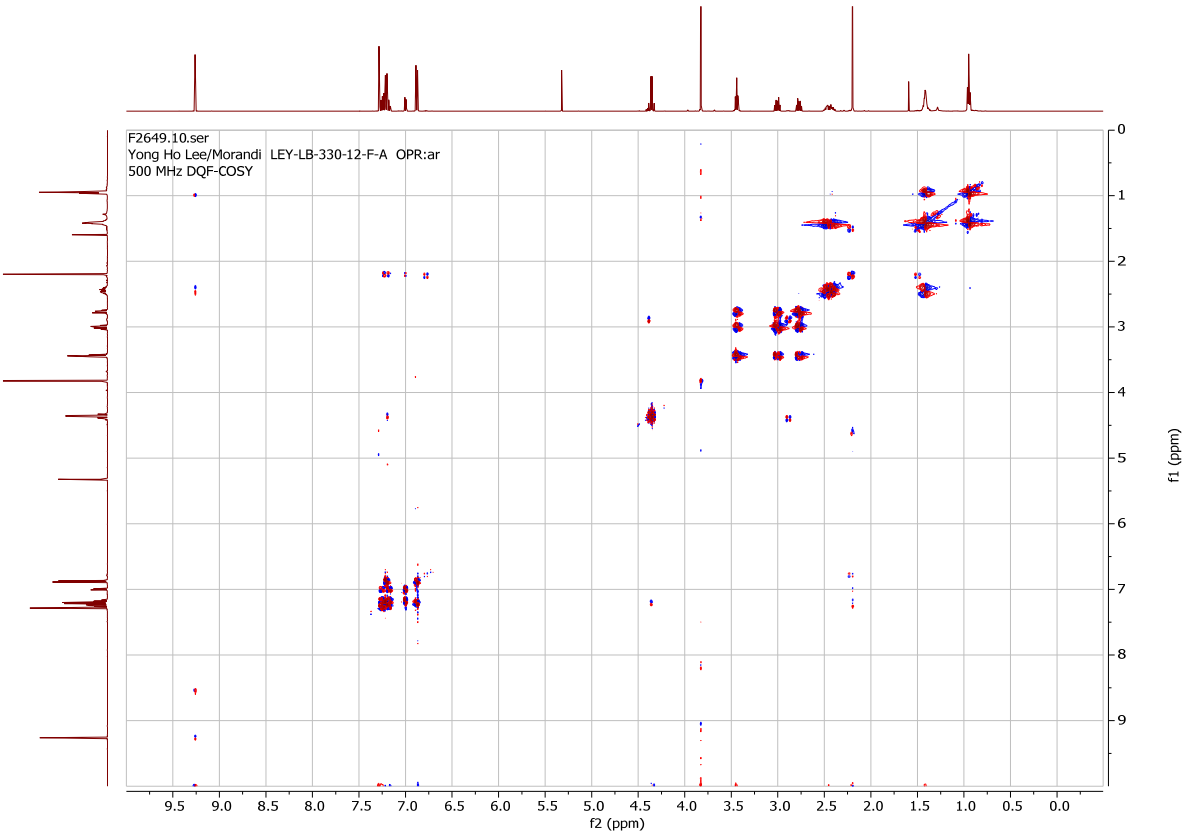
F2649.10.ser
Yong Ho Lee/Morandi LEY-LB-330-12-F-A OPR:ar
500 MHz DQF-COSY
f2 (ppm)
f1 (ppm)

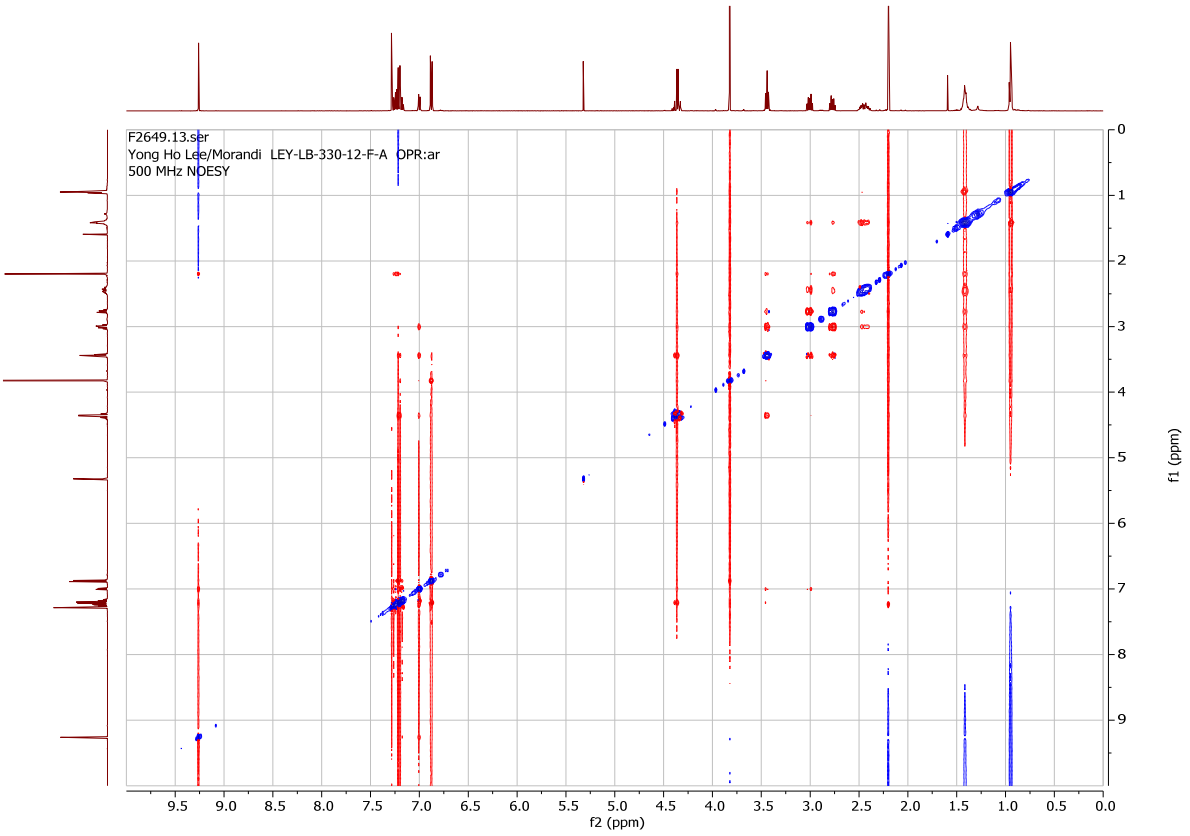
F2649.13.ser
Yong Ho Lee/Morandi LEY-LB-330-12-F-A OPR:ar
500 MHz NOESY
f2 (ppm)
f1 (ppm)

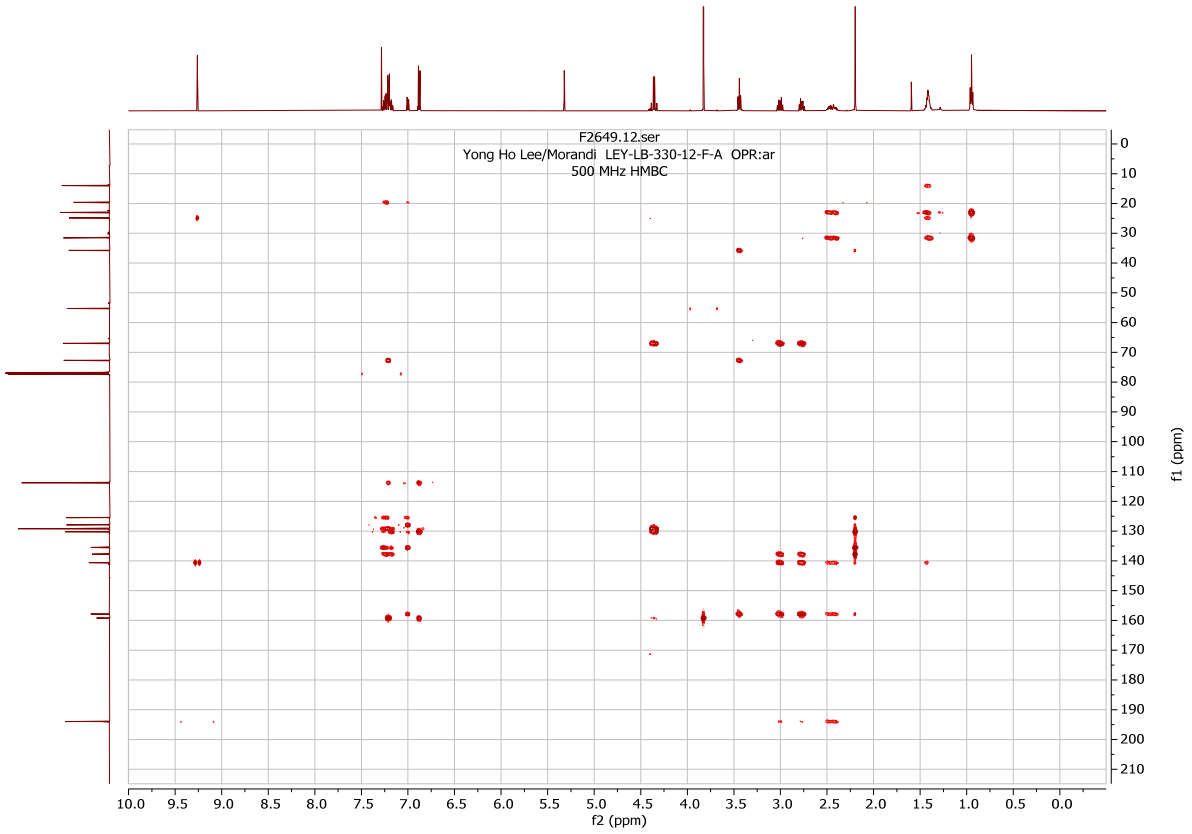
F2649.12.ser
Yong Ho Lee/Morandi LEY-LB-330-12-F-A OPR:ar
500 MHz HMBC
f1 (ppm)
f2 (ppm)

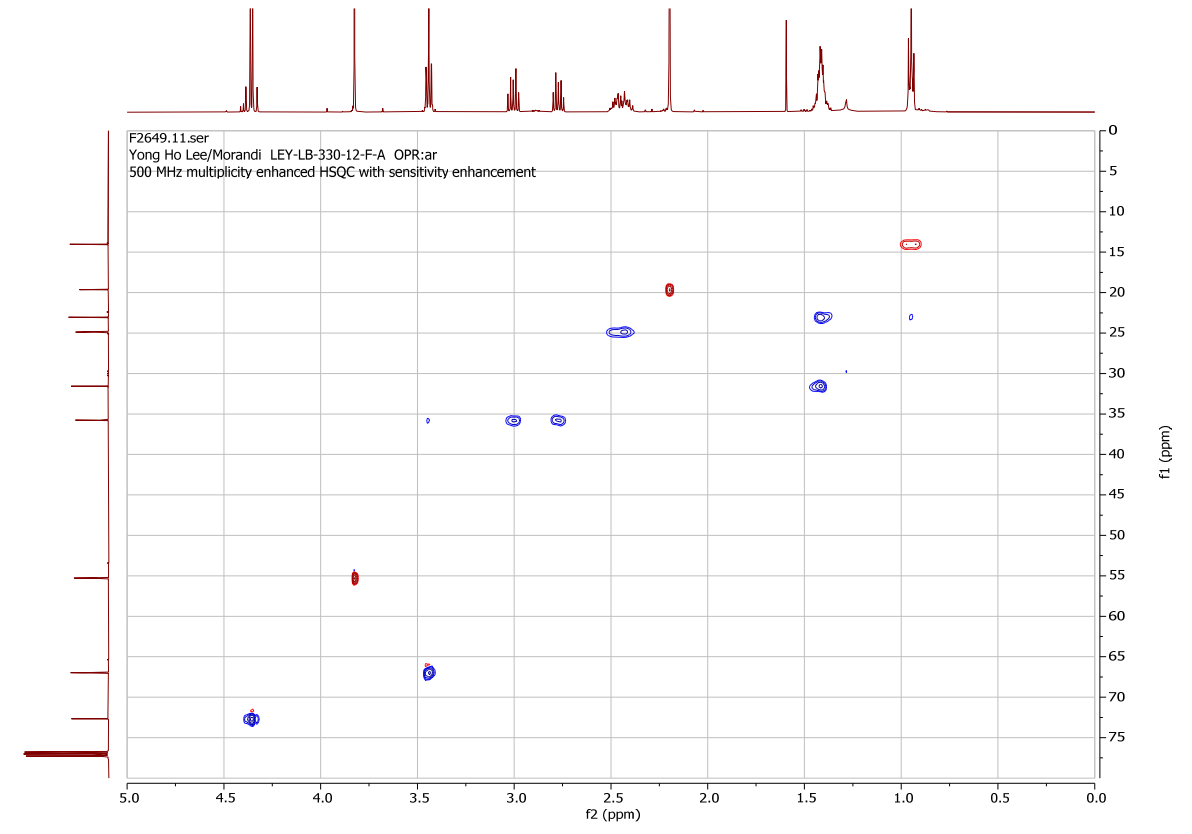
F2649.11.ser
Yong Ho Lee/Morandi LEY-LB-330-12-F-A OPR:ar
500 MHz multiplicity enhanced HSQC with sensitivity enhancement
f1 (ppm)
f2 (ppm)

(*Z*)-9-formyl-10-(*o*-tolyl)dodec-9-en-1-yl benzoate (**47-β-Ar, major**, an inseparable mixture of regioisomers, **β-Ar**/α-Ar = 53:47).

(*Z*)-10-formyl-9-(*o*-tolyl)dodec-9-en-1-yl benzoate (**47-α-Ar, minor**, an inseparable mixture of regioisomers, β-Ar/**α-Ar** = 53:47).

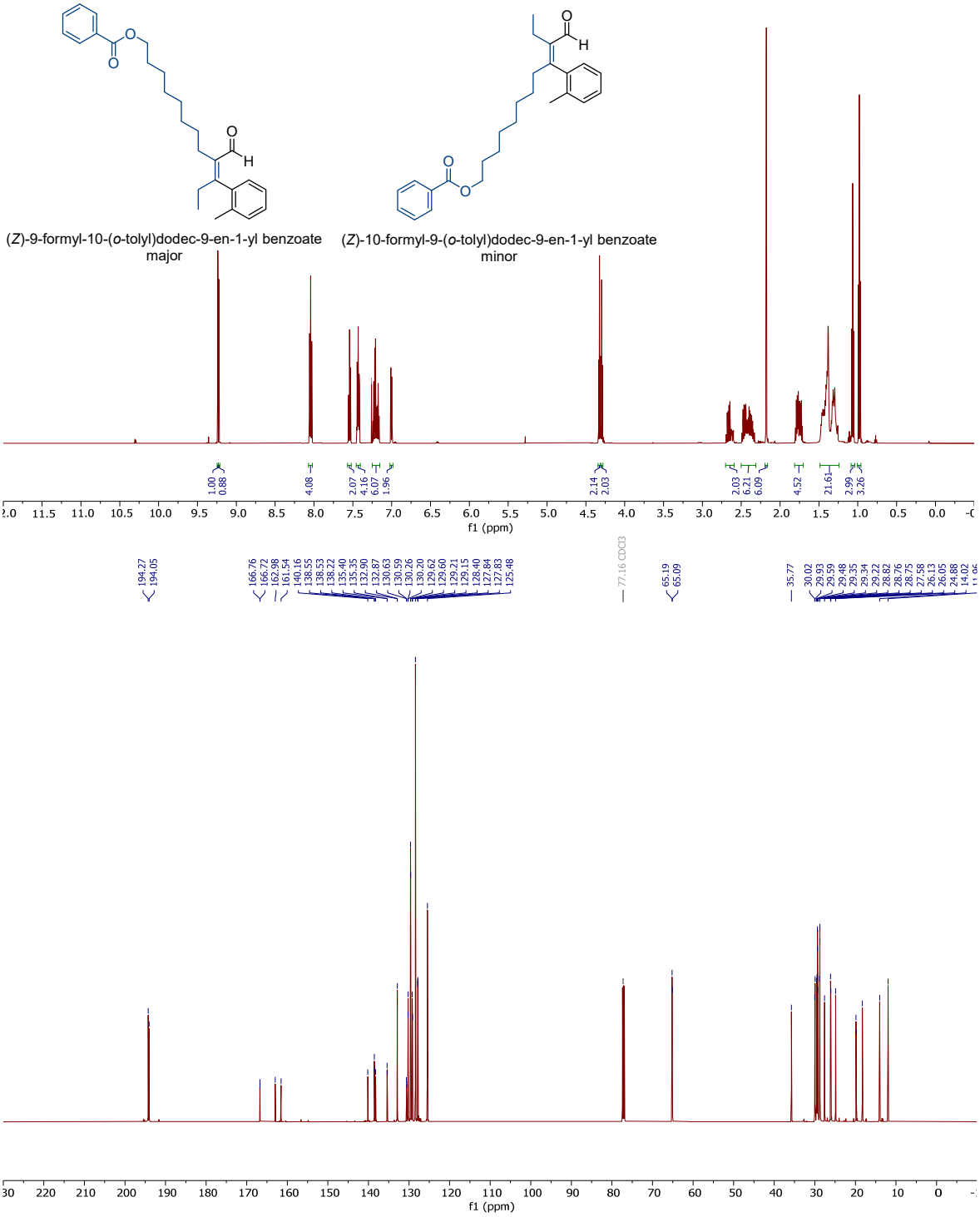

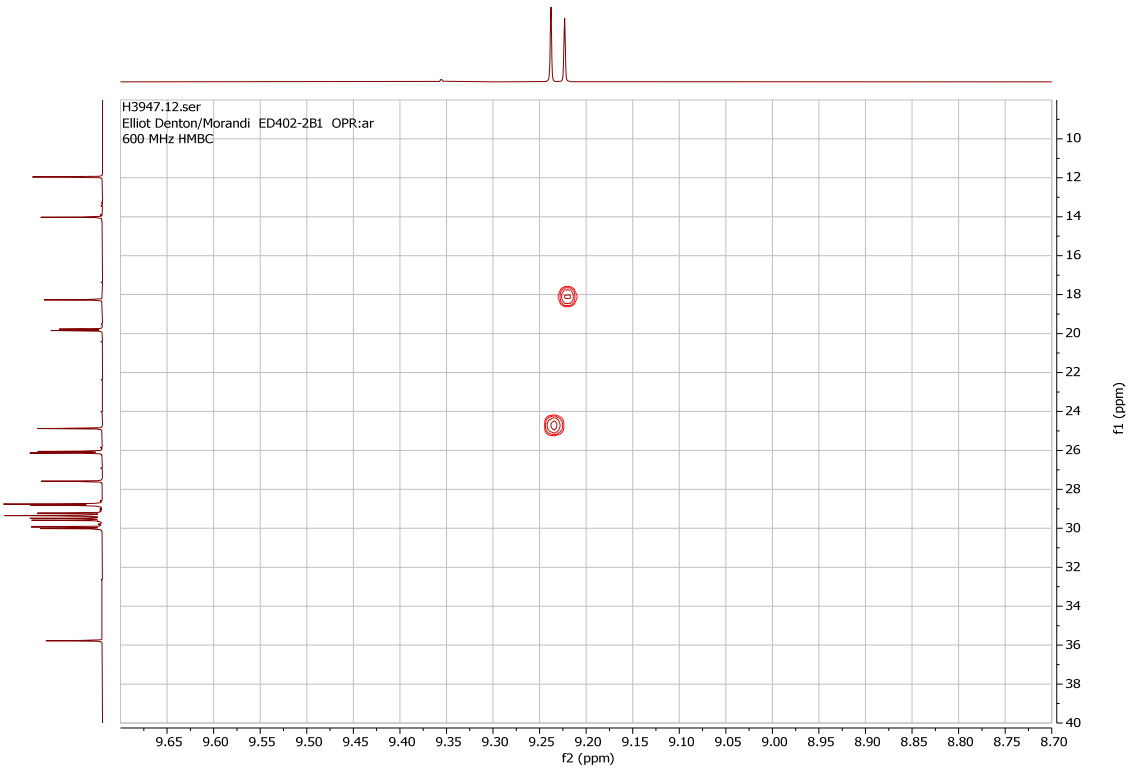
H3947.12.ser
Elliot Denton/Morandi ED402-2B1 OPR:ar
600 MHz HMBC
f2 (ppm)
f1 (ppm)

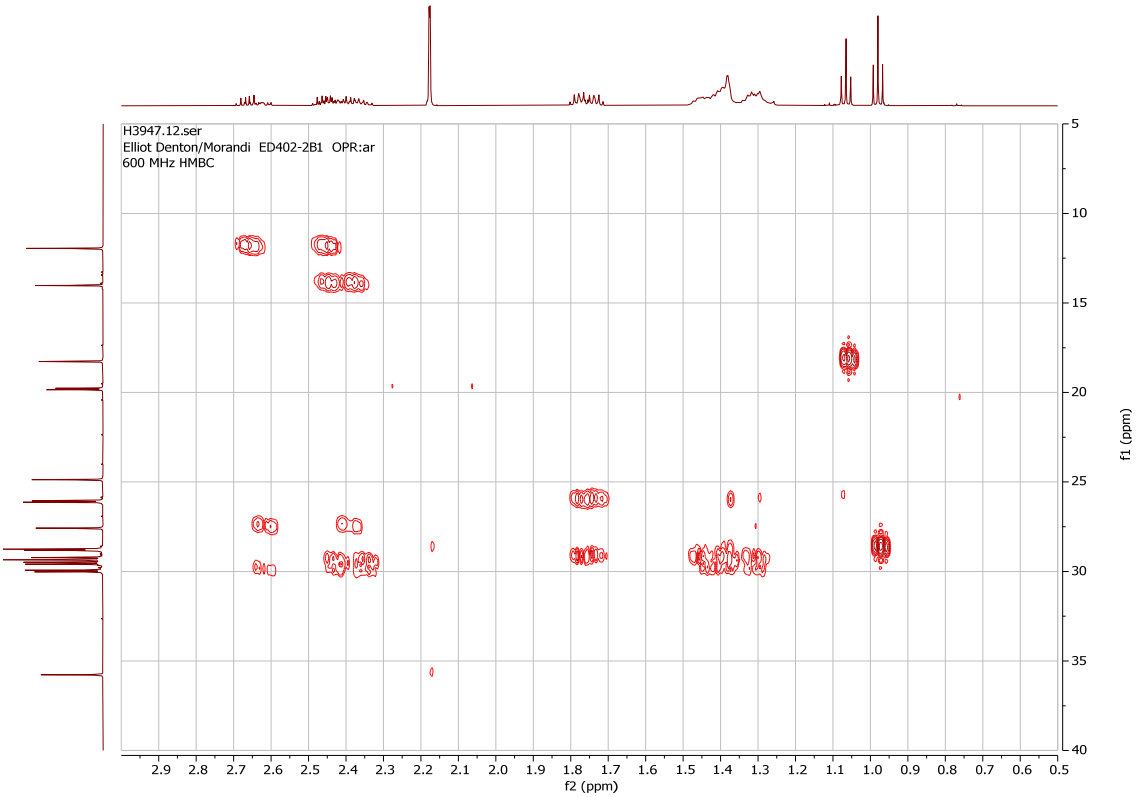
H3947.12.ser
Elliot Denton/Morandi ED402-2B1 OPR:ar
600 MHz HMBC
f2 (ppm)
f1 (ppm)

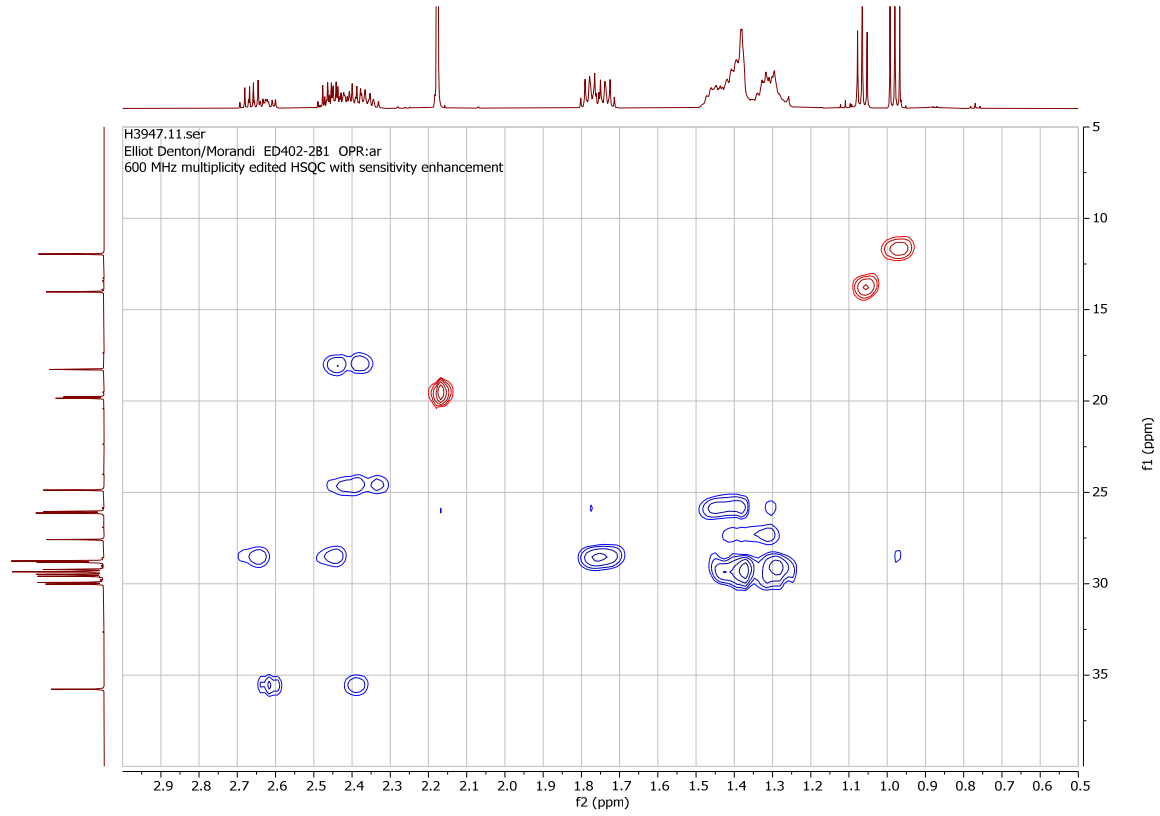
H3947.11.ser
Elliot Denton/Morandi ED402-2B1 OPR:ar
600 MHz multiplicity edited HSQC with sensitivity enhancement
f2 (ppm)
f1 (ppm)

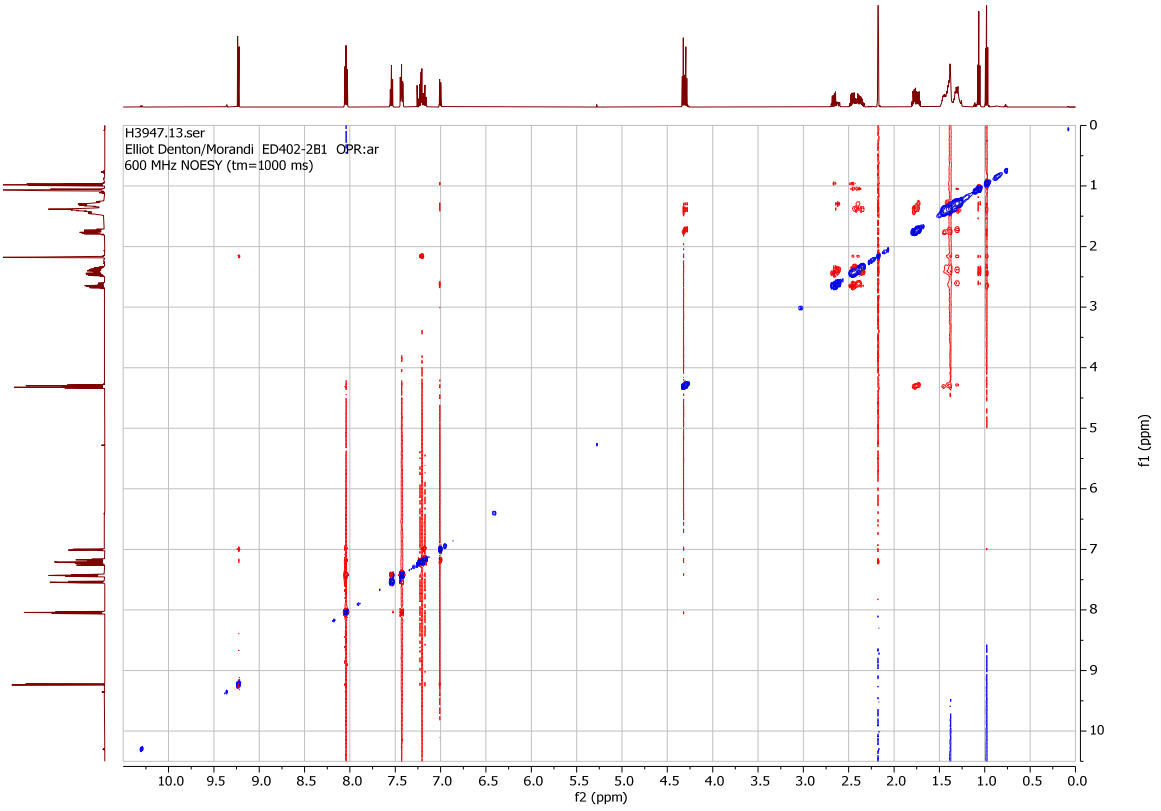
H3947.13.ser
Elliot Denton/Morandi ED402-2B1 OPR:ar
600 MHz NOESY (tm=1000 ms)
f2 (ppm)
f1 (ppm)

(*Z*)-5-formyl-6-(*o*-tolyl)dec-5-en-1-yl benzoate (**48-β-Ar, major**).

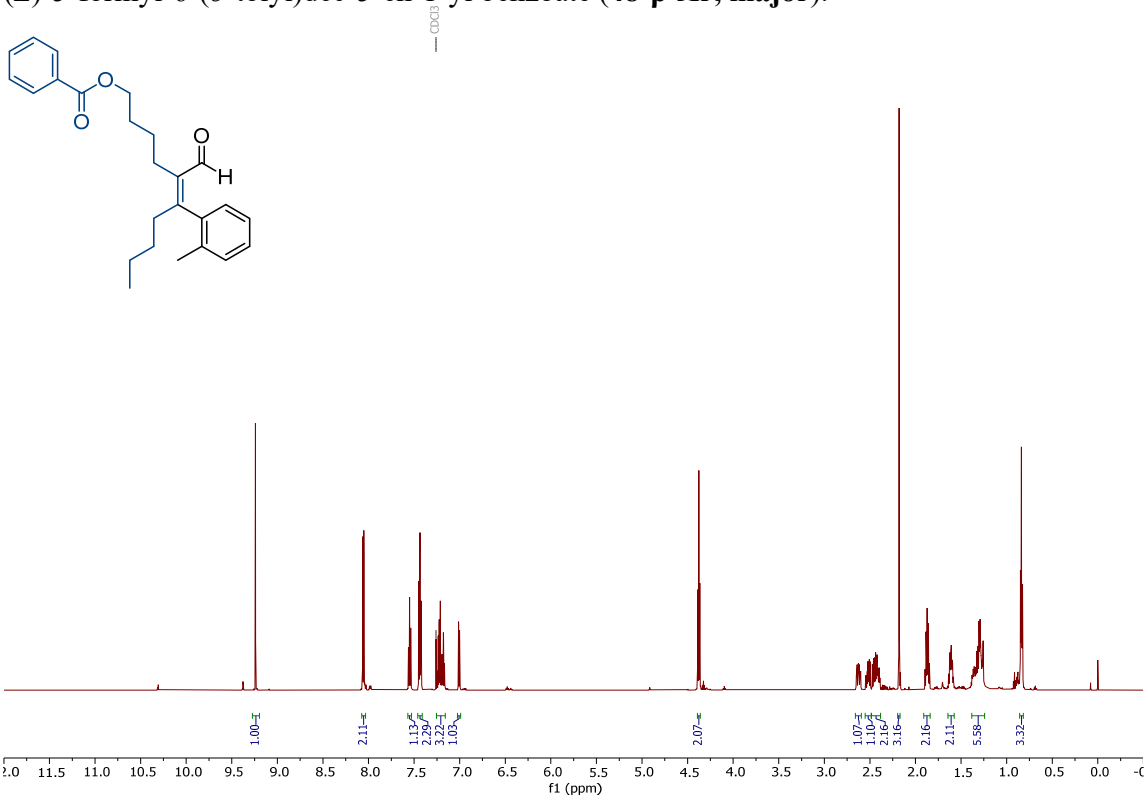

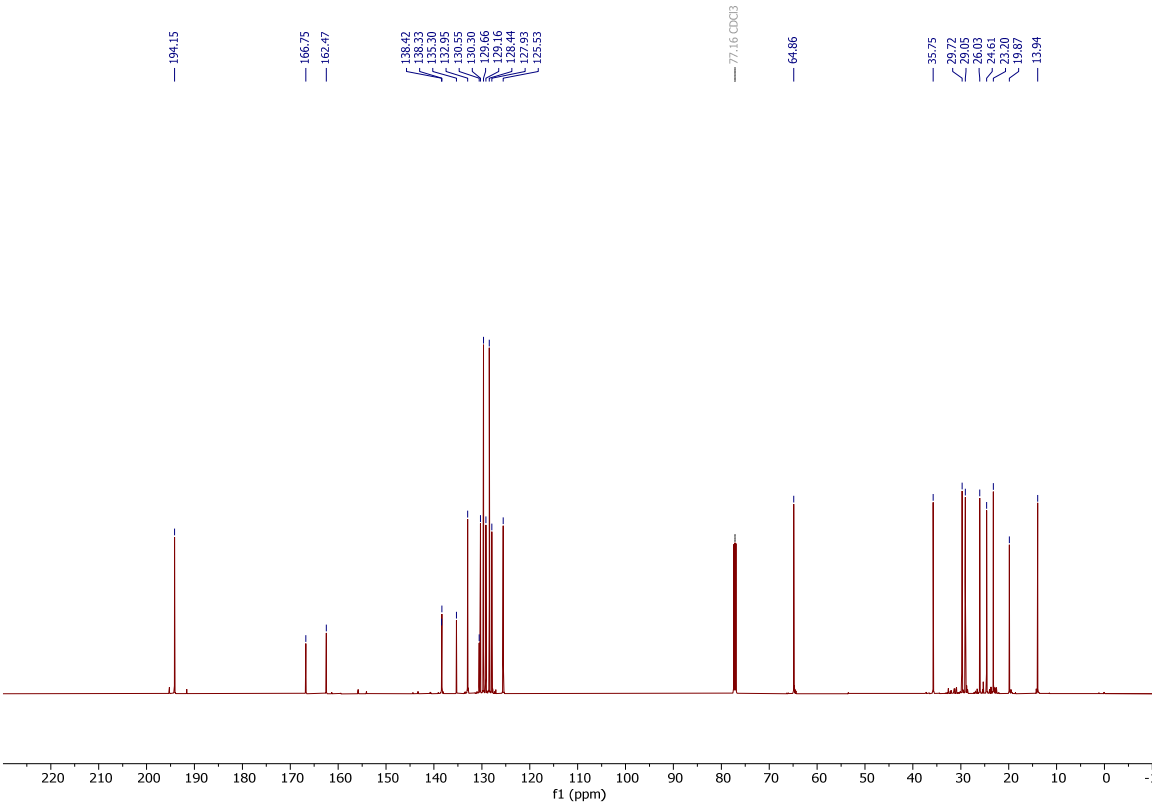

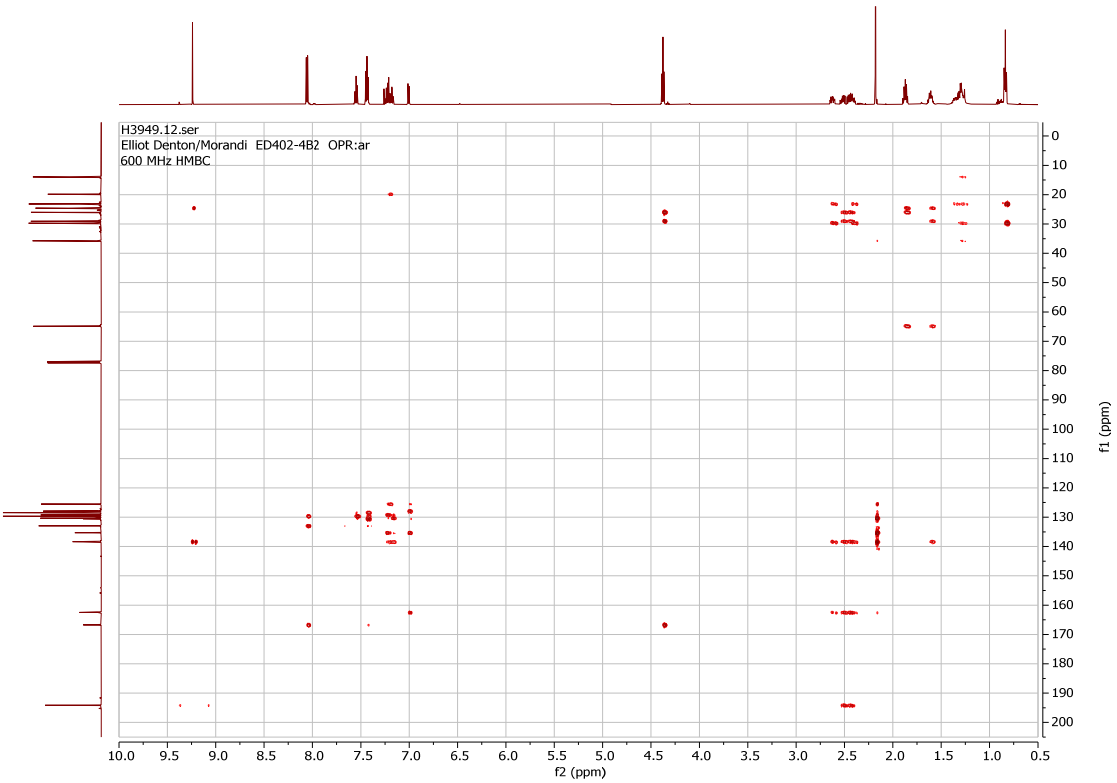
H3949.12.ser
Elliot Denton/Morandi ED402-4B2 OPR:ar
600 MHz HMBC
f2 (ppm)
f1 (ppm)

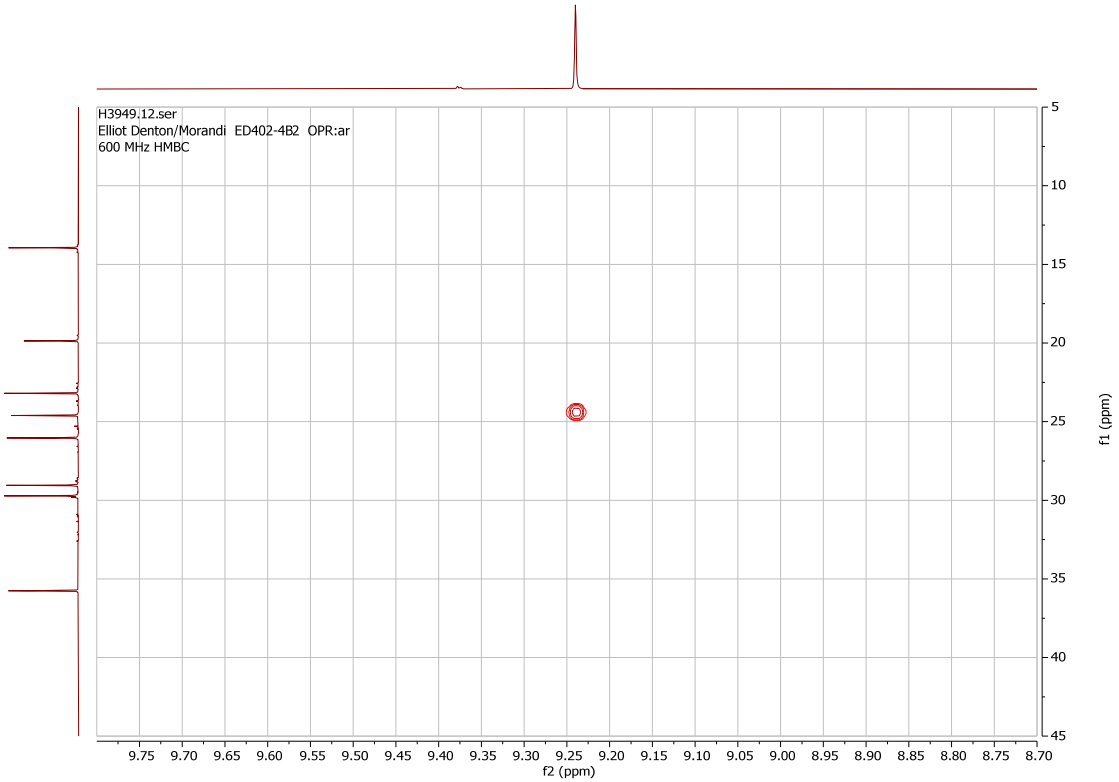
H3949.12.ser
Elliot Denton/Morandi ED402-4B2 OPR:ar
600 MHz HMBC
f2 (ppm)
f1 (ppm)

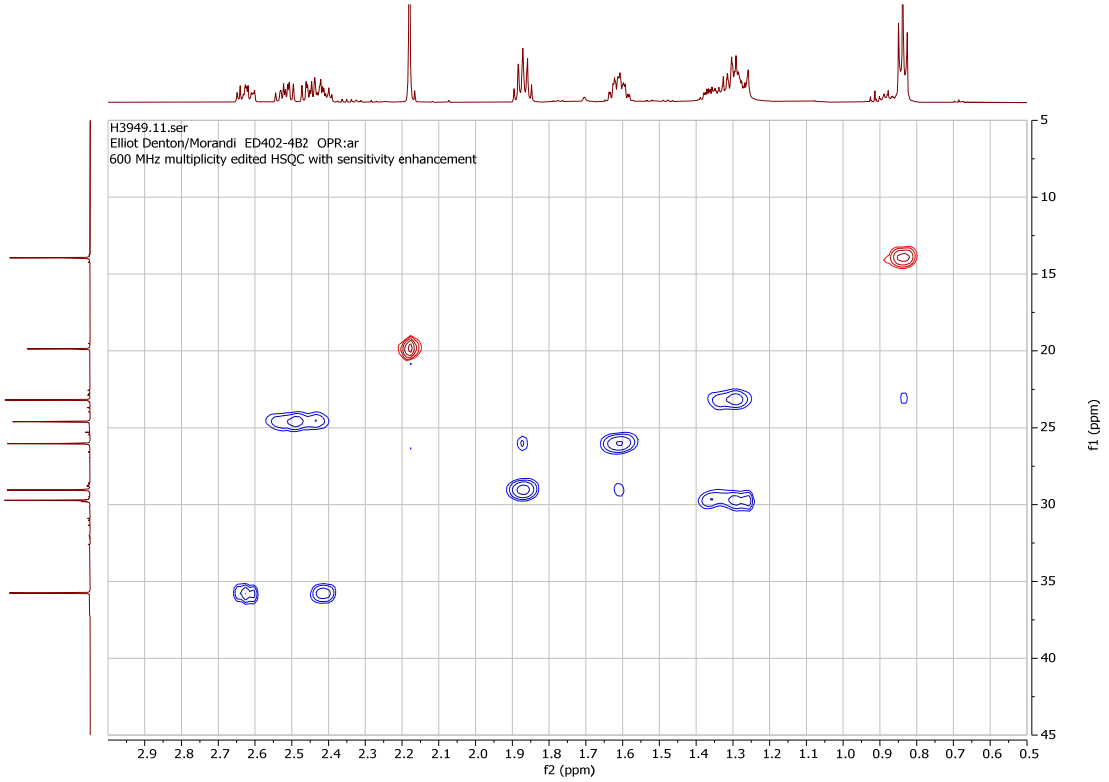
H3949.11.ser
Elliot Denton/Morandi ED402-4B2 OPR:ar
600 MHz multiplicity edited HSQC with sensitivity enhancement
f2 (ppm)
f1 (ppm)

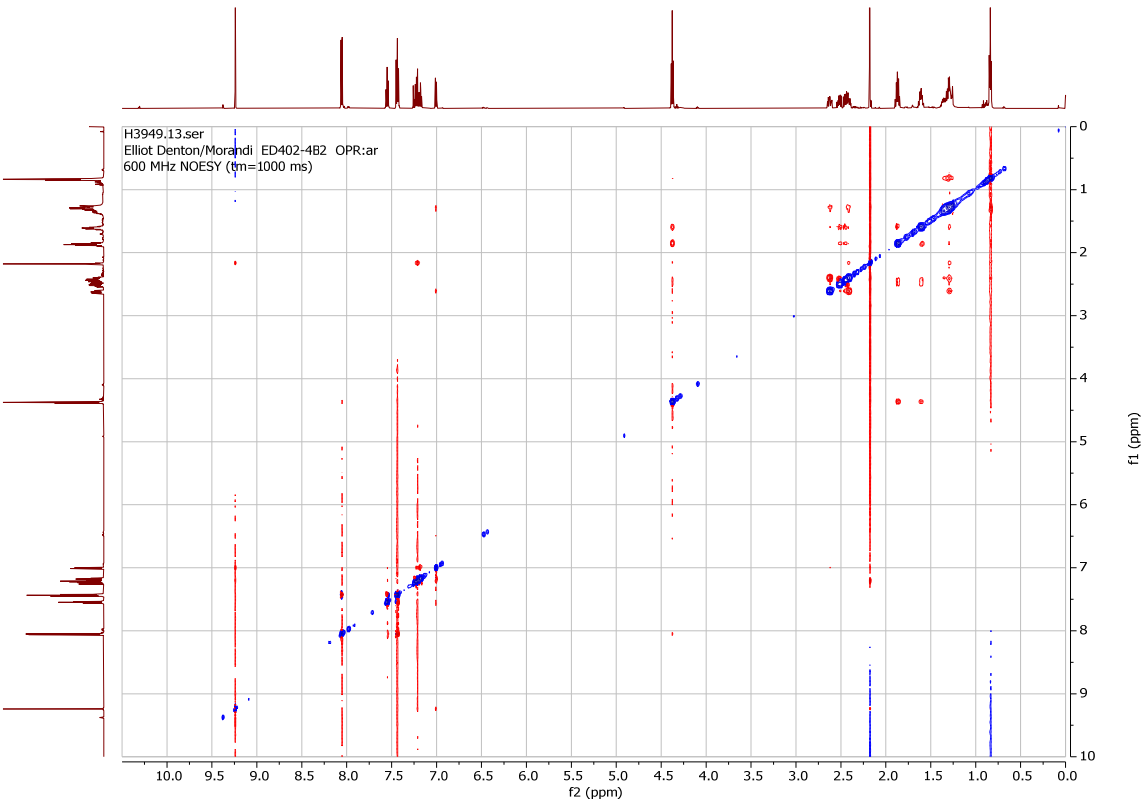
H3949.13.ser
Elliot Denton/Morandi ED402-4B2 OPR:ar
600 MHz NOESY (tm=1000 ms)
f2 (ppm)
f1 (ppm)

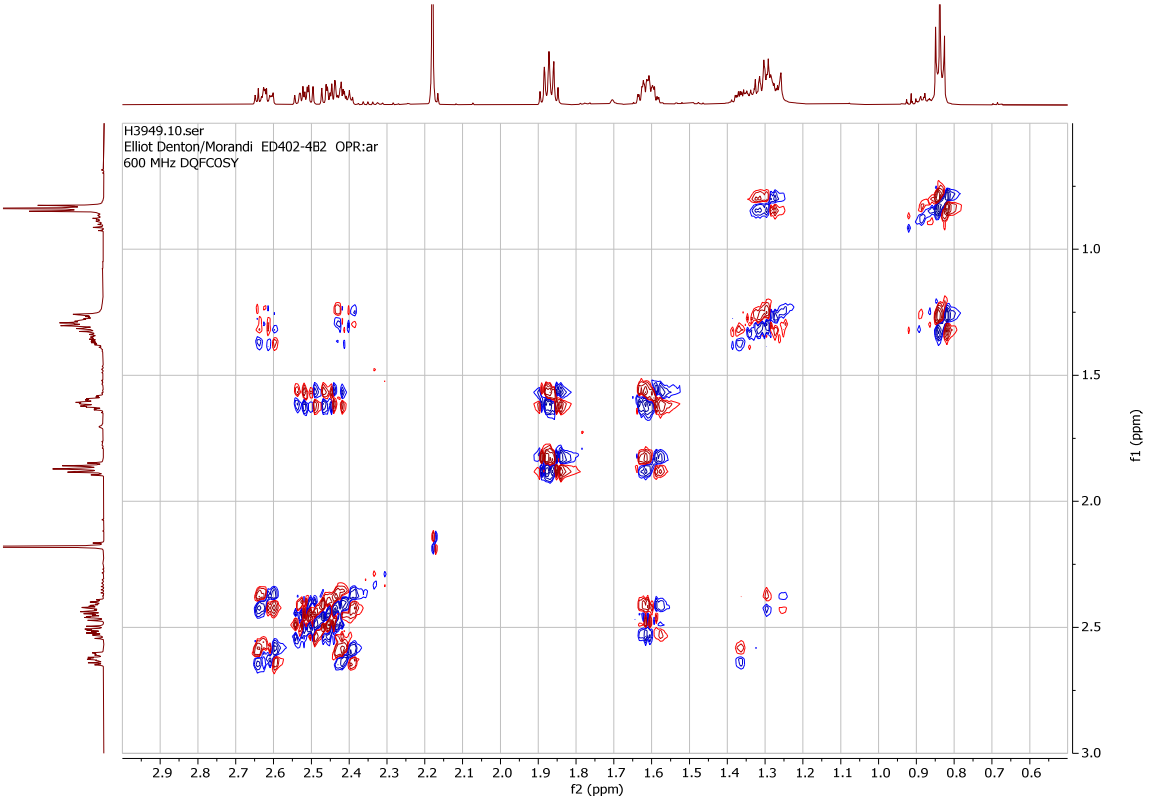
H3949.10.ser
Elliot Denton/Morandi ED402-4B2 OPR:ar
600 MHz DQFCOSY
f2 (ppm)
f1 (ppm)

(*Z*)-6-formyl-5-(*o*-tolyl)dec-5-en-1-yl benzoate (**48-α-Ar, minor**).

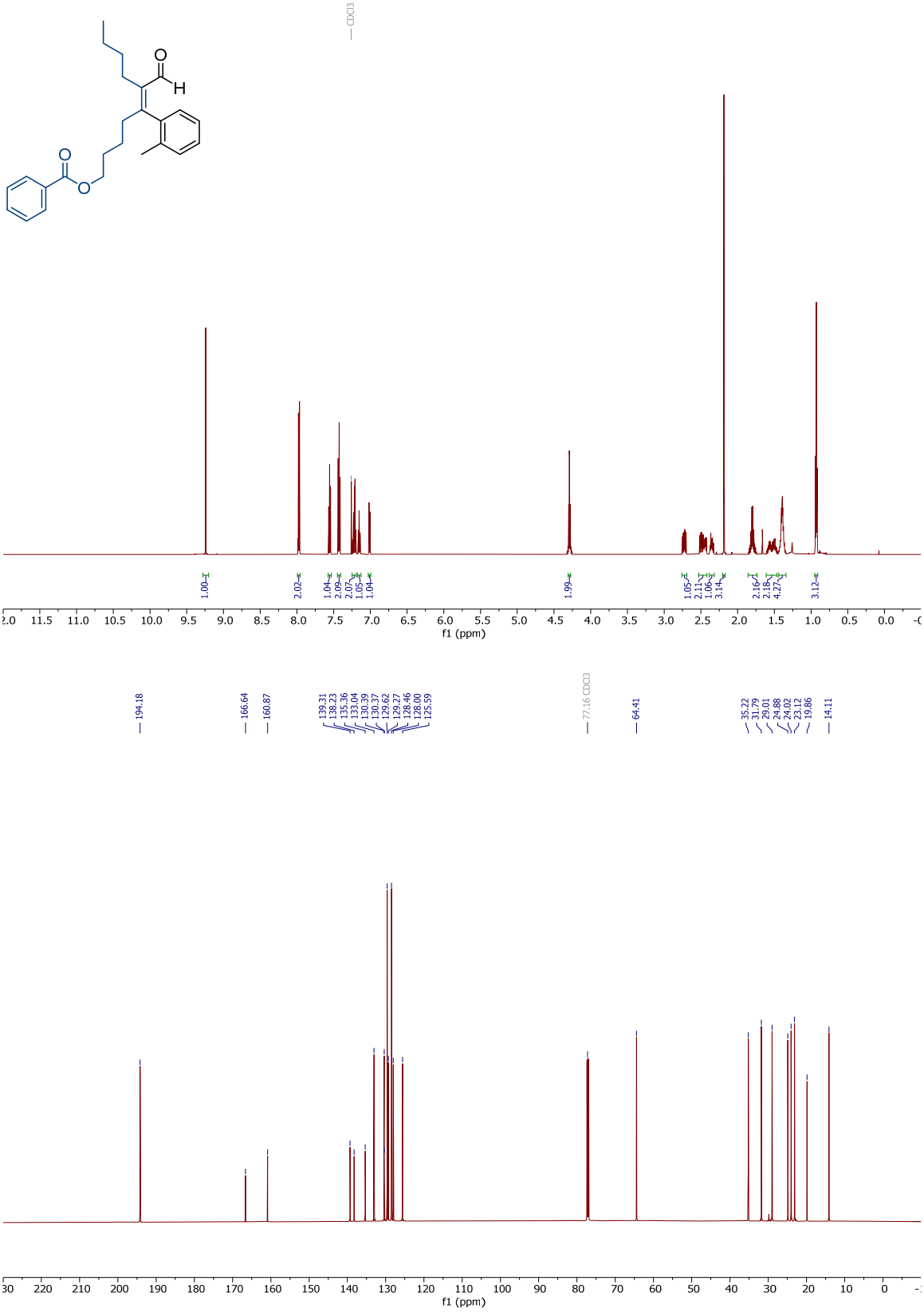

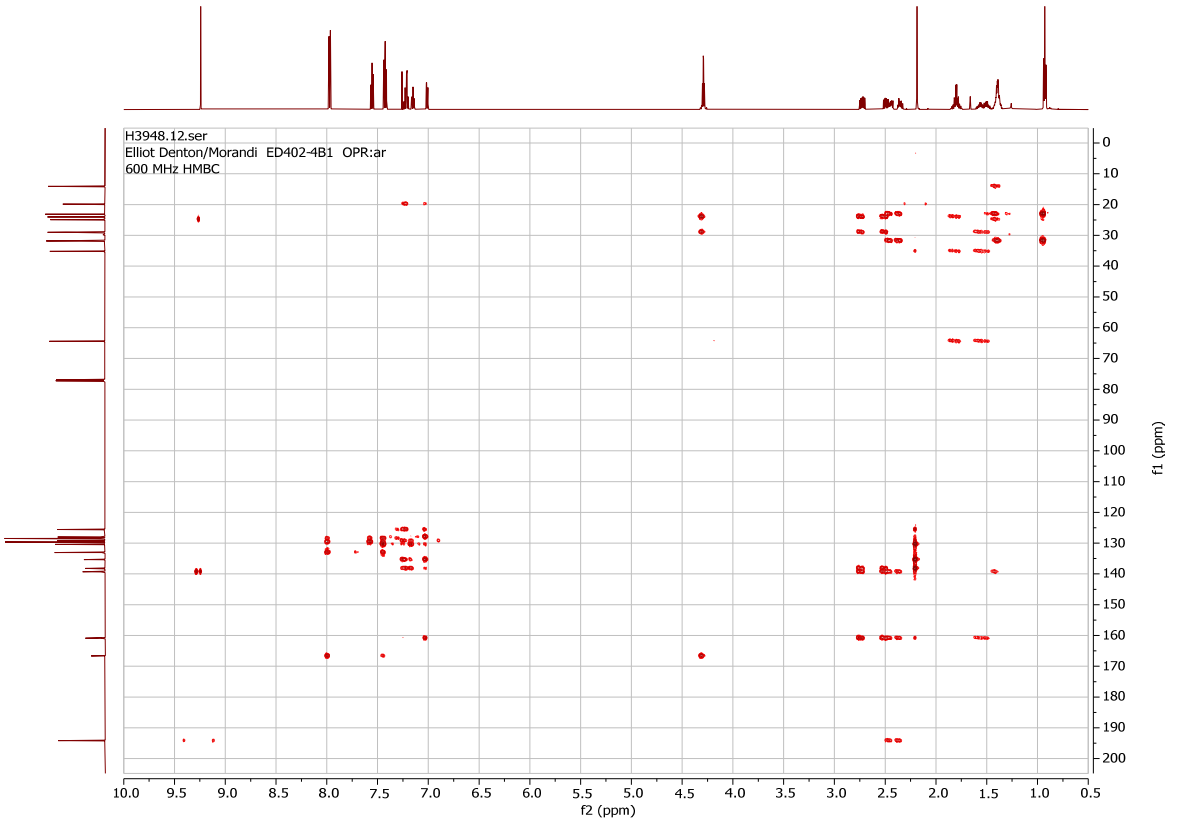
H3948.12.ser
Elliot Denton/Morandi ED402-4B1 OPR:ar
600 MHz HMBC
f2 (ppm)
f1 (ppm)

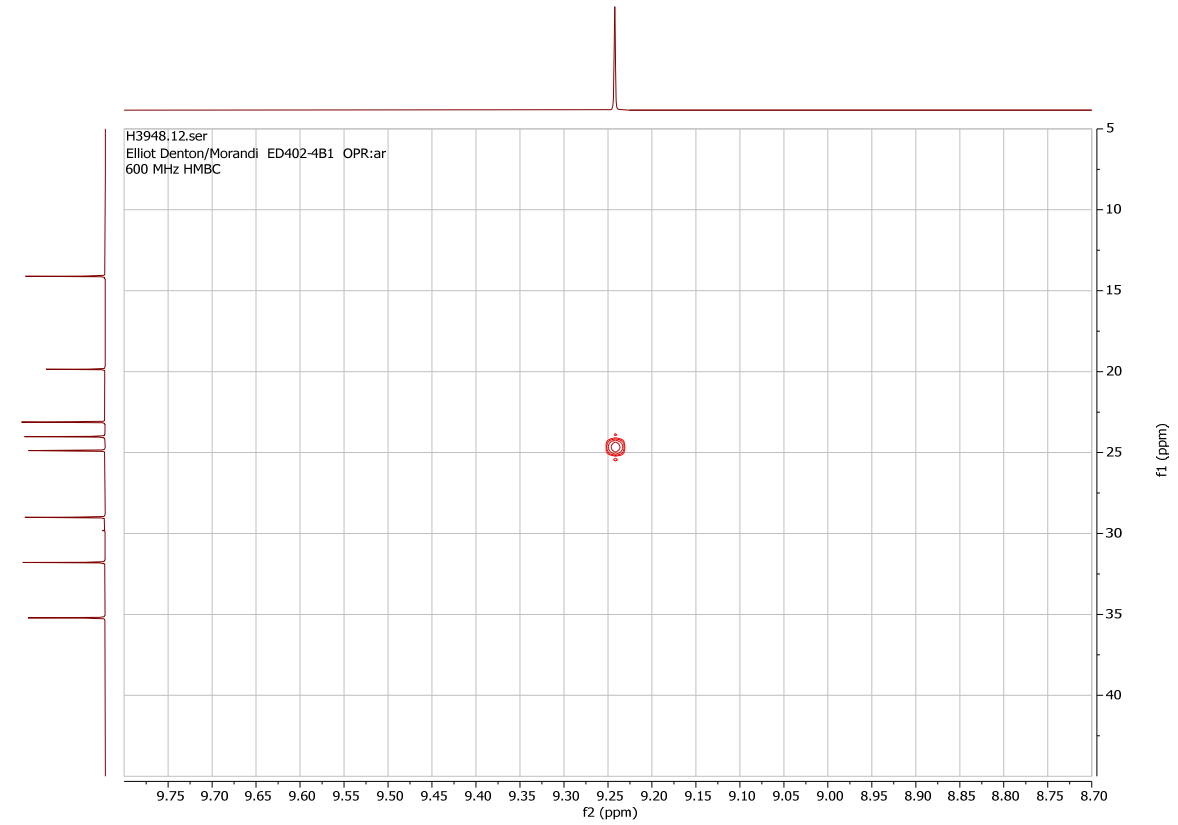
H3948.12.ser
Elliot Denton/Morandi ED402-4B1 OPR:ar
600 MHz HMBC
f2 (ppm)
f1 (ppm)

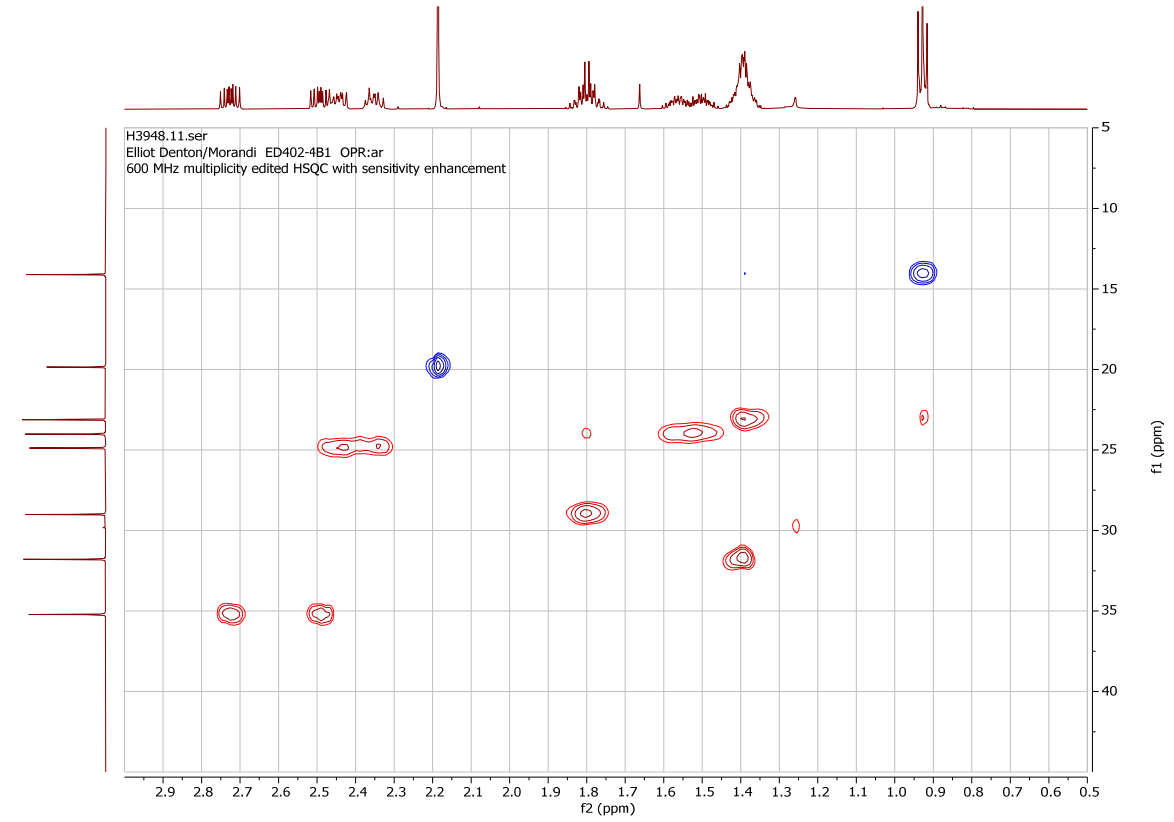
H3948.11.ser
Elliot Denton/Morandi ED402-4B1 OPR:ar
600 MHz multiplicity edited HSQC with sensitivity enhancement
f2 (ppm)
f1 (ppm)

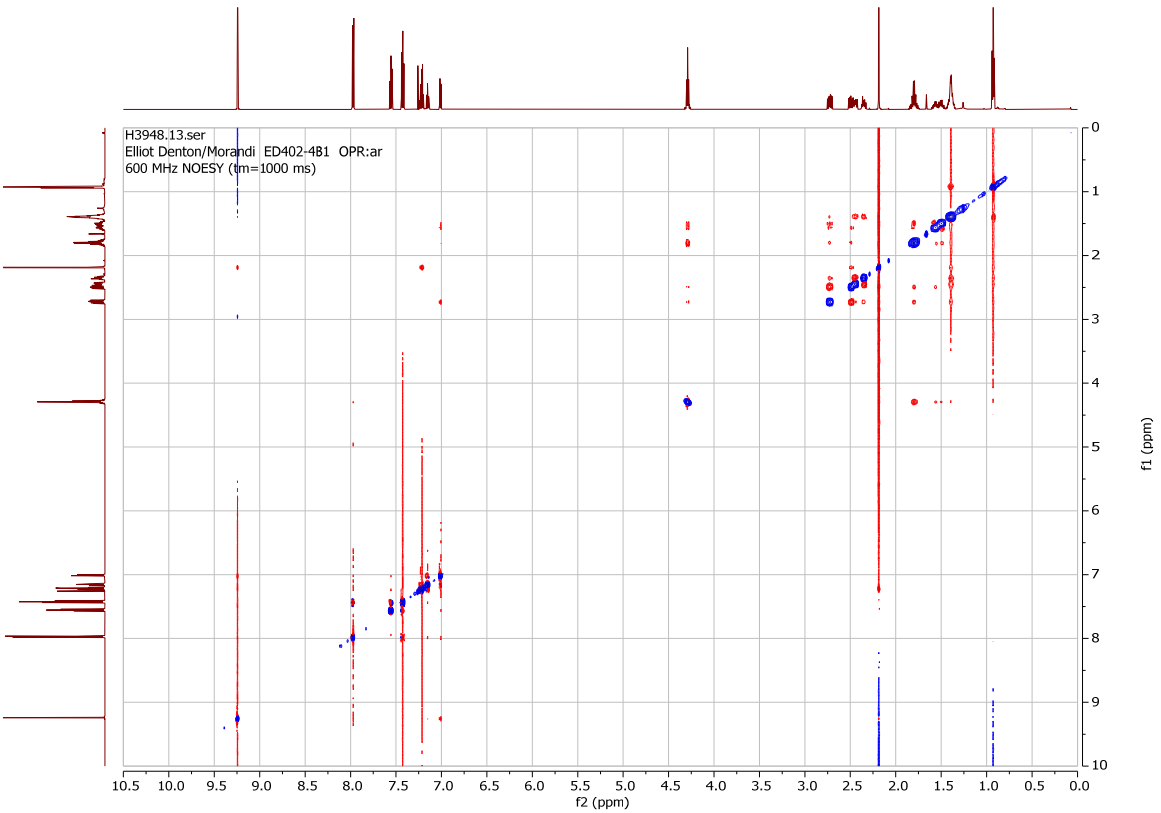
H3948.13.ser
Elliot Denton/Morandi ED402-4B1 OPR:ar
600 MHz NOESY (tm=1000 ms)
f2 (ppm)
f1 (ppm)

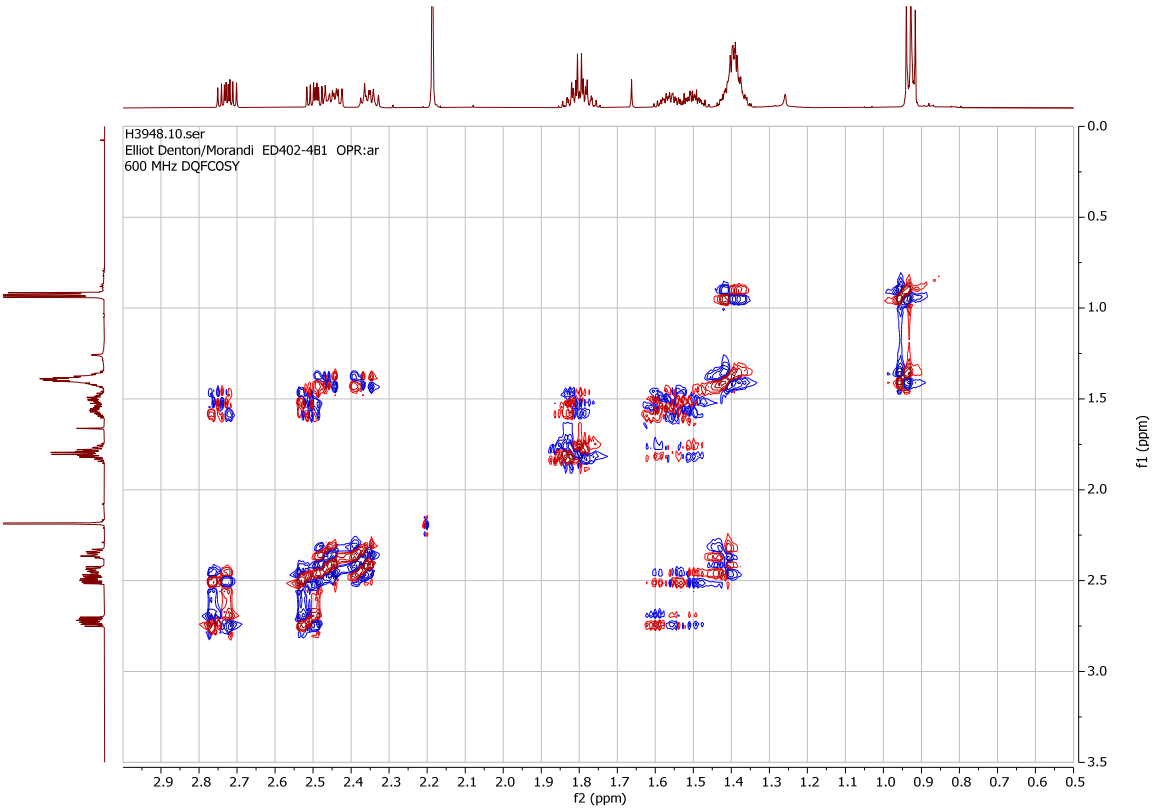
H3948.10.ser
Elliot Denton/Morandi ED402-4B1 OPR:ar
600 MHz DQFCOSY
f2 (ppm)
f1 (ppm)

Methyl (*E*)-2-formyl-3-mesityloct-2-enoate (**49**).

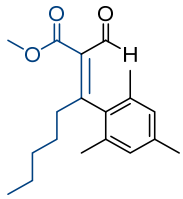

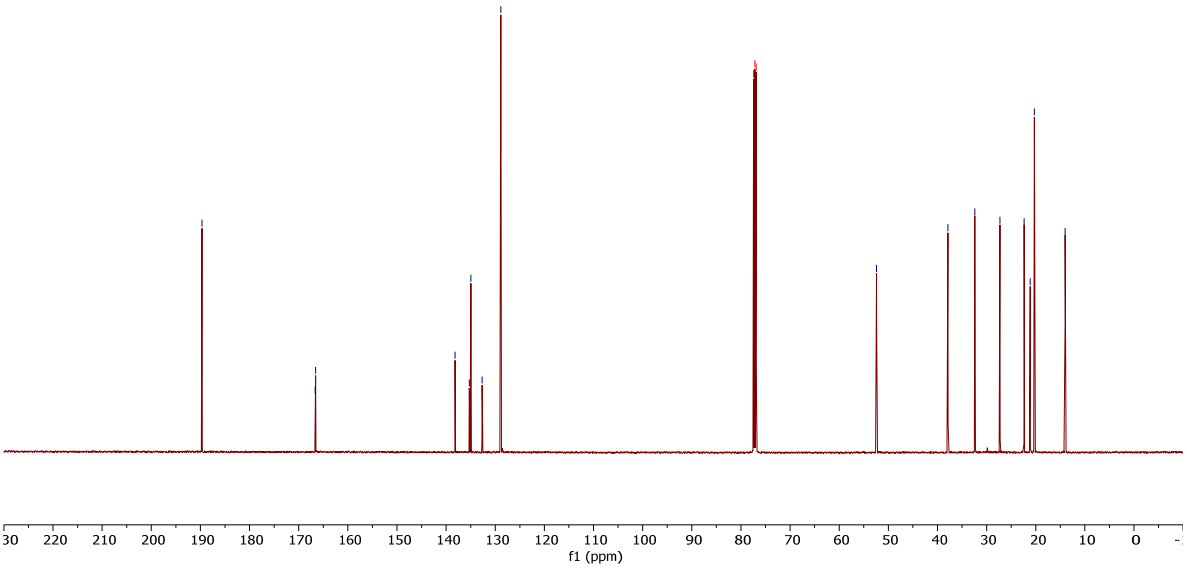

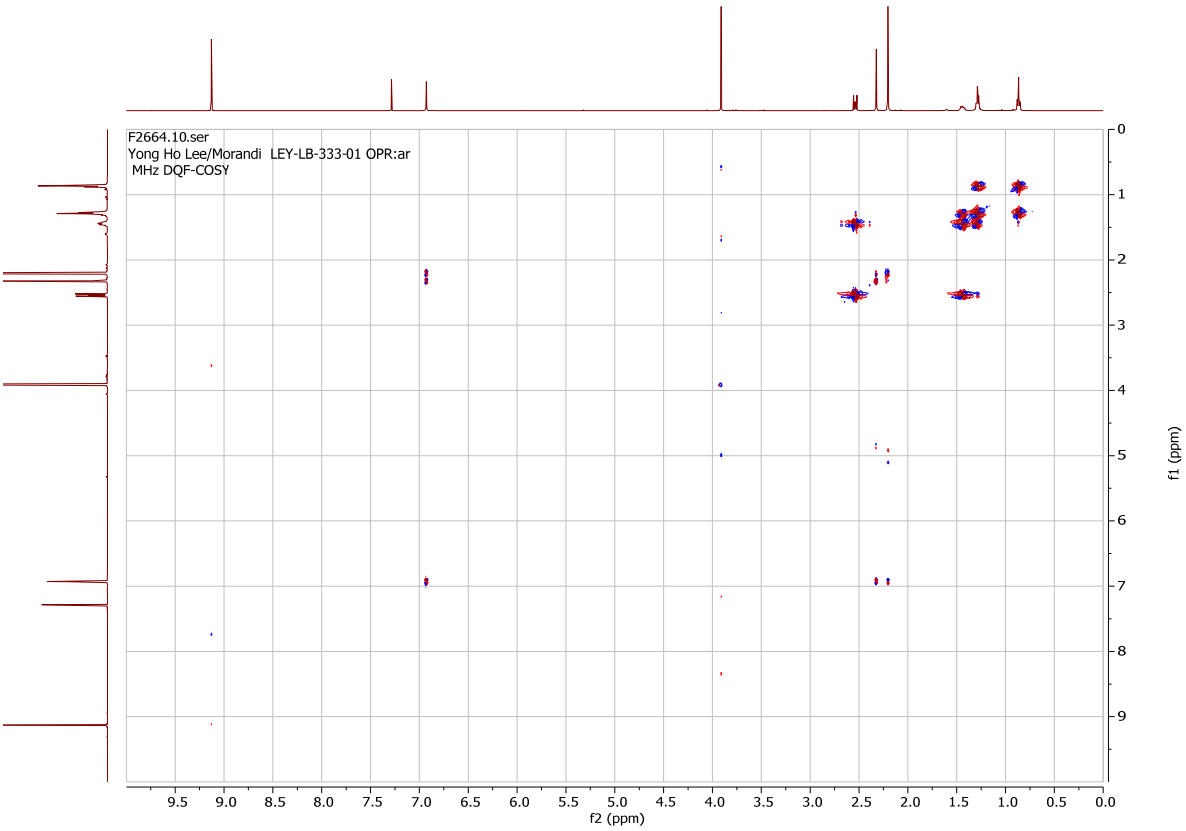
F2664.10.ser
Yong Ho Lee/Morandi LEY-LB-333-01 OPR:ar
MHz DQF-COSY
f2 (ppm)
f1 (ppm)

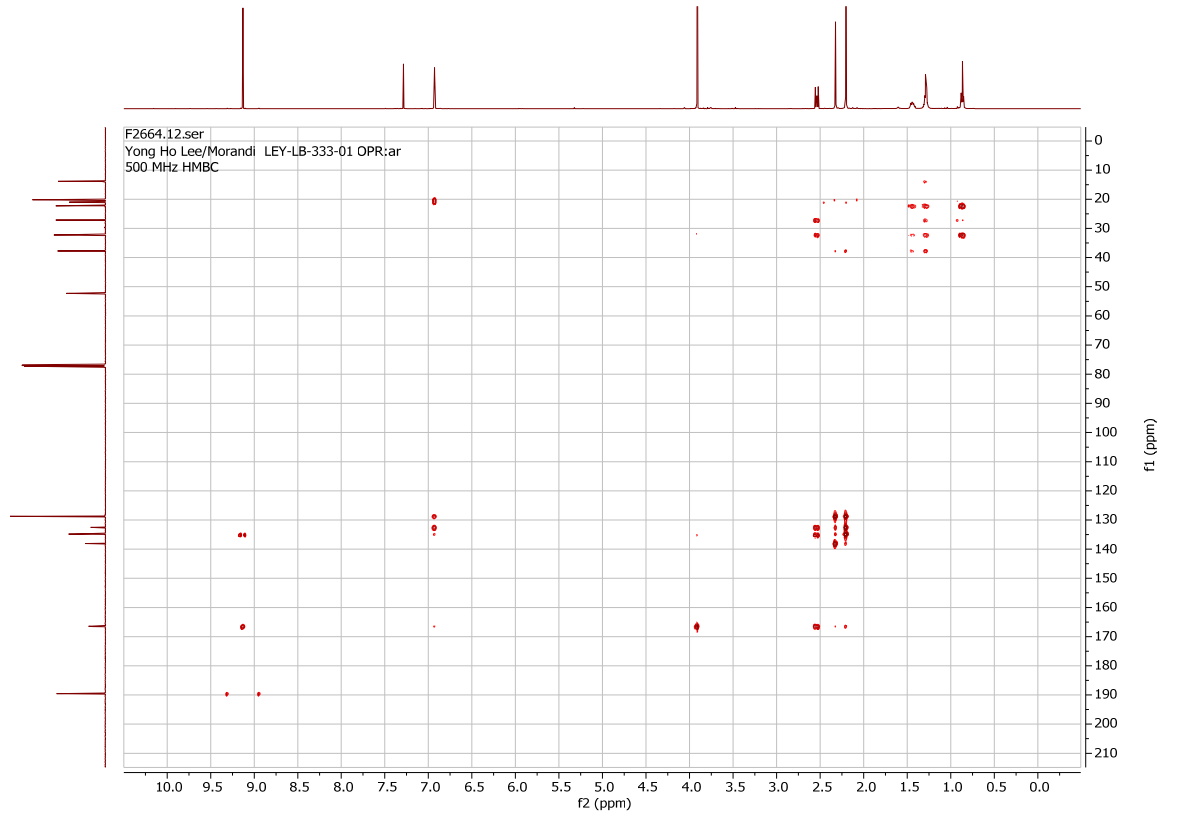
F2664.12.ser
Yong Ho Lee/Morandi LEY-LB-333-01 OPR:ar
500 MHz HMBC
f2 (ppm)
f1 (ppm)

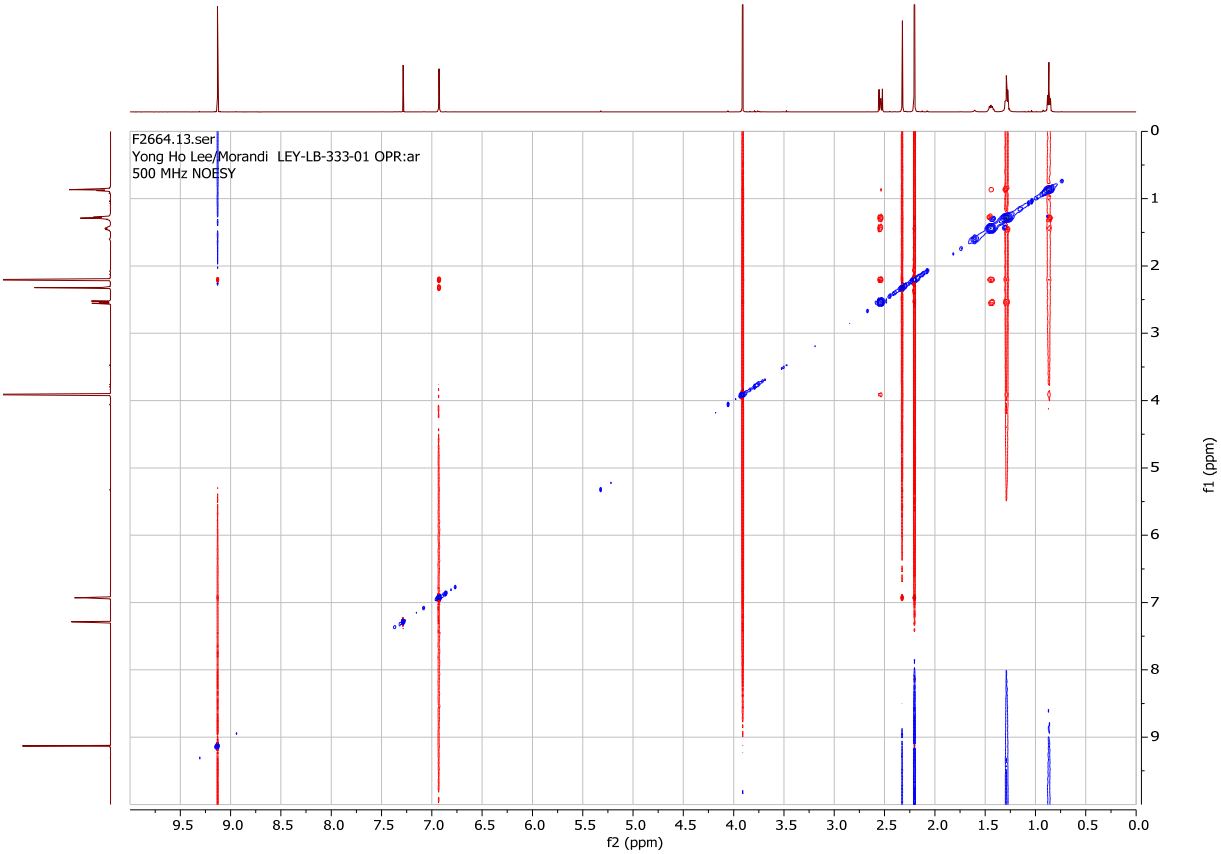
F2664.13.ser
Yong Ho Lee/Morandi LEY-LB-333-01 OPR:ar
500 MHz NOESY
f2 (ppm)
f1 (ppm)

(*Z*)-3-mesityl-2-methyl-3-phenylacrylaldehyde, A (**50-α-Ar**).

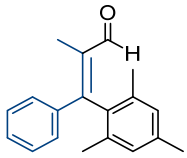

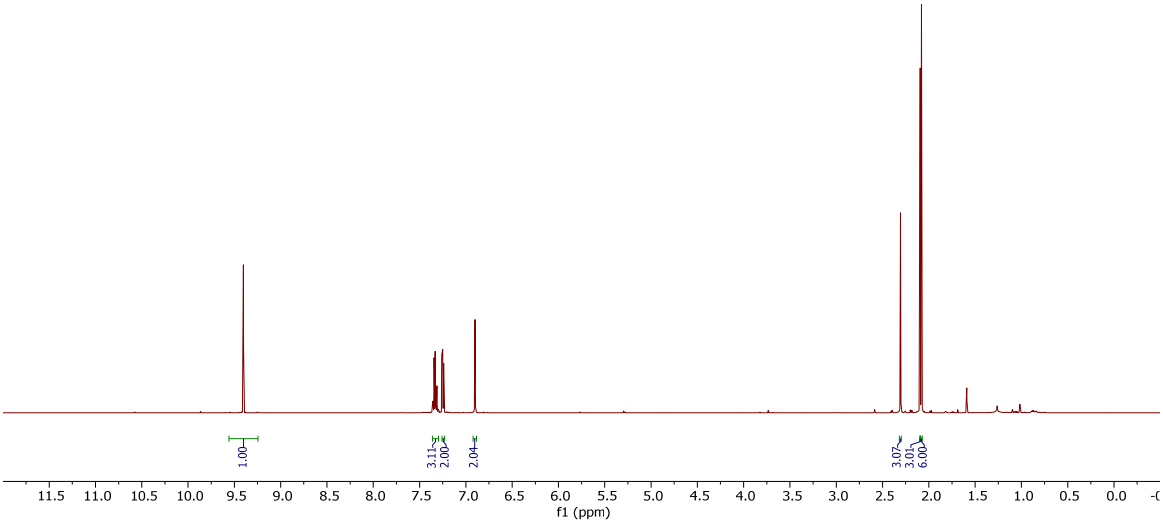

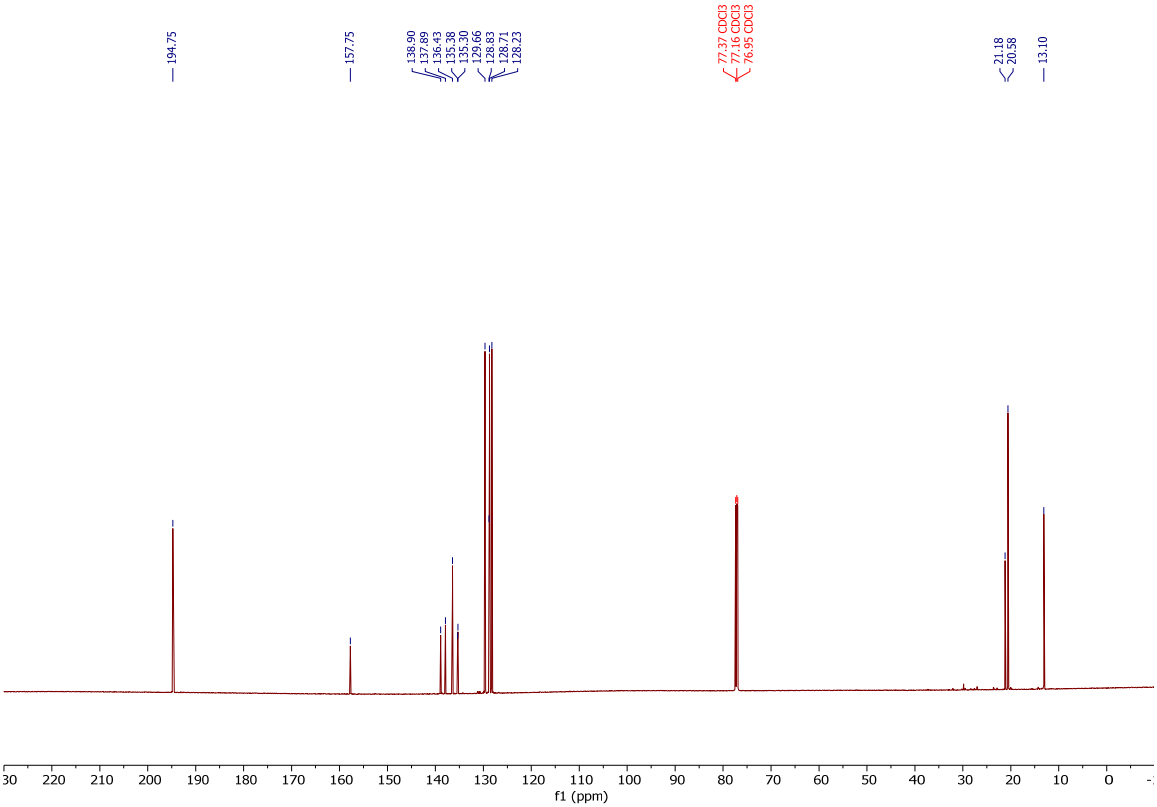

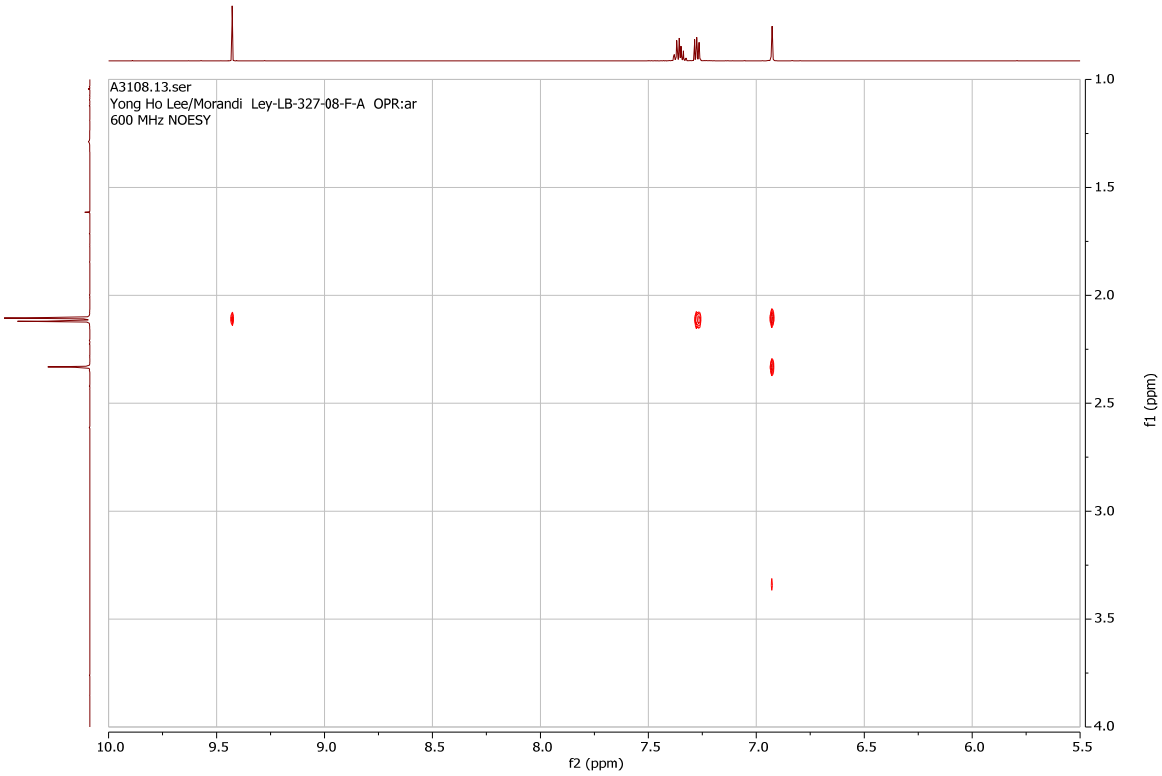
A3108.13.ser
Yong Ho Lee/Morandi Ley-LB-327-08-F-A OPR:ar
600 MHz NOESY
f2 (ppm)
f1 (ppm)

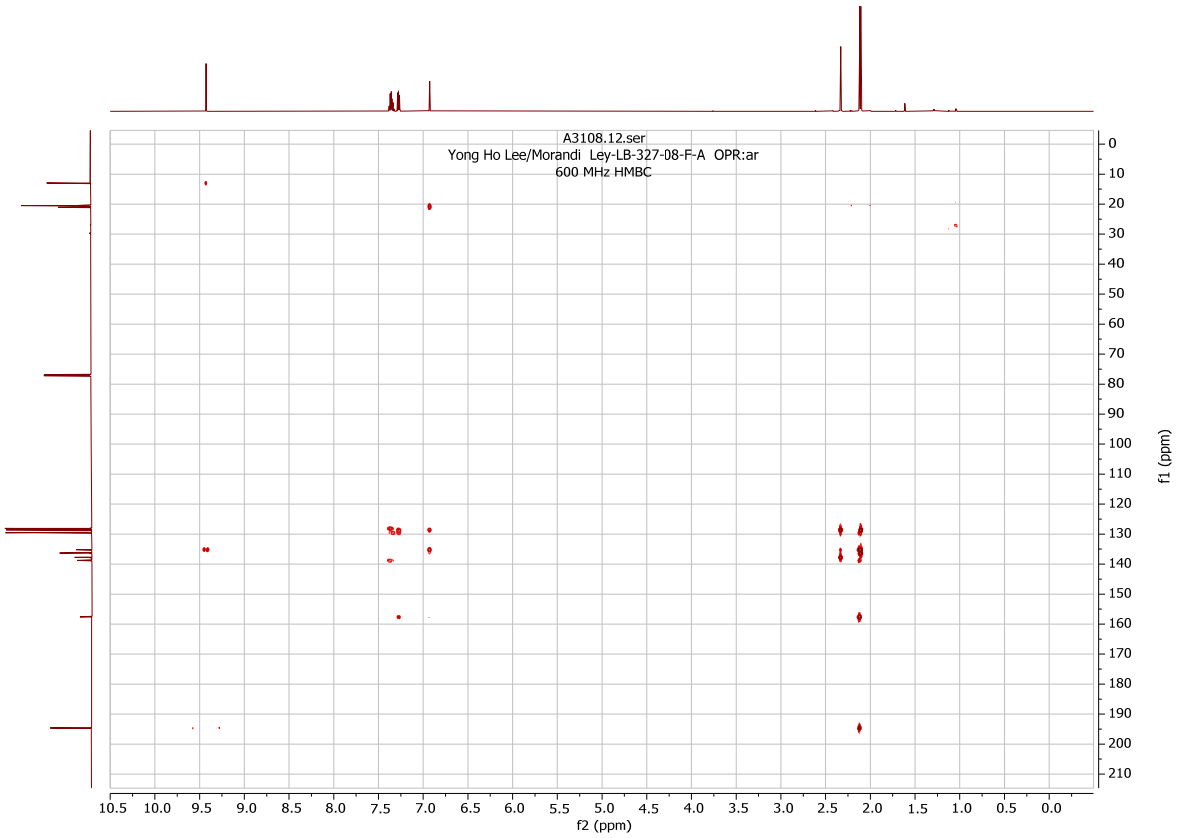
A3108.12.ser
Yong Ho Lee/Morandi Ley-LB-327-08-F-A OPR:ar
600 MHz HMBC
f2 (ppm)
f1 (ppm)

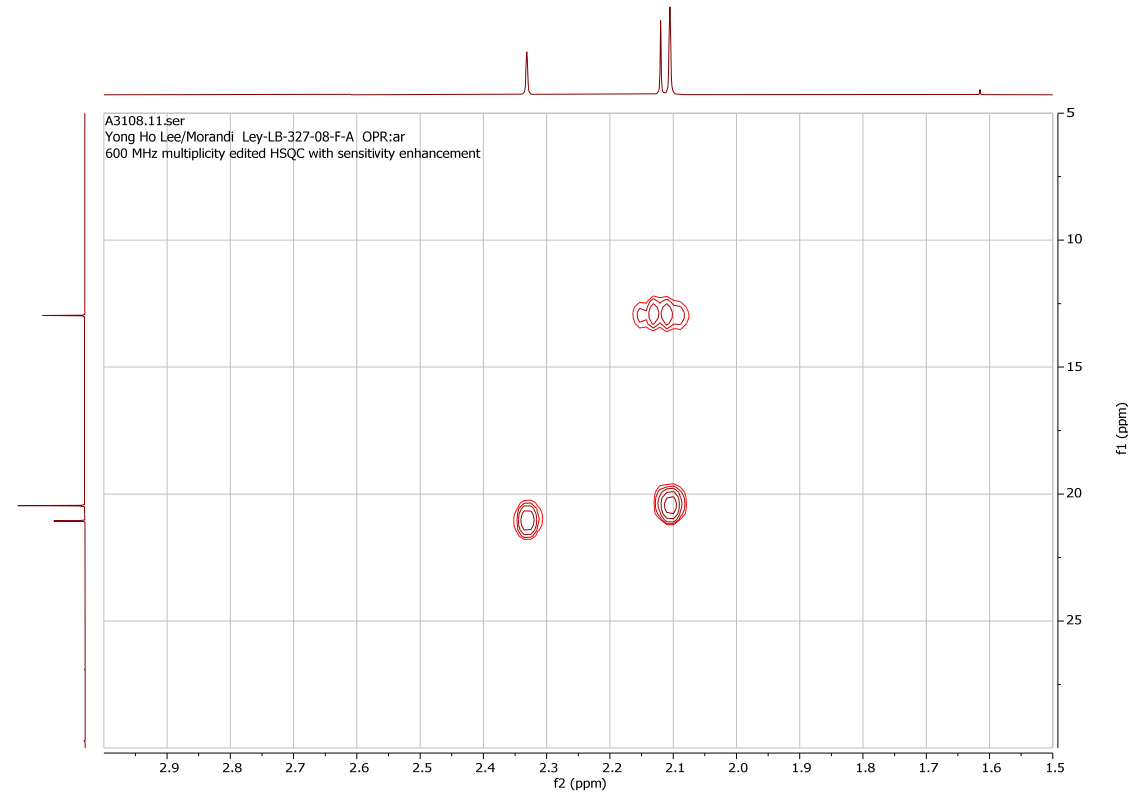
A3108.11.ser
Yong Ho Lee/Morandi Ley-LB-327-08-F-A OPR:ar
600 MHz multiplicity edited HSQC with sensitivity enhancement
f2 (ppm)
f1 (ppm)

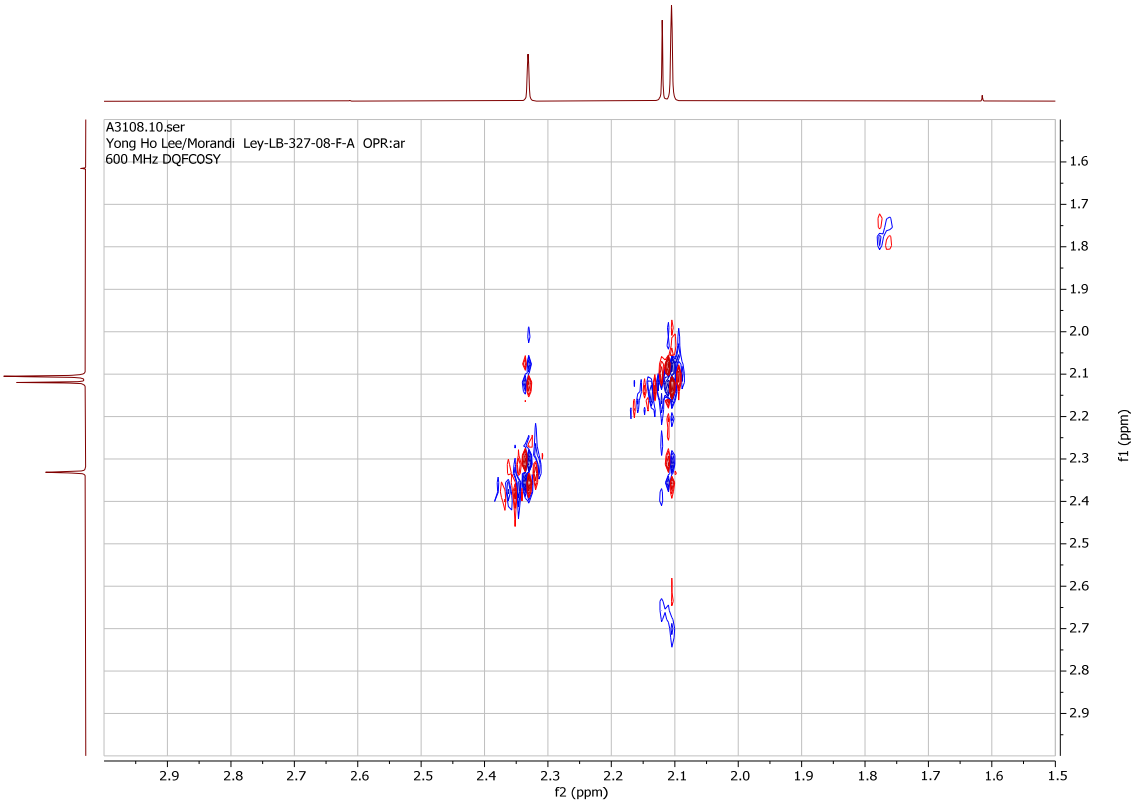
A3108.10.ser
Yong Ho Lee/Morandi Ley-LB-327-08-F-A OPR:ar
600 MHz DQFCOSY
f2 (ppm)
f1 (ppm)

(*Z*)-3-mesityl-2-phenylbut-2-enal, B (**50-β-Ar**).

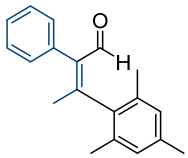

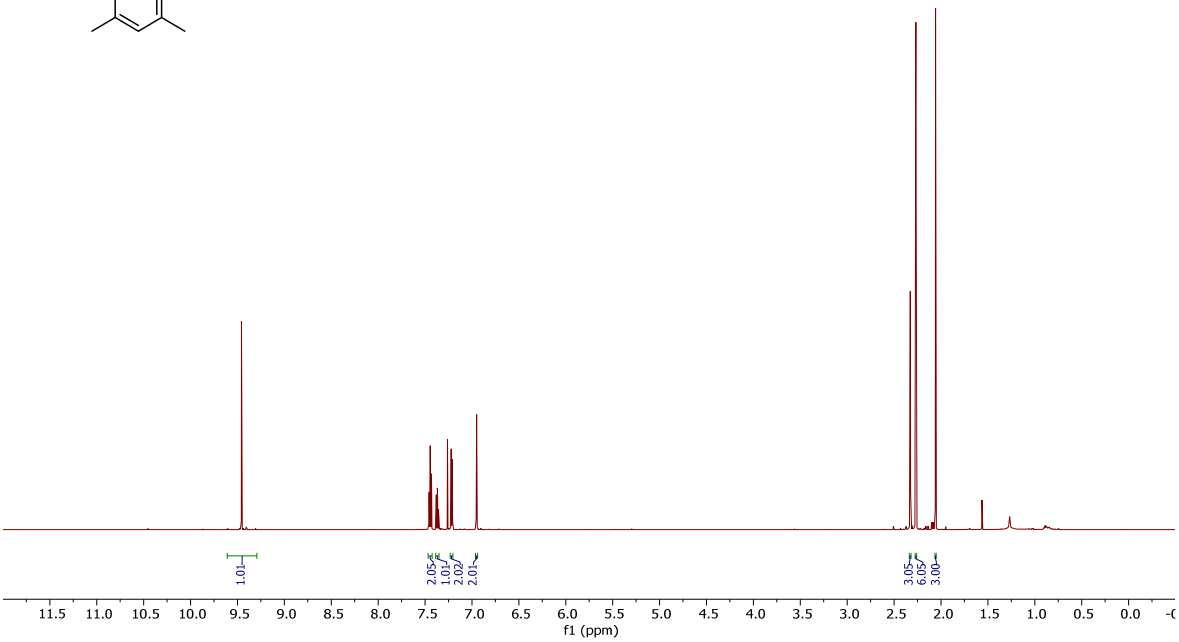

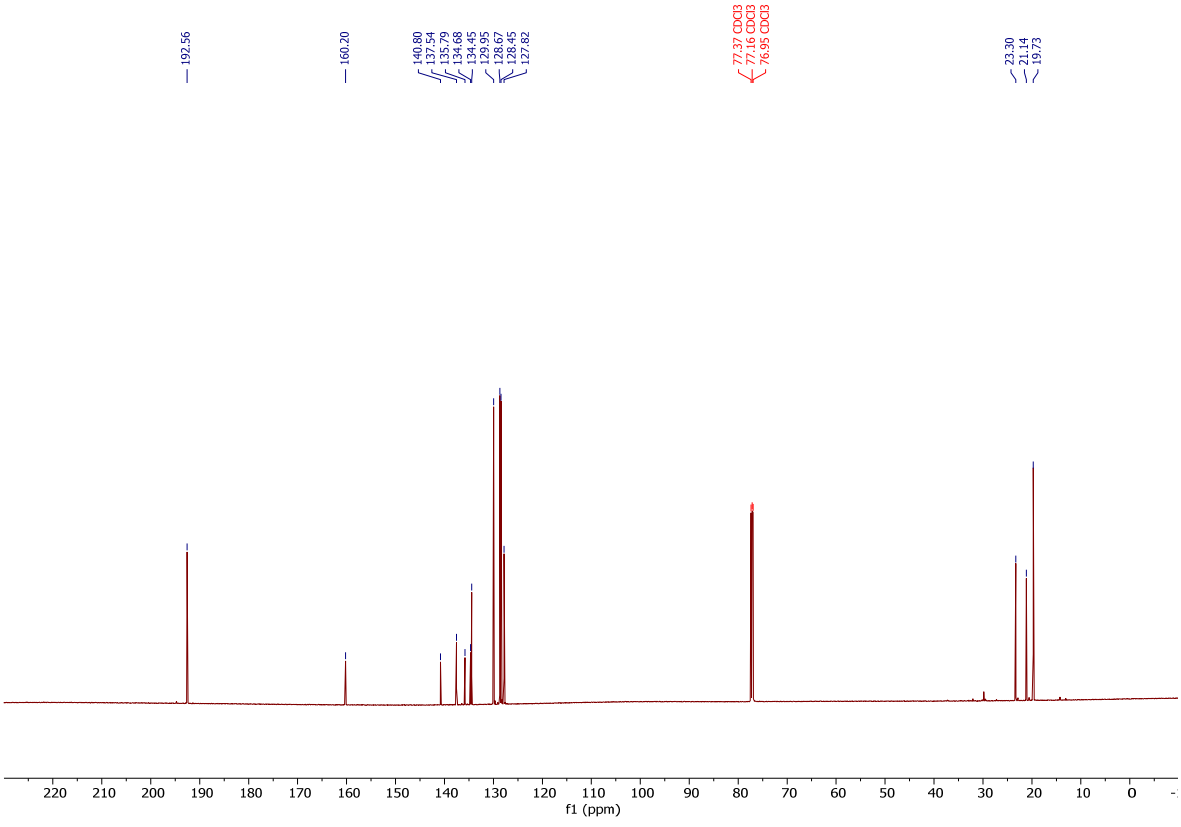

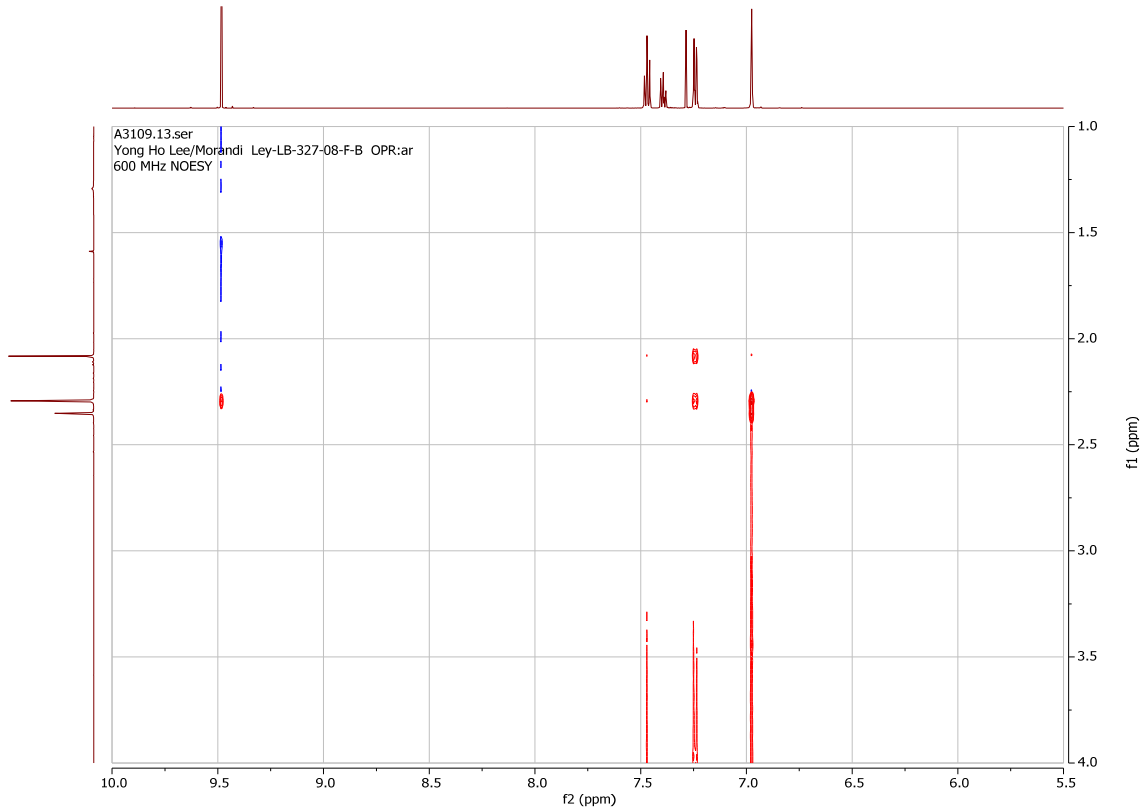
A3109.13.ser
Yong Ho Lee/Morandi Ley-LB-327-08-F-B OPR:ar
600 MHz NOESY
f2 (ppm)
f1 (ppm)

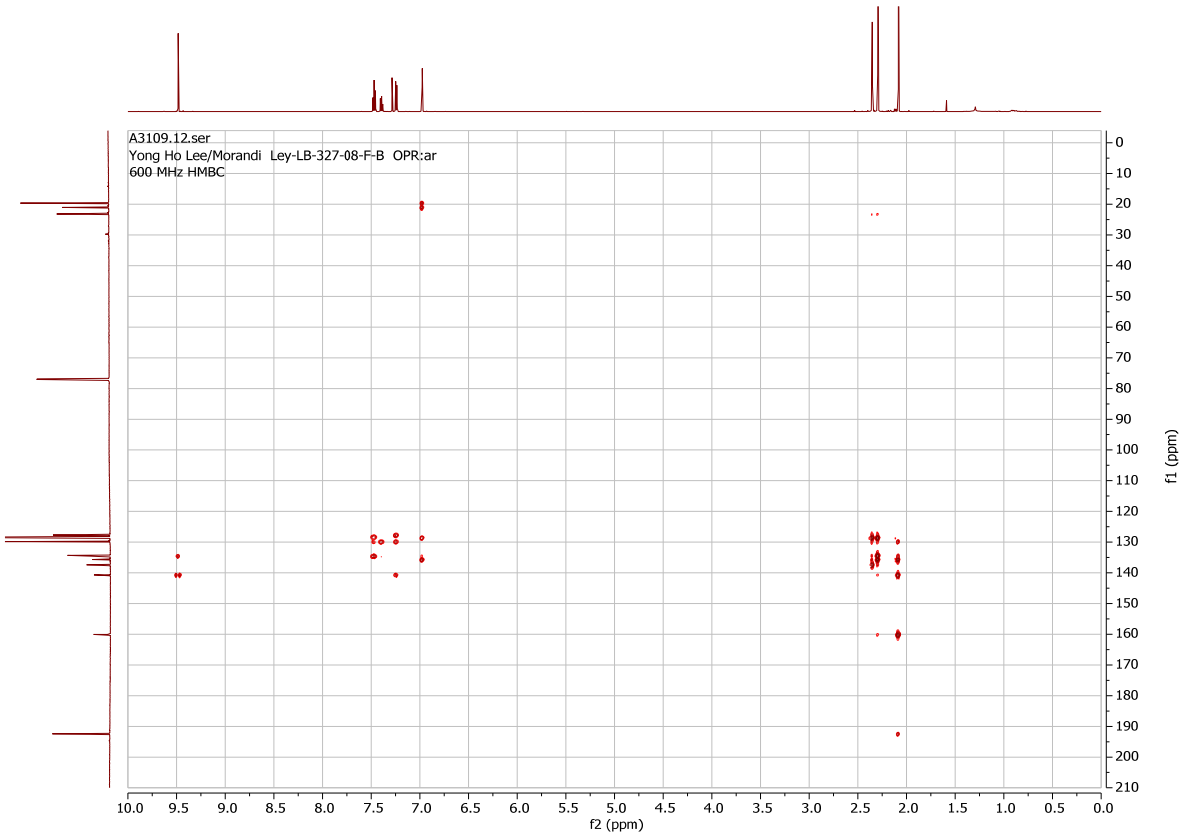
A3109.12.ser
Yong Ho Lee/Morandi Ley-LB-327-08-F-B OPR:ar
600 MHz HMBC
f2 (ppm)
f1 (ppm)

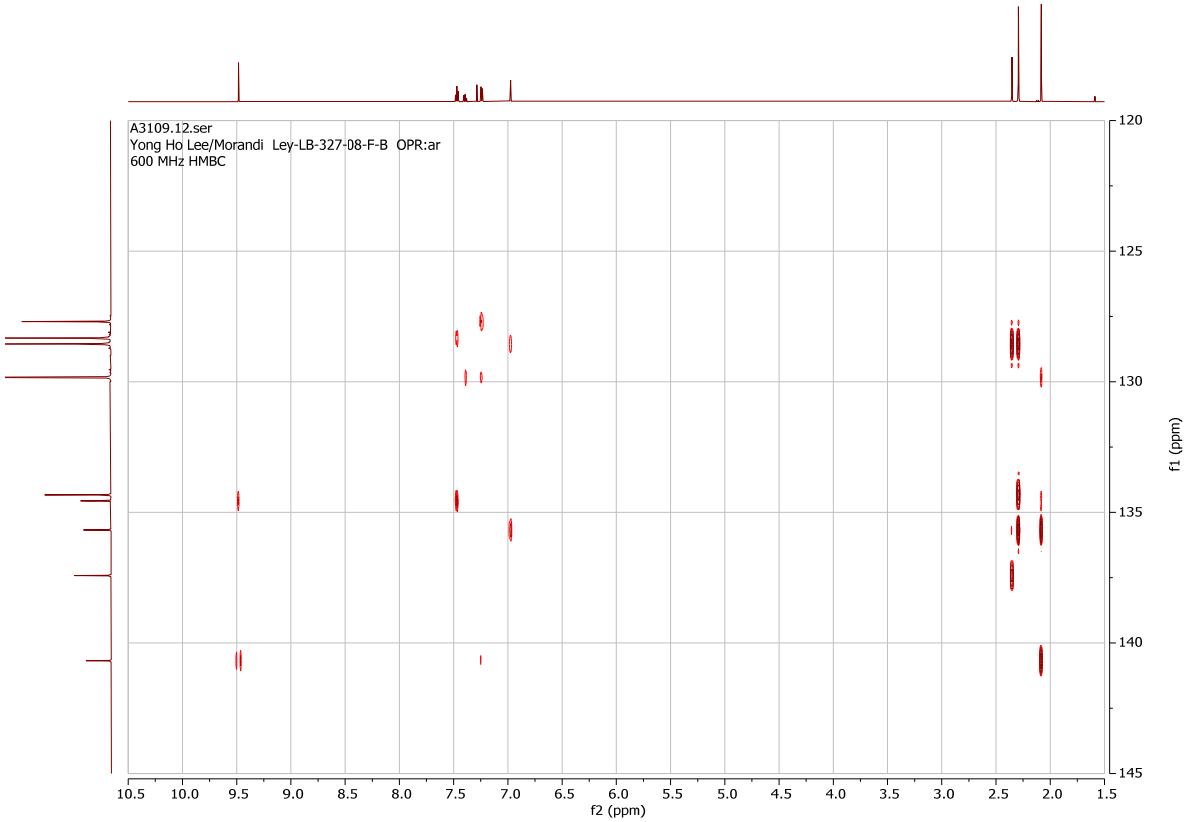
A3109.12.ser
Yong Ho Lee/Morandi Ley-LB-327-08-F-B OPR:ar
600 MHz HMBC
f2 (ppm)
f1 (ppm)

(*Z*)-2-(mesityl(phenyl)methylene)pentanal, A (**51-α-Ar, major**).

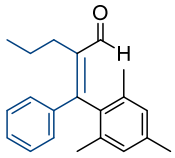

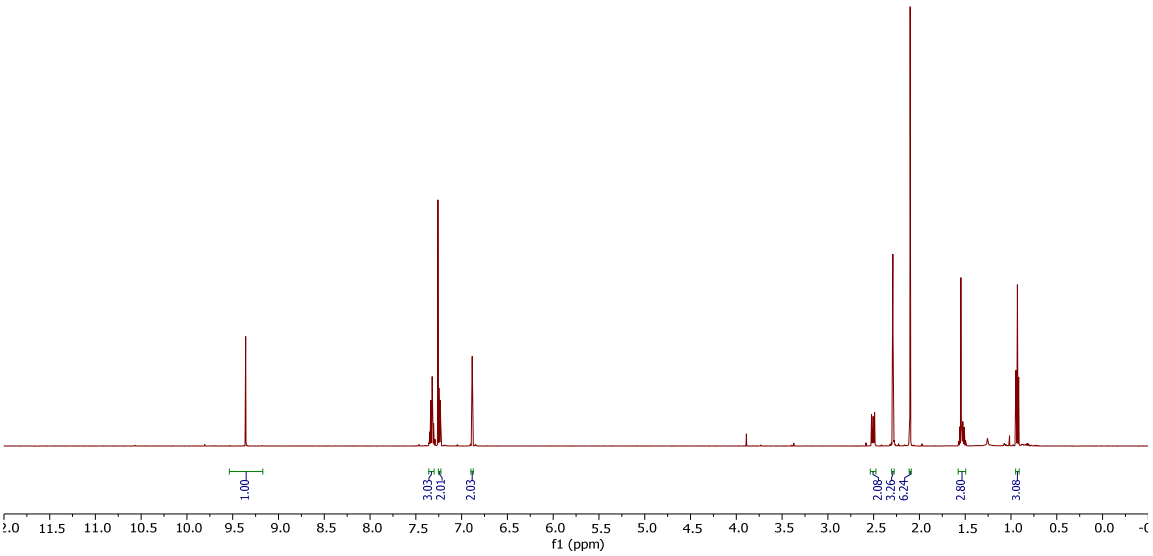

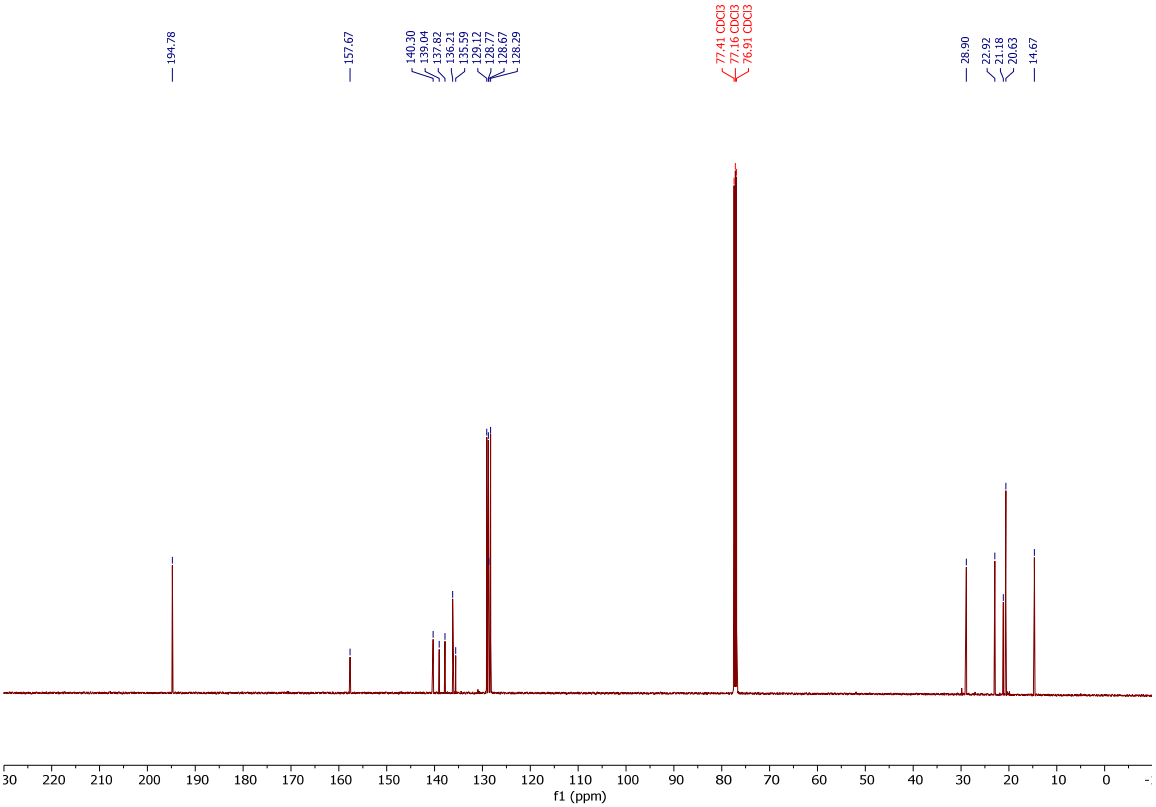

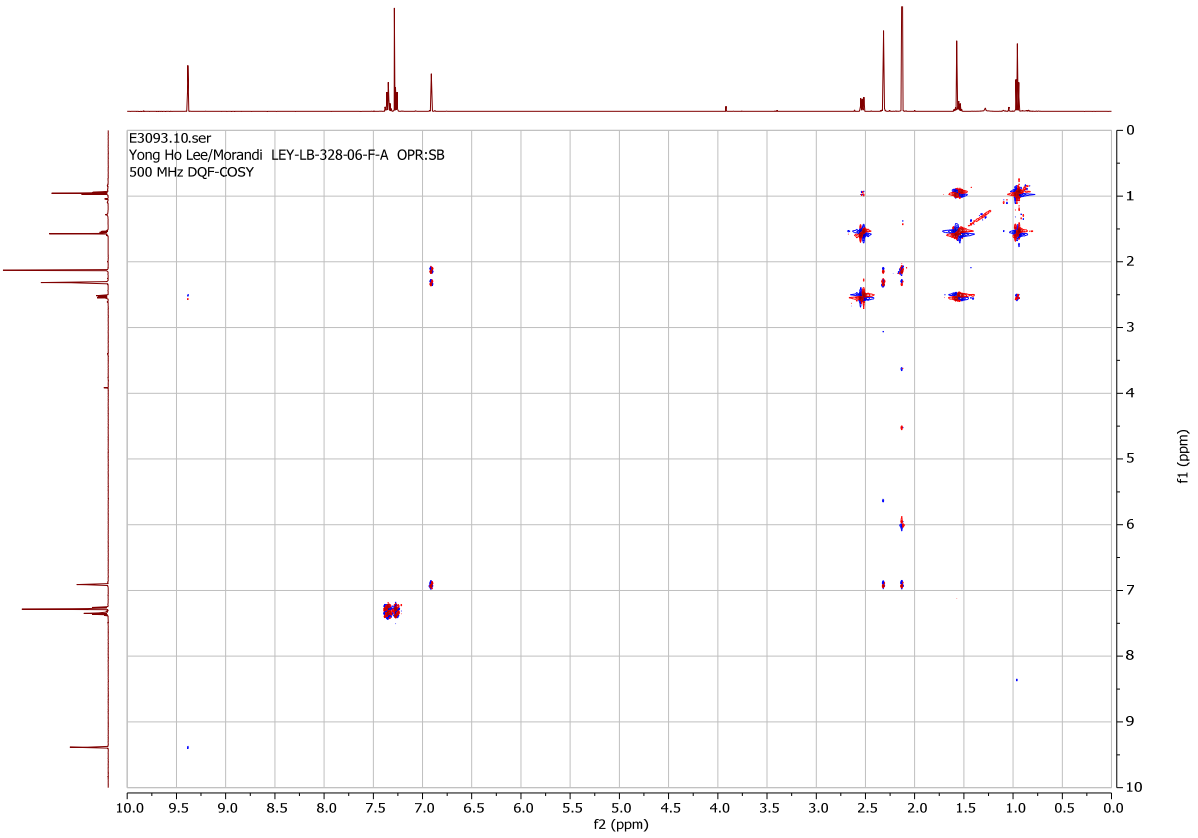
E3093.10.ser
Yong Ho Lee/Morandi LEY-LB-328-06-F-A OPR:SB
500 MHz DQF-COSY
f2 (ppm)
f1 (ppm)

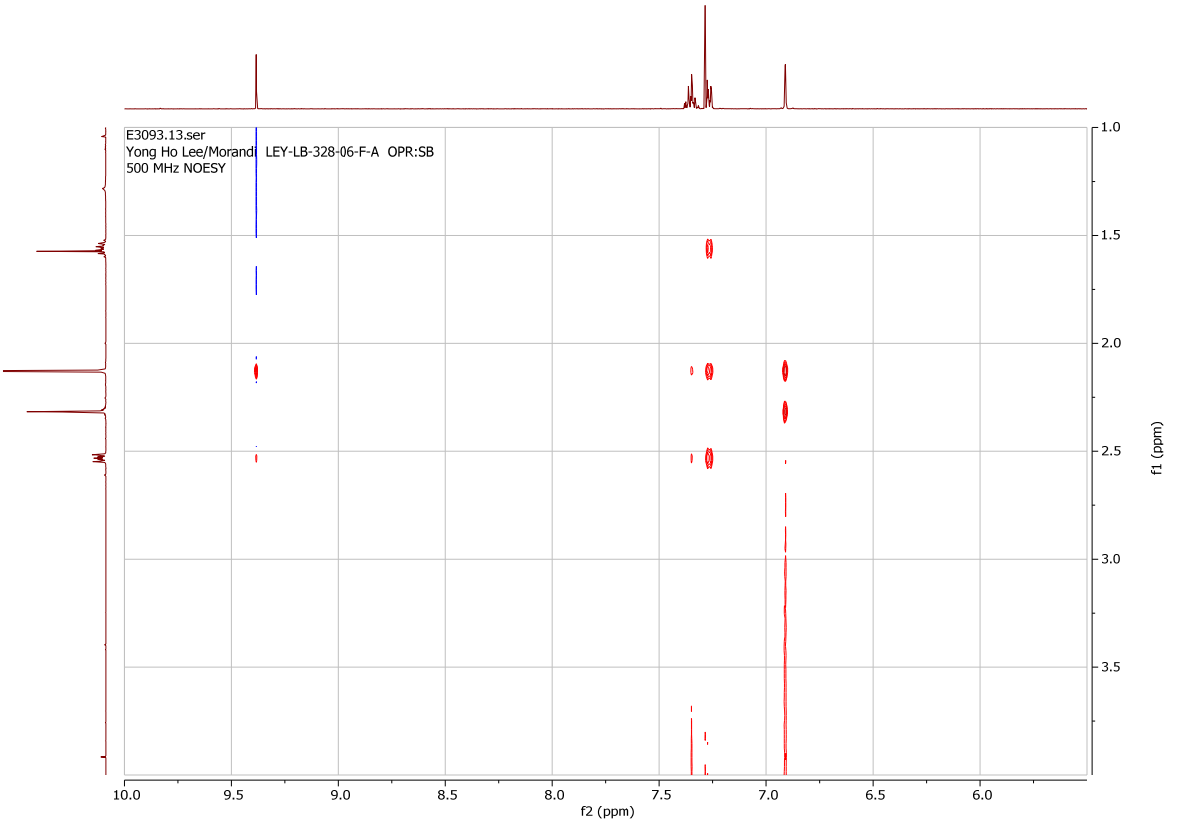
E3093.13.ser
Yong Ho Lee/Morandi LEY-LB-328-06-F-A OPR:SB
500 MHz NOESY
f2 (ppm)
f1 (ppm)

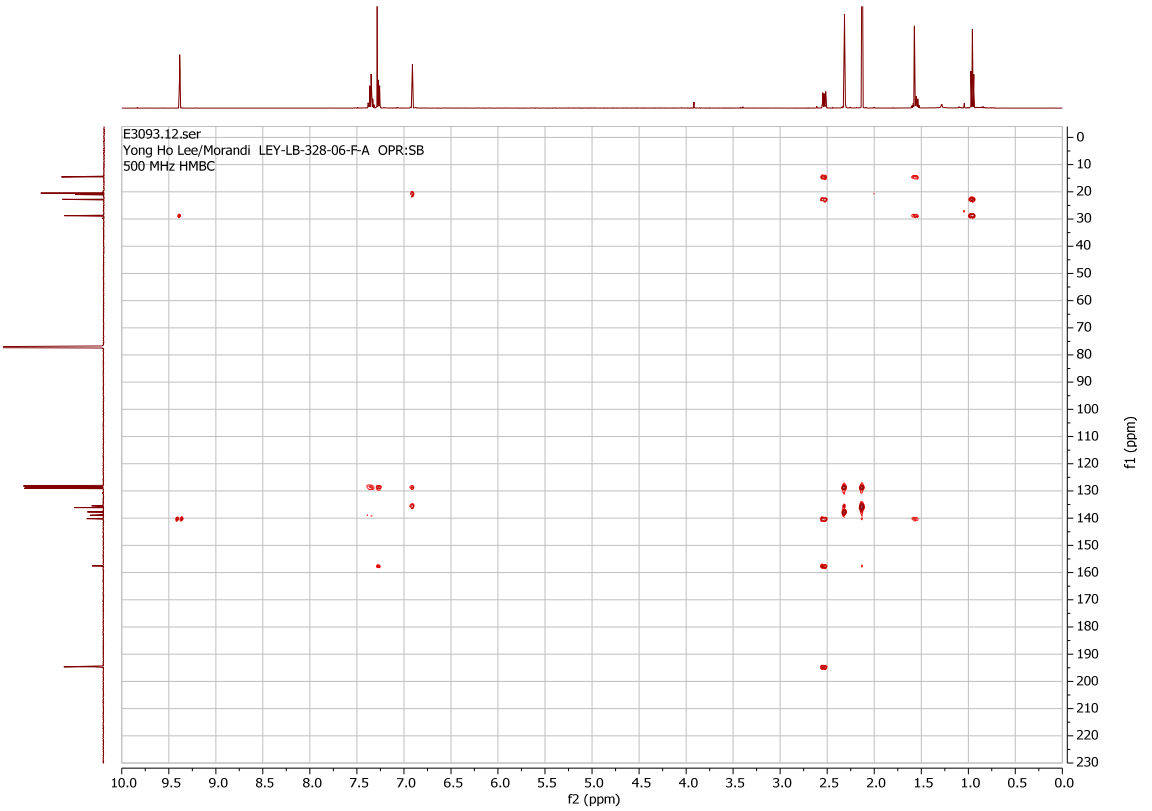
E3093.12.ser
Yong Ho Lee/Morandi LEY-LB-328-06-F-A OPR:SB
500 MHz HMBC
f2 (ppm)
f1 (ppm)

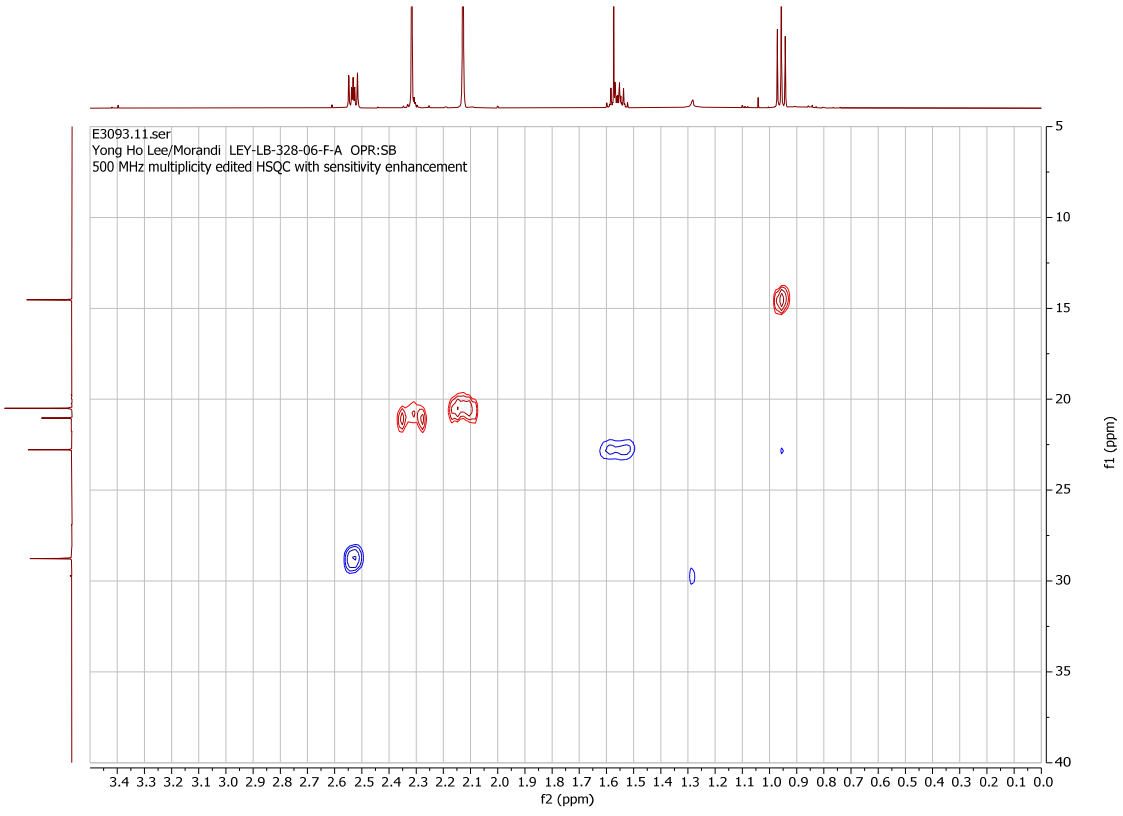
E3093.11.ser
Yong Ho Lee/Morandi LEY-LB-328-06-F-A OPR:SB
500 MHz multiplicity edited HSQC with sensitivity enhancement
f2 (ppm)
f1 (ppm)

(*Z*)-3-mesityl-2-phenylhex-2-enal, B (**51-β-Ar, minor**).

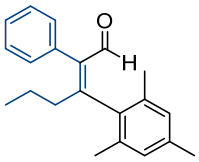

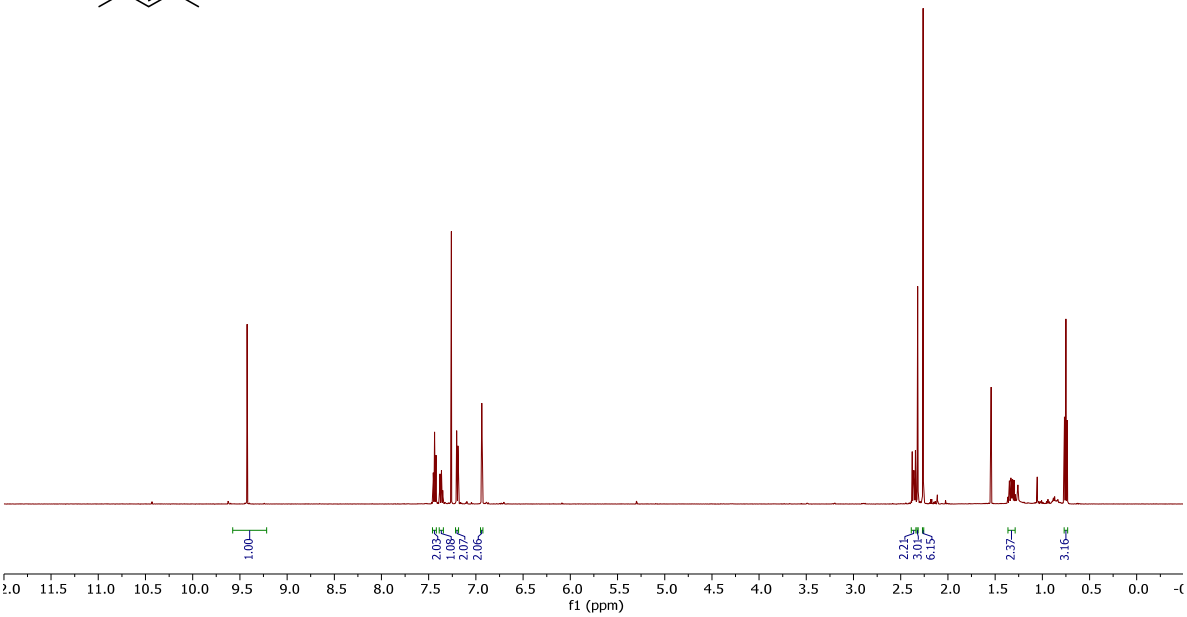

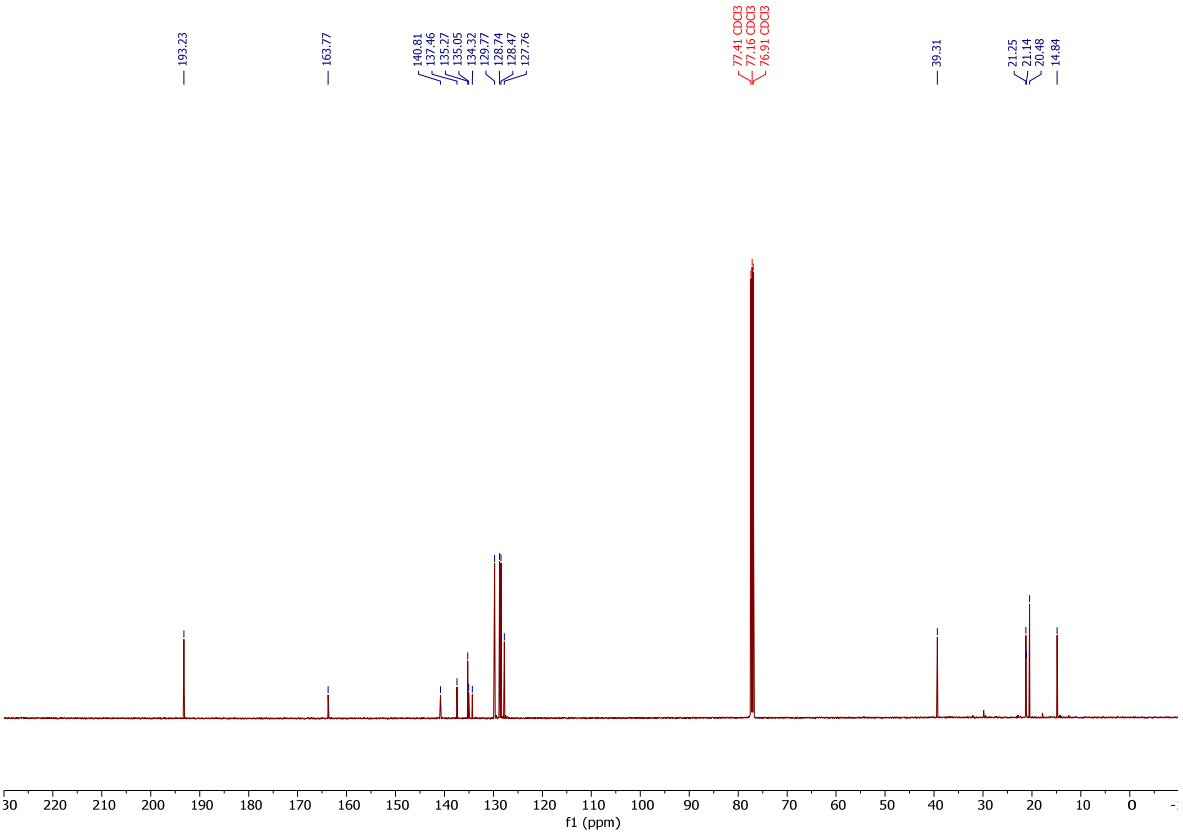

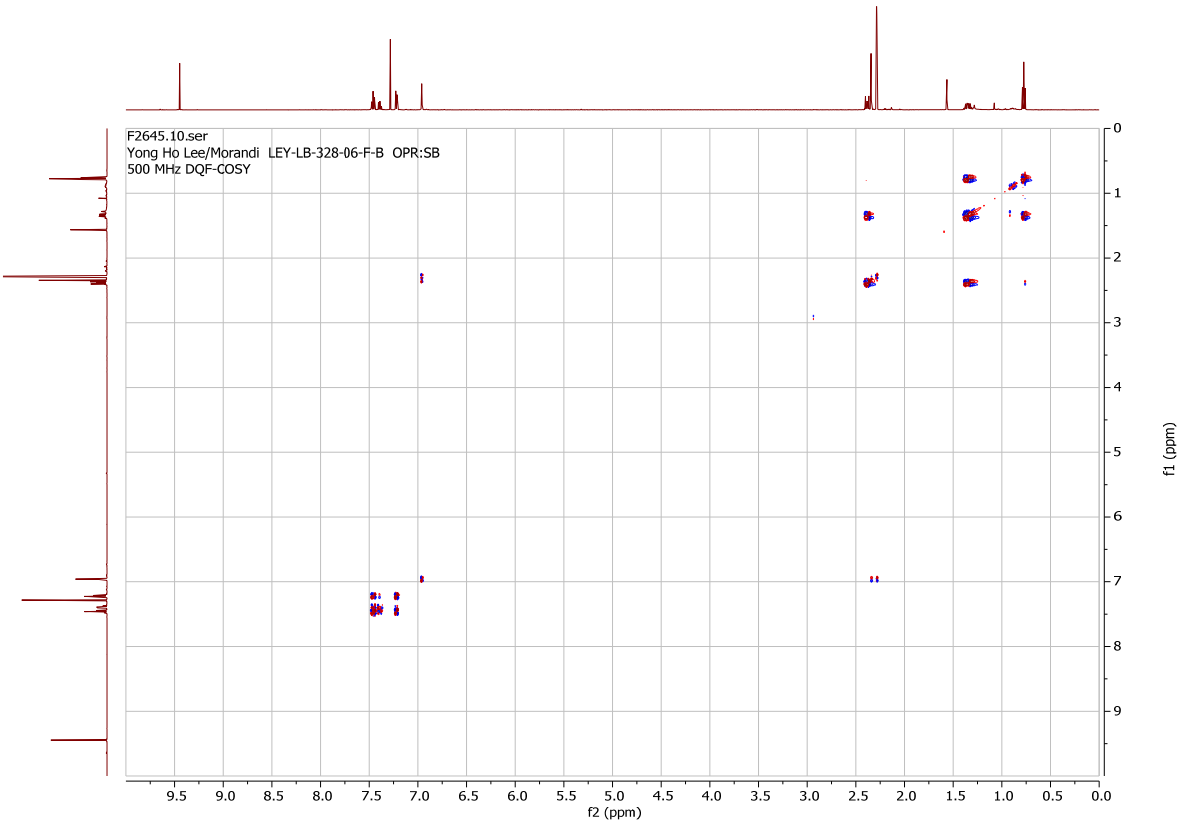
F2645.10.ser
Yong Ho Lee/Morandi LEY-LB-328-06-F-B OPR:SB
500 MHz DQF-COSY
f2 (ppm)
f1 (ppm)

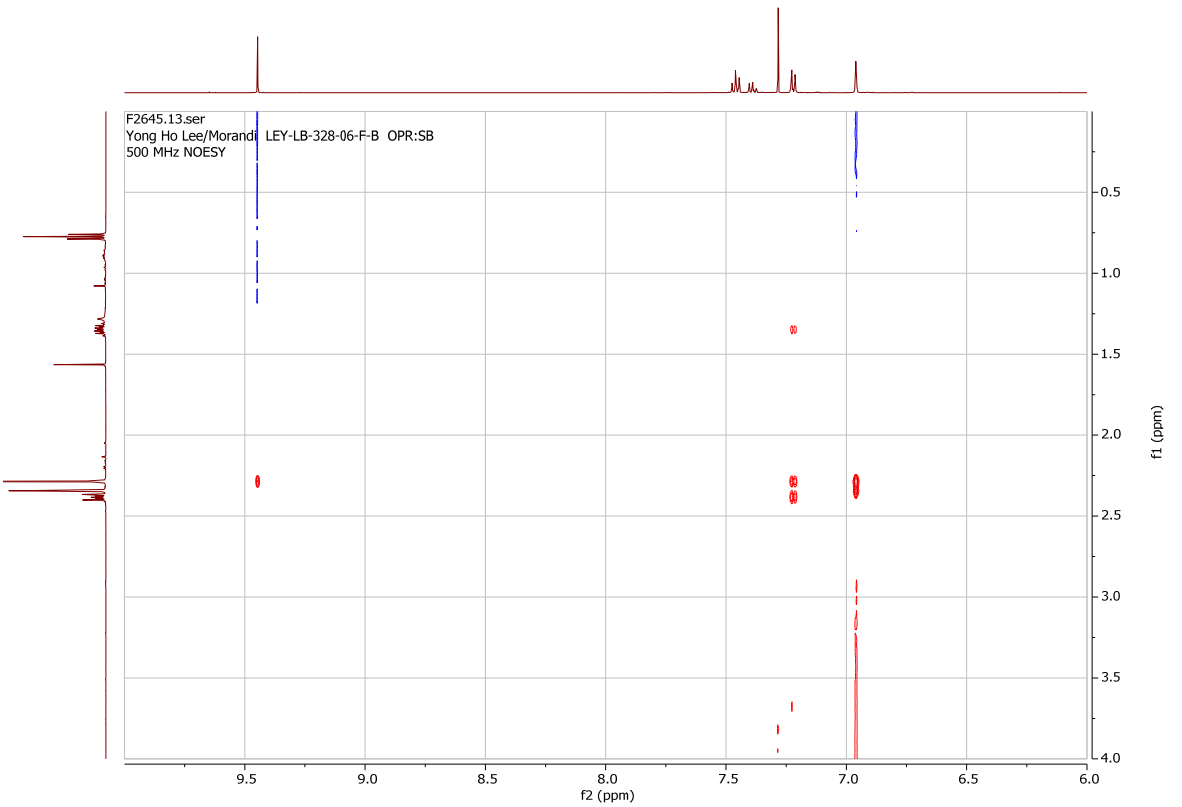
F2645.13.ser
Yong Ho Lee/Morandi LEY-LB-328-06-F-B OPR:SB
500 MHz NOESY
f2 (ppm)
f1 (ppm)

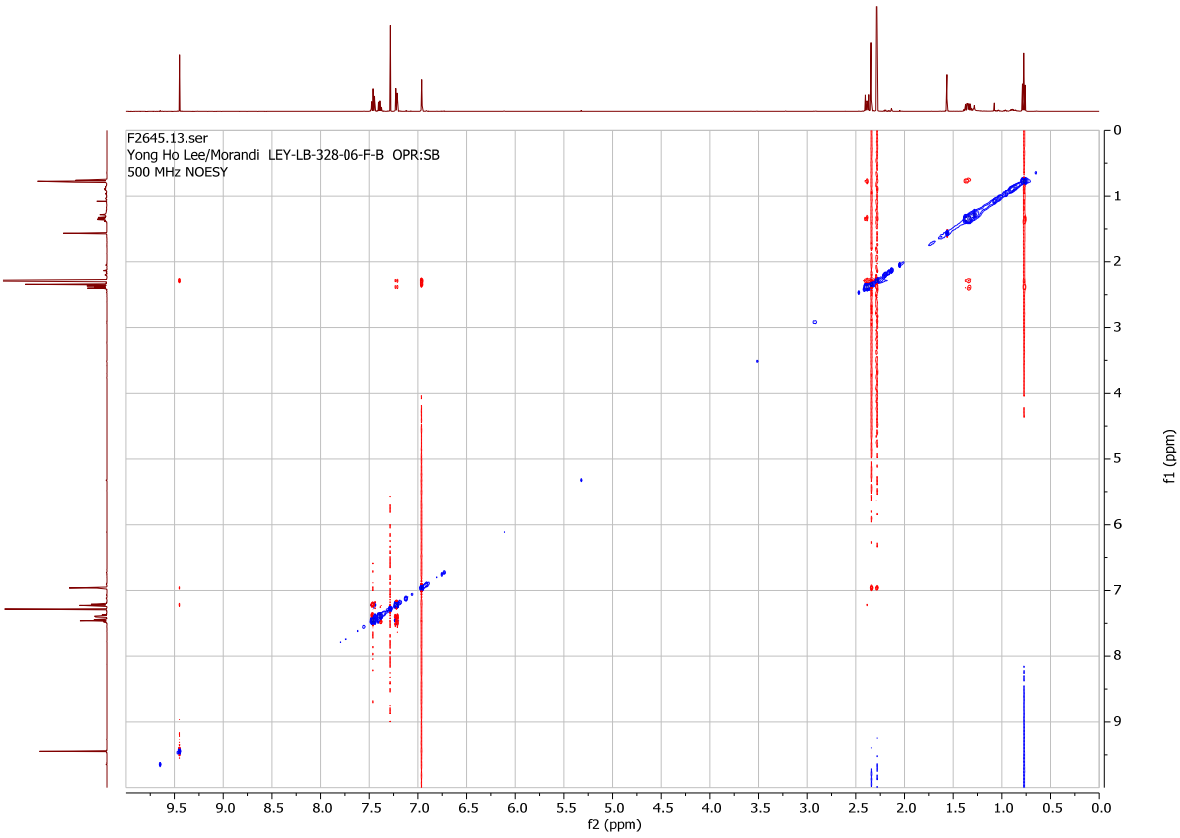
F2645.13.ser
Yong Ho Lee/Morandi LEY-LB-328-06-F-B OPR:SB
500 MHz NOESY
f2 (ppm)
f1 (ppm)

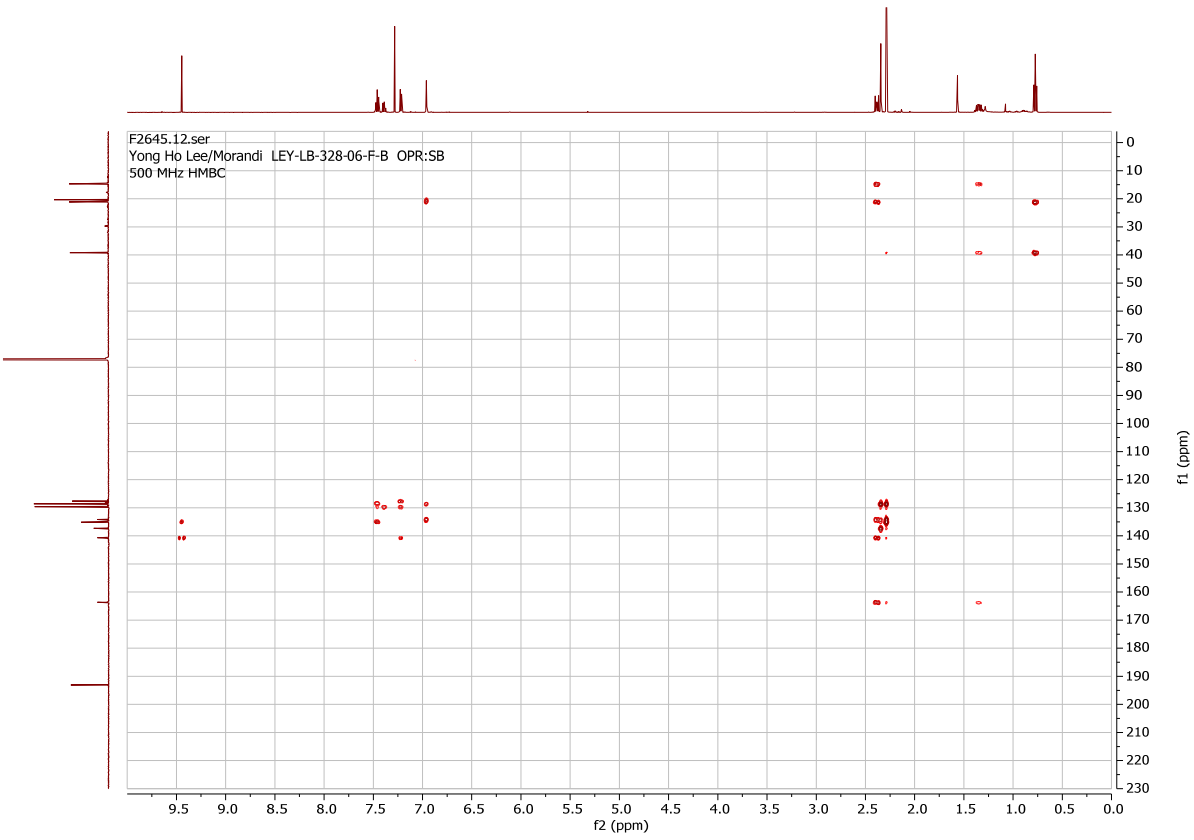
F2645.12.ser
Yong Ho Lee/Morandi LEY-LB-328-06-F-B OPR:SB
500 MHz HMBC
f2 (ppm)
f1 (ppm)

(*Z*)-2-(mesityl(phenyl)methylene)pent-4-enal (**52**).

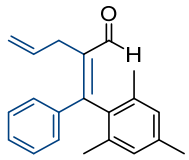

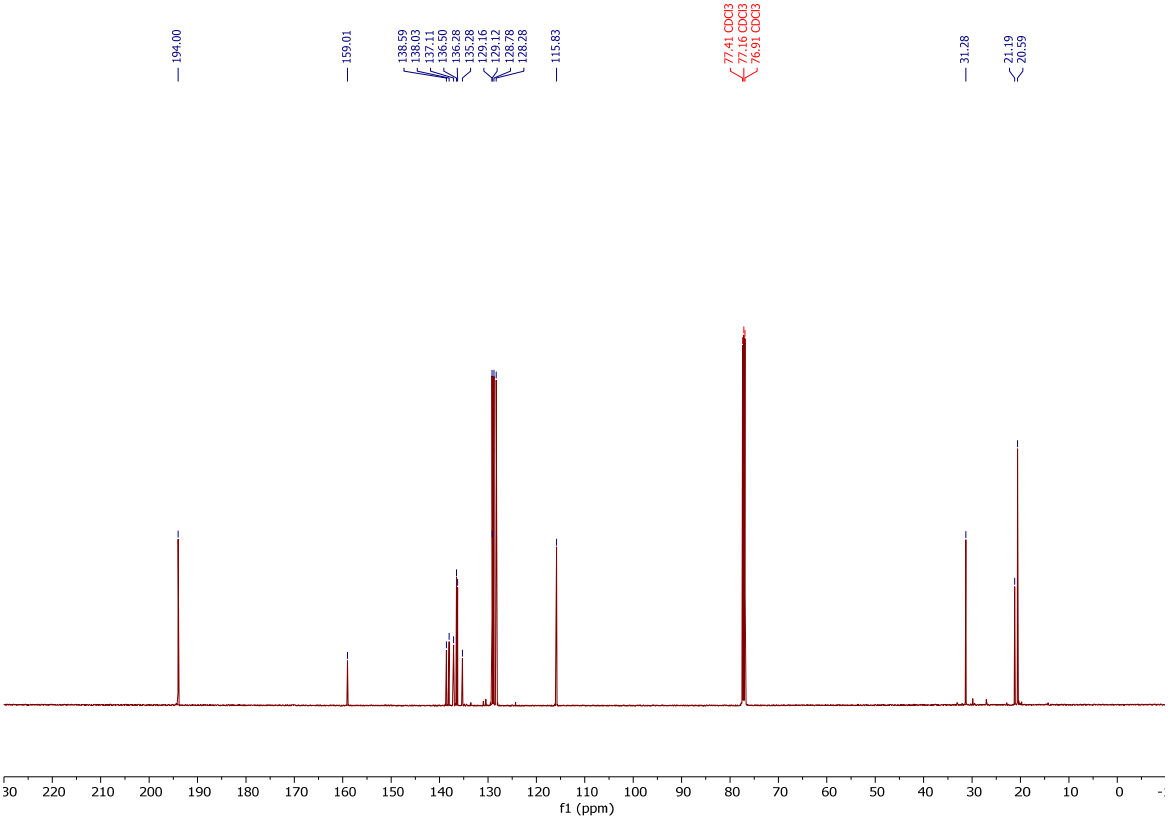

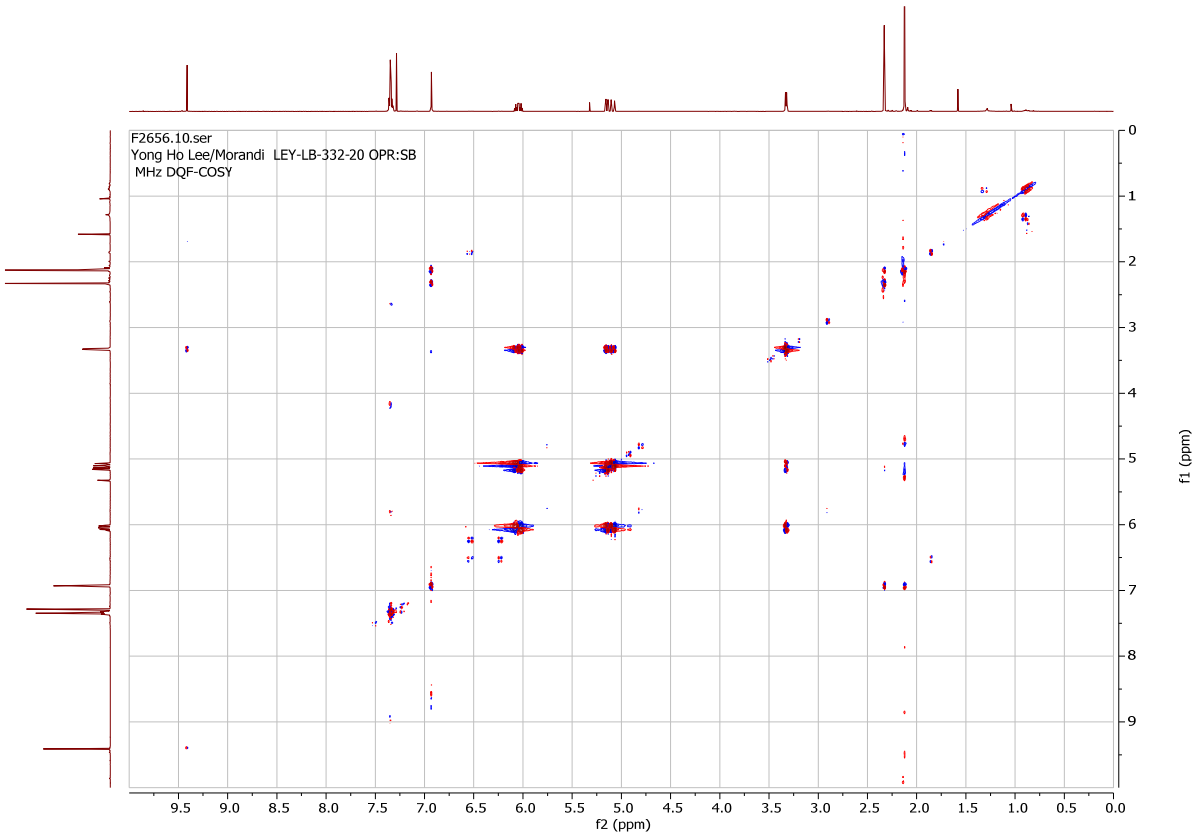
F2656.10.ser
Yong Ho Lee/Morandi LEY-LB-332-20 OPR:SB
MHz DQF-COSY
f2 (ppm)
f1 (ppm)

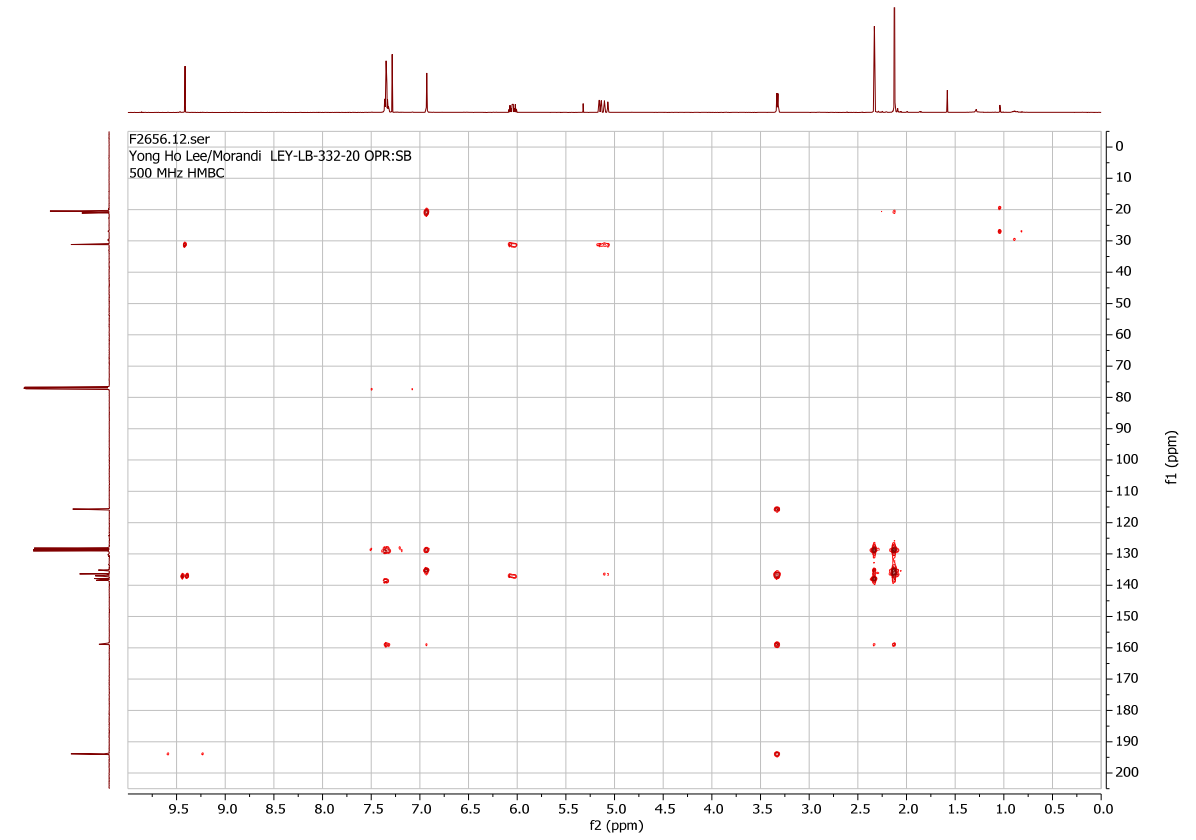
F2656.12.ser
Yong Ho Lee/Morandi LEY-LB-332-20 OPR:SB
500 MHz HMBC
f2 (ppm)
f1 (ppm)

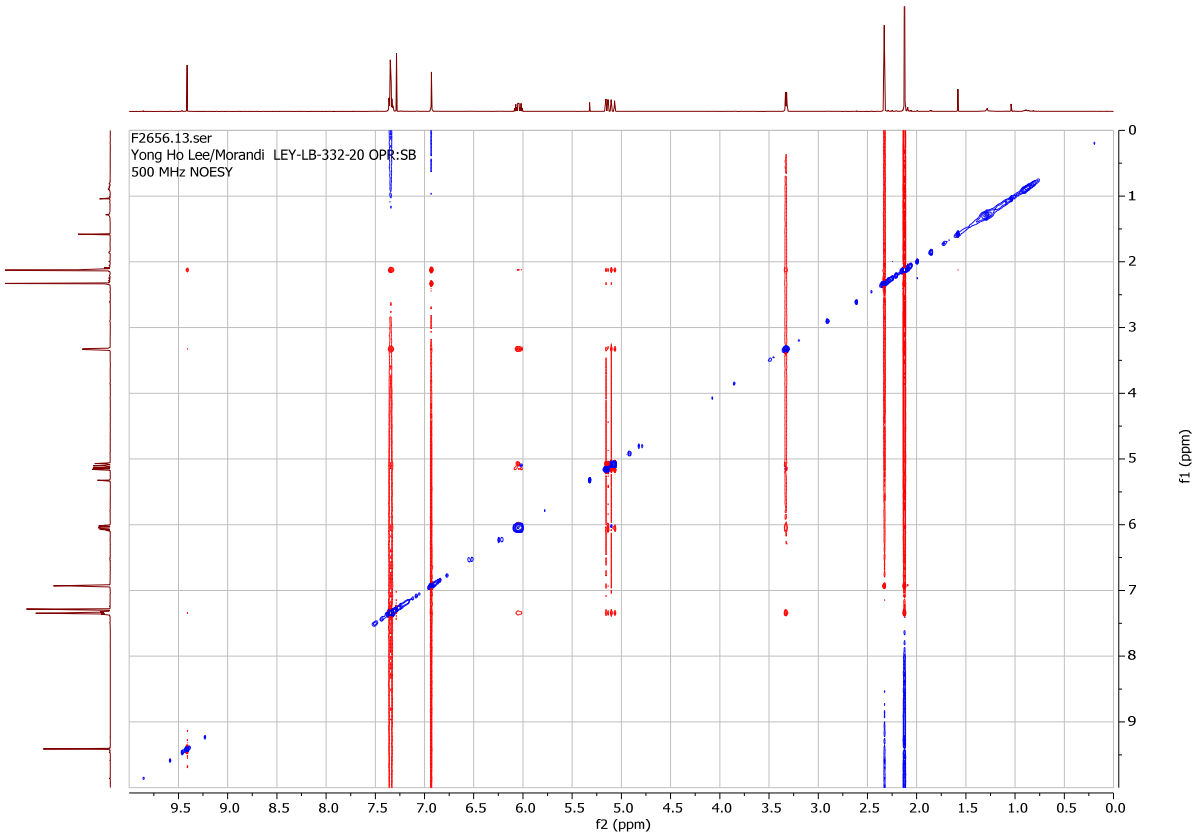
F2656.13.ser
Yong Ho Lee/Morandi LEY-LB-332-20 OPR:SB
500 MHz NOESY
f2 (ppm)
f1 (ppm)

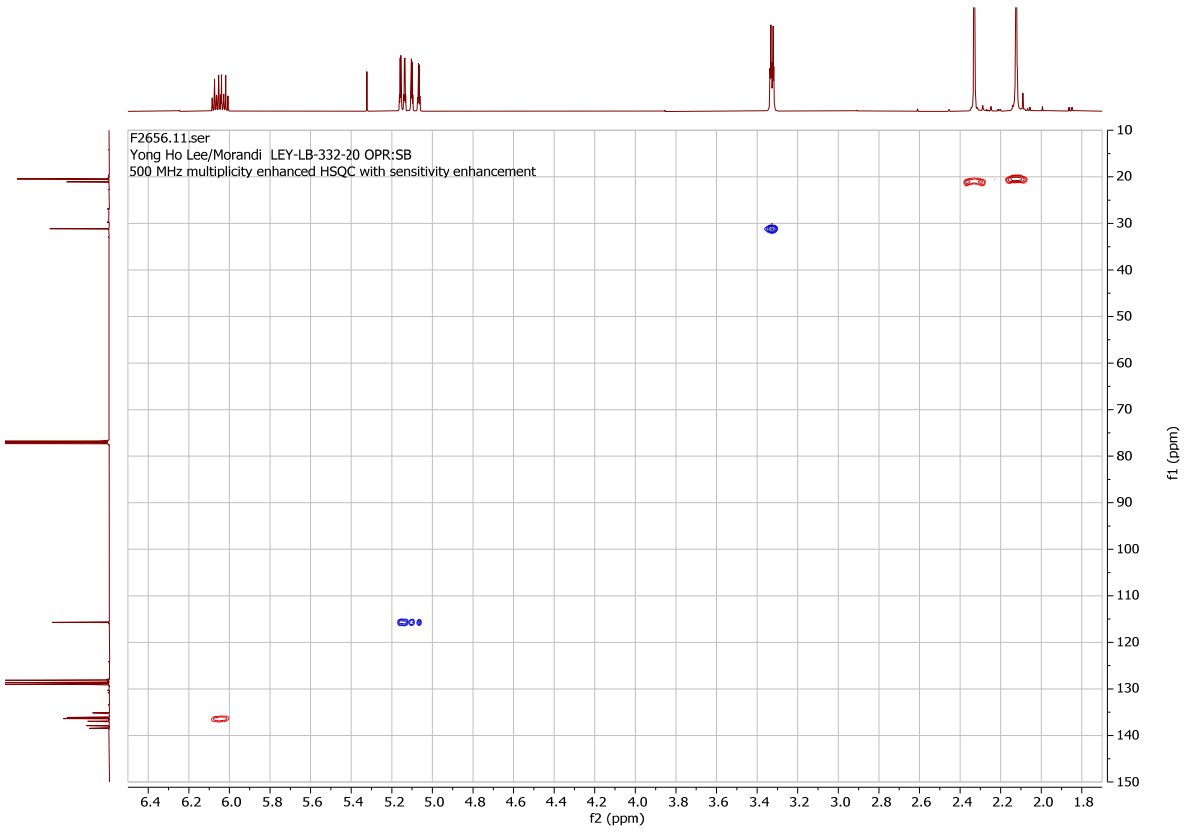
F2656.11.ser
Yong Ho Lee/Morandi LEY-LB-332-20 OPR:SB
500 MHz multiplicity enhanced HSQC with sensitivity enhancement
f2 (ppm)
f1 (ppm)

(*Z*)-*N*-(2-formyl-3-mesityl-3-phenylallyl)pivalamide (**53**).

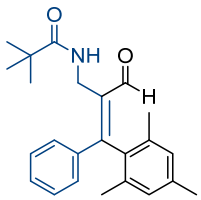

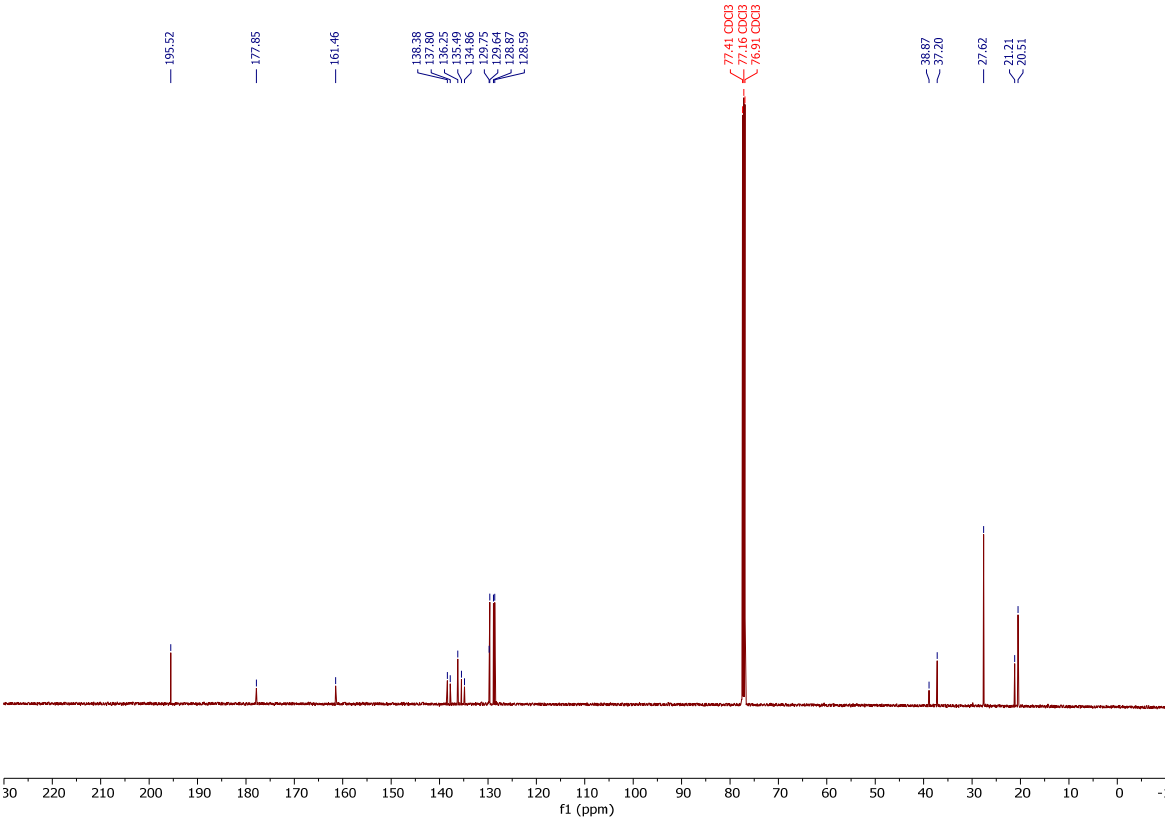

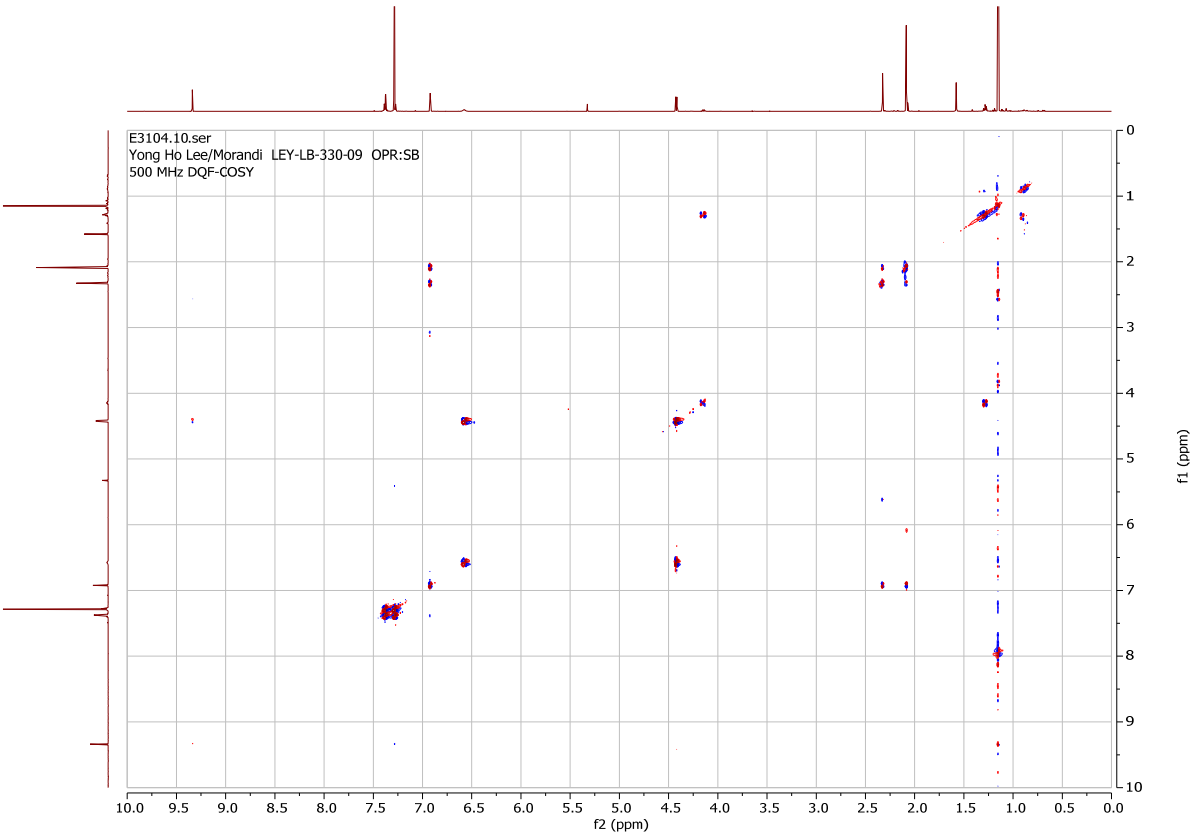
E3104.10.ser
Yong Ho Lee/Morandi LEY-LB-330-09 OPR:SB
500 MHz DQF-COSY
f2 (ppm)
f1 (ppm)

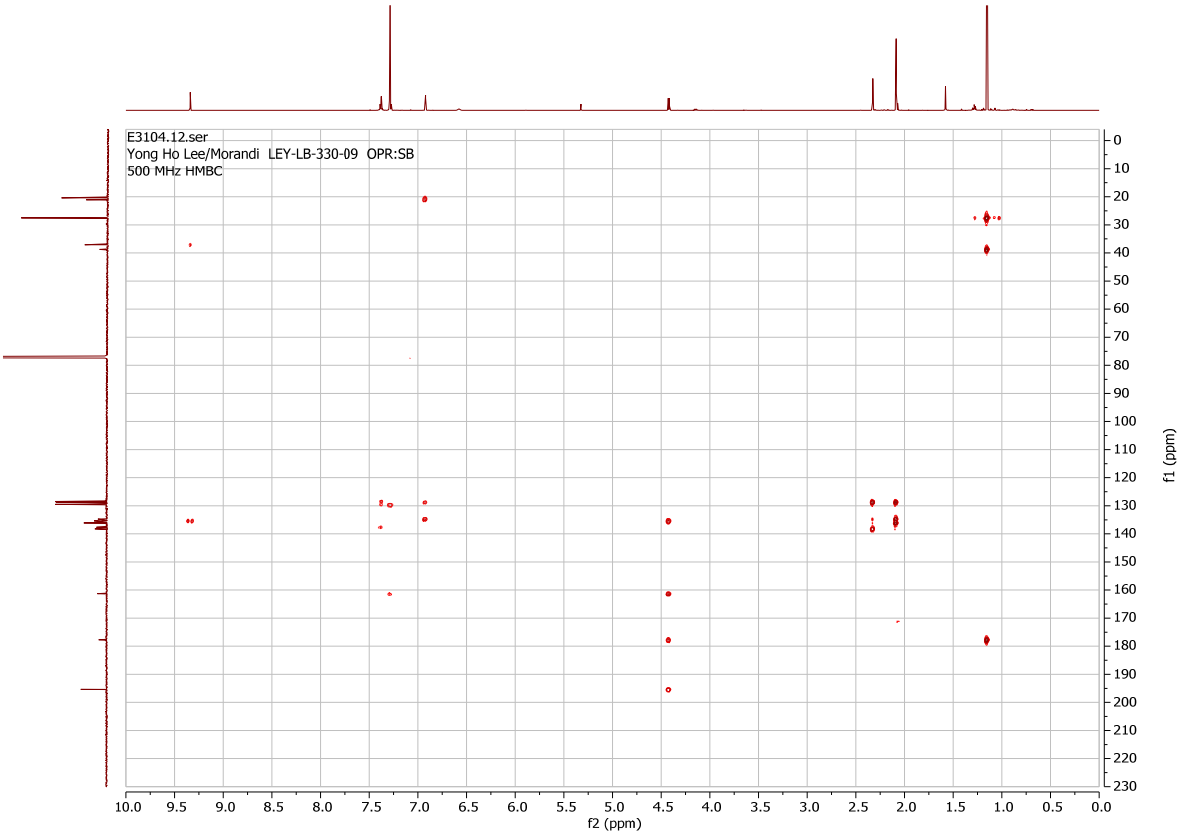
E3104.12.ser
Yong Ho Lee/Morandi LEY-LB-330-09 OPR:SB
500 MHz HMBC
f2 (ppm)
f1 (ppm)

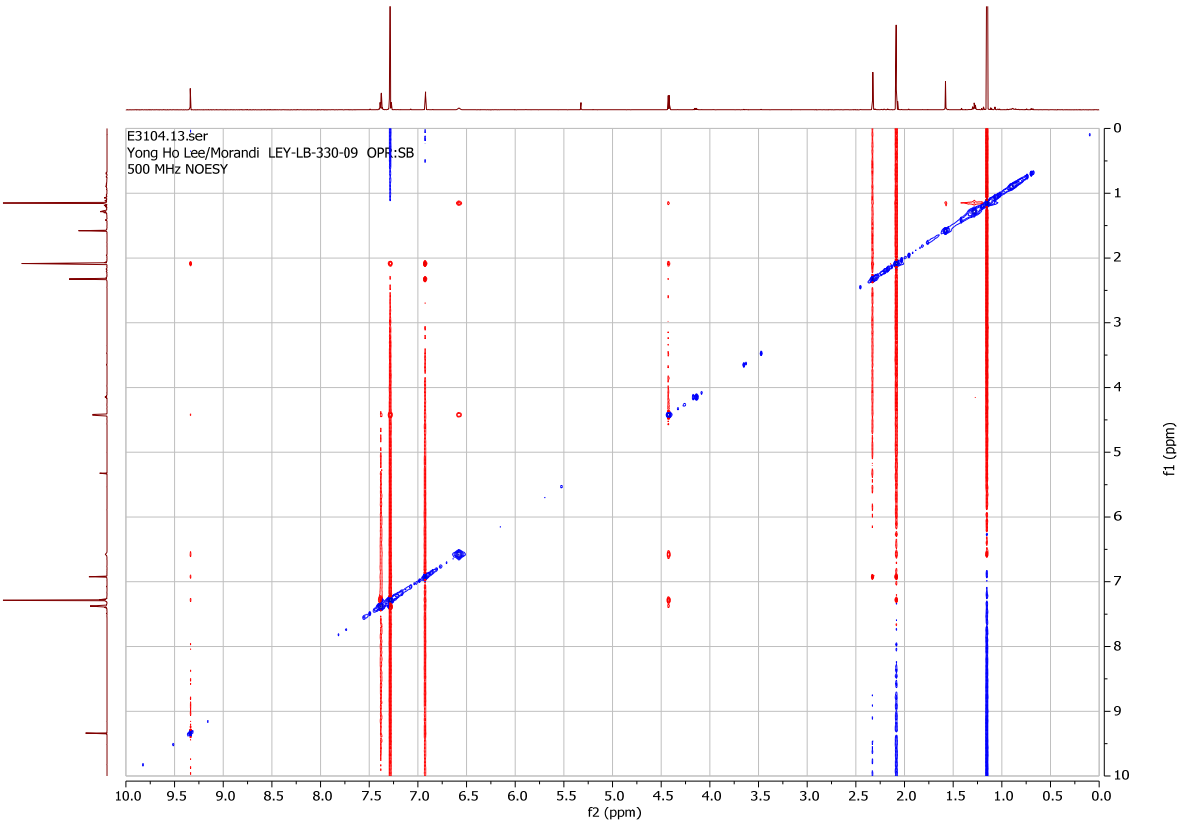
E3104.13.ser
Yong Ho Lee/Morandi LEY-LB-330-09 OPR:SB
500 MHz NOESY
f2 (ppm)
f1 (ppm)

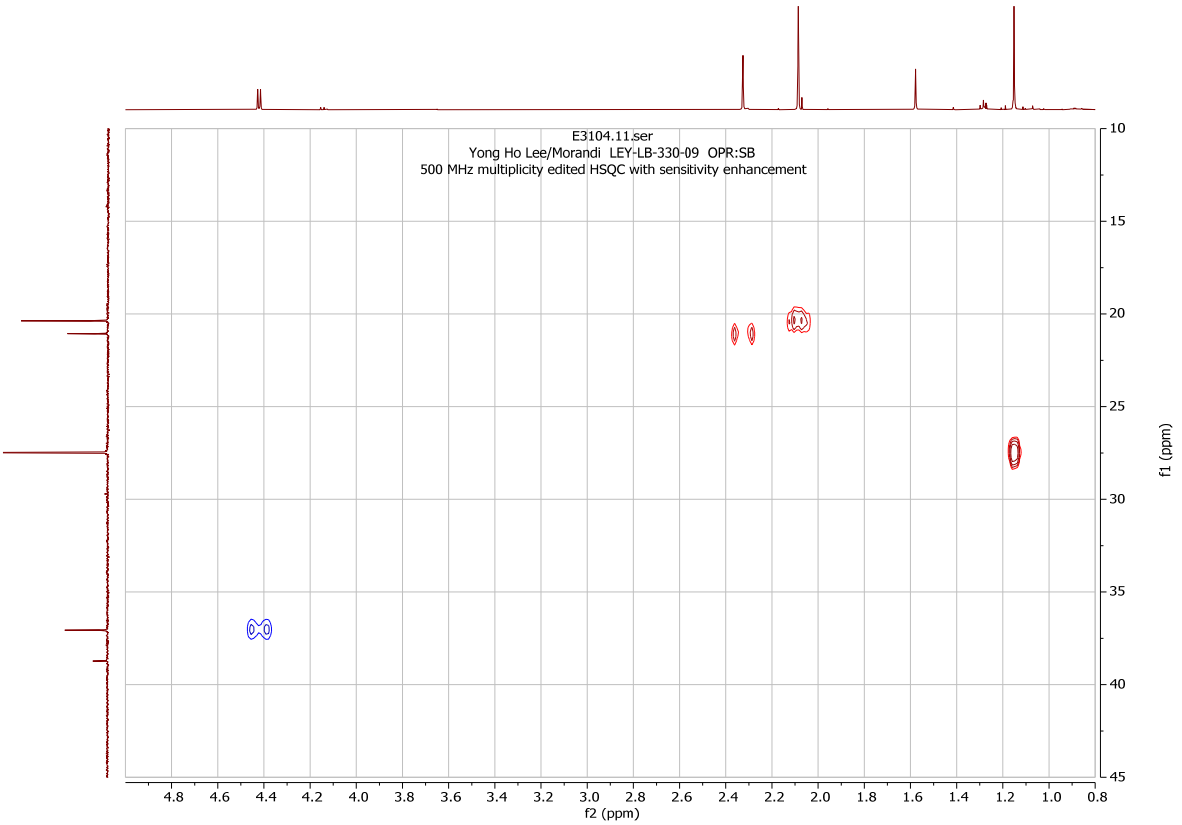
E3104.11.ser
Yong Ho Lee/Morandi LEY-LB-330-09 OPR:SB
500 MHz multiplicity edited HSQC with sensitivity enhancement
f2 (ppm)
f1 (ppm)

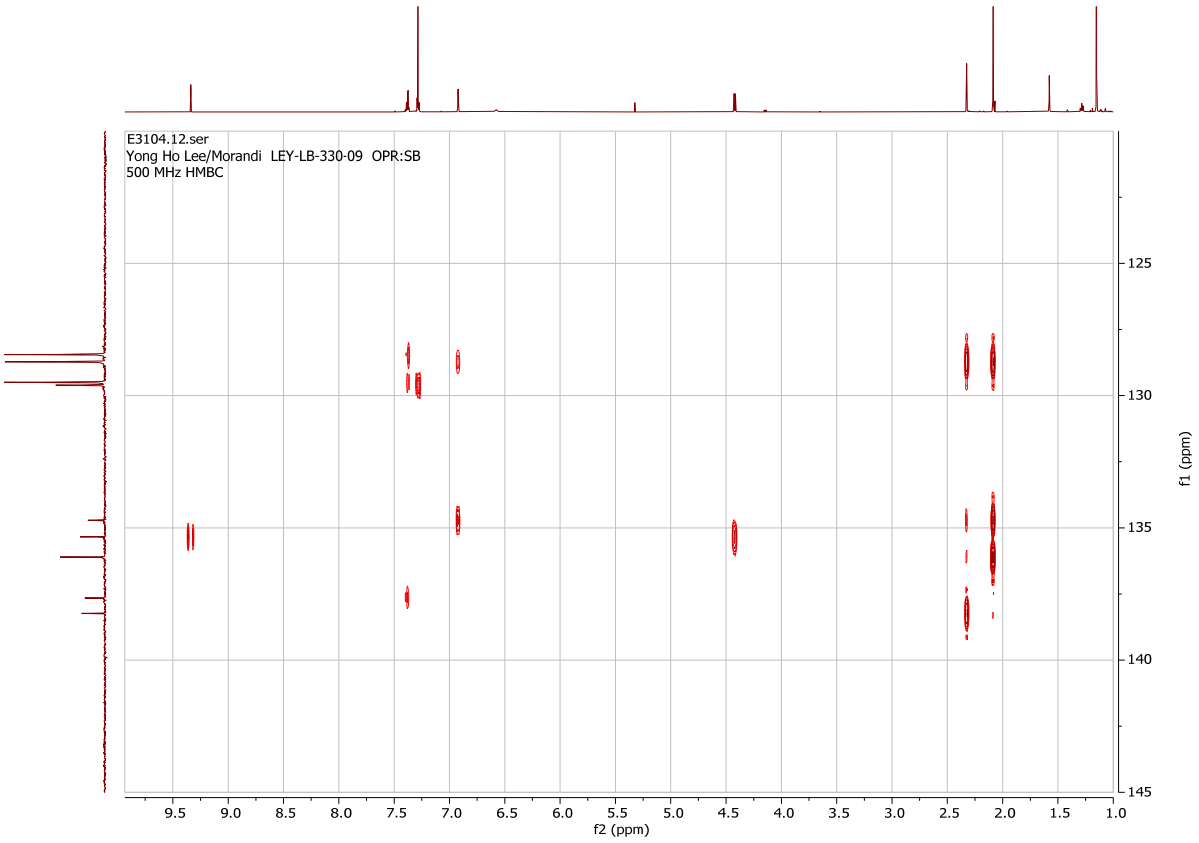
E3104.12.ser
Yong Ho Lee/Morandi LEY-LB-330-09 OPR:SB
500 MHz HMBC
125
130
135
140
145
f1 (ppm)
9.5
9.0
8.5
8.0
7.5
7.0
6.5
6.0
5.5
5.0
4.5
4.0
3.5
3.0
2.5
2.0
1.5
1.0
f2 (ppm)

(*E*)-3-mesityl-2-(trimethylsilyl)hex-2-enal (**54**).

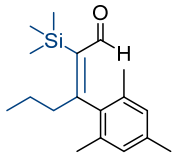

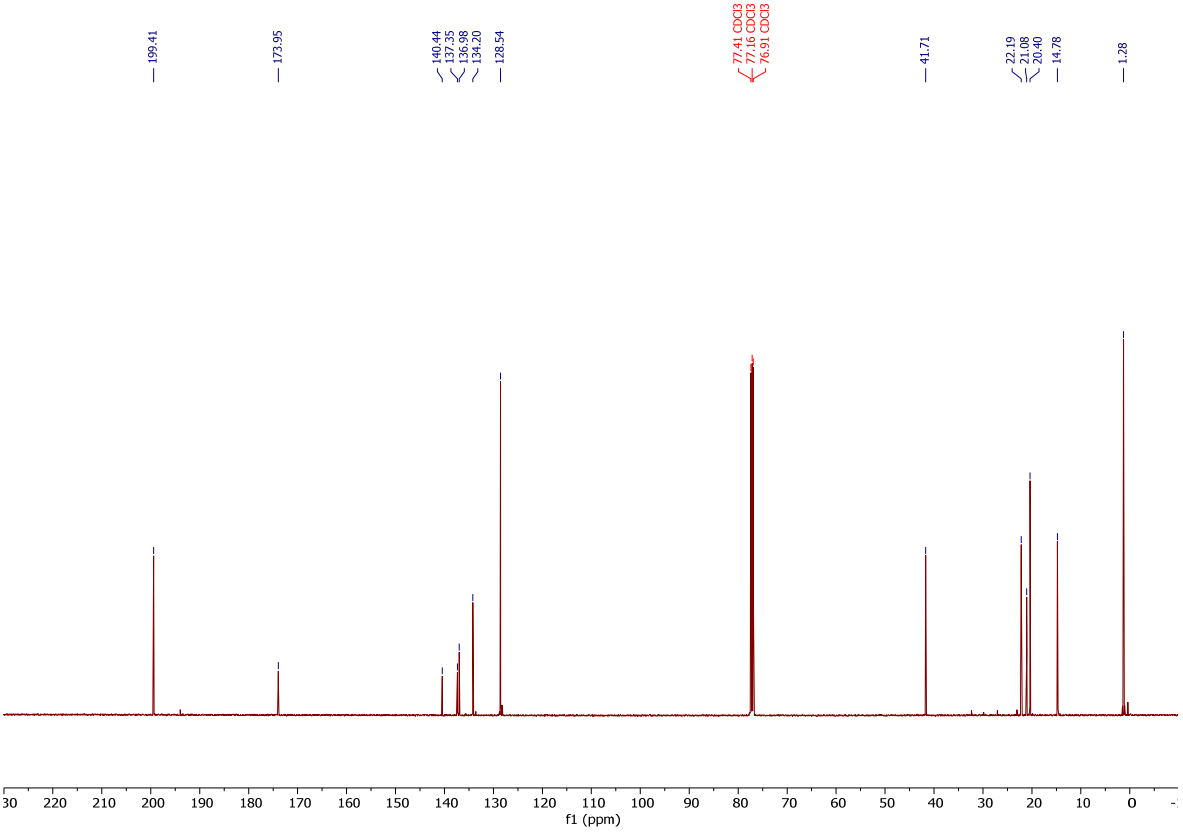

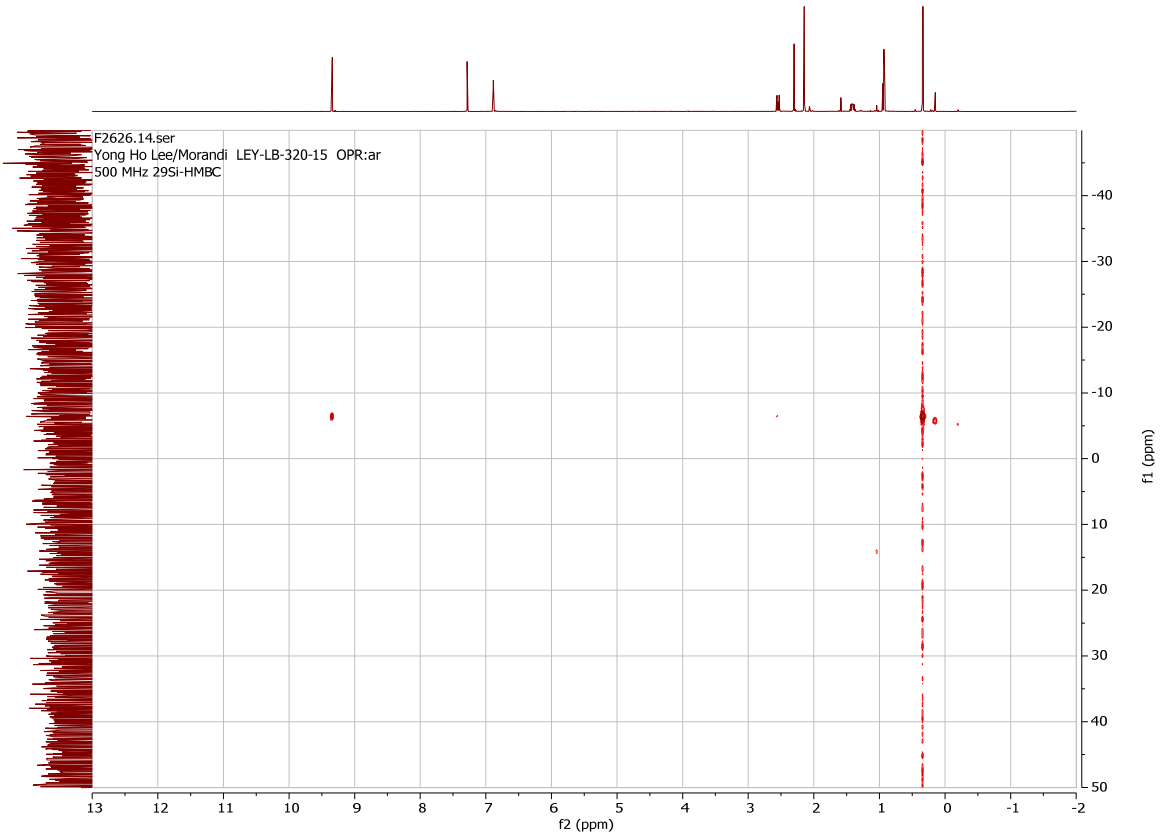
F2626.14.ser
Yong Ho Lee/Morandi LEY-LB-320-15 OPR:ar
500 MHz 29Si-HMBC
f2 (ppm)
f1 (ppm)

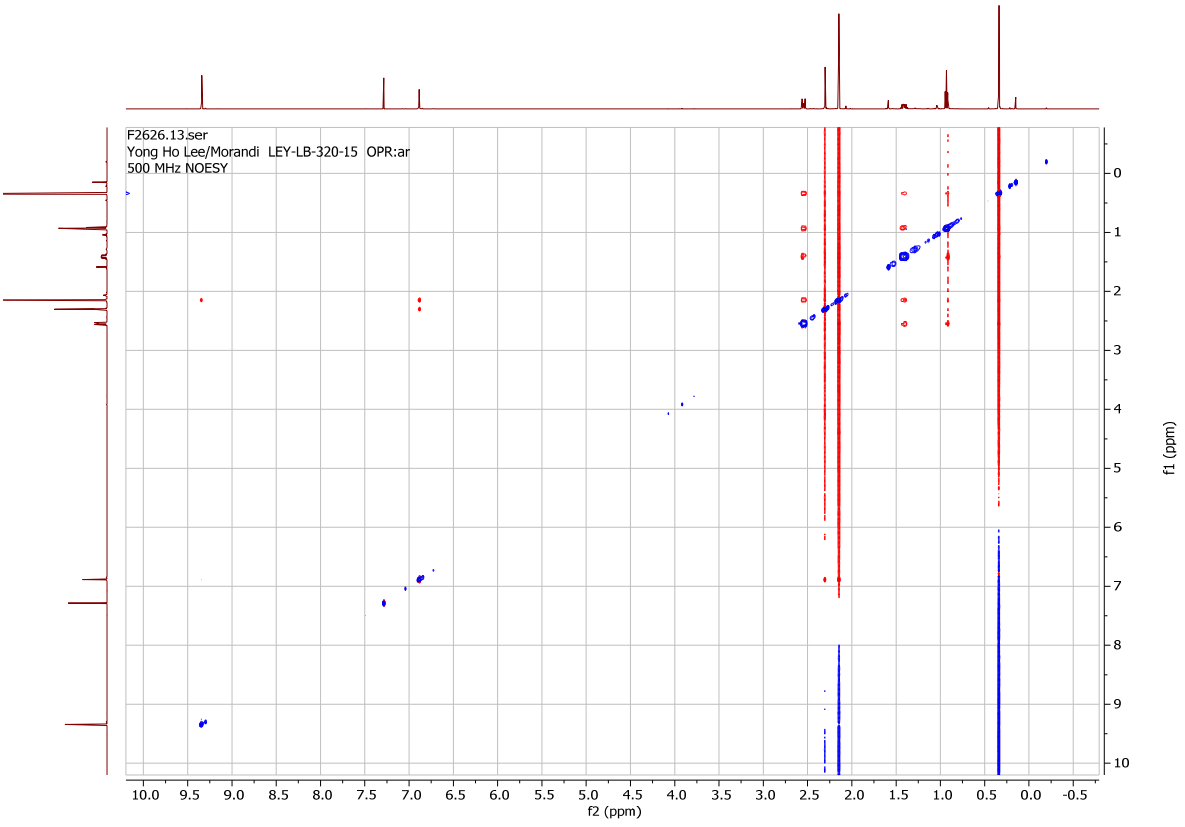
F2626.13.ser
Yong Ho Lee/Morandi LEY-LB-320-15 OPR:ar
500 MHz NOESY
f2 (ppm)
f1 (ppm)

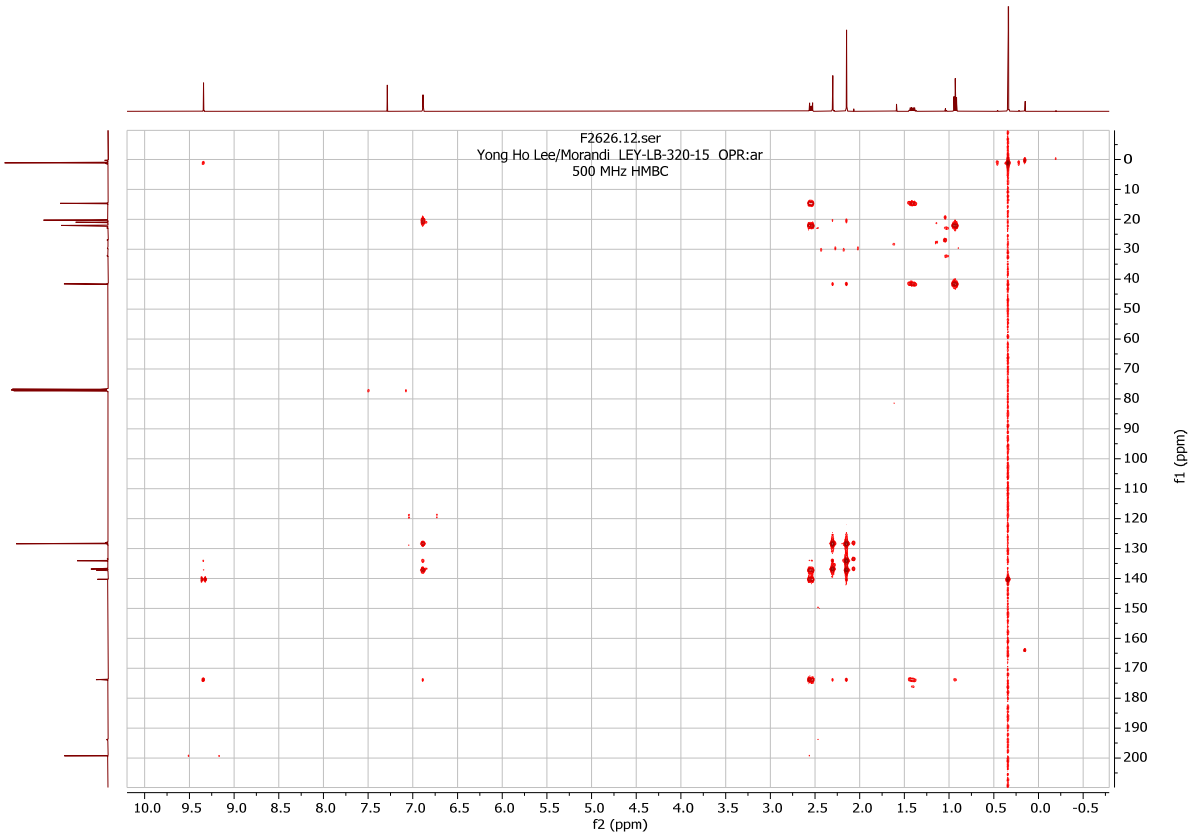
F2626.12.ser
Yong Ho Lee/Morandi LEY-LB-320-15 OPR:ar
500 MHz HMBC
f2 (ppm)
f1 (ppm)

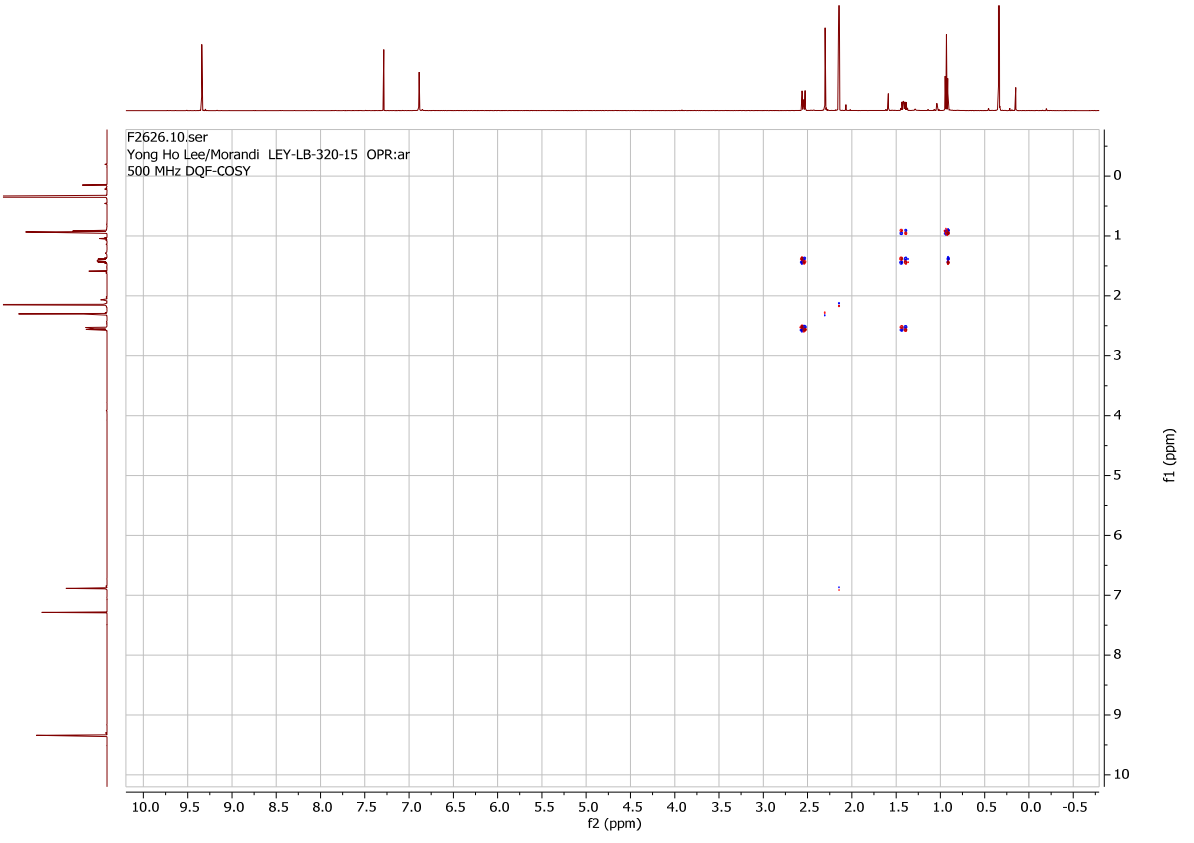
F2626.10.ser
Yong Ho Lee/Morandi LEY-LB-320-15 OPR:ar
500 MHz DQF-COSY
f2 (ppm)
f1 (ppm)

(*E*)-3-cyclopropyl-3-mesityl-2-(trimethylsilyl)acrylaldehyde (**55**).

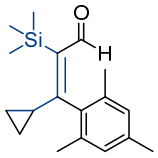

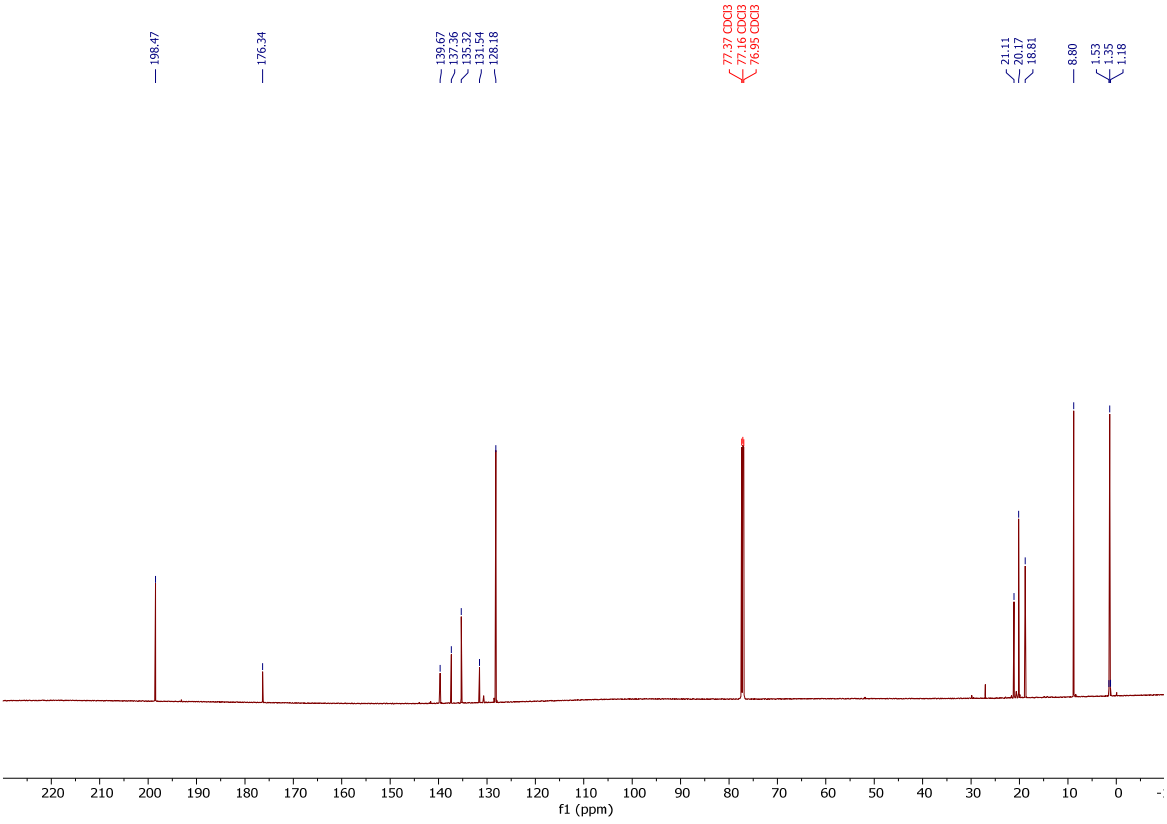

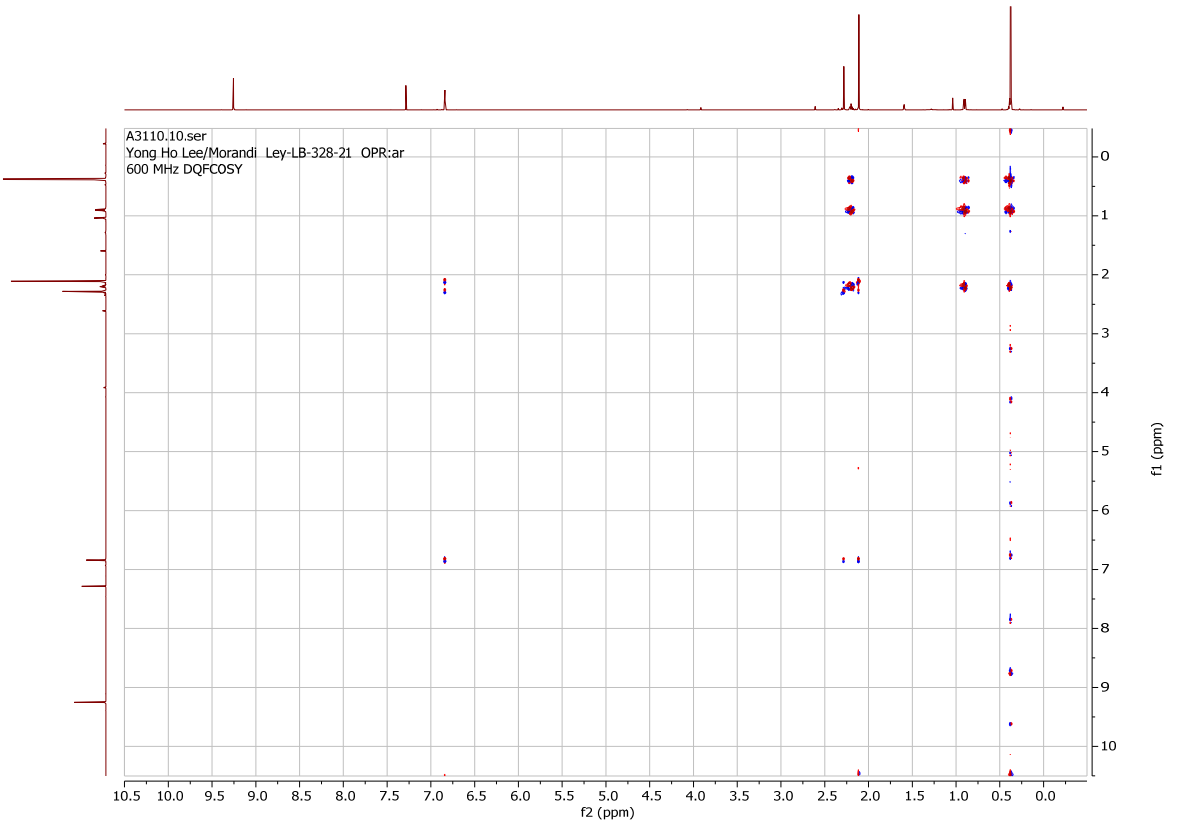
A3110.10.ser
Yong Ho Lee/Morandi Ley-LB-328-21 OPR:ar
600 MHz DQFCOSY
f2 (ppm)
f1 (ppm)

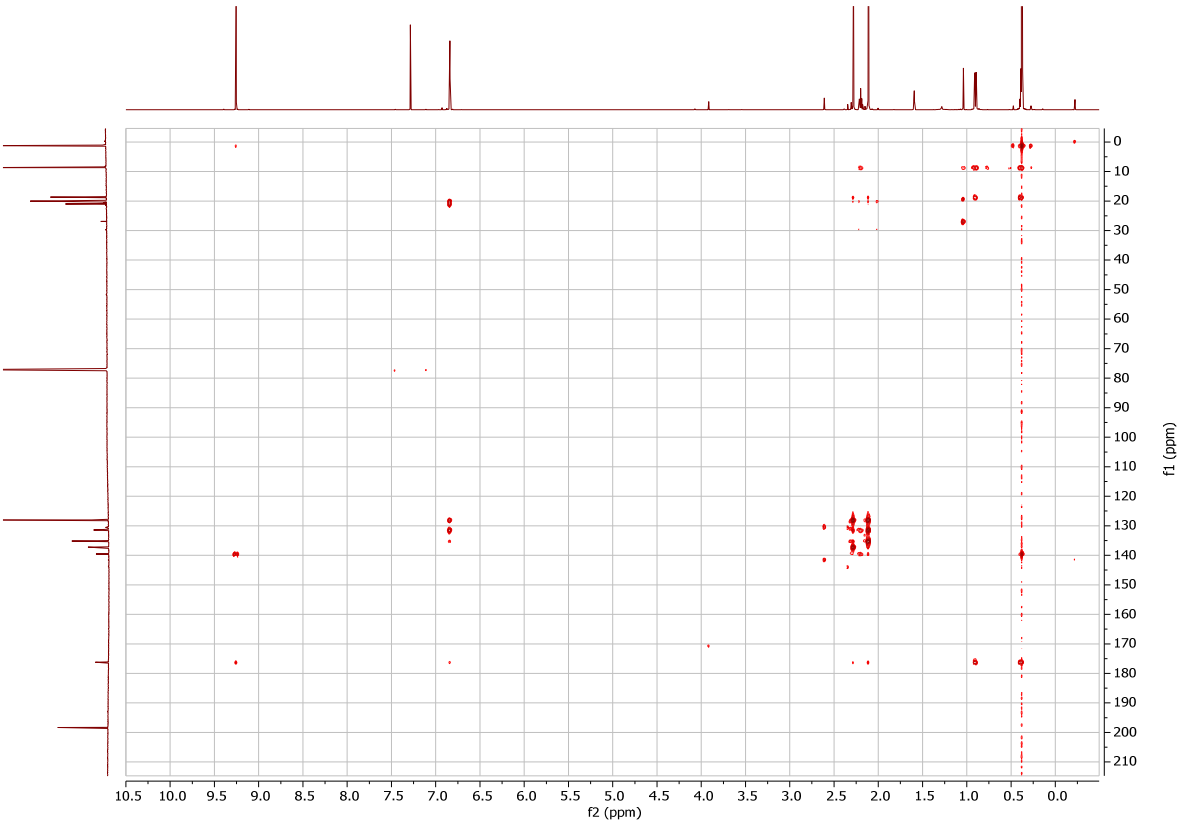
f2 (ppm)
f1 (ppm)

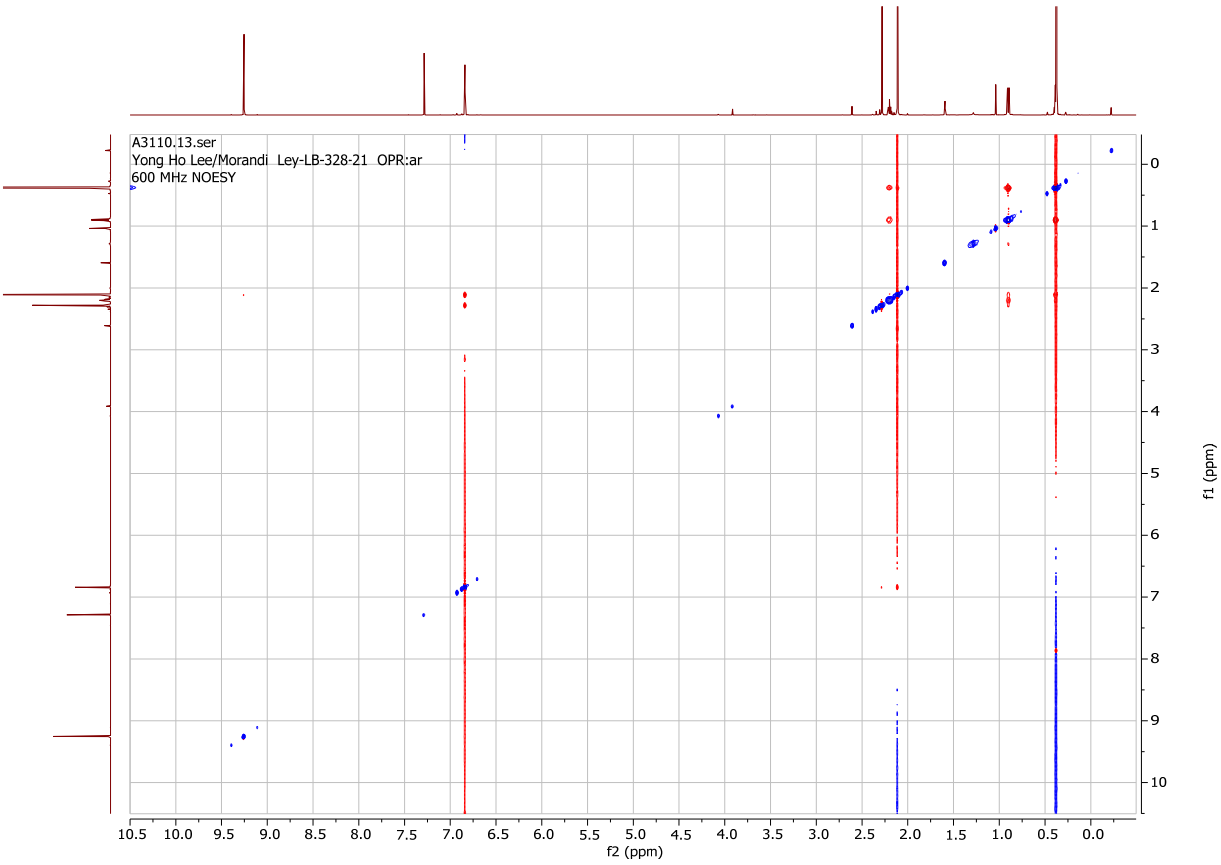
A3110.13.ser
Yong Ho Lee/Morandi Ley-LB-328-21 OPR:ar
600 MHz NOESY
f2 (ppm)
f1 (ppm)

(*E*)-3-mesityl-2-(triethylsilyl)oct-2-enal (**56**).

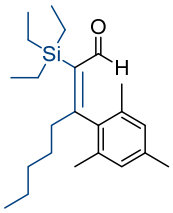

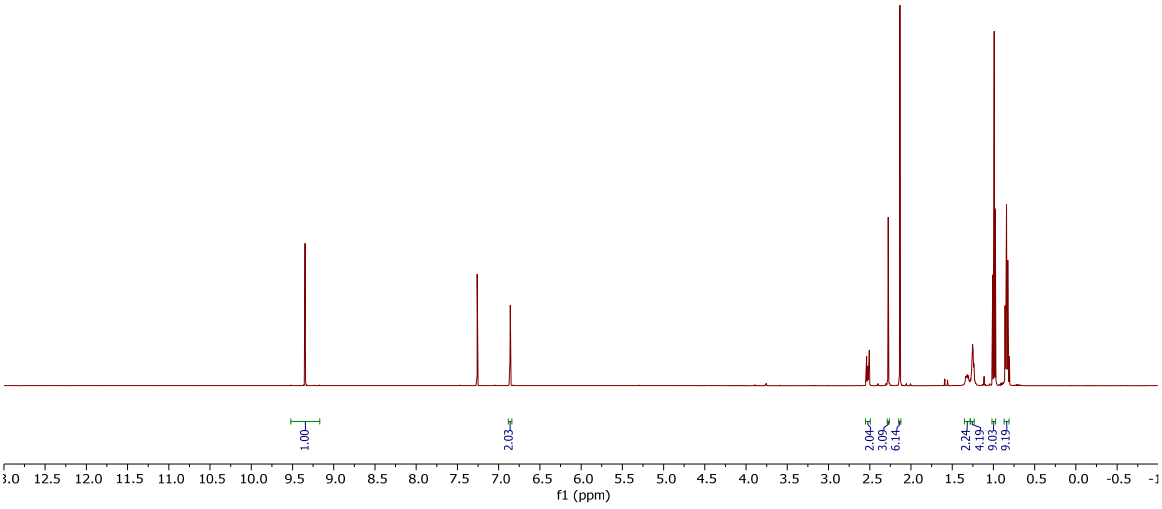

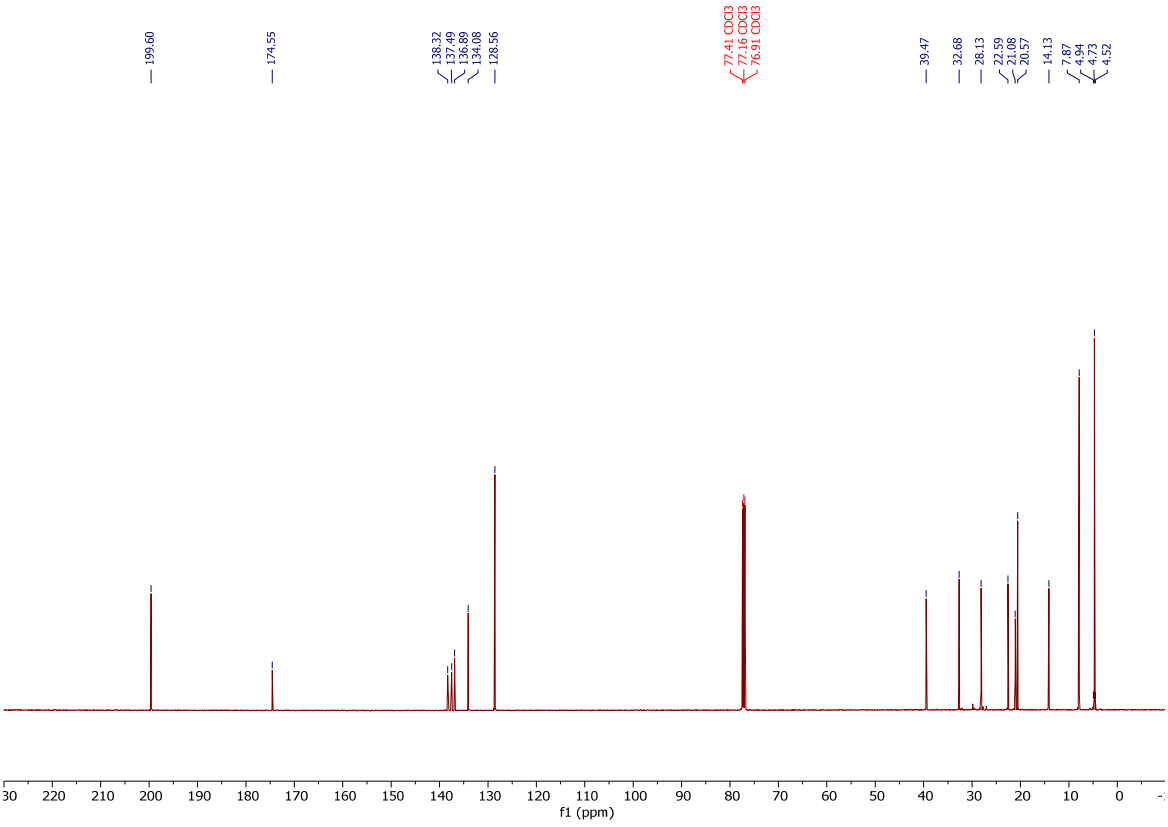

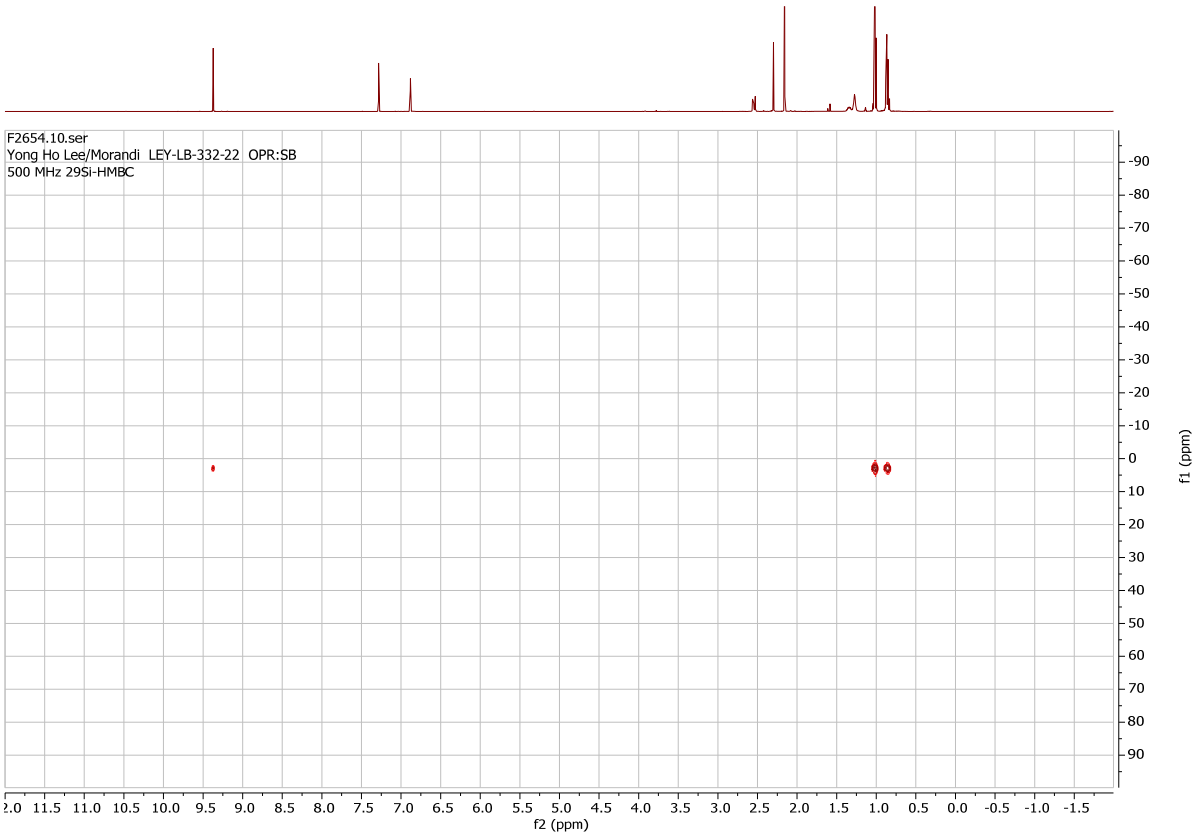
F2654.10.ser
Yong Ho Lee/Morandi LEY-LB-332-22 OPR:SB
500 MHz 29Si-HMBC
f2 (ppm)
f1 (ppm)

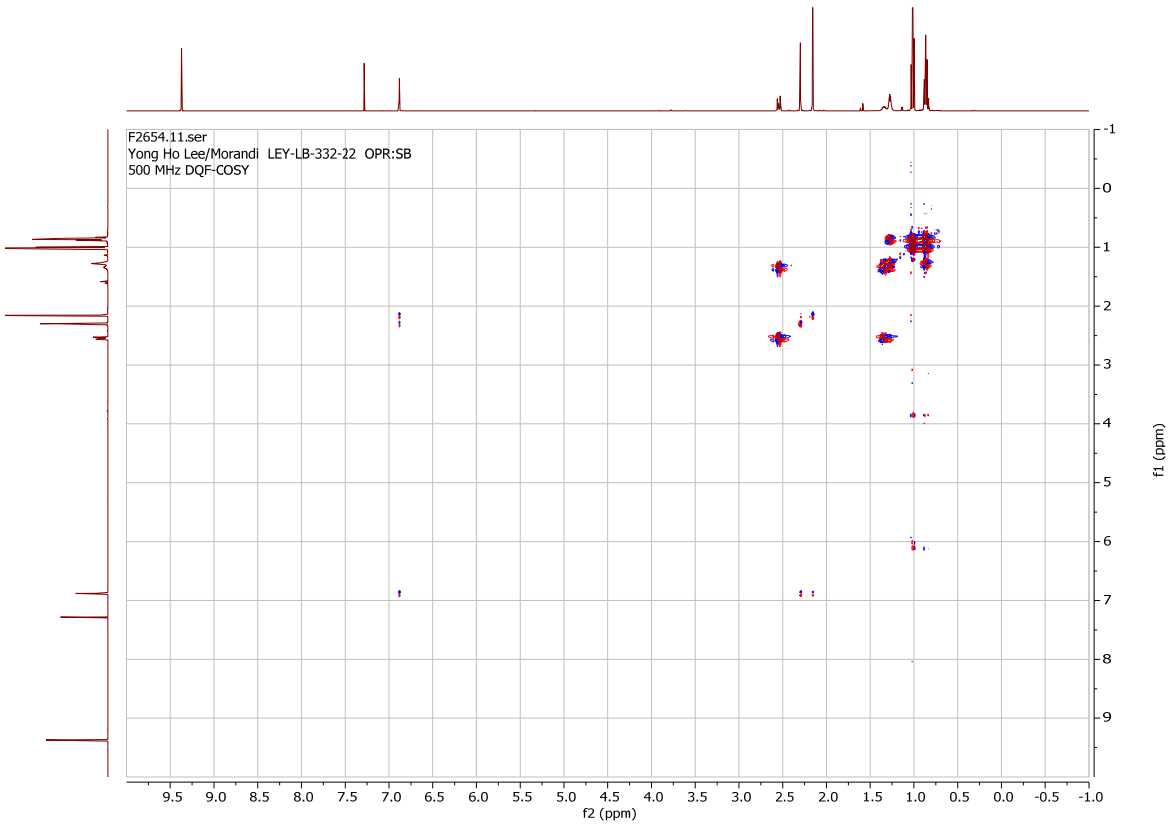
F2654.11.ser
Yong Ho Lee/Morandi LEY-LB-332-22 OPR:SB
500 MHz DQF-COSY
f2 (ppm)
f1 (ppm)

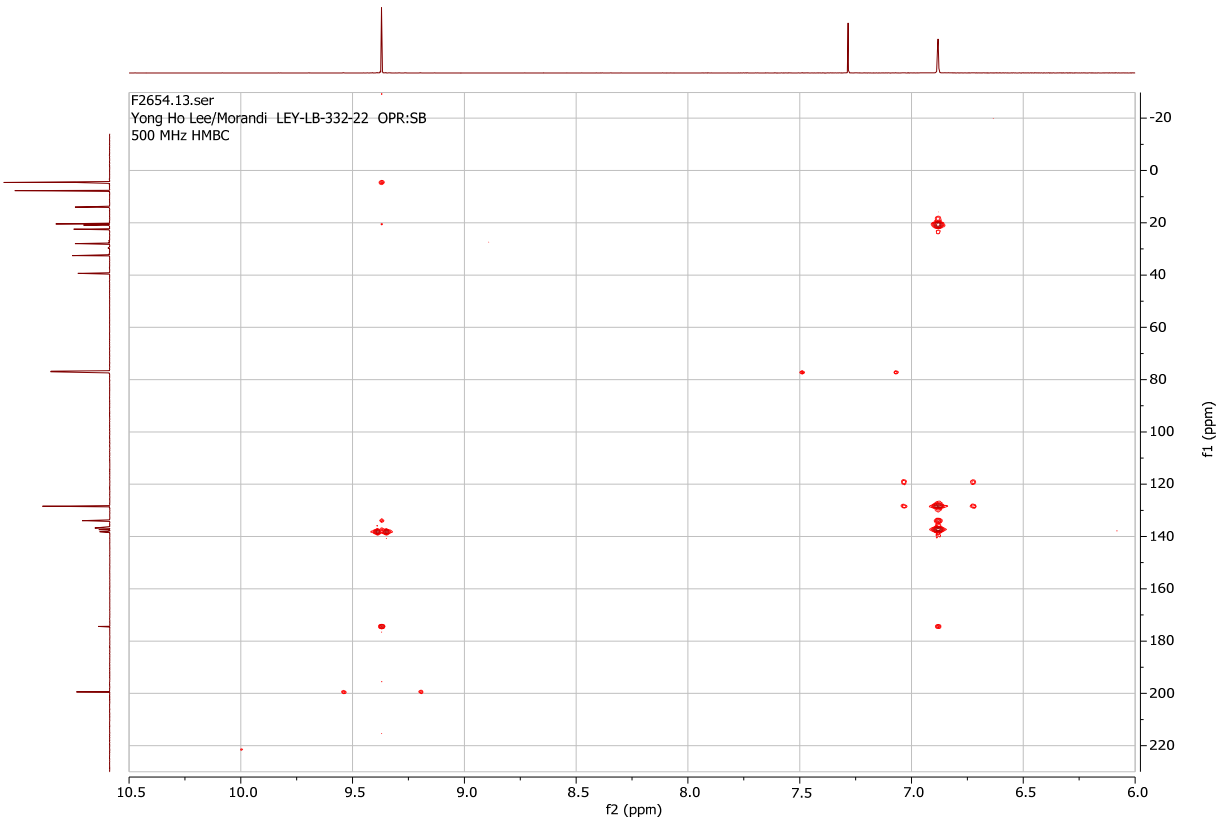
F2654.13.ser
Yong Ho Lee/Morandi LEY-LB-332-22 OPR:SB
500 MHz HMBC
f2 (ppm)
f1 (ppm)

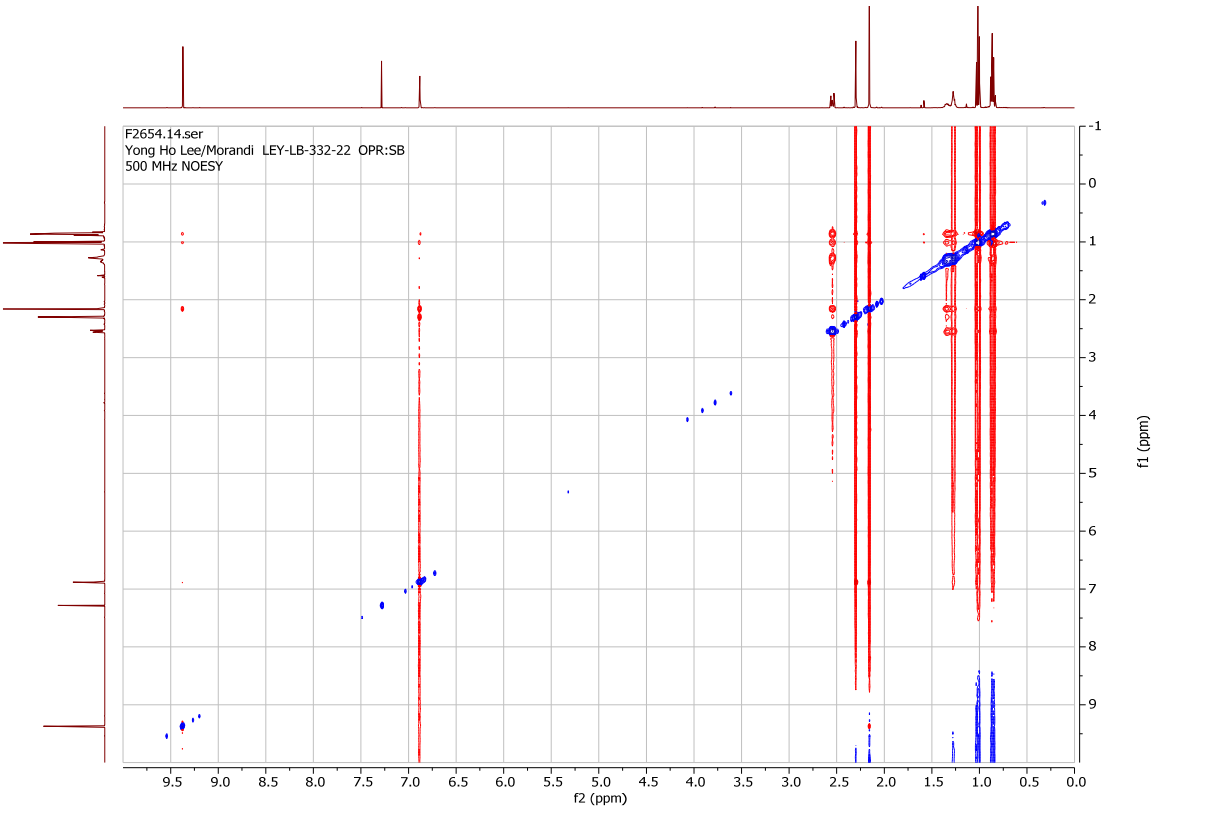
F2654.14.ser
Yong Ho Lee/Morandi LEY-LB-332-22 OPR:SB
500 MHz NOESY
f2 (ppm)
f1 (ppm)

(*E*)-3-mesityl-2-(triethylsilyl)-5-((triethylsilyl)oxy)pent-2-enal (**57**).

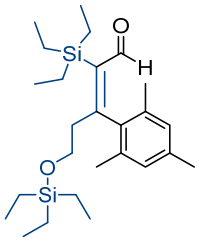

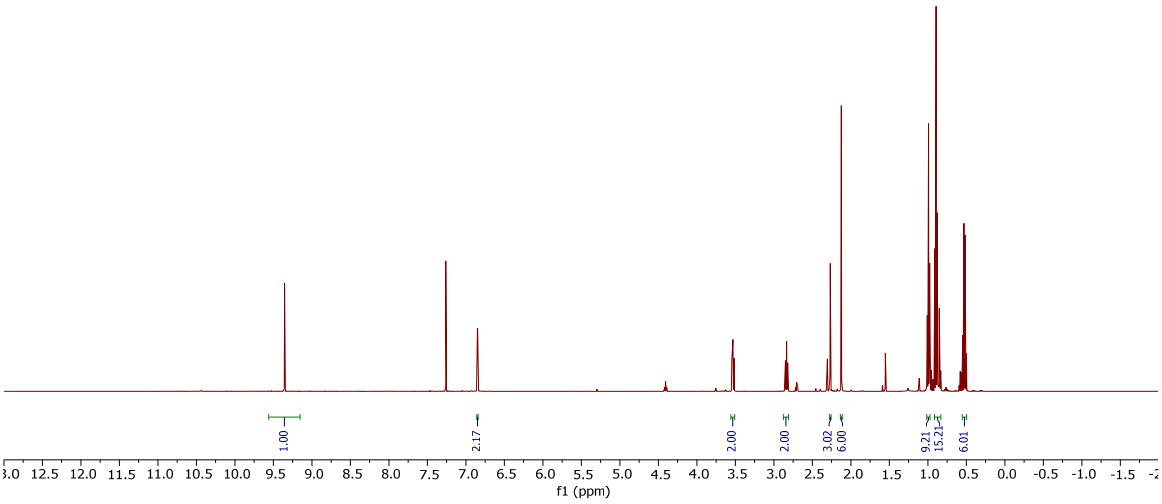

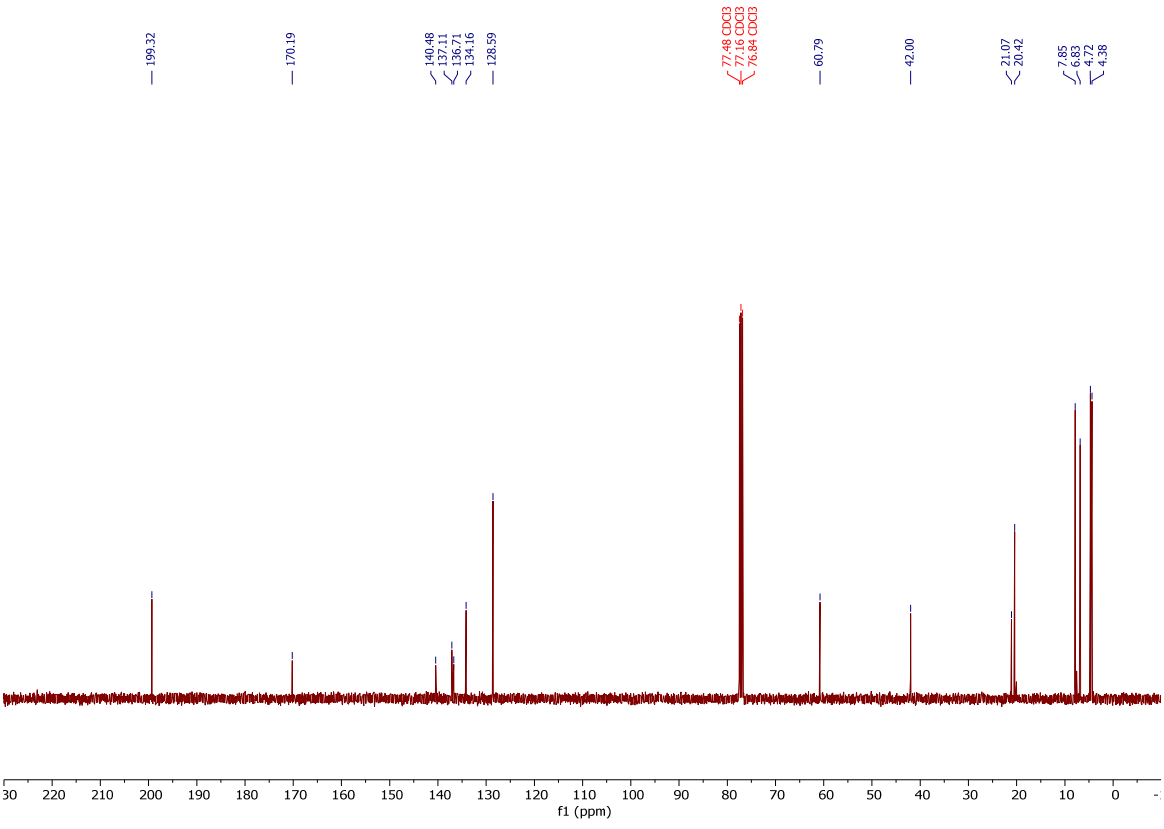

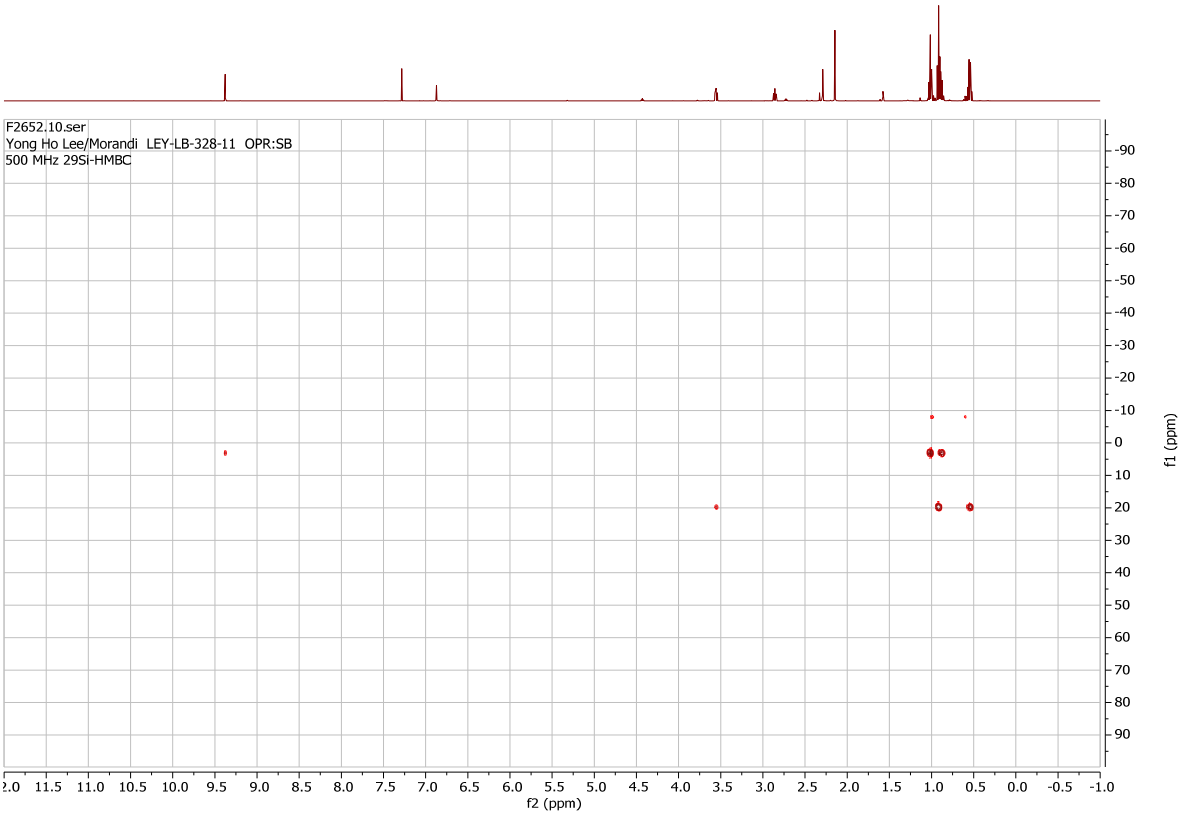
F2652.10.ser
Yong Ho Lee/Morandi LEY-LB-328-11 OPR:SB
500 MHz 29Si-HMBC
f2 (ppm)
f1 (ppm)

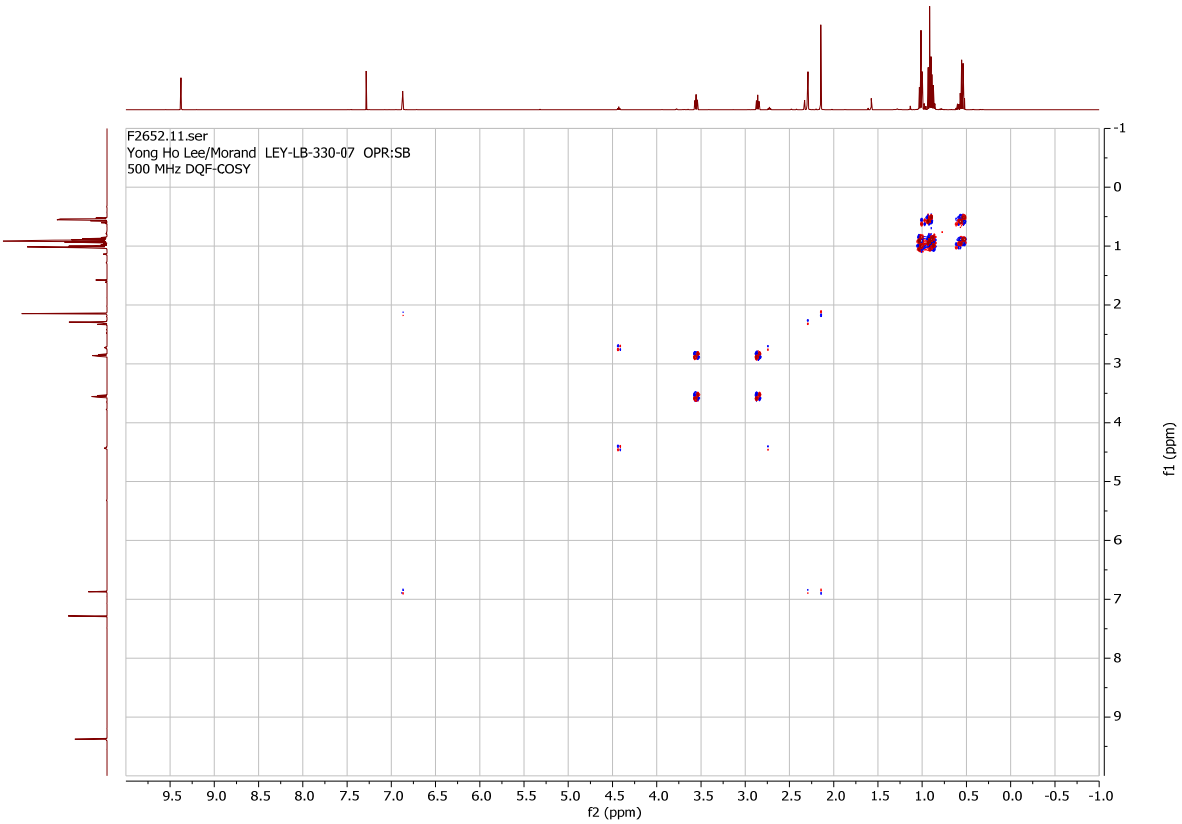
F2652.11.ser
Yong Ho Lee/Morand LEY-LB-330-07 OPR:SB
500 MHz DQF-COSY
f2 (ppm)
f1 (ppm)

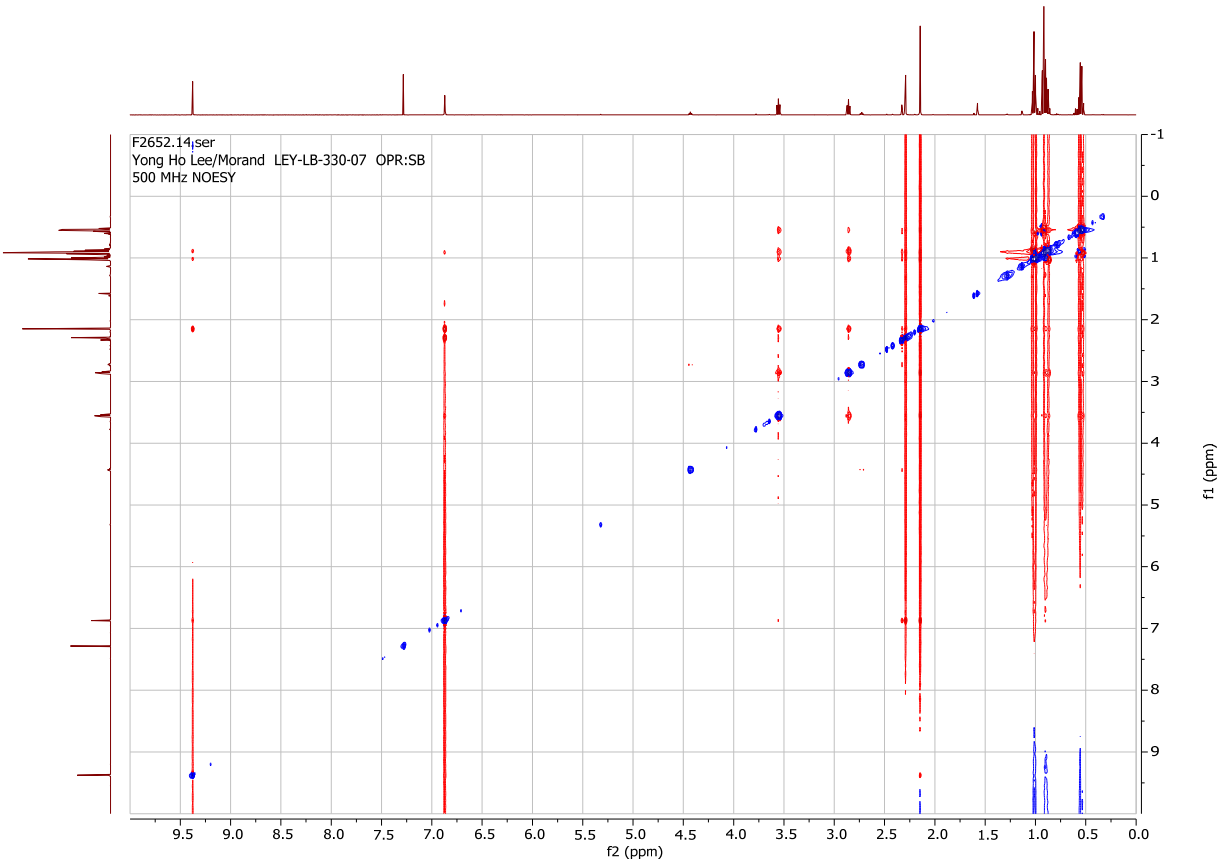
F2652.14.ser
Yong Ho Lee/Morand LEY-LB-330-07 OPR:SB
500 MHz NOESY
f2 (ppm)
f1 (ppm)

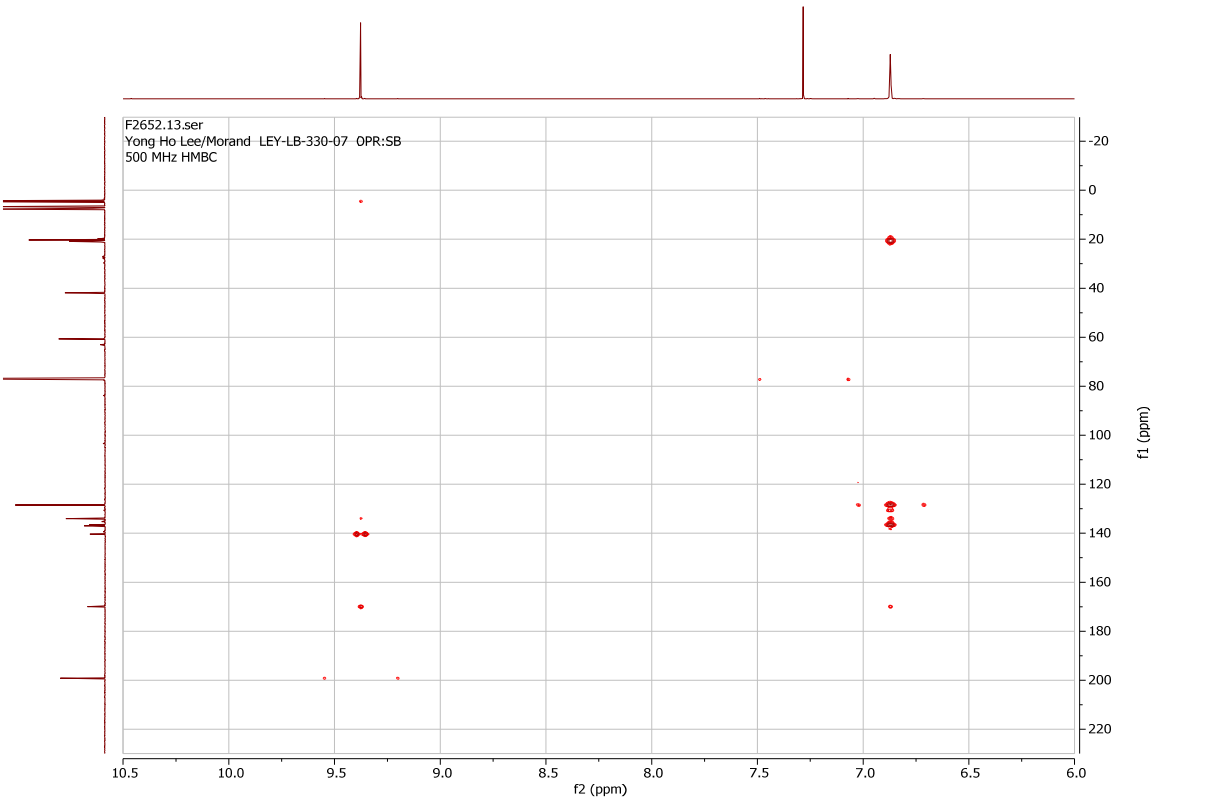
F2652.13.ser
Yong Ho Lee/Morand LEY-LB-330-07 OPR:SB
500 MHz HMBC
f2 (ppm)
f1 (ppm)

(*E*)-3-mesityl-3-phenyl-2-(trimethylsilyl)acrylaldehyde (**58**).

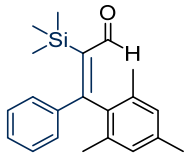

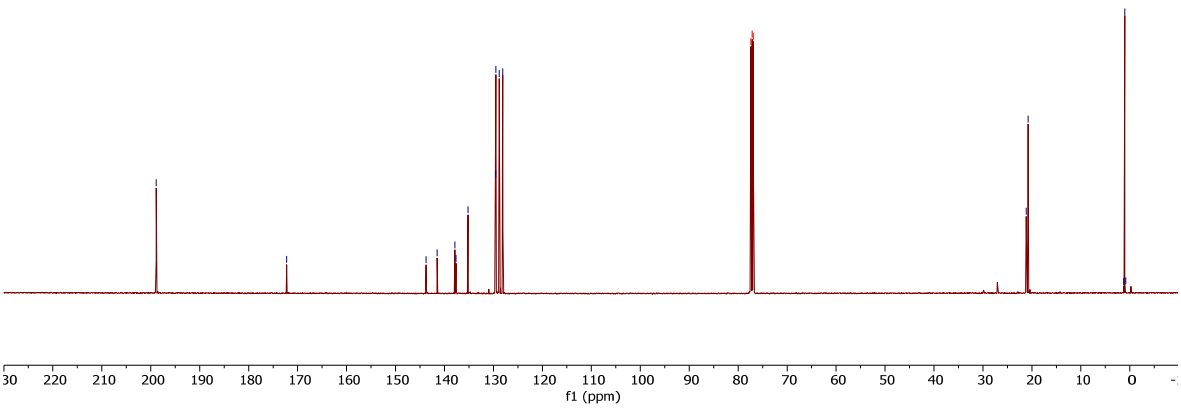

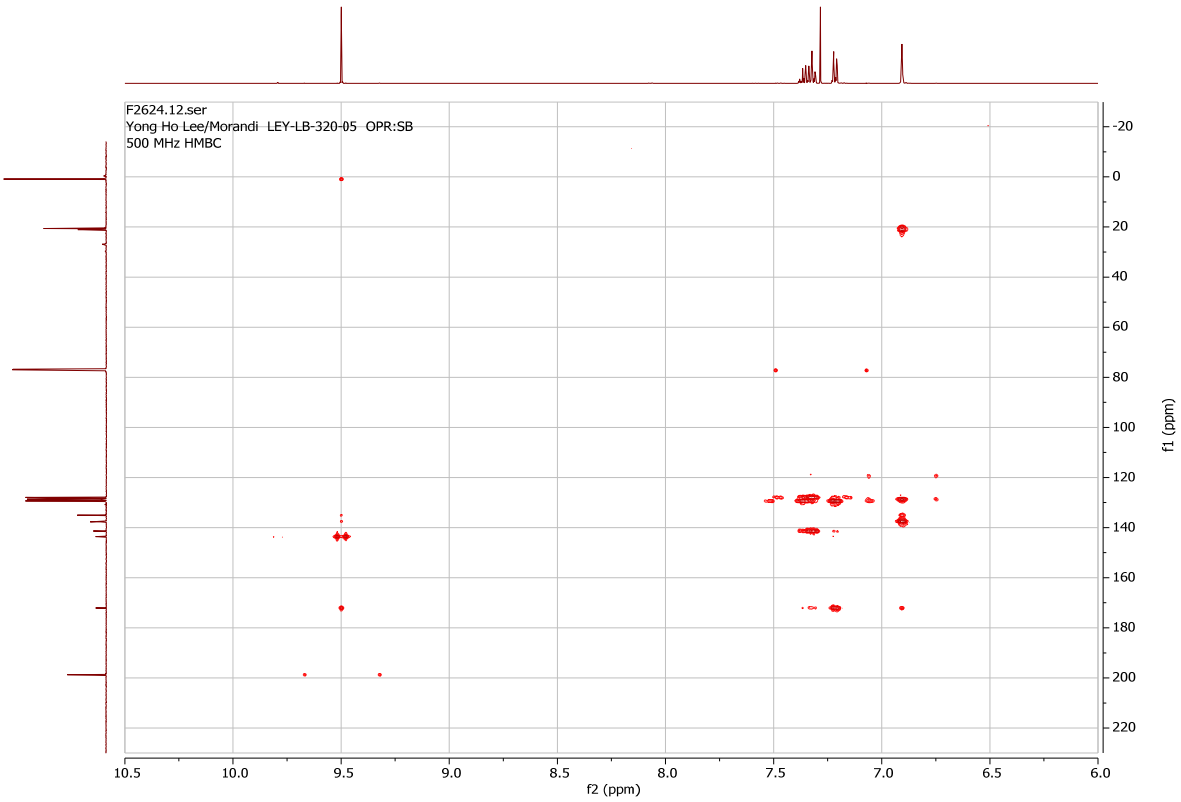
F2624.12.ser
Yong Ho Lee/Morandi LEY-LB-320-05 OPR:SB
500 MHz HMBC
f2 (ppm)
f1 (ppm)

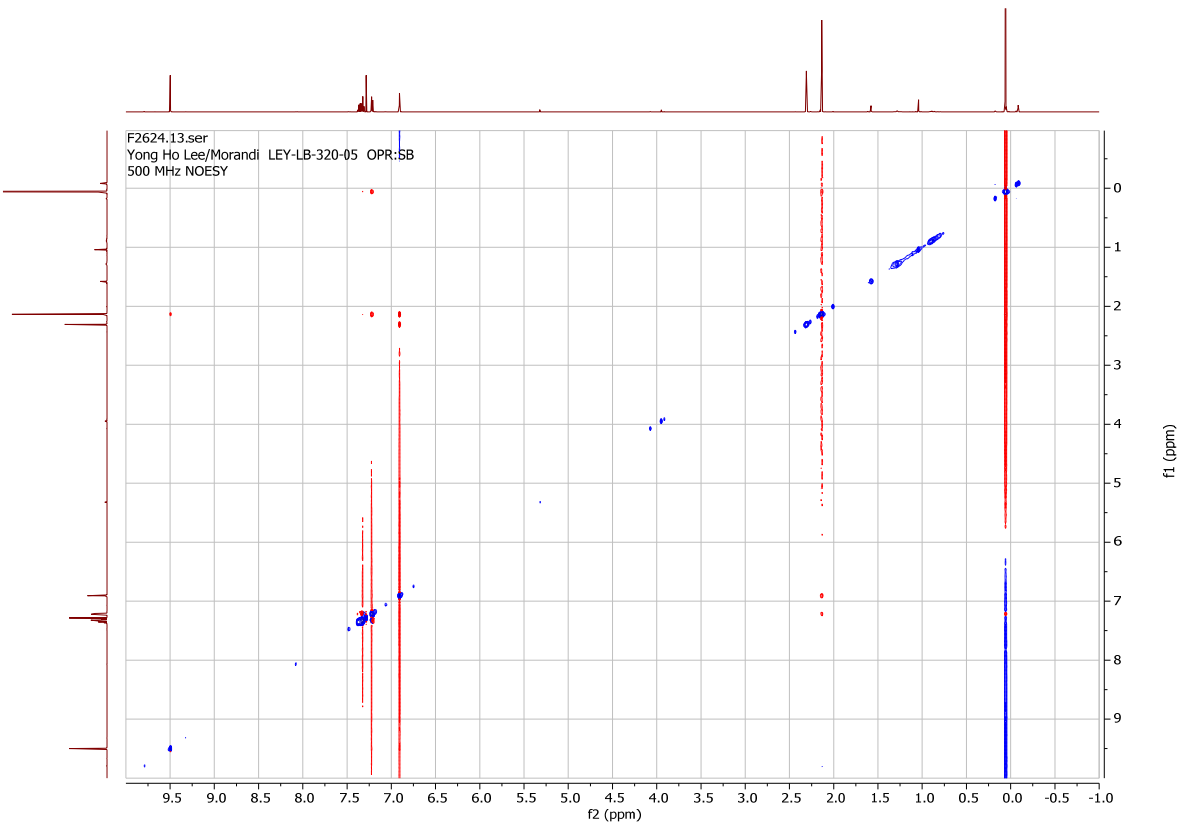
F2624.13.ser
Yong Ho Lee/Morandi LEY-LB-320-05 OPR:SB
500 MHz NOESY
f2 (ppm)
f1 (ppm)

(*E*)-3-mesityl-3-(4-methoxyphenyl)-2-(trimethylsilyl)acrylaldehyde (**59**).

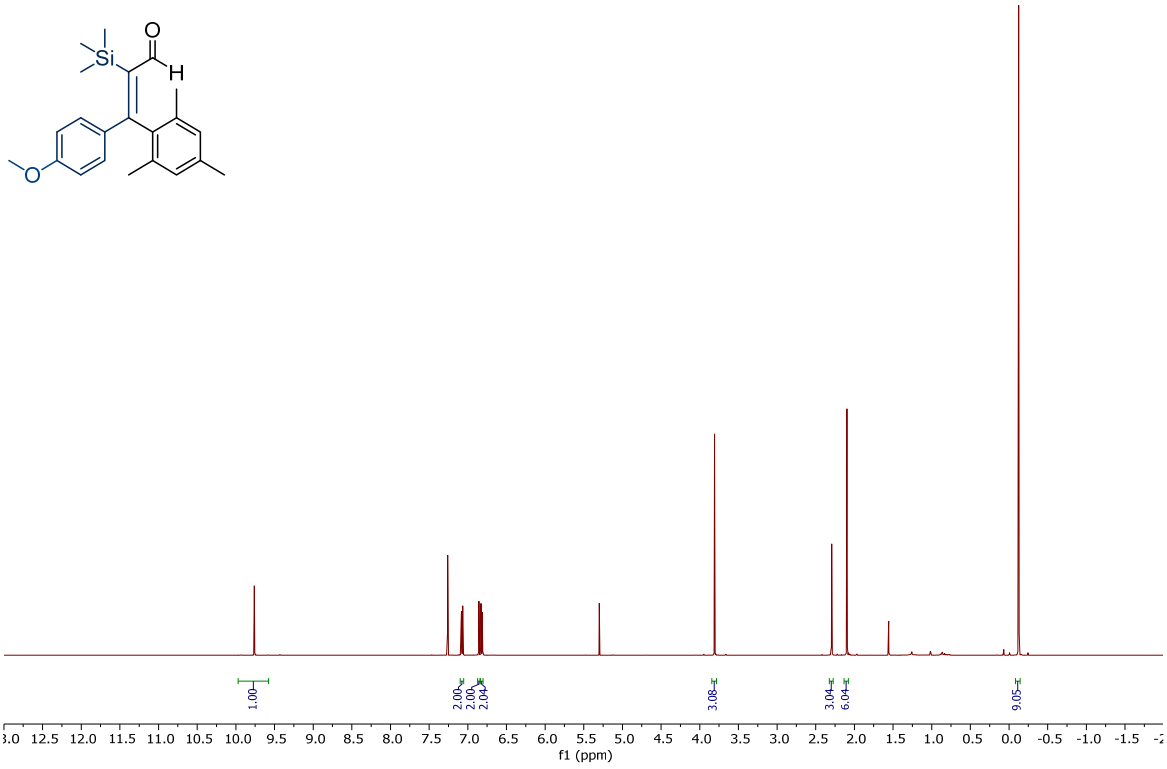

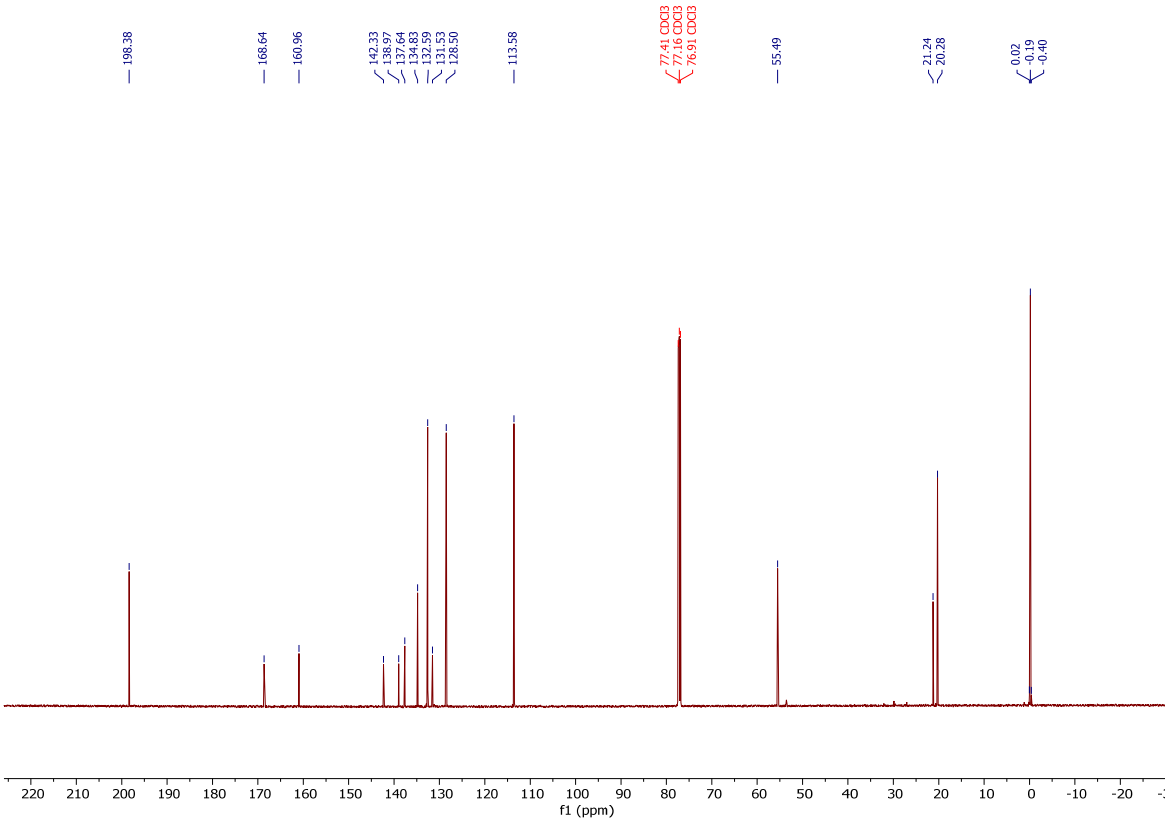

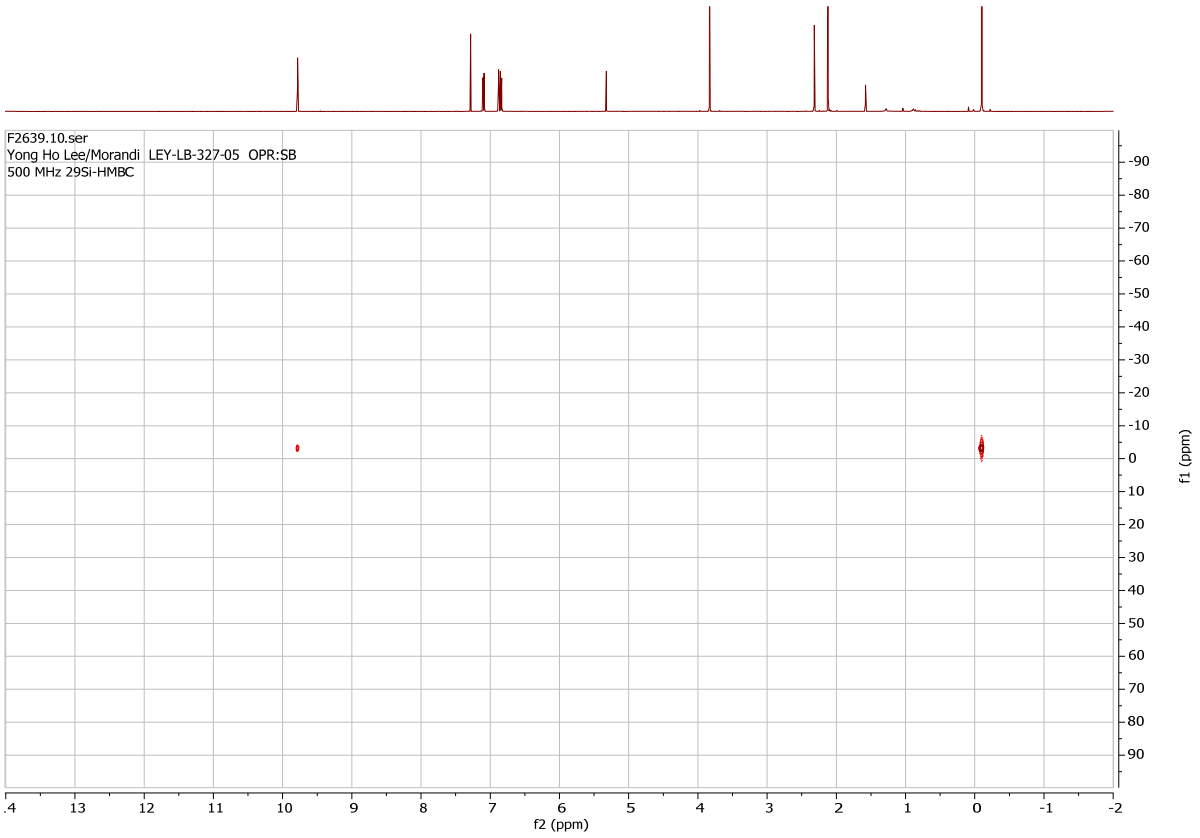
F2639.10.ser
Yong Ho Lee/Morandi LEY-LB-327-05 OPR:SB
500 MHz 29Si-HMBC
f2 (ppm)
f1 (ppm)

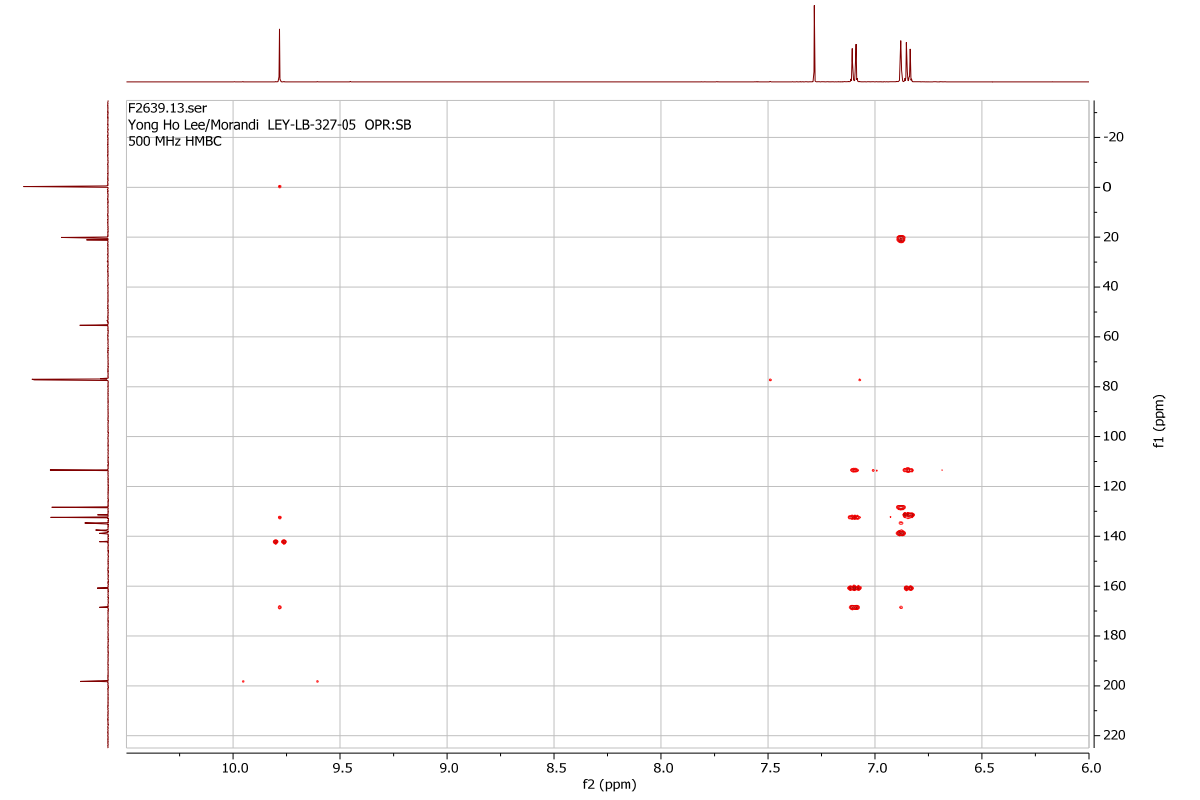
F2639.13.ser
Yong Ho Lee/Morandi LEY-LB-327-05 OPR:SB
500 MHz HMBC
f2 (ppm)
f1 (ppm)

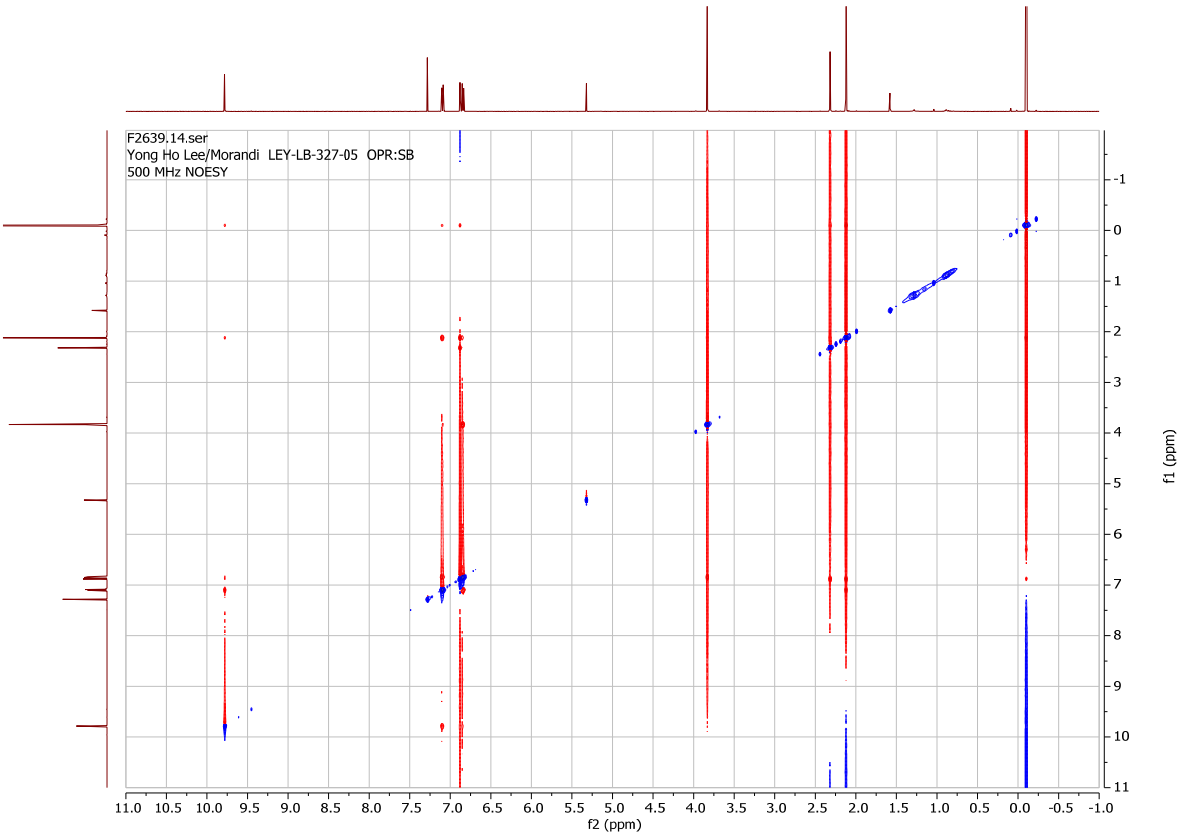
F2639.14.ser
Yong Ho Lee/Morandi LEY-LB-327-05 OPR:SB
500 MHz NOESY
f2 (ppm)
f1 (ppm)

(*E*)-4-(1-mesityl-3-oxo-2-(trimethylsilyl)prop-1-en-1-yl)benzonitrile (**60**).

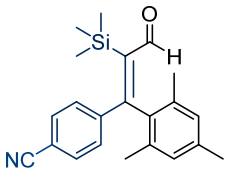

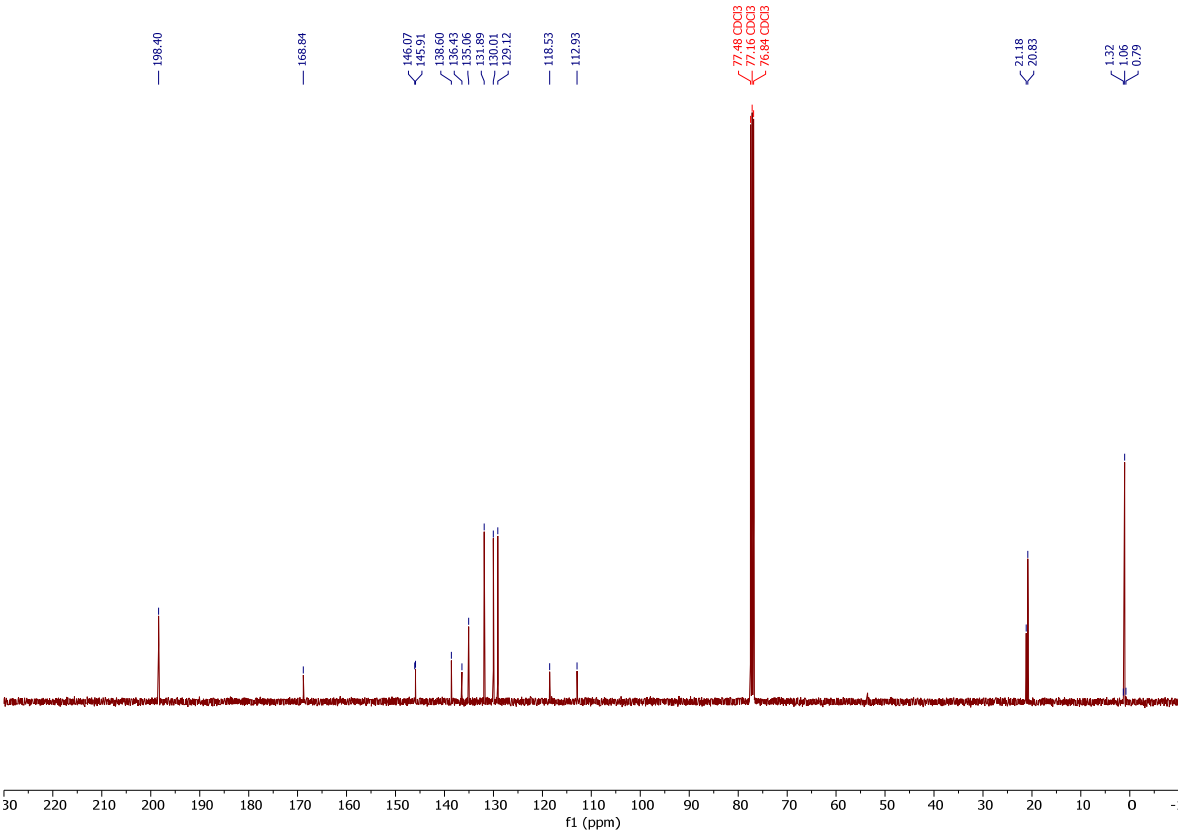

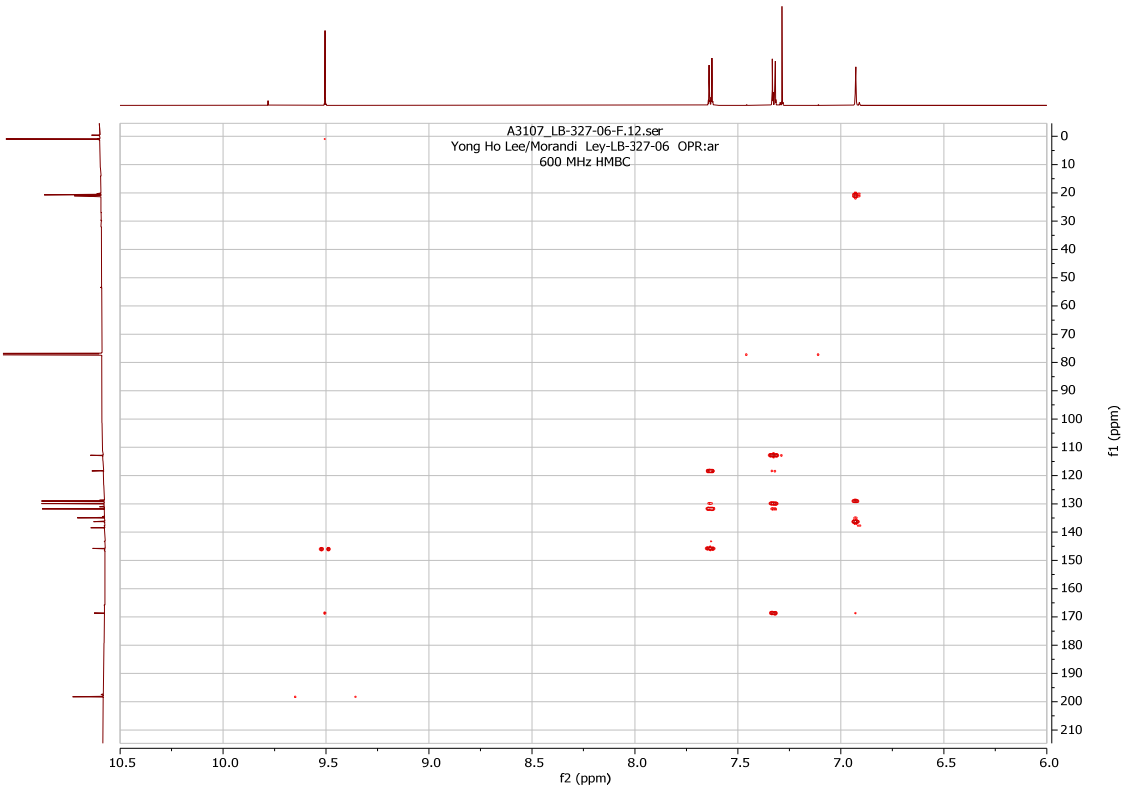
A3107_LB-327-06-F.12.ser
Yong Ho Lee/Morandi Ley-LB-327-06 OPR:ar
600 MHz HMBC
f2 (ppm)
f1 (ppm)

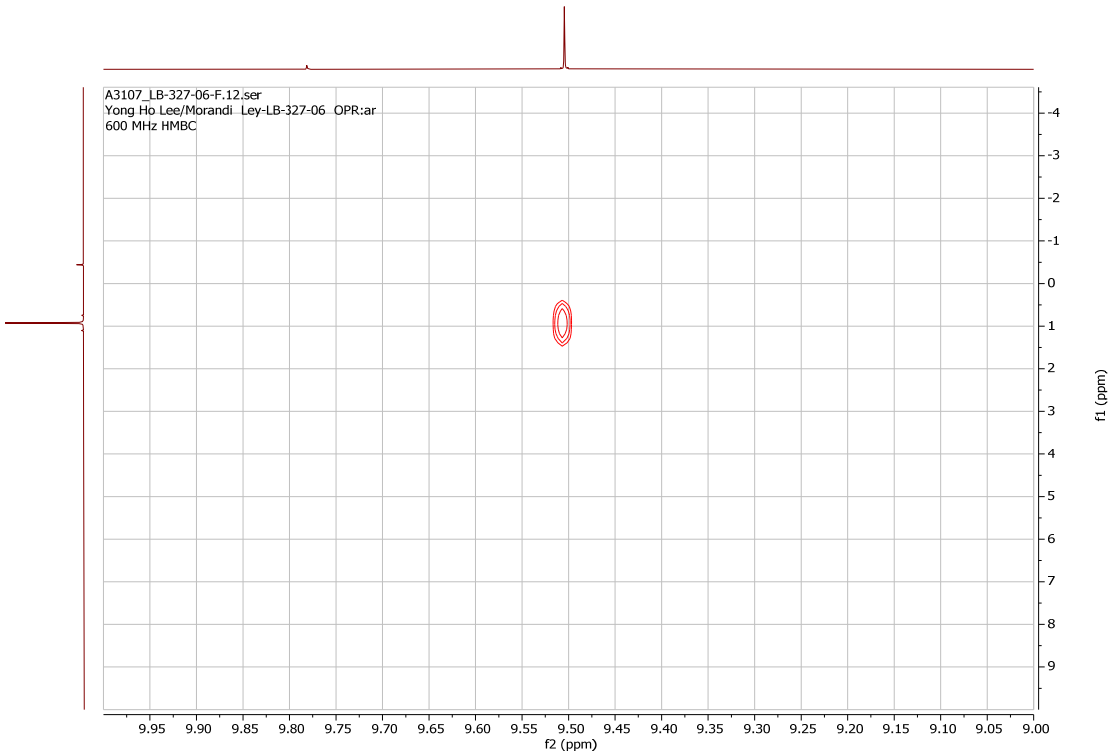
A3107_LB-327-06-F.12.ser
Yong Ho Lee/Morandi Ley-LB-327-06 OPR:ar
600 MHz HMBC
f2 (ppm)
f1 (ppm)

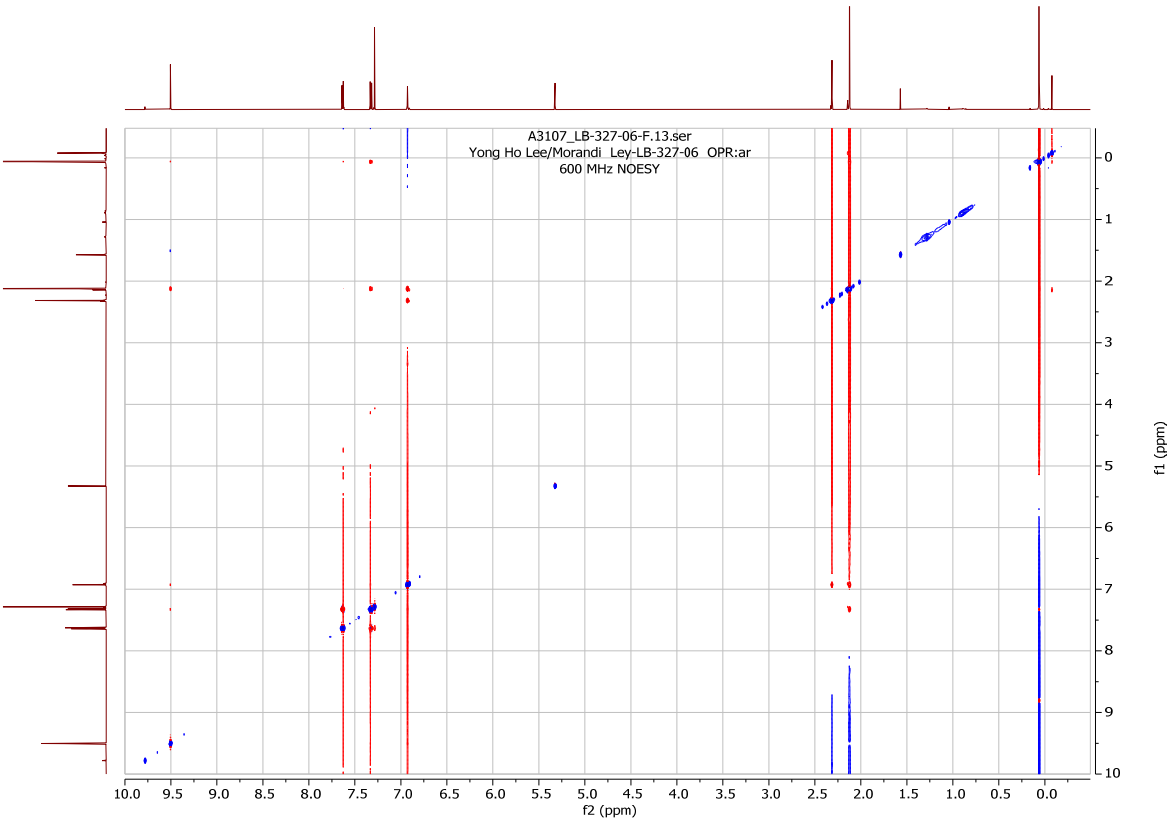
A3107_LB-327-06-F.13.ser
Yong Ho Lee/Morandi Ley-LB-327-06 OPR:ar
600 MHz NOESY
f2 (ppm)
f1 (ppm)

(*E*)-3-mesityl-3-(4-(trifluoromethyl)phenyl)-2-(trimethylsilyl)acrylaldehyde (**61**).

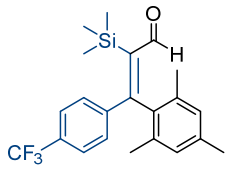

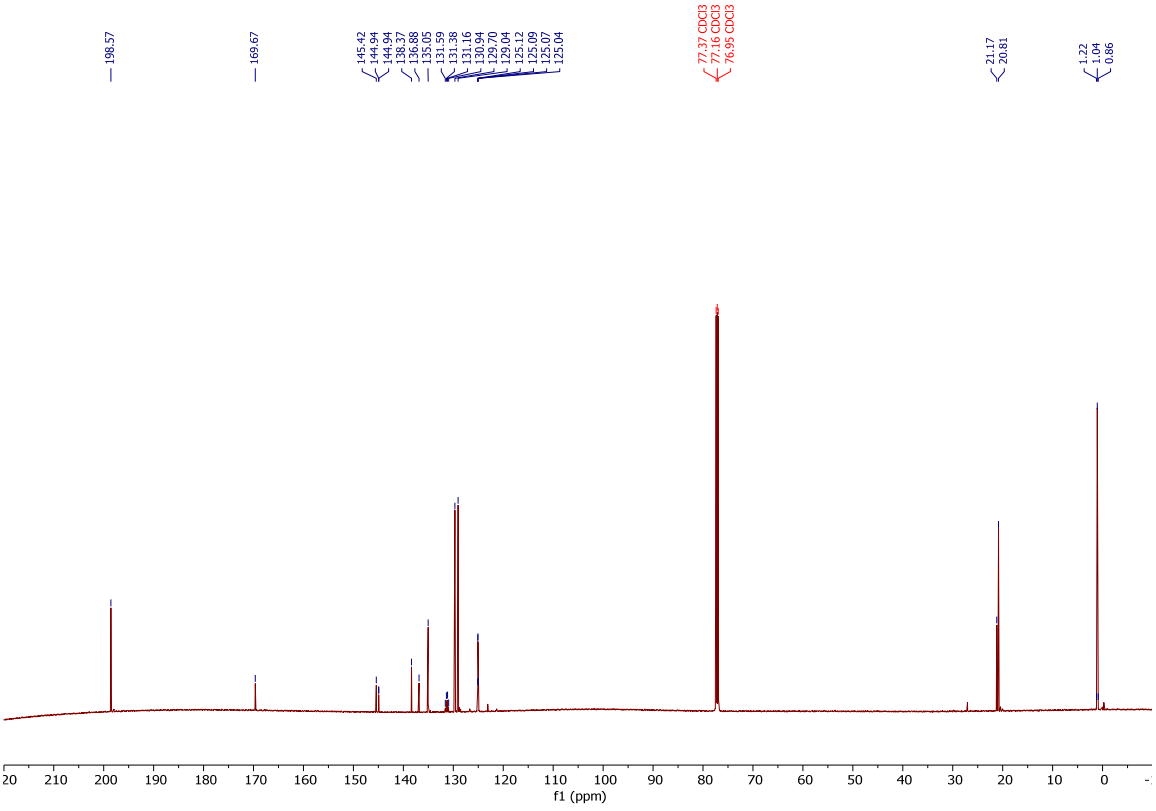

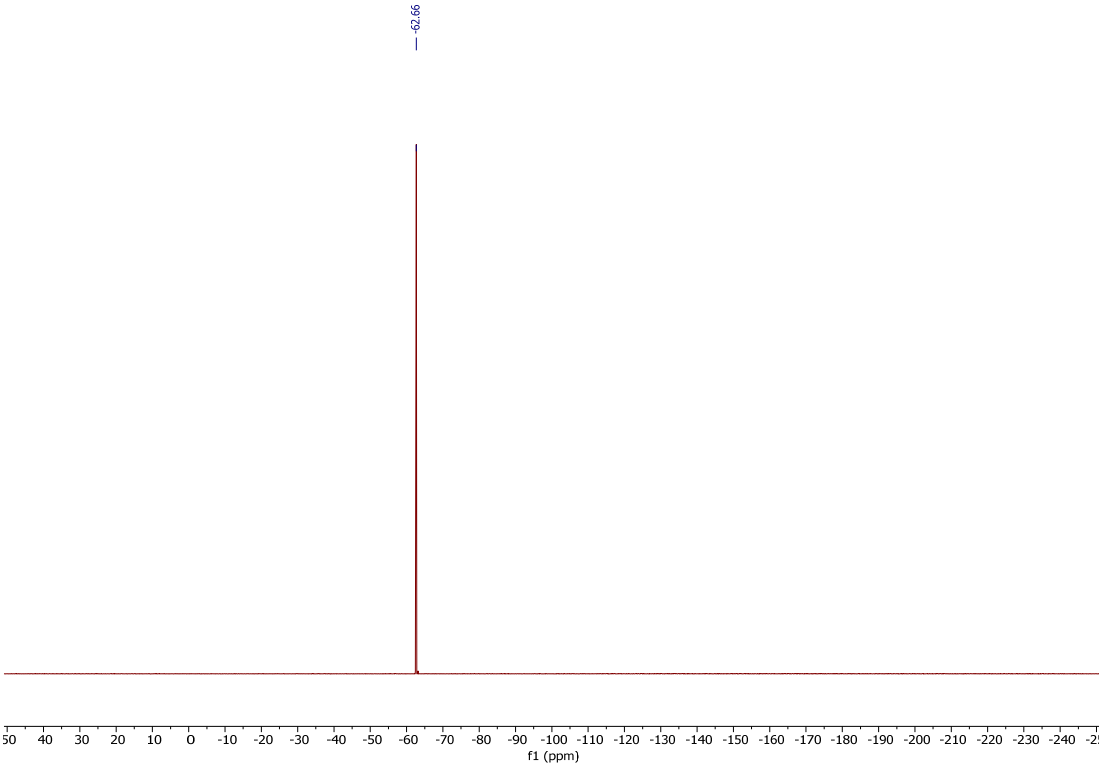
-62.66
50 40 30 20 10 0 -10 -20 -30 -40 -50 -60 -70 -80 -90 -100 -110 -120 -130 -140 -150 -160 -170 -180 -190 -200 -210 -220 -230 -240
f1 (ppm)

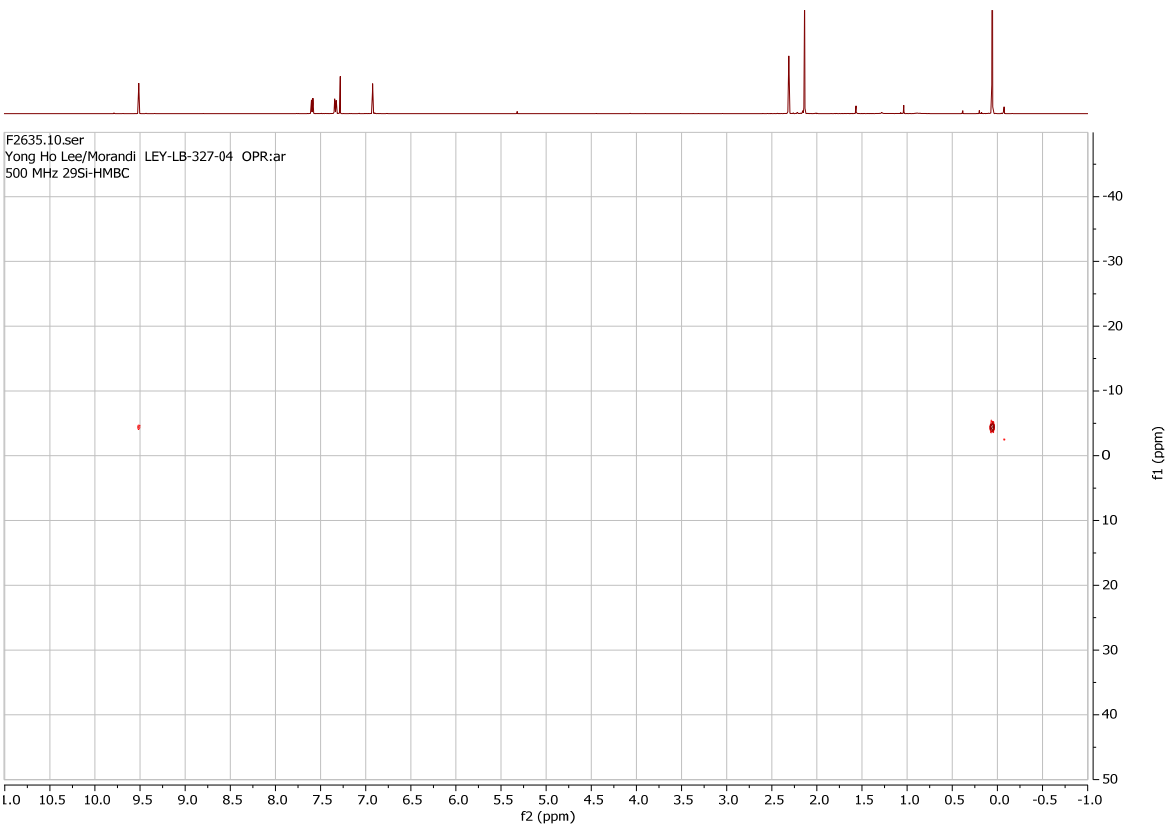
F2635.10.ser
Yong Ho Lee/Morandi LEY-LB-327-04 OPR:ar
500 MHz 29Si-HMBC
-40
-30
-20
-10
0
10
20
30
40
50
f1 (ppm)
1.0 10.5 10.0 9.5 9.0 8.5 8.0 7.5 7.0 6.5 6.0 5.5 5.0 4.5 4.0 3.5 3.0 2.5 2.0 1.5 1.0 0.5 0.0 -0.5 -1.0
f2 (ppm)

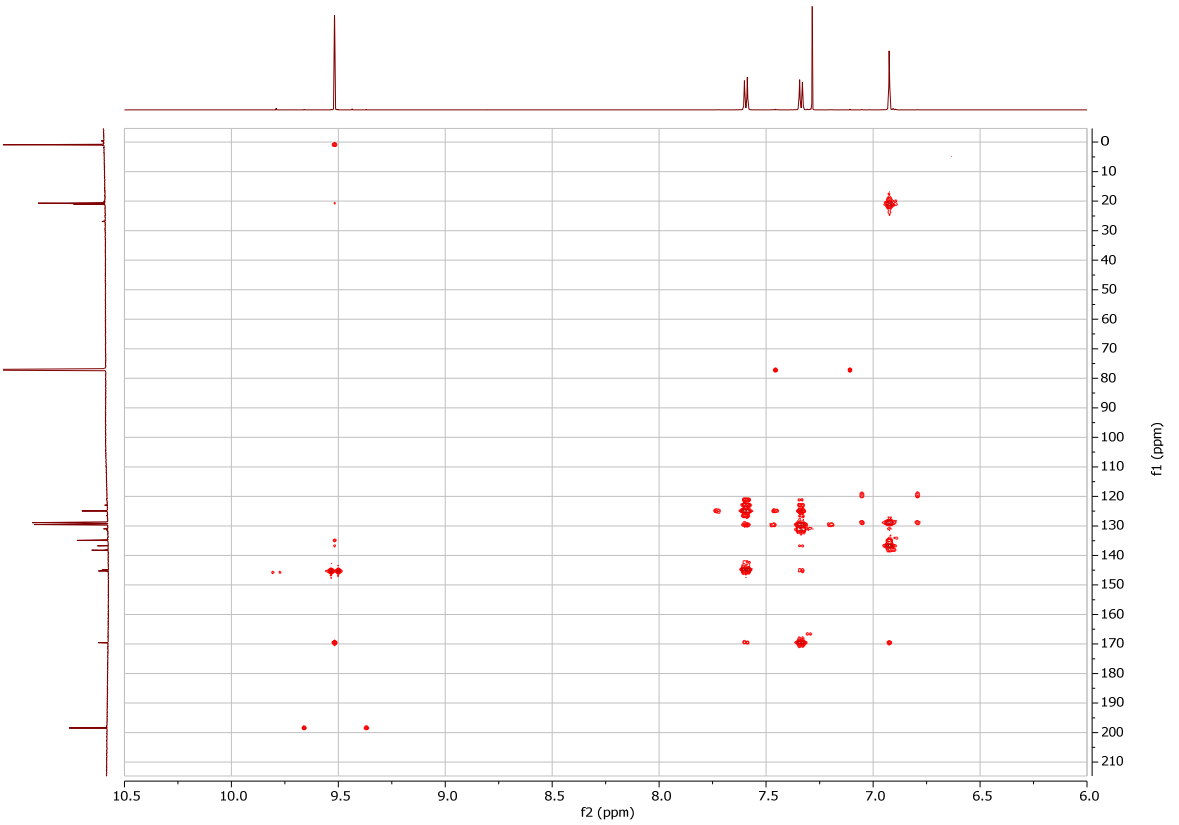
f2 (ppm)
f1 (ppm)

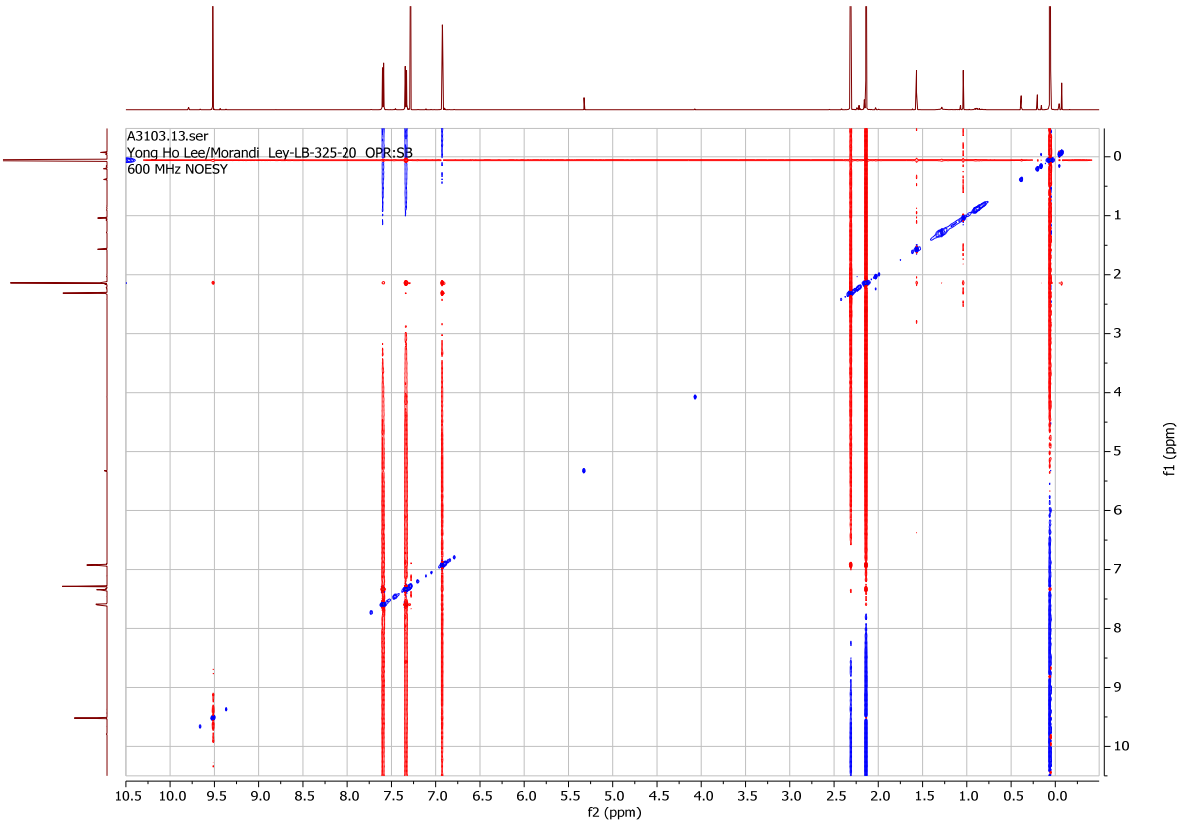
A3103.13.ser
Yong Ho Lee/Morandi Ley-LB-325-20 OPR:SB
600 MHz NOESY
f2 (ppm)
f1 (ppm)

(*E*)-3-(1-mesityl-3-oxo-2-(trimethylsilyl)prop-1-en-1-yl)benzaldehyde (**62**).

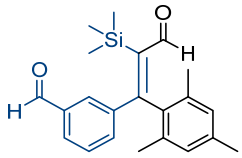

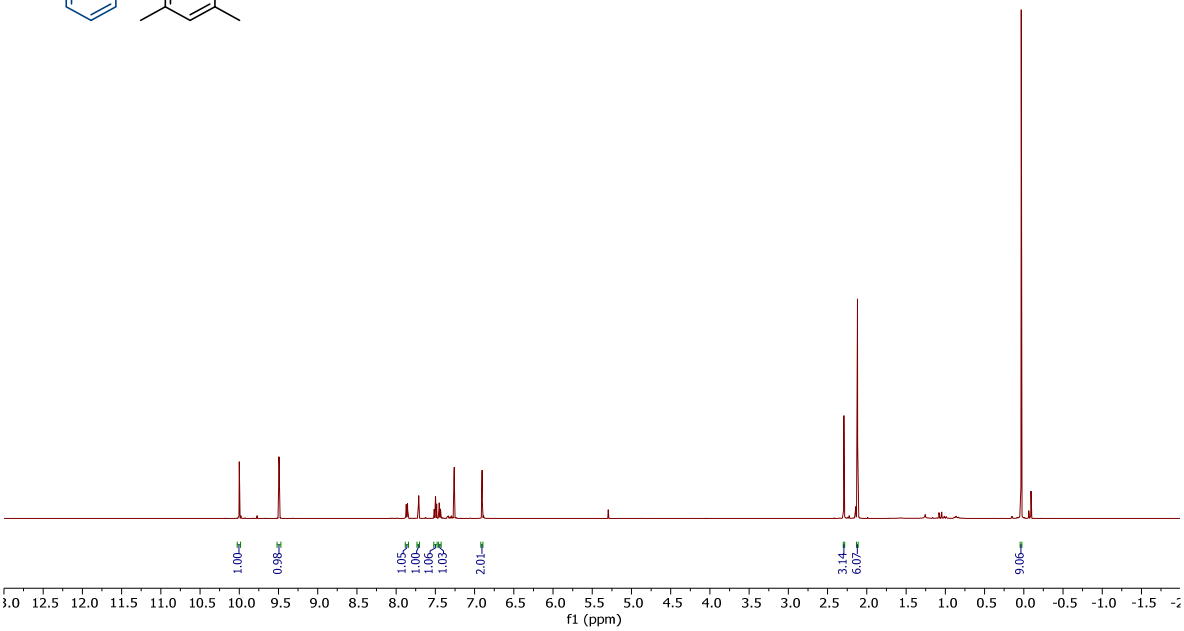

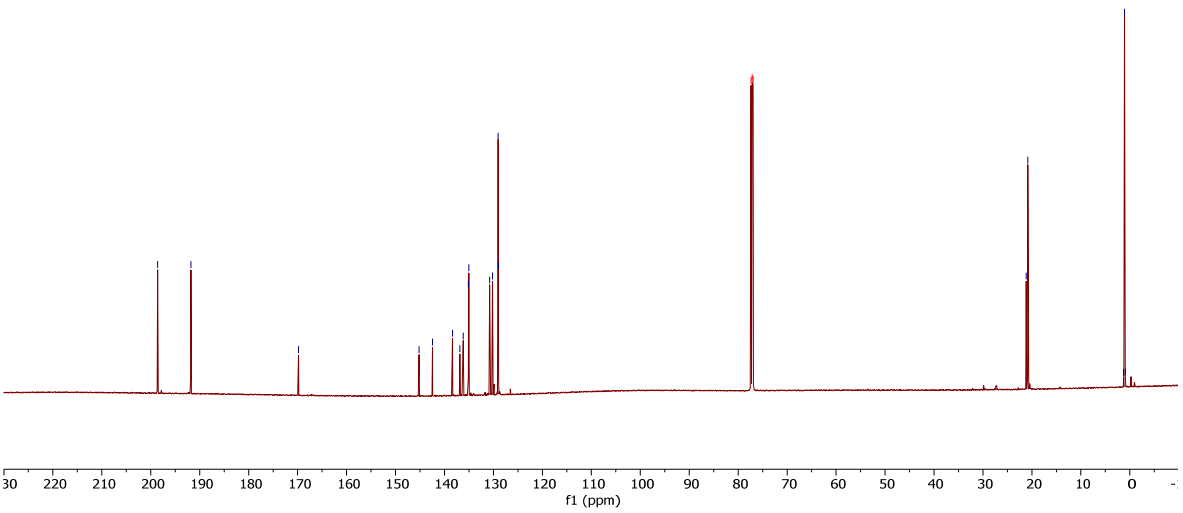

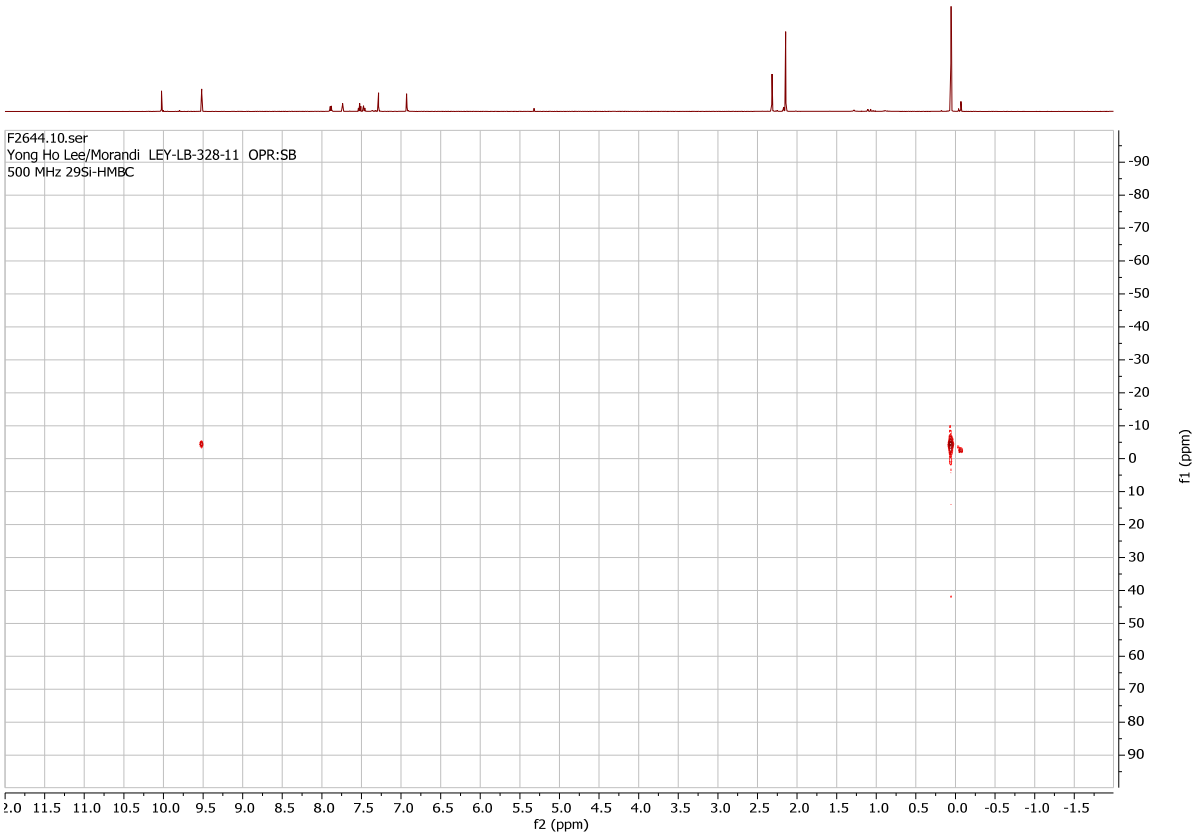
F2644.10.ser
Yong Ho Lee/Morandi LEY-LB-328-11 OPR:SB
500 MHz 29Si-HMBC
f2 (ppm)
f1 (ppm)

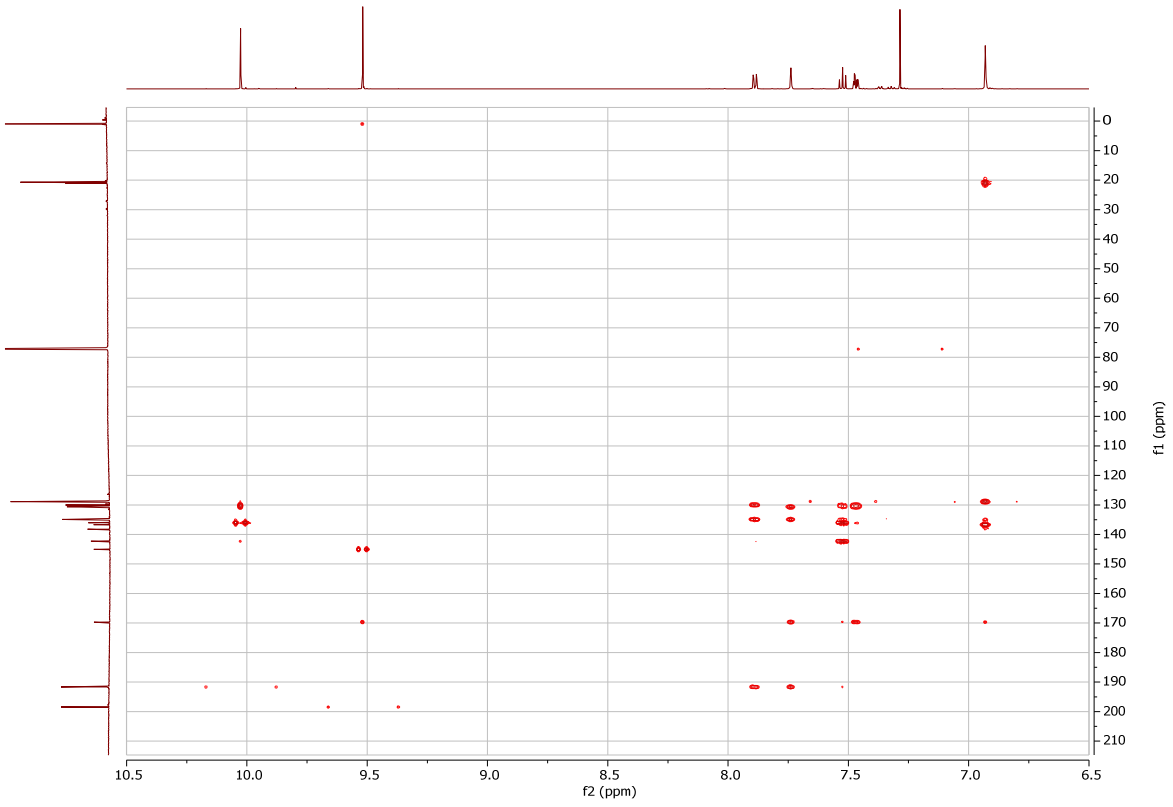
f2 (ppm)
f1 (ppm)

NOESY

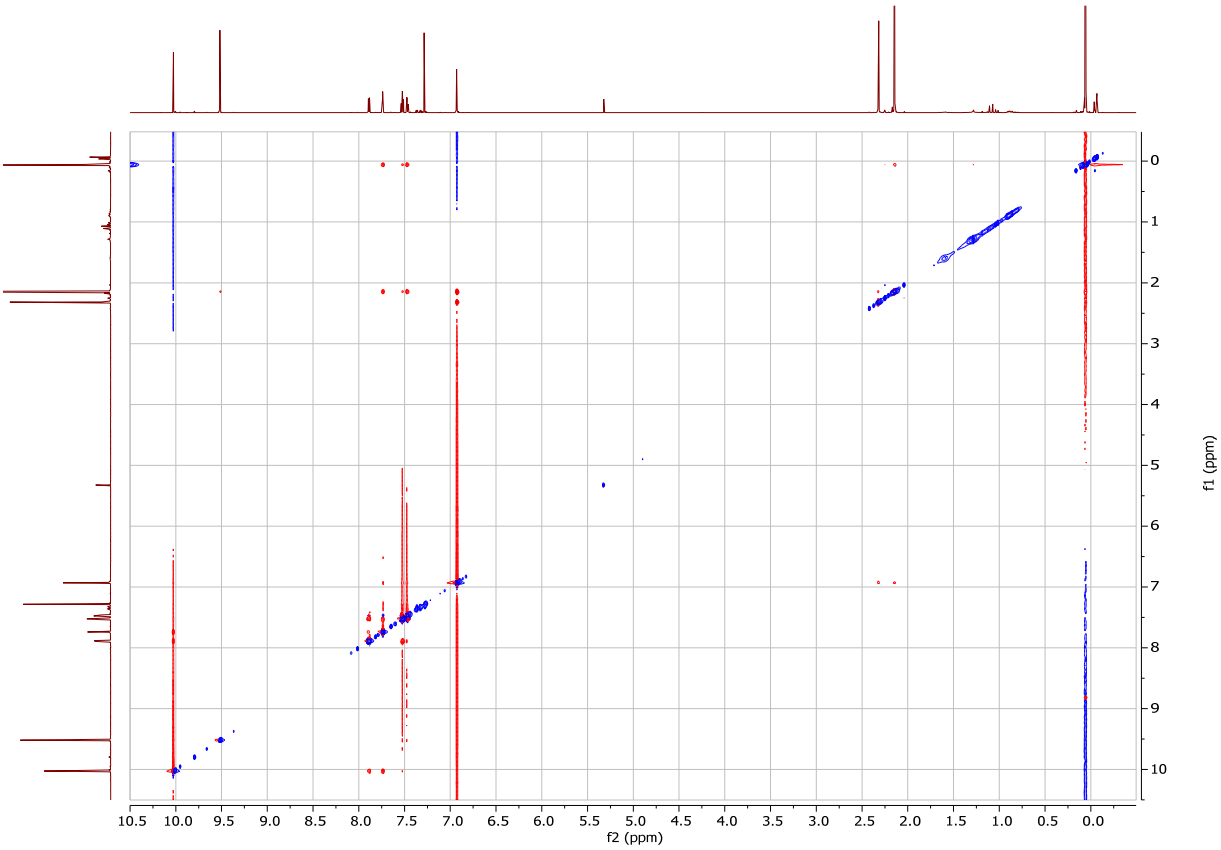

(*Z*)-3-mesityl-3-phenyl-2-(4,4,5,5-tetramethyl-1,3,2-dioxaborolan-2-yl)acrylaldehyde (**63**).

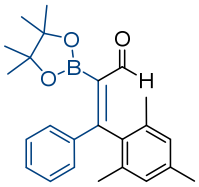

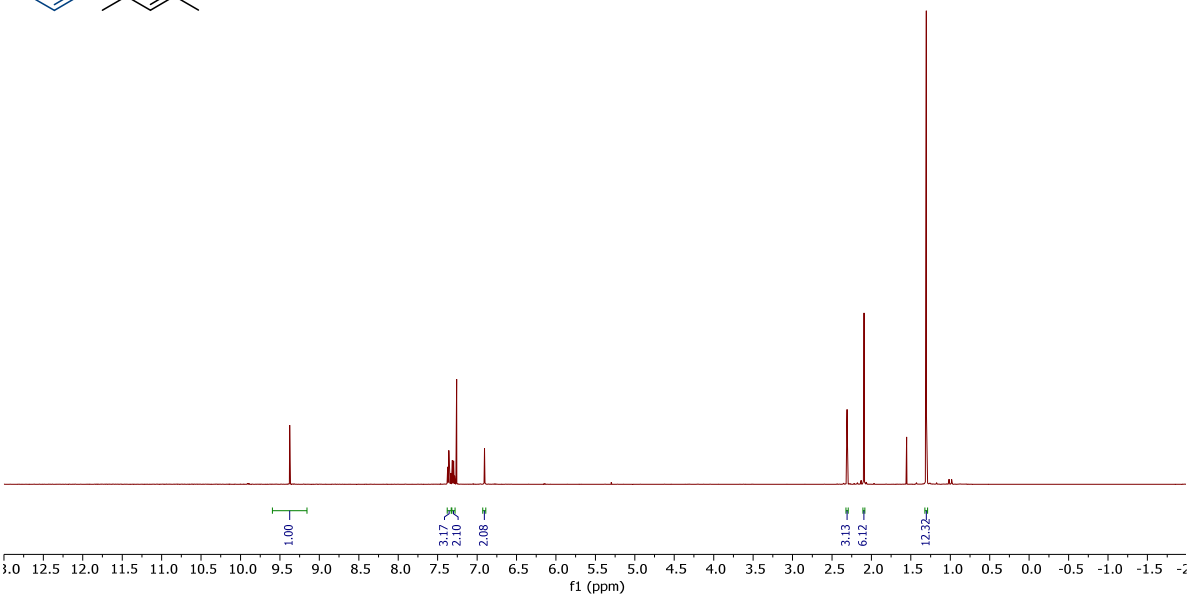

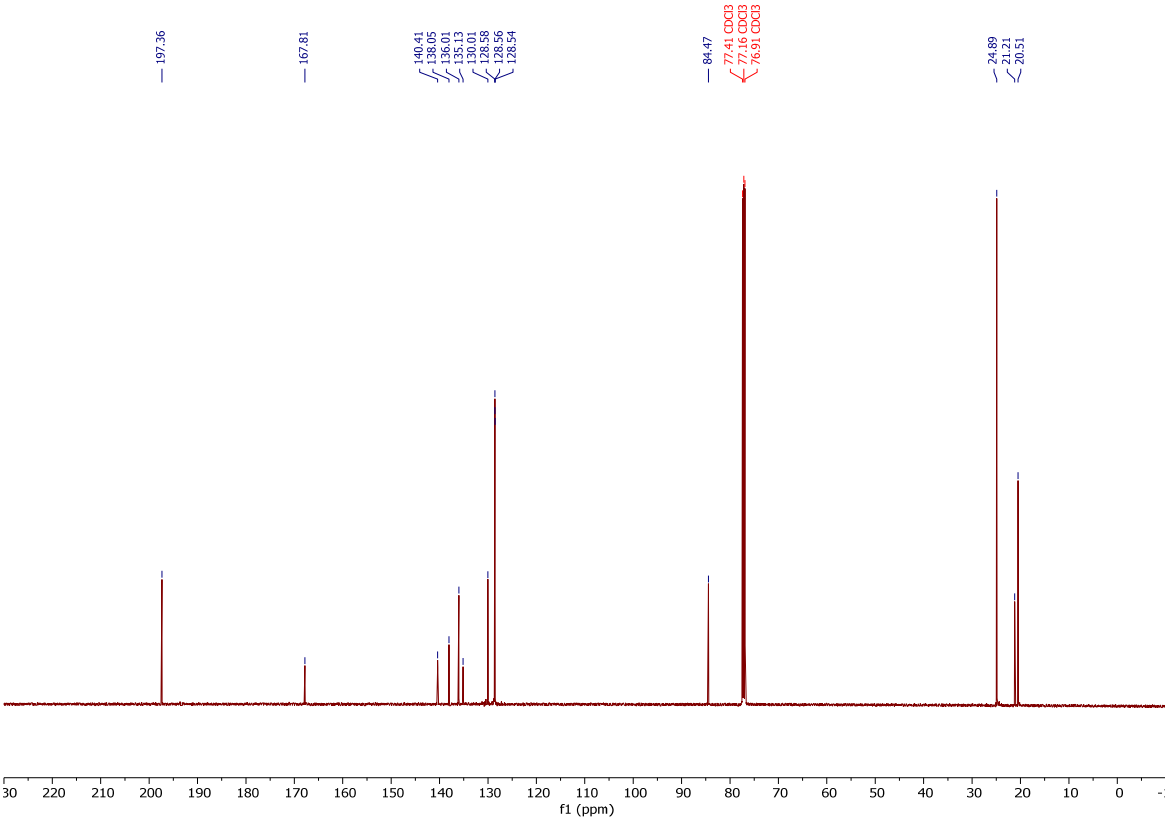

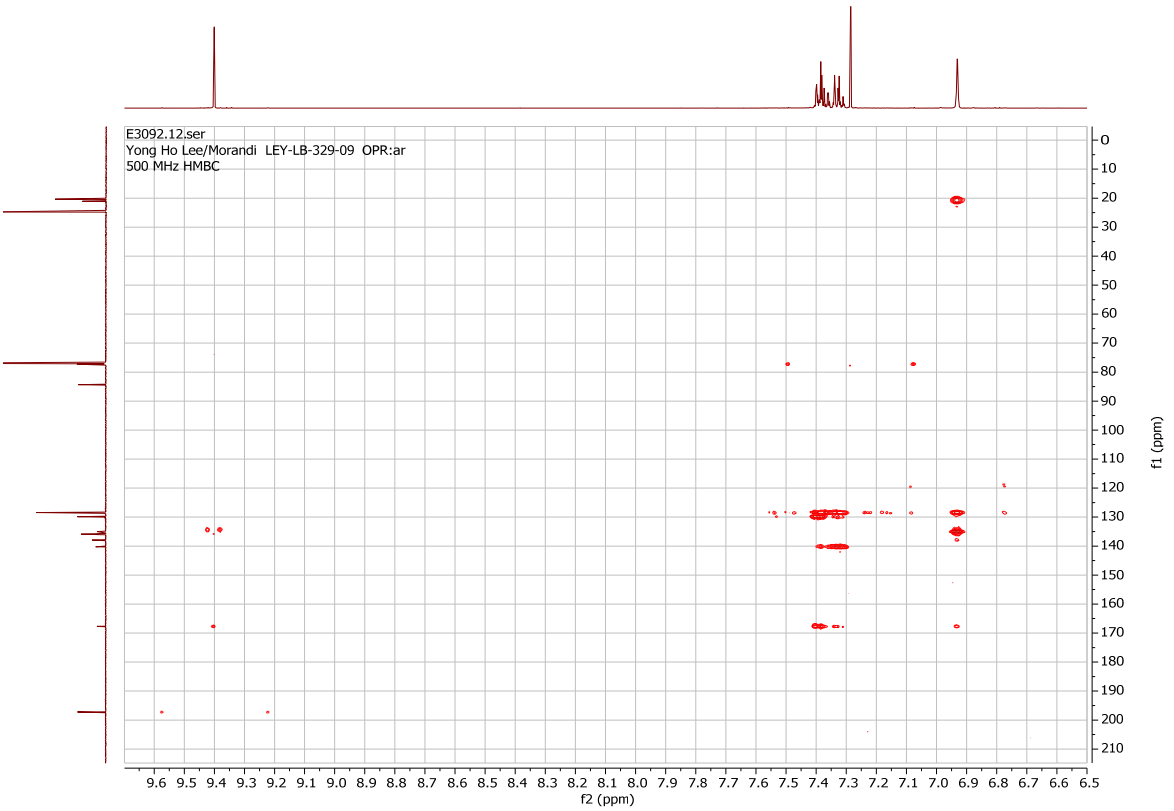
E3092.12.ser
Yong Ho Lee/Morandi LEY-LB-329-09 OPR:ar
500 MHz HMBC
f2 (ppm)
f1 (ppm)

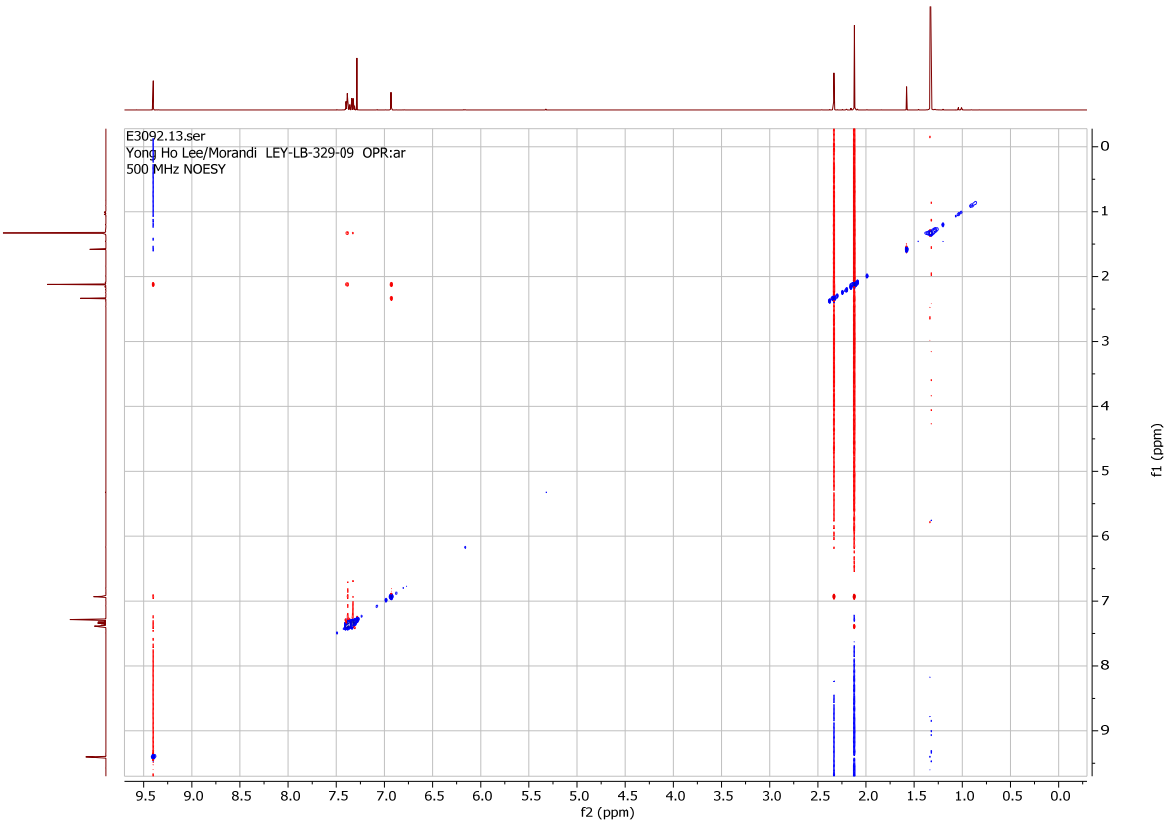
E3092.13.ser
Yong Ho Lee/Morandi LEY-LB-329-09 OPR:ar
500 MHz NOESY
f2 (ppm)
f1 (ppm)

(*Z*)-3-mesityl-2,3-diphenylacrylaldehyde (**64**).

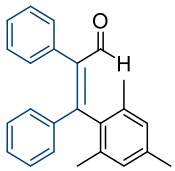

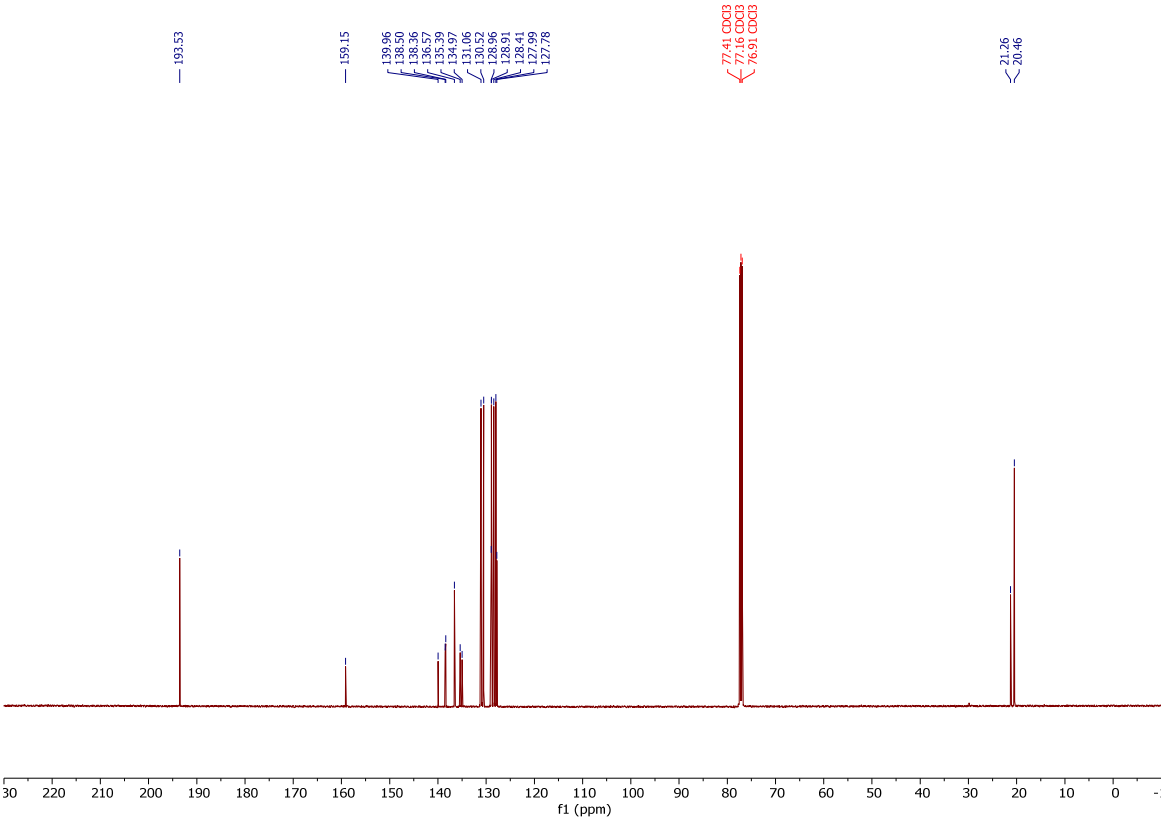

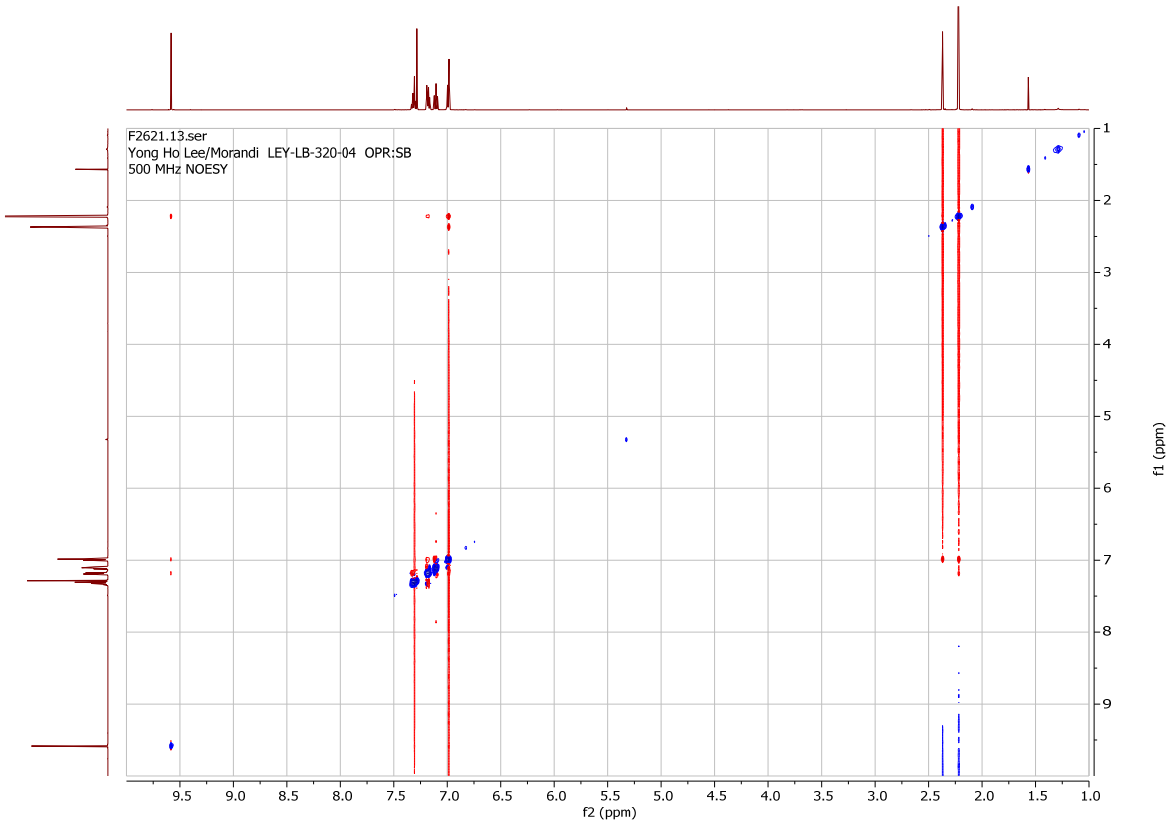
F2621.13.ser
Yong Ho Lee/Morandi LEY-LB-320-04 OPR:SB
500 MHz NOESY
f1 (ppm)
f2 (ppm)

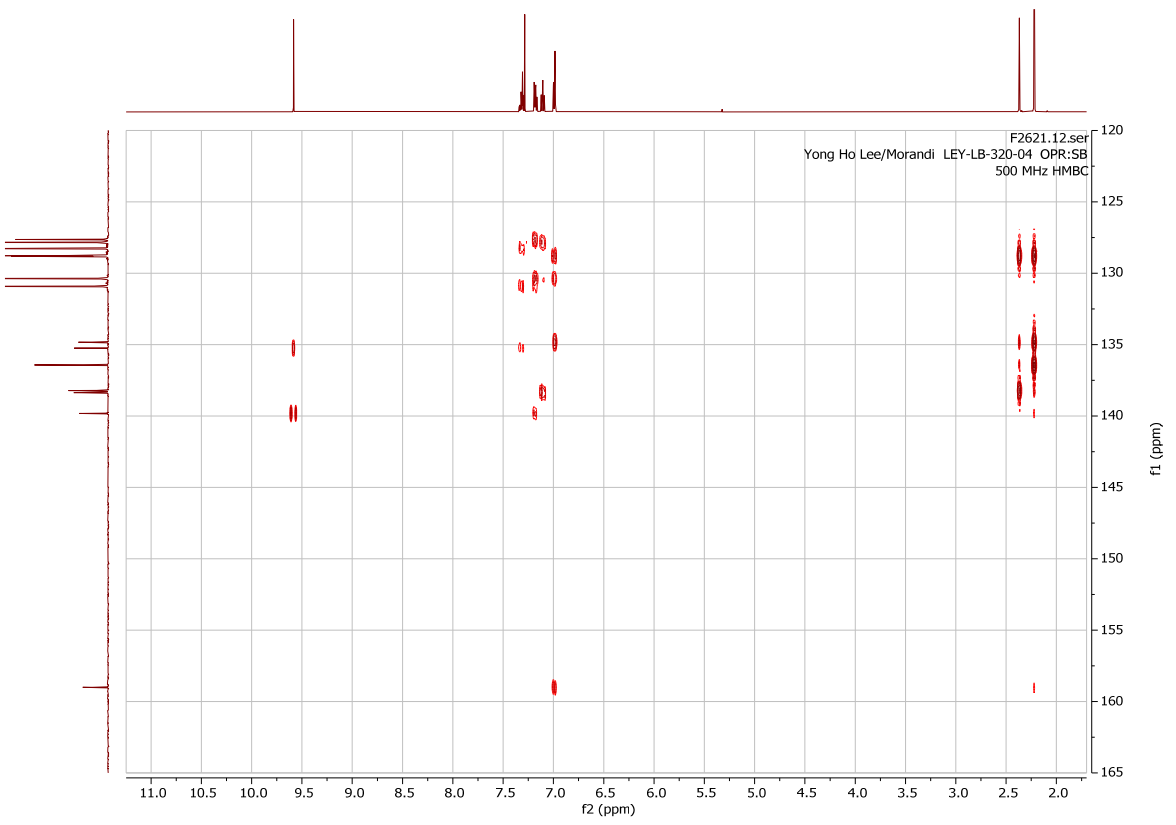
F2621.12.ser
Yong Ho Lee/Morandi LEY-LB-320-04 OPR:SB
500 MHz HMBC
f1 (ppm)
f2 (ppm)

14.2. Other chemodivergent transformations

(*E*)-2-butylhept-2-enal (**65**).

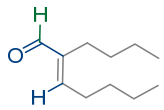

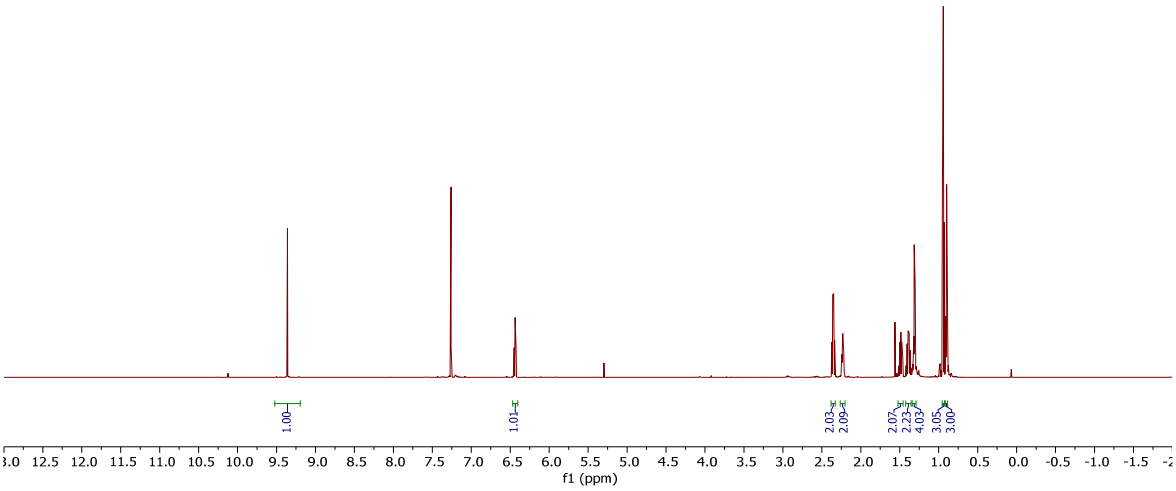

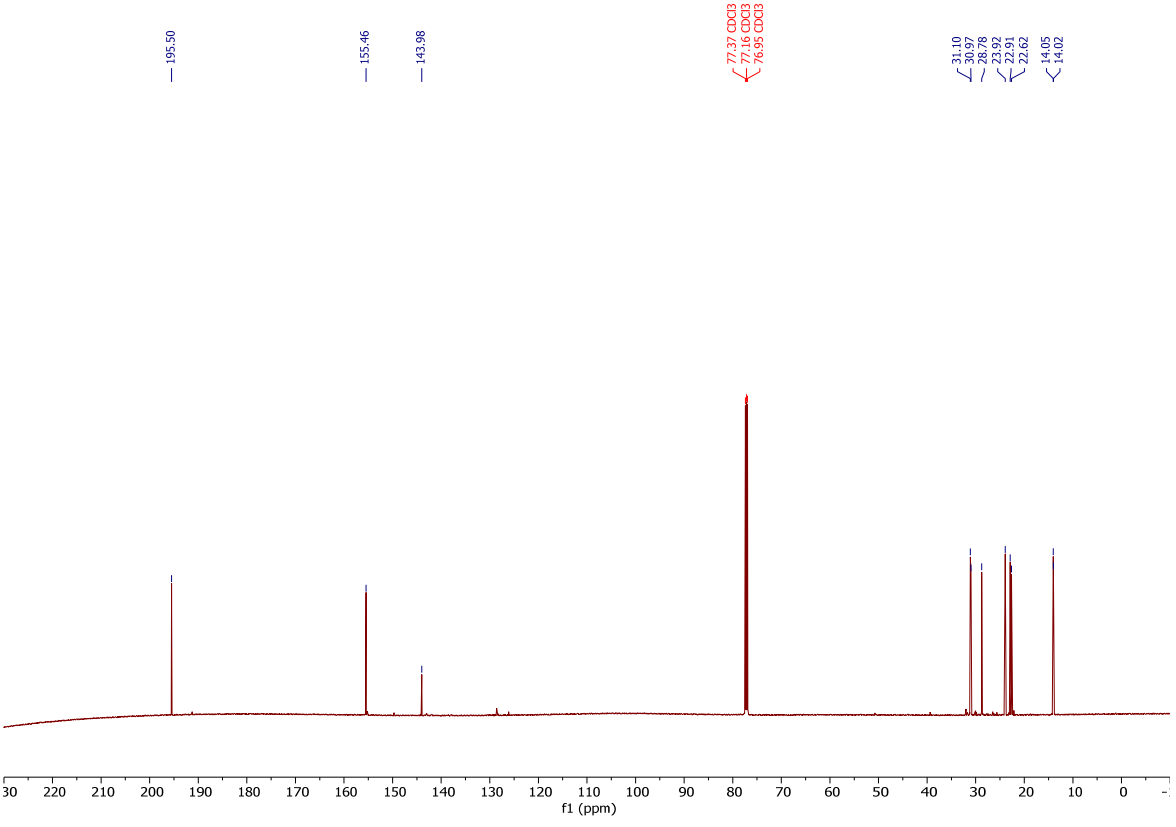

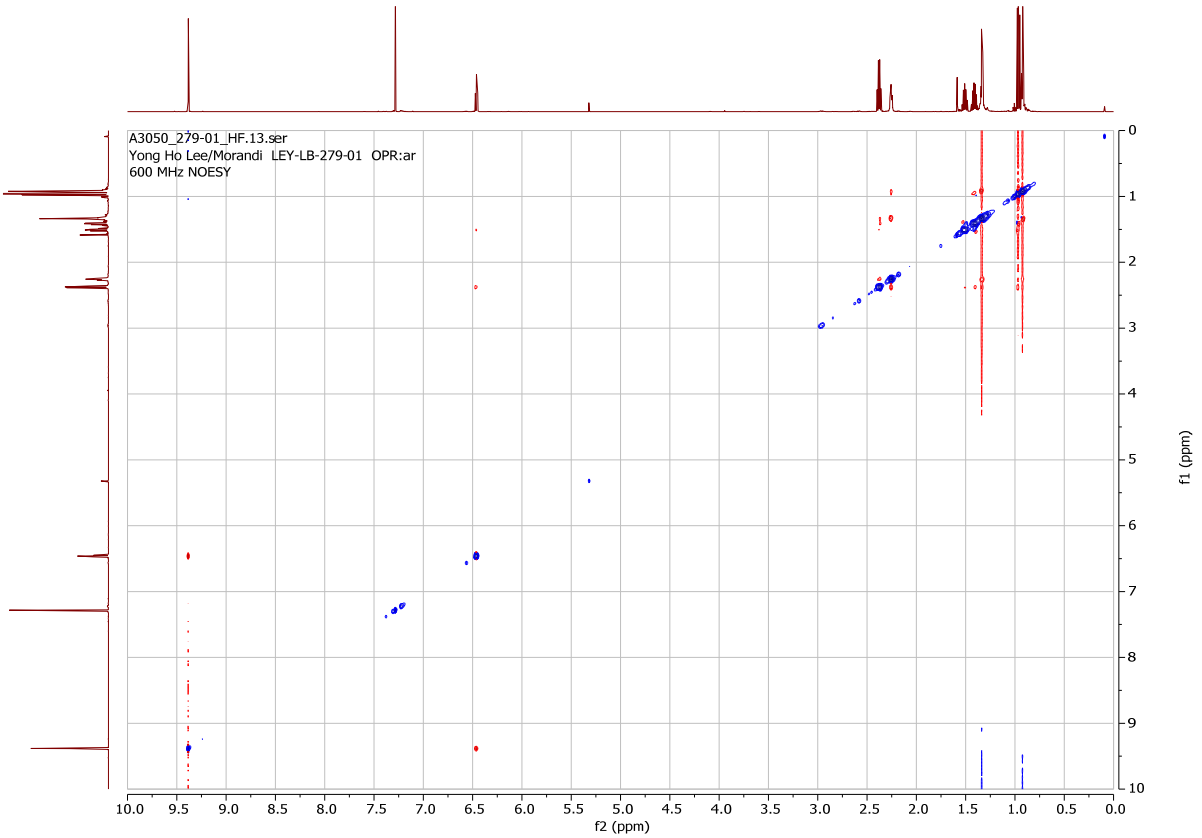
A3050_279-01_HF.13.ser
Yong Ho Lee/Morandi LEY-LB-279-01 OPR:ar
600 MHz NOESY
f2 (ppm)
f1 (ppm)

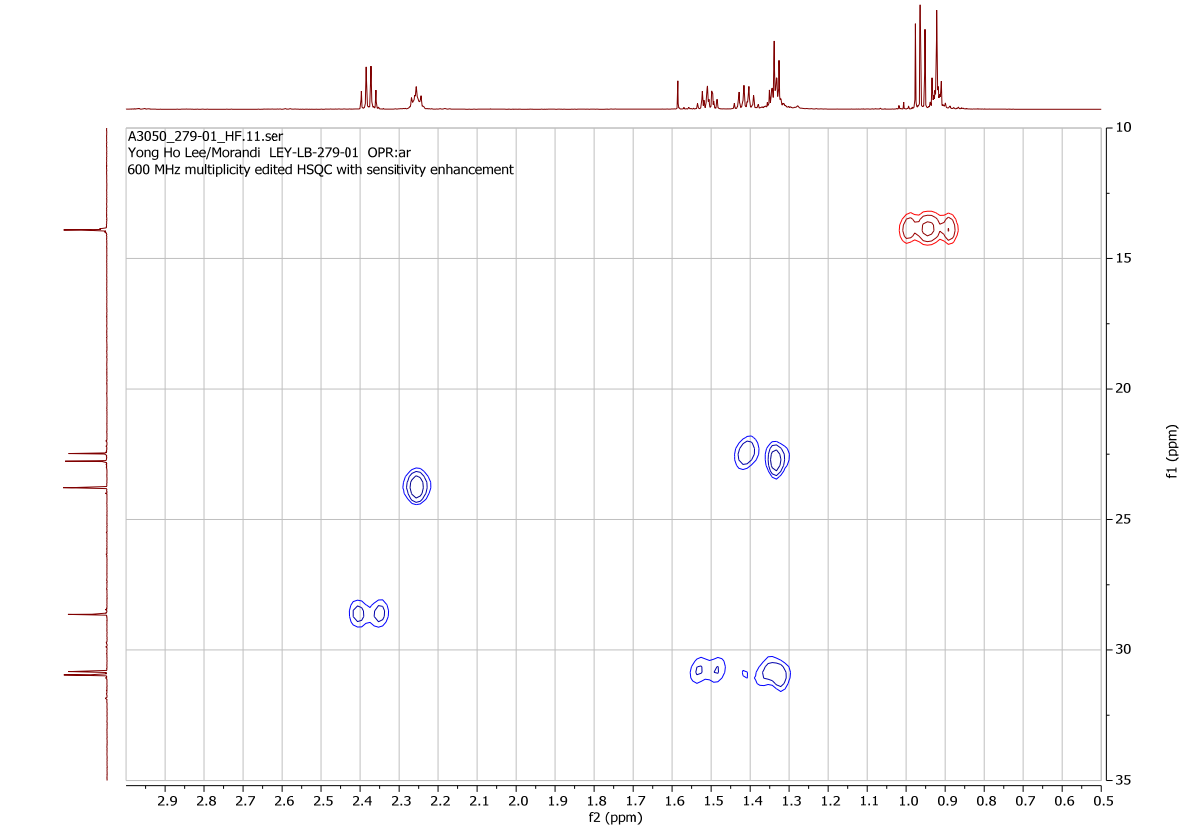
A3050_279-01_HF.11.ser
Yong Ho Lee/Morandi LEY-LB-279-01 OPR:ar
600 MHz multiplicity edited HSQC with sensitivity enhancement
f2 (ppm)
f1 (ppm)

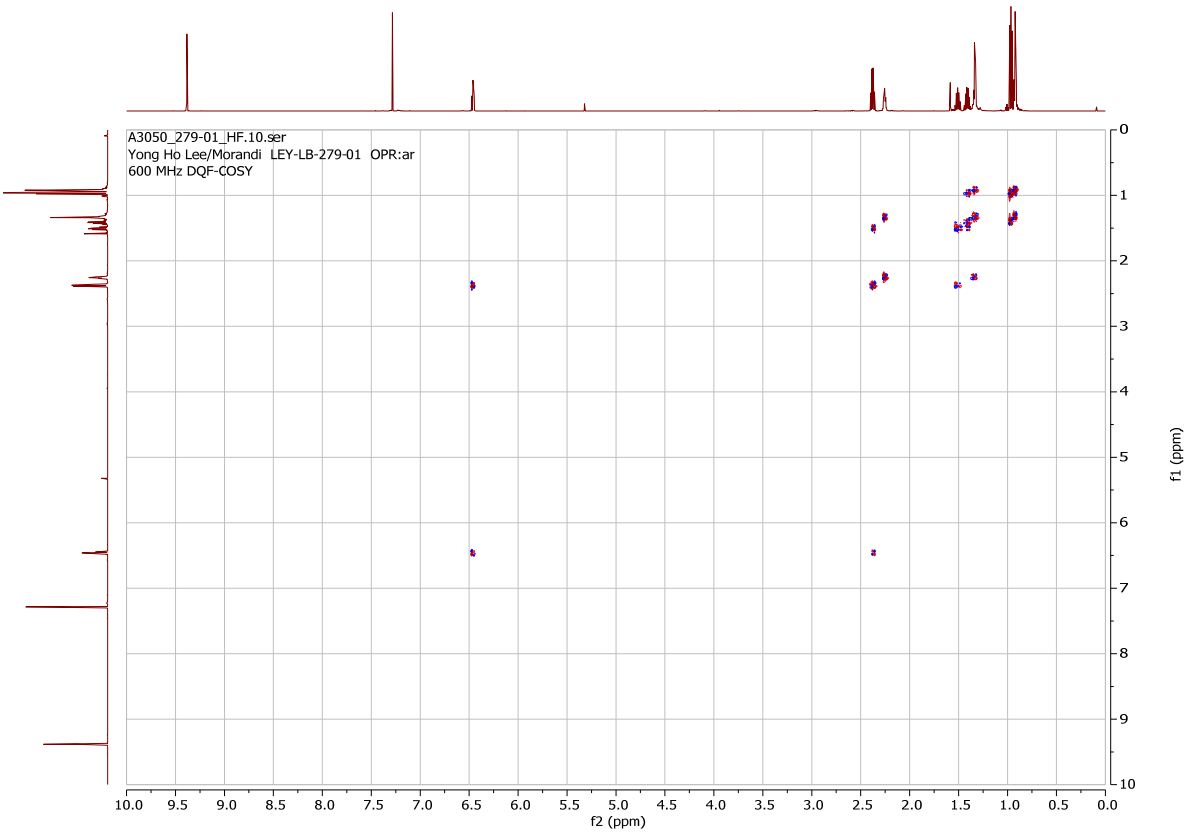
A3050_279-01_HF.10.ser
Yong Ho Lee/Morandi LEY-LB-279-01 OPR:ar
600 MHz DQF-COSY
f2 (ppm)
f1 (ppm)

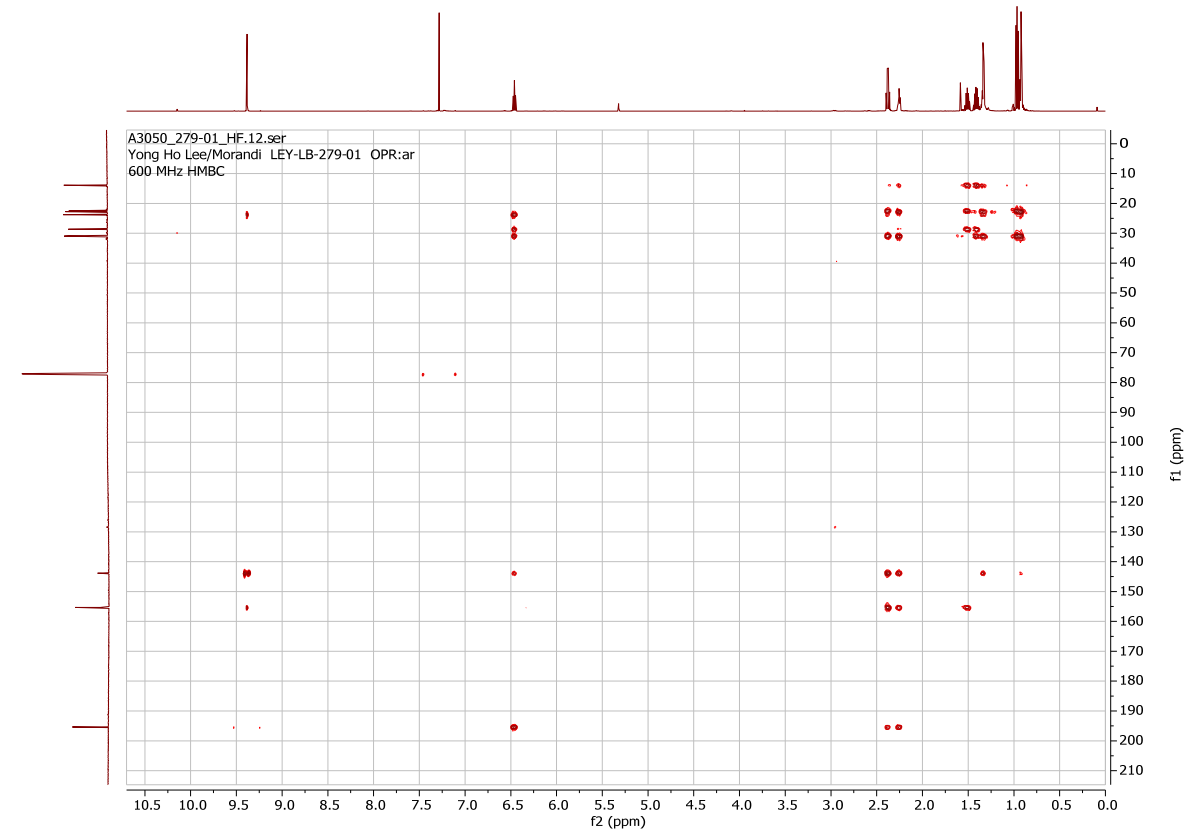
A3050_279-01_HF.12.ser
Yong Ho Lee/Morandi LEY-LB-279-01 OPR:ar
600 MHz HMBC
f2 (ppm)
f1 (ppm)

(*E*)-2-butylhept-2-enal-1-*d* (**68**).

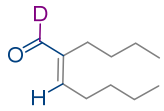

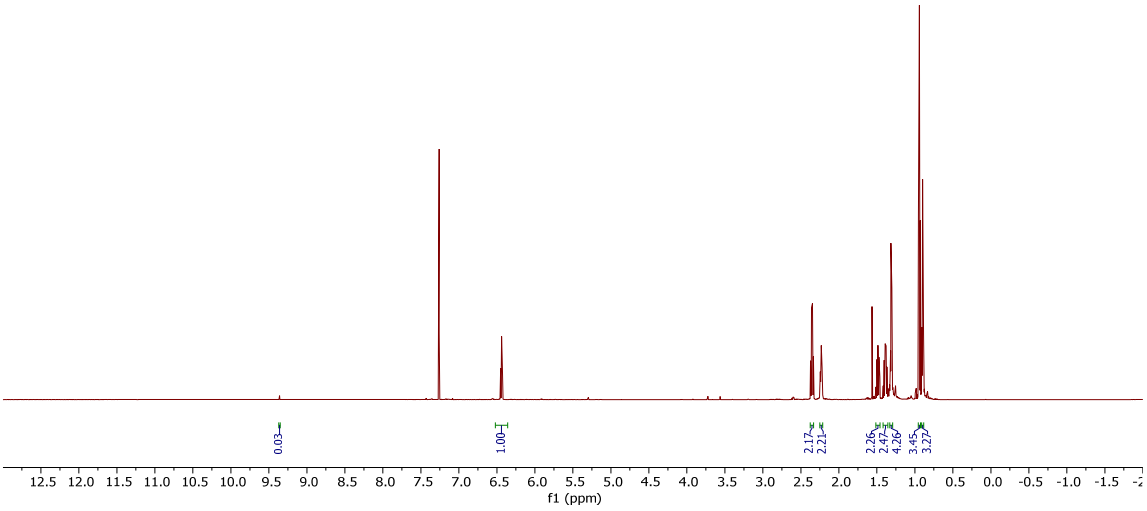

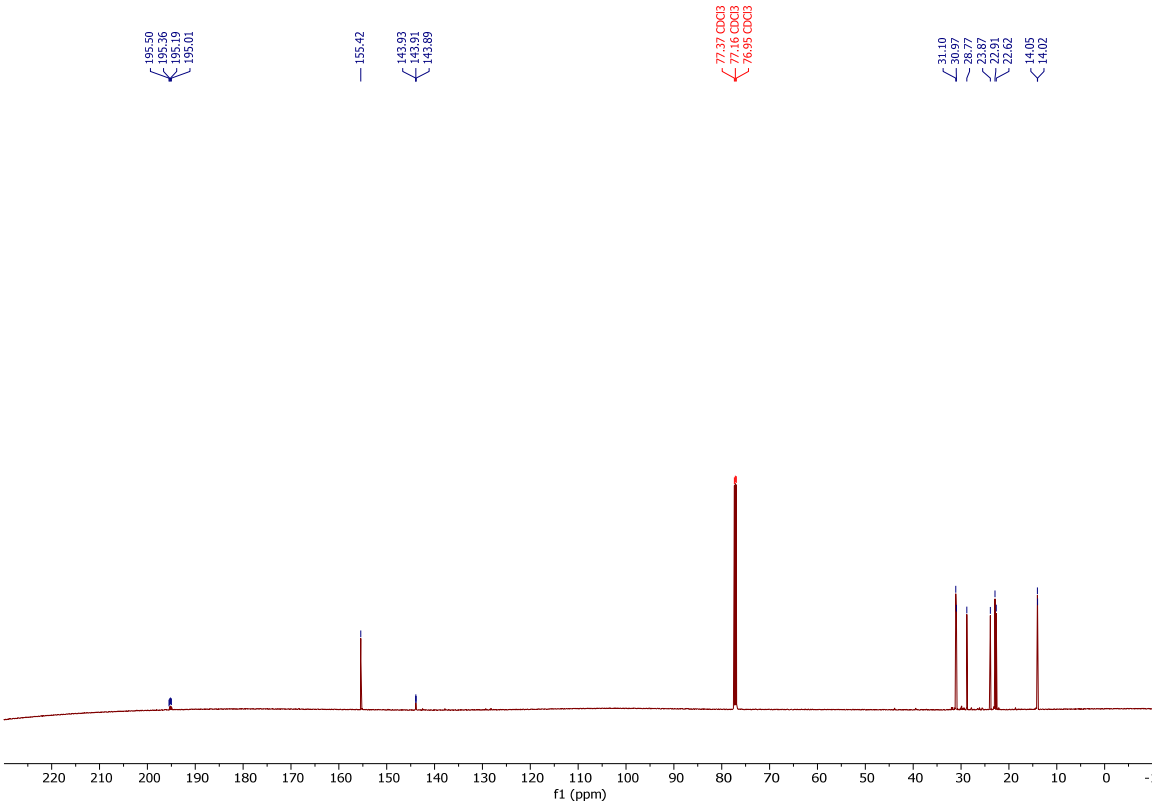

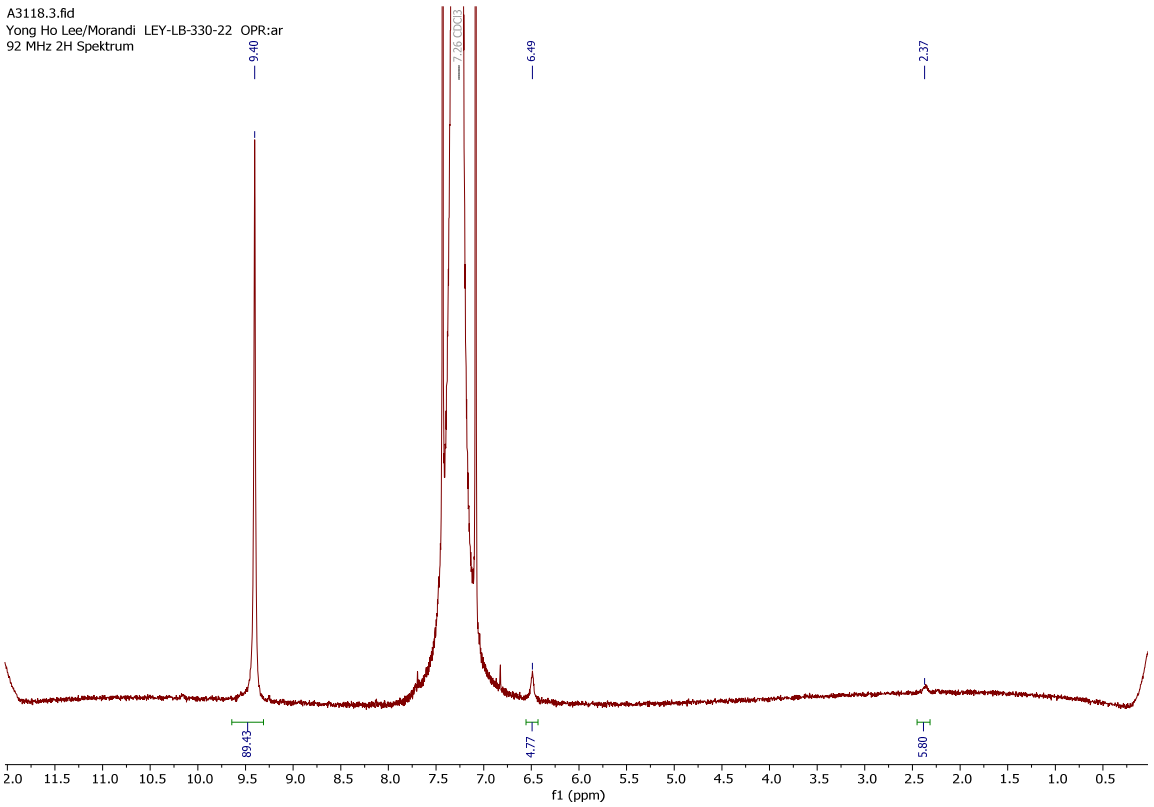
A3118.3.fid
Yong Ho Lee/Morandi LEY-LB-330-22 OPR:ar
92 MHz 2H Spektrum
9.40
7.26 CDCl3
6.49
2.37
89.43
4.77
5.80
f1 (ppm)

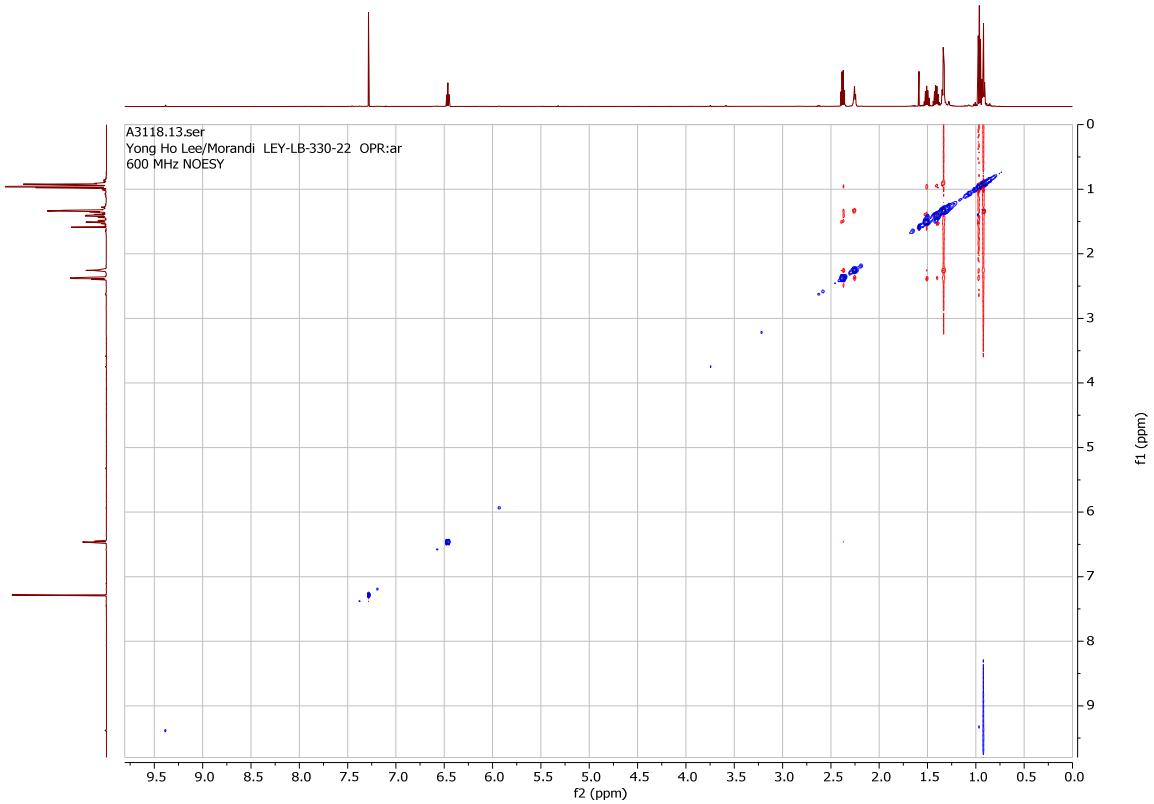
A3118.13.ser
Yong Ho Lee/Morandi LEY-LB-330-22 OPR:ar
600 MHz NOESY
f2 (ppm)
f1 (ppm)

(*Z*)-1-phenyl-2-propyl-3-(*o*-tolyl)hex-2-en-1-one (**66**).

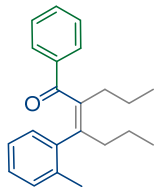

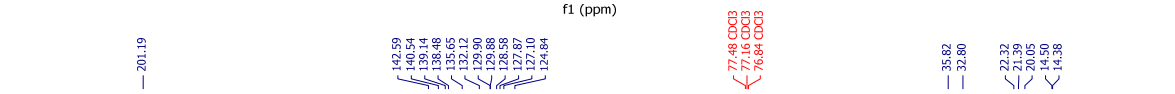

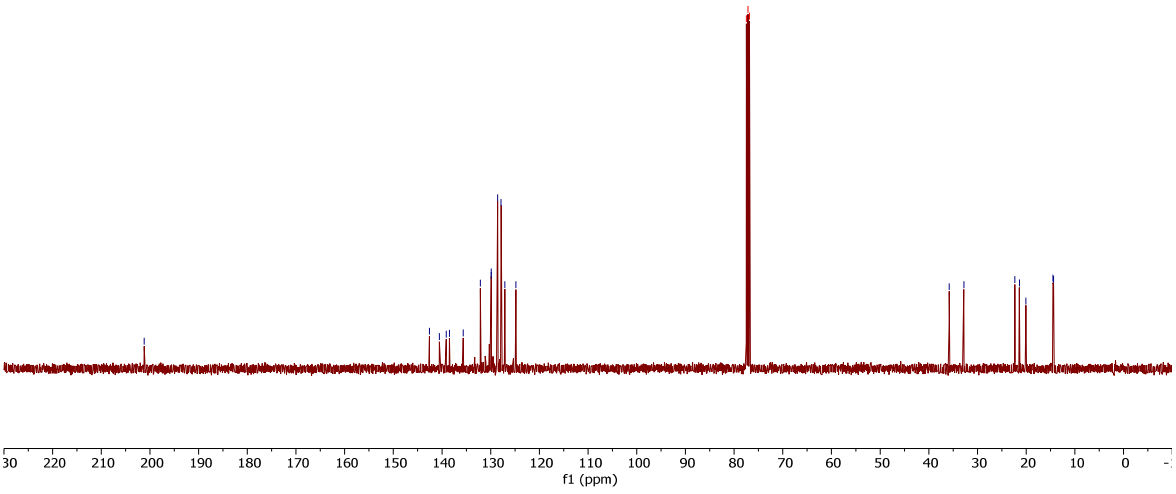

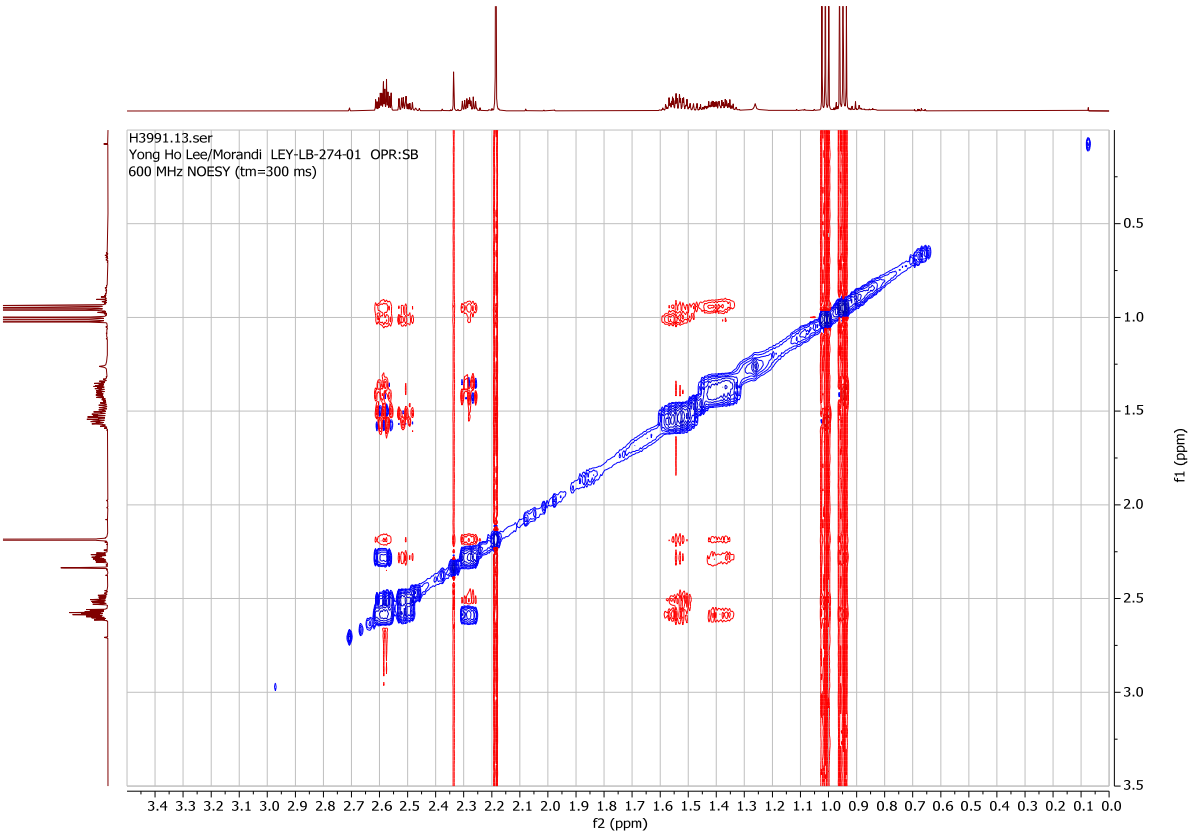
H3991.13.ser
Yong Ho Lee/Morandi LEY-LB-274-01 OPR:SB
600 MHz NOESY (tm=300 ms)
f1 (ppm)
f2 (ppm)

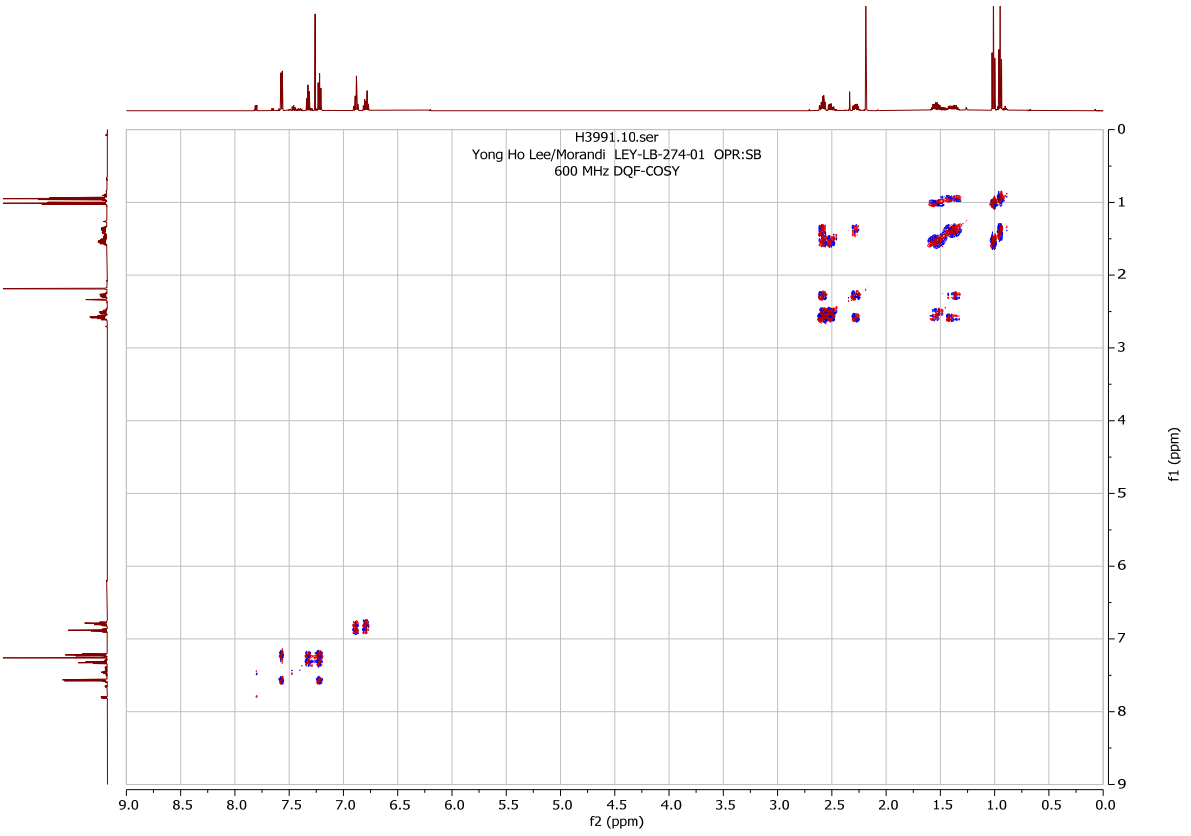
H3991.10.ser
Yong Ho Lee/Morandi LEY-LB-274-01 OPR:SB
600 MHz DQF-COSY
f1 (ppm)
f2 (ppm)

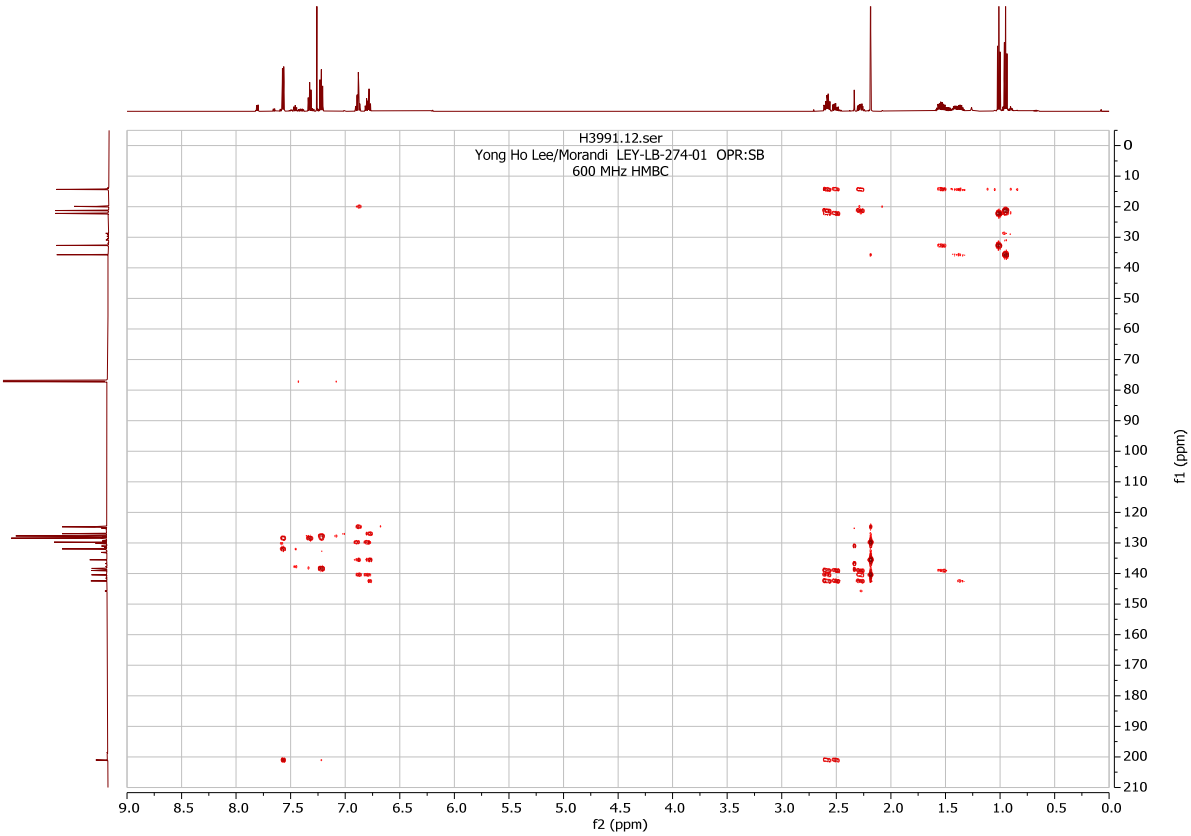
H3991.12.ser
Yong Ho Lee/Morandi LEY-LB-274-01 OPR:SB
600 MHz HMBC
f2 (ppm)
f1 (ppm)

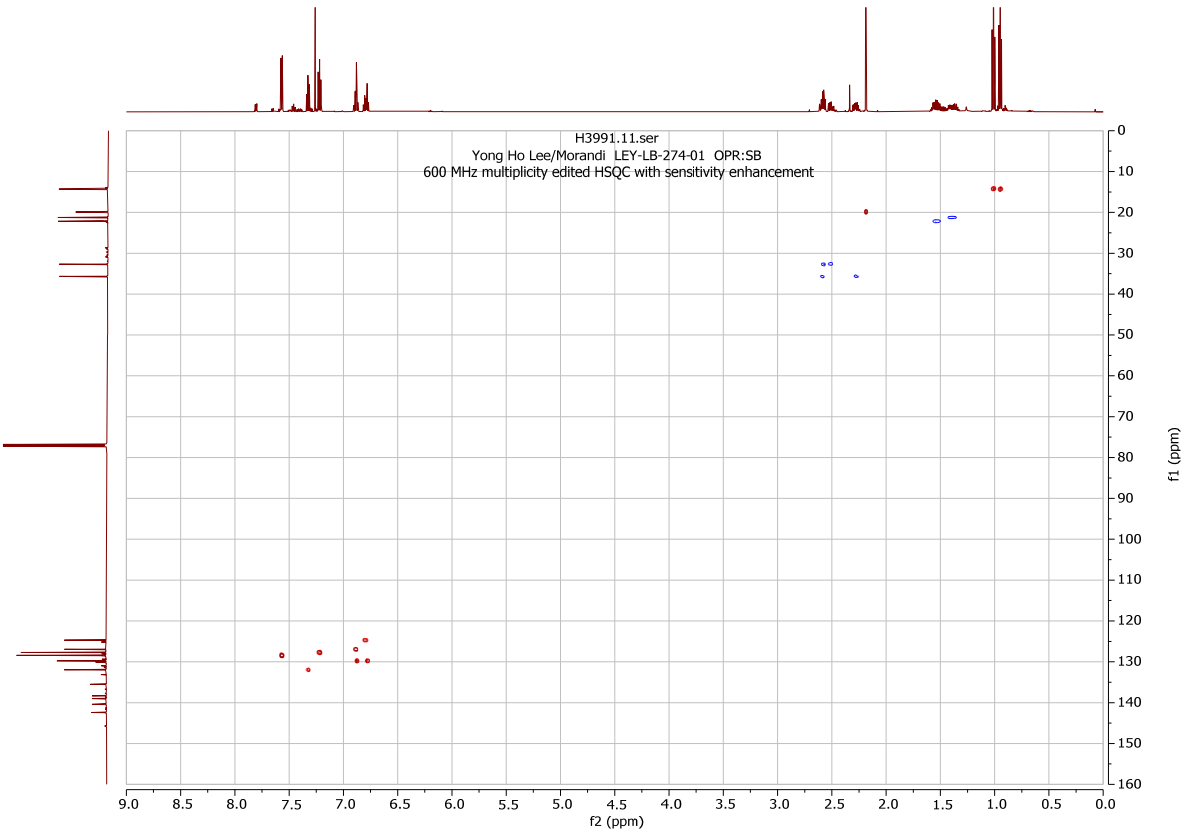
H3991.11.ser
Yong Ho Lee/Morandi LEY-LB-274-01 OPR:SB
600 MHz multiplicity edited HSQC with sensitivity enhancement
f2 (ppm)
f1 (ppm)

(*E*)-2-butyl-1-phenylhept-2-en-1-one (**67**).

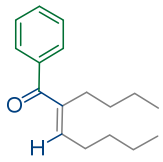

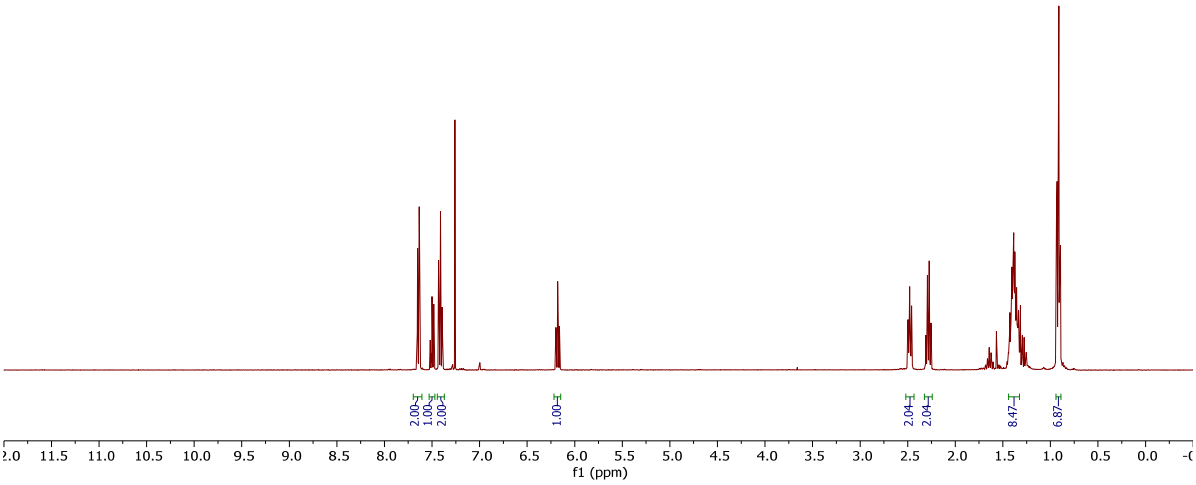

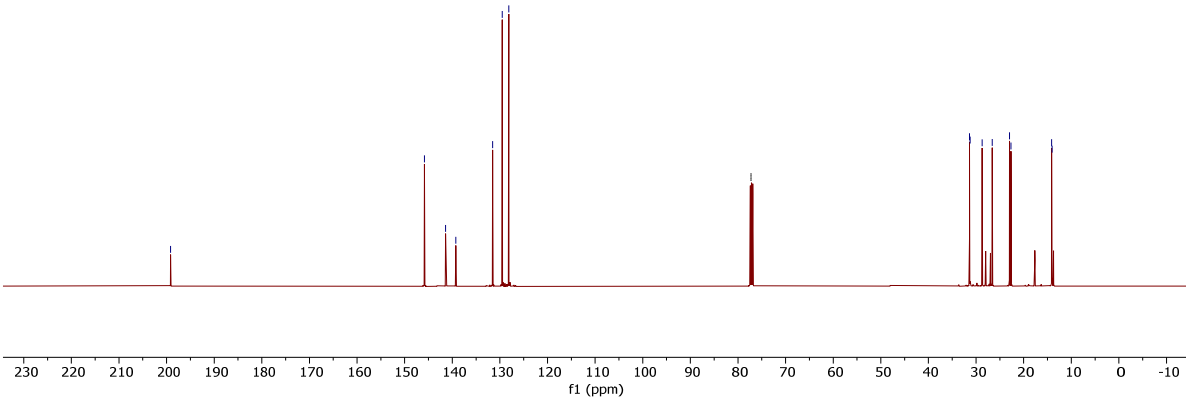

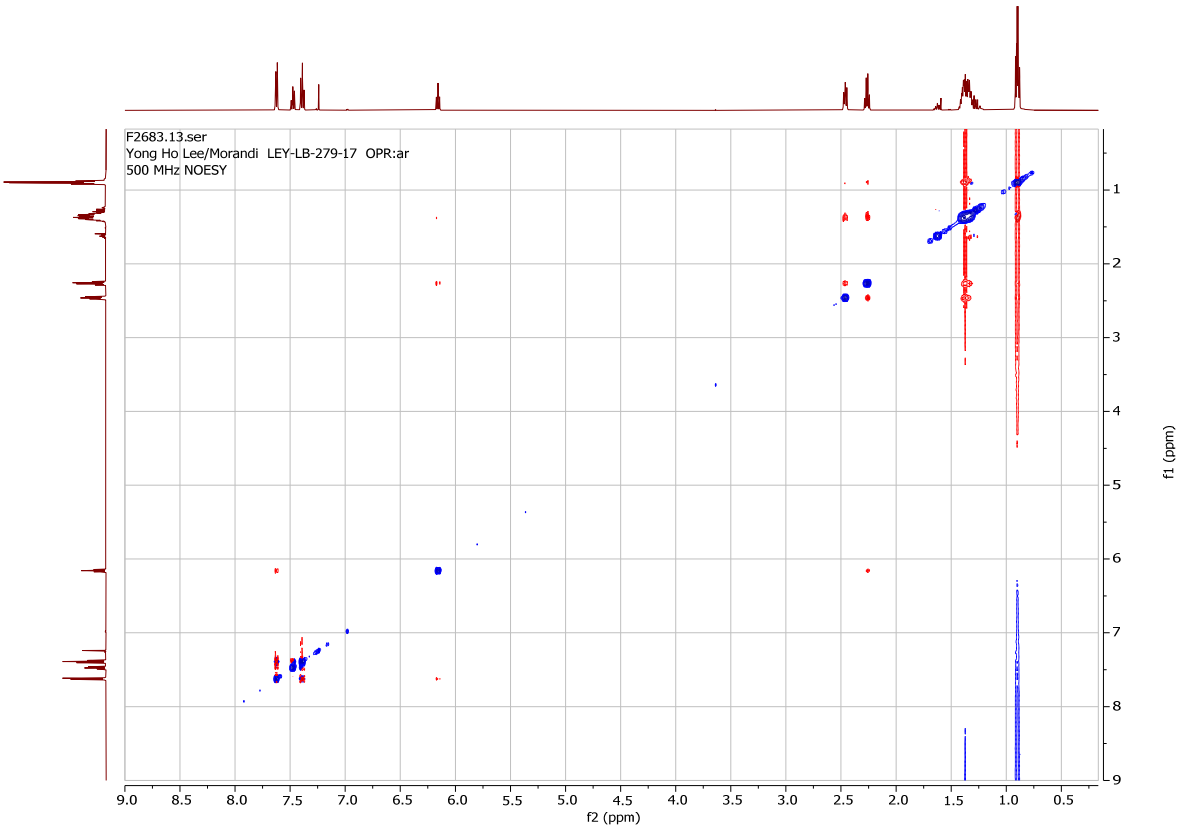
F2683.13.ser
Yong Ho Lee/Morandi LEY-LB-279-17 OPR:ar
500 MHz NOESY
f2 (ppm)
f1 (ppm)

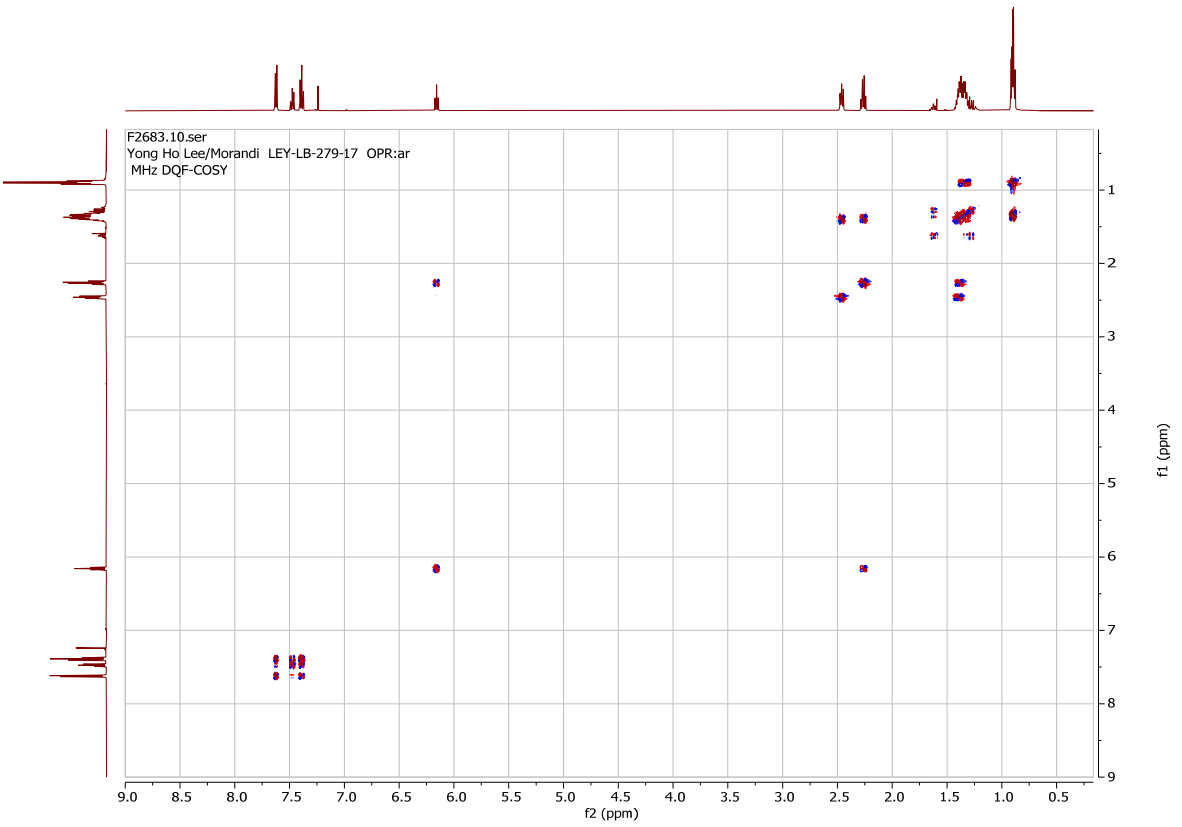
F2683.10.ser
Yong Ho Lee/Morandi LEY-LB-279-17 OPR:ar
MHz DQF-COSY
f2 (ppm)
f1 (ppm)

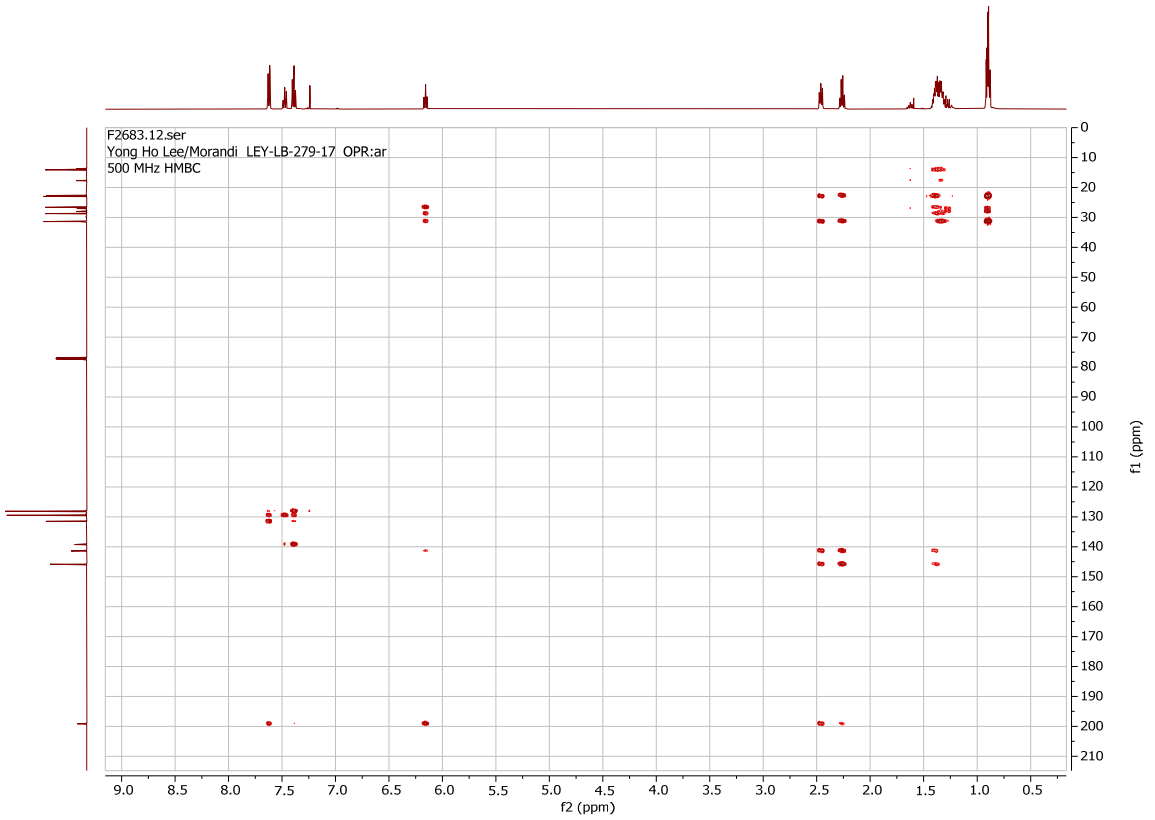
F2683.12.ser
Yong Ho Lee/Morandi LEY-LB-279-17 OPR:ar
500 MHz HMBC
f2 (ppm)
f1 (ppm)

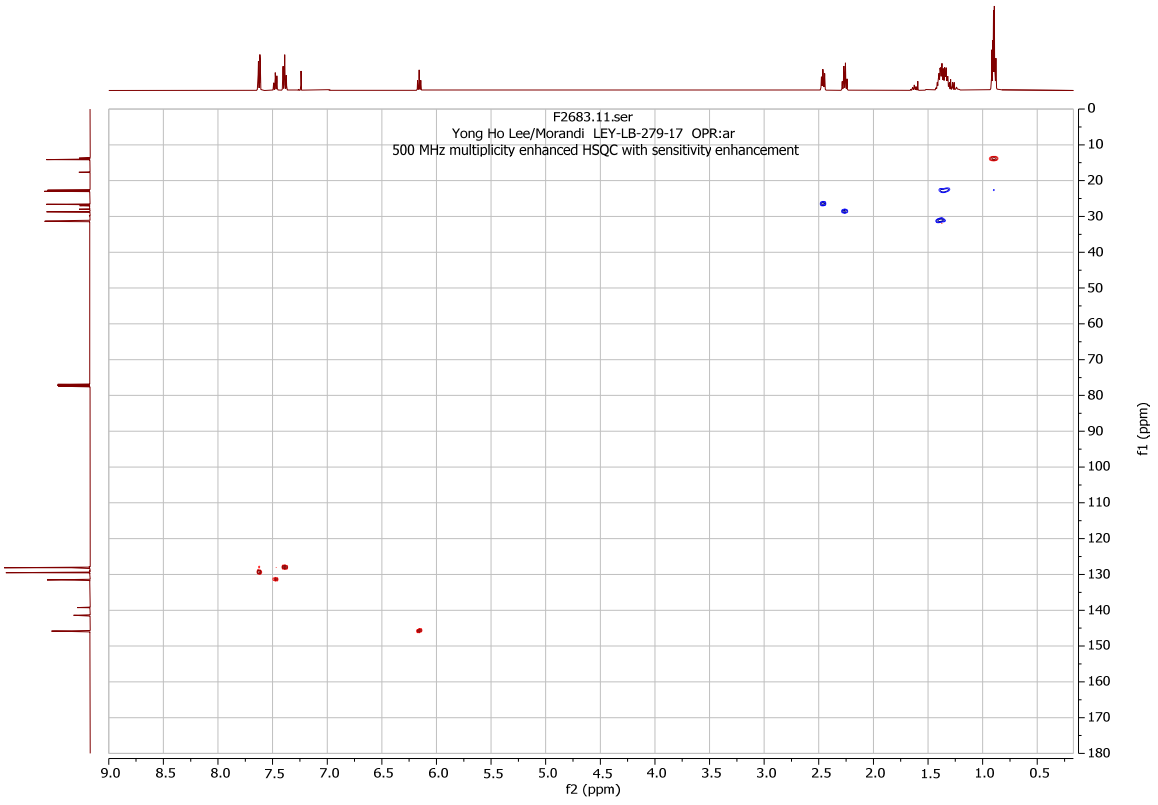
F2683.11.ser
Yong Ho Lee/Morandi LEY-LB-279-17 OPR:ar
500 MHz multiplicity enhanced HSQC with sensitivity enhancement
f2 (ppm)
f1 (ppm)

14.3. Phosphine ligands

1,4-Bis(diphenylphosphaneyl)benzene (**L23**)

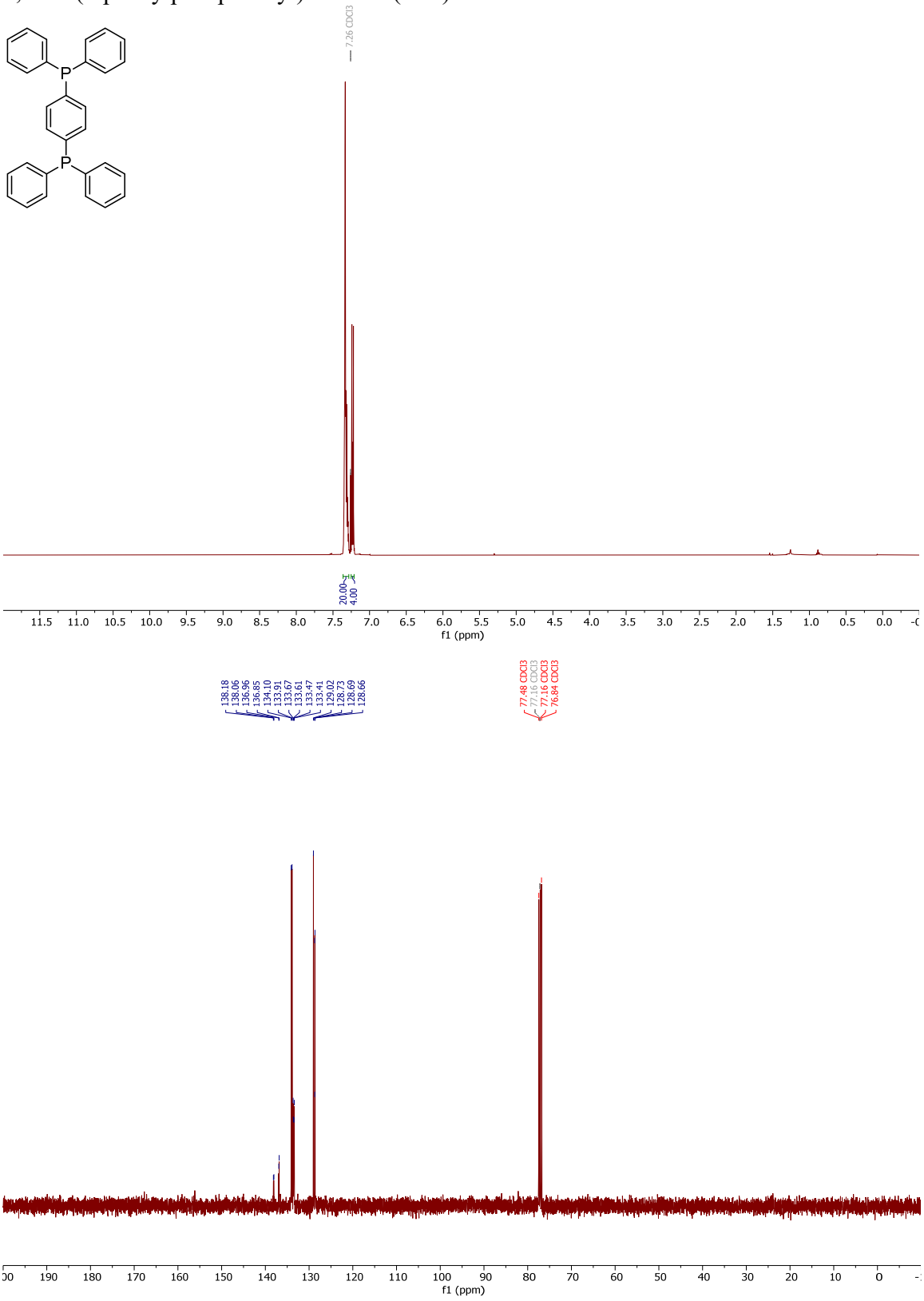

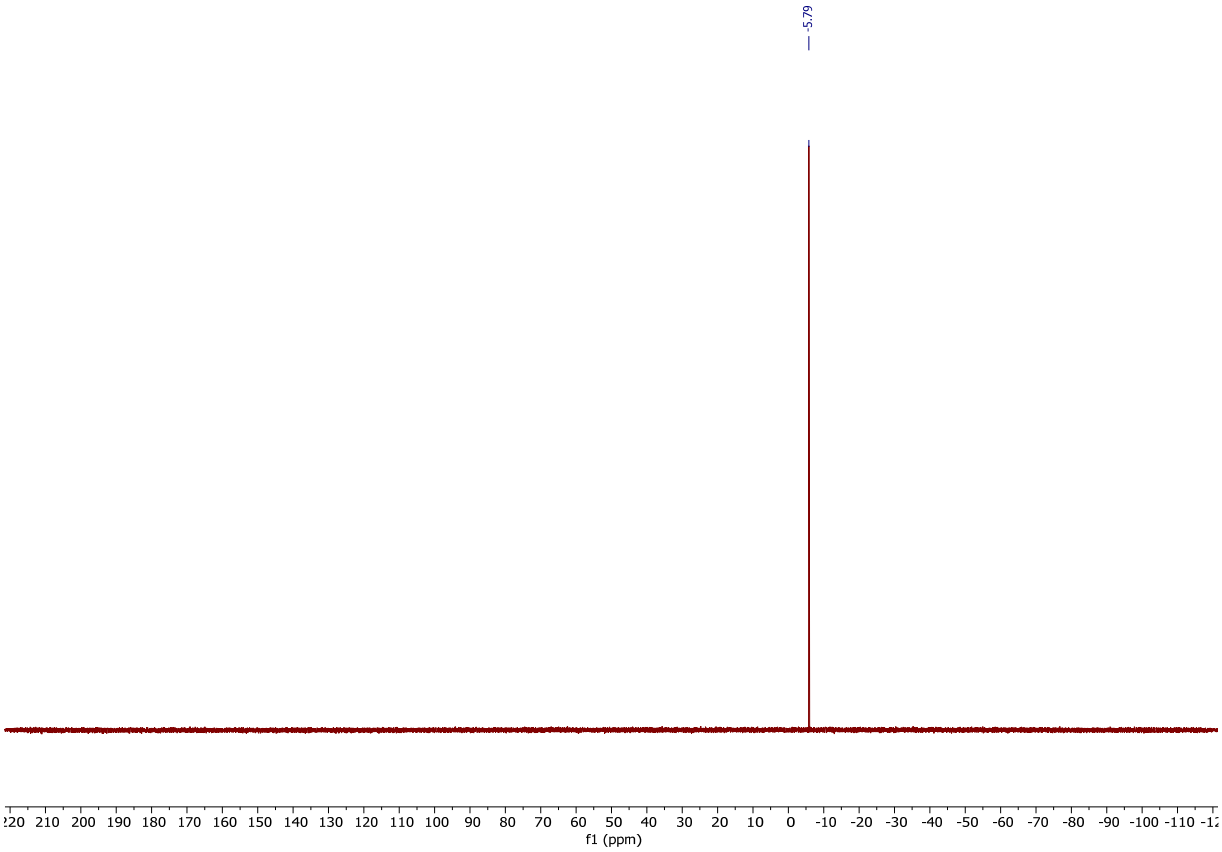
-5.79
220 210 200 190 180 170 160 150 140 130 120 110 100 90 80 70 60 50 40 30 20 10 0 -10 -20 -30 -40 -50 -60 -70 -80 -90 -100 -110
f1 (ppm)

4,6-Bis(diphenylphosphaneyl)dibenzo[b,d]furan (**L07**)

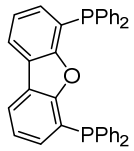

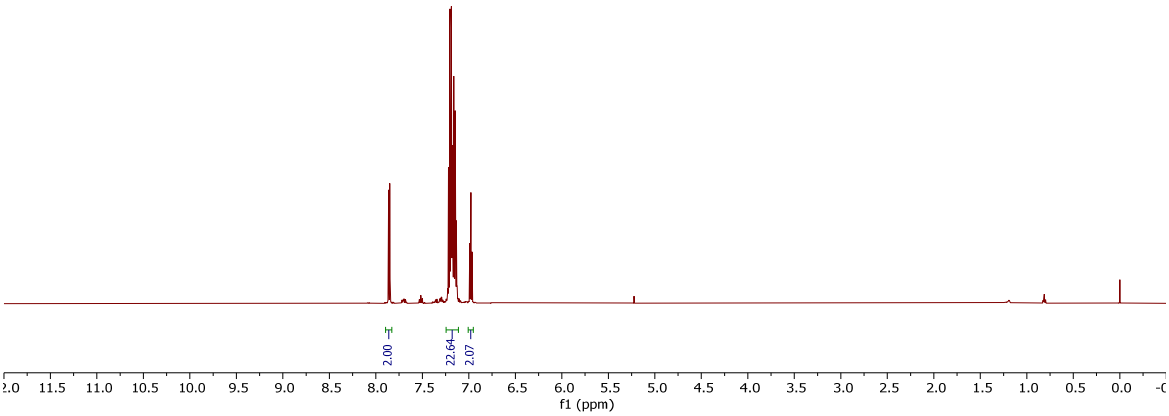

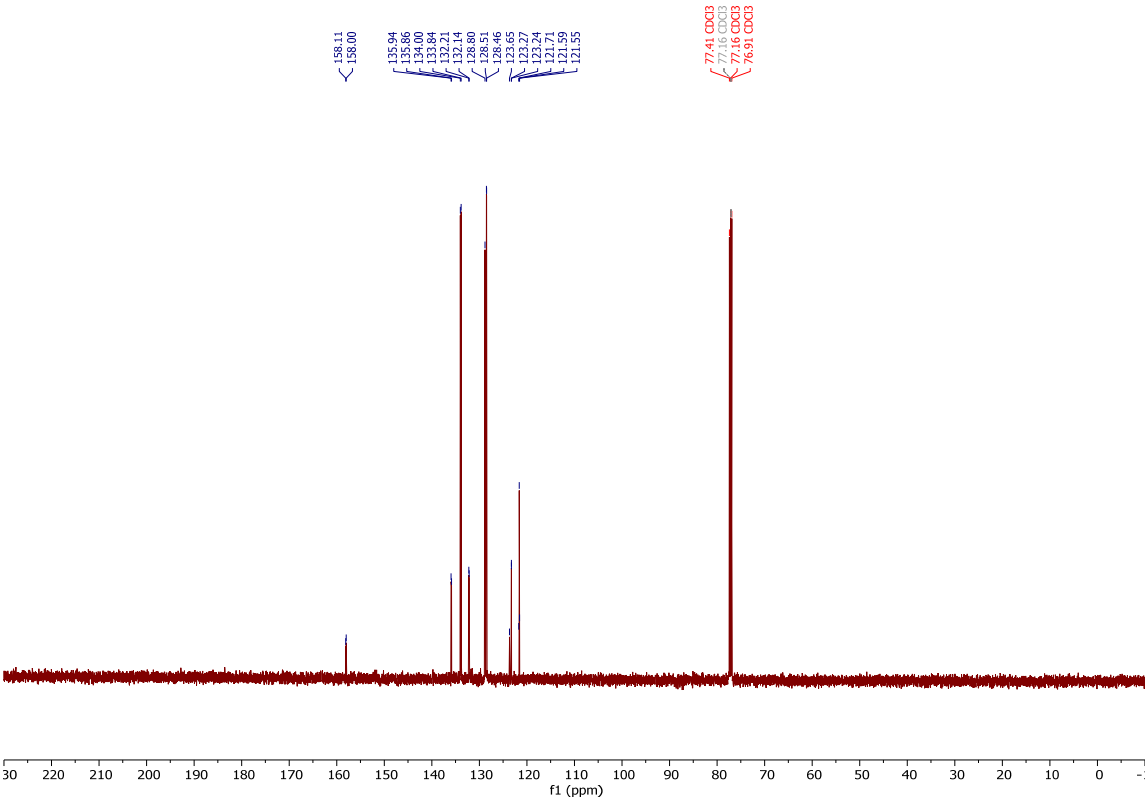

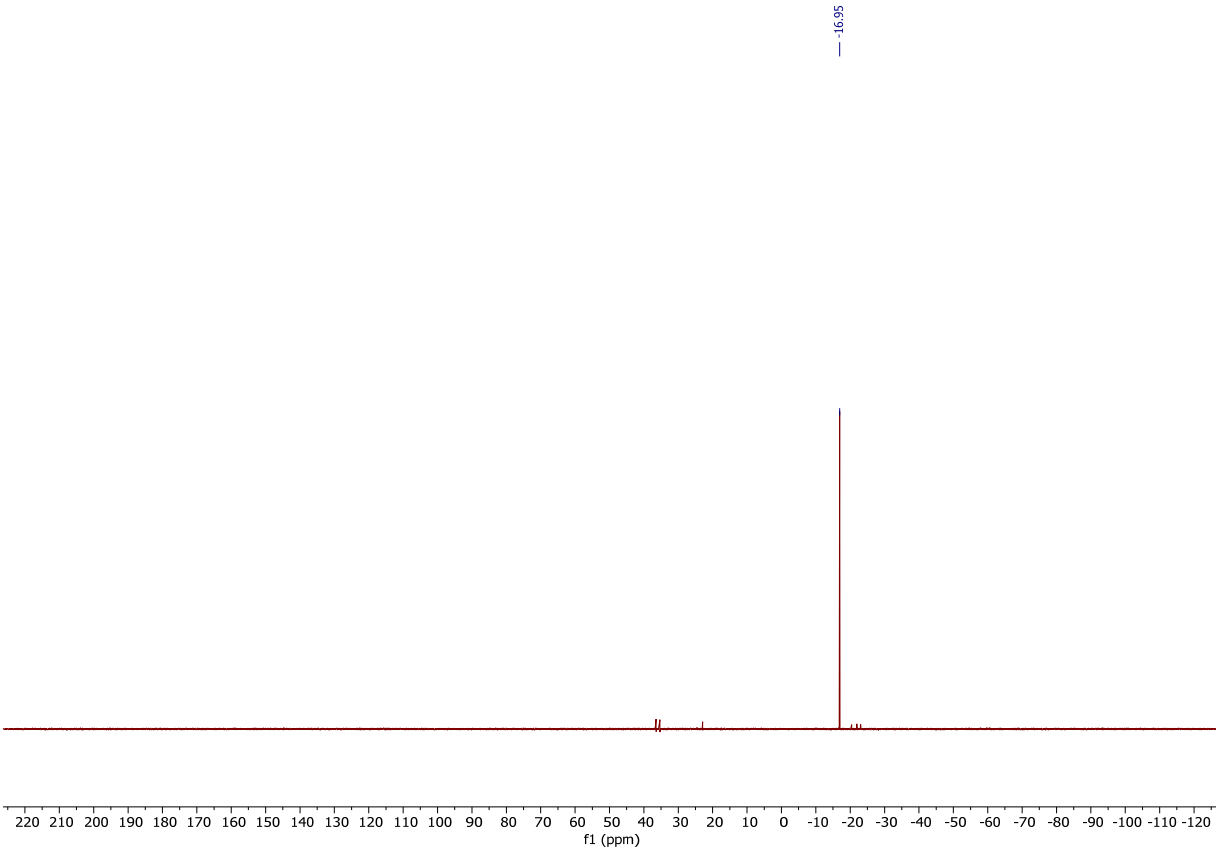
-16.95
220 210 200 190 180 170 160 150 140 130 120 110 100 90 80 70 60 50 40 30 20 10 0 -10 -20 -30 -40 -50 -60 -70 -80 -90 -100 -110 -120
f1 (ppm)

6,8-Bis(diphenylphosphaneyl)dinaphtho[2,1-b:1',2'-d]furan (U-DNFphos, **L08**)

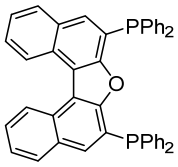

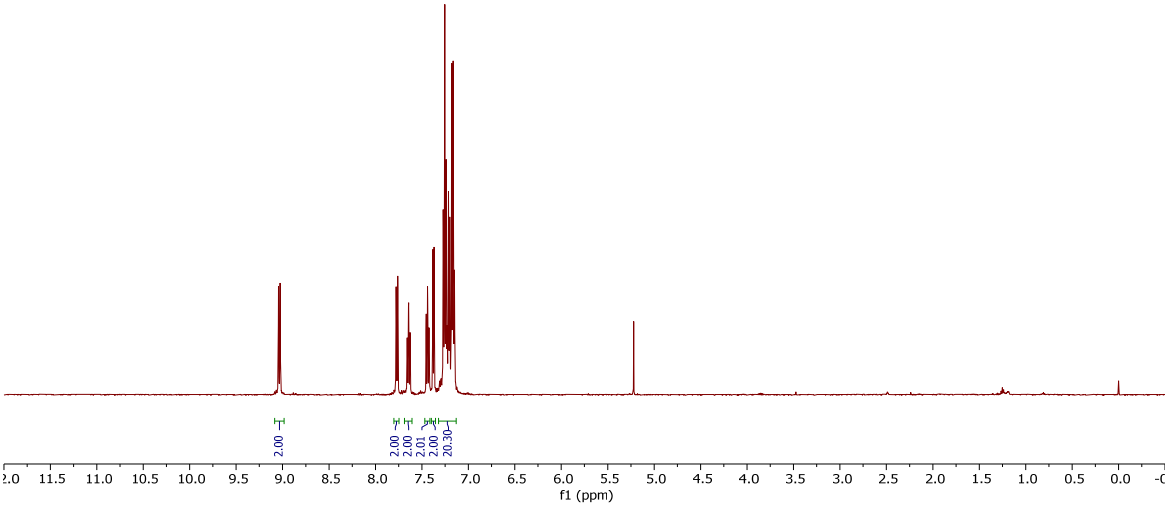

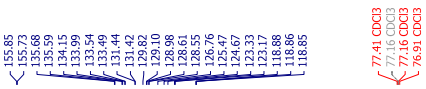

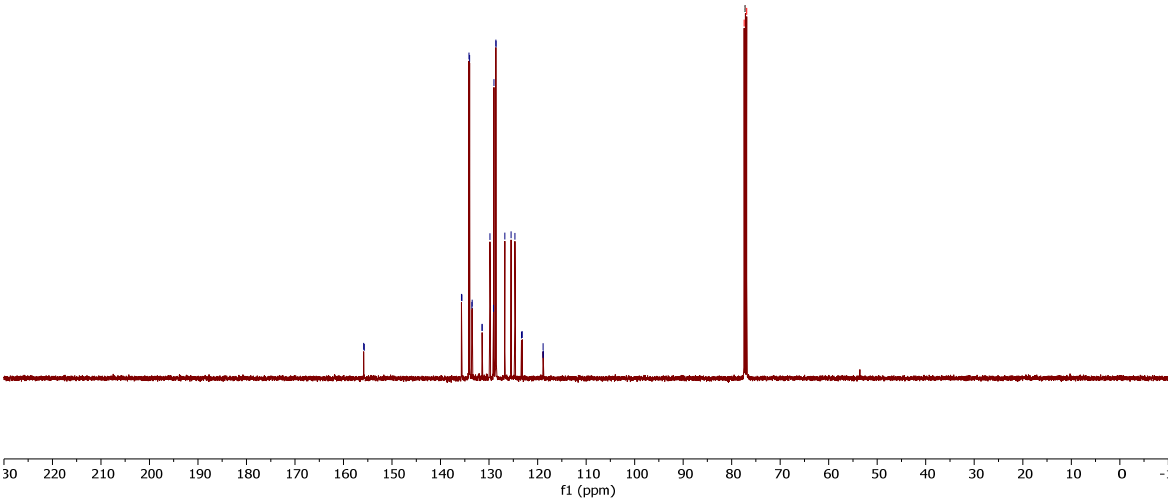

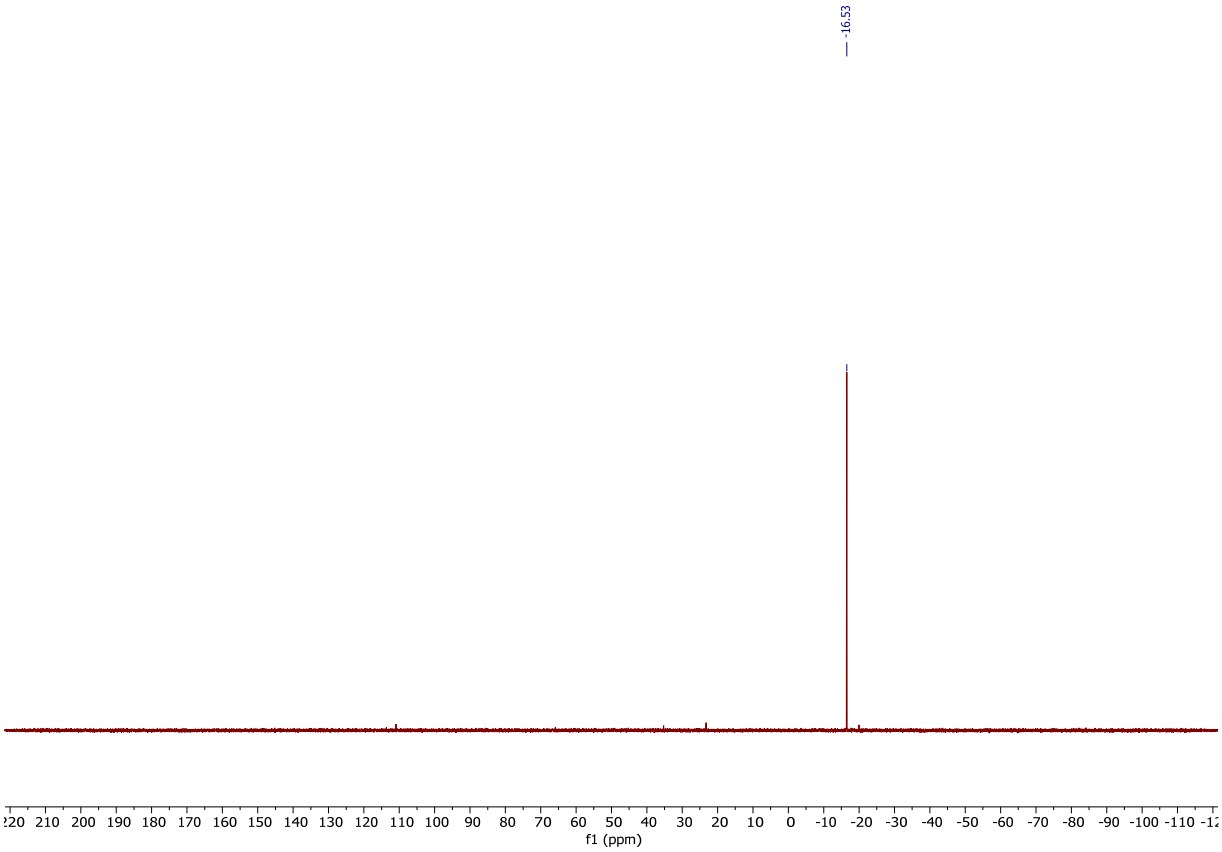
-16.53
220 210 200 190 180 170 160 150 140 130 120 110 100 90 80 70 60 50 40 30 20 10 0 -10 -20 -30 -40 -50 -60 -70 -80 -90 -100 -110
f1 (ppm)

3,3'-Bis((diphenylphosphaneyl)methyl)-2,2'-binaphthalene (VNAphos, **L25**)

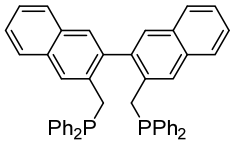

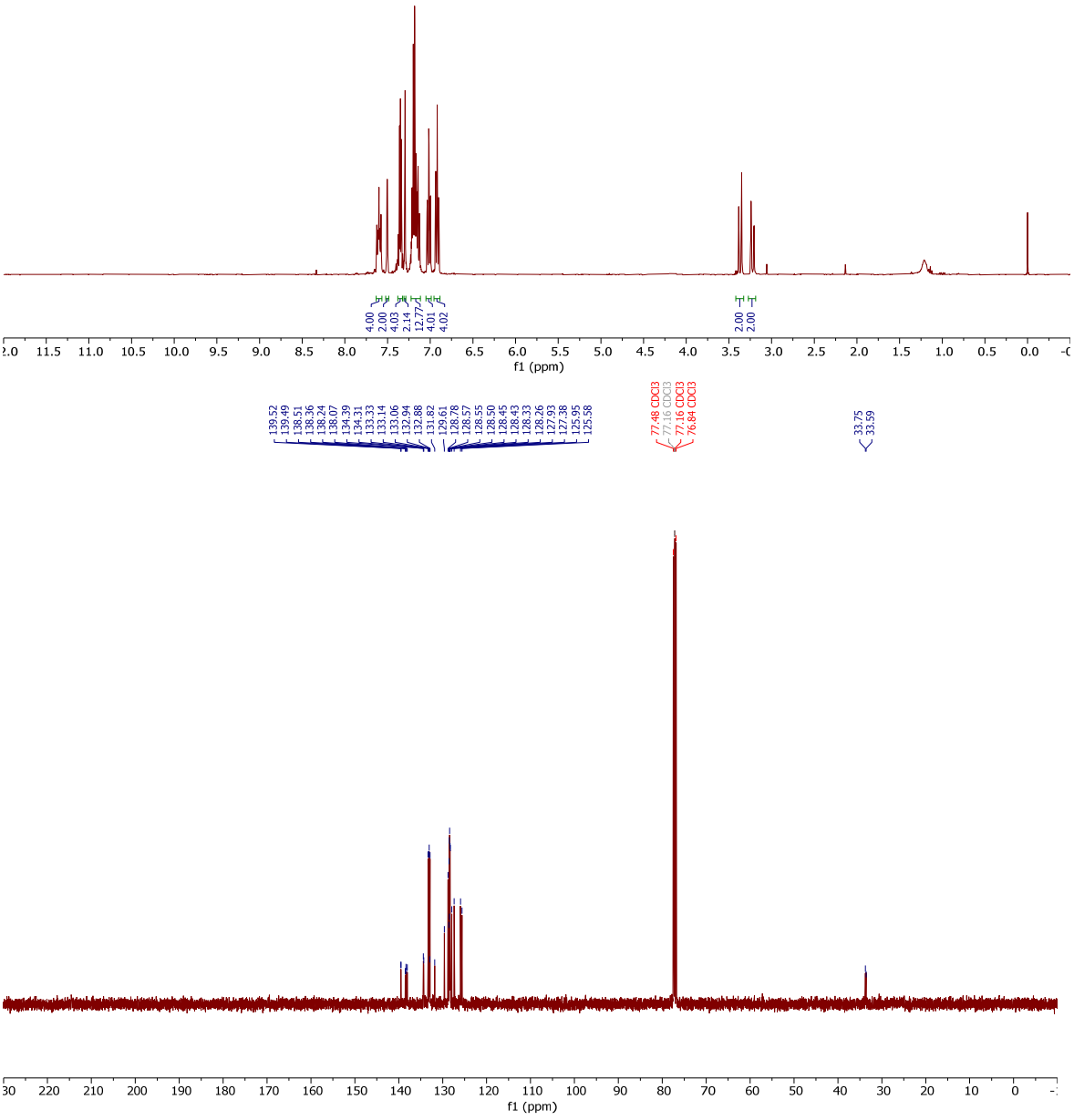

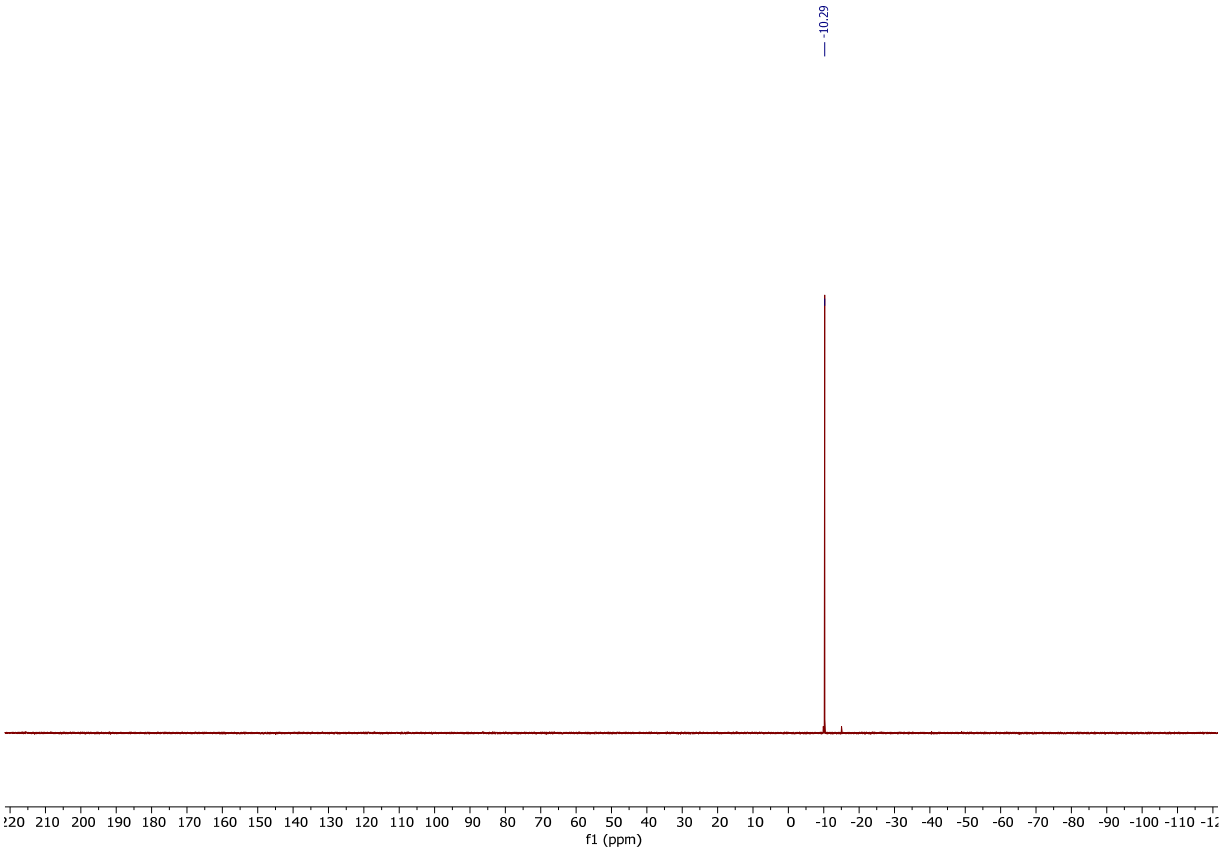
-10.29
220 210 200 190 180 170 160 150 140 130 120 110 100 90 80 70 60 50 40 30 20 10 0 -10 -20 -30 -40 -50 -60 -70 -80 -90 -100 -110 -12
f1 (ppm)

14.4. Acid chloride and alkyne substrates, etc.

2-Cyanobenzoyl chloride (**SAC-01**).

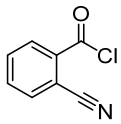

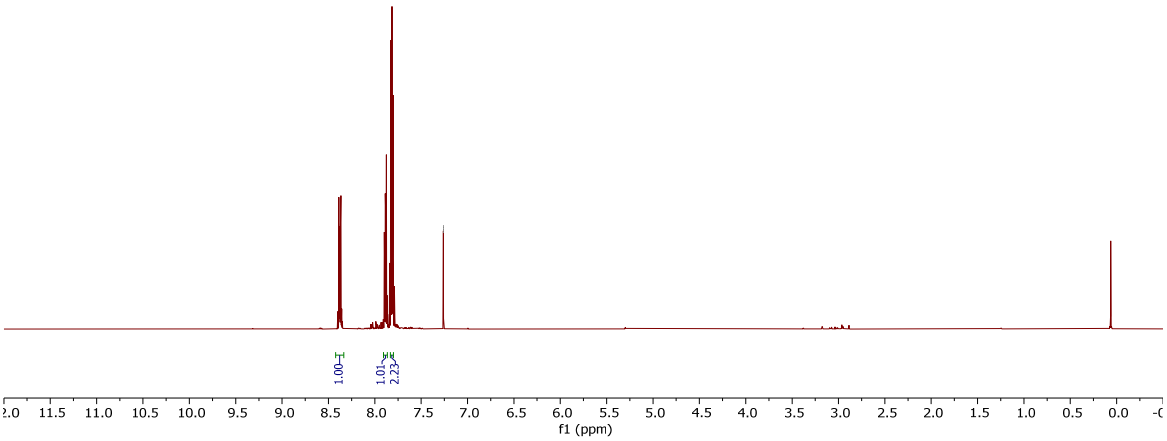

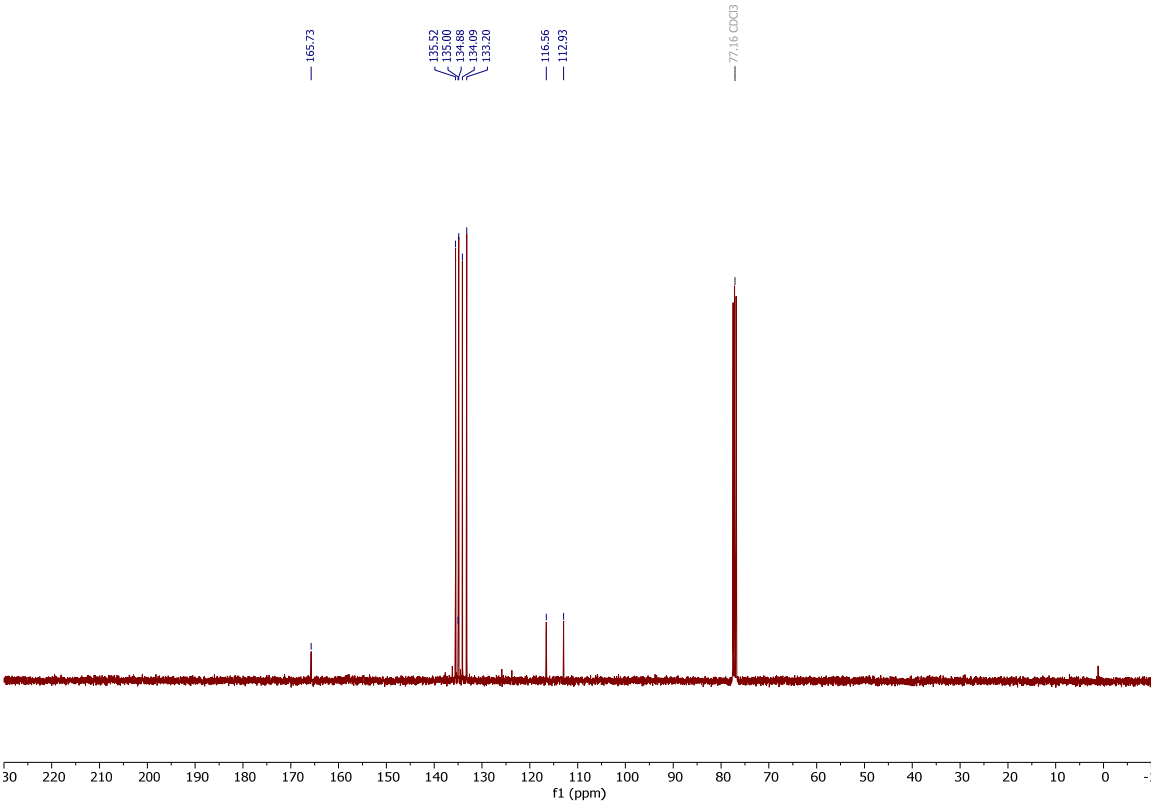

2-Methyl-6-(trifluoromethyl)nicotinoyl chloride (**SAC-02**).

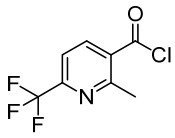

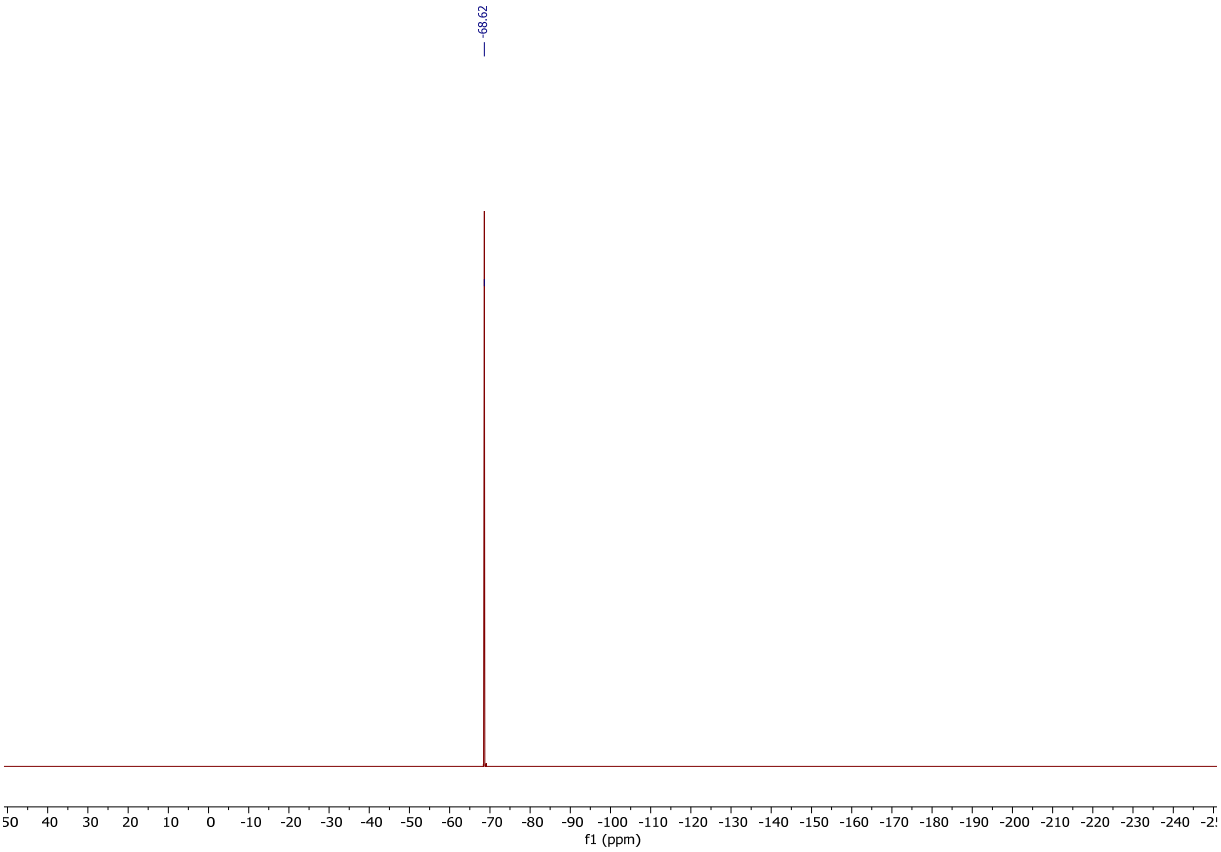
-68.62
50 40 30 20 10 0 -10 -20 -30 -40 -50 -60 -70 -80 -90 -100 -110 -120 -130 -140 -150 -160 -170 -180 -190 -200 -210 -220 -230 -240
f1 (ppm)

Benzoyl chloride-α-^{13}C (**SAC-03**).

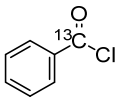

4-(4,4,5,5-Tetramethyl-1,3,2-dioxaborolan-2-yl)benzoyl chloride (**SAC-04**).

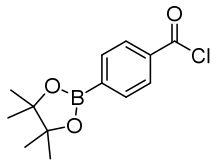

4-(*N*,*N*-Dipropylsulfamoyl)benzoyl chloride (**SAC-05**).

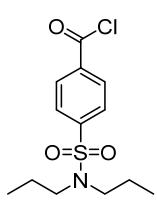

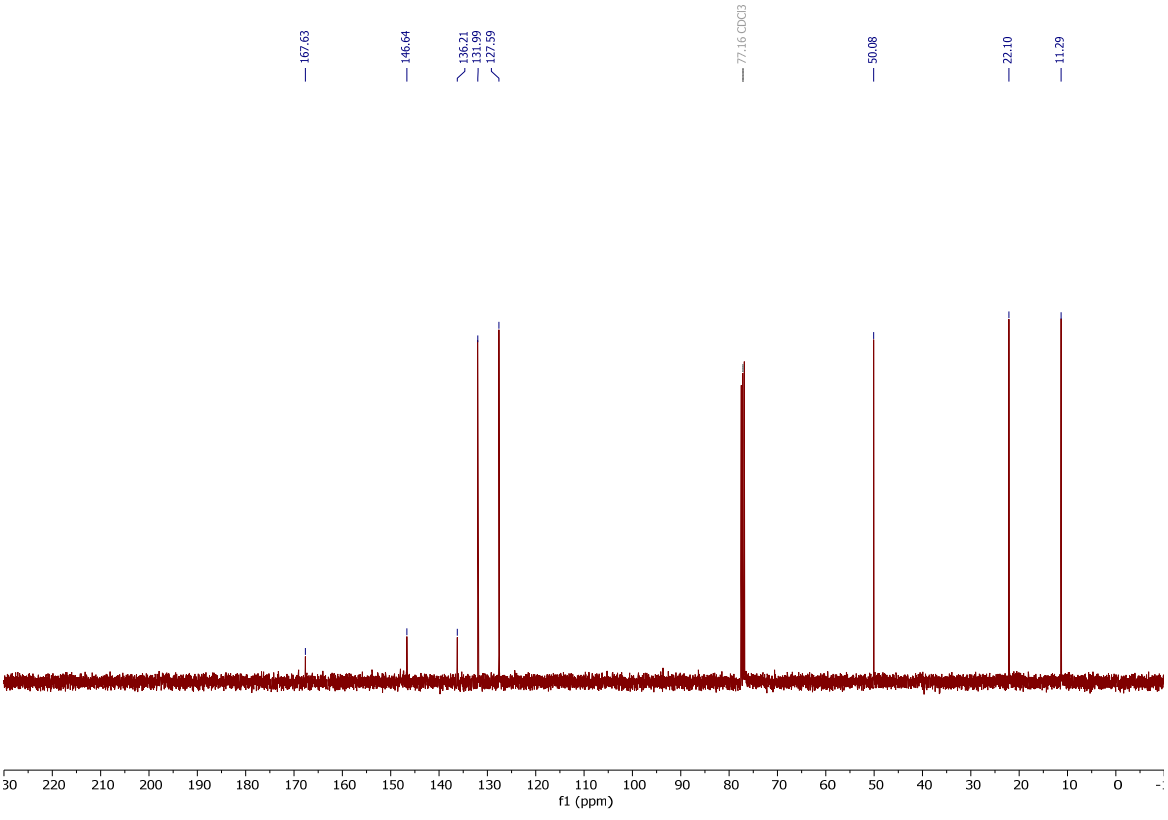

2-(3-Cyano-4-isobutoxyphenyl)-4-methylthiazole-5-carbonyl chloride (**SAC-06**).

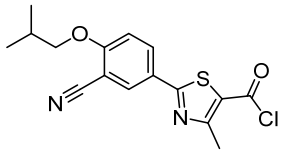

1,8-Diphenyloct-4-yne (**SAK-01**).

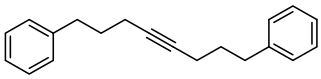

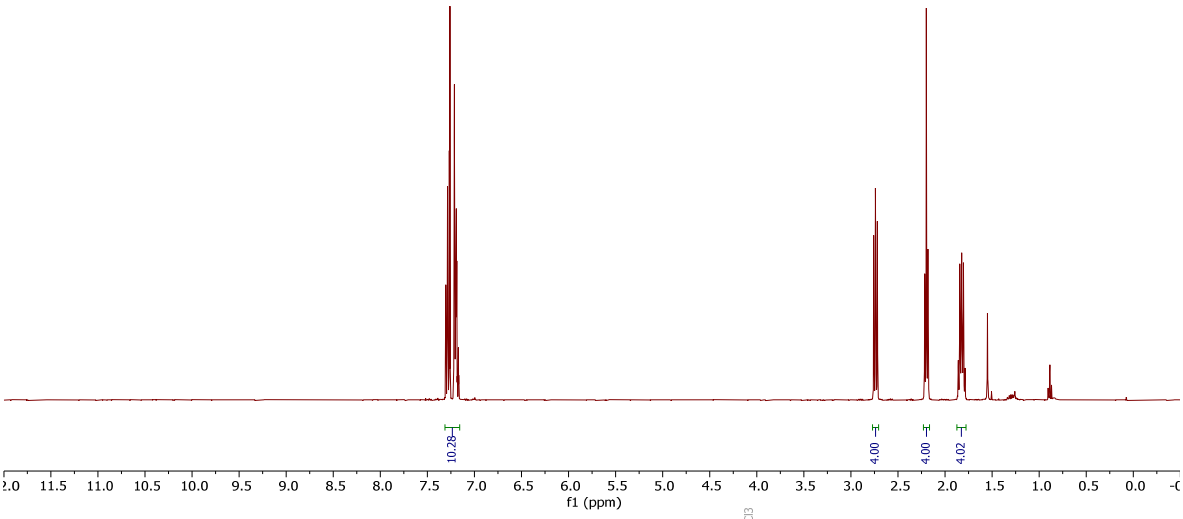

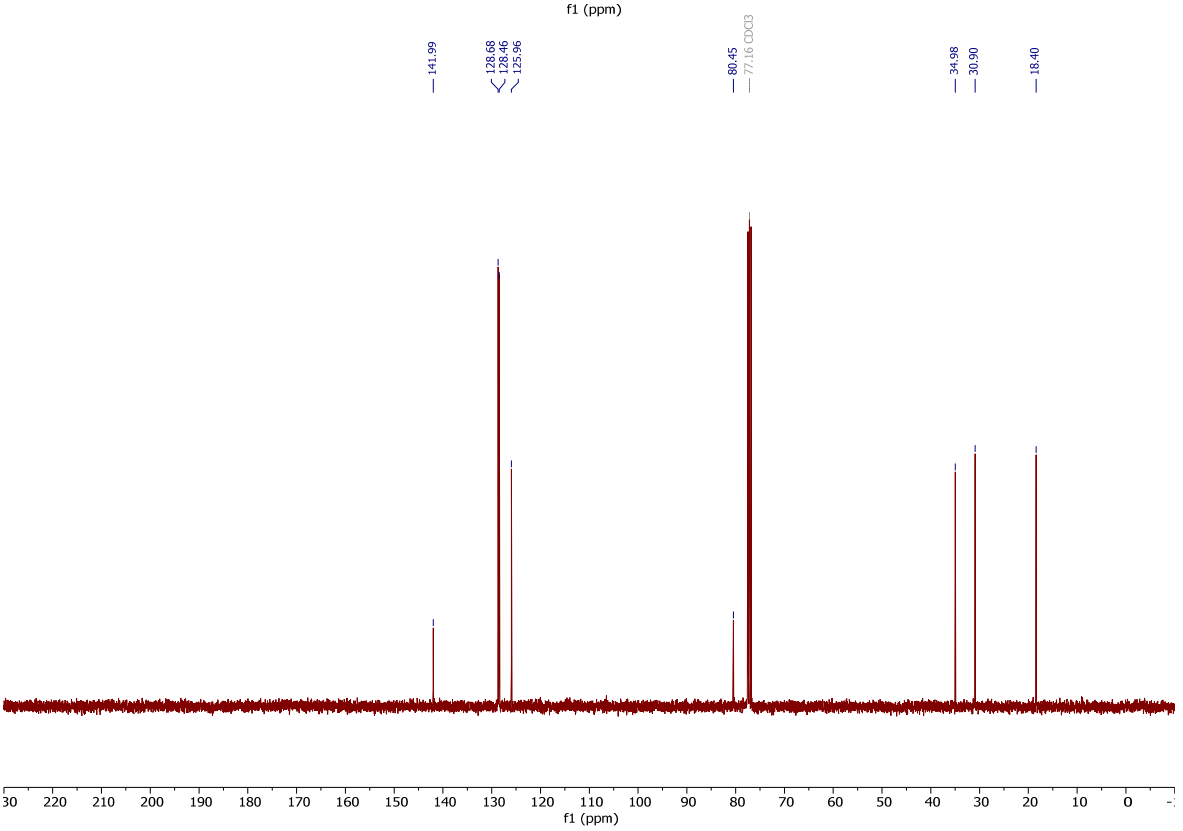

1,10-Dichlorodec-5-yne (**SAK-02**).

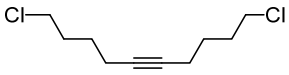

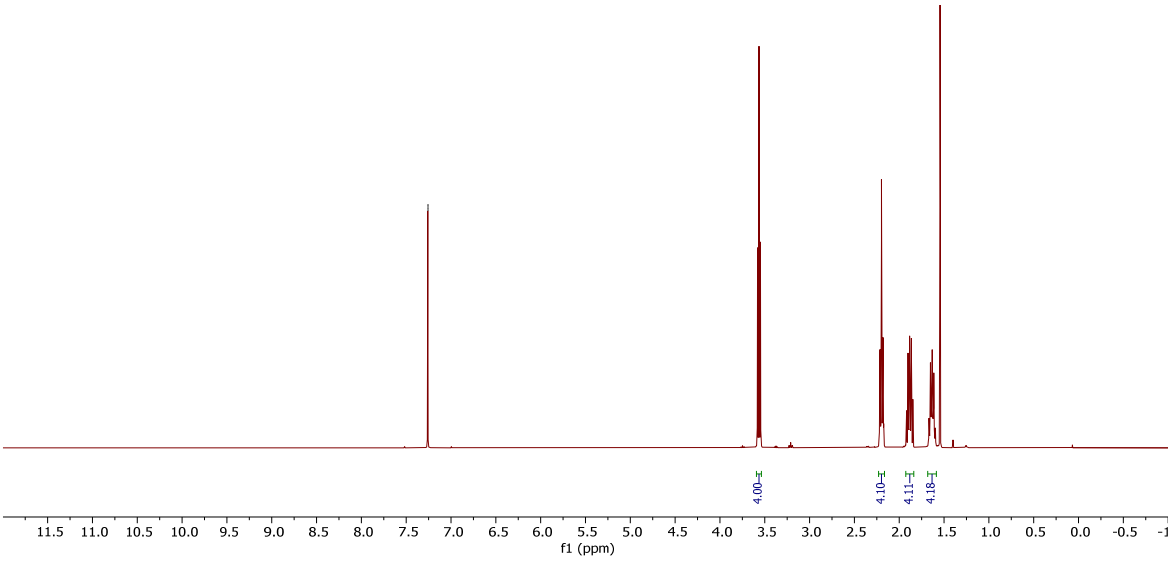

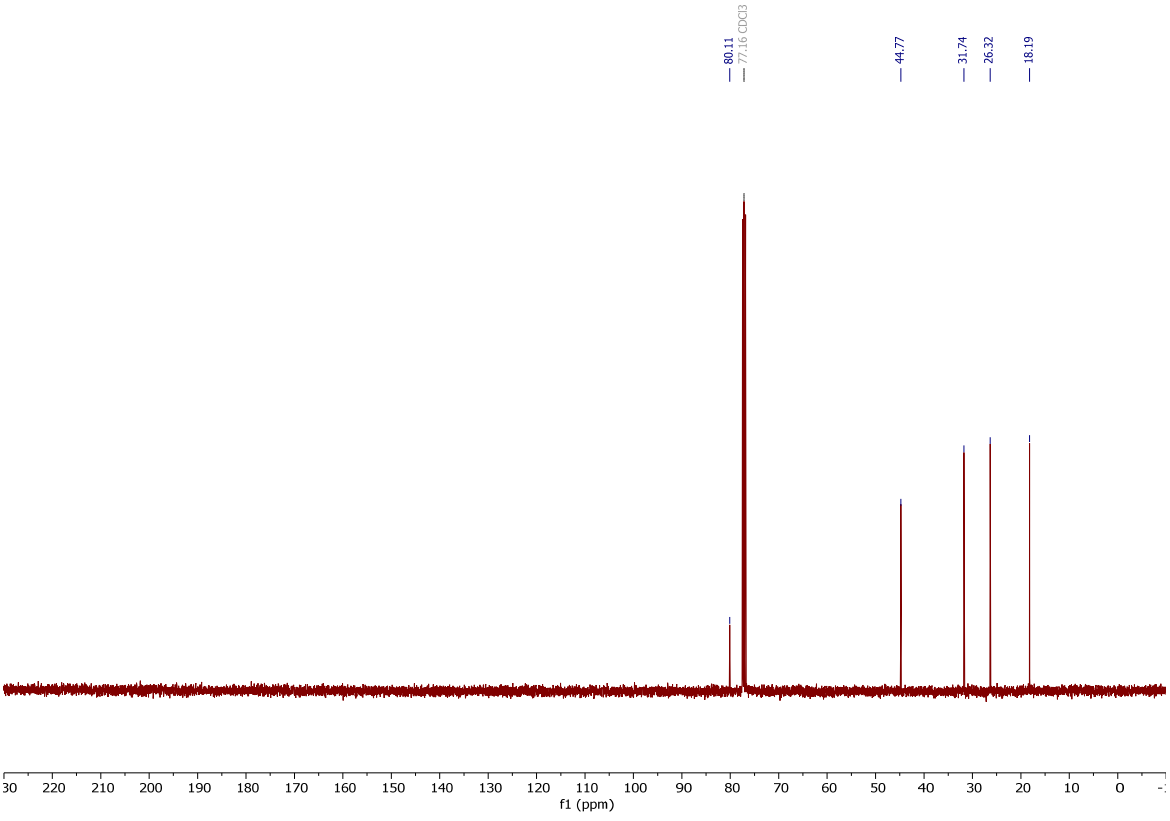

Hept-2-yn-1-yl benzoate (**SAK-03**).

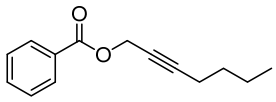

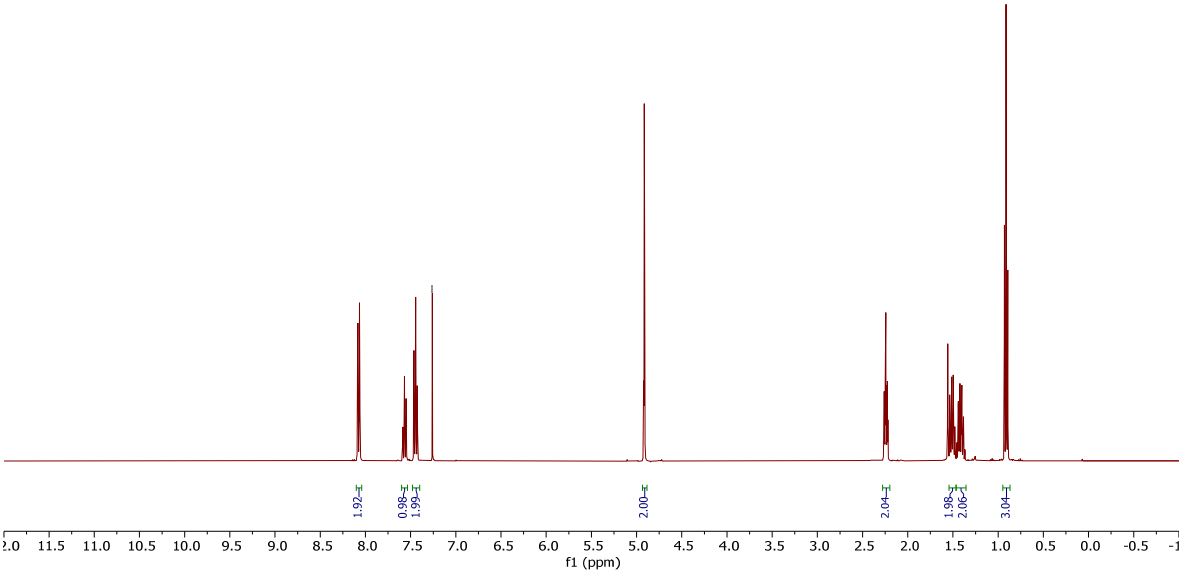

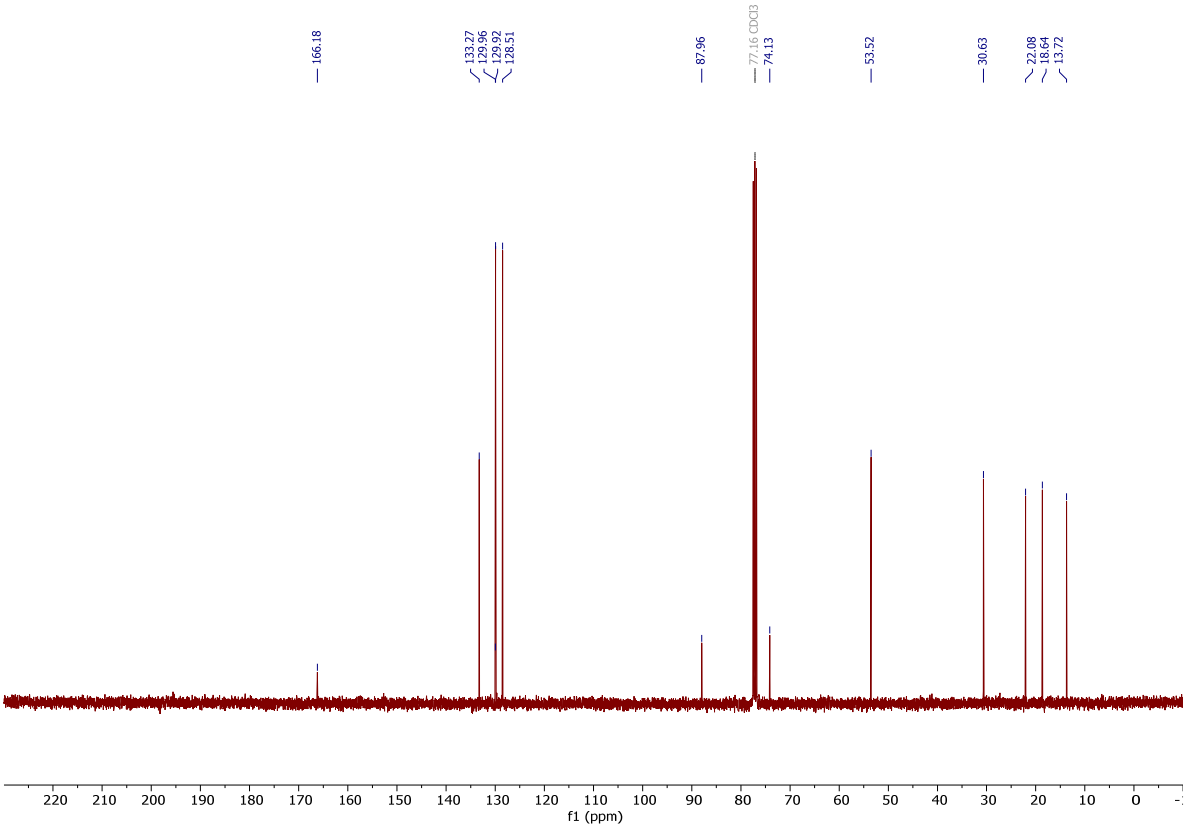

Oct-3-yn-1-yl benzoate (**SAK-04**).

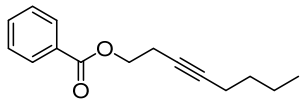

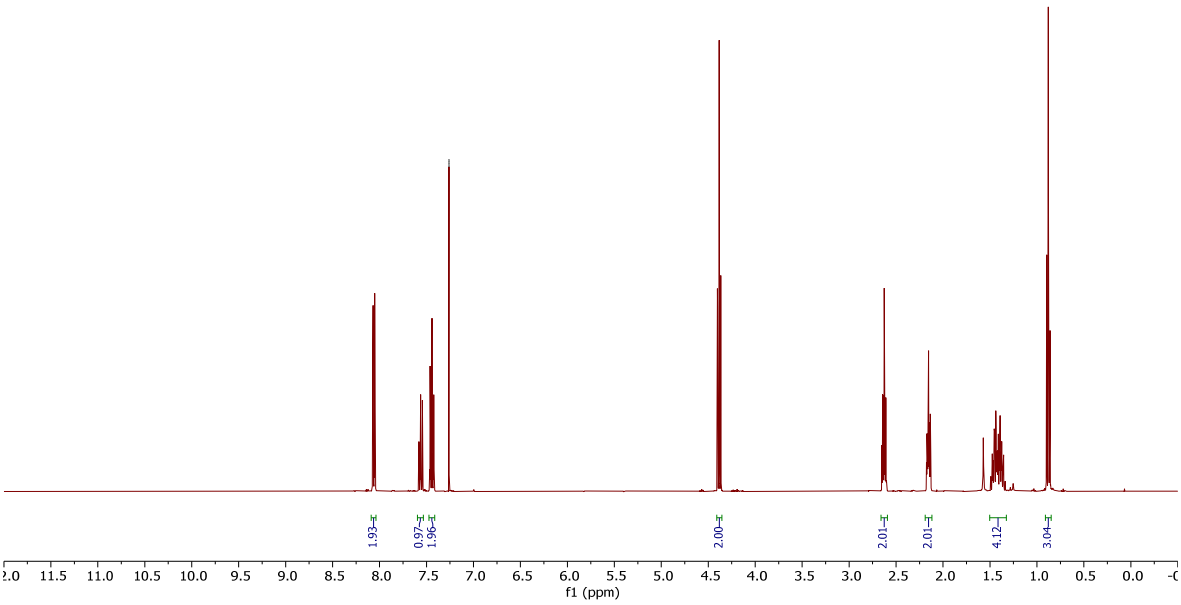

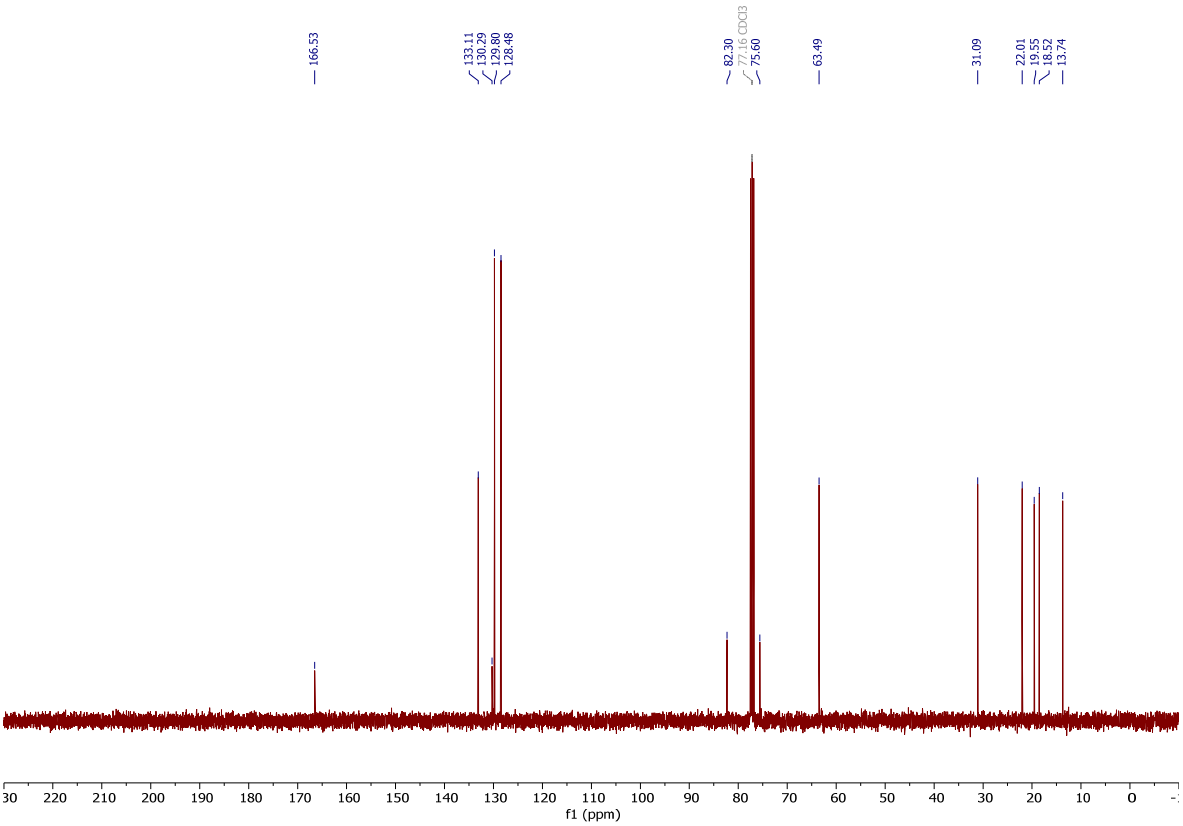

Oct-3-yn-1-yl butyrate (**SAK-05**).

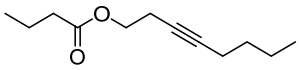

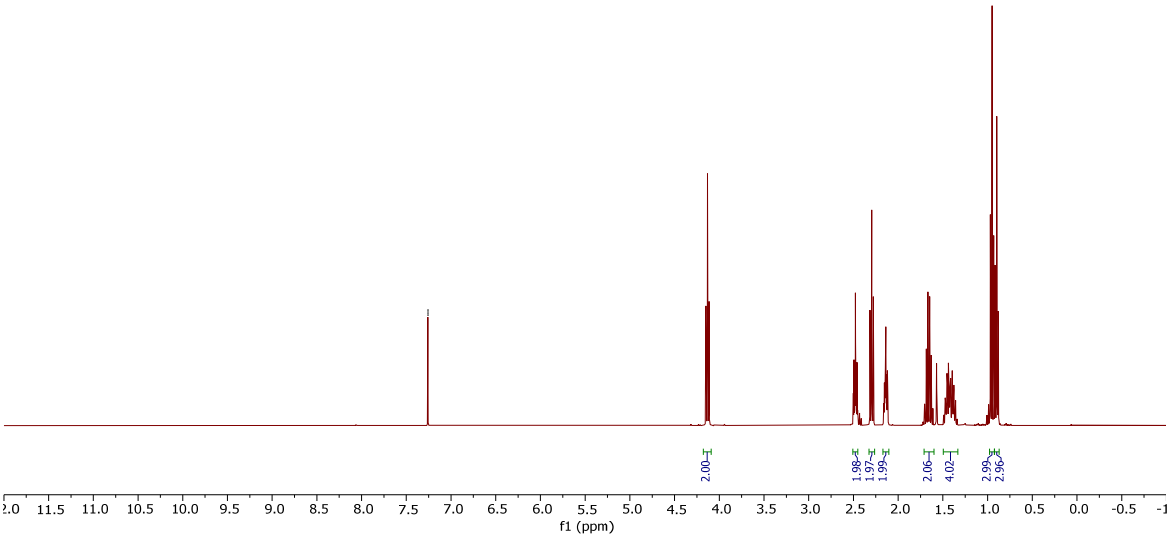

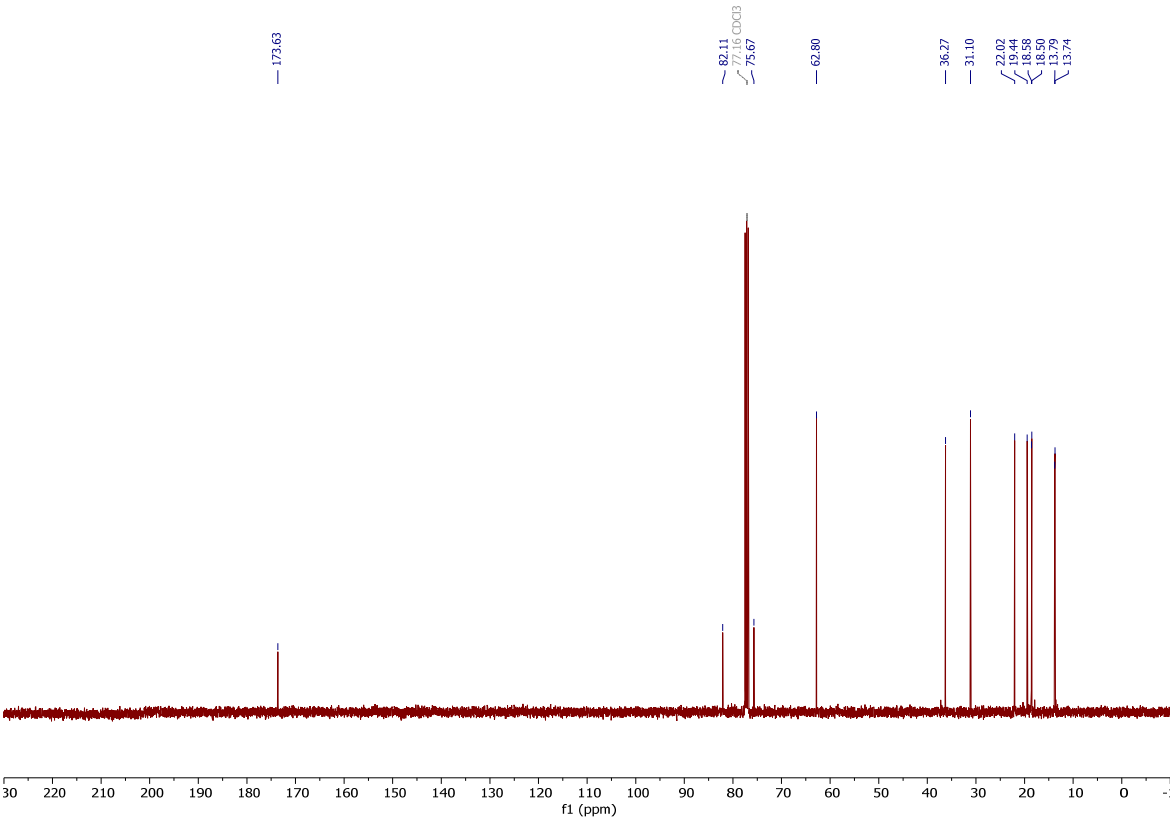

Oct-3-yn-1-yl diethylcarbamate (**SAK-06**).

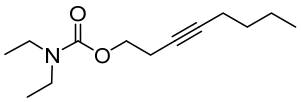

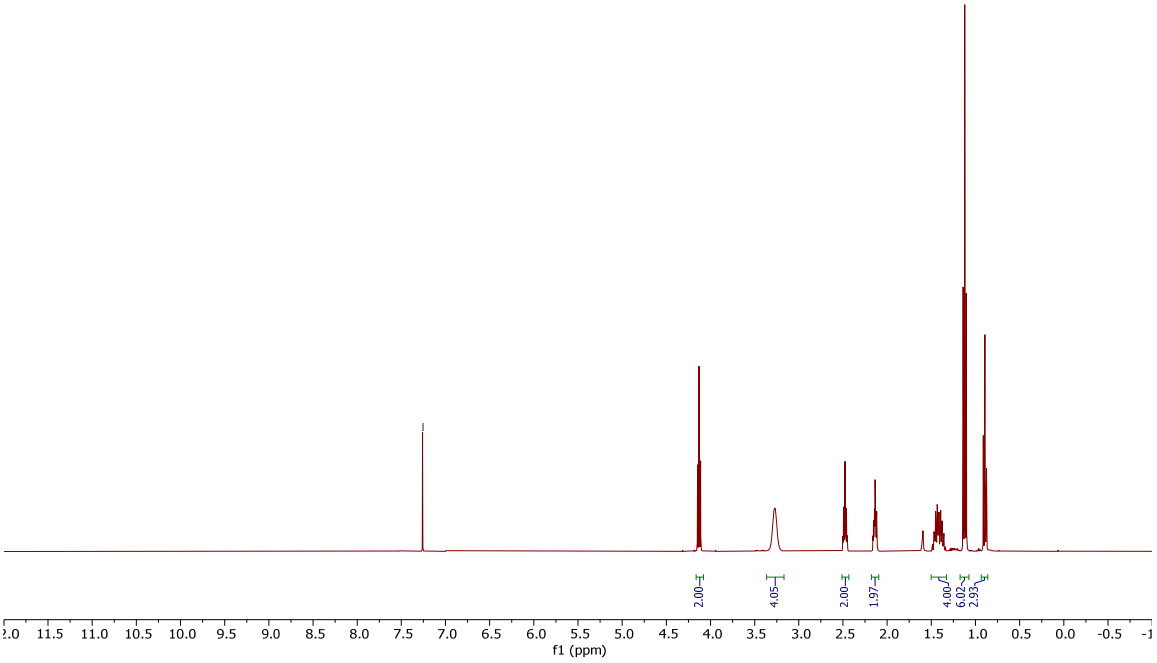

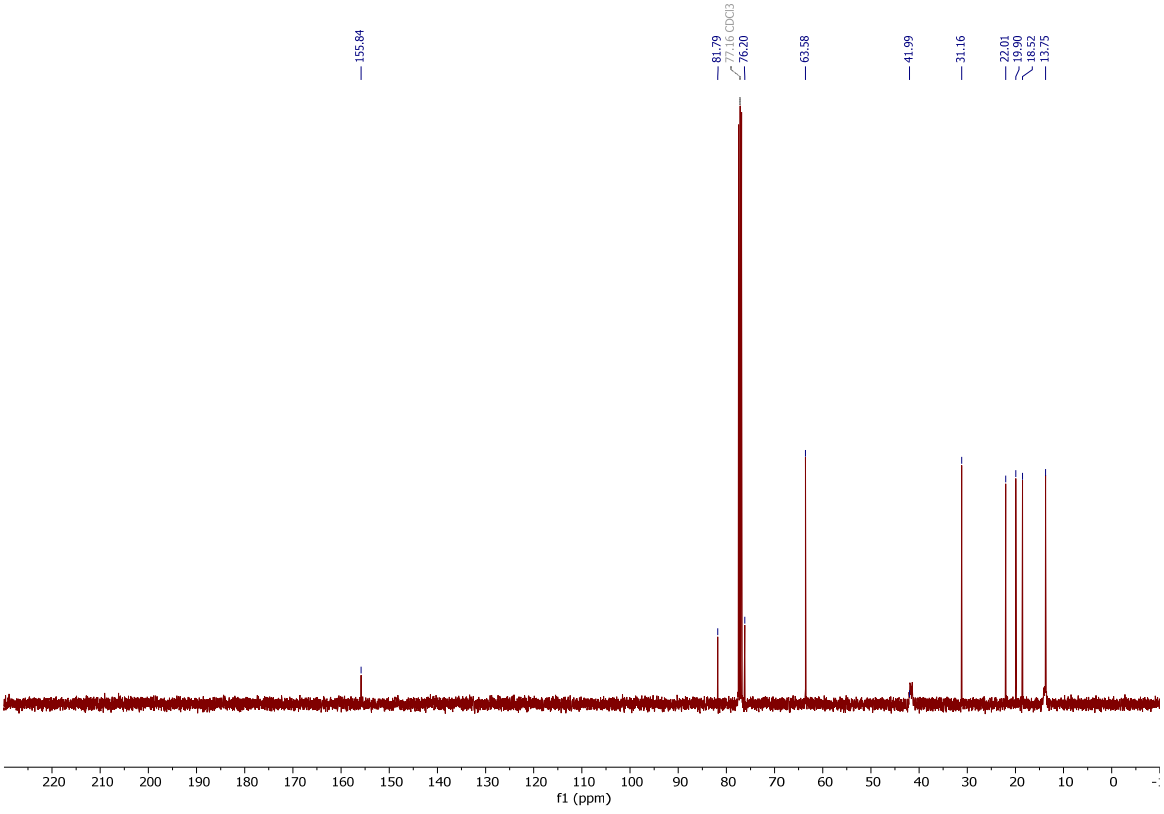

Dodec-9-yn-1-yl benzoate (**SAK-07**).

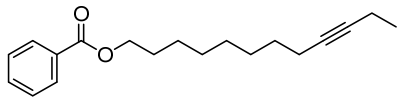

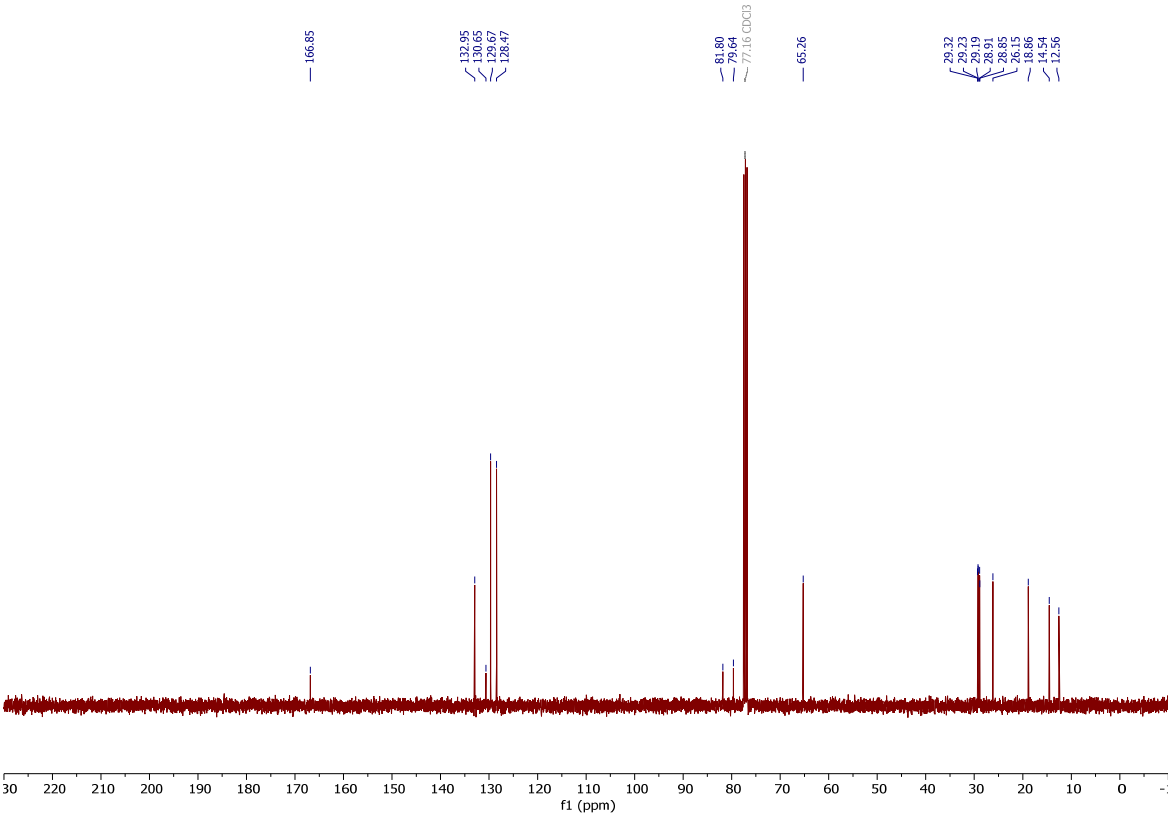

Dec-5-yn-1-yl benzoate (**SAK-08**)

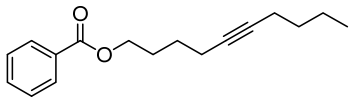

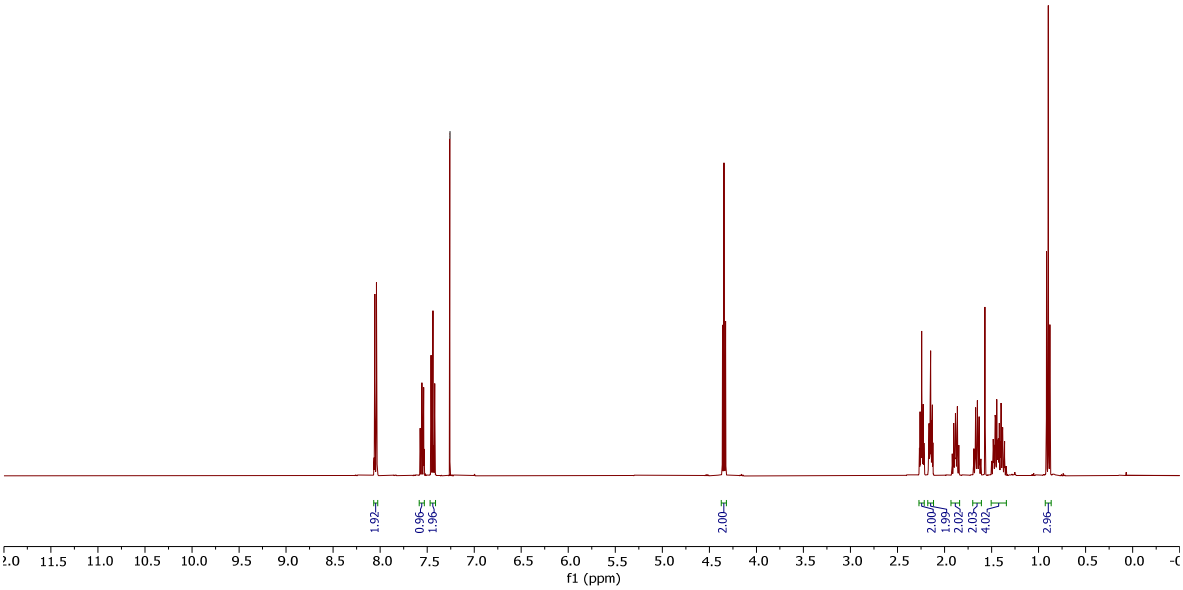

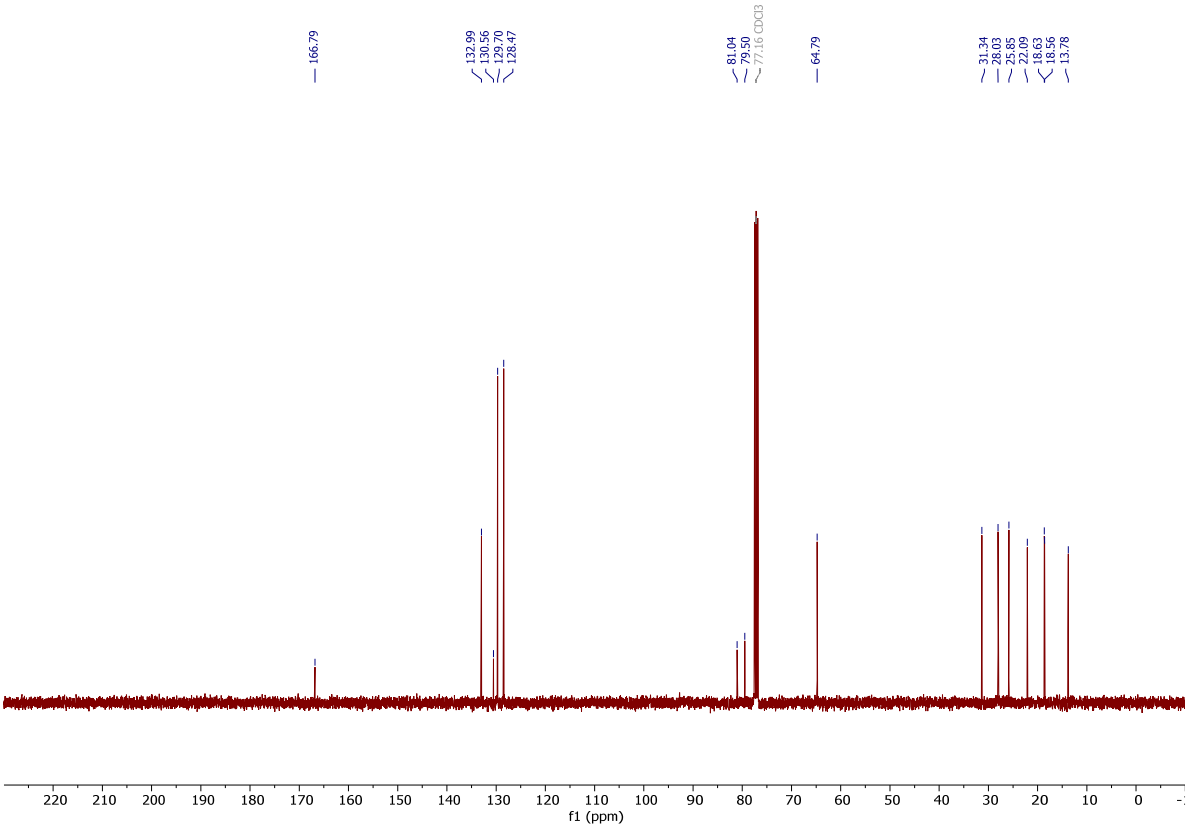

Methoxy-4-((oct-3-yn-1-yloxy)methyl)benzene (**SAK-09**).

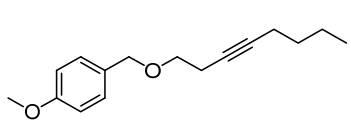

N-(3-Phenylprop-2-yn-1-yl)pivalamide (**SAK-10**).

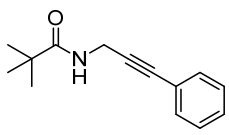

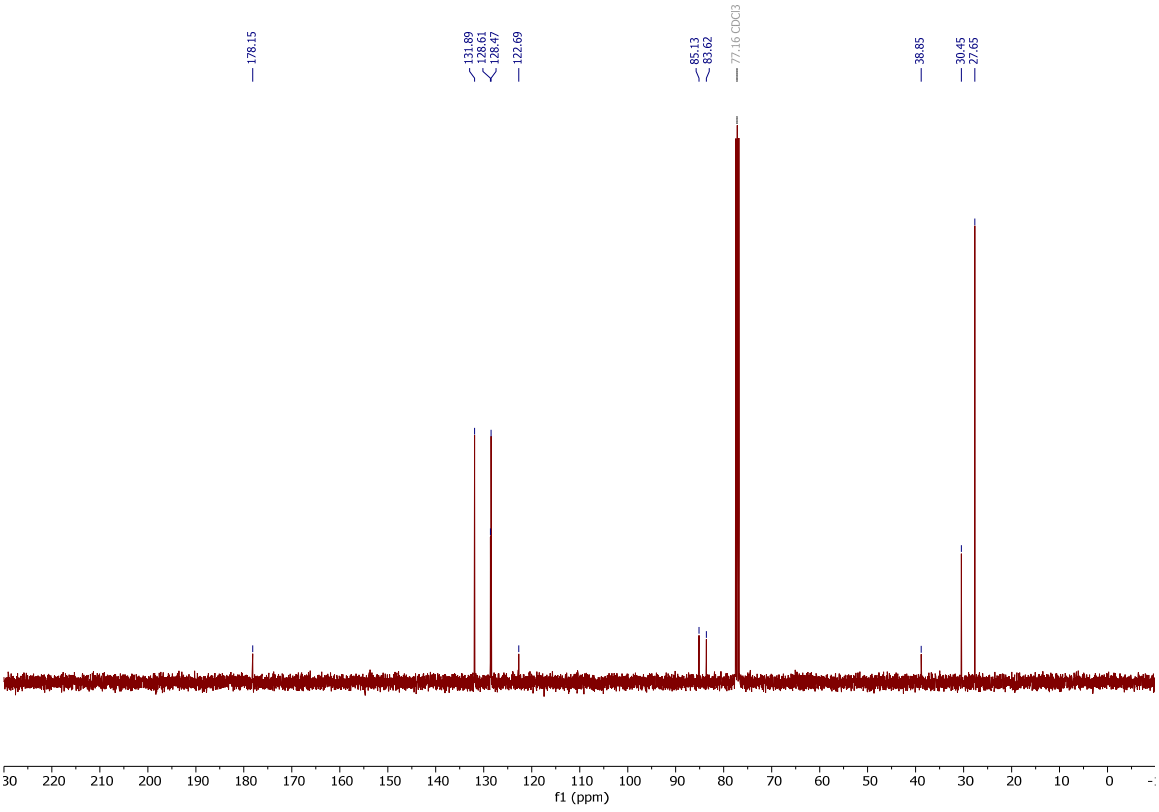

Triisopropylsilane-*d* (*i*Pr$_3$SiD).

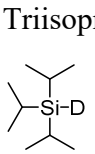

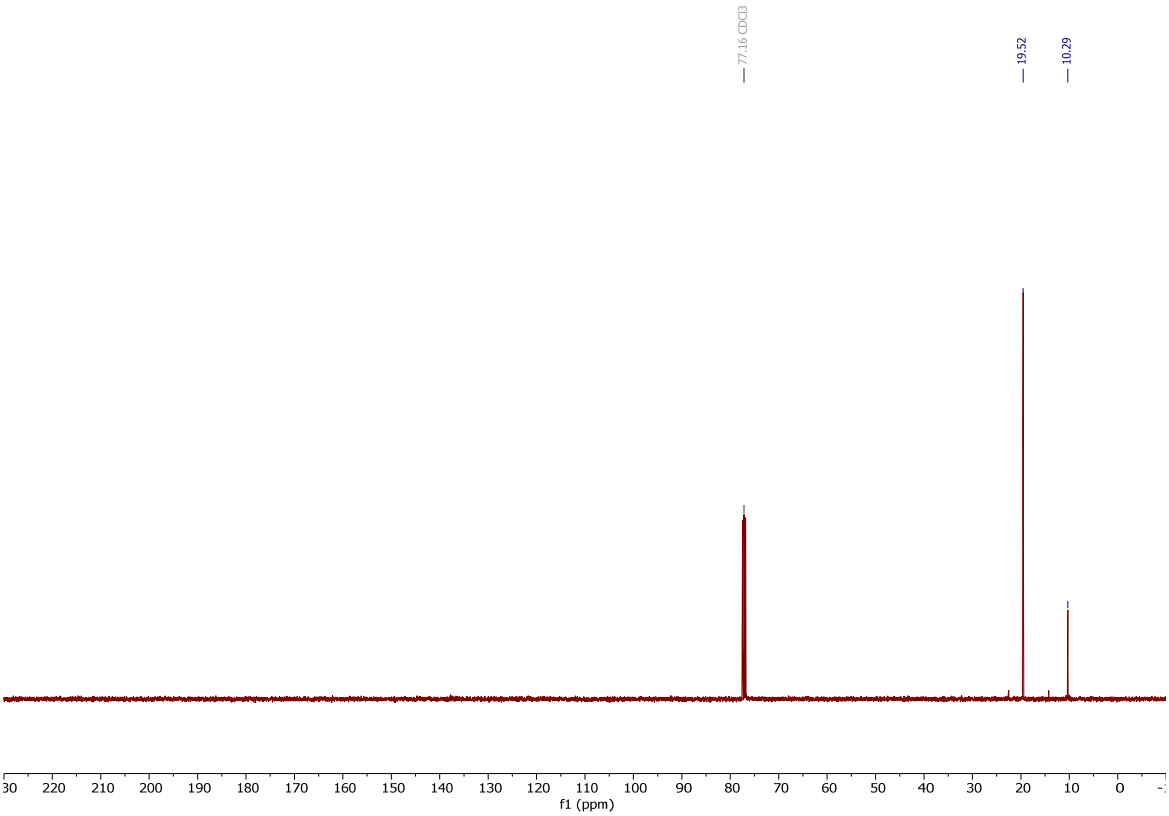

14. References

1. Wang, C., Mao, G.-L., Wang, Z.-H. & Xi, Z.-F. Facile synthesis of multiply substituted cyclopentadienes and conjugated dienals through reactions between 1,4-dilithio-1,3-dienes and carboxylic acid derivatives including acyl chlorides, anhydrides, and DMF. *Eur. J. Org. Chem.* 1267–1273 (2007).
2. Dai, J., Wang, M., Chai, G., Fu, C. & Ma, S. A practical solution to stereodefined tetrasubstituted olefins. *J. Am. Chem. Soc.* **138**, 2532–2535 (2016).
3. Chiachio, U. et al. Novel approach to the ring-opening of 4-isoxazolines: one-pot synthesis of α,β-enones. *Tetrahedron* **48**, 123–132 (1992).
4. Tan, G., Wu, Y., Shi, Y. & You, J. Syngas-free rhodium-catalyzed highly regioselective transfer hydroformylation of alkynes to α,β-unsaturated aldehydes. *Angew. Chem. Int. Ed.* **58**, 7440–7444 (2019).
5. Kokubo, K., Matsumasa, K., Miura, M. & Nomura, M. Rhodium-catalyzed reaction of aroyl chlorides with alkynes or alkenes in the presence of disilanes. *J. Organomet. Chem.* **560**, 217–222 (1998).
6. Fang, X., Cacherat, B. & Morandi, B. CO- and HCl-free synthesis of acid chlorides from unsaturated hydrocarbons via shuttle catalysis. *Nat. Chem.* **9**, 1105–1109 (2017).
7. Tsuda, T., Kiyoi, T. & Saegusa, T. Nickel(0)-catalyzed hydroacylation of alkynes with aldehydes to α,β-enones. *J. Org. Chem.* **55**, 2554–2558 (1990).
8. Dishington, A. P., Douthwaite, R. E., Mortlock, A., Muccioli, A. B. & Simpkins, N. S. Episulfone substitution and ring-opening reactions via α-sulfonyl carbanion intermediates. *J. Chem. Soc., Perkin Trans. 1*. 323–338 (1997).
9. Baldwin, R. A. & Washburn, R. M. Organometallic azides. I. preparation and reactions of diarylphosphinic azides. *J. Org. Chem.* **30**, 3860–3866 (1965).
10. Tunney, S. E. & Stille, J. K. Palladium-catalyzed coupling of aryl halides with (trimethylstannyl)diphenylphosphine and (trimethylsilyl)diphenylphosphine. *J. Org. Chem.* **52**, 748–753 (1987).
11. Sun, M., Zhang, H.-Y., Han, Q., Yang, K. & Yang, S.-D. Nickel-catalyzed C–P cross-coupling by C–CN Bond Cleavage. *Chem. Eur. J.* **17**, 9566–9570 (2011).
12. Kranenburg, M., van der Burgt, Y. E. M., Kamer, P. C. J. & van Leeuwen, P. W. N. M. New diphosphine ligands based on heterocyclic aromatics inducing very high regioselectivity in rhodium-catalyzed hydroformylation: effect of the bite angle. *Organometallics* **14**, 3081–3089 (1995).
13. Nakanishi, K. et al. Oligonaphthofurans: fan-shaped and three-dimensional π-compounds. *J. Am. Chem. Soc.* **136**, 7101–7109 (2014).
14. Devon, T. J., Phillips, G. W., Puckette, T. A., Stavinoha, J. L. & Vanderbilt, J. J. Chelate ligands for low pressure hydroformylation catalyst and process employing same. Patent US 4,694,109 (1987).

15. Suzuki, K., Kumamoto, N., Ito, N., Hatae, S. & Suzuki, H. Organic magnesium phosphide and method for producing same, organic magnesium phosphide complex and method for producing same, and method for producing organic phosphorus-containing compound using said phosphide. Patent WO 2018/008510; Patent EP 3,480,204 (2019).

16. Okamoto, T. et al. V-shaped organic semiconductors with solution processability, high mobility, and high thermal durability. *Adv. Mater.* **25**, 6392–6397 (2013).

17. Guan, B.-T. et al. Methylation of arenes via Ni-catalyzed aryl C–O/F activation. *Chem. Commun.* 1437–1439 (2008).

18. Budac, D. & Wan, P. Excited state carbon acid dissociation and competing photorearrangements of 5H-dibenzo[*a*,*c*]cycloheptene derivatives. *Can. J. Chem.* **74**, 1447–1464 (1996).

19. Lee, Y. H. & Morandi, B. Metathesis-active ligands enable a catalytic functional group metathesis between aroyl chlorides and aryl iodides. *Nat. Chem.* **10**, 1016–1022 (2018).

20. Kawasaki, Y., Ishikawa, Y., Igawa, K. & Tomooka, K. Directing group-controlled hydrosilylation: regioselective functionalization of alkyne. *J. Am. Chem. Soc.* **133**, 20712–20715 (2011).

21. Suri, S. C. & Marcischak, J. C. Efficient synthesis of 1,2-dicyclopropylethyne and (cyclopropylethynyl)cyclobutane from 1,2-di-(ω-haloalkyl)ethynes and 1-cycloalkyl-2-(ω-haloalkyl)ethynes. *Org. Prep. Proced. Int.* **45**, 154–164 (2013).

22. Borowiecki, P. & Dranka, M. A facile lipase-catalyzed KR approach toward enantiomerically enriched homopropargyl alcohols. *Bioorg. Chem.* **93**, 102754 (2019).

23. Sanz, R., Castroviejo, M. P., Fernández, Y., Fañanás, F. J. A new and efficient synthesis of 4-functionalized benzo[*b*]furans from 2,3-dihalophenols. *J. Org. Chem.* **70**, 6548–6551 (2005).

24. Mäsing, F., Wang, X., Nesse, H., Klingauf, J. & Studer, A. Facile light-mediated preparation of small polymer-coated palladium-nanoparticles and their application as catalysts for alkyne semi-hydrogenation. *Chem. Eur. J.* **23**, 6014–6018 (2017).

25. Walsh, K., Sneddon, H. F. & Moody, C. J. Sustainable, mild and efficient *p*-methoxybenzyl ether deprotections utilizing catalytic DDQ. *Tetrahedron* **70**, 7380–7387 (2014).

26. Wong, V. H. L., White, A. J. P., Hor, T. S. & Hii, K. K. Silver-catalyzed cyclization of propargylic amides to oxazolines. *Adv. Synth. Catal.* **357**, 3943–3948 (2015).

27. Cahard, E., Bremeyer, N. & Gaunt, M. J. Copper-catalyzed intramolecular electrophilic carbofunctionalization of allylic amides. *Angew. Chem. Int. Ed.* **52**, 9284–9288 (2013).

28. Kalyani, D., Deprez, N. R., Desai, L. V., Sanford, M. S. Oxidative C−H activation/C−C bond forming reactions: synthetic scope and mechanistic insights. *J. Am. Chem. Soc.* **127**, 7330−7331 (2005).

29. Gorunova, O. N. et al. When applying the mercury poisoning test to palladacycle-catalyzed reactions, one should not consider the common misconception of mercury(0) selectivity. *Organometallics* 37, 2842−2858 (2018).

30. Mato, M. & Echavarren, A. M. Donor rhodium carbenes by retro-Buchner reaction. *Angew. Chem. Int. Ed.* **58**, 2088−2092 (2019).

31. Shirakawa, E., Yamagami, T., Kimura, T., Yamaguchi, S. & Hayashi, T. Arylmagnesiation of alkynes catalyzed cooperatively by iron and copper complexes. *J. Am. Chem. Soc.* **127**, 17164-17165 (2005).

32. Dolomanov, O. V., Bourhis, L. J., Gildea, R. J., Howard, J. A. K. & Puschmann, H. OLEX2: a complete structure solution, refinement and analysis program. *J. Appl. Cryst.* **42**, 339−341 (2009).

33. Sheldrick, G. M. SHELXT – Integrated space-group and crystalstructure determination. *Acta Cryst.* A**71**, 3−8 (2015).

34. Sheldrick, G. M. Crystal structure refinement with SHELXL. *Acta Cryst.* C**71**, 3−8 (2015).

35. Sheldrick, G.M. A short history of SHELX. *Acta Cryst.* A**64**, 112−122 (2008).